THE ROLE OF VASCULAR ADHESION PROTEIN (VAP)-1 DURING INFLAMMATORY LIVER DISEASE

By

JOSEPH RICHARD TICKLE



A thesis submitted to
The University of Birmingham
for the degree of

DOCTOR OF PHILOSOPHY

Institute of Immunology and Immunotherapy
College of Medical and Dental Sciences
The University of Birmingham
July 2017

UNIVERSITY OF
BIRMINGHAM

University of Birmingham Research Archive

e-theses repository

This unpublished thesis/dissertation is copyright of the author and/or third parties. The intellectual property rights of the author or third parties in respect of this work are as defined by The Copyright Designs and Patents Act 1988 or as modified by any successor legislation.

Any use made of information contained in this thesis/dissertation must be in accordance with that legislation and must be properly acknowledged. Further distribution or reproduction in any format is prohibited without the permission of the copyright holder.

ABSTRACT

Liver disease is the fifth largest killer in the United Kingdom and with the numbers of diagnoses increasing each year there is an urgent need for novel therapeutic interventions. This thesis examines one potential target, Vascular Adhesion Protein (VAP)-1: an amine oxidase enzyme with reported adhesin functionality. The results herein confirm a primarily sinusoidal localisation of VAP-1, expression of which was upregulated in the liver during chronic inflammation correlated with diminished enzyme activity. Functional analysis of sinusoidal VAP-1 *in vitro* did not demonstrate any effect of inhibition on leukocyte recruitment, unlike that observed in other tissues. Furthermore, only neutrophils were capable of binding to recombinant VAP-1 under flow conditions. Further investigation highlighted the importance of this intimate relationship during neutrophil-endothelial interactions; revealing the first evidence that neutrophils also express catalytically active VAP-1. Neutrophil effector functions, such as the formation of extracellular traps, were also hindered by recombinant VAP-1. This was also observed in wild-type mice but not those expressing a catalytically inactive form of VAP-1 ($SSAO^{KO}$). Following acute injury, these mice also exhibited expanded intrahepatic macrophage and NKT cell populations compared to control. In combination, these data highlight the complex role that VAP-1 plays during inflammatory liver disease.

So it goes.

ACKNOWLEDGEMENTS

This project would not have been possible without the guidance and assistance of many other researchers and friends. First and foremost I would like to thank my supervisors, Dr Christopher Weston and Professor David Adams, for their support and invaluable scientific guidance over the course of this research.

I would like to thank all of my colleagues at the Centre for Liver Research who have helped me through the long days and nights of the last few years. Particular thanks to Dr Arjuna Singanayagam, Benjamin Wiggins, Robert Dinsdale, Dr Emma Shepherd and Gillian Muirhead for their technical support. I also owe heartfelt gratitude to Dr Daniel Patten for his supervision, encouragement and friendship.

Lastly, I am indebted to all my friends and family for their moral support. In particular I would like to thank Alex and my mum: their faith in me has been unwavering and their support unfailing. They have been my foundation and this thesis is dedicated to them.

TABLE OF CONTENTS

1. GENERAL INTRODUCTION 1

1.1 Overview 1

1.2 The human liver 2
1.2.1 Hepatic architecture 2
1.2.2 Hepatic cell populations 4
1.2.2.1 Hepatocytes 5
1.2.2.2 Hepatic sinusoidal endothelial cells 6
1.2.2.3 Cholangiocytes 8
1.2.2.4 Hepatic stellate cells 8

1.3 The hepatic immune environment 8
1.3.1 Liver-resident leukocytes 9
1.3.2 Hepatic immune tolerance 11
1.3.3 Hepatic immune activation 12

1.4 Hepatitis and inflammatory liver disease 14
1.4.1 Acute liver injury 14
1.4.2 Chronic xenobiotic-induced liver disease 16
1.4.3 Metabolic liver disease 17
1.4.4 Autoimmune liver diseases 18

1.5 Animal models of liver disease 19
1.5.1 Animal models of acute liver injury 19
1.5.2 Animal models of chronic liver disease 20

1.6 Leukocyte recruitment 22
1.6.1 Classical leukocyte adhesion cascade 22
1.6.1.1 Rolling 22
1.6.1.2 Activation and arrest 24
1.6.1.3 Crawling and migration 26
1.6.2 Sinusoidal leukocyte recruitment 27
1.6.2.1 Endothelial adhesion molecules 27
1.6.2.2 Endothelial chemokines 30
1.6.2.3 Recruitment via other sinusoidal cells 31

1.7 Vascular adhesion protein-1 33
1.7.1 Genomic organisation 33
1.7.2 Sites of expression 34
1.7.3 Protein structure 35
1.7.4 Soluble VAP-1 37
1.7.5 Amine oxidase activity 37
1.7.5.1 Substrates 39
1.7.5.2 Inhibition 40
1.7.6 Function of VAP-1 41
1.7.6.1 Detoxification of xenobiotic amines 41
1.7.6.2 Leukocyte recruitment 42
1.7.6.3 Glucose transport 46
1.7.6.4 Cell growth and development 47
1.7.7 Role in disease 47
1.7.7.1 Role in liver disease 49

1.8 Aims and Hypotheses 51

2. MATERIALS AND METHODS 53

2.1 Human Tissue 53
2.1.1 Cell and tissue culture 53
2.1.2 Isolation of hepatic sinusoidal endothelial cells 54
2.1.3 Other human cells 55
2.1.4 Isolation of human leukocyte subsets from peripheral blood 55
2.1.4.1 Peripheral blood lymphocyte isolation 55
2.1.4.2 T cell and natural killer cell isolation 55
2.1.4.3 Monocyte Isolation 56
2.1.4.4 B cell isolation 56
2.1.4.5 Neutrophil isolation 56

2.2 Immunohistochemistry 57
2.2.1 Frozen tissue 57
2.2.1.1 Picrosirius red staining 57
2.2.1.2 Chromogenic staining 58
2.2.1.3 Immunofluorescent Staining 58
2.2.2 Formalin-fixed tissue 59
2.2.2.1 Haematoxylin and eosin 59
2.2.2.2 Chromogenic staining 60
2.2.3 Immunocytochemistry 60
2.2.4 Visualisation and quantification 61
2.2.4.1 Quantification of stained area 62
2.2.4.2 Quantification of liver necrosis 62

2.3 Polymerase chain reaction 62
2.3.1 RNA extraction and cDNA synthesis 62
2.3.2 Quantitative polymerase chain reaction 63

2.4 VAP-1 amine oxidase activity assay 64
2.4.1 Sample preparation 64
2.4.2 Immunosorbance 65
2.4.3 Amplex UltraRed Assay 65
2.4.4 Cell-based assay 67

2.5 Western blotting 67
2.5.1 Sample preparation 67
2.5.2 Sodium dodecyl sulphate polyacrylamide gel electrophoresis 67
2.5.3 Western blot transfer 68
2.5.4 Membrane development 68
2.5.5 Quantification 69

2.6 Flow-based Adhesion Assays 69
2.6.1 Assay preparation 69
2.6.1.1 Cell-based assay preparation 69
2.6.1.2 Recombinant protein-based assay preparation 70
2.6.1.3 Leukocyte preparation 70
2.6.2 Conducting the flow-based adhesion assay 70
2.6.3 Analysis 72

2.7 Endothelial cell transfection 73
2.7.1 Electroporation 73
2.7.2 Transfection efficiency analysis 73
2.7.3 Time-course imaging 74
2.7.4 Measurement of VAP-1 amine oxidase activity 74
2.7.5 Flow-based adhesion assay 75
2.7.5.1 Standard flow-based adhesion assay 75
2.7.5.2 Confocal flow-based adhesion assay 75

2.8 Neutrophil function assays 76
2.8.1 Neutrophil VAP-1 amine oxidase activity assay 76
2.8.1.1 Neutrophil and endothelial cell amine oxidase activity assay 76
2.8.2 Fluorometric analysis of cell-free DNA 76
2.8.3 Visualization of ex vivo neutrophil extracellular traps 77
2.8.3.1 Neutrophil extracellular trap immunocytochemistry 78
2.8.4 Neutrophil H_2O_2-production assay 78

2.9 Murine Tissue 79
2.9.1 Animal husbandry 79
2.9.2 Acute carbon tetrachloride-induced liver injury 79
2.9.2.1 Wild-type time course experiment 79
2.9.2.2 Wild-type vs. $SSAO^{KO}$ experiment 80
2.9.3 Organ retrieval and preparation 80
2.9.4 Liver function tests 80
2.9.5 Leukocyte extraction from murine liver 80
2.9.5.1 Flow cytometric analysis of isolated leukocytes 81
2.9.6 Isolation of murine neutrophils from compact bone 81

2.10 Statistical Analysis 83

3. VAP-1 EXPRESSION, ACTIVITY AND LOCALISATION DURING HUMAN LIVER DISEASE 85

3.1 Introduction 85

3.2 Results 87
3.2.1 Characterisation of hepatic VAP-1 87
3.2.1.1 Hepatic VAP-1 localisation 87
3.2.1.2 Cell-specific VAP-1 expression 87
3.2.1.3 VAP-1 localisation during liver disease 90
3.2.1.4 AOC3 expression during liver disease 90
3.2.1.5 VAP-1 amine oxidase activity during liver disease 92
3.2.1.6 VAP-1 coverage, expression and activity correlations 96
3.2.1.7 VAP-1 and degree of hepatic fibrosis 97
3.2.2 Inhibition of hepatic VAP-1 99
3.2.2.1 Inhibition by semicarbazide 99
3.2.2.2 Inhibition by LJP-1586 101
3.2.2.3 Inhibition by methylxanthines 101

3.3 Discussion 107
3.3.1 Distribution of hepatic VAP-1 108
3.3.2 Characterisation of VAP-1 expression and activity 109
3.3.3 Inhibition of hepatic VAP-1 113
3.3.4 Chapter summary 117

4. THE ROLE OF VAP-1 IN LEUKOCYTE FUNCTION 118

4.1 Introduction 118

4.2 Results 120
4.2.1 VAP-1 and hepatic leukocyte recruitment 120
4.2.1.1 Effect of VAP-1 inhibition on lymphocyte recruitment to HSEC 120
4.2.1.2 Effect of serum on lymphocyte recruitment to HSEC 120
4.2.1.3 Effect of VAP-1 inhibition on recruitment of leukocyte subsets 123
4.2.1.4 Effect of TNFα on VAP-1 expression by HSEC 127
4.2.1.5 Transfection of HSEC with GFP-VAP-1 127
4.2.1.6 Neutrophil recruitment to GFP-VAP-1-transfected HSEC 135
4.2.1.7 Effect of rVAP-1 on neutrophil recruitment to HSEC 137

4.2.2 VAP-1 and neutrophil function....142
4.2.2.1 Neutrophil expression of VAP-1....142
4.2.2.2 Effect of inhibiting neutrophil VAP-1 on recruitment....145
4.2.2.3 Neutrophil VAP-1 activity and ROS production....147
4.2.2.4 Effect of rVAP-1 on neutrophil ROS production....149
4.2.2.5 Neutrophil VAP-1 activity and NETosis....149
4.2.2.6 Effect of rVAP-1 on NETosis....152

4.3 Discussion....160
4.3.1 Hepatic lymphocyte recruitment via VAP-1....161
4.3.2 Overexpression of GFP-VAP-1....165
4.3.3 Hepatic neutrophil recruitment via VAP-1....166
4.3.4 Expression of VAP-1 by neutrophils....169
4.3.5 Neutrophil-derived VAP-1 and recruitment....171
4.3.6 Functional consequence of neutrophil VAP-1 expression....172
4.3.7 Chapter summary....176

5. THE ROLE OF VAP-1 IN ACUTE LIVER DISEASE....178

5.1 Introduction....178

5.2 Results....181
5.2.1 Acute murine CCl_4 hepatotoxicity....181
5.2.1.1 Hepatotoxicity of CCl_4....181
5.2.1.2 Hepatic regeneration following acute CCl_4 injury....183
5.2.1.3 Inflammatory response to acute CCl_4 injury....183
5.2.1.4 Hepatic VAP-1 during acute CCl_4 injury....192
5.2.2 Role of VAP-1 activity in acute murine CCl_4 hepatotoxicity....194
5.2.2.1 Hepatic VAP-1 in $SSAO^{KO}$ mice following acute CCl_4 injury....194
5.2.2.2 Hepatotoxicity of CCl_4 in $SSAO^{KO}$ mice....194
5.2.2.3 Hepatic regeneration in $SSAO^{KO}$ mice following acute CCl_4 injury....196
5.2.2.4 Inflammatory response of $SSAO^{KO}$ mice to acute CCl_4 injury....197

5.3 Discussion....205
5.3.1 Acute murine liver injury model suitability....206
5.3.2 Characterisation of acute hepatic CCl_4 injury and regeneration....206
5.3.3 Consequence of VAP-1 activity during injury and regeneration....207
5.3.4 Characterisation of the acute inflammatory response to CCl_4 injury....208
5.3.5 Consequence of VAP-1 activity on inflammatory response....211
5.3.6 Changes in hepatic VAP-1 during acute CCl_4 hepatotoxicity....214
5.3.7 Chapter Summary....215

6. CONCLUSIONS AND FUTURE WORK....217

6.1 Overview....217

6.2 Summary of principle findings....218
6.2.1 VAP-1 and human liver disease....218
6.2.2 VAP-1 and leukocyte function....219
6.2.3 VAP-1 and acute murine liver injury....220

6.3 Study limitations....220

6.4 Translational implications....221

6.5 Future work....224

7. REFERENCES....228

LIST OF FIGURES

CHAPTER 1

1.1	Structure of the Human Liver	3
1.2	The cells of the Human Liver	5
1.3	Fenestrations of Hepatic Sinusoidal Endothelial Cells	7
1.4	Activation of the Inflammasome by DAMPs and PAMPs	13
1.5	The progression of Human Liver Disease	15
1.6	The leukocyte adhesion cascade	23
1.7	Structure and activation of integrin molecules	25
1.8	The sinusoidal leukocyte adhesion cascade	28
1.9	Leukocytes-hepatocyte interactions within the sinusoids	29
1.10	Structure of VAP-1	36
1.11	Leukocyte recruitment by VAP-1	38

CHAPTER 2

2.1	ImageJ quantification of immunohistochemical staining	61
2.2	Antibody-captured VAP-1 amine oxidase activity assay	66
2.3	Flow-based adhesion assay	71

CHAPTER 3

3.1	Localisation of hepatic VAP-1	88
3.2	VAP-1 expression by hepatic cell types	89
3.3	Expression of *Aoc3* mRNA by hepatic cell types	90
3.4	Localisation of hepatic VAP-1 during disease	91
3.5	Expression of hepatic VAP-1 during liver disease	93
3.6	Optimisation of antibody-capture Amplex UltraRed Assay	94
3.7	XY Comparison of VAP-1 staining, expression and activity between human liver tissue samples	95
3.8	XYZ Comparison of VAP-1 staining, expression and activity between human liver tissue samples	96
3.9	Extent of picrosirius red staining within human liver tissue samples	97
3.10	Comparison between VAP-1 and extent of fibrosis within human liver tissue samples	98
3.11	Inhibitory effect of semicarbazide on hepatic VAP-1 activity	100
3.12	Inhibitory effect of LJP-1586 on hepatic VAP-1 activity	102
3.13	Structure of Xanthine, Caffeine and Theobromine	103
3.14	Inhibitory effect of caffeine on hepatic VAP-1 activity	104
3.15	Optimisation of methylxanthines and amine oxidase activity	106

CHAPTER 4

4.1	Effect of VAP-1 inhibition on adhesion of PBLs to stimulated HSEC	121
4.2	HSEC viability in the presence of VAP-1 inhibitors	122
4.3	Effect of media on adhesion of PBLs to stimulated HSEC	123
4.4	HSEC viability in the presence of different culture media	124
4.5	Effect of VAP-1 inhibition on adhesion of leukocyte subsets to stimulated HSEC	125
4.6	Effect of VAP-1 inhibition on migration of leukocyte subsets across stimulated HSEC	126
4.7	Adhesion of leukocyte subsets to recombinant adhesion molecules	128
4.8	Interaction of leukocyte subsets with recombinant adhesion molecules	129
4.9	Effect of proinflammatory stimulation on HSEC VAP-1 expression	130
4.10	Optimisation of HSEC nucleofection with GFP-VAP-1	131
4.11	HSEC expression of GFP-VAP-1 over time	132
4.12	VAP-1 enzyme activity following transfection with GFP-VAP-1	134
4.13	Expression patterns of GFP-VAP-1 in HSEC	136
4.14	Effect of GFP-VAP-1 overexpression on adhesion of neutrophils to stimulated HSEC	138
4.15	Z-stack analysis of neutrophil interaction with GFP-VAP-1^{WT}	139

4.16	Time-lapse analysis of neutrophil interaction with GFP-VAP-1^{WT}	140
4.17	Effect of rVAP-1 on adhesion of neutrophils to stimulated HSEC	141
4.18	VAP-1 expression by human neutrophils	143
4.19	Effect of stimulation on VAP-1 expression by human neutrophils	144
4.20	Expression of *AOC3* mRNA by human leukocytes	145
4.21	VAP-1 amine oxidase activity of human neutrophils	146
4.22	Effect of VAP-1 inhibition on neutrophil adhesion	148
4.23	Effect of VAP-1 amine oxidase inhibition on neutrophil ROS production	150
4.24	Effect of VAP-1 substrates on neutrophil ROS production	151
4.25	Effect of recombinant VAP-1 protein on neutrophil ROS production	153
4.26	Effect of VAP-1 amine oxidase activity on NET production	154
4.27	Effect of recombinant VAP-1 protein on human NET production	156
4.28	Effect of recombinant VAP-1 protein on histone 3 citrullination	157
4.29	Effect of recombinant VAP-1 protein on NETosis	158
4.30	Effect of recombinant VAP-1 protein on murine NET production	159
4.31	A possible mechanism of VAP-1 in NETosis	175

CHAPTER 5

5.1	Effect of CCl_4 on serum ALT concentrations of WT mice	181
5.2	Effect of CCl_4 on hepatic necrosis of WT mice	182
5.3	Effect of CCl_4 on hepatic cleaved caspase-3 expression of WT mice	184
5.4	Effect of CCl_4 on hepatic Ki67 expression of WT mice	185
5.5	Effect of CCl_4 on hepatic PCNA expression of WT mice	186
5.6	Effect of CCl_4 on infiltrating hepatic $CD45^+$ cells in WT mice	187
5.7	Gating strategy for phenotypic analysis of WT murine intrahepatic leukocytes by flow cytometry	188
5.8	Effect of CCl_4 on intrahepatic lymphoid cells of WT mice	190
5.9	Effect of CCl_4 on intrahepatic myeloid cells of WT mice	191
5.10	Effect of CCl_4 on hepatic *Aoc3* expression of WT mice	192
5.11	Effect of CCl_4 on hepatic VAP-1 enzyme activity of WT mice	193
5.12	Effect of CCl_4 on hepatic VAP-1 of WT and $SSAO^{KO}$ mice	195
5.13	Effect of CCl_4 on serum liver enzyme concentrations of WT and $SSAO^{KO}$ mice	196
5.14	Effect of CCl_4 on hepatic necrosis of WT and $SSAO^{KO}$ mice	197
5.15	Effect of CCl_4 on hepatic cleaved caspase-3 expression of WT and $SSAO^{KO}$ mice	198
5.16	Effect of CCl_4 on hepatic Ki67 expression of WT and $SSAO^{KO}$ mice	199
5.17	Effect of CCl_4 on hepatic PCNA expression of WT and $SSAO^{KO}$ mice	200
5.18	Effect of CCl_4 on infiltrating hepatic $CD45^+$ cells in WT and $SSAO^{KO}$ mice	201
5.19	Gating strategy for phenotypic analysis of WT and $SSAO^{KO}$ murine intrahepatic myeloid leukocytes by flow cytometry	202
5.20	Effect of CCl_4 on intrahepatic lymphoid cells of WT and $SSAO^{KO}$ mice	203
5.21	Effect of CCl_4 on intrahepatic myeloid cells of WT and $SSAO^{KO}$ mice	204

LIST OF TABLES

CHAPTER 1

1.1	The effect of VAP-1 antibody blockade on leukocyte recruitment	44
1.2	The effect of VAP-1 amine oxidase inhibition on leukocyte recruitment	45

CHAPTER 2

2.1	Human staining antibodies (frozen tissue)	57
2.2	Fluorescent secondary antibodies	58
2.3	Murine staining antibodies (formalin-fixed tissue)	59
2.4	Primers for qPCR analysis	63
2.5	VAP-1 antibodies for immunosorbence	64
2.6	Western Blot primary antibodies	68
2.7	Western Blot secondary antibodies	69
2.8	Flow assay treatments	72
2.9	Transfection plasmids	73
2.10	Neutrophil experimental reagents	77
2.11	Neutrophil primary antibodies	78
2.12	Neutrophil secondary antibodies	79
2.13	Mouse liver flow cytometry antibodies – compensation and lymphoid panel	82
2.14	Mouse liver flow cytometry antibodies – myeloid panels	83

LIST OF ABBREVIATIONS

AGE	Advanced glycation end product
AIH	Autoimmune hepatitis
ALD	Alcohol-induced liver disease
ALDH	Aldehyde dehydrogenase
ALF	Acute liver failure
ALT	Alanine transaminase
AOC	Amine-oxidase copper containing
APC	Antigen presenting cell
aSMA	Anti-smooth muscle antibody
AST	Aspartate transaminase activity
BEC	Biliary epithelial cell
CCl_4	Carbon tetrachloride
CCR	Chemokine receptor
CD	Cluster of differentiation
CitH3	Citrullinated histone 3
ConA	Concavalin A
CYP450	Cytochrome P450
DC	Dendritic cell
DAMP	Danger associated molecular pattern
ECM	Extracellular matrix
EpCAM	Epithelial cell adhesion molecule
ER	Endoplasmic reticulum
GAPDH	Glyceraldehyde 3-phosphate dehydrogenase
GFP	Green Fluorescent Protein
H&E	Haematoxylin and eosin
HEV	High endothelial venules
HGF	Hepatocyte growth factor
HRP	Horseradish peroxidase
HS	Human serum
HSC	Hepatic stellate cell
HSEC	Hepatic sinusoidal endothelial cell
ICAM	Intracellular cell adhesion molecule
IFN	Interferon
Ig	Immunoglobulin
IL	Interleukin
IQR	Interquartile range
KC	Kupffer cell
KW	Kruskal-Wallis
LOX(L)	Lysyl oxidase (like)
LPS	Lipopolysaccharide
MAdCAM	Mucosal addressin cell adhesion molecule
MAO	Monoamine oxidase
MCD	Methyl choline deficient
MDSC	Myeloid-derived suppressor cell
MHC	Major histocompatibility complex
M-MDSC	monocyte myeloid-derived suppressor cell
MMP	Matrix metalloproteinase
NADPH	Nicotinamide adenine dinucleotide phosphate
NAFLD	Non-alcoholic fatty liver disease
NASH	Non-alcoholic steatohepatitis
NANB	Non-A Non-B hepatitis
NE	Neutrophil elastase

NET	Neutrophil extracellular trap
NF*k*B	Nuclear factor kappa B
NK	Natural killer
NL	Normal liver
NOX	NADPH oxidase
PAD	Protein arginine deiminase
PAMP	Pathogen-associated molecular pattern
PBC	Primary biliary cirrhosis
PBL	Peripheral blood leukocyte
PBS	Phosphate-buffered saline
PKC	Protein kinase C
PMN-MDSC	Neutrophil Myeloid-derived suppressor cell
POD	Paracetamol overdose
PRR	Patten recognition receptor
PSC	Primary sclerosing cholangitis
qPCR	Quantitative real-time PCR
RAGE	Receptor for advanced glycation end products
ROS	Reactive oxygen species
SD	Standard deviation
Siglec	sialic-acid-binding immunoglobulin-like lectin
SMI	Small molecule inhibitors
SNL	Steatotic normal
SSAO	Semicarbazide-sensitive amine oxidase
sVAP-1	Soluble VAP-1
T_c	Cytotoxic T-cell
TCR	T-cell receptor
TGF	Transforming growth factor
T_h	Helper T-cell
TNF	Tumour necrosis factor
TPQ	Topoquinone
VAP	Vascular adhesion protein
VAP-1^{Y471F}	Catalytically inactive VAP-1
VAP-1^{WT}	Catalytically active VAP-1
VCAM	Vascular cell adhesion molecule
VEGF	Vascular endothelial growth factor
WT	Wild-type
Y471F	Tyrosine-471 to Phenylalanine mutation

1

GENERAL INTRODUCTION

1.1 Overview

The anatomical feature of the liver whereby the organ receives blood directly from the gut has resulted in the adaptation of a highly specialised local immune environment. Harmless commensals and food-borne antigens from the gastrointestinal tract must be effectively tolerated while appropriate immune responses are mounted against pathogenic organisms. Fundamental to this immune regulation are the interactions between the liver and circulating peripheral blood leukocytes that occur within the hepatic blood channels: the sinusoids. Here, highly specialised hepatic sinusoidal endothelial cells that form a physical barrier between hepatocytes and the sinusoidal lumen are capable of determining the fate of this specific immune response: tolerance or activation. Constitutive expression of molecules necessary for receptor-mediated endocytosis, antigen presentation and leukocyte adhesion on the endothelial surface

allow for efficient, but frequently complex, communication between cell types. One such molecule called Vascular Adhesion Protein (VAP)-1 is an amine oxidase with adhesion molecule functionality that plays an important role in hepatic leukocyte recruitment and has been implicated in the pathogenesis of inflammatory liver disease.

The intention of this thesis is to examine VAP-1 expression across a spectrum of liver diseases and to interrogate some of the functions of VAP-1 within the hepatic environment with a view to elucidate more about the mechanism of action.

1.2 The human liver

The liver is the largest internal organ; located in the upper right abdomen it receives blood via a dual blood supply: 25-30% is oxygenated and supplied by the hepatic artery directly from the heart, while the remaining 70-75% is nutrient-rich deoxygenated blood entering from the gastrointestinal tract via the hepatic portal vein. As a consequence, the highly vascularised liver receives the highest cardiac output of all the organs, with 30% of the total blood volume passing through it each minute (Sheth and Bankey, 2001), supporting the role of the liver in filtration of the blood from the gut, in addition to extensive exocrine and endocrine functions

1.2.1 Hepatic architecture

The human liver consists of four distinct anatomical lobes, which can be further subdivided into eight functionally independent segments as seen in Figure 1.1A (Abdel-Misih and Bloomston, 2010). Blood is supplied to the centre of each segment by a branch of the hepatic artery and hepatic portal vein. The blood percolates through the segment to the hepatic veins in the periphery that in turn lead to the vena cava. Each segment also contains a central duct, which drains bile away from the liver and towards the duodenum and gallbladder.

Individual segments consist of thousands of functional subunits known as lobules (Figure 1.1B). The classic hepatic lobule is the unit drained by a single portal vein: it is a hexagonal structure with a central hepatic vein and a single portal triad at each of the six vertices. Each portal triad is composed of five structures: a hepatic arteriole, hepatic portal venule, bile duct, lymphatic vessels and a branch of the vagus nerve. Blood from the artery and portal vein combines within the sinusoids: the vessels that radiate out

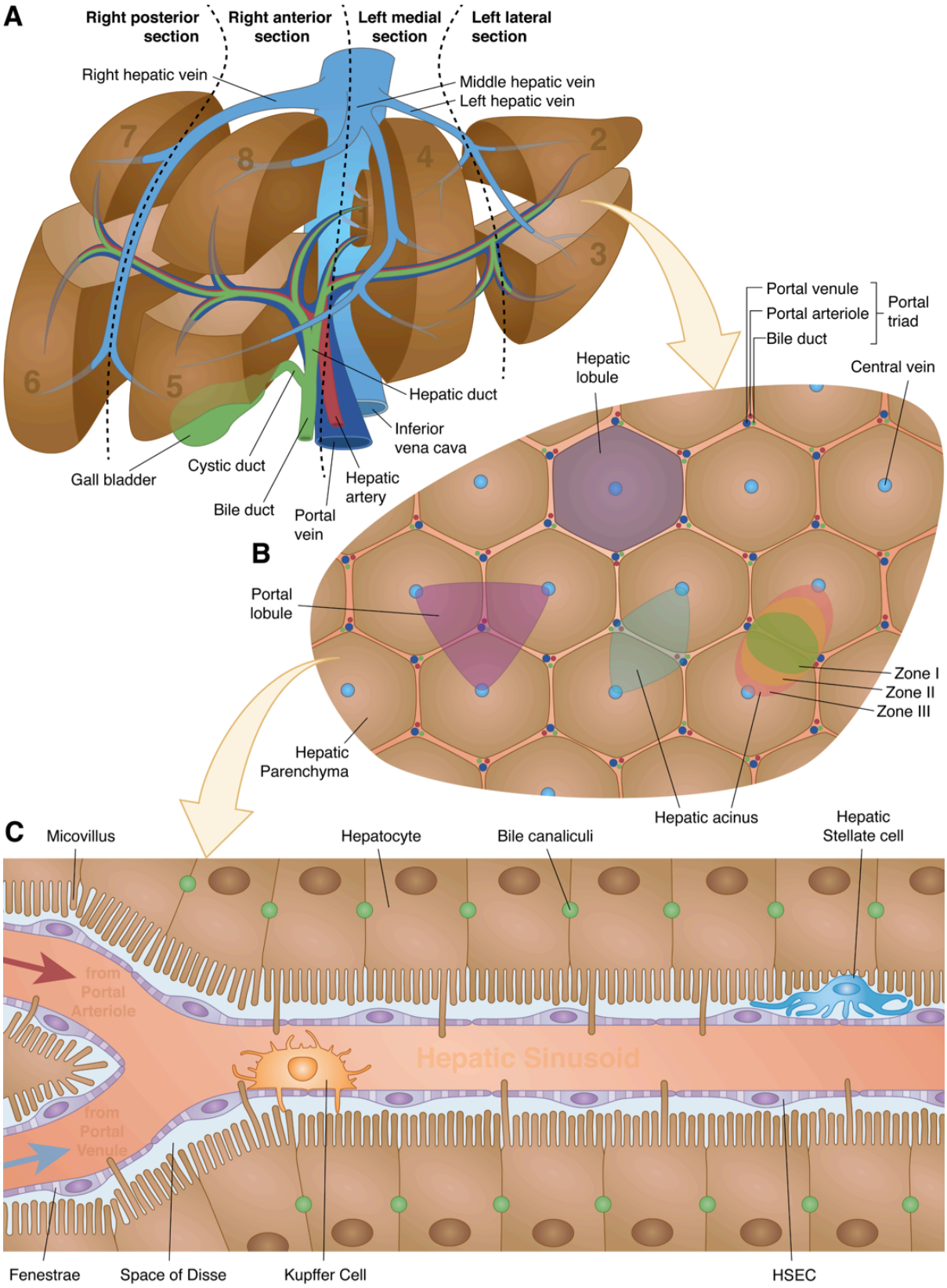

A
Right posterior section
Right anterior section
Left medial section
Left lateral section
Right hepatic vein
Middle hepatic vein
Left hepatic vein
7
8
4
2
3
6
5
Hepatic duct
Inferior vena cava
Gall bladder
Cystic duct
Bile duct
Portal vein
Hepatic artery
Portal venule
Portal arteriole
Bile duct
Portal triad
Hepatic lobule
Central vein
B
Portal lobule
Zone I
Zone II
Zone III
Hepatic Parenchyma
Hepatic acinus
C
Micovillus
Hepatocyte
Bile canaliculi
Hepatic Stellate cell
from Portal Arteriole
Hepatic Sinusoid
from Portal Venule
Fenestrae
Space of Disse
Kupffer Cell
HSEC

Figure 1.1 Structure of the Human Liver. (**A**) Division of the liver into 8 distinct structural lobes, each of which receives blood from a branch of the hepatic artery and hepatic portal vein and drains through the hepatic vein to the inferior vena cava and to the heart. Each is also connected to the bile ducts, which drain bile to the gall bladder. (**B**) The structure of the hepatic parenchyma, which can be structurally divided into hepatic and portal lobules, or into by metabolic activity into the hepatic acinus. This can be further subdivided into zones I, II and III by the distance from the portal triad and therefore oxygen blood. (**C**) The structure of the hepatic sinusoids, which drain blood from the portal triad to the central vein. The sinusoids are lined with highly specialised hepatic sinusoidal endothelial cells (HSEC) that separate the lumen from the parenchymal hepatocytes.

from the central vein (Figure 1.1C). Between each of the sinusoids are cords of hepatic parenchymal cells called hepatocytes, which are separated from the sinusoids by the perisinusoidal space, or space of Disse. This space largely consists of blood plasma but is characterised by components of the extracellular matrix (ECM) such as collagen III, proteoglycans and fibronectin (Abdel-Misih and Bloomston, 2010).

The liver microarchitecture can also be viewed as the hepatic acinus, which depicts the region supplied and drained by the portal triad. The structure is rhombus-shaped with two veins and two portal triads at opposing vertices. The acinus is a more accurate depiction from a metabolic perspective as it can be divided into three zones according to oxygen exposure (Abdel-Misih and Bloomston, 2010). Those hepatocytes in zone 1, closest to the arteriole (periportal), are best oxygenated but are also first exposed to blood-borne pathogens and toxins (Gebhardt, 2014). Zone 3 is proximal to the central vein (centrilobular) and is therefore low in oxygen and rich in waste products such as metabolites (Gebhardt, 2014).

The final histological division of the liver parenchyma is the portal lobule, which describes the area drained by any single bile duct. This triangular structure is centred on a portal triad, with central veins at each of the vertices (Abdel-Misih and Bloomston, 2010).

1.2.2 Hepatic cell populations

The liver is largely composed of hepatocytes: comprising approximately 60-80% of the total liver cell population and accounting for over 90% of the total liver volume (Daoust and Cantero, 1959; Kmieć, 2001). The hepatocytes are arranged in plates averaging two cells thick, which radiate out from the central vein and are separated by hepatic sinusoids. The remaining non-parenchymal cells are mostly located within this sinusoidal region and are summarised in Figure 1.2.

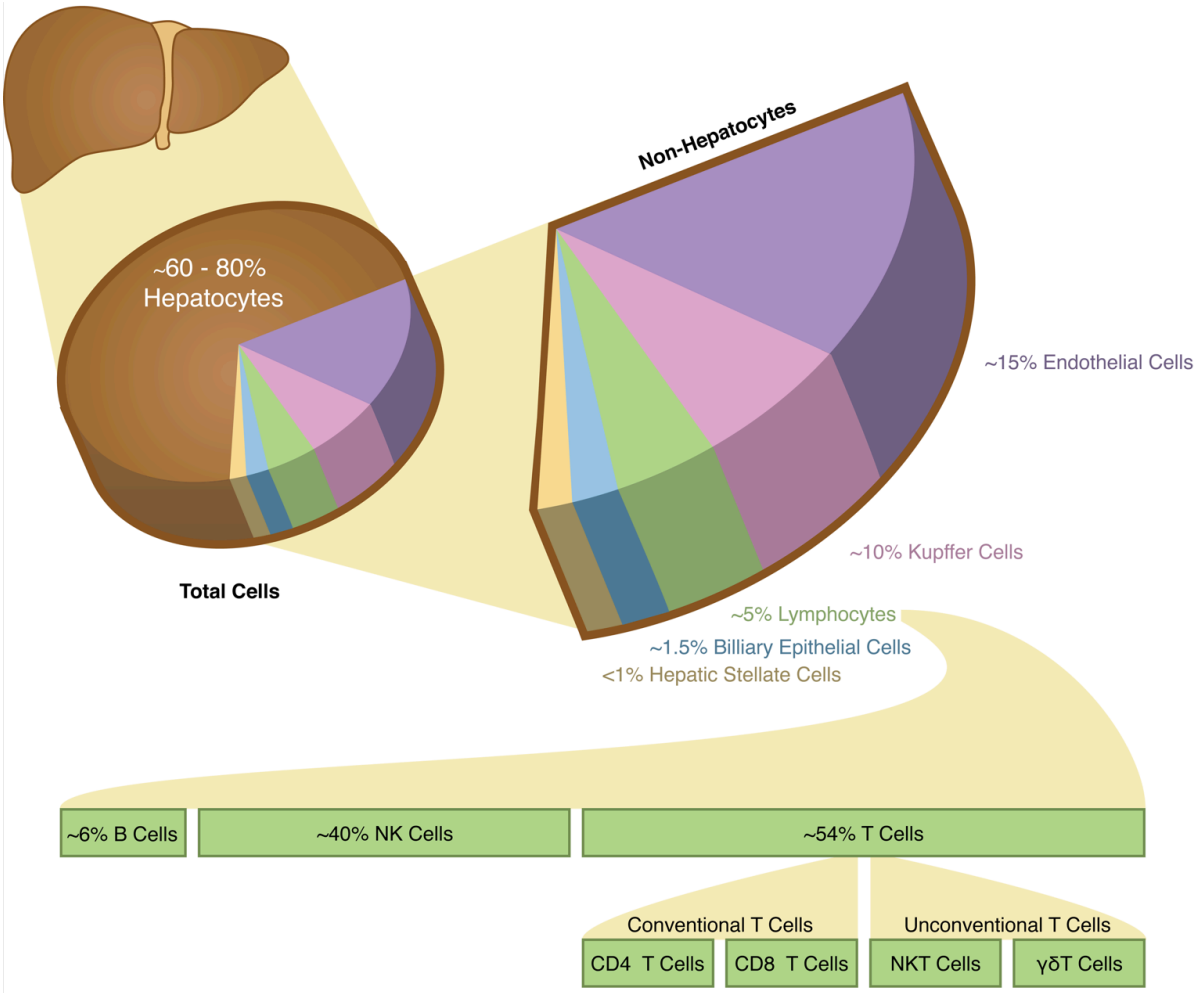


Figure 1.2 The cells of the Human Liver. Hepatocytes carry out the majority of liver functions and therefore form the largest proportion of hepatic cells (between approximately 60 – 80%). The remaining cells are endothelial cells, Kupffer cells, Biliary Epithelial Cells, Hepatic Stellate Cells and lymphocytes. Over half of these lymphocytes are T cells, approximately 40% are Natural Killers (NK) cells and the rest are B cells. The T cell population is highly diverse, but consists of conventional $CD4^+$ and $CD8^+$ T cells and unconventional NKT cells and those expression receptors such as γδ.

1.2.2.1 Hepatocytes

As the most abundant cell type within the liver, the vast majority of hepatic functions are carried out within hepatocytes: specialised epithelial cells that contain large amounts of mitochondria and extensive smooth and rough endoplasmic reticulum (ER). These components allow for the synthesis and secretion of a large variety of growth factors, cytokines, plasma proteins, blood clotting factors and complement components. Hepatocytes are critical to the metabolism of many drugs and toxins due to the expression of molecules such as the family of cytochrome P450 enzymes (CYP450) (Zanger and Schwab, 2013). The majority of lipid, carbohydrate and amino acid

metabolism also occurs within hepatocytes, with functional heterogeneity observed across the hepatic acinus: periportal cells in zone 1 exhibit higher numbers of mitochondria and enzymes corresponding to oxidative metabolism whereas centrilobular hepatocytes favour glycolysis and liponeogenesis (Katz, 1992).

The hepatocyte cell surface is heavily coated with microvilli, which extend into the perisinusoidal space to facilitate the efficient exchange of molecules and absorption of nutrients. Bile is also synthesised within hepatocytes and is drained directly into bile canaliculi.

1.2.2.2 Hepatic sinusoidal endothelial cells

Hepatic sinusoidal endothelial cells (HSEC) are the second most abundant cell within the liver. HSEC form the walls of the hepatic sinusoids; acting as a barrier between the parenchyma and peripheral blood. Unlike the microvasculature of most other organs the HSEC monolayer is very thin and lacks an underlying basement membrane and tight junctions, creating a discontinuous vascular lining (Sørensen et al., 2015).

HSEC are a major site of the elimination of many molecules from the circulation and are able to actively control their transport across the monolayer because of high endocytotic activity (Tavassoli et al., 1986). This is due to the presence of numerous endocytotic vesicles and lysosome-like vacuoles present within HSEC (Braet and Wisse, 2002) combined with expression of a range of endocytosis receptors for both soluble and colloidal ligands. These include the mannose receptor, hyaluronan receptor, Immunoglobulin-G (IgG) Fc receptor, collagen α-chain receptor and a host of scavenger receptors (Elvevold et al., 2004). Interestingly, HSEC receptor expression exhibits zonal heterogeneity, for example periportal and centrilobular HSEC exhibit different levels of junctional adhesion molecule-1 (Khandoga et al., 2005), caveolin-1 (Ogi et al., 2003) and galactose and mannose receptors (Dini and Carla, 1998).

HSEC are antigen-presenting cells (APCs), capable of antigen cross-presentation to lymphocytes on major histocompatibility complex class I and II (MHC I and MHC II) molecules at their cell surface (Berg et al., 2006; Limmer et al., 2005, 2000). HSEC are as competent as dendritic cells (DCs) at cross-presentation but are around one hundred-fold more pronounced at antigen uptake (Schurich et al., 2009) and the process is much more rapid than in traditional APCs (Knolle and Wohlleber, 2016).

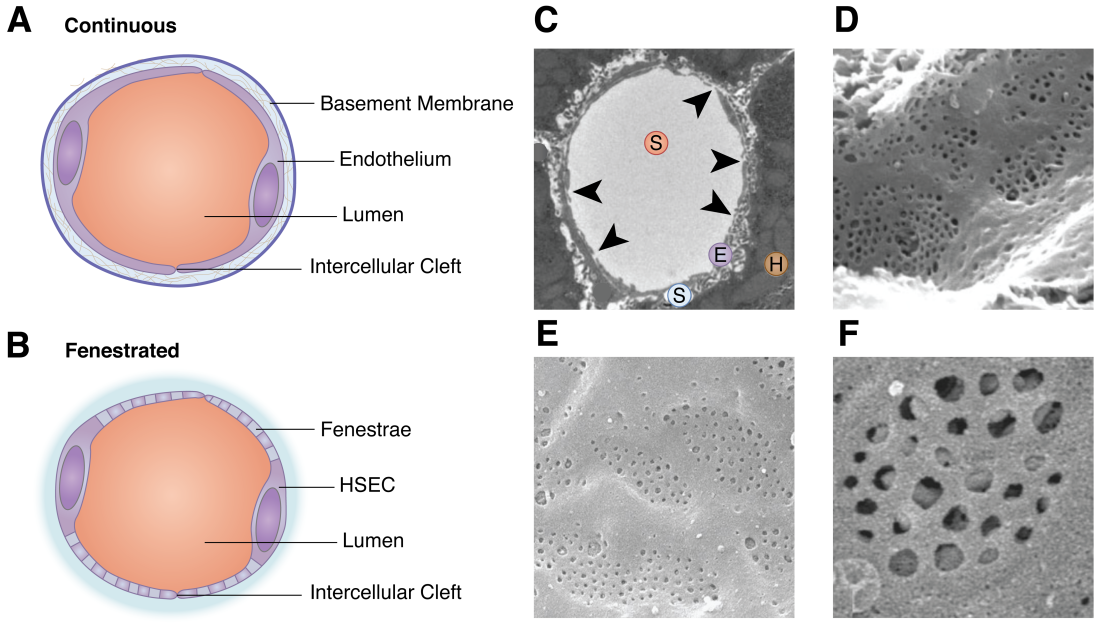


Figure 1.3 Fenestrations of Hepatic Sinusoidal Endothelial Cells. (**A**) The structure of most blood vessels consists of a continuous endothelial monolayer, lined by a basement membrane consisting primarily of extracellular matrix components. (**B-F**) Hepatic sinusoidal endothelial cells contain many large (100-200 nm) cytoplasmic holes called fenestrae thereby allowing them to act as physical sieves. *S*, Sinusoidal lumen; *E*, Endothelium; *H*, Hepatocytes; *S*, Stellate Cells. Arrows indicate fenestrae. Image C, D & F from Warren et al., 2006, Image E from Wisse et al., 2010.

HSEC are also able to control molecular transport by physical filtration. Unlike most other vascular endothelial cells they contain many large (100-200 nm) cytoplasmic holes called fenestrae, as seen in Figure 1.3 (Braet and Wisse, 2002). These fenestrations occupy between 6-8% of the endothelial surface, decreasing in size but increasing in number from periportal to centrilobular regions (Aird, 2007). Along with the lack of a basement membrane, fenestrations allow the HSEC to act as a sieve: selectively obstructing particles from diffusing in to or out of the perisinusoidal space, facilitated by the low shear flow rate within the sinusoids of between 25-250 μm/min (MacPhee et al., 1995). This process is not passive: molecular passaging is tightly regulated and HSEC can exclude translocation of macromolecules as small as 12 nm (Kempka and Kolb-Bachofen, 1988).

HSEC are also able to facilitate leukocyte extravasation via expression of a range of adhesion molecules that, in combination with the narrow diameter (7-12 μm) and low flow rate (MacPhee et al., 1995), promotes interactions between HSEC and peripheral blood leukocytes. This process is discussed in depth within section 1.6.

1.2.2.3 Cholangiocytes

Bile is secreted by hepatocytes and drains from the liver via the bile ducts, which are lined with highly specialised biliary epithelial cells (BEC), named cholangiocytes. Cholangiocytes can be broadly categorized as either large or small, which are found in either the large or small bile ducts, respectively. These cells not only differ morphologically but also functionally: large cholangiocytes have a low nucleus/cytoplasm ratio with abundant organelles and are therefore more specialized for the modification of bile (Benedetti et al., 1996; Tabibian et al., 2013).

Cholangiocytes have immunomodulatory function via expression of MHC, lymphocyte adhesion molecules and through secretion of cytokines and chemokines (Chuang et al., 2009; Fava et al., 2005). Cholangiocytes are also the target of the immune system in several hepatobiliary diseases, known as cholangiopathies, during which their barrier function is disrupted (as described in section 1.4.5). Large cholangiocytes are more susceptible to this damage, whereas small cholangiocytes appear more resistant and are capable of replenishing the biliary epithelium through enhanced proliferation (Alvaro et al., 2007; Francis et al., 2008; Mancinelli et al., 2010).

1.2.2.4 Hepatic stellate cells

Hepatic stellate cells (HSCs) are star-shaped pericytes located within the perisinusoidal space that are present at an approximate ratio of one for every twenty hepatocytes (Moreira, 2007). HSCs are involved in the regulation of retinoid homeostasis and store approximately 80% of the total retinoids in the whole body (Blomhoff et al., 1992). HSCs become activated during pathological conditions such as liver cirrhosis; characterised by the loss of retinoids and proliferation at a very high rate while secreting large amounts of ECM components such as collagen, proteoglycan and glycoprotein (Senoo, 2004). Their morphology also changes to resemble that of a fibroblast or myofibroblast.

1.3 The hepatic immune environment

The liver is central to metabolism and clearance of toxins but it is also a highly specialised immunological organ. This is necessary due to the high volume of blood it receives directly from the gut, which is rich in oxygen and nutrients, but also contains blood-borne pathogens and pathogen-derived molecules (Lumsden et al., 1988; Son et al.,

2010). The liver is therefore one of the first lines of defence between the host and external environment.

The normal liver contains large numbers of both infiltrated and resident leukocytes, which constitute approximately 5-8% of all cells within the liver: totalling an estimated 10^{10} cells (Morsy et al., 2005). The majority of these cells are of the innate immune system that are enriched within the liver (Li and Diehl, 2003). The cells of this system are fast mobilising and specifically targeted towards invading organisms through pattern-recognition receptors (PRRs) that recognize specific structures called pathogen-associated molecular patterns (PAMPs) (Janeway and Medzhitov, 2002). PRRs fall into three distinct categories: membrane-bound, phagocytic or secreted. The majority of secreted PRRs within the circulation (80-90%) are biosynthesised by hepatocytes, including components of the complement system (Gao et al., 2008). Hepatocytes upregulate the production of these secreted PRRs in response to inflammatory cytokines such as tumour necrosis factor-α (TNFα) and interferon-γ (IFNγ), which primes the immune response. This rapid upregulation is reliably observed in response to inflammation, therefore hepatocyte-derived soluble PRRs, such as C-reactive protein, are used as diagnostic markers of acute and chronic inflammatory disease states (Verma et al., 2005).

1.3.1 Liver-resident leukocytes

80-90% of all tissue macrophages within the body are found within the liver, constituting approximately 35% of non-parenchymal cells (Bilzer et al., 2006). Contrary to most monocyte and macrophage populations, these Kupffer cells (KCs) are static and bound to HSEC within the sinusoidal lumen where they are exposed to the contents of the blood. They are distributed between zones 1, 2 and 3 of the acinus in a ratio of 4:3:2 so are therefore more concentrated at the first point of contact with potentially pathogen-laden blood (Parker and Picut, 2005). KCs play a dominant role in clearing particles from the circulation and are uniquely able to capture bacteria from blood flow. Once captured, KCs are able to phagocytose the bacteria or recruit neutrophils to internalize and kill the pathogen (Rakhmilevich, 1995), resulting in production of proinflammatory cytokines such as TNFα or interleukin-1 (IL-1); thereby acting as immune sentinels, activating the immune response to the presence of harmful pathogens (Olynyk et al., 1994; Shi et al., 2004). KCs are also important APCs, capable of licensing $CD8^+$ effector cells through the

expression of MHC and costimulatory molecules. However, they are poor activators of the adaptive immune response under basal conditions and help maintain homeostasis via the secretion of IL-10 (Knolle et al., 1998; You et al., 2008).

Early work indicated that KCs derive from differentiated bone marrow-derived monocytes that migrate into the liver (Gale et al., 1978), however they are now believed to originate from the foetal yolk sack (Epelman et al., 2014). The tissue-resident KCs and infiltrated macrophages are therefore thought to be distinct cellular subsets, although distinguishing between them is often difficult. The infiltrating monocytes that differentiate into macrophages can be divided into two distinct subsets that display differential expression of CD14 and CD16. Classical $CD14^{hi}CD16^{low}$ monocytes are considered to have proinflammatory activity whereas $CD14^{low}CD16^{hi}$ cells have a more immunomodulatory function and are thought to form a larger proportion of tissue-resident macrophages (Heymann et al., 2009).

Natural Killer (NK) cells are highly enriched within the liver: constituting between 30-50% of total hepatic lymphocytes in humans and 10% in mice (Doherty and O'Farrelly, 2000; Dong et al., 2004). NK cells are large, highly cytotoxic, granular lymphocytes that target pathogens and virally infected hepatocytes. They do this mainly by cell-mediated lysis via the release of preformed cytolytic granules containing perforin and granzyme (Notas et al., 2009). They are also capable of secreting large amounts of proinflammatory cytokines in response to activation, such as IFNγ (Crispe, 2009). Both functions are also inherent to $CD3^+$ Natural Killer T (NKT) cells, which are also enriched within the liver and constitute between 5-10% of liver lymphocytes in humans and 30-40% in mice (Doherty and O'Farrelly, 2000; Dong et al., 2004; Matsuda et al., 2008).

The intrahepatic T cell population also differs from the peripheral blood. Conventional $CD4^+$ helper (T_h) and $CD8^+$ cytotoxic T cells represent a ratio of 2:1 in the circulation, whereas this is reversed within the liver. Hepatic $CD4^+$ and $CD8^+$ T cells are capable of recognising a wide range of antigens in the context of MHC I and II, respectively, due to a diverse repertoire of αβ-T cell receptors (αβTCR). The liver also contains a range of less common $CD3^+$ cell types such as $CD4^+CD8^+$ and $CD4^-CD8^-$ as well as over 5 times more cells expressing the γδTCR than in peripheral blood (Norris et al., 1998).

The professional APCs of the liver, DCs, scavenge antigen from the blood and mature as they traverse the sinusoids. They then exit via the central vein or cross the HSEC

monolayer to the perisinusoidal space and drain via the lymphatics, transporting antigens to regional lymph nodes. However, under basal conditions, hepatic DCs are considerably less efficient at T cell activation than those from other tissues (Matsuno et al., 1996; Pillarisetty et al., 2004; Tokita et al., 2008). Hepatic DCs therefore play a key role in the balance between liver tolerance and immunity.

Antibody-producing B cells constitute approximately 6% of adult intrahepatic lymphocytes (Doherty and O'Farrelly, 2000). Conventional B cells (B2) are derived from bone marrow, however during early human life the neonatal liver is the primary site of B cell production (Asma et al., 1984). Compared to other lymphoid subsets, relatively little is known about the resident B cell population. However they are thought to exhibit increased expression of proinflammatory IFNγ, IL-6 and TNFα and minimal IL-10 in response to lipopolysaccharide (LPS) stimulation than those found within secondary lymphoid tissue. This may suggest a proinflammatory rather than regulatory function of these cells (Zhang et al., 2013).

1.3.2 Hepatic immune tolerance

It is essential that the liver maintains immune tolerance in order to prevent an inappropriate or disproportionate response to non-pathogenic exogenous material or commensals entering via the portal vein. The liver therefore exhibits a highly tolerogenic phenotype largely due to the antigen-presenting capabilities of most hepatic cell types: HSEC, hepatocytes and HSCs can all endocytose exogenous antigens and directly present them to T lymphocytes on MHC molecules (Chen et al., 2005; Franco et al., 1988; Knolle and Limmer, 2003; Winau et al., 2007). Antigen cross-presentation within the liver typically results in immune tolerance rather than activation (Bowen et al., 2005).

HSEC are critical to this process due to their high endocytotic capabilities and efficiency at presenting blood-derived antigen in the context of MHC I: HSEC can present orally administered antigen within 2 hours of ingestion (Limmer et al., 2005). This cross-priming by HSEC leads to antigen-specific induction of $CD8^+$ T cell tolerance and secretion of anti-inflammatory cytokines such as IL-10 and IL-4 by $CD4^+$ T cells (Berg et al., 2006; Klugewitz and Blumenthal-Barby, 2002; Limmer et al., 2005). This is thought to be due to the expression of programmed death-ligand 1 (PD-L1) on the HSEC surface,

which is reciprocally upregulated upon cognate antigen recognition, further contributing to immune tolerance (Diehl et al., 2008).

Hepatocytes, HSEC, HSCs, KCs and hepatic lymphocytes all express members of the Toll-like receptor (TLR) family (Seki and Brenner, 2008). These PRRs recognise a wide range of pathogen-derived molecules and upon stimulation result in cellular activation, cytokine production and modification of cellular function (Jenne and Kubes, 2013). However, the response to TLR ligands in the liver often differs from the response observed in other tissues. For example, LPS from the membrane of Gram-negative bacteria is a potent immune activator in circulating leukocytes, however it can be immunosuppressive within the liver. This is important because portal blood can be one hundred times more concentrated than peripheral venous blood due to continuous supply from the gut (Lumsden et al., 1988). The liver must therefore be more tolerant of these PAMPs in order to avoid a constant state of inflammation.

Repeat exposure of HSEC to LPS results in a refractory state whereby T cell adhesion and activation is downregulated (Uhrig et al., 2005). Similarly upon stimulation with LPS, KCs secrete a range of mediators including IL-10, which is crucial for the maintenance of hepatic tolerance, and is coupled to downregulation of MHC molecule expression by HSEC, further reducing T cell activation (Knolle et al., 1998).

1.3.3 Hepatic immune activation

Despite the default tolerogenic hepatic environment, a robust immune response can be generated in the liver with appropriate and sufficient stimulation. The hepatic immune environment can be activated in response to pathogen-derived molecules (PAMPs), but also to endogenous ligands in response to sterile injury. These endogenous damage-associated molecular patterns (DAMPs) are released upon tissue injury and activate PRRs on liver cells (Kubes and Mehal, 2012). DAMPs such as high mobility group protein B1 (HMGB1) are actively released by damaged hepatocytes. Other DAMPs are more passively released: either during necrotic cell death, such as double stranded DNA (dsDNA), histones or adenosine triphosphate (ATP); or upon destruction of cell structures, such as uric acid crystals or cholesterol. These DAMPs also bind to PRRs and can result in activation of the inflammasome: intracellular multi-protein complexes expressed by myeloid cells and regulate the activation of caspase-1 as summarised in

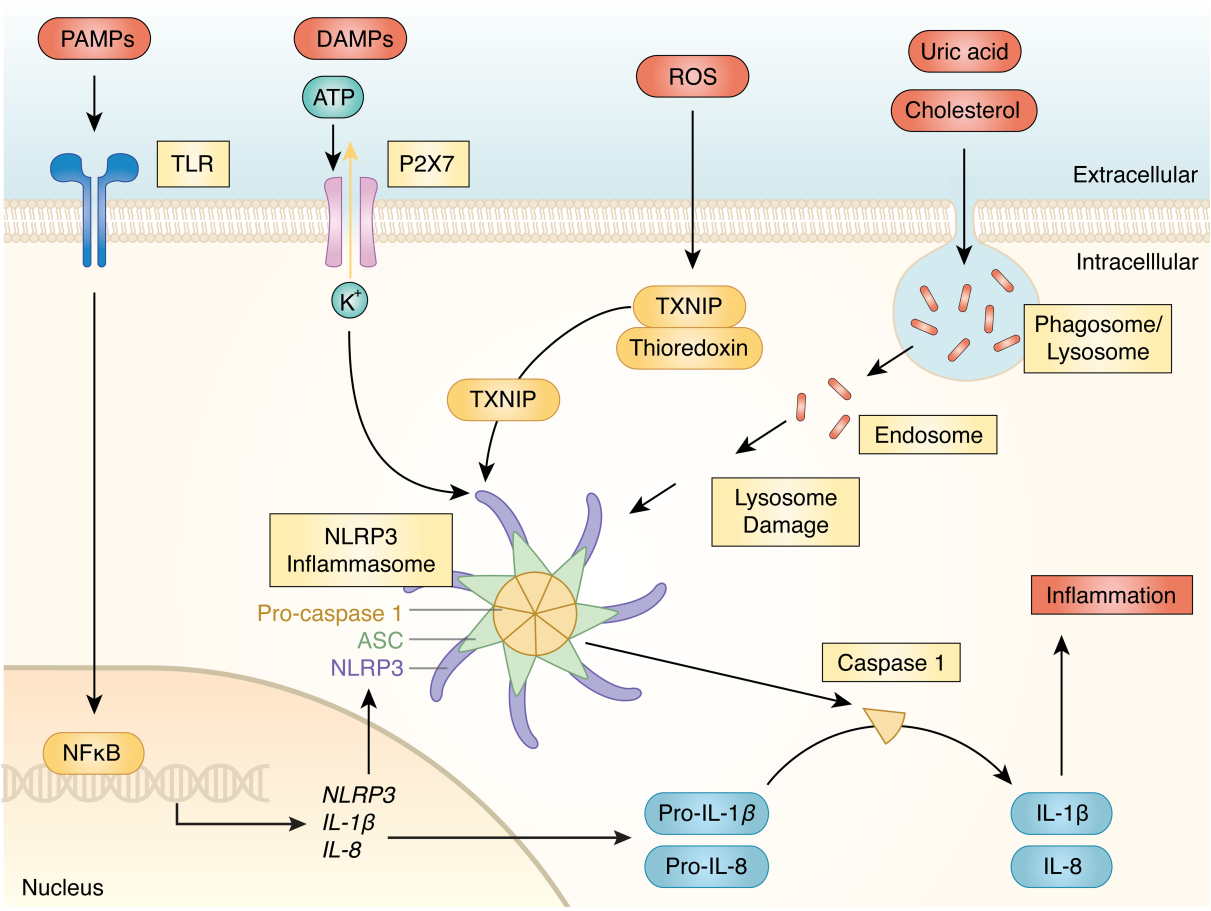


Figure 1.4 Activation of the Inflammasome by DAMPs and PAMPs. Activation of toll-like receptors (TLRs) by pathogen-associate molecular patterns (PAMPS) leads to activation and translocation of NFκB to the nucleus. This results in upregulation of *NLRP3*, promoting assembly of the inflammasome, and upregulation of the pro-forms of IL-1β and IL-8. Activation of the inflammasome results in activation of Caspase 1, which can then cleave these pro-forms into mature active inflammation-causing IL-1β and IL-8. Damage associated molecular patterns (DAMPs) can also induce potassium efflux via the ATP-gated ion channel P2X7, which can in turn activate the inflammasome directly. Similarly, intensive oxidative stress (ROS) and lysosomal rupture from phagocytosis of crystals such as uric acid or cholesterol can also initiate inflammasome activation.

Figure 1.4. Upon stimulation by DAMPs, they exacerbate the proinflammatory response by promoting the maturation of the inflammatory cytokines IL-1β and IL-18 (Guo et al., 2015). These cytokines are involved in an array of cellular activities such as cell proliferation, differentiation and apoptosis. However, the main effect of PAMPs and DAMPs is the rapid recruitment of large numbers of peripheral blood leukocytes to the liver, giving rise to the condition known as hepatitis (Kubes and Mehal, 2012).

1.4 Hepatitis and inflammatory liver disease

Inflammation of the liver, or hepatitis, is characterised as a marked increase in leukocyte recruitment from normal levels in response to injury. Clinically, this corresponds with the presence of hepatic enzymes in serum, such as alanine aminotransferase (ALT) or aspartate aminotransferase (AST). Generally this is rapidly resolved upon removal of the insult and parenchymal cells can regenerate and replace the necrotic or apoptotic cells. However, if the damage continues then the inflammation persists resulting in matrix deposition, parenchymal cell death and angiogenesis (Figure 1.5). These processes are the hallmarks of progressive fibrosis - the wound-healing response by the liver to repeated injury. The activation of HSCs is at the core of fibrosis, stimulating their differentiation into myofibroblast-like cells, which migrate and accumulate at sites of damage and secrete large amount of ECM, such as collagen. Continued damage can lead to disruption of hepatic architecture by large bridging fibrotic scars across the parenchyma. This may result in loss of function, known as cirrhosis, with potential for liver failure or development of hepatocellular carcinoma (HCC).

Initial hepatitis can be instigated by a variety of insults, but the most common can be grouped by those caused by viral pathogens, autoimmunity, hepatotoxic chemicals or metabolic mechanisms. While many inflammatory mechanisms are conserved, the nature and extent of the initial insult broadly dictates the composition of the leukocytic infiltrate.

1.4.1 Acute liver injury

Acute liver disease, or acute hepatitis, is defined as that lasting less than six months and often results in acute liver failure (ALF). The majority of ALF cases in the Western world are due to paracetamol overdose (POD), whereas in the developing world viral infections are the predominant cause. However due to a decline in paracetamol overdoses in the United Kingdom, seronegative hepatitis is the most common cause of liver transplantation due to ALF (Bernal, 2003; Germani et al., 2012). The diagnosis of seronegative hepatitis, or non-A non-B (NANB) hepatitis, is one of exclusion and although a viral aetiology is assumed (rather than autoimmune), very little is known about this condition (Donaghy et al., 2013; Wigg et al., 2005). The proportion of

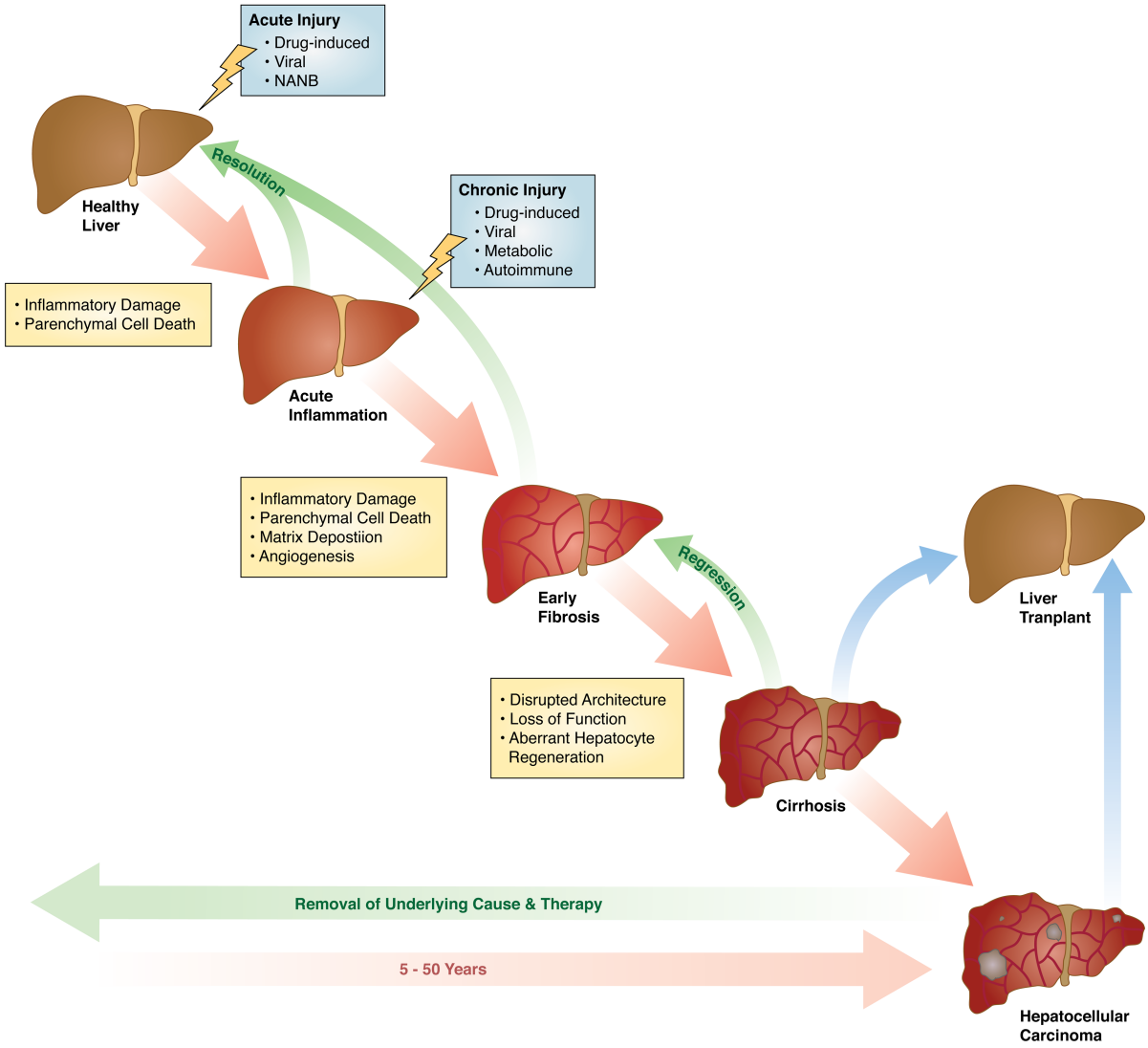


Figure 1.5 The progression of Human Liver Disease. Initial injury to the liver results in inflammatory damage and parenchymal death. Continuation of this damage leads to fibrosis, characterised by angiogenesis and matrix deposition by activate hepatic stellate cells, and finally cirrhosis. The regenerative capacity of the liver means that removal of the underlying cause of damage results in regression, however without therapy or liver transplant it is likely that hepatocellular carcinoma will develop.

transplantations for NANB across Europe has steadily decreased over the last 30 years, however this may represent improved diagnosis over this period (Germani et al., 2012).

N-acetyl-p-aminophenol (paracetamol) is metabolized by CYP450 within hepatocytes into the toxic metabolite N-acetyl-p-benzoquinone (NAPQI). This can then form adducts with mitochondrial proteins resulting in subsequent hepatocyte necrosis and DAMP release (Krenkel et al., 2014). DAMPs such as HMGB1 activate KCs, stimulating the

inflammasome and secretion of chemokines including CCL2 and CXCL16, which confer monocyte, neutrophil and NKT cell recruitment (Fisher et al., 2013; Holt et al., 2008; Szabo and Csak, 2012; et al., 2013).

Monocyte recruitment during paracetamol-induced injury, as well as proliferation of resident cells, results in a greatly expanded hepatic macrophage population (Antoniades et al., 2012). Neutrophils are also recruited to the periphery of necrotic areas; they then follow a mitochondrial formyl-peptide gradient into the inner site (McDonald et al., 2010). However, despite a large influx, the evidence is quite conflicting as to whether their presence affects outcome or severity of the liver damage (Cover et al., 2006; James et al., 2003; Marques et al., 2012; Williams et al., 2010). T cells and NK cells are also recruited in large numbers during POD and subsequently contribute to the pathogenesis in an IFNγ-dependent manner (Ishida et al., 2002; Krenkel et al., 2014).

1.4.2 Chronic xenobiotic-induced liver disease

As the key site of drug metabolism, the liver is particularly susceptible to drug-induced damage. The most prevalent form worldwide is alcoholic liver disease (ALD), accounting for three-quarters of deaths from liver disease (Williams et al., 2014). The initial stage of the disease is characterised by steatosis: the accumulation of fat within the liver caused by an ethanol-dependent increase in fatty acid synthesis and inhibition of fatty acid oxidation within hepatocytes (Gao and Bataller, 2011). The metabolism of ethanol within hepatocytes also generates reactive oxygen species (ROS) and free radicals that cause lipid peroxidation, resulting in apoptosis and necrosis. This triggers an inflammatory response called alcoholic steatohepatitis that is dominated by cells of the innate immunity.

The gut microbiota are altered with chronic ethanol consumption leading to an increase in the proportion of Gram-negative bacteria (Bull-Otterson et al., 2013). Ethanol also increases gut permeability, resulting in elevated intrahepatic LPS concentrations (Rao, 2009), which induces KC activation and subsequent production of proinflammatory cytokines such as TNFα and IFNβ (Hritz et al., 2008; Yin et al., 1999). However, chronic LPS administration alone cannot mimic ALD injury in mice, suggestive of a multifactorial mechanism (Deaciuc et al., 1999).

Ethanol also directly affects other hepatic cells: sensitising hepatocytes to proinflammatory stimulation and skewing HSCs towards an activated phenotype (Roychowdhury et al., 2014; Wang et al., 2006). Leukocytes are also affected, such as promotion of an anti-inflammatory infiltrating monocyte phenotype and suppression of NK cell and neutrophil functions such as oxidative burst and chemokine expression (Collier and Pruett, 2000; Patel et al., 1996; Szabo et al., 1996; Taïeb et al., 2002). These contradicting effects of ethanol may explain why the majority of heavy drinkers do not develop ALD.

Neutrophils are present in the alcoholic liver in large numbers due to increased aldehyde products of lipid peroxidation and upregulation of cytokines and chemokines such as IL-8, CXCL1 and IL-17 (Curzio et al., 1984; Dominguez et al., 2009). Such cellular infiltration correlates with hepatocyte apoptosis, but it is unclear whether the neutrophils directly contribute to the pathophysiology (Ziol et al., 2001).

Although there is a clear immune-mediated response during ALD, targeting this alone has not been particularly successful as a treatment for the disease in previous studies (Naveau et al., 2004; Spahr et al., 2002; Tilg et al., 2003).

1.4.3 Metabolic liver disease

Liver disease can be caused by disruption to cellular metabolism, through either inherited or acquired mechanisms. The most prevalent hereditary disorders are *HFE* haemochromatosis, Wilson's disease and α1-antitrypsin deficiency; caused by accumulation of iron, copper or α1-antitrypsin, respectively, within hepatocytes resulting in apoptosis and subsequent hepatitis.

Non-alcoholic steatohepatitis (NASH) is the most prevalent form of liver dysfunction in the Western world (Anstee et al., 2013). It is characterised by steatohepatitis in the absence of excessive alcohol consumption, commonly associated with overnutrition and obesity. While it is thought that around 20-30% of the Western adult population live with relatively benign hepatic steatosis, called non-alcoholic fatty liver disease (NAFLD), only approximately 25% of those develop steatohepatitis, fibrosis and cirrhosis (Preiss and Sattar, 2008; Williams et al., 2011). Similarly to ALD, the precise reason for progression of the disease in only a small proportion of individuals currently remains unknown, however it is likely that more than simple fat deposition is required.

Although the initial causative agent is different, the pathophysiology of NASH and ALD are broadly similar due to the commonality of steatohepatitis. Similarly to ALD, NASH is associated with a change in the composition and prevalence of gut microbiota (Spencer et al., 2011; Wigg et al., 2001). In particular, alcohol-producing *Escherichia* species are abundant in the gut of NASH patients, which may increase gut permeability to molecules such as LPS (Baker et al., 2010; Zhu et al., 2013). Activation of KCs via TLR4 has been proposed as a critical component of NASH pathogenesis, although the activation pathway may differ to that observed in ALD (Petrasek et al., 2013; Rivera et al., 2007). Also similarly to ALD, LPS stimulation alone during a high fat diet is not sufficient to transition from steatosis to NASH, suggestive of a more complex mechanism (Liang et al., 2014).

The innate immune response is key to NASH inception whereas the adaptive response appears to be crucial for disease progression. Neutrophil accumulation is a prominent feature of the disease, demonstrating characteristic localisation around steatotic hepatocytes (Rensen et al., 2009). Neutrophils may even enhance fibrosis in NASH by stimulating HSC proliferation (Ibusuki et al., 2013). T_h1 cells, that can stimulate a proinflammatory macrophage response through the secretion of IFNγ, are elevated in NASH livers (Sutti et al., 2014). The frequency of NKT cells is reduced in steatotic livers but the numbers are dramatically increased during NASH (Adler et al., 2011; Li et al., 2005; Tajiri et al., 2009) where they may play a role in pathogenesis by promoting hepatocyte lipid uptake (Wolf et al., 2014). Mice lacking NKT cells also appear to be protected from fibrosis (Syn et al., 2010).

1.4.4 Autoimmune liver diseases

There are three main autoimmune liver diseases: autoimmune hepatitis (AIH), primary biliary cholangitis (PBC) and primary sclerosing cholangitis (PSC). AIH is the most common, accounting for around 20% of chronic liver disease (CLD) in Caucasian populations (Blachier et al., 2013). AIH is characterised by a loss of immune tolerance to antigens on hepatocytes, resulting in destruction of the hepatic parenchyma by autoreactive T cells. PBC and PSC, during which T cells are targeted towards cholangiocytes, are both considerably less prevalent. Although the precise aetiologies of these diseases remains unclear, all involve a genetic susceptibility in combination with environmental factors and a coinciding associated inflammatory bowel disease.

T cells form the majority of the inflammatory infiltrate in all three diseases, with a preponderance of IFNγ-secreting T_h1 cells (Lohr et al., 1996; Tjandra et al., 2000) and elevated T_h17 fraction (Katt et al., 2013; Lan et al., 2009; Zhao et al., 2011). The IL-17-secreting T_h17 subset has also been implicated in the pathogenesis of numerous other inflammatory and autoimmune diseases (Bettelli et al., 2007). Their infiltration in PSC and PBC livers may be due to the expression of pro-T_h17 cytokines (such as IL-6 and IL-1β) by cholangiocytes in response to PAMPs (Harada et al., 2009). IL-17 can also induce IL-6 expression in hepatocytes, which may form a positive feedback loop and exacerbate inflammation in AIH (Zhao et al., 2011). Conversely, while intrahepatic T_h17 cell numbers are elevated, T_{reg} numbers are decreased and their function impaired during autoimmune liver diseases (Ferri et al., 2010; Garetto et al., 2015; Sebode et al., 2014).

1.5 Animal models of liver disease

Currently, no animal models of liver disease are available that exhibit all attributes of the human condition, only imitating certain characteristics. It is therefore important to select the most appropriate model for investigation of the particular research question. Mice are often used to study liver disease due their genetic similarity to humans while also being small with a short gestational period allowing ease of husbandry and genetic manipulation.

1.5.1 Animal models of acute liver injury

Paracetamol-overdose has also been used due to the similarities to the human condition, however in the past there has been a lack of reproducibility reflected by unpredictable dose response and time to death (Newsome et al., 2000). Recently there has been more success with murine paracetamol-overdose models with clear similarities to human pathophysiology (McGill et al., 2012). Equally, there has been little progression in viral models due to the specificity of the hepatitis viruses to humans and non-human primates. Carbon tetrachloride (CCl_4) is one of the most widely used models of acute hepatitis and been routinely implemented for over fifty years. Similarly to paracetamol, CCl_4 is metabolised by CYP450 within hepatocytes. Homolytic cleavage forms the trichloromethyl radical, which then rapidly reacts with surrounding macromolecules, enhancing lipid peroxidation and disrupting calcium homeostasis, resulting in reversible

centrilobular necrosis (Benedetti et al., 1974; Boll et al., 2001; Slater et al., 1964). This triggers a typical wound healing response, including phagocytic and inflammatory leukocyte recruitment to clear dead cells, which are rapidly replaced following proliferation of parenchymal and non-parenchymal cells (Starkel and Leclercq, 2011). Typically, the murine inflammatory response lasts approximately 72 hours (Karlmark et al., 2009). Acute thioacetamide (TAA)-induced injury works via a similar mechanism to CCl_4: reactive metabolites bind to proteins and lipids resulting in oxidative stress and centrilobular necrosis. TAA, however, elicits more periportal infiltrate and pronounced ductal proliferation (Wallace et al., 2015). Acute intravenous concanavalin A (Con A) dosing is also often used to model liver injury, but represents a T cell-mediated hepatitis or cytokine storm. The injury is therefore largely associated with T helper cell recruitment within 24 hours of treatment (Heymann et al., 2015).

1.5.2 Animal models of chronic liver disease

If mice are continually dosed with CCl_4 or TAA then chronic hepatitis, fibrosis and subsequent HCC develop. This similarity to the human condition but without aetiology-specific mechanism has resulted in these hepatotoxins being the most widely employed models to study fibrosis. Upon cessation of treatment, fibrosis within livers treated with either toxin will undergo spontaneous resolution, although this is considerably slower during the TAA model (Iredale et al., 1998; Zimmermann et al., 1987). It must be noted, however, that the speed and extent of resolution in murine models far exceeds that observed for fibrotic human livers.

Although various models of specific chronic liver disease have been developed, none are able to fully recapitulate the human condition, highlighting the fact that these diseases are multifactorial and still relatively understudied. Models of ALD differ largely because of the rapid metabolism of ethanol by rodents and inconsistent intake due to their aversion to alcohol (Starkel and Leclercq, 2011). This can be overcome by models such as Lieber-DeCarli, whereby ethanol is incorporated into a liquid diet at 36% of total calories (Lieber and DeCarli, 1986). Blood alcohol levels are raised sufficiently in these mice to exhibit hepatic lesions, steatosis, KC activation, ROS generation and hepatocyte death but without necrosis or fibrosis (Leo and Lieber, 1983). NAFLD pathogenesis has been imitated in several transgenic mouse models, including mutations in leptin (*ob/ob*) or the leptin receptor (*db/db*), however these animals exhibit obesity and steatosis, but do

not progress to steatohepatitis or fibrosis without a secondary insult (Anstee and Goldin, 2006; Reddy, 2001). Altered diet models of NAFLD have been quite successful, such as the methionine- and choline-deficient diet (MCD). This high fat (10%) and high sucrose (40%) diet is deficient in methionine and choline, thus inhibiting mitochondrial β-oxidation and low-density lipoprotein synthesis (Anstee and Goldin, 2006). Mice fed this diet rapidly exhibit steatohepatitis with subsequent necrosis and fibrosis, despite a loss of up to 10% body weight (Gao et al., 2004). Other variations of high fat content diets used to induce NASH, include the Western lifestyle model (WLM) and fast-food diet (FF). These models show strong similarities to the human condition, recapitulating features such as obesity, insulin resistance, steatohepatitis and fibrosis, although to a lesser degree than MCD diet (Charlton et al., 2011; Lieber et al., 2004).

Autoimmune disorders involve a complex combination of genetic and environmental factors, although several murine models exist. For example, autoimmune hepatitis can be mimicked by injection of an adenoviral vector expressing human CYP450 2D6 (Ad-CYP2D6), triggering an immune response to mouse CYP2D6 (Hintermann et al., 2012; Holdener et al., 2008). CYP2D6 has been identified as an autoantigen in human AIH therefore the disorders are mechanistically similar (Mizutani et al., 2008). Double congenic NOD.c3c4 mice spontaneously develop PBC-like leukocytic infiltration around bile ducts followed by fibrosis (Irie et al., 2006). Anti-mitochondrial antibodies (AMA) similar to those present in the human condition are also observed in these animals (Irie et al., 2006; Oertelt et al., 2006). *Mdr2*$^{-/-}$ mice are the most common and robust animal model of PSC. These animals lack the multi-drug resistance gene (MDR)-2 that mediates the transport of phospholipids during bile secretion, thus exhibit high biliary concentrations of toxic and damage-inducing free bile acids. Over time these animals develop hepatitis, fibrosis and HCC (Katzenellenbogen et al., 2007; Lammert et al., 2004).

Animal models provide a useful tool for studying liver diseases, however there are several key caveats for their use. One major limitation is the clear differences in the immune systems between humans and mice. This is highly significant when considering the strong immune element of each of the conditions. Furthermore, the majority of models lack a number of critical factors that are observed in the human conditions, and therefore data must be considered with some reservation.

1.6 Leukocyte recruitment

The key stage in an immune response is the recruitment of peripheral blood leukocytes from circulation to sites of damage or infection; however disruption of the balance of these responses can be devastating for the organism. The process is therefore highly complex and involves sequential and overlapping processes mediated by both leukocytes and endothelial cell monolayers that line blood vessels; these processes carefully control which leukocytes are able to migrate into a tissue at any given time, following which their fate is determined by responses to signals from the local microenvironment.

1.6.1 Classical leukocyte adhesion cascade

In the majority of tissues extravasation occurs within specialised high endothelial venules (HEV). These post-capillary venules are present in most secondary lymphoid organs but are also seen in non-lymphoid organs during chronic inflammation (Ager and May, 2015). The conventional multistep adhesion cascade paradigm of leukocyte extravasation was described as occurring in three discrete steps: rolling, adhesion and migration, as illustrated in Figure 1.6 (Adams and Shaw, 1994; Butcher, 1991). However, slow rolling, adhesion strengthening and intraluminal crawling have more recently been generally accepted as additional steps in the process (Ley et al., 2007).

1.6.1.1 Rolling

The first contact between the endothelium and leukocyte is mediated by the selectin family of type I transmembrane glycoproteins and results in reversible rolling interactions. E-selectin and P-selectin are expressed on the surface of inflamed endothelium and have long consensus repeat domains allowing them to extend into the vessel lumen and tether passing leukocytes (Patel et al., 1995). Upon stimulation from proinflammatory factors, P-selectin is rapidly released from intracellular stores called Weibel-palade bodies, whereas E-selectin requires *de novo* synthesis (Kansas, 1996; Kiskin et al., 2010). Surface-presented selectins interact with a variety of sialyl-Lewis X tetrasaccharide-related ligands on the leukocyte surface, such as P-selectin glycoprotein ligand-1 (PSGL-1), CD44 and E-selectin ligand 1 (ESL1) if they are appropriately glycosylated (Hidalgo et al., 2007; McEver and Cummings, 1997). Another family member, L-selectin is expressed by a variety of leukocytes and is considerably shorter in length than the others, however it is localised to protruding microvilli at the cell surface

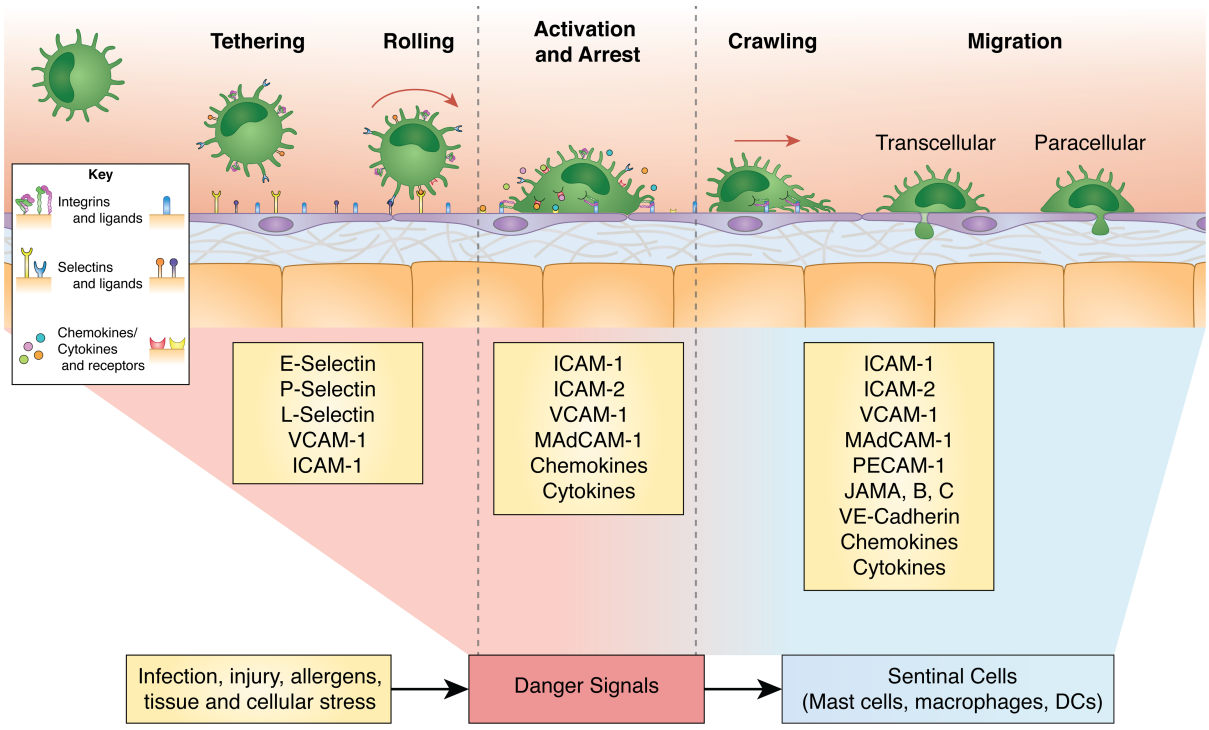


Figure 1.6 The leukocyte adhesion cascade. In response to a variety of inflammatory trigger, danger signals are released thereby stimulating the recruitment of leukocytes to the affected tissues. Initially leukocytes are tethered from the circulating blood by long selectin molecules. As the cells roll along the vessel wall and begin to slow they interact with integrins and sample the microenvironment for appropriate chemotactic signals. The interaction of integrins and their cognate ligands triggers cytoskeletal rearrangements, promoting the transmigration across the endothelial monolayer, which along with interaction of chemokines and G-protein coupled receptors, induced firm adhesion and activation of the leukocyte. The leukocyte then crawls along the luminal surface searching for transmigration signals. Upon location of these signals, the leukocyte migrates across the endothelial monolayer and can pass through the basements membrane to the damaged tissue. This can take place either through intercellular junctions (paracellular) or directly through the endothelial cell body (transcellular). *ICAM, intracellular cell adhesion molecules; VCAM, vascular cell adhesion molecules, VE-cadherin, vascular endothelial cell cadherin; JAM, junctional adhesion molecule; DC, dendritic cell.*

for optimal interactions (Kansas, 1996). The interactions between L- and P-selectin and their ligands are shear stress-dependent, therefore requiring flow for successful binding (Finger et al., 1996; Lawrence et al., 1997). The hydrodynamic force of blood flow is also the impetus behind rolling, however the rate is dictated by the molecular interactions (Tedder et al., 1995). P-selectin supports faster rolling, whereas E-selectin exhibits reduced rolling velocity (Kanwar et al., 1995; Kunkel and Ley, 1996). This may allow time for integrin-activation through a p38 mitogen-activated protein kinase (MAPK)-dependent pathway (Simon et al., 2000).

1.6.1.2 Activation and arrest

Leukocyte activation and arrest is primarily dependent on the role of integrins: heterodimeric membrane-bound glycoproteins comprising of one α and one β chain as seen in Figure 1.7A (Harburger and Calderwood, 2009). They are expressed on the leukocyte surface and bind to ECM proteins or immunoglobulin superfamily members on endothelial cells, such as intercellular adhesion molecule-1 (ICAM-1) and vascular cell adhesion molecule-1 (VCAM-1). The subunits are joined non-covalently, allowing for a wide variety of combinations and formation of multimeric structures, thereby conferring a large molecular variety.

The most relevant integrins for leukocyte binding are the β_2 (CD18) subfamily, which consists of four heterodimers including lymphocyte function-associated antigen 1 (LFA-1, CD11a or αLβ2) and macrophage-1 antigen (Mac-1, CD11b or $\alpha_M\beta_2$). While LFA-1 is ubiquitously expressed among leukocytes, Mac-1 is confined primarily to cells of the myeloid lineage (Harris et al., 2000). The β2 subfamily primarily binds ICAM-1 and ICAM-2 on endothelium (Makgoba et al., 1988). The α_4 (CD49d) integrin also plays a significant role in leukocyte adhesion, in particular as part of the very late antigen-4 (VLA-4, CD29 or $\alpha_4\beta_1$) dimer and lymphocyte Peyer's patch adhesion molecule (LPAM or $\alpha_4\beta_7$). These integrins can also facilitate lymphocyte rolling via interactions between VLA-4 and VCAM-1 or LPAM and mucosal addressin cell adhesion molecule-1 (MAdCAM-1) (Huo et al., 2000; Petrovic et al., 2004; Singbartl et al., 2001).

The differential expression of integrins and their receptors is thought to dictate the specificity of leukocyte arrest. However, the clustering of these molecules as well as their adhesiveness (termed valency) is also important. These properties are all affected by the local presence of chemokines (Constantin et al., 2000; D'Ambrosio et al., 2002) Chemokines are both expressed and transcytosed by endothelial cells and presented on glycosaminoglycans at their surface in response to proinflammatory cytokines (Johnson et al., 2005; Middleton et al., 1997). The process of rolling allows leukocytes to sample these and other chemoattractants within the endothelial microenvironment via chemokine receptors. The differential expression of these receptors adds a further level of specificity to leukocyte migration.

The binding of chemokines to their G-protein coupled receptors (GPCR) can also trigger conformational changes in the integrin extracellular domains, altering their

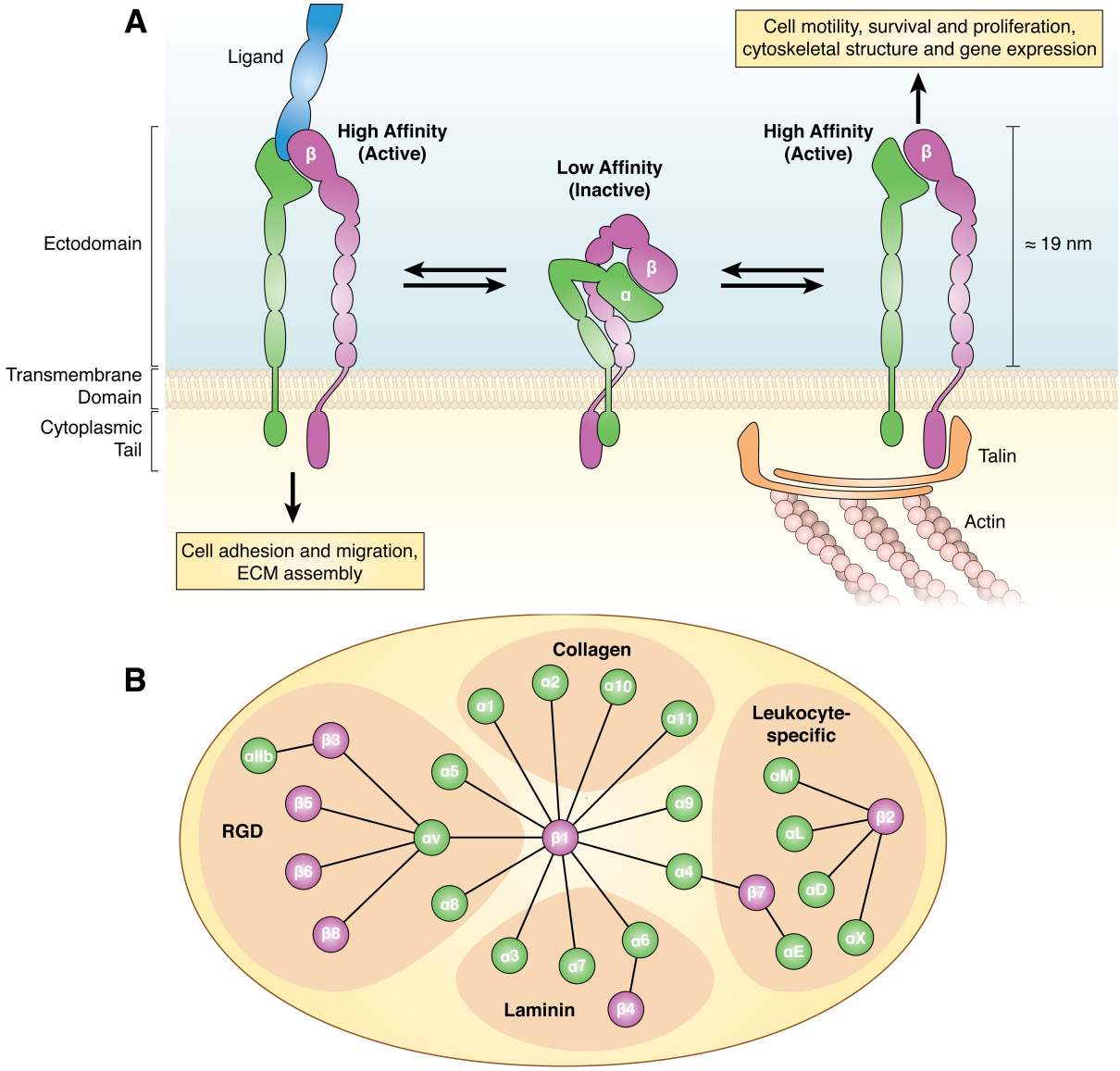


Figure 1.7 Structure and activation of integrin molecules. (**A**) Integrins comprise of a large extracellular region and short intracellular tail. They exist as heterodimers of α and β subunits in the bent low affinity conformation when inactive. Upon binding of the their ligand they adopt an extended active conformation, which can result in cell adhesion and migration and assembly of extracellular matrix (ECM), known as 'outside-in' signalling. Similarly, binding of the Talin head/actin structure to the intracellular domain also induces the active confirmation, leading to cell motility, survival, proliferation, changes to the cytoskeletal structure and altered gene expression, known as 'inside-out' signalling. (**B**) 8 β subunits can associate with 18 α subunits to form 24 distinct integrin heterodimers. These can be classified by their ligand specificity and restricted expression. For example the β2 and β7 subunits are restricted to leukocytes.

ligand-binding affinity in a process called "inside out" signalling, also illustrated in Figure 1.7 (Chan et al., 2001; Giagulli et al., 2004). This increased affinity results in firm adherence to the endothelium. In turn, integrin-ligand binding causes "outside in"

signalling, resulting in intracellular signalling to regulate changes in cell motility, proliferation and apoptosis (Giagulli et al., 2006; Shattil, 2005).

1.6.1.3 Crawling and migration

Once firmly adhered to vascular endothelium, a large proportion of leukocytes laterally migrate along the vessel wall in a process known as intraluminal crawling (Auffray et al., 2007; Heit et al., 2006). The cells flatten, send out pseudopods and crawl in a millipede-like fashion in search of exit cues independent of the direction of flow (Schenkel et al., 2004; Shulman et al., 2009). This process is thought to be integrin dependent: via Mac-1 in monocytes and neutrophils and via LFA-1 for lymphocytes (Phillipson et al., 2009; Shulman et al., 2009). Leukocyte arrest is dependent on increased integrin affinity in response to cytokines presented on the endothelial glycocalyx (Tanaka et al., 1993).

The vast majority of transendothelial migration (diapedesis) takes place between adjacent cells (paracellular), although migration through the cell body (transcellular) has been documented (Nourshargh and Alon, 2014). Regardless of migration route, docking structures, or 'transmigratory cups' are observed on the apical surface of endothelium. The endothelial cells extend out pseudopod-like membrane protrusions that are enriched in ICAM-1, VCAM-1 and actin filaments (Barreiro et al., 2002; Carman and Springer, 2004; Carman et al., 2007). The formation of these structures is dependent on the phosphorylation of cortactin, a cytoplasmic protein involved in actin rearrangement (Yang et al., 2006). Deficiency in cortactin is associated with decreased leukocyte extravasation in vivo (Schnoor et al., 2011). Once the leukocyte begins transmigration, these structures progress to surround the whole leukocyte, thereby maintaining the endothelial cell membrane integrity (Phillipson et al., 2009). Signalling through these multimeric ICAM-1 and VCAM-1 structures results in phosphorylation of vascular endothelial (VE)-cadherin (Dejana, 2004), a key gatekeeper of endothelial function integrity which is able to both impede or facilitate the progress of extravasating leukocytes (Schulte et al., 2011). Phosphorylation of VE-cadherin weakens the cell-cell junctions, allowing for paracellular migration to occur, an effect that is amplified by ICAM-1 and VCAM-1 signalling through increased intracellular Ca^{2+} concentration and subsequent cell contraction and further junction weakening (Huang et al., 1993).

Paracellular migration is actively mediated by the engagement of adhesion molecules expressed between endothelial cells, namely the junctional adhesion molecules (JAMs), endothelial cell-selective adhesion molecule (ESAM), ICAM-1 and -2, platelet/endothelial cell adhesion molecule (PECAM-1) and CD99 (Ley et al., 2007). These integrins either interact with their relevant ligands or form homodimeric interactions to guide the leukocyte across the endothelial monolayer (Ley et al., 2007). The identity of the molecules that engage in these interactions depends on a complex interplay between tissue- and leukocyte-specific expression as well as cytokine and chemokine stimulation.

Little is known about the mechanisms behind transcellular migration, however it is thought that the ligation of ICAM-1 triggers the translocation of apical ICAM-1 to caveolae: small "cup-like" invaginations in the cell membrane, rich in caveolin-1 and F-actin (Millán et al., 2006). Leukocyte protrusions then penetrate into these domains with ICAM-1 and caveolin-1 clustering around. This results in actin- and vimentin-stabilised channel formation, which the leukocyte is then able to pass through (Millán et al., 2006; Nieminen et al., 2006). PECAM-1, CD99 and JAM-A also appear to be translocated to these sites of paracellular migration (Carman et al., 2007; Mamdouh et al., 2009). Despite mounting evidence for this pathway, it is still unclear why leukocytes that appear to use the same rolling and adhesion mechanisms, would undergo transcellular rather than paracellular migration.

1.6.2 Sinusoidal leukocyte recruitment

In most organs leukocyte extravasation occurs in HEV, whereas in the liver a much smaller proportion occurs within such post-sinusoidal venules; the majority of leukocytes adhering to HSEC that line the hepatic sinusoids (Wong et al., 1997). Within portal and central venules of the liver, leukocytes are thought to undergo diapedesis via the classical adhesion cascade as outlined above (Lee and Kubes, 2008). In contrast, leukocyte extravasation within the sinusoids has distinct mechanistic differences, primarily due to structural and functional differences in HSEC compared to other vascular endothelial beds as outlined in Figure 1.8 and described below.

1.6.2.1 Endothelial adhesion molecules

A major difference in the leukocyte adhesion mechanism within the sinusoids is evidenced by the lack of E- and P-selectin expression on HSEC, resulting in

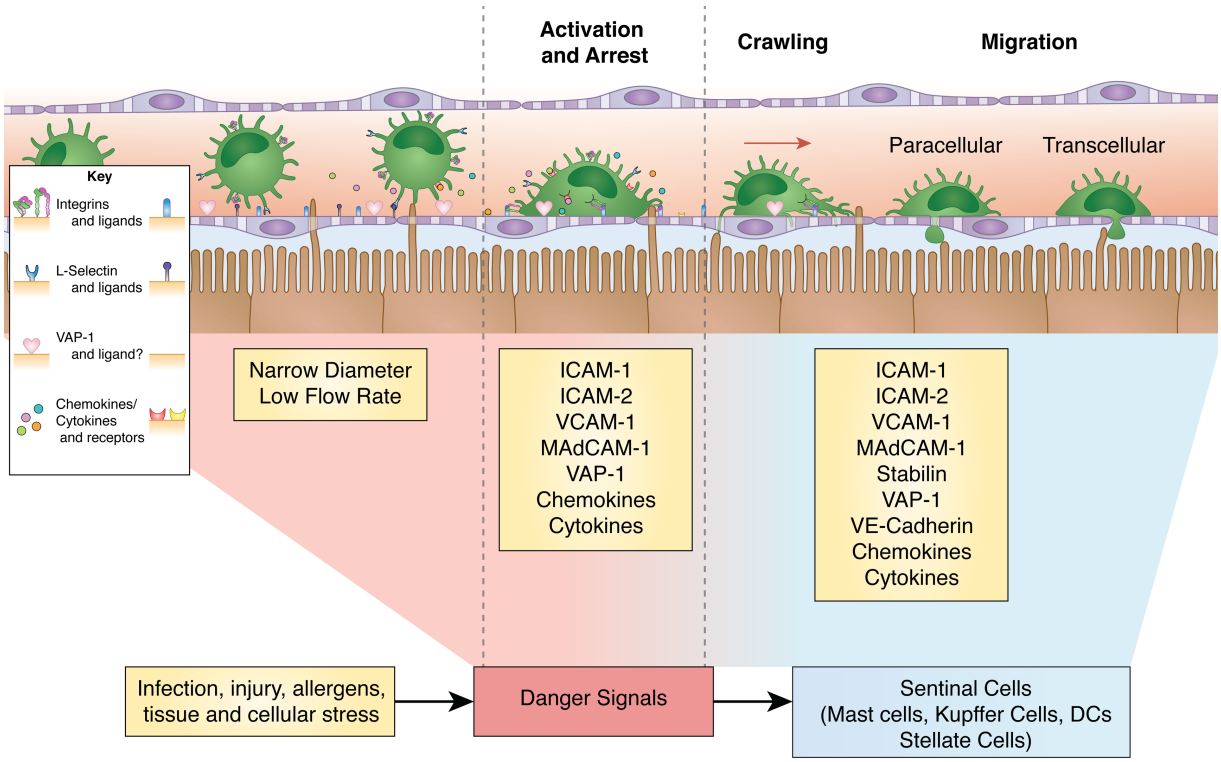


Figure 1.8 The sinusoidal leukocyte adhesion cascade. Leukocyte recruitment within the sinusoids differs considerably to other tissues, primarily due to structural differences. The narrow diameter and low shear flow rate within the sinusoids allows for selectin-independent capture, therefore no initial tethering and tolling stages occur. The fenestrated endothelium allows for interactions and signalling between leukocytes and underlying hepatocytes through the monolayer. Furthermore, sinusoidal endothelial cells express additional molecules involved in recruitment, such as VAP-1 and Stabilin.
ICAM, intracellular cell adhesion molecules; VCAM, vascular cell adhesion molecules, VE-cadherin, vascular endothelial cell cadherin; JAM, junctional adhesion molecule; VAP-1, vascular adhesion protein-1; DC, dendritic cell.

selectin-independent capture (Adams and Shaw, 1994; Steinhoff et al., 1993; Wong et al., 1997). The adhesion cascade model describing the sinusoids therefore only occurs in two discrete steps - adhesion and migration - due to greatly attenuated rolling (Fox-Robichaud and Kubes, 2000). This is made possible by the unique sinusoidal structure. The low shear rate of flow (25-250 μm/min) along with the narrow diameter of sinusoids (5-7 μm) not only allows efficient exchange of nutrients and toxins, but also increases contact between leukocyte and endothelium as they traverse the liver microvasculature (MacPhee et al., 1995). The HSEC fenestrae and lack of a basement membrane also allows hepatocyte microvilli and leukocyte protrusions to extend across the endothelial monolayer, thereby promoting direct interactions between the cells and

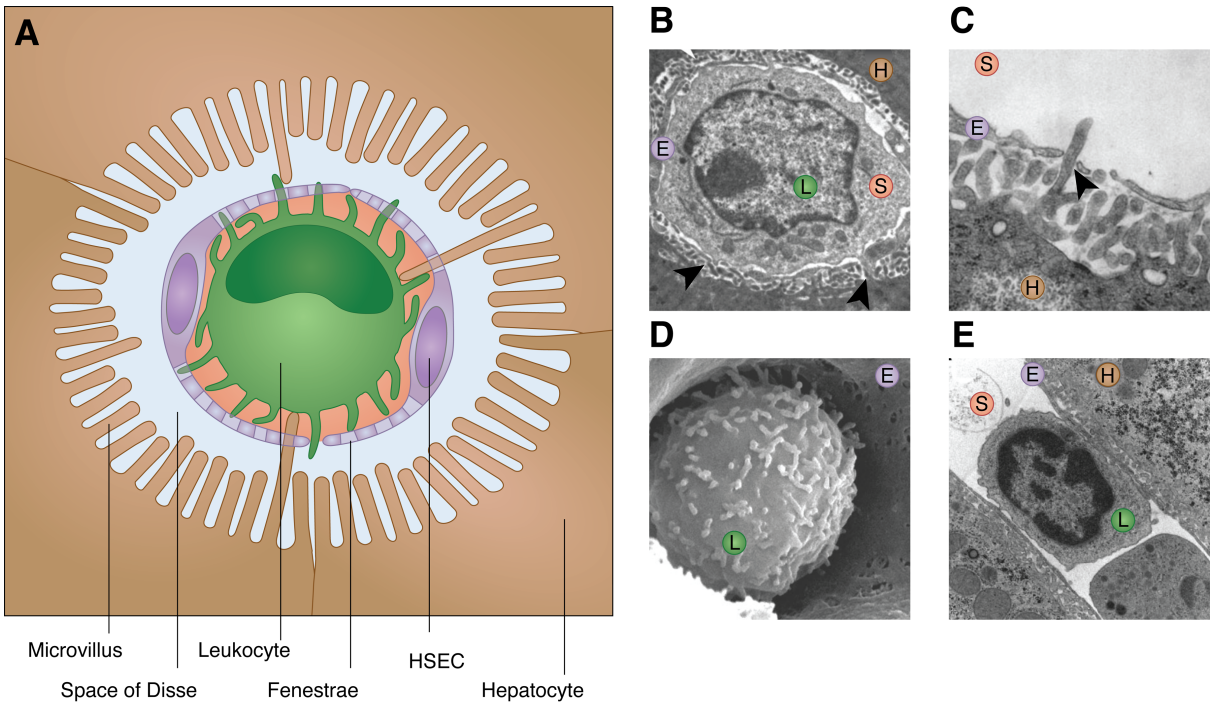


Figure 1.9 Leukocytes-hepatocyte interactions within the sinusoids. The narrow sinusoidal diameter forces the leukocytes to squeeze through the sinusoids, promoting an intimidate contact with the endothelium. Hepatocytes are able to project their microvilli into the sinusoidal lumen through the large endothelial fenestrae (black arrows), thereby promoting the interaction between these two cells without the need for migration. This allows for signalling and sampling of the local environment. (**A** & **B**) Illustrate luminal cross-section. (**C**) Hepatocyte microvilli projection through fenestrae. (**D** & **E**) The narrow diameter of the sinusoids forces the interaction between leukocytes and endothelium. *S*, Sinusoidal lumen; *E*, Endothelium; *H*, Hepatocytes; *L, Leukocyte*. Arrows indicate fenestrae. Image B-E from Warren et al., 2006.

sensing of transmigratory signals, shown in Figure 1.9 (Guidotti et al., 2015; Warren et al., 2006).

It was originally hypothesised that leukocytes adhered within sinusoids via physical trapping, however a range of other molecules are now thought to play a role. Lymphocyte capture in the sinusoids is primarily integrin-dependent; ICAM-1 is constitutively expressed by HSEC and mice deficient in ICAM-1 expression exhibit reduced sinusoidal leukocyte adhesion (Iigo et al., 1997; Wong et al., 1997). Although HSEC do not constitutively express VCAM-1, it is upregulated during inflammatory liver disease (Steinhoff et al., 1993; Volpes et al., 1992) and antibody blockade of both ICAM-1 and VCAM-1 leads to a reduction in lymphocyte adhesion to inflamed HSEC in culture (Edwards et al., 2005; Lalor et al., 2006). Effector $CD8^+$ T cells tether to HSEC primarily via ICAM-1/LFA-1 interactions, while naïve cells may also use the VCAM-1/ α_4-integrin mechanism (Bertolino et al., 2005; John and Crispe, 2004; Sato et al., 2006).

$CD4^+$ T cells may also bind via ICAM-1/LFA-1, particularly those of the T_h1 lineage (Bonder et al., 2005). Neutrophils are thought to bind via differential routes depending on injury; sterile injury appears to be dependent on ICAM-1/Mac-1 interactions but during bacterial infection neutrophils bind hyaluronan (HA) on the HSEC surface via CD44 (McDonald et al., 2008). Lymphocytes have also been observed to adhere by this route in other tissues, but this has yet to be demonstrated within the liver.

HSEC express low levels of PECAM-1 and JAMs, resulting in less tightly regulated cell junctions and ease of paracellular transmigration (Scoazec and Feldmann, 1994). They also express a range of non-classical endothelial adhesion molecules to facilitate diapedesis, some of which are more generally associated with leukocyte trafficking within the lymphatics, such as stabilin-1 and vascular adhesion protein-1 (VAP-1). Stabilin-1 is a member of the scavenger receptor family and has been shown to internalise modified LDLs, whole bacteria and advanced glycation end products (AGE) (Politz et al., 2002; Tamura et al., 2003). It also supports T and B cell migration in the draining lymph nodes and T cell migration across HSEC *in vitro* (Karikoski et al., 2009; Shetty et al., 2011). VAP-1 mediates lymphocyte adhesion to hepatic sinusoidal endothelium both *in vitro* and *in vivo* (Bonder et al., 2005; Lalor et al., 2002). Stabilin-1 and VAP-1 may also localise with ICAM-1 in hepatic 'transmigratory cup' structures to facilitate T cell migration (Shetty et al., 2011). During inflammatory liver disease HSEC also express MAdCAM-1, which is normally confined to mucosal endothelium in the bowel (Adams and Eksteen, 2006; Liaskou et al., 2011). This interaction may account for the adhesion of activated gut-derived T cells in inflammatory bowel disease (IBD) (Grant et al., 2001).

1.6.2.2 Endothelial chemokines

Within the sinusoids, chemokines initiate the first step in leukocyte adhesion and are also crucial for subsequent transmigration. HSEC are able to instigate cell-specific leukocyte diapedesis via chemokine presentation, achieved by expression, capture or transcytosis. One example of control by chemokine expression is the ability of HSEC to direct neutrophil chemotaxis by upregulation of CXCL1 and CXCL2, observed in both sterile and non-sterile injury (Bajt et al., 2001; McDonald et al., 2012; Patrick et al., 2007). This is a key interaction in neutrophil extravasation; blocking CXCL2 or CXCL1 from binding their receptor (CXCR2) results in critically reduced hepatic neutrophil

recruitment (Li, 2003). HSEC are also able to capture and present passing chemokines on proteoglycans within the endothelial cell glycocalyx (Curbishley et al., 2005; Middleton et al., 2002). One important example is that of CXCR3 ligands such as IFN-inducible protein-10 (IP-10), which are secreted by all hepatic cell types upon the appropriate stimulation (Maher, 1995; Morland et al., 1997; Shiratori et al., 1993). These ligands are present at higher concentrations in a range of CLDs with corresponding upregulation of CXCR3 on effector T cells (Apolinario et al., 2002; Butera et al., 2005; Curbishley et al., 2005; Nishioji et al., 2001). HSEC can also take up chemokines secreted by other cells via the basolateral surface and transcytose them in clathrin-coated vesicles to their luminal surface for presentation (Neumann et al., 2015). This has specifically been demonstrated for the proinflammatory chemokines CXCL9 and CXCL10, which are presented to $CD4^+$ T cells for interaction via CXCR3 and subsequent transmigration (Schrage et al., 2008). A similar mechanism may also be important for T_h17 recruitment to the liver (Oo et al., 2012).

1.6.2.3 Recruitment via other sinusoidal cells

HSEC are capable of orchestrating diapedesis in their own right, but other cells within the sinusoids can facilitate the process. As previously discussed, lymphocytes can be activated by sinusoidal-resident KCs via MHC molecules, however KCs also constitutively express adhesion molecules, such as ICAM-1 and VCAM-1, which can be upregulated upon exposure to LPS (van Oosten et al., 1995). This has been demonstrated in bacterial insult models following which neutrophils accumulate around KCs in an ICAM-1-dependent manner (Gregory et al., 2002) or where depletion of KCs dramatically decreased neutrophil binding within the sinusoids (Ebe et al., 1999). Taken together, these data suggest KCs may directly facilitate neutrophil binding. Similarly, invariant NKT (*i*NKT) cells cluster around KCs in a CXCR3-dependent manner and form stable contacts via CD1d (Lee et al., 2010). Hepatic NKT cells express ICAM-1, which is thought to be vital for adhesion within the sinusoids in an LFA-1-dependent manner (Emoto et al., 1999). As HSEC are not thought to express LFA-1 it is possible that LFA-1-expressing KCs support this interaction. KCs also transiently interact with T cells, but this appears to have a negligible effect on intrahepatic accumulation (Sitia et al., 2011).

Platelets are also capable of facilitating leukocyte adhesion within the sinusoids, and may in fact be critical for adhesion of some leukocyte subsets during disease. Platelets are known to form complexes with neutrophils, monocytes and lymphocytes in the circulation, the numbers of which increase during inflammatory disease states (Furman et al., 1998; Green et al., 2015; Ott et al., 1996; Pamuk et al., 2007). These platelet-leukocyte structures appear to enhance leukocyte rolling and adhesion within HEV (Diacovo et al., 1996). The cells were originally proposed to interact primarily via P-selectin on the platelet surface to PSGL1 (Hamburger and McEver, 1990; Jungi et al., 1986). However, more recently an additional role of leukocyte Mac-1 has been elucidated in which it is capable of binding both glycoprotein Ib (GPIb) and JAM-C on platelets, with the latter capable of mediating binding to surface-adherent platelets (Ehlers et al., 2003; Santoso et al., 2002; Simon et al., 2000). Platelets are also able to bind to KCs through classic GPIIb interactions with von Willebrand factor (vWF) (Wong et al., 2013) and can adhere to endothelial cells: a process that occurs rapidly after injury and is subsequently followed by leukocyte recruitment (Croner et al., 2006). Several studies also suggest that sinusoidal recruitment of $CD8^+$ T cells may be dependent on platelets. These cells accumulate rapidly in mouse sinusoids after Hepatitis B Virus infection via a mechanism independent of PSGL-1, VLA-4, LFA-1, PECAM-1 and VAP-1 on HSEC and T cells as well as CD44 and chemokines on the leukocytes (Guidotti et al., 2015). The depletion of platelets in the same mouse model lead to a corresponding reduction in cytotoxic T cells bound within the sinusoids, which could be reversed by platelet transfusion (Iannacone et al., 2005). While the precise mechanism of binding remains elusive, the platelets must also be activated to support lymphocyte recruitment as inhibition of activation pathways results attenuation of binding (Cattaneo, 2004; Iannacone et al., 2005).

Inhibition of platelet adhesion to HSEC also resulted in reduced neutrophil recruitment in a mouse model of sterile injury (Slaba et al., 2015). However, platelets also reciprocally bind to neutrophils, preferentially adhering to endothelial-bound neutrophils over activated endothelium (Clark et al., 2007). This interaction is dependent on TLR4-activation of platelets by circulating LPS and leads to rapid neutrophil activation and the formation of neutrophil extracellular traps (NETs) (Clark et al., 2007). NETs consist of extracellular fibres of decondensed chromatin and proteins from the cytosol and granules, which are able to bind and immobilise pathogens

(Brinkmann et al., 2004). There are many NET-associated proteins; most are cationic in order to bind DNA and bactericidal in nature, such as histones, defensins, neutrophil elastase (NE), myeloperoxidase (MPO) and the bactericidal/permeability-increasing protein (Urban et al., 2009). Platelet-induced NETs have been shown to enhance both bacterial and viral capture within the liver and limit dissemination (Jenne et al., 2013; McDonald et al., 2012). They are formed via a specialised cell death programme termed NETosis, which is distinct from normal apoptosis or necrosis (Gupta et al., 2010). The exact mechanism of NETosis still remains elusive, but appears to be dependent on the production of superoxide by nicotinamide adenine dinucleotide phosphate (NADPH) oxidase (NOX) (Fuchs et al., 2007; Steinberg and Grinstein, 2007). Some studies have suggested that this is dependent on activation of peptidylarginine deiminase 4 (PAD4), which converts positively charged arginine residues of Histone H3 to uncharged citrulline side chains and subsequent rapid chromatin decondensation (Wang et al., 2009, 2004). However, more recent analysis has demonstrated that PAD4 activation and H3 citrullination are not universal features of NETs (Konig and Andrade, 2016).

1.7 Vascular adhesion protein-1

One of the atypical adhesion molecules implicated in recruitment of immune cells to the human liver is VAP-1. This protein is a glycosylated type II membrane protein that associates as a homodimer; it is also a member of the copper containing amine oxidase family and therefore exhibits primary amine oxidase activity. The dual functionality of VAP-1 has resulted in a large body of literature describing roles in a wide range of somewhat disparate cellular mechanisms and pathologies (Tipton et al., 2003).

1.7.1 Genomic organisation

Human VAP-1 is the product of the *AOC3* gene located on chromosome 17q21 and consists of four exons (Kaitaniemi et al., 2013). It lies between two other members of the copper containing amine oxidase (AOC) family: *AOC2* and *AOC4*. The final member of this family, *AOC1*, is located on chromosome 7q36 (Schwelberger, 2010). Most mammals express orthologs of all four AOC genes, however *AOC4* in humans is a non-functioning pseudogene due to an internal stop codon (Schwelberger, 2007). Mice and rats also only express small fragment of the 5' region of *AOC4*, however the four genes exhibit between

40-90% sequence homology with identical exon-intron organization, suggesting a common evolutionary origin (Schwelberger, 2010).

Kaitaniemi and colleagues have also documented a shorter splice variant of VAP-1 (VAP-1Δ3) within the lung (Kaitaniemi et al., 2013). It is widely expressed at the mRNA level but the protein does not exhibit any amine oxidase activity. It is capable of dimerising with the full length VAP-1, resulting in diminished cell surface expression and total enzymatic activity (Kaitaniemi et al., 2013).

1.7.2 Sites of expression

VAP-1 was originally described in the vessels of the tonsil, peripheral lymph node and inflamed rheumatoid synovium, however expression in almost all adult mammalian tissues has since been recorded (Salmi and Jalkanen, 1992). During foetal development, VAP-1 is first expressed within the vascular system and adipose tissue followed by the sensory organs, smooth muscle and skeletal elements (Valente et al., 2008). It therefore follows that in developed adults VAP-1 expression is highest in highly vascularised tissues such as the lungs, heart, gut and adipose and is upregulated during inflammation (Jaakkola et al., 2000). VAP-1 expression within the liver tissue is comparably lower than other tissues, however hepatic vascular endothelial cells, HSEC and HSCs are believed to constitutively express high levels (Hsia et al., 2016; Lalor et al., 2002; Weston et al., 2015).

VAP-1 is predominantly expressed by vascular endothelial cells, smooth muscle cells, adipocytes and more recently in HSCs (Hernandez et al., 2006; Jalkanen and Salmi, 2001; Weston et al., 2015; Zorzano et al., 2003). It primarily localises to the extracellular plasma membrane, with particularly high concentrations within caveolae of adipocytes and smooth muscle (Jaakkola et al., 1999; Souto et al., 2003). Endothelial VAP-1 may be stored in cytoplasmic granules, distinct from Weibel-Palade bodies, and trafficked to the cell surface upon inflammatory stimulation (Salmi and Jalkanen, 1995). A recent study also identified mitochondrial aldehyde dehydrogenase-2 (ALDH2) as a VAP-1 binding partner by co-immunoprecipitation, suggesting a potential mitochondrial localisation of VAP-1 (Ke et al., 2016).

1.7.3 Protein structure

Despite the somewhat low sequence homology across species, the tertiary structure of the AOC family of proteins is evolutionarily conserved, with all but *Escherichia coli* exhibiting similar conformations (Parsons et al., 1995). Each are formed of three domains (D2, D3 and D4), which bind together non-covalently via the D4 domain to form a heart-shaped homodimer as illustrated in Figure 1.10 (Airenne et al., 2005). The active site is buried deep within the protein and is therefore only accessible via a cavity between the D3 and D4 domains, the size of which dictates substrate specificity. The catalytic reaction involves a highly conserved aspartic acid residue and a trihydroxyphenylalanine quinone (TPQ) cofactor: an essential post-translationally modified tyrosine residue located within residue D4 (Salminen et al., 1998; Smith-Mungo and Kagan, 1998). The generation of the TPQ cofactor requires the presence of a copper (II) ion, which is coordinated by three conserved histidine residues (Airenne et al., 2005).

The human VAP-1 homodimer is around 180 kDa in weight and resembles that of the other AOC family members. A short four amino acid N-terminal tail forms the only intracellular part of the molecule and contains no classical signal transduction domains (Smith et al., 1998). This is followed by another short transmembrane region and the extracellular D2, D3 and D4 domains, consisting of residues 55-169, 170-300 and 301-761, respectively. The key tyrosine residue that forms the TPQ cofactor lies at residue 471. The channel between domains D3 and D4 that leads to the active site is blocked by a hydrophobic leucine residue (Leu469), which is thought to guard substrate entry (Airenne et al., 2005). VAP-1 is unique among other AOC proteins in that it also contains an Arg-Gly-Asp (RGD) motif at the C-terminal residues 726-728 (Salmi et al., 2000; Smith et al., 1998). The RGD motif is found within many integrin ligands involved in cell-cell and cell-matrix adhesion, including fibronectin and vWF (Takagi, 2004).

VAP-1 also has six N-linked glycosylation sites, which are fully glycosylated, and three potential O-linked glycosylation sites that are not utilised (Maula et al., 2005; Salmi and Jalkanen, 1996). All of the N-linked sites are highly conserved between all mammalian amine oxidases, in particular the N1 (Asn137), N2 (Asn232), N4 (Asn592) and N6 (Asn666) sites (Maula et al., 2005).

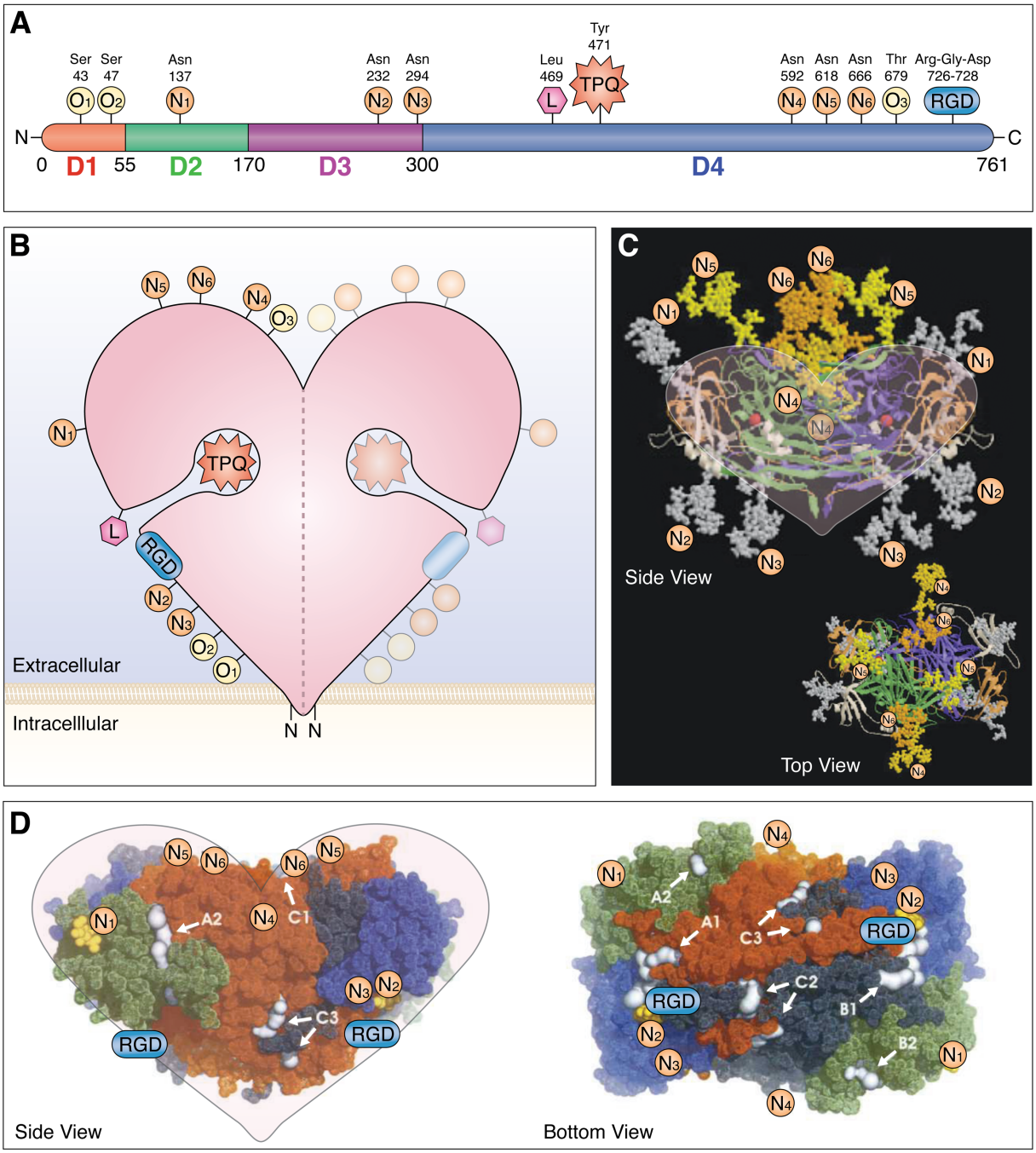


Figure 1.10 Structure of VAP-1. (**A**) VAP-1 is a 761 amino acid protein consisting of 4 domains. The N-terminal D1 domain contains the short cytoplasmic tail and membrane-spanning region. The C-terminal D4 domain is the largest and contains both the active site topoquinone (TPQ) cofactor and RGD domains. (**B**) The RGD motif lies at the edge of the active site channel, which is guarded by a hydrophobic leucine residue. (**C** & **D**) VAP-1 contains 3 O- and 6 N-glycosylation sites. N1, N4, N5 and N6 are found on the apical surface and are thought to be involved in leukocyte adhesion.

1.7.4 Soluble VAP-1

In addition to a membrane-bound ectoenzyme, VAP-1 also exists in a soluble form (sVAP-1) that circulates within the blood (Kurkijärvi et al., 1998). Soluble VAP-1 is catalytically active and accounts for the majority of plasma amine oxidase activity of any mammals that do not express the full-length *AOC4* gene, including both mice and men (Schwelberger, 2007; Stolen et al., 2004). Structurally sVAP-1 is highly similar to the membrane bound form including its glycosylation and dimerisation states, however a blocked N-terminus has hampered efforts to sequence the circulating protein. *Aoc3*$^{-/-}$ mice lack detectable serum amine oxidase activity, suggesting VAP-1 as the primary source (Stolen et al., 2004). Overexpression of membrane-bound VAP-1 on endothelial cells also confers higher levels of sVAP-1 in the blood; it is therefore likely that the membrane-bound protein undergoes cleavage and is subsequently released into serum (Stolen et al., 2004). This is consistent with enzymatic cleavage of many other surface-expressed leukocyte-endothelial cell adhesion molecules that are also released into the circulation, including ICAM-1, VCAM-1, CD44 and selectins (Bazil, 1995). In adipocytes VAP-1 release is stimulated by TNFα and low dose isoproterenol, and can be inhibited by the metalloproteinase (MMP) inhibitor batimastat (Abella et al., 2004; García-Vicente et al., 2005). Similarly, incubation with a specific inhibitor of MMP9 with or without MMP2 resulted in reduced sVAP-1 release from retinal capillary endothelial cells *in vitro* under high glucose conditions (Murata et al., 2012). However the precise mechanism leading to release of soluble VAP-1 is yet to be described.

The liver is thought to be the primary source of sVAP-1, although some evidence indicates bone tissue as a significant contributor (Ekblom et al., 1999; Kurkijärvi et al., 1998). Circulating concentrations of sVAP-1 are elevated in many inflammatory conditions, however the full implications of this are yet to be explored. Soluble VAP-1 has recently also been shown to act as a leukocyte chemotactic factor and lymphocytes pretreated with sVAP-1 demonstrate enhanced binding to VAP-1-transfected endothelial cells (Kurkijärvi et al., 1998; Weston et al., 2015).

1.7.5 Amine oxidase activity

Amine oxidases catalyse the oxidative deamination of a variety of amines to yield the corresponding aldehyde, ammonia and hydrogen peroxide. VAP-1 favours deamination of primary amines via formation of a transient Schiff base with the TPQ to release the

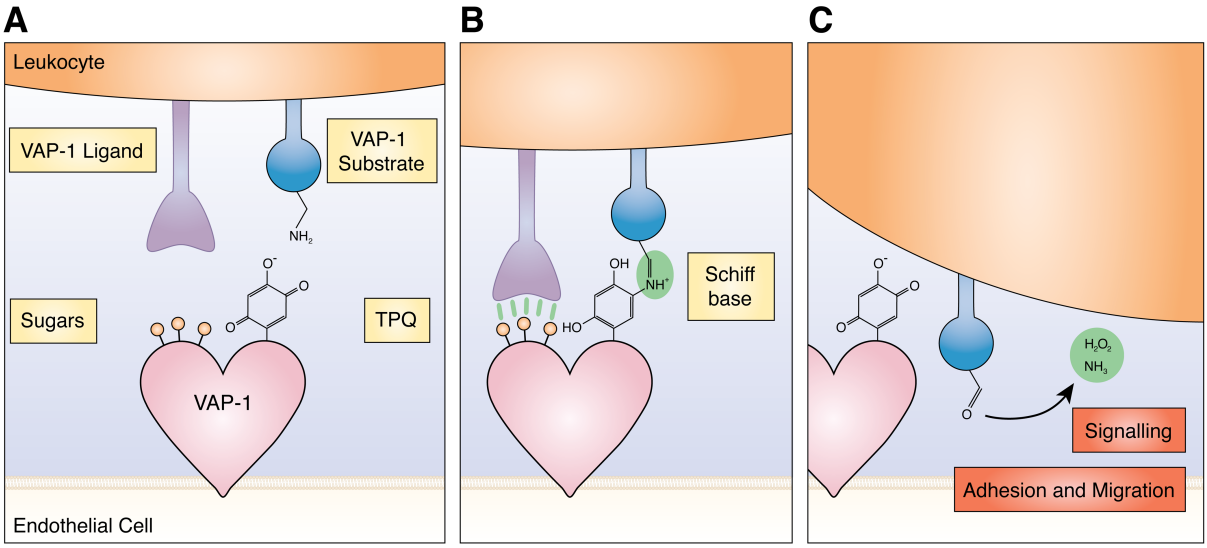


Figure 1.11 Leukocyte recruitment by VAP-1. The amine oxidase activity and adhesin functionality of VAP-1 are thought to be discrete, but both are involved in the recruitment of leukocytes. The carbohydrate decoration of VAP-1 is likely to be involved in a ligand interaction. Any substrate would require a primary aldehyde group to form a Schiff base intermediate with the topoquinone (TPQ) active site residue. The substrate is then spontaneously converted to an aldehyde while releasing H_2O_2 and NH_3, which are involved in localised signalling mechanisms. Although these molecules may be discrete, a single molecule may also exhibit both functions.

corresponding aldehyde. This is followed by hydrolyzation of the reduced TPQ with oxygen to yield hydrogen peroxide and ammonia, illustrated in Figure 1.11. Mutation of the key TPQ-forming tyrosine-471 to a phenylalanine residue (VAP-1^{Y471F}) elicits a structurally identical but enzymatically inactive form of VAP-1 (Koskinen et al., 2004). Knock-out, knock-in mice have since been bred that are deficient in *Aoc3* expression and only express the murine equivalent of VAP-1^{Y471F} (Jalkanen et al., 2007).

VAP-1 was originally described as semicarbazide-sensitive amine oxidase (SSAO) due to its sensitivity to inhibition by carbonyl-group reagents such as semicarbazide. This nomenclature is somewhat misleading as in fact all copper-containing amine oxidases are sensitive to inhibition by semicarbazide, including lysyl oxidase (LOX) (Smith-Mungo and Kagan, 1998). While SSAO is now largely recognised as VAP-1 alone, in some literature it has been used to describe any TPQ cofactor-containing AOC protein (O'Sullivan et al., 2003). However, SSAO has always been categorised as distinct from the flavin-containing monamine oxidase family (MAO). These enzymes are usually bound intracellularly to mitochondria and are not inhibited by semicarbazide but are sensitive to clorgyline and pargyline.

1.7.5.1 Substrates

The substrate specificity is used as one of the defining features of the amine oxidases, although there is cross-reactivity between some members. However the literature is highly conflicting - perhaps due to the apparent inter-species differences in substrate specificity and difficulty in obtaining preparations of active, purified protein (O'Sullivan, 2004). VAP-1 is therefore reported to deaminate a wide range of amines; both aliphatic and aromatic. The optimum substrate, however, is definitively the non-physiological amine benzylamine (Shen et al., 2012).

Dietary amines are a likely source of VAP-1 substrate, particularly due to the high VAP-1 expression in the liver and gut. Substrates for VAP-1 such as methylamine and tyramine are both found in alcohol as well as seafood and fermented foods (Benedetti et al., 2007; Mitchell and Zhang, 2001; Young et al., 1982). High concentrations of methylamine are also present in cigarette smoke and fumes from pollution, which may provide a substrate for lung-expressed VAP-1 (Schmeltz, 1977). Similarly xenobiotics such as mescaline and the anti-malarial drug primaquine are readily oxidised by VAP-1 (Tipton and Benedetti, 2001).

Bacterial pathogens also produce several VAP-1 substrates, including branched chain amines (such as isoamylamine), aminoacetone and cysteamine (Bukowski et al., 1999; Ghenghesh and Drucker, 1988; Shen et al., 2012). Cysteamine is also produced by pantetheinase during coenzyme A synthesis and may be involved in the oxidative stress response (Berruyer et al., 2004). Similarly, aminoacetone is also a product of mitochondrial metabolism of threonine and glycine and is not a substrate for MAO, suggesting a potential substrate for ALDH2-bound mitochondrial VAP-1 (Lyles and Chalmers, 1992; O'Sullivan, 2004).

Some neurosignalling molecules, such as dopamine, also make excellent substrates for VAP-1. Interestingly, serotonin is oxidised by VAP-1 from dental pulp cells but not from any other tissues, highlighting a potential tissue-dependant substrate specificity of VAP-1 (O'Sullivan et al., 2003). Similarly, sVAP-1 produced in a *Drosophila* cell line showed little activity with histamine as a substrate but VAP-1 from adipose and gut tissue showed levels comparable to benzylamine oxidation (Iffiú-Soltész et al., 2010; Shen et al., 2012). In fact VAP-1-deficient mice exhibit no benzylamine or histamine

oxidation in adipose tissue, suggesting VAP-1 as the primary source of activity (Iffiú-Soltész et al., 2010).

1.7.5.2 Inhibition

As an SSAO, the classical small molecule inhibitor (SMI) of VAP-1 is semicarbazide: an active-site-directed irreversible inhibitor that forms a non-covalently bound complex with VAP-1 (Lizcano et al., 1996). Other carbonyl reagents, such as hydrazine derivatives also inhibit VAP-1 but in a reversible manner (Lizcano et al., 1996; Magyar et al., 2001). During the search for an endogenous substrate of VAP-1, some physiological amines have also been found to exert an inhibitory effect on bovine VAP-1, including glucosamine and caffeine (Olivieri et al., 2011). Caffeine was shown to inhibit bovine sVAP-1 in a non-competitive or mixed manner and rats that were treated with caffeine over 10 days exhibited a dose-dependent decrease in SSAO activity (Che et al., 2012; Olivieri and Tipton, 2011). An endogenous inhibitor of VAP-1 has also been reported in human serum but this has not been fully identified and characterised (Buffoni et al., 1983).

While these molecules inhibit VAP-1 enzyme activity, they also inhibit other amine oxidases, such as MAO and LOX, due to high structural homology. In fact in previous studies semicarbazide and hydroxylamine have widely been used as VAP-1 inhibitors, which also potently inhibit all AOCs (Lyles, 1996). Discovery of VAP-1 specific inhibitors has therefore been hampered by similar sensitivities across amine oxidases, however several VAP-1-specific inhibitors have recently been developed. These primarily fall into two groups: reversible inhibitors and mechanism-based, irreversible inhibitors based on allylamines or hydrazines. The latter set of compounds form covalent bonds with the TPQ cofactor and have proven to be highly potent and specific. One of the first compounds was produced by La Jolla Pharmaceutical Company and named LJP-1586. LJP-1586 is an allylamine with an IC_{50} value of around 30 nM for human umbilical cord VAP-1 and under 10 nM or rat and mouse VAP-1 (Foot et al., 2013; O'Rourke et al., 2007). Pharmaxis Ltd. has more recently developed several VAP-1 inhibitors including PXS-4728A and PXS-4681A. These two molecules are both low molecular weight fluoroallylamines that potently inhibit VAP-1 across species with IC_{50} values less than 10 nM (Foot et al., 2013; Schilter et al., 2015).

1.7.6 Function of VAP-1

The wide range of expression sites, coupled with its amine oxidase activity, broad substrate specificity and interaction with leukocytes has led to much speculation about the physiological role of VAP-1. Mice deficient in VAP-1 (*Aoc3*$^{-/-}$) and those that express the catalytically inactive VAP-1^{Y471F} (SSAO^{KO}) develop normally with no overt phenotype (Jalkanen et al., 2007; Stolen et al., 2005). However, these animals have been instrumental in the elucidation of VAP-1 function in health and disease. Over time it has become apparent that VAP-1 may in fact be multifunctional depending on tissue-specificity. Currently the involvement of VAP-1 can be broadly divided into four categories: the detoxification of xenobiotic amines, the modulation of leukocyte adhesion, the regulation of glucose uptake and cell growth and development (Lalor et al., 2007).

1.7.6.1 Detoxification of xenobiotic amines

The extracellular localisation of the catalytic domain of membrane-bound VAP-1 suggests a role in the inactivation of potentially toxic amines in the blood. This is in contrast to MAOs, which may be more efficacious at deaminating VAP-1 substrates but do not encounter the substrate due to their intracellular localization. This hypothesis is supported by high expression of VAP-1 at sites of xenobiotic entry: expression within the gut and liver vasculature expose VAP-1 directly to dietary amines while expression within the lung exposes VAP-1 to inhaled volatile amines. As previously mentioned, methylamine found food, drinks and cigarette smoke is an excellent substrate for VAP-1 and would therefore be readily metabolised by VAP-1 at each of these sites. Any amines that avoid oxidation at initial entry could be metabolised by the high amine oxidase activity within the blood conferred by sVAP-1.

This function of VAP-1 is challenged somewhat by the fact that many of the aldehyde products of the VAP-1-catalysed reaction are more toxic than the substrates. Furthermore, many of these aldehyde products do not make good substrates for subsequent metabolic enzymes such as aldehyde dehydrogenase, aldehyde oxidase, aldehyde reductase and alcohol dehydrogenase. This is particularly true for the three most well documented endogenous VAP-1 substrates: methylamine, aminoacetone and allylamine (O'Sullivan, 2004). However, these molecules may alter the function of the VAP-1-expressing cells or affect other cells in a paracrine manner and provide a 'danger' signal. The oxidative deamination of methylamine produces highly toxic formaldehyde,

which is capable of cross-link primary amino groups in proteins and DNA. This process has also been documented after incubation of SSAO-rich tissues with methylamine (Gubisne-Haberle, 2004). The deamination of allylamine by VAP-1 to acrolein induces hypercontraction of blood vessels and is cytotoxic to vascular smooth muscle cells (Conklin et al., 2011, 1998). Increased blood acrolein concentration results in a corresponding increase in circulating platelet-leukocyte aggregate levels and an increased risk of cardiovascular disease (DeJarnett et al., 2014). VAP-1 also catalyses the formation of methylgloxal from aminoacetone, which subsequently reacts with proteins to form AGEs in smooth muscle cells (Mathys et al., 2002). These AGEs exert their main effect via interaction with their receptors (RAGE) on endothelium and leukocytes, thereby activating downstream inflammatory responses such as cytokine and chemokine production (Hofmann et al., 1999).

Hydrogen peroxide (H_2O_2) produced during the VAP-1-catalysed reaction may also have great physiological significance, although any effect could only be local to the VAP-1 molecule due to the particularly short half-life and ability to diffuse across cell membranes. However, the role of H_2O_2 as a local signalling molecule is well documented, with additional implications in cell proliferation, differentiation, migration and apoptosis (Forman et al., 2010; Rhee, 2006). Low levels of H_2O_2 are able to stimulate proliferation and enhanced survival in a wide variety of cell types (Stone and Collins, 2002). There is also growing evidence to support a complex role for H_2O_2 in leukocyte recruitment.

The ammonia by-product of the VAP-1 catalysed reaction is highly toxic and is normally metabolised to urea within the liver. However, it is capable of inducing immune dysfunction, such as impairing neutrophil phagocytosis and increasing oxidative burst (Shawcross et al., 2008). A recent link has also been proposed between ammonia signalling in the liver and hepatic fibrosis, through induced HSC ER stress and ROS production (Jalan et al., 2016).

1.7.6.2 Leukocyte recruitment

Since its discovery, VAP-1 has been described as a mediator of leukocyte adhesion (Salmi and Jalkanen, 1992). In the first identification study, an antibody raised against VAP-1 decreased lymphocyte binding to HEV and affinity-isolated VAP-1 *in vitro*. Since then, decreased leukocyte adhesion via antibody blockade of VAP-1 has been demonstrated in

multiple inflamed and vascularised organs such as ischemic heart (Jaakkola et al., 2000), inflamed skin (Arvilommi et al., 1996), the gut (Salmi et al., 1993) and the liver (McNab et al., 1996). Incubation of VAP-1 with monoclonal antibody does not appear to inhibit the enzymatic activity of the protein to small substrates *in vitro* or *in vivo*, therefore suggesting an alternative mode of action (Kiss et al., 2008; Salmi et al., 2001). However, inhibition of VAP-1 amine oxidase activity with SMIs also results in a reduction in leukocyte adhesion, although there is no synergistic or additive effect exhibited upon combined inhibition (Koskinen et al., 2004; Lalor et al., 2002; Marttila-Ichihara et al., 2006; Salmi et al., 2001). Both activities of VAP-1 are therefore required for leukocyte diapedesis, suggesting leukocytes bind VAP-1 via the antibody-defined surface epitope whilst also presenting substrate to the active site.

The most probable regions of leukocyte interaction with VAP-1 are the RGD motif and carbohydrate decoration. The RGD motif of VAP-1 is located at the tip

of a looped region at the extracellular surface by the entrance to the active site - the ideal conformation for ligand recognition (Airenne et al., 2005). While some proteins that contain the RGD motif serve to block integrin-ligand interactions, HEV cells transfected with VAP-1 lacking this motif exhibited significantly diminished leukocyte adhesion, however similar effects were not recapitulated with a single D/A point mutation (de Oliveira et al., 2014; Salmi et al., 2000). This suggests a functional, but perhaps not critical, role for this motif. The N-glycosylation sites N4, N5 and N6 are also located on the top of the VAP-1 molecule and are therefore also in optimum positions for leukocyte interaction (Airenne et al., 2005). Mutation of any of these residues also results in reduced, but not abolished, leukocyte adhesion under non-static conditions (Maula et al., 2005). Interestingly, mutation of these residues, which are located distal to the substrate-binding channel, also results in increased amine oxidase activity. This may be due to steric hindrance caused by the long, charged carbohydrate molecules when they are present (Maula et al., 2005). VAP-1 may also be alternatively glycosylated in different tissues, which may explain the variability in leukocyte binding, substrate specificity and activity (Jaakkola et al., 1999).

The early VAP-1 antibody blockade experiments demonstrated a decrease in total peripheral blood mononuclear cell (PBMC) adhesion (Salmi and Jalkanen, 1992). Since then many additional studies have also been conducted investigating the effect of VAP-1

	Human			Mouse			Rat			Rabbit
	R	A	M	R	A	M	R	A	M	A
Leukocyte	5(2)	57(18)	57(3)	40(1)	25(2)	51(4)	25(2)	38(2)		28(4)
Neutrophils		40(2)		80(2)	0(1)	27(4)	0(1)	44(1)	69(1)	
Monocytes		63(2)	40(1)			55(3)				
Macrophage		0(1)			0(1)					0(1)
Lymphocytes		38(4)	0(1)		43(4)	32(3)				-27(1)
CD8		75(4)			0(1)					
CD4		6(4)			10(1)					
Th1				0(1)	0(2)					
Th2				75(1)	73(2)					
Treg		0(1)	65(1)		0(1)					
NK		65(1)								
NKT										
B Cell		10(1)								

Table 1.1 The effect of VAP-1 antibody blockade on leukocyte recruitment. A summary of the literature examining the effect of VAP-1 antibody blockade on the proportion of rolling (R), adherent (A) and migrated (M) leukocyte subsets across different endothelial monolayers. Numbers indicate the percentage inhibition and the number of experiments investigating the topic.
(Tohka *et al.*, 2001; Salmi and Jalkanen, 1992; Salmi *et al.*, 1993; Salmi and Jalkanen, 1996; McNab *et al.*, 1996; Salmi *et al.*, 1997b, 1997a; Vicente-Manzanares and Sánchez-Madrid, 2004; Salmi *et al.*, 1998; Smith *et al.*, 1998; Yoong *et al.*, 1998; Jaakkola *et al.*, 2000, 1999; Salmi *et al.*, 2000, 2001; Irjala *et al.*, 2001; Kurkijärvi *et al.*, 2001; Lalor *et al.*, 2002; Martelius *et al.*, 2004; Bonder *et al.*, 2005; Edwards *et al.*, 2005; Kirton *et al.*, 2005; Salmi and Jalkanen, 2006; Merinen *et al.*, 2005; Marttila-Ichihara *et al.*, 2010; Aspinall *et al.*, 2010; Shetty *et al.*, 2011; Tuncer *et al.*, 2013)

inhibition on leukocyte migration, a summary of which can be seen in Table 1.1 and Table 1.2. Most studies have examined the effect on total PBMC populations and have replicated the original finding: inhibition of VAP-1, either by antibody blockade or SMI, leads to approximately 50% inhibition of PBMC adherence. The literature becomes more convoluted when examining the role of VAP-1 in the migration of specific subsets, also shown in Table 1.1 and Table 1.2. The conflicting data make it hard to draw firm conclusions as to which cells are recruited in a VAP-1-dependent manner. Neutrophils and monocytes are relatively well studied and show repeatable reductions in rolling, adhesion and transmigration whereas there appears to be no effect on macrophages *in vitro*, although effects have been shown *in vivo* (Bour et al., 2009; Nakao et al., 2011). Lymphocytes exhibit the most varied levels of inhibition, suggesting potential key differences between these subsets. In humans, $CD8^+$ and not $CD4^+$ T cells appear to interact with VAP-1, an effect that may be reversed in mice. The conflicting data on which leukocyte subsets are recruited are likely due to different experimental conditions (including different antibodies and SMIs and experimental systems) and different tissues in question. A study by Marttila-Ichihara and colleagues also suggested that inhibition of VAP-1 via antibody blockade affected adhesion of different subsets to

	Human			Mouse			Rat			Rabbit
	R	A	M	R	A	M	R	A	M	A
Leukocyte		50[1]	80[1]				30[1]	45[1]		80[1]
Neutrophils	30[2]	50[1]	48[2]	55[1]	75[2]					30[1]
Monocytes										
Macrophage					48[2]	0[1]				-36[1]
Lymphocytes			0[1]							-64[1]
CD8						0[2]				0[1]
CD4						25[2]				70[1]
Th1						0[1]				
Th2						50[1]				
Treg										
NK						0[1]				
NKT						0[1]				
B Cell						-45[1]				

Table 1.2 The effect of VAP-1 amine oxidase inhibition on leukocyte recruitment. A summary of the literature examining the effect of VAP-1 inhibition on the proportion of rolling (R), adherent (A) and migrated (M) leukocyte subsets across different endothelial monolayers. Numbers indicate the percentage inhibition and the number of experiments investigating the topic.
(Lalor *et al.*, 2002; Koskinen *et al.*, 2004; Edwards *et al.*, 2005; Salmi *et al.*, 2001; Xu *et al.*, 2006; Marttila-Ichihara *et al.*, 2006; Martelius *et al.*, 2004; Nakao *et al.*, 2011; Lee *et al.*, 2012; Tuncer *et al.*, 2013; Weston *et al.*, 2015)

inhibition with SMI ($CD8^+$ T cells or monocytes and neutrophils, respectively) therefore suggesting different mechanisms of action (Marttila-Ichihara et al., 2010). Further study is clearly required to fully elucidate these mechanisms.

Leukocyte recruitment via VAP-1 is independent of classical ligands such as L-selectin, PSGL-1 and α_4 integrin (Salmi et al., 1997), therefore the leukocyte ligand remained elusive until relatively recently. Various amino sugars have been investigated and the binding of VAP-1 active site proposed, including galactosamine, mannosamine and glucosamine (O'Sullivan et al., 2003). However, a phage-display screening initially identified Sialic acid binding Ig-like lectin-10 (Siglec 10) and later Siglec 9 as potential counterreceptors of VAP-1 (Aalto et al., 2011; Kivi et al., 2009). The authors proposed that the interaction takes place via an arginine amino group binding the TPQ cofactor and functioning as a substrate (Aalto et al., 2011; Kivi et al., 2009). The most recent study from this group suggests a multifaceted interaction via both glycan-mediated and protein-protein interactions between VAP-1 and separate domains of Siglec 9 (Elovaara et al., 2016). Despite the authors demonstrating the binding capacity of the molecules, some scepticism remains around the proposal. Firstly, due to the lack of a primary amine, arginine is an unlikely substrate for VAP-1. Secondly, the proposed residues are not conserved within the mouse orthologue (Siglec G) therefore implying fundamental interspecies differences in the VAP-1 recruitment mechanism. However, the Siglec

molecules are known to bind to sialic acids such as those that decorate the surface of VAP-1 (Kivi et al., 2009), which may therefore explain at least some of the attraction between the molecules. Lastly, expression of Siglec 9 is only highly expressed by monocytes and neutrophils whereas weaker expression is observed on minor populations of NK cells, B cells and T cells (Zhang et al., 2000). Siglec 10, however, is only found on B cells and NK cells, with low levels on monocyte and eosinophils (Aalto et al., 2011; Munday et al., 2001). The lack of lymphoid expression of Siglec 9 and 10 implies that either other VAP-1 binding partners remain to be elucidated, or that lymphocyte recruitment via VAP-1 occurs independently of a direct ligand interaction.

H_2O_2 produced during the VAP-1-catalysed reaction may also be key to its function as an adhesion molecule. Mechanistically, VAP-1 is only capable of binding to certain molecules, such as the amino sugars galactosamine, glucosamine and mannose, in the presence of H_2O_2; specifically H_2O_2 formed as a product of SSAO-catalysed oxidation (O'Sullivan et al., 2007). H_2O_2 is capable of modulating the microenvironment, thereby priming the traditional leukocyte extravasation cascade. H_2O_2 is a chemotactic agent in its own right and can recruit leukocytes to the site of injury (Niethammer et al., 2009) but also treatment of lymphocytes with H_2O_2 can lead to ligand-independent activation (Reth, 2002). H_2O_2 is also involved in cross-talk between VAP-1 and other adhesion molecules: H_2O_2 generated by VAP-1 can also induce the expression of adhesion molecules (P- and E-selectins) and chemokines (including MCP-1 and IL-8) both *in vitro* and *in vivo* (Jalkanen et al., 2007; Lalor et al., 2007; Salter-Cid et al., 2005). The deamination of methylamine by VAP-1 in the presence of TNFα can also induce the expression of MAdCAM-1 on endothelial cells (Liaskou et al., 2011). Moreover, SSAO inhibition has led to diminished P-selectin expression in an *in vivo* mouse model of eye inflammation (Noda et al., 2008).

1.7.6.3 Glucose transport

The most abundant glucose transporter within adipocytes and smooth muscle cells, glucose transporter type-4 (GLUT4), is localised to intracellular vesicles. Upon binding of insulin to its receptor, the GLUT4-containing vesicles are transported to the plasma membrane where it functions to traffic glucose into the cell. Interestingly, these vesicles also contain relatively high concentrations of catalytically active VAP-1 (Enrique-Tarancón et al., 1998). The H_2O_2 formed during amine oxidation of VAP-1 is

able to activate the insulin receptor in the absence of insulin, resulting in subsequent GLUT-4 translocation and glucose transport (Horie et al., 2008). In this way, VAP-1 substrates are also capable of acting in an insulinomimetic manner, increasing glucose transport into the cell (El Hadri et al., 2002; Enrique-Tarancón et al., 2000; Morin et al., 2001). In fact, chronic administration of VAP-1 substrates improves the glucose tolerance of diabetic mice and those fed a high-fat diet (Abella et al., 2003; Iffiú-Soltész et al., 2010).

1.7.6.4 Cell growth and development

The maturation of adipocytes appears to correlate with VAP-1 expression, with very low levels expressed by preadipocytes and much higher levels in mature cells (Moldes et al., 1999; Raimondi et al., 1990). Similarly, the treatment of adipocytes with VAP-1 substrates induces maturation in a dose-dependent manner (Fontana et al., 2001; Mercier et al., 2001). This effect can be reversed by the addition of catalase or by inhibition of VAP-1, possibly suggesting an H_2O_2-dependent mechanism, although inhibition of MAO had no effect (Mercier et al., 2001).

The function of LOX in ECM deposition and angiogenesis is well documented, and VAP-1 also appears to have a similar role (Shih et al., 2013). Both *Aoc3*$^{-/-}$ and SSAO^{KO} mice exhibit defective tumour angiogenesis (Marttila-Ichihara et al., 2009). This effect can also be induced by treatment with VAP-1 SMI but not antibody blockade, demonstrating the importance of enzyme activity (Marttila-Ichihara et al., 2010). IL-1β can induce angiogenesis in the inflamed cornea with particularly high expression of VAP-1 within the neovasculature (Nakao et al., 2011). Inhibition of VAP-1 can block this angiogenesis but has no effect on vascular endothelial growth factor-A (VEGF-A)-induced angiogenesis (Nakao et al., 2011). Inhibition of VAP-1 also results in aberrant collagen and elastin deposition by smooth muscle cells and mice chronically treated with VAP-1 SMI developed large aortic lesions (Langford et al., 2002, 1999). Both *Aoc3*$^{-/-}$ mice and those treated with an SMI exhibited increased arterial diameter, further implicating VAP-1 in arterial wall remodelling (Langford et al., 1999; Mercier et al., 2006).

1.7.7 Role in disease

The diverse expression and functions of VAP-1 has resulted in its implication in a wide range of disease pathogeneses, particularly as expression of VAP-1 is upregulated at

sites of inflammation and therefore correlates with inflammatory conditions (Salmi et al., 1993). For example, inhibiting the amine oxidase activity of VAP-1 leads to suppression of inflammation and leukocyte recruitment to the gut in models of ulcerative colitis (Salter-Cid et al., 2005), to inflamed joints in arthritis (Marttila-Ichihara et al., 2006; Tábi et al., 2013), the eye in models of uveitis (Noda et al., 2008) and diabetic retinopathy (Noda et al., 2009), to the lungs in cigarette smoke-induced chronic obstructive pulmonary disease (Jarnicki et al., 2016), to ischemic heart (Jaakkola et al., 2000) and into solid melanoma and lymphoma tumours (Marttila-Ichihara et al., 2010). VAP-1 is also highly expressed at sites of metastatic tumour attachment where it can aid myeloid cell recruitment (Ferjančič et al., 2013). Inhibition of VAP-1 decreases the incidence and severity of inflammation in mouse models of multiple sclerosis (O'Rourke et al., 2007) and kidney fibrosis (Wong et al., 2014) and reduces intestinal and lung damage during ischemia-reperfusion injury (Kiss et al., 2008). VAP-1 inhibition also decreases neurologic dysfunction in rats following subarachnoid haemorrhage (Xu et al., 2014). The glucose-controlling function of VAP-1 also means that addition of VAP-1 substrate and vanadate increases acute glucose tolerance in type II diabetic mice, and also normalizes hyperglycemia, stimulates glucose transport in adipocytes and reverses muscle insulin resistance in the long term (Abella et al., 2003).

There is also a large body of literature describing alterations in serum sVAP-1 concentrations in a range of disease states. Serum sVAP-1 concentrations are significantly higher during many inflammatory conditions, such as multiple sclerosis (Airas et al., 2006; Yanaba et al., 2013), atherosclerosis (Karádi et al., 2002), Psoriasis vulgaris (Ataseven and Kesli, 2016; Madej et al., 2007; Nemati et al., 2013), atopic eczema (Madej et al., 2006), chronic kidney disease (Lin et al., 2008) and during septic shock (Sallisalmi et al., 2012). Levels are also elevated in smokers (Wang et al., 2013) and those suffering from hypertension (Maciorkowska et al., 2015) and congestive heart failure (Boomsma and van Veldhuisen, 1997) and correlates with an increase in body mass index (Garpenstrand et al., 1999). Concentrations are also raised in patients suffering from type II diabetes (Elliott et al., 1991; Garpenstrand et al., 1999; Hayes and Clarke, 1990; Li et al., 2009) and sVAP-1 titre is a good indicator of end stage renal disease (Li et al., 2016)and mortality from cardiovascular and cancer in diabetic patients (Li et al., 2011). However, the picture with cancer sufferers is less clear; sVAP-1 levels are higher in patients with small cell lung cancer (Garpenstrand et al., 2004) and levels

are a good indicator of all-cause mortality in colorectal cancer sufferers (Li et al., 2014). Low serum VAP-1 titre is also a good indicator of poor prognosis in patients suffering from colorectal cancer (Toiyama et al., 2009) and gastric cancer (Kaplan et al., 2014; Yasuda et al., 2011). However, concentrations are lower in those suffering from thyroid cancer (Hu et al., 2016), prostate cancer (Chen et al., 2013) and colorectal cancer (Ward et al., 2016). Interestingly sVAP-1 levels are also significantly lower in patients who have suffered from severe burns (Lewinsohn, 1977).

1.7.7.1 Role in liver disease

VAP-1 plays a crucial role in homeostasis of the liver and there is increasing evidence for a role in the pathogenesis of both acute and chronic inflammatory liver disease. Patients suffering from ALD, PBC, PSC, NAFLD and NANB hepatitis have significantly raised sVAP-1 levels compared to healthy controls, whereas patients suffering from POD and AIH showed no median difference in concentration (Kurkijärvi et al., 2000, 1998; Weston et al., 2015). The enzymatic activity of sVAP-1 in these patients was higher in hepatic compared to portal veins, suggesting the liver as a potential source of the protein (Kurkijärvi et al., 2000).

The constitutive expression of VAP-1 on cultured HSEC and the function of this in leukocyte adhesion and transendothelial migration have been well documented (Edwards et al., 2005; Lalor et al., 2002, 2007; Shetty et al., 2011; McNab et al., 1996; Weston et al., 2015). This has also been demonstrated in a chronic CCl_4 model of hepatitis in mice, during which *Aoc3*$^{-/-}$ mice or those treated with VAP-1 antibody exhibited significantly lower levels of injury than wild-type (WT) or untreated animals (Weston et al., 2015). This correlated with lower numbers of liver-infiltrating leukocytes in *Aoc3*$^{-/-}$ mice at the point of maximum injury, including: $CD4^+$ and $CD8^+$ lymphocytes, B cells, NK cells, NKT cells and myeloid cells (Weston et al., 2015).

Although serum VAP-1 titre is reduced, VAP-1 expression is higher in the livers of patients suffering acute liver failure from either POD or NANB (Tuncer et al., 2013). In an acute Con A model of hepatitis in mice, antibody blockade of VAP-1 reduced the rolling of neutrophils and T_h2 (but not T_h1) cells within the hepatic sinusoids (Bonder et al., 2005; Lee et al., 2013); this diminished recruitment of T_h2 cells was also replicated in

an acute model of Con A-treated *Aoc3*$^{-/-}$ mice, in which VAP-1 knockout correlated with lower levels of hepatic injury compared to WT littermates (Lee et al., 2013).

The role of VAP-1 in the pathogenesis of NAFLD has been suggested since the discovery of the link between VAP-1 activity and hepatic glucose uptake (Karim et al., 2014). *Aoc3*$^{-/-}$ mice receiving the MCD diet demonstrated lower levels of steatohepatitis and liver infiltration of CD4^{+} lymphocytes, NKT and myeloid cells than WT animals (Weston et al., 2015). WT mice treated with VAP-1 antibody exhibited comparably low levels of steatohepatitis to *Aoc3*$^{-/-}$ mice, however only the proportion of intrahepatic macrophages was decreased (Weston et al., 2015). *Aoc3*$^{-/-}$ mice fed the WLM diet exhibited a similar phenotype to the MCD model in terms of reduced injury and CD4^{+} and NKT cell infiltration (Weston et al., 2015). Similarly, this was also replicated in SSAO^{KO} mice treated with the WLM reinforcing the importance of enzyme activity to function (Weston et al., 2015).

VAP-1 has previously been implicated in matrix remodelling because its overexpression in smooth muscle cells results in deposition of collagen and elastin (Langford et al., 2002). The ECM-depositing cells of the liver, HSCs, are also capable of *de novo* synthesis of VAP-1 mRNA, which can be stimulated by platelet-derived growth factor-β (PDGFβ) and TGFβ1 (Weston et al., 2015). The *Aoc3*$^{-/-}$ and antibody-treated mice above also exhibited decreased levels of fibrosis during the chronic injury models, suggesting a potential role within the liver (Weston et al., 2015). Furthermore, SSAO^{KO} mice also demonstrated decreased fibrosis during WLM, further supporting the important role of the amine oxidase activity (Weston et al., 2015). One potential mechanism of action may be the formation of AGEs by the catalysis aminoacetone and methylamine. The interactions of AGEs and their receptors have been shown to evoke inflammatory responses, including by hepatocytes, and have suggested involvement in NASH and liver cirrhosis (Hyogo and Yamagishi, 2008).

VAP-1 is also highly expressed on the vasculature in HCC and in the tumour margin where it is capable of supporting adhesion of T cells (Yoong et al., 1998). Patients with HCC caused by progressive ALD and NAFLD also had higher sVAP-1 levels than those with cirrhosis alone (Kemik et al., 2010).

1.8 Aims and Hypotheses

A large body of literature has developed around VAP-1 since its discovery including its structure, expression patterns and functions. Although our current broad picture of VAP-1 is therefore fairly well developed, many of these studies report conflicting data, thereby highlighting potential key differences between tissue- and organism-specificity, experimental methods and choice of inhibitors.

Recent studies from groups such as our own have suggested an important role for VAP-1 in multiple liver diseases; however characterisation of VAP-1 expression has been somewhat limited. Very few studies have examined expression of VAP-1 in the human liver due to the restricted availability of tissue. Of the few studies that have been published, the focus has been primarily on histological analysis and restricted to only a few disease types. To the author's knowledge, no work has examined the activity of hepatic VAP-1 and how this may be linked to the development and progression of inflammatory liver disease. This has lead to the first hypothesis to be examined:

Hypothesis 1. Hepatic VAP-1 expression and activity is differentially regulated during inflammatory liver disease and may be linked to development of specific pathophysiologies.

One possible mechanism by which VAP-1 enzyme activity may affect disease progression is through leukocyte recruitment. However, it is still unclear whether the catalytic activity of VAP-1 is critical for this process or discrete from its adhesive capacity, particularly within the hepatic environment. Understanding the mechanism of VAP-1-dependent adhesion is also fundamental to elucidating the leukocyte specificity of VAP-1 recruitment. A wide range of leukocyte have been suggested to interact with VAP-1, despite the proposed ligands of VAP-1, Siglec 9 and 10, exhibiting limited expression to specific immune subsets. This may highlight key mechanistic different between different cell types and has driven the second hypothesis to be investigated:

Hypothesis 2. Hepatic VAP-1 is involved in the recruitment of specific leukocyte subsets and the amine oxidase activity is important for this functionality.

Although many leukocyte subsets have been suggested as VAP-1 interactants, neutrophils in particular have shown a propensity for recruitment. Furthermore, the

catalytic activity of VAP-1 is thought to be critical for recruitment of this specific subtype. These cells also exhibit expression of Siglec molecules and are known to migrate in response to H_2O_2. These findings indicate an important relationship between neutrophils and VAP-1 that will be explored in this thesis:

Hypothesis 3. VAP-1 is involved in the recruitment of neutrophils and may impact their effector functions.

During the acute stage of hepatitis, collateral immune cell-mediated damage is thought to contributes to and often dominate the pathogenic mechanism. The role of VAP-1 as a mediator of leukocyte recruitment to the liver may therefore implicate VAP-1 in the pathogenesis of acute liver injury and possibly acute liver failure. Much of the work to date has focused on VAP-1 in chronic inflammatory liver disease, therefore the final hypothesis of this thesis is that:

Hypothesis 4. VAP-1 amine oxidase activity is involved in the pathogenesis of acute liver injury.

It is unclear whether VAP-1 is only important in a proportion or all liver diseases and much of the mechanistic detail is still lacking. The broad intention of this thesis is therefore to examine VAP-1 expression across the liver diseases and to interrogate some of the functions of hepatic VAP-1 with hopes to offer insight into the mechanisms by which its effects are exerted. More specifically:

Aim 1. To determine and compare hepatic VAP-1 expression during health and across inflammatory liver diseases.

Aim 2. To interrogate the adhesin functionality of hepatic VAP-1: the importance of amine oxidase activity to this process and leukocyte specificity.

Aim 3. To investigate the effect of VAP-1 on neutrophil function.

Aim 4. To investigate the role of VAP-1 amine oxidase activity in a murine model of acute liver injury.

2

MATERIALS AND METHODS

2.1 Human Tissue

Human liver tissue was acquired from explanted livers removed at time of transplantation, or from healthy donors surplus to transplantation requirements. Peripheral blood was obtained from healthy volunteers or from patients suffering from haemochromatosis as part of routine treatment. All blood and tissue were obtained through the Queen Elizabeth Hospital (Birmingham, UK) with local research ethics committee approval (tissue: 06/Q2702/61, blood: 04/Q2708/41) and informed patient consent.

2.1.1 Cell and tissue culture

Cell and tissue culture was carried out in a standard class II microflow safety cabinet, unless otherwise stated. Aseptic technique was maintained by swabbing with Trigene

(Tristel Solution Ltd, UK) followed by industrial methylated spirit (IMS; Adams Healthcare, UK). All cells were maintained in humidified incubators at 37˚C and 5% CO_2. Viability and growth was monitored with an inverted phase contrast microscope (Olympus IX50). All well plates, flasks, tubes and stripettes used for culture were purchased from Corning Costar (UK).

For passage, adherent cells were trypsinised with the addition of 37˚C TrypLE Express (Invitrogen, UK) with gentle agitation until cells detached. Cells were aspirated before centrifugation (300 *x g*, 5 minutes). The resulting pellet was then resuspended in the appropriate media before reseeding for subsequent culture.

Cell viability was quantified by Trypan-blue (Life Technologies, UK) exclusion. Cells were counted with the use of a haemocytometer (MerckMillipore, UK).

2.1.2 Isolation of hepatic sinusoidal endothelial cells

HSEC were isolated as previously described (Lalor et al., 2006). In brief, ~30 g human liver tissue was finely diced before collagenase-digestion (0.2% $^{w}/_{v}$ collagenase type Ia; Sigma-Aldrich, UK) for 30 minutes at 37˚C and 5% CO_2. The resultant mixture was filtered in excess of sterile phosphate-buffered saline (PBS; Oxoid, UK). Non-parenchymal cells were subsequently isolated via density gradient centrifugation using 33/77% $^{w}/_{v}$ Percoll (Amersham Biosciences, UK) at 600 *x g* for 25 minutes, brake-free. Cholangiocytes were then removed by immunomagnetic selection using anti-HEA125-conjugated Dynabeads (20 minutes, 37˚C, 5% CO_2; Invitrogen, UK) and discarded. HSEC were then positively selected with anti-CD31-conjugated Dynabeads (30 minutes, 4˚C). HSEC-bead conjugates were then resuspended in HSEC media consisting of human endothelial serum free media (SFM; Invitrogen) supplemented with heat-inactivated AB human serum (10% $^{v}/_{v}$; HD supplies, UK), VEGF (10 ng/mL; PeproTech, UK), HGF (10 ng/mL; PeproTech), L-glutamine (2 mM), penicillin (100 U/mL) and streptomycin (100 µg/mL). Cells were cultured in flasks pre-coated overnight in rat-tail collagen (RTC; 220 µg/mL in PBS; Sigma-Aldrich) at 37°C with 5% CO_2. All cells were used within 7 passages of isolation.

2.1.3 Other human cells

Human embryonic kidney cell line HEK293 (Originally purchased from ECCAC, UK) were cultured in DMEM (Invitrogen) supplemented with heat inactivated foetal calf serum (HI-FCS; 10% $^{v}/_{v}$; Invitrogen), L-glutamine (2 mM), penicillin (100 U/mL) and streptomycin (100 µg/mL).

Primary human hepatic stellate cells (HSCs) and activated liver myofibroblasts (aLMFs) were a kind gift from Dr Emma Shepherd, Birmingham, UK.

2.1.4 Isolation of human leukocyte subsets from peripheral blood

All leukocyte subsets were isolated from ethylenediaminetetraacetic acid (EDTA)-treated peripheral blood and used on the same day as venesection.

2.1.4.1 Peripheral blood lymphocyte isolation

Peripheral blood lymphocytes (PBLs) were isolated via density gradient centrifugation over Lymphoprep (Stemcell technologies, Canada) for 25 minutes at 600 *x g*. The lymphocyte layer was then washed with MACS buffer (PBS containing FCS (2% $^{v}/_{v}$; Invitrogen) and EDTA (1 mM; Sigma-Aldrich)) before centrifugation for 10 minutes at 200 *x g* to deplete platelets. Resulting peripheral blood mononuclear cells (PBMC) were then resuspended in lymphocyte media (RPMI-1640 (Sigma-Aldrich) supplemented with FCS (10% $^{v}/_{v}$), L-glutamine (2 mM), penicillin (100 U/mL) and streptomycin (100 µg/mL)). Cells were then incubated for one hour at 37°C with 5% CO_2 to deplete monocytes by plastic adherence before being washed with PBS and resuspended in lymphocyte media.

2.1.4.2 T cell and natural killer cell isolation

$CD4^+$ and $CD8^+$ T cells and natural killer (NK) cells were isolated by negative immunomagnetic selection using a $CD4^+$ or $CD8^+$ T cell or NK isolation kit (Miltenyi Biotec, UK).

Briefly, PBMC fraction was isolated using a Lymphoprep gradient as in 2.1.4.1 and resuspended in MACS buffer (40 µL per 10^7 cells). Cells were first incubated with a biotin-conjugated antibody cocktail (10 µL per 10^7 cells, 5 minutes, 4°C). A further volume of MACS buffer was then added (30 µL per 10^7 cells) along with a MicroBead

cocktail (20 µL per 10^7 cells, 10 minutes, 4°C). Cells were then loaded into LS columns (Miltenyi Biotec) within a magnetic field, and enriched unlabelled cell suspension collected for further downstream use. $CD4^+$ and $CD8^+$ T cells routinely constituted >95% purity whereas NK cells were >85% pure, as confirmed by multi-colour flow cytometry.

2.1.4.3 Monocyte Isolation

$CD14^+$ monocytes were isolated by positive immunomagnetic selection using CD14 isolation kit (Miltenyi Biotec).

Cells were isolated as in 2.1.4.2 but using CD14 MicroBeads. Following elution of unlabelled cell fraction, the column was removed from the magnetic field and $CD14^+$ bead-conjugated cells eluted and collected for further downstream use. Monocytes were routinely >90% pure as confirmed by multi-colour flow cytometry.

2.1.4.4 B cell isolation

B cells were isolated by negative immunomagnetic selection using an EasySep human B cell enrichment kit (Stemcell). Briefly, PBMC fraction was isolated using a lymphoprep gradient as in 2.1.4.1 and resuspended to 5 x 10^7 cells/mL in MACS buffer. Cells were first incubated with an Enrichment Cocktail (50 µl/mL, 10 minutes, room temperature (RT)) before adding Magnetic Particles (75 µl/mL, 5 minutes, RT). Cells were then placed into "The Big Easy" magnet (Stemcell) for 5 minutes before the enriched unlabelled cell suspension was collected for further downstream use. B cells were routinely >90% pure as confirmed by multi-colour flow cytometry.

2.1.4.5 Neutrophil isolation

Neutrophils were isolated from whole blood using a Percoll density gradient. First 2% $^{w}/_{v}$ dextran (Pharmacosmos, DK) was added to the EDTA-treated blood (1:6, 30 minutes, RT) in order to sediment red blood cells. The leukocyte-rich plasma was then layered onto 56/80% $^{w}/_{v}$ Percoll gradient at a ratio of 5:3 mL before centrifugation (20 minutes, 220 *x g*, no brake). Neutrophils were aspirated from the 56/80% boundary and resuspended in neutrophil media consisting of RPMI-1640 supplemented with L-glutamine (2 mM), penicillin (100 U/mL) and streptomycin (100 µg/mL). Cells were then centrifuged (450 *x g*, 10 minutes) before resuspension of pellet in neutrophil media for

further downstream use. Neutrophils were routinely >75% pure as confirmed by multi-colour flow cytometry.

2.2 Immunohistochemistry

2.2.1 Frozen tissue

All human immunohistochemistry was performed on frozen tissue. At the time of explant, liver tissue was cut into ~1 cm^3 cubes and snap frozen in liquid nitrogen before being mounted in Tissue-Tek embedding compound (Sakura Finetek, NL). 7 µm sections were cut and placed onto poly-L-lysine-coated glass slides (0.01% $^{w}/_{v}$; VWR, UK) before fixing in acetone (5 minutes; Thermo Fisher Scientific, UK) and storage at -20˚C. Prior to staining, sections were allowed to warm to RT before re-fixing in acetone (5 minutes). A list of antibodies used for immunohistochemistry on frozen tissue can be found in Table 2.1.

2.2.1.1 Picrosirius red staining

Sections were rinsed in water before submerging in phosphomolybdic acid (0.5% $^{v}/_{v}$; 5 minutes; Sigma-Aldrich). Connective tissue was then stained by submerging in saturated aqueous picric acid solution (1 hour; Sigma-Aldrich) containing Direct Red 80 (0.1%; Sigma Aldrich). The sections were then washed twice in aqueous glacial acetic acid (0.1 M; Sigma-Aldrich). Finally, sections were dehydrated in three sequential alcohol solutions (99% $^{v}/_{v}$ for 3 minutes) and cleared twice in xylene (Pioneer Research

	Target	Clone	Isotype	Supplier	Working conc
Chr	VAP-1	TK8-14	Mm IgG_{2a}	eBioscience	0.25 µg/mL
FI	VAP-1	TK8-14	Mm IgG_{2a}	eBioscience	10 µg/mL
	VAP-1	174-5	Mm IgG_1	Hycult Biotech	10 µg/mL
	CD31	JC70A	Mm IgG_1	Dako	10 µg/mL
	CK18	DC10	Mm IgG_1	Dako	4 µg/mL
	EpCAM	1B7	Mm IgG_1	eBioscience	10 µg/mL
	αSMA	1A4	Mm IgG_{2a}	Dako	0.35 µg/mL
IMC	N/A	X0943	Mm IgG_{2a}	Dako	*Assay Dependent*
	N/A	X0931	Mm IgG_1	Dako	*Assay Dependent*

Table 2.1 Human staining antibodies (frozen tissue); Chr, Chromogenic; FI, Fluorescent.

Chemicals Ltd, UK) before cover slips were attached with DPX mounting medium (CellPath, UK).

2.2.1.2 Chromogenic staining

All incubation steps were carried out in a humidified chamber with gentle agitation at RT unless otherwise stated. Prior to staining, sections were encircled with wax pen (Dako) before hydrating in TBS-T, consisting of Tris-buffered saline (pH 7.6; Sigma-Aldrich) and Tween 20 (0.05% $^{v}/_{v}$; Sigma-Aldrich). Endogenous peroxidase activity was quenched with H_2O_2 (0.3% $^{v}/_{v}$ in methanol, 5 minutes; Sigma-Aldrich), before washing in TBS-T and blocking with horse serum (2.5% $^{v}/_{v}$, 20 minutes; Vector laboratories, UK). Sections were then incubated with primary antibody in TBS-T containing FCS (0.5% $^{v}/_{v}$) overnight at 4˚C. Slides were washed twice with TBS-T followed by incubation with ImmPRESS universal HRP-conjugated antibody (30 minutes; Vector laboratories). Slides were washed again twice before incubation with 3,3'-Diaminobenzidine (DAB peroxidase; Vector laboratories) as per manufacturer's instructions until the desired stain was achieved. Nickel chloride solution was added in some incidence to produce a grey-black stain. IMCs were run simultaneously to indicate any non-specific binding. Sections were washed with TBS-T before counterstaining with Mayer's haematoxylin (30 seconds; Pioneer Research Chemicals Ltd.). Finally sections were washed with water before mounting coverslips with Shandon Immu-Mount (Thermo Fisher Scientific).

2.2.1.3 Immunofluorescent Staining

All incubation steps were carried out in a humidified chamber with gentle agitation at RT unless otherwise stated. Prior to staining, sections were encircled with wax pen before permeabilising with Triton X-100 in PBS (0.3% $^{v}/_{v}$, 5 minutes; Sigma-Aldrich). The sections were then blocked with goat serum (10% $^{v}/_{v}$; Sigma-Aldrich) in PBS-T consisting of PBS and Triton X-100 (0.1% $^{v}/_{v}$; 10 minutes). Primary antibody was added

Source	Target	Target Isotype	Fluorophore	Supplier	Working conc
Goat	Mouse	IgG_{2a}	AlexaFluor 488	Thermo Fisher	4 µg/mL
Goat	Mouse	IgG_{2a}	AlexaFluor 546	Thermo Fisher	4 µg/mL
Goat	Mouse	IgG_1	AlexaFluor 488	Thermo Fisher	4 µg/mL
Goat	Mouse	IgG_{2a}	AlexaFluor 546	Thermo Fisher	4 µg/mL

Table 2.2 Fluorescent secondary antibodies

to the sections in PBS-T supplemented with goat serum (2% v/v) and incubated overnight at 4°C. Sections were washed in PBS-T and incubated with fluorescently conjugated secondary antibodies (Table 2.2) in PBS-T supplemented with goat serum (2% v/v) for 1 hour at room temperature protected from light. Finally, sections were washed with PBS-T and mounted with ProLong diamond antifade mountant containing the nuclear stain 4',6-diamidino-2-phenylindole (DAPI; Thermo Fisher Scientific, UK) and stored at 4°C protected from light until visualisation.

2.2.2 Formalin-fixed tissue

All mouse tissue immunohistochemistry was performed on formalin-fixed tissue. At the time of explant, liver tissue was cut into ~2 cm x ~2 cm x ~1 cm cuboids and fixed in neutral-buffered formalin (4% v/v; CellPath, UK) before being paraffin-embedded and stored at RT. Sections of 5 µm thickness were cut and fixed onto microscope slides (X-tra Adhesive, Leica, DE). Prior to staining, sections were dewaxed in xylene (3 x 5 minutes; Pioneer Research Chemicals Ltd.) before rehydration in three sequential alcohol solutions (99% v/v for 3 minutes) followed by water (2 x 3 minutes). A list of antibodies used for immunohistochemistry of formalin-fixed tissue can be found in Table 2.3.

2.2.2.1 Haematoxylin and eosin

For haematoxylin and eosin (H&E) staining, sections were first dewaxed and rehydrated. Nuclei were then stained by submerging in Harris haematoxylin (Pioneer Research Chemicals Ltd.). They were then washed in water followed by acid alcohol (0.3% v/v; Pioneer Research Chemicals Ltd.). The sections were then washed with water, submerged in Scott's tap water substitute (Pioneer Research Chemicals Ltd.) and then washed again with water. The cytoplasm was then stained by submerging in eosin (Pioneer Research Chemicals Ltd.) followed by washing with tap water before

	Target	Clone	Isotype	Supplier	Working	pH	PBS
Chr	CD45	30-F11	Rt IgG_{2b}	eBioscience	5 µg/mL	High	PBS
	Ki67	16A8	Rt IgG_{2a}	BioLegend	5 µg/mL	High	PBS
	Cleaved	N/A	Rb Poly	Cell Signalling	1/150	Low	TBS
IMC	N/A	eB149/10H5	Rt IgG_{2b}	eBioscience	*Assay Dependent*		
	N/A	RTK2758	Rt IgG_{2a}	BioLegend	*Assay Dependent*		

Table 2.3 Murine staining antibodies (formalin-fixed tissue); Chr, Chromogenic.

dehydrating through three 99% v/v alcohol solutions and xylene (as described in 2.2.2) and then cover slipped using DPX mounting medium (CellPath, UK).

2.2.2.2 Chromogenic staining

Following dewaxing and rehydration, endogenous peroxidase activity was quenched by incubation with H_2O_2 (0.3% v/v in methanol, 10 minutes) and then washed in buffer consisting of either PBS or TBS and Tween 20 (0.1% v/v) depending on antibody (see Table 2.3). Antigen retrieval was performed in either high or low pH buffer (Vector Laboratories) dependent on antibody (see Table 2.3). Slides were placed in pre-warmed buffer and heated for 30 minutes then left to cool (10 minutes). The buffer was further cooled by the steady addition of cold water until the temperature of the slides had reached RT.

All further incubation steps were carried out in a humidified chamber with gentle agitation at RT unless otherwise stated. Sections were encircled with wax pen before washing in buffer. Non-specific binding was blocked by incubation with casein (1x diluted in buffer, 30 minutes; Vector Laboratories). Sections were then incubated with primary antibody diluted in casein blocking solution (1 hour). Slides were washed thoroughly in buffer before addition of Immpress HRP-conjugated secondary antibody (Vector Laboratories) corresponding to source of primary antibody (30 minutes). Following washing twice with buffer, staining was visualised with DAB peroxidase (Vector Laboratories) as per manufacturer's instructions until the desired stain was achieved. IMCs were run simultaneously to control for non-specific binding. Sections were washed with buffer before counterstaining with Mayer's haematoxylin (30 seconds; Pioneer Research Chemicals Ltd.). Finally sections were washed with water before dehydration and mounting with DPX as in 2.2.2.1.

2.2.3 Immunocytochemistry

For immunocytochemistry, cells were first fixed with paraformaldehyde in PBS (PFA; 4% v/v, 20 minutes, RT; Sigma-Aldrich) before washing thoroughly with PBS. Immunofluorescent staining was carried out as in 2.2.1.2.

If fluorescent actin staining was also required cells were incubated with Phalloidin-633 (5 units, Life Technologies, UK) in PBS-T supplemented with bovine serum albumin

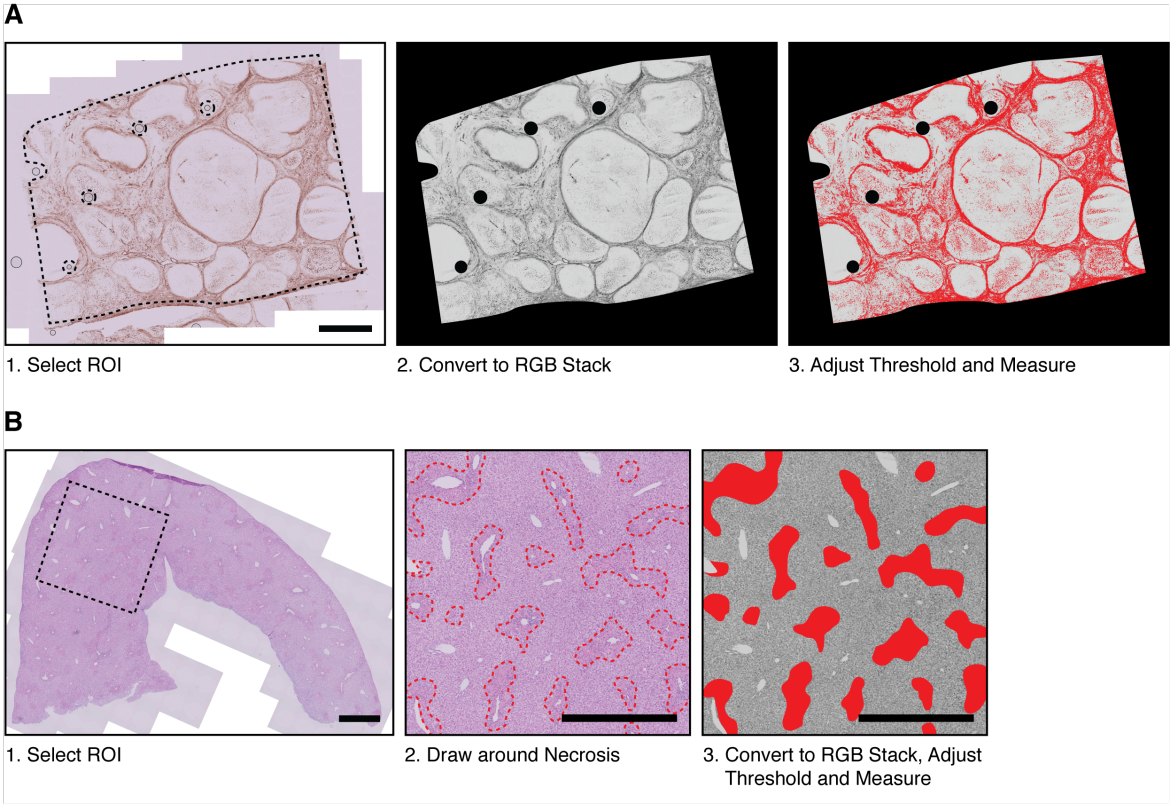


Figure 2.1 ImageJ quantification of immunohistochemical staining. Images taken using the Axio Scan.Z1 were exported at 50% total size to allow for a manageable file size. (**A**) The region of interest (ROI) selected in ImageJ. The selection was drawn ~100 μm of the tissue edge and any breaks or tissue damage. The image was then separate into red, green and blue channels of which the blue channel was chosen. Thresholding was manually adjusted until the majority of stained regions were highlighted in multiple samples. All subsequent tissue was analysed using consistent threshold settings. The highlighted area was then measured and expressed as a proportion of tissue area. (**B**) The extent of liver necrosis was quantified by first selecting a 2.5 mm x 2.5 mm square tissue section, ensuring selection was at least 100 μm from the tissue edge and any damage. The necrotic areas were then manually highlighted using Photoshop CS6 as shown in panel 2, filled and quantified via the method described above.

(BSA; 1% $^{v}/_{v}$, 20 minutes RT, protected from light) between incubation with secondary antibody and addition of mountant.

2.2.4 Visualisation and quantification

Fluorescently stained sections were imaged by confocal microscopy on either an Axiovert 200 or LSM 780 both running Zen v2.3 (blue edition) software (Carl Zeiss).

All chromogenically stained slides were imaged in full on an Axio Scan.Z1 at 10x magnification running Zen v2.3 (blue edition) software (Carl Zeiss, UK).

2.2.4.1 Quantification of stained area

Quantification of stained area was carried out using ImageJ software v1.7 (NIH, USA) and can be seen in Figure 2.1A. First, the image was exported at 50% total size in order to achieve a manageable file size. The region of interest was selected by drawing ~100 μm of tissue edge and excluding any breaks or damage created during sectioning or staining. The image was then converted to an RGB stack and threshold adjusted on the blue channel. Threshold setting remained constant throughout each staining protocol. The threshold area was then measured and expressed as a proportion of total tissue area.

2.2.4.2 Quantification of liver necrosis

First, the image was exported at 50% total size in order to achieve a manageable file size. The region of interest was selected by randomly choosing a 2.5 mm x 2.5 mm square of the tissue section (Figure 2.1B). One restriction was that the square must be >100 μm from the tissue edge or any major damage created during sectioning or staining before proceeding. The necrotic area was then drawn around in Photoshop CS6 (Adobe, USA) and filled in black. The image was then assessed using ImageJ as in 2.2.4.1.

2.3 Polymerase chain reaction

2.3.1 RNA extraction and cDNA synthesis

Total RNA was extracted and purified using an RNeasy mini kit (QIAGEN, DE) as per the manufacturer's instructions including on-column treatment with DNase I (QIAGEN). Snap frozen tissue (~30 mg) was first mechanically digested with a MACS M-tube in a gentleMACS dissociator (Miltenyi Biotec). Frozen cell pellets (5-10 x 10^7 cells) were resuspended in buffer RLT and passed 10 times through a 20G needle. Following

purification, RNA was stored at -80°C for cDNA synthesis.

Prior to synthesis, RNA was thawed and the concentration and purity of the sample determined using a Nanophotometer (Implen, Germany). An absorbance ratio 260/280 of >1.8 was used as an indication of a pure mRNA sample. cDNA was synthesised (typically from 1 μg mRNA) by reverse transcription (RT) using a high-capacity cDNA reverse transcription kit (Thermo Fisher Scientific) including RNase inhibitor and random

Target species	Target Gene	Primer/Probe ID	Supplier
Human	*AOC3*	Hs00186647_m1	Thermo Fisher Scientific
Human	*GAPDH*	Hs99999905_m1	Thermo Fisher Scientific
Human	*18S*	Hs99999901_s1	Thermo Fisher Scientific
Human	*SRSF4*	Hs00194538_m1	Thermo Fisher Scientific
Murine	*Aoc3*	Mm00839624_m1	Thermo Fisher Scientific
Murine	*Gapdh*	Mm99999916_g1	Thermo Fisher Scientific

Table 2.4 Primers for qPCR analysis

primers as per the manufacturer's instructions. The quantity of RNA was kept constant between test groups. Appropriate negative controls were run simultaneously (no template and no reverse transcriptase).

2.3.2 Quantitative polymerase chain reaction

Murine and human VAP-1 gene expression (*Aoc3*/*AOC3*) was analysed by quantitative polymerase chain reaction (qPCR) using TaqMan fluorogenic 5' FAM-labelled probes and specific primers mixes (Table 2.4) and TaqMan gene

expression master mix (Thermo Fisher Scientific) according to the manufacturer's instructions. Reactions were conducted in a total volume of 10 µL in a MicroAmp optical 384-well reaction plate (Thermo Fisher Scientific). A LightCycler 480 II (Roche Life Science, UK) was used with cycling conditions:

95°C for 15 seconds, 60°C for 1 minute and 72°C for 1 second. Negative controls from RT-PCR and additional no RNA negative controls were run simultaneously. Threshold cycle (Ct) values of *AOC3*/*Aoc3* were normalised to relative housekeeping gene(s), calculated according to the $2^{-\Delta\Delta Ct}$ method (Livak and Schmittgen, 2001) . In the case of human liver, *AOC3* was normalised to both *18S* and *SRSF4* to account for variability across the diseases. Each sample was run in triplicate.

2.4 VAP-1 amine oxidase activity assay

2.4.1 Sample preparation

For analysis of VAP-1 activity within human or murine liver, snap frozen tissue (~60 mg) was first mechanically digested with a MACS M-tube in a gentleMACS dissociator (Miltenyi Biotec) along with 1.2 mL lysis buffer consisting of sterile PBS (Sigma-Aldrich) and Triton X-100 (0.2% $^{v}/_{v}$; Sigma Aldrich). Sample was recovered by centrifugation (10^3 *x g*, 2 minutes) before incubation on ice with agitation (20 minutes). Suspension was then centrifuged at 10^4 *x g* for 10 minutes, supernatant removed and centrifuged again to ensure pelleting of debris. The protein concentration of the supernatant was determined by bicinchoninic acid (BCA) assay (Thermo Fisher Scientific) as per manufacturer's instructions using BSA (Sigma-Aldrich) diluted in lysis buffer as standard. Colorimetric analysis was performed using a Synergy HT multi-mode microplate reader (Biotek, UK) running Gen5 software version 2.0 and cells were diluted to 2 mg/mL and stored at -20°C until required.

For analysis of VAP-1 activity within HSEC or neutrophils, frozen cell pellets (5-10 *x* 10^7 cells) were resuspended in lysis buffer and passed 10 times through a 20G needle. Cells were then incubated on ice, centrifuged and supernatant collected and diluted to 2 mg/mL as above.

HSEC and neutrophil-conditioned media was simply aspirated and subsequently centrifuged at 10^4 *x g* for 10 minutes to pellet debris. Concentration and storage conditions were as described above.

Clone	Isotype	Reported Species reactivity	Supplier
TK8-14	Mm IgG_{2a}	Human	eBioscience
174-5	Mm IgG_1	Human	Hycult Biotech
TK8-18	Mm IgG_{2a}	Human	*
EB07582	Gt Polyclonal	Human / Rat / Mouse	Everest Biotech
7-106	Rt IgG_{2b}	Mouse	**
7-88	Rt IgG_{2b}	Mouse	Hycult Biotech
393112	Mm IgG_{2b}	Human / 50% Mouse	R&D Systems

Table 2.5 VAP-1 antibodies for immunosorbence.
** A kind gift from BioTie Therapies (Turku, Finland)*
*** A kind gift from Prof. Sirpa Jalkanen (Turku, Finland)*

2.4.2 Immunosorbance

Nunc MaxiSorp (Sigma-Aldrich) high affinity protein-binding plates were coated with the anti-VAP-1 antibody (100 µL, 5 µg/mL, unless otherwise stated) in carbonate coating buffer, pH 9.5, consisting of sodium hydrogen carbonate (0.1 M; Sigma-Aldrich) and sodium carbonate (0.034 M; Sigma-Aldrich) in sterile water, and sealed overnight at 4°C. VAP-1 antibodies can be found in. The plate was brought to RT and washed thoroughly with wash buffer consisting of sterile PBS (Sigma-Aldrich) and Tween 20 (0.05% $^{v}/_{v}$; Sigma Aldrich). Non-specific binding was blocked with BSA (1% $^{v}/_{v}$ in sterile PBS, 1 hour). Plate was washed again and samples (2 mg/mL) were added and incubated overnight at 4°C. All samples were used on day of preparation to ensure reliability. Plates were then washed three times, allowing one minute between washes to increase stringency.

2.4.3 Amplex UltraRed Assay

VAP-1 catalysis of primary amine oxidation results in H_2O_2 production, the rate of this production as detected by the formation of a fluorescent product from Amplex UltraRed forms the basis of this assay.

Wells containing captured VAP-1 were incubated with benzylamine (1 mM; Sigma-Aldrich), Amplex UltraRed (40 µM; Thermo Fisher Scientific) and horseradish peroxidase (HRP; 2 U/mL; Sigma-Aldrich) in sterile PBS (Sigma-Aldrich) to a total volume of 200 µL. Kinetic analysis of fluorescence from peroxidised Amplex UltraRed was measured using a Synergy HT multi-mode microplate reader (Biotek) running Gen5 software version 2.0. Readings at excitation 530 nm and emission 590 nm were taken every 5 minutes for one hour. An H_2O_2 (Sigma-Aldrich) standard curve (0.2 – 3.0 µM) was prepared and run simultaneously and used to calculate enzyme activity (Figure 2.2).

Semicarbazide (Sigma-Aldrich), LJP-1586 (a gift from Sirpa Jalkanen, Turku, Finland), caffeine (Sigma-Aldrich) and theobromine (Sigma-Aldrich) were added to reaction mixture when necessary.

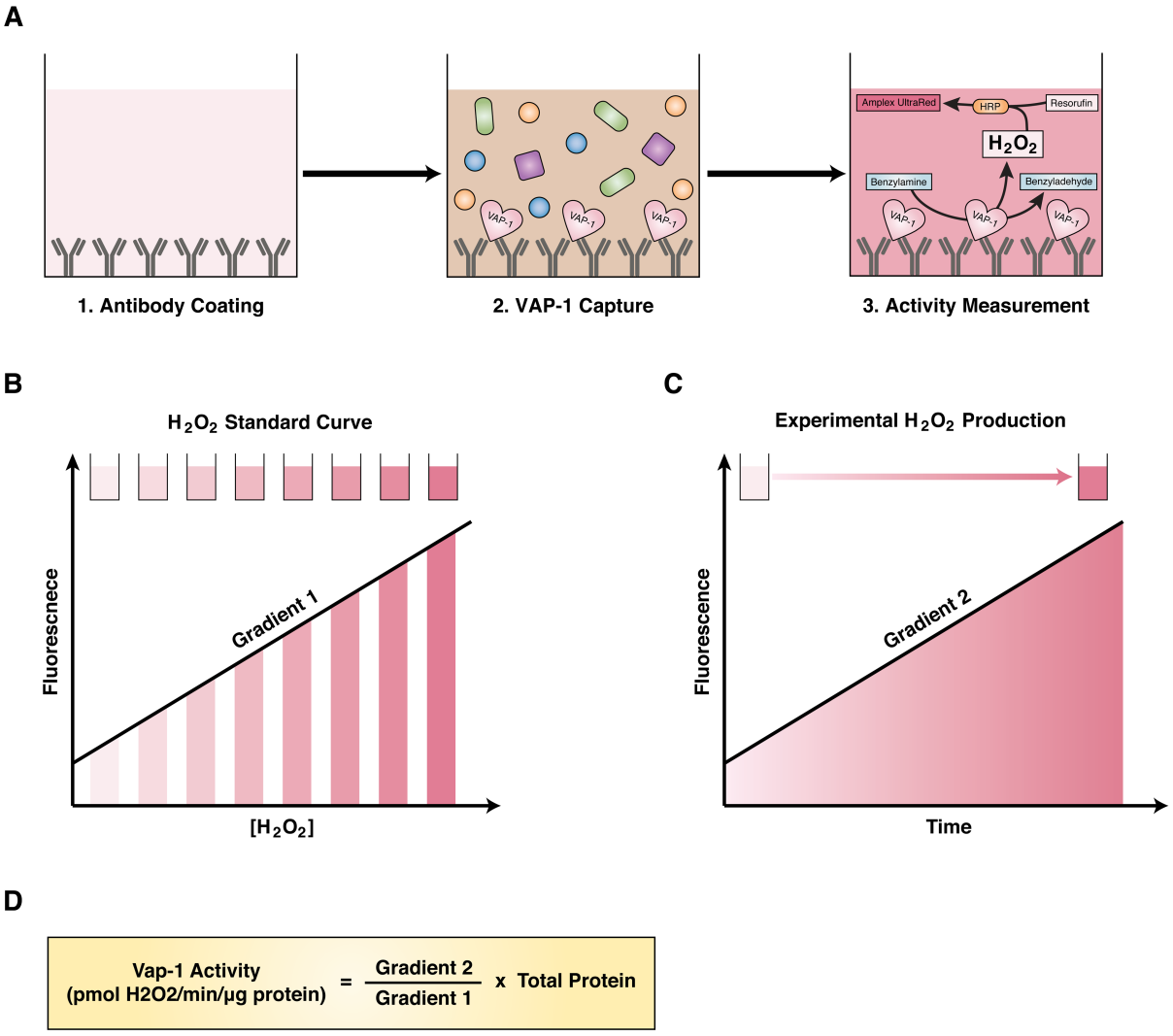


Figure 2.2 Antibody-captured VAP-1 amine oxidase activity assay. (**A**) High affinity protein-binding plates were first coated with anti-VAP-1 antibody and blocked with BSA before being incubated with the VAP-1 containing mixture. The plate was left overnight to ensure all VAP-1 was captured from solution and washed thoroughly to remove any non-specifically bound compounds. VAP-1 activity was then measured in the presence of benzylamine using the Amplex UltraRed assay. Briefly, the H_2O_2 peroxide produced during the VAP-1-catalysed reaction enabled the conversion of colourless resorufin to the fluorescent Amplex UltraRed compound by horseradish peroxidase (HRP). Kinetic analysis of fluorescence was measured by taking readings at excitation 530 nm and emission 590 nm every 5 minutes for one hour. (**B**) An H_2O_2 standard curve (0.2 – 3.0 µM) was run simultaneously and compared to (**C**) experimental data by the equation shown in (**D**). VAP-1 activity was defined as the gradient of the experimental curve divided by the gradient of the standard curve multiplied by the amount of total protein.

2.4.4 Cell-based assay

Cell-based amine oxidase assays were carried out by first seeding HSEC into a 96-well plate. A confluent T75 was trypsinised, the cells washed with PBS and resuspended in complete HSEC medium (10 mL; as in 2.1.2). Cells were added to each desired well (100 μL) and allowed to adhere (24 hours, 37°C, 5% CO_2). Media was then aspirated and reaction carried out as in 2.4.3. VAP-1 activity was determined by calculating the difference in activity ± semicarbazide (500 μM, Sigma-Aldrich).

2.5 Western blotting

2.5.1 Sample preparation

For analysis of protein presence within human or murine liver, snap frozen tissue (~80 mg) was first added to lysis buffer (1.6 mL) consisting of CellLytic MT (Sigma-Aldrich) supplemented with cOmpleteULTRA protease inhibitor cocktail (Sigma-Aldrich). Tissue was then processed as in 2.4.1 but with incubation on ice for one hour.

Similarly, frozen cell pellets (5-10 x 10^7 cells) were resuspended in lysis buffer consisting of CellLyticM (Sigma-Aldrich) supplemented with cOmpleteULTRA and processed as in 2.4.1 but with incubation on ice for one hour.

2.5.2 Sodium dodecyl sulphate polyacrylamide gel electrophoresis

Protein samples were separated by sodium dodecyl sulphate polyacrylamide gel electrophoresis (SDS-PAGE) using the Mini-PROTEAN tetra cell system (Bio-Rad Laboratories, UK). Protein samples were first diluted in 5x loading buffer consisting of PBS containing Trizma base (200 mM, pH 6.8; Sigma-Aldrich), glycerol (20% $^{w}/_{v}$; Sigma-Aldrich), sodium dodecyl sulphate (SDS; 10% $^{w}/_{v}$; Sigma-Aldrich), bromophenol blue (0.05% $^{w}/_{v}$; Sigma-Aldrich) and β-mercaptoethanol (βME; 10 mM; Sigma-Aldrich), boiled (100°C, 2 minutes) then centrifuged at 10^4 x g to pellet any insoluble matter.

Gels of 1.5 mm thickness were prepared using a discontinuous system of a stacking gel on top of resolving gel. Gels consisted of Protogel 30% degassed acrylamide (Geneflow) and water to the desired proportions and prepared in ProtoGel resolving buffer (Geneflow) or ProtoGel stacking buffer (Geneflow). The gels were polymerised with

ammonium persulphate (APS; 2.6 mM; Sigma-Aldrich) and N,N,N',N'-tetramethylethylenediamine (TEMED; 400 mM; Sigma-Aldrich). The completed gel was loaded into the apparatus and Tris-Glycine-SDS-PAGE buffer added (Geneflow). Samples were then loaded (20 µL) along with PageRuler prestained protein ladder (5 µL; Thermo Fisher Scientific) and electrophoresed at 200 V until the dye front reached the bottom of the gel.

2.5.3 Western blot transfer

The resolving gel was then transferred onto nitrocellulose (Geneflow) pre-soaked in Tris-Glycine Electro-Blotting Buffer (Geneflow). This was then sandwiched between filter paper (Bio-Rad) and foam pads (also soaked in buffer) within a cassette as part of the Mini Trans-Blot cell (Bio-Rad). The cell was then filled with transfer buffer along with an ice pack and current of 100 V applied (1 hour) with agitation via magnetic stirrer. The transfer cell was then dismantled and effective transfer evaluated by immersion of membrane in Ponceau S solution (5 minutes; Sigma-Aldrich). The membrane was then washed thoroughly with water and transferred to the development stage.

2.5.4 Membrane development

Following protein transfer, membranes were blocked in milk solution consisting of PBS or TBS (dependent on antibody, see Table 2.6) supplemented with Tween 20 (0.02% $^{v}/_{v}$) and non-fat dry milk powder (5% $^{w}/_{v}$; Marvel, UK) with constant agitation (1 hour, RT). Primary antibody solution was then diluted (Table 2.6) in fresh milk solution and membrane incubated with constant agitation (overnight, 4°C). Membrane was thoroughly washed with PBS or TBS containing Tween 20 (0.02% $^{v}/_{v}$, PBS-T) and incubated with relevant HRP-conjugated secondary antibody diluted in milk solution

	Target	Clone	Isotype	Supplier	Working conc	TBS or PBS
Human	VAP-1	393112	Mm IgG_{2b}	R&D Systems	1 µg/mL	PBS
	β-Actin	BA3R	Mm IgG_{2b}	Thermo Fisher	1 µg/mL	PBS
Mouse	Cleaved PARP	E51	Rb IgG	Abcam	0.4 µg/mL	TBS
	PCNA	D3H8P	Rb IgG	Cell Signaling	1/1000	PBS
	β-Actin	BA3R	Mm IgG_{2b}	Thermo Fisher	1 µg/mL	PBS

Table 2.6 Western Blot primary antibodies

Source	Target	Target Isotype	Conjugate	Supplier	Working
Goat	Mouse	IgG	HRP	Dako	1/5000
Goat	Rabbit	IgG	HRP	Dako	1/5000

Table 2.7 Western Blot secondary antibodies

shown in Table 2.7 (1 hour, RT). The membrane was then washed thoroughly with PBS-T (30 minutes) and Supersignal West Pico chemiluminescent substrate (Thermo Fisher Scientific) was then added as per manufacturer's instructions (5 minutes). Chemiluminescence was detected using the PXi 6 Touch gel imaging system (Syngene, UK).

Membranes were then incubated with Restore Western blot stripping buffer (30 minutes, RT; Thermo Fisher Scientific), blocked with milk solution (1 hour, RT) and reprobed with housekeeping antibodies as per the method described above.

2.5.5 Quantification

Semi-quantitative analysis of band densities was carried out using ImageJ software v1.7 (NIH) using the inbuilt gel image analysis functionality. Band densities were normalised to housekeeping protein expression.

2.6 Flow-based Adhesion Assays

2.6.1 Assay preparation

2.6.1.1 Cell-based assay preparation

Prior to conducting the flow-based adhesion assay, a six-channel µ-Slide $VI^{0.4}$ (ibidi, DE) was first coated with RTC (220 µg/mL in PBS, 40 µL per channel, 37°C, 1 hour; Sigma-Aldrich). The slide was then washed thoroughly with PBS and seeded with HSEC: a fully confluent T75 was trypsinised, washed and resuspended in 2 mL complete HSEC media (2.1.2) and 70 µL of cell suspension was then added to each channel. Cells were allowed to adhere (3 hours, 37°C, 5% CO_2) on a slide rack to ensure full gaseous exchange. Media was then changed and cells incubated overnight (37°C, 5% CO_2). HSEC

were then stimulated with tumour necrosis factor-α (TNFα, Peprotech, UK) in complete HSEC media unless otherwise stated (10 ng/mL, 24 hours) before flow assay. During media changes, channels were never emptied fully so as not to damage or detach HSEC.

2.6.1.2 Recombinant protein-based assay preparation

Six-channel µ-Slides VI$^{0.4}$ were coated with recombinant VAP-1 (rVAP-1; R&D Systems, UK) or recombinant VCAM-1 (rVCAM-1; R&D Systems) suspended in sterile PBS (10 µg/mL unless otherwise stated, 37°C, 2 hours). A control lane was simultaneously treated with BSA (0.5% $^{v}/_{v}$, Sigma-Aldrich). For conditions where lanes were first treated with rVAP-1 and then rVCAM-1, the slide was washed with sterile PBS after one hour of incubation before the second protein as added for the remaining hour. After two hours, all lanes were washed thoroughly with sterile PBS before blocking with BSA in sterile PBS (1% $^{v}/_{v}$, 30 minutes, 37°C). Slides were then washed thoroughly with sterile PBS before use in the assay.

2.6.1.3 Leukocyte preparation

PBLs or isolated leukocyte subsets were isolated as in 2.1.4 and always used within 12 hours of venesection. Prior to the flow-based adhesion assay cells were pelleted by centrifugation, viability confirmed by Trypan-blue exclusion before being resuspended at 10^6 cells/mL in flow assay medium consisting of human endothelial SFM supplemented with BSA (0.5% $^{v}/_{v}$). Cells were allowed to rest prior to conducting the assay (20 minutes, 37°C, 5% CO_2).

2.6.2 Conducting the flow-based adhesion assay

The experimental apparatus were assembled as shown in Figure 2.3 and described in (Shetty et al., 2014). Briefly, a chamber was warmed to 37°C and the µ-Slide VI placed on the stage of an inverted microscope housed within the chamber. A syringe pump was then connected to one port of the slide via silicone tubing (1 mm internal diameter; Thermo Fisher Scientific), ensuring both syringe and tubing contained liquid in order to normalise pressure. The barrels of two syringes (5 mL and 10 mL) with plungers removed were then connected to an electronic solenoid valve via silicone tubing. The

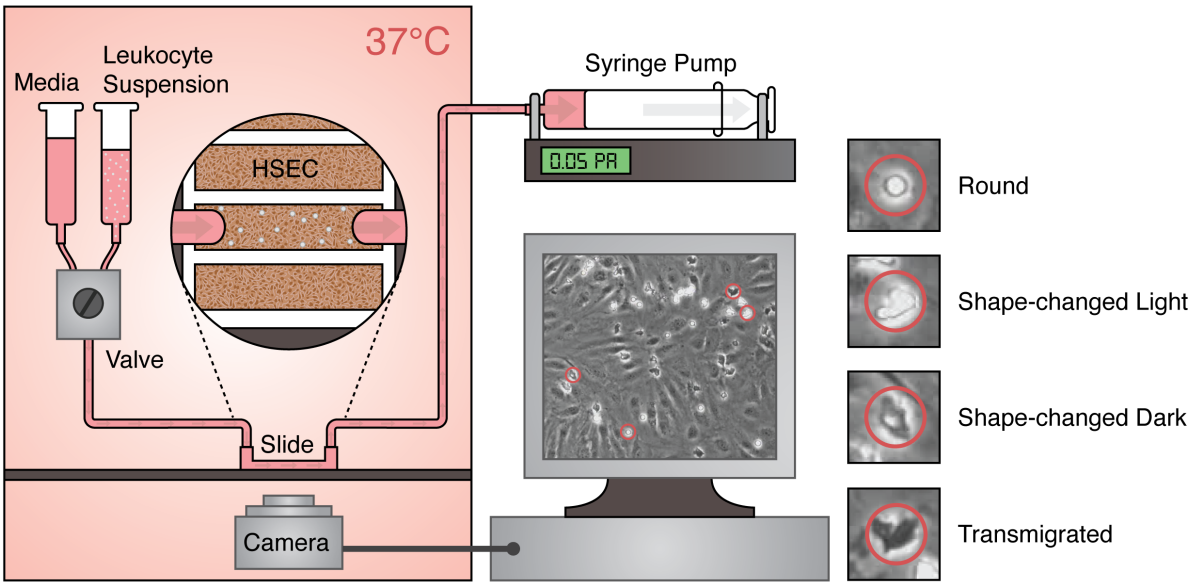


Figure 2.3 Flow-based adhesion assay. A slide flow assay microslide containing endothelial cells or recombinant protein was placed on an inverted microscope (not shown) within a transparent chamber maintained at 37°C to improve cell viability. The suspension of leukocyte was drawn through the slide via a syringe-driven pump at a consistent shear stress similar to that within the hepatic sinusoids (0.05 Pa, 0.5 dyne/cm^2). An electronic solenoid valve allowed for the switching between the cell suspension or media with no dead space. The assay was recorded in real-time by a phase-contrast camera connected to a computer. Still images were taken of the video and cells manually designated as round, shape-changed light, shape-change dark or transmigrated due to their appearance.

valve was in turn connected to the second port of the µ-Slide VI via silicone tubing (1 mm internal diameter; Thermo Fisher Scientific). One syringe contained flow assay medium (10 mL; as in 2.6.1.3) and the other the leukocyte suspension (5 mL). The leukocytes were then perfused through the chamber at a shear stress similar to that within the hepatic sinusoids (0.05 Pa, 0.5 dyne/cm^2, 5 minutes) followed by a wash phase of flow assay media (3 minutes). Phase contrast video was then recorded during the proceeding 2 minutes at 10x magnification using WinTV software v7 (Hauppauge, USA) ensuring capture of 10 – 12 fields of view along the median of the chamber for offline analysis. Sequential fields were recorded in the opposite direction to flow in order to eliminate counting cells twice should they detach and reattach during the recording phase.

Treatment of HSEC monolayer or recombinant protein with inhibitor/antibody was conducted sequentially during assay to ensure exact treatment times. This was always for 20 minutes (37°C) in flow assay media at concentration in Table 2.8 unless otherwise stated. All experimental parameters and controls were run at the same time to increase comparability.

Treatment	Clone	Isotype	Supplier	Working Conc
Anti-VAP-1	TK8-14	Mm IgG_{2a}	eBioscience	10 µg/mL
Anti-VCAM-1	BBA5	Mm IgG_1	R&D Systems	10 µg/mL
IMC	N/A	Mm IgG_{2a}	Dako	10 µg/mL
IMC	N/A	Mm IgG_1	Dako	10 µg/mL
Semicarbazide	N/A	N/A	Sigma-Aldrich	500 µM
LJP-1586	N/A	N/A	*	500 nM
Caffeine	N/A	N/A	Sigma-Aldrich	200 µM

Table 2.8 Flow assay treatments
** A kind gift from Prof. Sirpa Jalkanen (Turku, Finland)*

2.6.3 Analysis

Offline analysis was conducted by taking still images of fields of view and counting cells using the cell counter plugin for ImageJ software v1.7 (NIH). Cells were assigned either rolling, round, shape-changed light, shape-changed dark or transmigrated as in Figure 2.3. The mean number of cells in each group was calculated throughout the fields of view and normalised to the image area per million cells perfused by the following equation:

$$N = \frac{n}{c \times f \times t \times A}$$

N is the normalised number of cells

n is the mean number of cells per field

c is the concentration of cells perfused (cells/mL)

f is flow rate (mL/minute)

t is the bolus time (minute)

A is the area of view (mm^2)

The number of total adherent cells was the sum of all rolling, round, shape-changed and transmigrated cells. The percentage of cell in each group was also calculated as a proportion of the total number of cells.

Vector	Amount per transfection	Supplier
pmaxGFP	2 ng	Lonza
GFP-VAP-1^{WT}	5 ng	Generon*
GFP-VAP-1^{Y471F}	5 ng	Generon*
pLifeAct-Ruby	5 ng	Generon*

Table 2.9 Transfection plasmids
**Initial constructs were prepared by Dr Weston (Birmingham, UK).*

2.7 Endothelial cell transfection

2.7.1 Electroporation

HSEC and HEK293 cells were transiently transfected with plasmid DNA via electroporation using a Nucleofector II/2b (Lonza, UK). Plasmids were prepared in-house by Dr Christopher Weston (Birmingham, UK) and based on the pcDNA6.2 TOPO plasmid provided with the Vivid colors pcDNA 6.2/N–EmGFP-GW/TOPO mammalian expression vector kit (Thermo Fisher).

Cells were trypsinised and reseeded into clean flasks 24 hours prior to transfection procedure to increase transfection efficiency. On the day of transfection, cells were again trypsinised then washed in PBS before 10^6 cells per reaction were transferred into 15mL Falcon tubes. Cells were then centrifuged (90 *x g*, 10 minutes) before resuspending in Basic Endothelial Nucleofection solution (100 µL per reaction; Lonza). Cells were then aliquoted into separate Eppendorf tubes containing DNA for transfection (see Table 2.9). Cell-DNA suspension was then transferred into a single use Amaxa aluminium electrode cuvette (Lonza), placed into the Nucleofector II/2b and transfected using the settings described in chapter 4.2.1.5. Cells were then transferred into complete cell media using single use pipettes (Lonza) and centrifuged (8 *x* 10^3 *x g*, 5 minutes). Transfected cells were resuspended in relevant complete media for further downstream use.

2.7.2 Transfection efficiency analysis

Transfected cells were seeded into T25 flasks and incubated for 24 hours to allow for plasmid expression (37˚C, 5% CO_2). Cells were then trypsinised, washed in PBS and analysed by flow cytometry in order to determine the transfection efficiency of different

Nucleofector II/2b programs. Transfected HSEC and stably transfected LX2 cells that had been blasticidin-selected (5×10^5) were resuspended in MACS buffer as in 2.1.4.1 (10^6 cells/mL) and incubated with VAP-1-APC or mouse IgG_{2a}-APC (5 µL; both conjugated in-house by Dr Christopher Weston, Birmingham, UK) in 5 mL polypropylene round-bottomed Falcon tubes and protected from light with gentle agitation (100 µL total, 30 minutes, 4˚C; BD Biosciences). A SYTOX Blue dead cell stain (Thermo Fisher Scientific) was also included as a viability marker as per manufacturer's instructions. Cells were then washed thoroughly in MACS buffer and resuspended for analysis using a CyAn ADP 9-colour flow cytometer (Beckman Coulter Inc.). Data analysis was performed using FlowJo v10.2 (FlowJo LLC).

2.7.3 Time-course imaging

HSEC transfected with GFP-VAP-1^{WT}, GFP-VAP-1^{Y471F} or positive control (pmaxGFP) were resuspended in complete HSEC media (10^5 cells/mL) and seeded into an RTC-coated 24-well plate in quadruplicate (1 mL/well). Real-time image capture was then performed using a Cell-IQ system (Chip-man Technologies, Finland). Inter-well spaces were filled with water to decrease evaporation. Cells were incubated for 72 hours with phase and GFP-channel images taken of each well every 30 minutes (37˚C, 5% CO_2 in air). Images were then analysed offline using ImageJ software v1.7 (NIH) to determine total fluorescent area as per the threshold method in 2.2.4.1.

2.7.4 Measurement of VAP-1 amine oxidase activity

VAP-1 amine oxidase activity of transfected HSEC and HEK293 cells was determined by the cell-based Amplex UltraRed assay as described in 2.4.4. Transfected and untransfected cells were seeded into two RTC-coated 48-well plate (5×10^4 cells/well) in complete media (125 µL). Cells were allowed to adhere (4 hours, 37˚C, 5% CO_2) before changing media (with or without TNFα (10 ng/mL)). After 24 hours (37˚C, 5% CO_2) cell-conditioned media was removed from one plate for antibody capture assay as previously described and cell-based Amplex UltraRed assay performed on remaining cells. Remaining plate was left for an additional 24 hours before undergoing the same process.

2.7.5 Flow-based adhesion assay

2.7.5.1 Standard flow-based adhesion assay

HSEC were first transfected with GFP-VAP-1^{WT}, GFP-VAP-1^{Y471F} or a positive control (pLifeAct-Ruby). LifeAct was chosen in this instance due to its small size (17 amino acids) and evidence to suggest that it does not interfere with cellular processes (Riedl et al., 2008). Following transfection, cells were resuspended in complete HSEC media (140 µL) and seeded into two channels of an RTC-coated six-channel µ-Slide $VI^{0.4}$ (70 µL; ibidi). Cells were allowed time to adhere to the plastic (2 hours, 37˚C, 5% CO_2) before changing to media supplemented with TNFα (10 ng/mL, 24 hours, 37˚C, 5% CO_2). Flow assay was then carried out as previously described in 2.6.2.

2.7.5.2 Confocal flow-based adhesion assay

Following transfection, cells were resuspended in HSEC media (150 µL) and seeded into an RTC-coated µ-Slide $I^{0.6}$ (ibidi). Cells were allowed time to adhere to the plastic (2 hours, 37˚C, 5% CO_2) before changing to media supplemented with TNFα (10 ng/mL, 24 hours, 37˚C, 5% CO_2). Freshly isolated leukocytes were incubated with CellTracker Red CMTPX dye (Thermo Fisher Scientific) as per the manufacturer's instructions and rested prior to use in assay (20 minutes, 37˚C, 5% CO_2). For some experiments nuclei were visualised by incubation with DRAQ5 fluorescent probe solution (Thermo Fisher Scientific) as per the manufacturer's instructions immediately before use.

Flow-based adhesion assay was carried out using the ibidi Pump System (ibidi). In brief, the µ-Slide I was connected to Fluidic unit (ibidi) containing two tubes: one filled with flow assay media and the other with cells suspended in flow assay media (10^6 cells/mL). The Fluidic unit was in turn connected to the ibidi Pump, controlled via a laptop running PumpControl software (ibidi). The experiment (excluding laptop) was assembled within a heat-controlled chamber around the stage of an LSM 780 confocal microscope (Carl Zeiss). Once the system had been degassed, the cells were flowed in a continuous and unidirectional manner (0.05 Pa, 5 minutes). Interactions between leukocytes and HSEC were observed over the course of 3 hours with constant recirculation of cells. Timecourses were carried out using Zen v2.3 (blue edition) software (Carl Zeiss).

2.8 Neutrophil function assays

2.8.1 Neutrophil VAP-1 amine oxidase activity assay

To evaluate intracellular and extracellular VAP-1 amine oxidase activity, neutrophils were suspended in neutrophil media (1 x 10^7 cells/mL) consisting of phenol red-free RPMI-1640 (Thermo Fisher Scientific) supplemented with L-glutamine (2 mM), penicillin (100 U/mL) and streptomycin (100 µg/mL). Cells were then stimulated with human Interferon-γ (IFNγ; Peprotech) or TNFα (10 ng/mL, 3 hours, 37˚C and 5% CO_2). Cells were then centrifuged (450 *x g*, 10 minutes) and conditioned media aspirated and retained. The neutrophils were lysed as described in 2.4.4.1 and VAP-1 amine oxidase activity was determined from lysed cells and conditioned media as described in 2.4.4.

2.8.1.1 Neutrophil and endothelial cell amine oxidase activity assay

HSEC were seeded into an RTC-coated 24-well plate with 4% of a confluent T-75 flask (approximately 10^5 cells) in each well in complete HSEC media and allowed to adhere (24 hours, 37˚C and 5% CO_2). HSEC were then incubated with either media alone, LPS (100 ng/mL) or TNFα (10 ng/mL, 24 hours, 37˚C and 5% CO_2). Freshly isolated neutrophils (2.1.4.5) suspended in neutrophil media were then also stimulated with the same treatments (1 hour, 37˚C and 5% CO_2). Both neutrophils and HSEC were then washed thoroughly before adding neutrophils to the HSEC suspended in 500 µL neutrophil media (10^6 cells/well, 3 hours, 37˚C and 5% CO_2). Cell-conditioned media was then aspirated and centrifuged to pellet cells and debris (10^4 *x g*, 10 minutes). VAP-1 amine oxidase activity was then determined by antibody capture and Amplex UltraRed assay as described in 2.4.4. VAP-1 activity was determined as the difference in activity ± LJP-1586 (500 nM).

2.8.2 Fluorometric analysis of cell-free DNA

Neutrophils were isolated as described in 2.1.4.5 and resuspended in phenol red-free neutrophil media (2 x 10^6 cells/mL) as in 2.8.1. Stimulation treatments (Table 2.10) were prepared in a clear flat bottomed 96-well plate at twice the desired final concentration in neutrophil media (100 µL) in duplicate. Neutrophils were then added and plate was incubated to allow stimulation to occur (3 hours, 37˚C and 5% CO_2). Supernatant was

Treatment	Abbreviation	working conc.	Supplier
Phorbol myristate acetate	PMA	25 nM	Sigma-Aldrich
Lipopolysaccharide	LPS	100 ng/mL	Sigma-Aldrich
Human Tumour necrosis factor-α	TNFα	10 ng/mL	Peprotech
Mouse Tumour necrosis factor-α	TNFα	10 ng/mL	Peprotech
Recombinant human VAP-1	rVAP-1	500 ng/mL	R&D Systems
Recombinant mouse VAP-1	rVAP-1	500 ng/mL	R&D Systems
LJP-1586	N/A	500 nM	*
Benzylamine	N/A	100 nM	Sigma-Aldrich
Histamine	N/A	100 nM	Sigma-Aldrich
Cysteamine	N/A	100 nM	Sigma-Aldrich

Table 2.10 Neutrophil experimental reagents
** A kind gift from Prof. Sirpa Jalkanen (Turku, Finland)*

then aspirated, transferred to a sterile Eppendorf tube and centrifuged to pellet cellular debris (2.2 x 10^3 x g, 10 minutes). Neutrophil supernatant was then transferred to a second clear flat-bottomed 96-well plate (100 µL) and incubated with SYTOX Green nucleic acid stain (1 µM, 10 minutes, RT; Thermo Fisher Scientific). Fluorescence from labelled cell-free DNA (cfDNA) was then quantified using a Synergy HT multi-mode microplate reader (Biotek) running Gen5 software version 2.0 with excitation and emission set at 485 and 528 nm, respectively. For calibration a λ-DNA (Thermo Fisher Scientific) standard curve was prepared and run simultaneously (0 – 1000 ng).

2.8.3 Visualization of ex vivo neutrophil extracellular traps

In order to visualize neutrophil extracellular traps (NETs) neutrophils were isolated as described in 2.1.4.5 and resuspended in neutrophil media (1 x 10^6 cells/mL). Autoclaved glass coverslips (12 mm; VWR) were then placed into the bottom of wells of a 24-well plate. Neutrophil suspension was then gently added to the surface of each coverslip (2 x 10^5 cells/well) and allowed to adhere (20 minutes, 37˚C and 5% CO_2). Stimulation treatments (Table 2.10) were then added at twice the desired final concentration in neutrophil media (200 µL) and incubated (3 hours, 37˚C and 5% CO_2). Media was then gently aspirated, taking care not to disturb NETs and cells fixed by the addition of PFA (4% $^{v}/_{v}$, 400 µL, 20 minutes). Coverslips were carefully washed with PBS to remove any residual PFA.

Target	Clone	Isotype	Supplier	Working conc
VAP-1	TK8-14	Mm IgG_{2a}	eBioscience	10 µg/mL
Histone H3	polyclonal	Rb IgG	abcam	1 µg/mL
Neutrophil	polyclonal	Rb IgG	abcam	10 µg/mL
IMC	X0943	Mm IgG_{2a}	Dako	*Assay Dependent*
IMC	polyclonal	Rb IgG	Dako	*Assay Dependent*

Table 2.11 Neutrophil primary antibodies

2.8.3.1 Neutrophil extracellular trap immunocytochemistry

All steps in the fluorescent staining of NETs were conducted by upturning the coverslip onto a drop of each liquid. First, coverslips were carefully removed from the 24-well plate and permeabilised with Triton X-100 in PBS (0.3% $^{v}/_{v}$, 5 minutes). The coverslips were washed in PBS before incubation in SYTOX Green nucleic acid stain (1 µM, 20 minutes, RT) diluted in PBS within a humidified chamber protected from light. All remaining steps were carried out protected from light. Coverslips were washed in PBS and blocked with goat serum (10% $^{v}/_{v}$) in PBS-T consisting of PBS and Triton X-100 (0.1% $^{v}/_{v}$; 10 minutes) before incubation with primary antibody (Table 2.11) diluted in PBS-T supplemented with goat serum (2% $^{v}/_{v}$; 1 hour, RT) in a humidified chamber. Sections were washed in PBS and incubated with fluorescently conjugated secondary antibodies (Table 2.12) in PBS-T supplemented with goat serum (2% $^{v}/_{v}$, 1 hour, RT). Finally, sections were washed with PBS and mounted with Shandon Immu-Mount. Coverslips were stored at 4°C protected from light until visualisation using an LSM 780 running Zen v2.3 (blue edition) software (Carl Zeiss).

2.8.4 Neutrophil H_2O_2-production assay

Neutrophils were isolated as described in 2.1.4.5 and resuspended in phenol red-free neutrophil media (2 x 10^6 cells/mL) as in 2.8.1. Stimulation treatments (Table 2.10) in neutrophil media (100 µL) at quadruple the desired final concentration were added in duplicate to a clear flat bottomed 96-well plate. Neutrophils were then added (10^5 cells/well) along with phenol red-free RPMI-1640 (100 µL) containing Amplex UltraRed (40 µM) and HRP (2 U/mL). Kinetic analysis of fluorescence was measured using a Synergy HT multi-mode microplate reader (Biotek) running Gen5 software version 2.0. Readings at excitation 530 nm and emission 590 nm were taken every 2.5 minutes for 30

Source	Target	Target Isotype	Fluorophore	Supplier	Working conc
Goat	Mouse	IgG_{2a}	AlexaFluor 546	Thermo Fisher	4 µg/mL
Goat	Mouse	IgG_{2a}	AlexaFluor 488	Thermo Fisher	4 µg/mL

Table 2.12 Neutrophil secondary antibodies

minutes. An H_2O_2 standard curve (0.2 – 3.0 µM) was prepared and run simultaneously and used to calculate enzyme activity.

2.9 Murine Tissue

2.9.1 Animal husbandry

C57BL/6 mice expressing VAP-1 with a point mutation at Tyrosine-471 to a phenylalanine residue ($SSAO^{KO}$) were a kind gift from Biotie Therapies and are described in (Weston et al., 2015). Age- and sex-matched WT animals were supplied by a contract breeder (Charles River, UK). Animals were housed in accordance with established care protocols at the University of Birmingham. All procedures using mice underwent ethical review and were performed in accordance with the Animals (Scientific Procedures) Act of 1986 under Home Office Project License 70/7933.

2.9.2 Acute carbon tetrachloride-induced liver injury

2.9.2.1 Wild-type time course experiment

Groups of five 7-week-old male WT C57BL/6 mice were administered either a single dose of carbon tetrachloride (CCl_4; 1 mL/kg; Sigma-Aldrich) prepared in mineral oil (Sigma-Aldrich) or mineral oil alone via intraperitoneal (IP) infusion. 48 or 72 hours later blood was then drawn via cardiac puncture under isofluorane anaesthesia before sacrifice by cervical dislocation.

2.9.2.2 Wild-type vs. SSAO^{KO} experiment

Groups of seven 8-12-week old age-matched WT C57BL/6 or SSAO^{KO} mice were administered with carbon tetrachloride (CCl_4; 1 mL/kg) prepared in mineral oil (Sigma-Aldrich) via intraperitoneal (IP) infusion. 48 hours later blood was then drawn via cardiac puncture under isofluorane anaesthesia before sacrifice by cervical dislocation.

2.9.3 Organ retrieval and preparation

Following sacrifice, the liver was perfused with PBS (10 mL) by intra-cardiac injection following disconnection of the hepatic portal vein, to remove peripheral blood. The liver was then harvested and divided into lobes. The lower ¼ of the left lateral lobe was placed in neutral-buffered formalin (4% $^{v}/_{v}$; CellPath) for future paraffin embedding for immunohistochemistry. The remainder of the left lateral lobe and left medial lobe were placed in RPMI-1640 for leukocyte extraction. The right medial lobe was divided equally in half and snap-frozen in liquid nitrogen for VAP-1 enzyme assay analysis. The remaining right lateral and caudate lobes were also snap frozen for Western blot analysis.

2.9.4 Liver function tests

Blood taken via cardiac puncture (0.7 – 1.0 mL) prior to sacrifice was allowed to clot (1 hour, RT) before serum was aspirated and centrifuged (10^4 *x g*; 10 minutes) to sediment erythrocytes. Serum was again carefully aspirated into 13 mm false-bottomed sample tubes and assayed for alanine aminotransferase (ALT) and aspartate aminotransferase (AST) as markers of hepatocyte damage at Birmingham Women's Hospital clinical biochemistry department.

2.9.5 Leukocyte extraction from murine liver

Intrahepatic leukocytes were isolated from the left medial lobe and ¾ of the left lateral lobe on the same day as sacrifice. The lobes were first weighed and then mechanically digested using a MACS C-tube in a gentleMACS dissociator (Miltenyi Biotec) in a volume of RPMI-1640 (3 mL). The homogenate was then passed through a 70 μm strainer (BD Falcon, UK) and cells pelleted by centrifugation (600 *x g*, 5 minutes). The cell pellet was resuspended in RPMI-1640, layered onto an Optiprep gradient (1.09

g/mL; Axis-Shield, UK) and centrifuged (1000 *x g*, 25 minutes, without brake). Leukocytes were removed from between the Optiprep-RPMI interface, washed with RPMI-1640 and resuspended in MACS buffer consisting of PBS containing FCS (2% $^{v}/_{v}$; Invitrogen) and EDTA (1 mM; Sigma-Aldrich).

2.9.5.1 Flow cytometric analysis of isolated leukocytes

Isolated hepatic leukocytes were characterised using multi-colour flow cytometry as outlined in 2.1.4.6. In brief, the cells were first resuspended in MACS buffer (2 mL) and incubated with a LIVE/DEAD Fixable near-IR dead cell stain (Thermo Fisher Scientific) as per manufacturer's instructions. They were then washed thoroughly with MACS buffer before dividing into thirds for incubation with either the lymphoid or myeloid cell panels (Table 2.13) of fluorochrome-labelled antibodies. In the case of myeloid panels, cells were incubated with antibodies against Ly6G, Ly6C or Gr-1 prior to incubation with F4/80 antibody to alleviate any steric hindrance effects (Rose et al., 2012). The remaining third were either incubated with control antibodies (IMC or fluorescent minus one (FMO)) or CD45-conjugated antibodies used for compensation. Following incubation with antibodies (30 minutes, 4˚C, in the dark with agitation) cells were washed thoroughly with MACS buffer before fixation with Cytofix fixation buffer (BD Biosciences) as per the manufacturer's instructions. Cells were then stored at 4˚C and protected from light for subsequent analysis using a CyAn ADP 9-colour flow cytometer (Beckman Coulter Inc., USA). Data analysis was performed using Summit software v4.3 (Dako) or FlowJo v10.2 (FlowJo LLC). Cells were analysed within 48 hours of fixation to ensure cell viability and reliability of data. Cell number was determined with the use of AccuCheck counting beads (Thermo Fisher Scientific) as per the manufacturer's instructions.

2.9.6 Isolation of murine neutrophils from compact bone

10-20-week old WT C57BL/6 or SSAO^{KO} mice were sacrificed by cervical dislocation. The legs were amputated and all soft tissue removed from around the femur and tibia. The bones were sterilised with IMS and stored on ice while remaining animals were processed.

Panel	Target	Clone	Isotype	Fluorophore	Supplier	Working conc
Compensation	CD45	30-F11	Rt IgG_{2b}	PB	BioLegend	10 µg/mL
	CD45	30-F11	Rt IgG_{2b}	BV510	BioLegend	10 µg/mL
	CD45	30-F11	Rt IgG_{2b}	FITC	BioLegend	10 µg/mL
	CD45	30-F11	Rt IgG_{2b}	PE	BioLegend	10 µg/mL
	CD45	30-F11	Rt IgG_{2b}	PerCPCy5.5	BioLegend	10 µg/mL
	CD45	30-F11	Rt IgG_{2b}	APC	BioLegend	10 µg/mL
Lymphoid panel	CD19	6D5	Rt IgG_{2a}	PB	BioLegend	0.25 µg/mL
	IMC	RTK2758	Rt IgG_{2a}	PB	BioLegend	0.25 µg/mL
	CD3	17A2	Rt IgG_{2b}	BV510	BioLegend	10 µg/mL
	IMC	RTK4530	Rt IgG_{2b}	BV510	BioLegend	10 µg/mL
	CD49b	DX5	Rt IgM	FITC	BioLegend	25 µg/mL
	IMC	RTK2118	Rt IgM	FITC	BioLegend	25 µg/mL
	CD4	RM4-5	Rt IgG_{2a}	PE	BioLegend	0.1 µg/mL
	IMC	RTK2758	Rt IgG_{2a}	PE	BioLegend	0.1 µg/mL
	CD45	30-F11	Rt IgG_{2b}	PerCPCy5.5	BioLegend	0.1 µg/mL
	IMC	RTK4530	Rt IgG_{2b}	PerCPCy5.5	BioLegend	0.1 µg/mL
	CD8a	53-6.7	Rt IgG_{2a}	APC	BioLegend	0.1 µg/mL
	IMC	RTK2758	Rt IgG_{2a}	APC	BioLegend	0.1 µg/mL
	IMC	RTK2758	Rt IgG_{2a}	FITC	BioLegend	25 µg/mL
	CD11b	M1/70	Rt IgG_{2b}	PE	BioLegend	10 µg/mL
	IMC	RTK4530	Rt IgG_{2b}	PE	BioLegend	10 µg/mL

Table 2.13 Mouse liver flow cytometry antibodies – compensation and lymphoid panel

Under a standard class II microflow safety cabinet the bone ends were removed with scissors and the marrow flushed out with sterile PBS containing EDTA (PBS-E; 0.1% $^{w}/_{v}$; 5 mL/bone; Sigma-Aldrich) using a 25G needle. A single cell suspension was then formed by repeated aspiration with a 19G needle and subsequently passed through a 70 µm strainer (BD Falcon). Cells were then washed thoroughly and resuspended in PBS-E (1 mL). Ice-cold water (4 mL, 30 seconds) was added to lyse erythrocytes followed by equilibration of isotonicity with 4x PBS (2 mL) and removal of debris by passing through a 70 µm strainer. The suspension was then layered onto an equal parts 72/64/52% $^{w}/_{v}$ Percoll gradient and centrifuged (30 minutes, 10^3 *x g*, no brake). Neutrophils were aspirated from the 72/64% boundary and washed thoroughly with PBS before resuspending in neutrophil media consisting of RPMI-1640 supplemented with L-glutamine (2 mM), penicillin (100 U/mL) and streptomycin (100 µg/mL) for further downstream use.

Panel	Target	Clone	Isotype	Fluorophore	Supplier	Working conc
Myeloid panel 1	CD3	17A2	Rt IgG_{2b}	BV510	BioLegend	10 µg/mL
	IMC	RTK4530	Rt IgG_{2b}	BV510	BioLegend	10 µg/mL
	CD11b	M1/70	Rt IgG_{2b}	FITC	BioLegend	2.5 µg/mL
	IMC	RTK4530	Rt IgG_{2b}	FITC	BioLegend	2.5 µg/mL
	Gr-1	RB6-8C5	Rt IgG_{2b}	PE	BioLegend	1 µg/mL
	IMC	RTK4530	Rt IgG_{2b}	PE	BioLegend	1 µg/mL
	CD45	30-F11	Rt IgG_{2b}	PerCPCy5.5	BioLegend	0.1 µg/mL
	IMC	RTK4530	Rt IgG_{2b}	PerCPCy5.5	BioLegend	0.1 µg/mL
	F4/80	BM8	Rt IgG_{2a}	APC	BioLegend	2 µg/mL
	IMC	RTK2758	Rt IgG_{2a}	APC	BioLegend	2 µg/mL
Myeloid panel 2	CD3	17A2	Rt IgG_{2b}	BV421	BioLegend	10 µg/mL
	IMC	RTK4530	Rt IgG_{2b}	BV421	BioLegend	10 µg/mL
	CD19	6D5	Rt IgG_{2a}	BV421	BioLegend	10 µg/mL
	IMC	RTK2758	Rt IgG_{2a}	BV421	BioLegend	10 µg/mL
	CD49b	DX5	Rt IgM	PB	BioLegend	25 µg/mL
	IMC	RTK2118	Rt IgM	PB	BioLegend	25 µg/mL
	Ly6G	1A8	Rt IgG_{2a}	BV510	BioLegend	10 µg/mL
	IMC	RTK2758	Rt IgG_{2a}	BV510	BioLegend	10 µg/mL
	F4/80	BM8	Rt IgG_{2a}	FITC	BioLegend	25 µg/mL
	IMC	RTK2758	Rt IgG_{2a}	FITC	BioLegend	25 µg/mL
	CD11b	M1/70	Rt IgG_{2b}	PE	BioLegend	10 µg/mL
	IMC	RTK4530	Rt IgG_{2b}	PE	BioLegend	10 µg/mL
	CD45	30-F11	Rt IgG_{2b}	PerCPCy5.5	BioLegend	10 µg/mL
	IMC	RTK4530	Rt IgG_{2b}	PerCPCy5.5	BioLegend	10 µg/mL
	Ly6C	HK1.4	Rt IgG_{2c}	APC	BioLegend	10 µg/mL
	IMC	RTK4174	Rt IgG_{2c}	APC	BioLegend	10 µg/mL

Table 2.14 Mouse liver flow cytometry antibodies – myeloid panels

2.10 Statistical Analysis

The distribution of continuous variables was assessed via the Kolmogorov-Smirnov method. Non-normal data are presented using the median and interquartile range (IQR) unless otherwise specified. The Mann-Whitney (MW) test was conducted when comparing between two independent groups, and analysis of variance through Kruskal-Wallis (KW) test with Dunn's post-hoc correction for multiple-groups. Normally distributed data are presented using the mean and standard deviation (SD) unless

otherwise stated. Statistically significant differences between related groups were tested using *t* test. Two-way ANOVA with Holm-Sidak post-hoc correction was used for analysis of two variables. Measures of statistical dependence between two continuous variables were conducted using Spearman's rank correlation coefficient (*r*) and slopes assessed to be non-zero by linear regression analysis.

3

VAP-1 EXPRESSION, ACTIVITY AND LOCALISATION DURING HUMAN LIVER DISEASE

3.1 Introduction

VAP-1 expression has been recorded in almost all mammalian organs, however particularly high levels are exhibited on the surface of cells within highly vascularised tissue beds such as the lungs, heart, gut and adipose (Jaakkola et al., 2000). Here VAP-1 functions to mediate leukocyte recruitment from peripheral blood (Salmi and Jalkanen, 1992). Accordingly, elevated levels of VAP-1 have been associated with a range of inflammatory conditions, implicating the protein in a wide range of disease pathogeneses (Salmi et al., 1993). This observation has led to particular interest in its potential as a possible therapeutic target for treatment of inflammatory disorders ranging from

ulcerative colitis (Salter-Cid et al., 2005) to arthritis (Marttila-Ichihara et al., 2006; Tábi et al., 2013) and kidney fibrosis (Wong et al., 2014).

Although VAP-1 expression within the liver is comparably lower than other tissues, hepatic vascular endothelial cells, HSEC and HSCs are believed to constitutively express high levels (Lalor et al., 2002; McNab et al., 1996; Weston et al., 2015). Furthermore, VAP-1 expression is elevated during inflammatory liver disease (Trivedi et al., 2017; Kurkijärvi et al., 2000, 1998; McNab et al., 1996; Tuncer et al., 2013). In line with other vascular tissues, the elevated expression of VAP-1 within HSEC of the sinusoids appears to facilitate leukocyte migration into the liver from the circulation, thereby possibly underlying the disease mechanism (Edwards et al., 2005; Lalor et al., 2002, 2007; Shetty et al., 2011). Likewise expression of VAP-1 has been observed within the fibrotic scar in patients with NASH, indicating a potential additional role for VAP-1 in hepatic fibrogenesis (Hsia et al., 2016; Weston et al., 2015). VAP-1 may also play an aetiology-specific function, for example the altered expression of VAP-1 in steatotic liver disease has been linked to its role in glucose transport within adipocytes (Karim et al., 2014; Weston et al., 2015).

Despite these advances in our knowledge, there has been very little work conducted into the correlation of VAP-1 expression and disease progression and even fewer investigations examining how VAP-1 enzyme activity is altered in these conditions. It is therefore still unclear whether there is a correlation between the presence of VAP-1 and the aetiology or extent of liver disease. The true therapeutic value of VAP-1 may therefore be yet undiscovered.

In this chapter, hepatic VAP-1 is characterised across a range of liver diseases from those that mainly affect the parenchyma (ALD, NASH) or biliary tree (PBC, PSC), and encompass steatotic diseases, autoimmune diseases and acute NANB hepatitis. Specifically the expression, enzyme activity and sensitivity of VAP-1 to small molecule inhibitors are described in an attempt to determine whether certain liver diseases are more susceptible to disruption of VAP-1 function in a therapeutic setting.

3.2 Results

3.2.1 Characterisation of hepatic VAP-1

3.2.1.1 Hepatic VAP-1 localisation

Immunohistochemical analysis was used to determine the localisation of VAP-1 within the healthy human liver and to elucidate changes during cirrhosis. Pathological control tissue was taken from organs that were rejected from transplant and assessed for steatosis and inflammation by an independent pathologist. Normal tissue was designated as that with a score of 1 out of 5 in each of these categories, whereas steatotic normal (SNL) were graded between 2 and 4. Normal tissue sections exhibited VAP-1 expression across the parenchyma, confined primarily to vascular structures: sinusoids, portal vessels and central veins (A). Sinusoidal VAP-1 staining was most pronounced within centrilobular regions, with considerably lower periportal presence. Sinusoidal staining was also observed within the cirrhotic liver, however VAP-1 levels appeared to correlate with proximity to fibrotic lesions within these samples (Figure 3.1B). Sinusoidal VAP-1 staining was strongest within sinusoids at sites distal to these lesions. The most dramatic difference within cirrhotic samples was the particularly concentrated VAP-1 staining within the fibrotic scar itself, this was accompanied by VAP-1-positive neovessels within the lesion. Comparisons between different aetiologies of liver disease are described below in section 3.2.1.3.

3.2.1.2 Cell-specific VAP-1 expression

The cell-specific expression of hepatic VAP-1 was examined at protein level by confocal fluorescent immunohistochemistry. Human liver sections taken from normal or chronically diseased tissue were simultaneously probed with antibodies raised against VAP-1 and phenotypic cell markers for hepatocytes (Cytokeratin 18; CK18), cholangiocytes (Epithelial Cell Adhesion Molecule; EpCAM), endothelial cells (CD31) or stromal cells (α-smooth muscle actin; αSMA). Multicolour confocal microscopy revealed that VAP-1 did not colocalise with hepatocyte or cholangiocyte markers within the liver (Figure 3.2A and 3.2B) but was co-expressed on cells with CD31- or αSMA-positivity, indicative of endothelial and stromal cell expression, respectively (Figure 3.2C and 3.2D). VAP-1 gene expression (*AOC3*) was confirmed at the messenger RNA (mRNA) level in

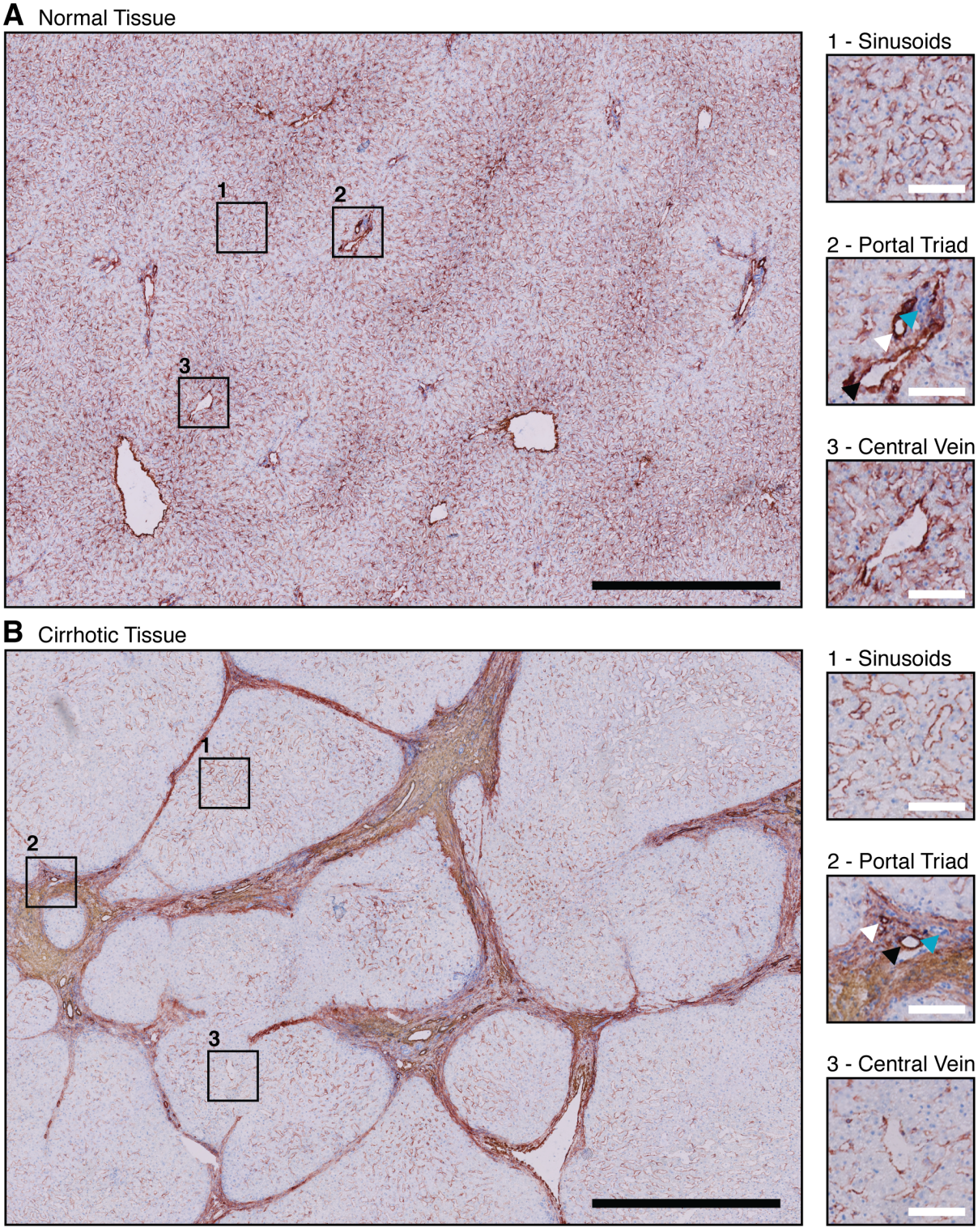


Figure 3.1 Localisation of hepatic VAP-1. Representative immunohistochemical staining of (**A**) Normal human liver tissue and (**B**) Chronically diseased human ALD liver tissue for the presence of VAP-1 (red) and counterstained with haemotoxylin (blue). VAP-1 was predominantly located within the sinusoids, central vein, hepatic artery (White arrowheads) and portal vein (black arrowheads). Bile ducts (blue arrowheads) were negative. Black boxes relate to magnified regions. Black bar: 1 mm, white bar: 100 µm.

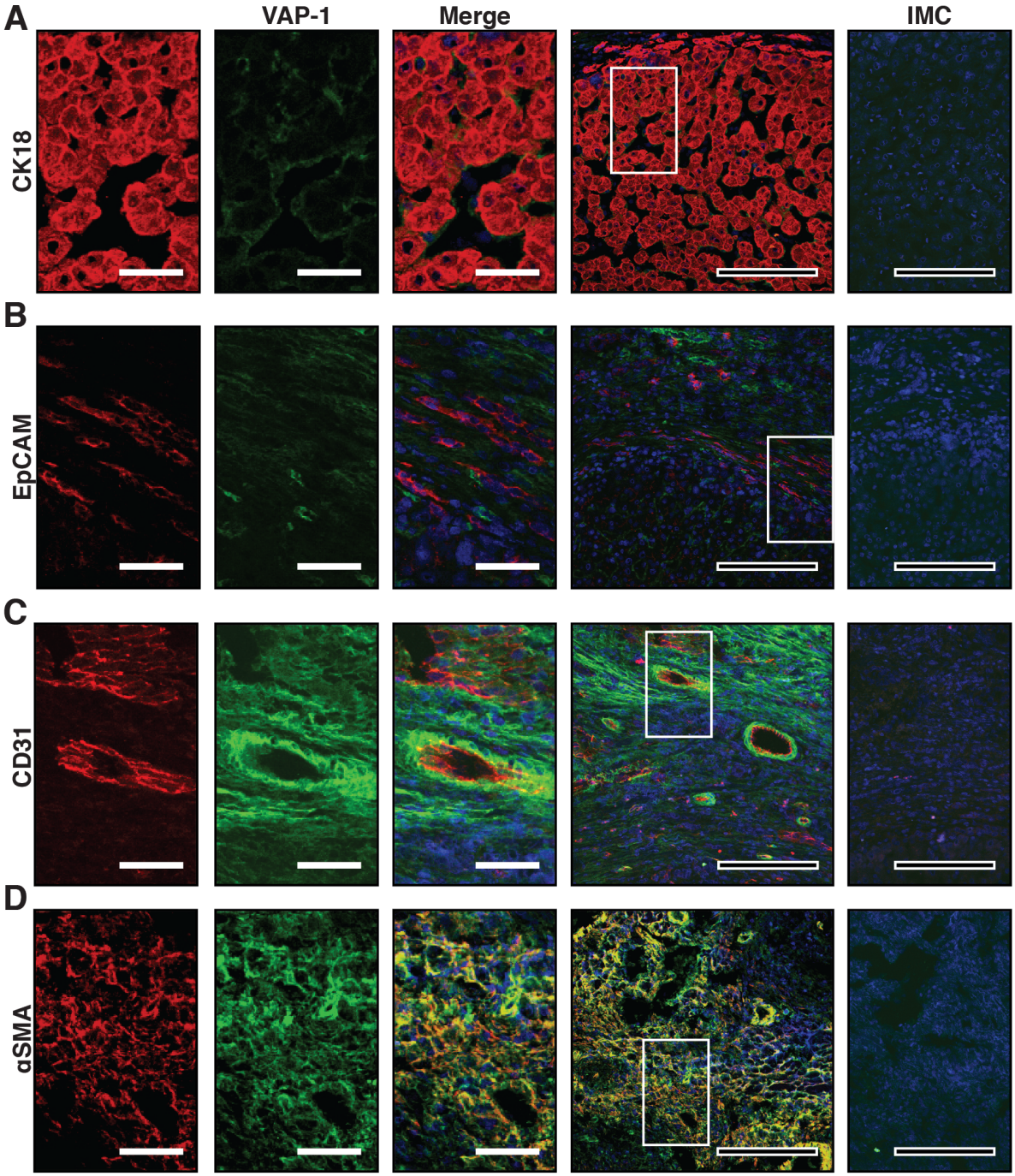


Figure 3.2 VAP-1 expression by hepatic cell types. Fluorescent immunohistochemical staining of chronically inflamed human liver tissue for VAP-1 (green) and cell-specific markers (red). VAP-1 was absent from hepatocytes (**A**, CK18) and cholangiocytes (**B**, EpCAM) but colocalised with endothelium (**C**, CD31) and fibroblasts (**D**, αSMA). White box indicates magnified region. IMC = Isotype matched control. White bar: 50 μm, black bar: 200 μm.

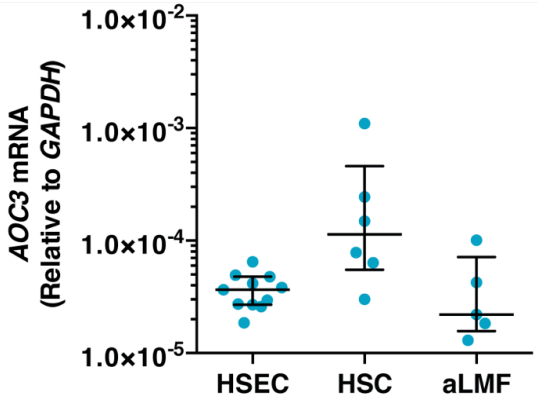


Figure 3.3 Expression of *AOC3* mRNA by hepatic cell types. qPCR analysis demonstrated *AOC3* mRNA was expressed by isolated human HSEC, HSCs and aLMFs. Data shown as median (IQR). Each dot represents separate preparations (n = 5-11).

primary HSEC and stromal cells isolated from both normal (HSC) and cirrhotic (activated liver myofibroblasts; aLMFs) human livers as seen in Figure 3.3.

3.2.1.3 VAP-1 localisation during liver disease

To determine changes in VAP-1 localisation during specific liver diseases, a cohort of human tissue samples were analysed by immunohistochemistry including normal, chronic steatotic and autoimmune diseases and acute NANB hepatitis. Hepatic VAP-1 localisation was similar between each of the examined aetiologies (taking into consideration structural pathophysiological differences): VAP-1 was present within the sinusoids and blood vasculature (in particular the central vein) but absent from bile ducts (Figure 3.4). VAP-1 staining was also highly concentrated throughout all fibrotic lesions. Despite structural differences and extent of fibrosis, the total VAP-1-positive area was broadly similar between normal, chronic and acutely diseased liver sections (Figure 3.5A and 3.5B).

3.2.1.4 *AOC3* expression during liver disease

Following immunohistochemical analysis, *AOC3* mRNA was assayed in the same liver samples by qPCR analysis to determine differences in VAP-1 gene expression. Expression was normalised to two housekeeping genes, *18S* and *SRSF4*, to take account of any changes in expression between disease states.

These were chosen as genes that exhibit the lowest modification in hepatic expression during the disease state (Boujedidi et al., 2012). Tissue from normal and steatotic

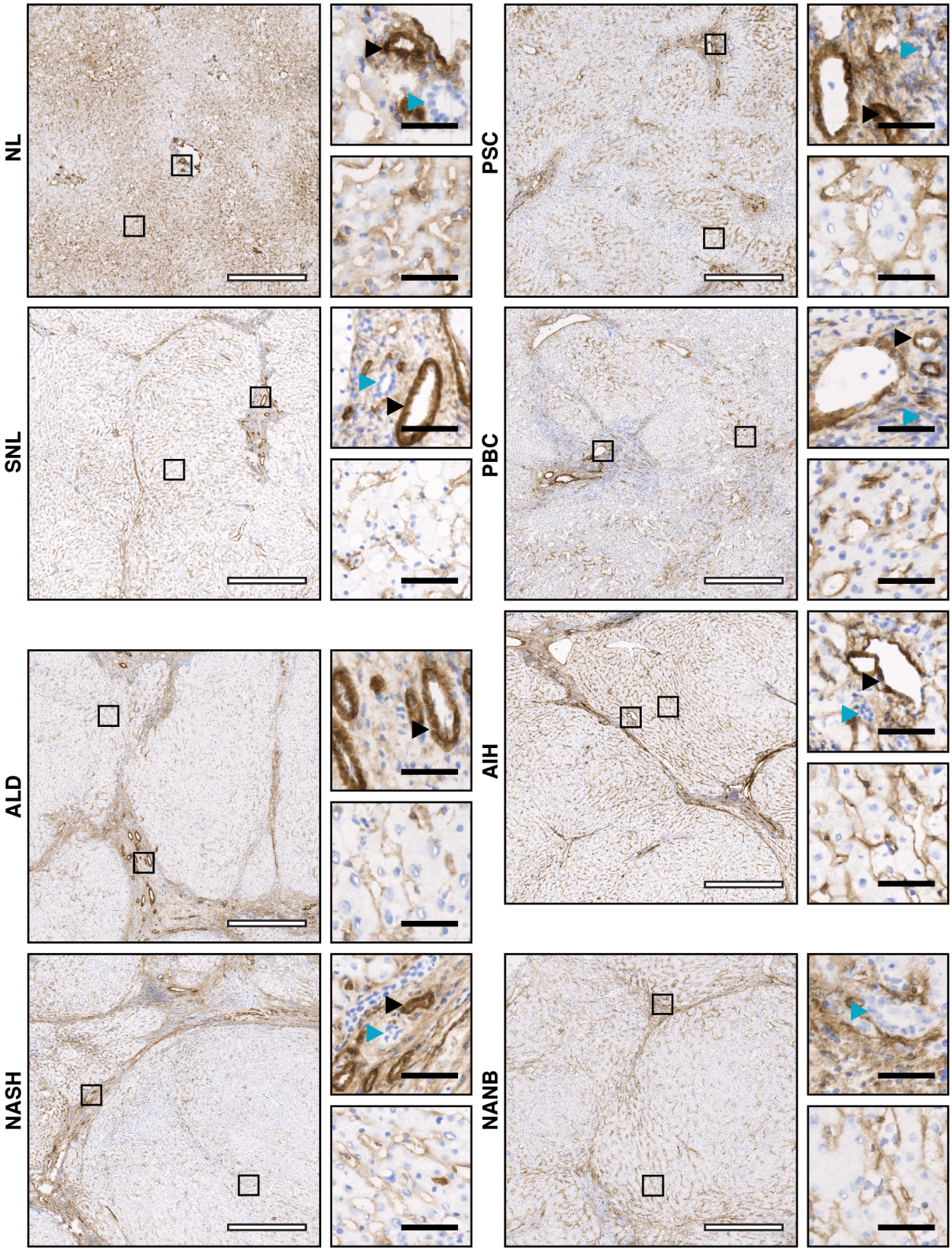


Figure 3.4 Localisation of hepatic VAP-1 during disease. Representative immunohistochemical staining of Normal and diseased human liver tissue for the presence of VAP-1 (brown) and counterstained with haemotoxylin (blue). VAP-1 localisation was broadly similar between the diseases: predominantly located within the sinusoids, central vein, hepatic artery and portal vein while Bile ducts (blue arrows) and hepatocytes were negative. Black arrow heads indicate positive blood vasculature. Black boxes relate to magnified regions. White bar: 500 µm, black bar: 50 µm.

normal livers exhibited comparably low levels of *AOC3* mRNA relative to the housekeeping genes: 8.34 x 10^{-5} (7.44 x 10^{-5} – 9.02 x 10^{-5}) and 6.63 x 10^{-5} (5.13 x 10^{-5} - 6.90 x 10^{-5}), respectively (Figure 3.5C). Expression within diseased livers was considerably broader ranging but exhibited an overall trend for higher expression. Average ratios for disease aetiologies lay within two distinct groups: ALD, PSC and PBC; and NASH, AIH and NANB. The former median values were between 8.79 x 10^{-5} - 1.36 x 10^{-4} whereas the latter exhibited the highest expression between 1.85 x 10^{-4} - 2.73 x 10^{-4}. When data from all chronic disease samples were combined, *AOC3* expression was significantly higher than within normal tissue ($p \leq 0.05$; Figure 3.5D).

3.2.1.5 VAP-1 amine oxidase activity during liver disease

Hepatic VAP-1 enzymatic activity was also quantified within the patient cohort using a novel modified Amplex UltraRed assay. During this assay, H_2O_2 production was fluorometrically quantified over the course of one hour - by means of a well described coupled enzyme assay - and used as a surrogate for amine oxidase activity. VAP-1 in each sample of tissue lysate was first captured by an antibody that had been adsorbed onto a Maxisorp multiwell plate to exclude contributions from other hepatic amine oxidases. Anti-VAP-1 antibody clone TK8-18 was chosen for this purpose as it was the only clone available that both effectively captured VAP-1 from solution and did not have any discernable effect on its catalytic activity (Figure 3.6A). In order to determine the amount of TK8-18 required to capture VAP-1 from tissue samples, increasing concentrations of the antibody were used to capture 200 ng recombinant VAP-1 protein (equivalent to 1000 ng/mL), representing the approximate upper limit of soluble VAP-1 found in human serum (Weston et al., 2015). VAP-1 amine oxidase activity of the captured protein was then assessed by Amplex UltraRed assay using benzylamine as a substrate. Increasing the concentration of plate-bound TK8-18 led to a corresponding increase in VAP-1 activity (Figure 3.6B). The enzyme activity saturated at concentrations of TK8-18 higher than approximately 5 µg/mL, although the upper asymptote was not fully reached, suggesting effective capture of the whole sample. Recombinant VAP-1 was then titrated onto a capturing concentration of 5 µg/mL TK8-18 to ensure that the limit of linearity was not reached (Figure 3.6C). The assay exhibited linearity up to and including 500 ng protein (equivalent to 2500 ng/mL) and therefore

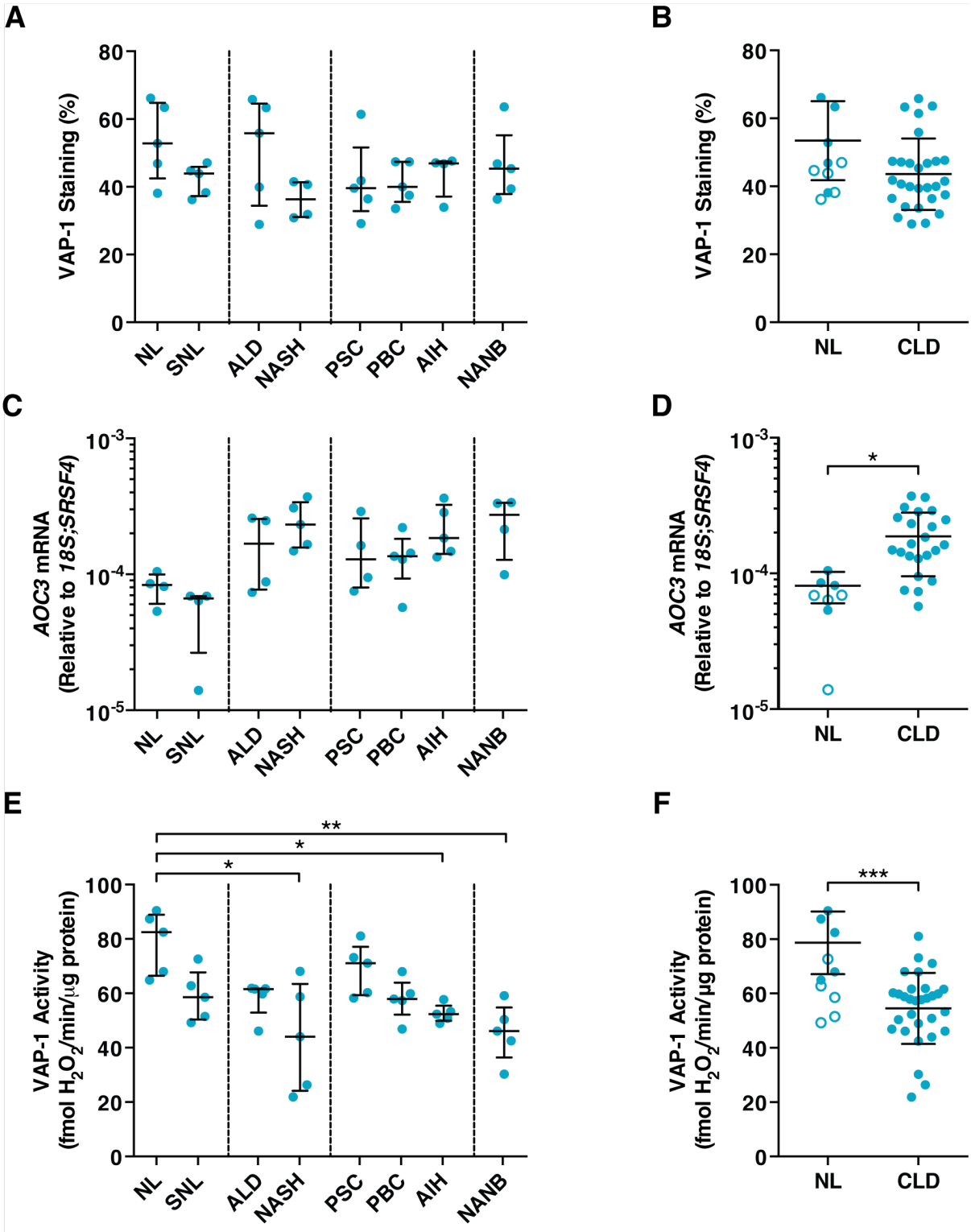


Figure 3.5 Expression of hepatic VAP-1 during liver disease. Human tissue samples were analysed for (**A** & **B**) VAP-1^{+} area following immunohistochemical tissue staining, (**C** & **D**) *AOC3* mRNA expression by qPCR analysis and (**E** & **F**) VAP-1 amine oxidase activity by antibody-capture Amplex UltraRed assay. Each horizontal pair represent the same data set (n = 4 - 5). Each point represents an individual patient sample. Circles indicate SNL samples shown for illustrative purposes only and were excluded from analysis. Data shown as median (IQR) and analysed by KW test with Dunn's post-hoc correction (**A**, **C** & **E**) and mean (SD) and analysed by t test (**B**, **D** & **F**). * $p \leq 0.05$, ** $p \leq 0.01$, *** $p \leq 0.001$.

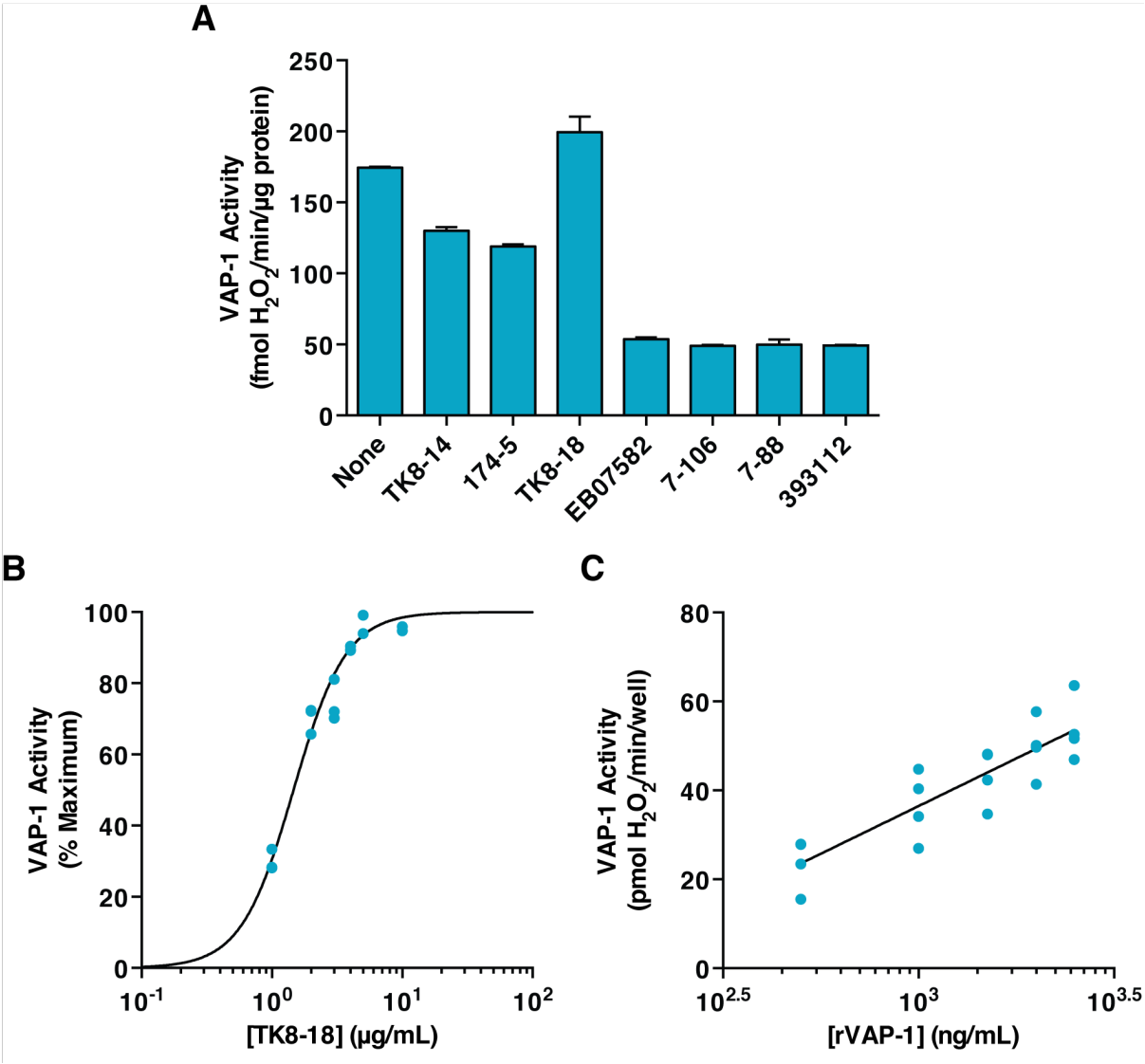


Figure 3.6 Optimisation of antibody-capture Amplex UltraRed Assay. (**A**) Amine oxidase activity of 1µg rVAP-1 either uncaptured or following capture with different antibody clones (n = 2). (**B**) Amine oxidase activity of 1 µg rVAP-1 following capture with increased concentration of TK8-18 antibody, normalised to maximum activity (n = 3). (**C**) Amine oxidase activity of rVAP-1 following capture with 5 µg/mL TK8-18 antibody (n = 4).

was considered effective up to at least these experimental concentrations of VAP-1 without saturation.

The highest median VAP-1 amine oxidase activity (82.5 fmol H_2O_2/min/µg protein (68.0 - 87.4 fmol H_2O_2/min/µg protein)) was detected within normal liver tissue (Figure 3.5E). The amine oxidase activity of samples derived from AIH and NANB livers were significantly lower than those for non-diseased samples (52.3 fmol H_2O_2/min/µg protein (50.9 – 53.29 fmol H_2O_2/min/µg protein), $p \leq 0.05$; and 46.1 fmol H_2O_2/min/µg protein

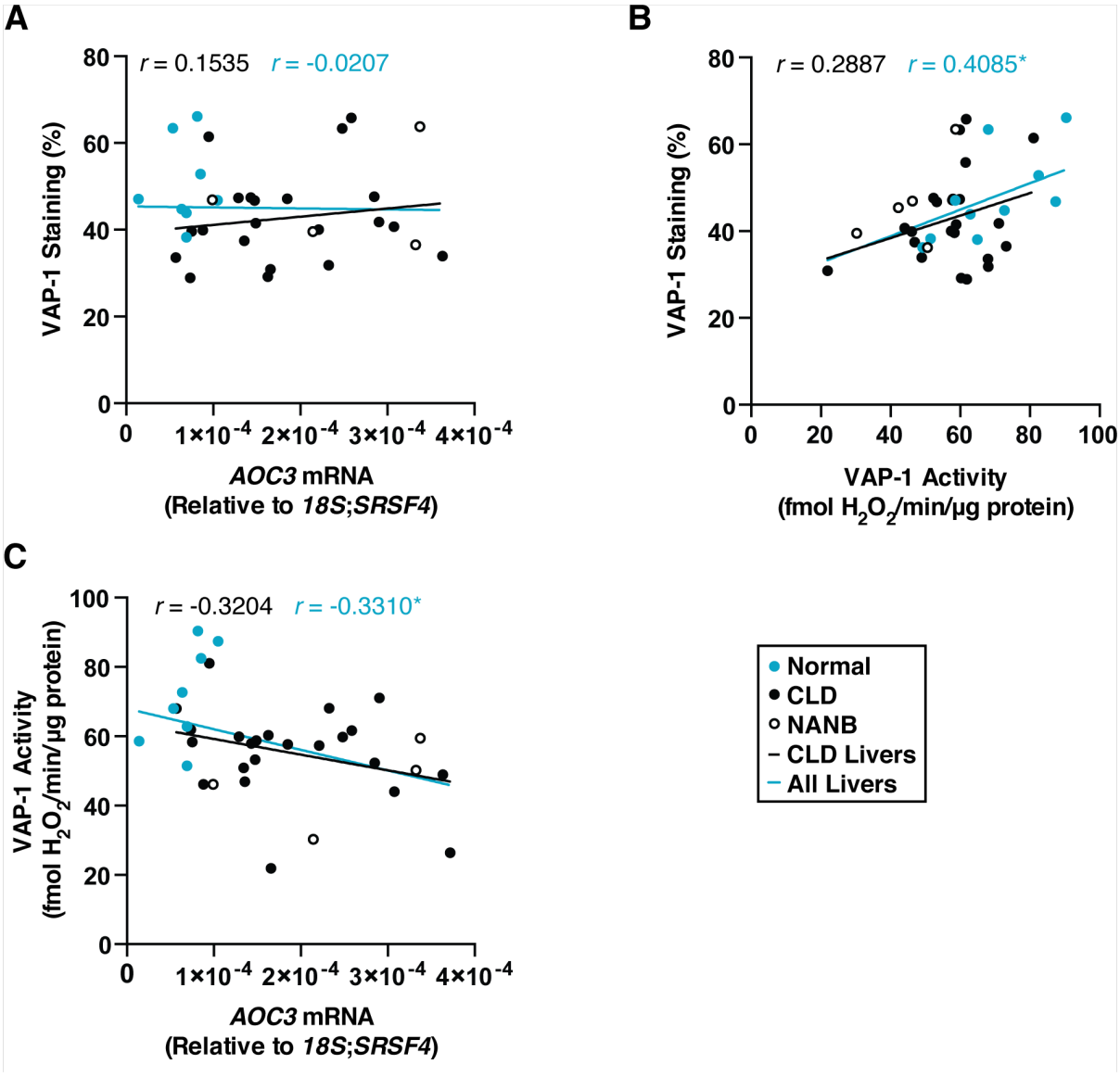


Figure 3.7 XY Comparison of VAP-1 staining, expression and activity between human liver tissue samples. Human tissue samples were analysed for VAP-1$^+$ area following immunohistochemical tissue staining, *AOC3* mRNA expression by qPCR analysis and VAP-1 amine oxidase activity by antibody-capture Amplex UltraRed assay and subsequently plotted for comparison. (**A**) VAP-1 positively stained area and mRNA expression, (**B**) VAP-1 positively stained area and amine oxidase activity and (**C**) VAP-1 amine oxidase activity and mRNA expression. Normal (blue dots) includes NL and SNL samples; CLD (black dots) includes ALD, NASH, PSC, PBC and AIH samples. Black lines and Pearson coefficients (r) relate only to samples from CLD, blue lines and Pearson coefficients (r) relate to all samples. Slopes were assessed to be non-zero by linear regression analysis. * $p \leq 0.05$.

(42.5 – 50.4 fmol H_2O_2/min/µg protein), $p \leq 0.01$, respectively) as was the lowest activity found within NASH livers (44.0 fmol H_2O_2/min/µg protein (26.4 – 58.8 fmol H_2O_2/min/µg protein), $p \leq 0.01$). When data from all chronic disease samples were combined, VAP-1 activity was significantly lower than within normal tissue (Figure 3.5F).

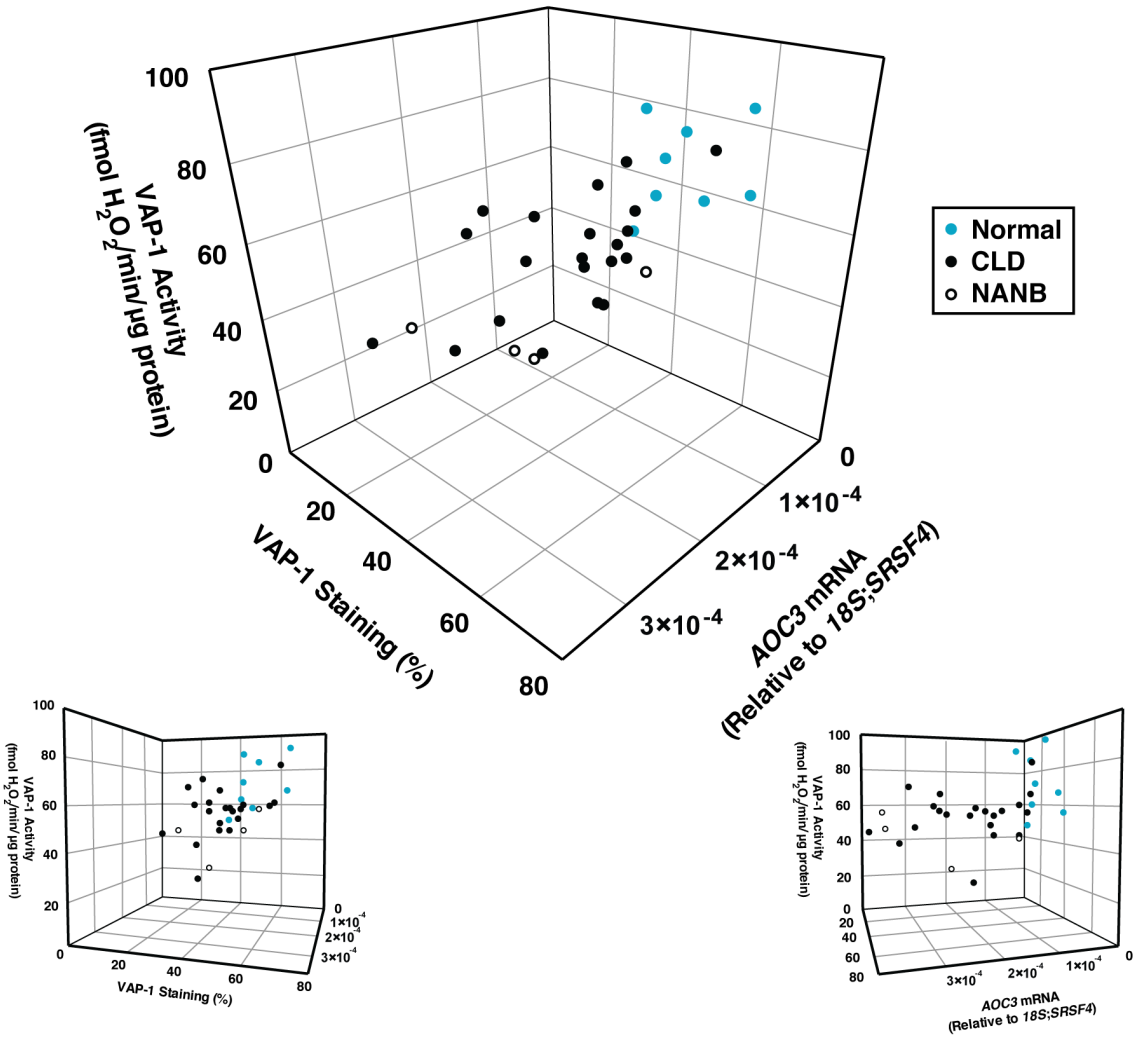


Figure 3.8 XYZ Comparison of VAP-1 staining, expression and activity between human liver tissue samples. Human tissue samples were analysed for VAP-1^{+} area following immunohistochemical tissue staining, *AOC3* mRNA expression by qPCR analysis and VAP-1 amine oxidase activity by antibody-capture Amplex UltraRed assay and subsequently plotted for comparison. Normal (blue dots) includes NL and SNL samples. CLD (black dots) includes ALD, NASH, PSC, PBC and AIH samples. Lower figures represent different orientations of central figure.

3.2.1.6 VAP-1 coverage, expression and activity correlations

The characterisation of hepatic VAP-1-stained area, mRNA expression and amine oxidase activity data from the matched samples derived from the same cohort of patients, therefore allowed for comparison to investigate and elucidate common trends (Figure 3.7). Separate linear correlation coefficients were calculated for CLD samples and all combined samples to ascertain whether fundamental changes occured within the chronic disease state. No correlation was observed between VAP-1 immunohistochemical

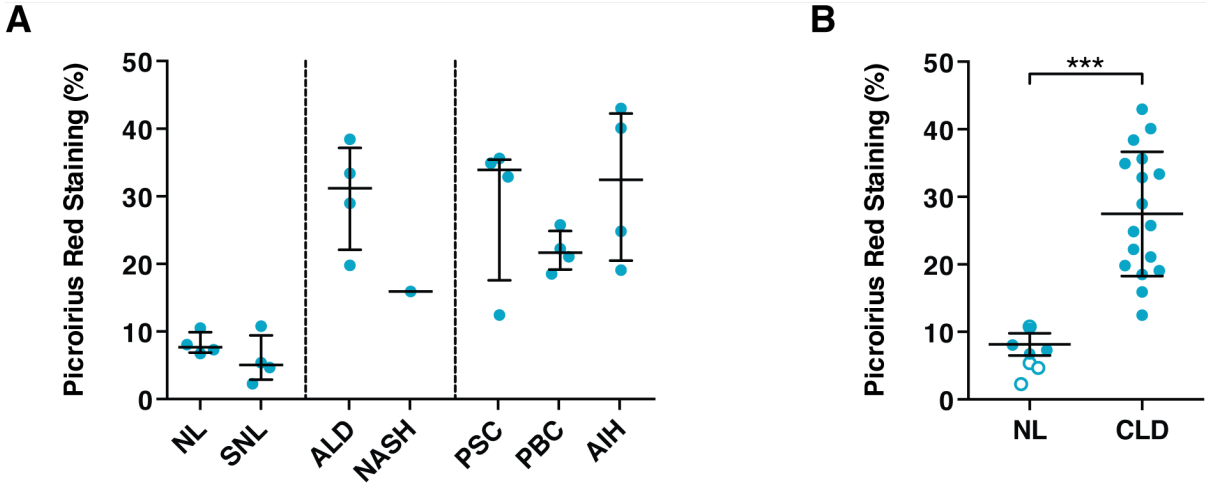


Figure 3.9 Extent of picrosirius red staining within human liver tissue samples. (**A**) Picrosirius red staining was elevated in chronically diseased liver tissue samples. (**B**) Represents the same combined dataset shown in (**A**) (n = 1 - 4). Each point represents an individual patient sample. Circles indicate SNL samples shown for illustrative purposes only and were excluded from analysis. Data shown as median (IQR) and analysed by KW test with Dunn's post-hoc correction (**A**) and mean (SD) and analysed by t test (**B**). *** $p \leq 0.001$.

staining and *AOC3* mRNA when considering only chronically diseased livers (r = 0.1535, p = 0.507) or all measured samples (r = -0.0207, p = 0.909) as seen in Figure 3.7A. The extent of VAP-1 staining positively correlated with increased VAP-1 enzymatic activity, although this correlation was only significantly non-zero when considering all livers (r = 0.4085, p = 0.0109) rather than CLD in isolation as shown in Figure 3.7B. Similarly, VAP-1 activity and mRNA expression were negatively correlated when all samples were considered (r = -0.3310, p = 0.019; Figure 3.7C). All coefficients of determination (r^2) were below 0.17, suggesting low degrees of linear-correlation.

Three-dimension representation of these data (Figure 3.8) highlighted the discrete clustering of normal and steatotic normal samples. These samples exhibited high levels of VAP-1 staining coverage and enzyme activity but low levels of mRNA expression. Samples from NANB livers do not form any such obvious group in terms of these parameters.

3.2.1.7 VAP-1 and degree of hepatic fibrosis

Immunohistochemical analysis demonstrated VAP-1 positivity of fibrotic lesions within liver tissue samples. In order to evaluate whether changes in hepatic VAP-1 correlated with the extent of fibrosis, the collagen content of samples was analysed by picrosirius

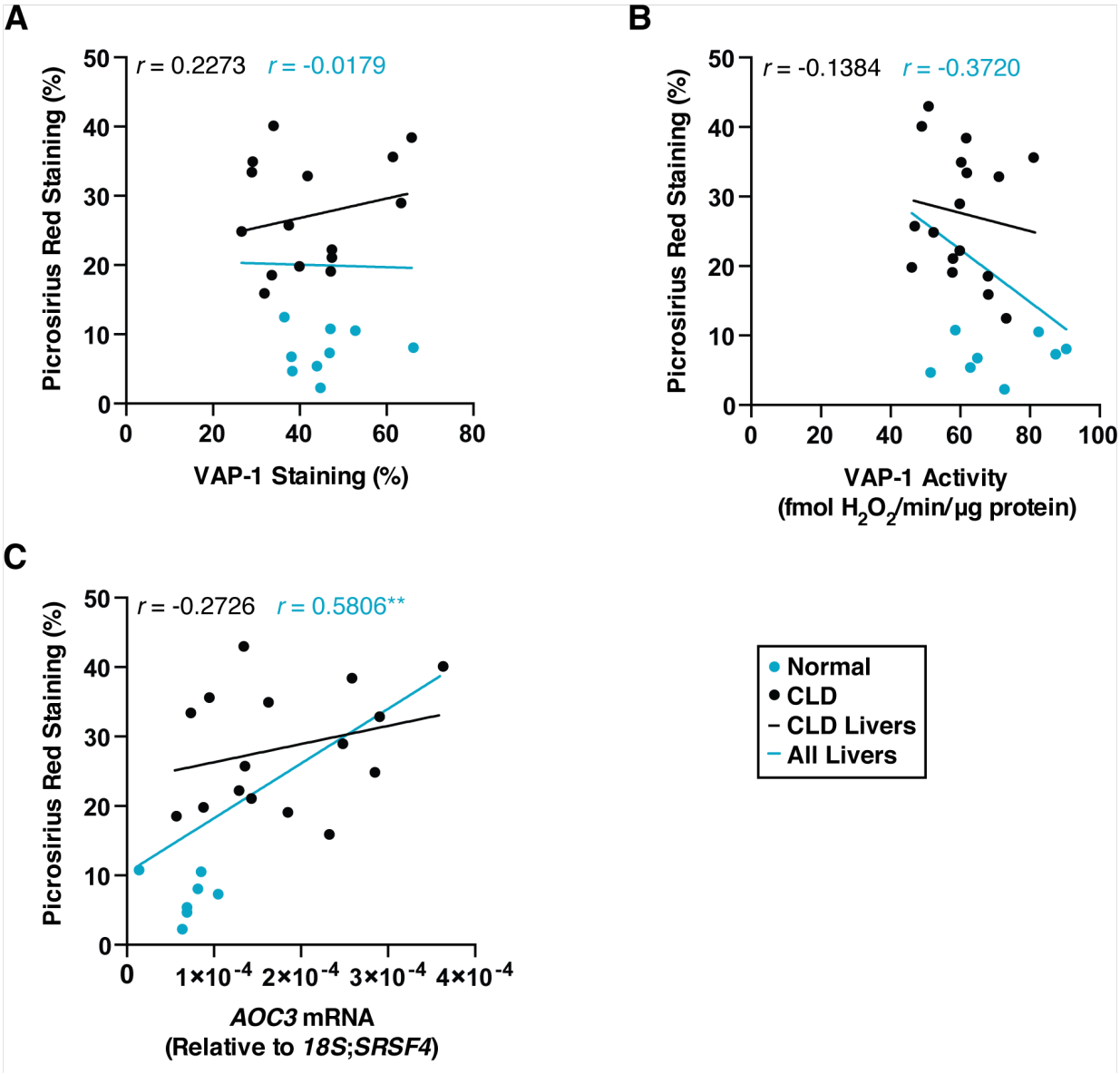


Figure 3.10 Comparison between VAP-1 and extent of fibrosis within human liver tissue samples. The level of fibrosis in human tissue samples, quantified by picrosirius red stain was plotted for comparison against (**A**) VAP-1^{+} area following immunohistochemical tissue staining, (**B**) *AOC3* mRNA expression by qPCR analysis and (**C**) VAP-1 amine oxidase activity by antibody-capture Amplex UltraRed assay. Normal (blue dots) includes normal and fatty donor samples; CLD (black dots) includes ALD, NASH, PSC, PBC and AIH samples. Black lines and Pearson coefficients (*r*) relate only to samples from CLD, blue lines and Pearson coefficients (*r*) relate to all samples. Slopes were assessed to be non-zero by linear regression analysis. Data in (**A**) was analysed by KW test with Dunn's post-hoc correction, however relationships were not significant. ** $p \leq 0.01$.

red histological stain and quantified by ImageJ analysis. Normal and steatotic normal livers exhibited low levels of picrosirius red staining, indicating low levels of fibrosis as expected (8.09% (7.69 – 9.30%) and 4.70% (3.49 – 7.75%), respectively). Staining levels were higher in all chronically diseased samples but were considerably broader ranging

(Figure 3.9A). However, when combined picrosirirus red staining was significantly elevated in chronically diseased tissue ($p \leq 0.001$; Figure 3.9B).

No significantly non-zero correlations existed between picrosirius red staining and VAP-1 staining (r = 0.2273), activity (r = -0.1384) or mRNA expression (r = -0.2726) within chronically diseased tissue samples (Figure 3.10). Picrosirius red staining did however positively correlate with *AOC3* mRNA expression when normal livers were also included within the cohort (r = 0.5806, p = 0.004; Figure 3.9D).

3.2.2 Inhibition of hepatic VAP-1

3.2.2.1 Inhibition by semicarbazide

Semicarbazide (Figure 3.11A) is the archetypal inhibitor of VAP-1, therefore the properties of the interaction with hepatic VAP-1 were characterised by immunosorbent Amplex UltraRed assay. Proof of concept was first demonstrated by measuring the activity of 200 ng of captured recombinant VAP-1 in the presence of semicarbazide (Figure 3.11B). VAP-1 activity decreased in response to increasing concentrations of semicarbazide until baseline levels (typically occurring through autoxidation of the Amplex UltraRed dye) were recorded above approximately 500 μM. Similar dose-response curves were then generated for VAP-1 captured from pooled normal, CLD and NANB liver tissue lysates prepared at a concentration of 2 mg/mL, despite presumably consisting of a mixture of soluble and membrane forms of VAP-1 rather than pure soluble protein (Figure 3.11C). There was no discernible difference in the inhibition of VAP-1 captured from each pooled sample, demonstrated by the similarity of dose-response curves (r^2 = 0.7759 – 0.9173). Statistical analysis could not reject the null hypothesis of a shared IC_{50} of 81.44 ± 1.05 μM (p = 0.2831).

In order to test for differences in VAP-1 semicarbazide-sensitivity between different individual healthy and diseased livers, the amine oxidase activity of antibody-captured VAP-1 was recorded in the absence or presence of 500 μM semicarbazide. This approach also minimised any potential cross-contamination from other amine oxidases (such as those from the lysysl oxidase family), which would not interact with the plate-bound antibody. Semicarbazide significantly inhibited VAP-1 activity across all liver samples

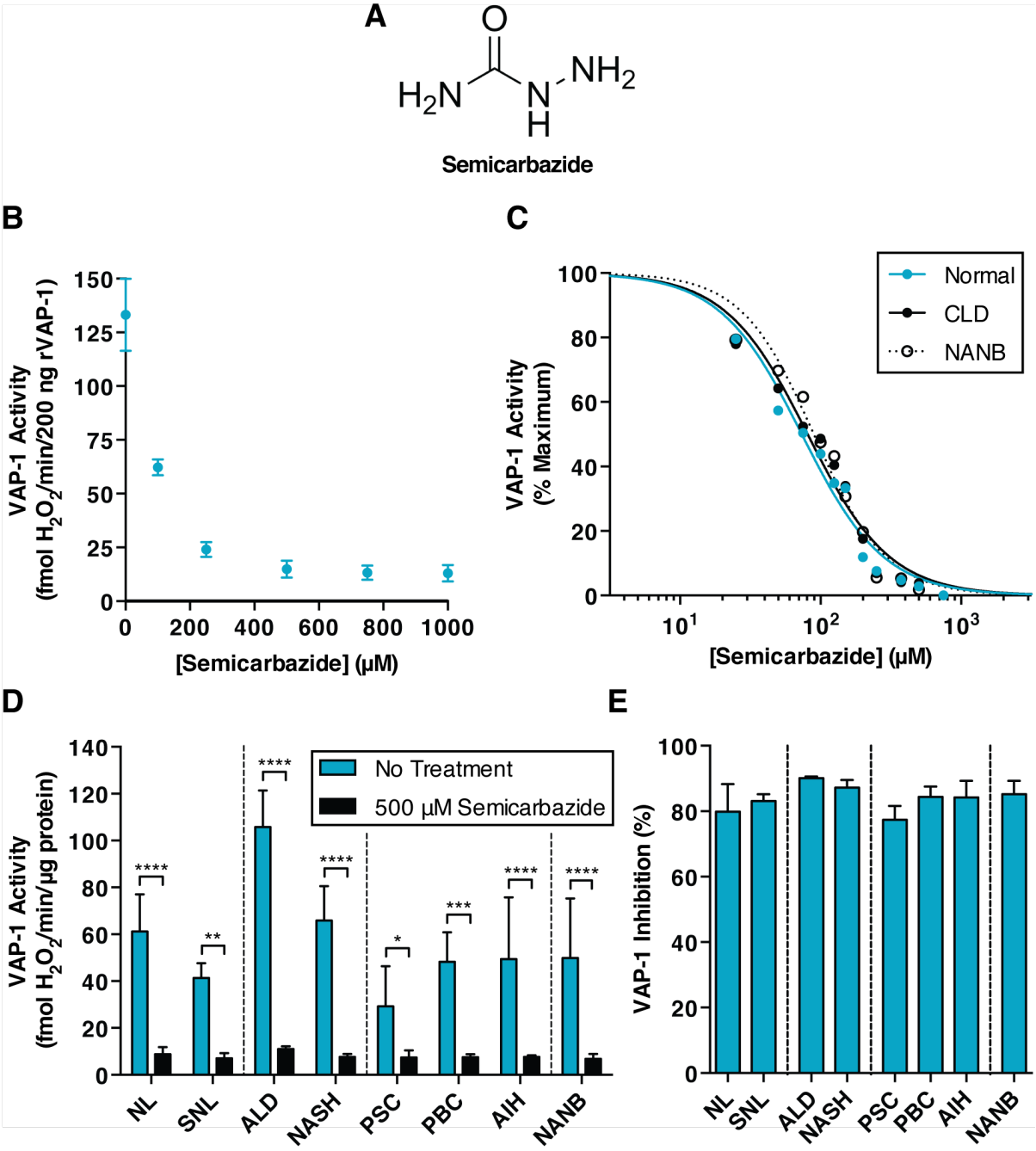


Figure 3.11 Inhibitory effect of semicarbazide on hepatic VAP-1 activity. (**A**) Structure of Semicarbazide. (**B**) Inhibition of 200 ng rVAP-1 by semicarbazide (n = 3). (**C**) Inhibition of VAP-1 captured from liver tissue by semicarbazide. CLD represents combined tissue samples from ALD, NASH, PSC and PBC (n = 3). (**D**) Amine oxidase activity of VAP-1 captured from human liver tissue in the presence and absence of 500 μM semicarbazide (n = 5). (**E**) Proportion of total VAP-1 activity inhibited by 500 μM semicarbazide in (**D**) across liver tissue samples (n = 5). Data shown as mean (SD) (**B**), mean (**C**) and median (IQR) (**D** & **E**) and were analysed by two-way ANOVA with Holm-Sidak post-hoc correction (**D**) and KW test with Dunn's post-hoc correction (**E**). * $p \leq 0.05$, ** $p \leq 0.01$, *** $p \leq 0.001$, **** $p \leq 0.0001$.

equally at this concentration (Figure 3.11D) representing between approximately 75% - 90% inhibition of total VAP-1 activity (Figure 3.11E).

3.2.2.2 Inhibition by LJP-1586

Following the successful determination of sensitivity of hepatic VAP-1 to semicarbazide from across multiple disease samples, a similar approach was taken to study a VAP-1-specific inhibitor, namely LJP-1586 (Z-3-fluoro-2-(4-methoxybenzyl)allylamine; Figure 3.12A) that has been used in a number of studies to preferentially inhibit SSAO activity (Filip et al., 2016; Marttila-Ichihara et al., 2010; O'Rourke et al., 2008; Xu et al., 2015). The immunocapture Amplex UltraRed assay was used to determine changes in VAP-1 amine oxidase activity in the presence and absence of 500 nM LJP-1586. VAP-1 activity from all tissues was significantly decreased in the presence of the inhibitor compared to untreated VAP-1 (Figure 3.12B). The proportion of activity inhibited was largely similar between the individual tissue samples, regardless of disease state, representing median values of approximately 55% - 70% inhibition (Figure 3.12C). However, VAP-1 isolated from NANB livers was inhibited to a significantly lesser degree than VAP-1 from normal liver tissue (56.2% (55.3 – 57.1%) and 70.1% (69.8 – 70.2%), respectively).

Treatment of hepatic VAP-1 with 500 nM LJP-1586 inhibited the amine oxidase activity to approximately 20 fmol H_2O_2/min/μg protein: twice the baseline activity recorded after treatment with 500 μM semicarbazide (approximately 10 fmol H_2O_2/min/μg protein). However, if samples were preincubated with LJP-1586 for one hour prior to running the assay the baseline activity dropped to approximately 5 fmol H_2O_2/min/μg protein. This is exhibited as an increase of approximately 15 fmol H_2O_2/min/μg protein total VAP-1 inhibition seen in Figure 3.12D. This time-dependent inhibition corresponds to a significant increase in inhibition of approximately 20% - 30% when the assay is run after one hour of pretreatment (1-2 hours) rather than immediately (0-1 hours) as shown in Figure 3.12E.

3.2.2.3 Inhibition by methylxanthines

Methylxanthines are methylated forms of the purine base xanthine (Figure 3.13) and are involved in a variety of physiological functions (Monteiro et al., 2016). One particularly well-characterised member of this group is caffeine, which has been previously

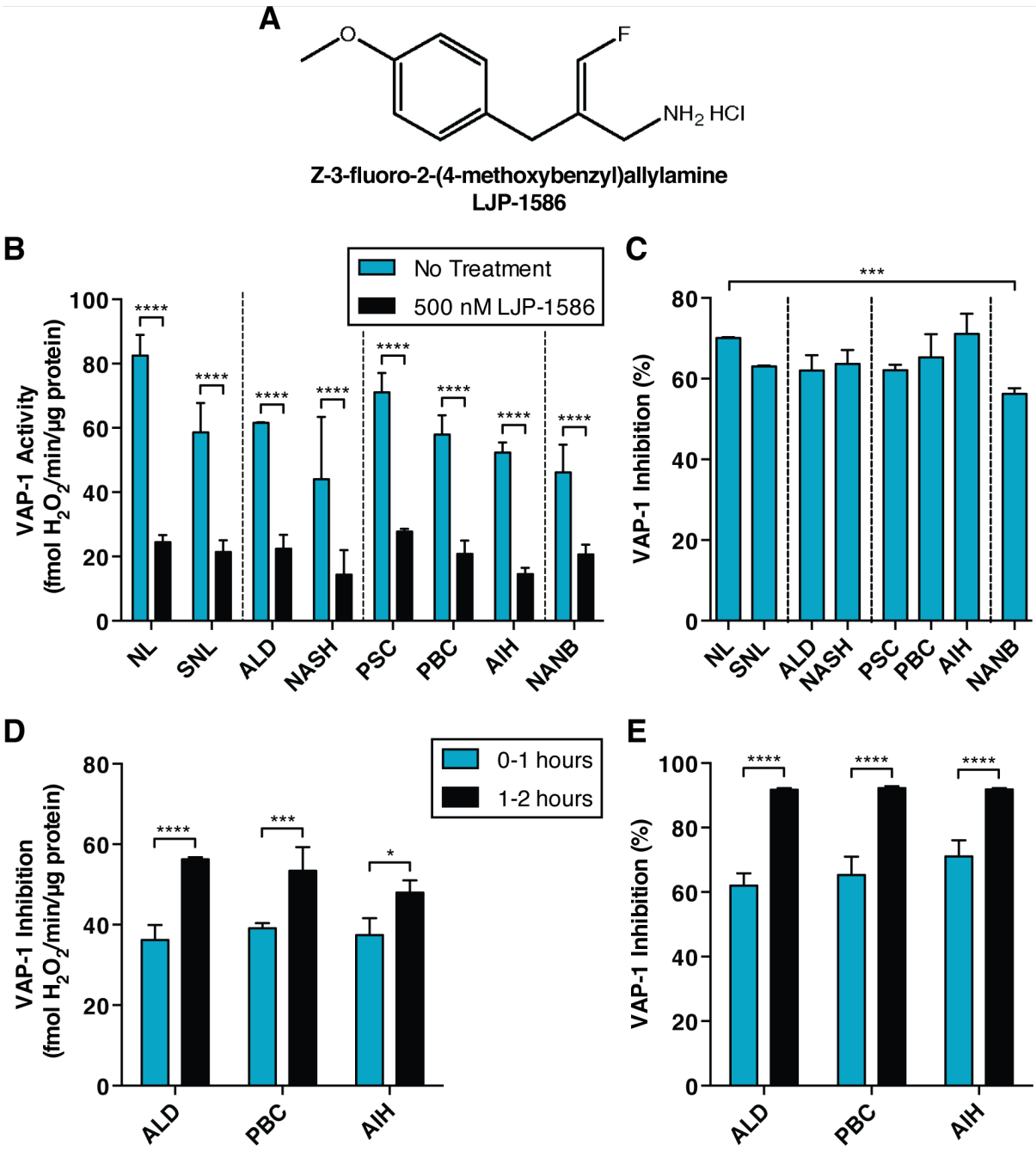


Figure 3.12 Inhibitory effect of LJP-1586 on hepatic VAP-1 activity. (**A**) Structure of LJP-1586. (**B**) Amine oxidase activity of VAP-1 captured from human liver tissue in the presence and absence of 500 nM LJP-1586 (n = 5). (**C**) The proportion of VAP-1 activity without treatment that is inhibited by the addition of 500 nM LJP-1586 across liver tissue samples shown in (A) (n = 5). (**D**) The difference in the amine oxidase activity of VAP-1 captured from ALD, PBC or AIH liver tissue, with and without the presence of 500 nM LJP-1586. All activities were measured over a period of one hour, black lines indicate VAP-1 that was preincubated with LJP-1586 for one hour prior to measurement (n = 3). (**E**) Data shown in (**D**) represented as proportion of total VAP-1 activity. Data shown as median (IQR) and were analysed by two-way ANOVA with Holm-Sidak post-hoc correction (**B**, **D** & **E**) and KW test with Dunn's post-hoc correction (**C**). * $p \leq 0.05$, *** $p \leq 0.001$, **** $p \leq 0.0001$.

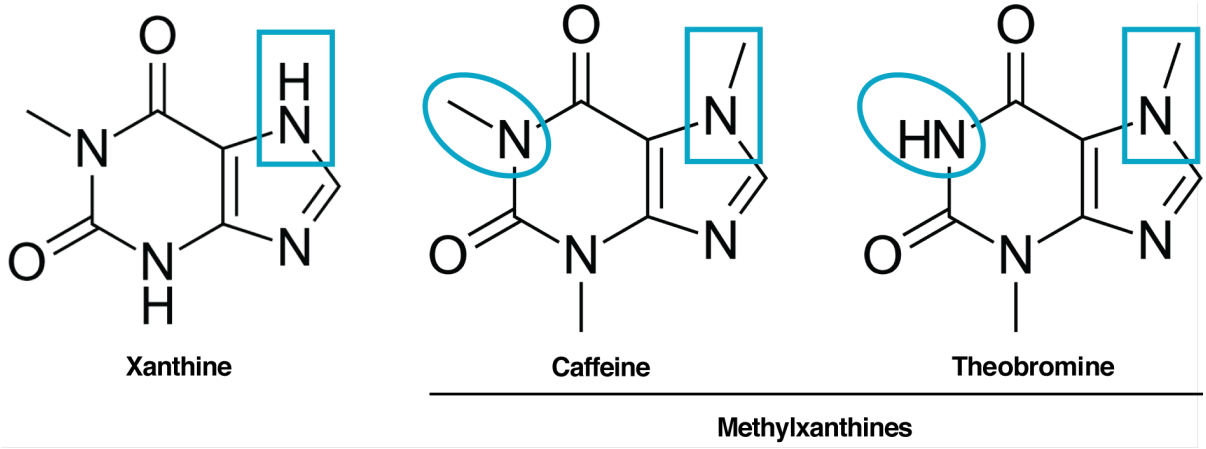


Figure 3.13 Structure of Xanthine, Caffeine and Theobromine. Caffeine and Theobromine are methylated forms of the purine base xanthine, this group is highlighted with rectangles. Caffeine differs from theobromine in structure by the presence of an additional methyl group, highlighted with ovals.

demonstrated to inhibit bovine VAP-1 in a non-competitive manner (Olivieri and Tipton, 2011). Given the structural differences between bovine and human VAP-1 the immunosorbent Amplex UltraRed assay was used to determine whether a similar effect was observed with human hepatic VAP-1. In pilot studies using recombinant VAP-1, caffeine was effectively capable of reducing the amine oxidase activity of recombinant VAP-1 in a dose-dependent manner within the micromolar range (Figure 3.14A). Although the linear relationship between caffeine concentration and VAP-1 activity was low, the correlation was still statistically significant ($r^2 = 0.2391$, $p = 0.0464$). A similar effect was also demonstrated using pooled VAP-1 from normal and diseased liver tissue (Figure 3.14B) although no significant difference in dose-response curves was found between these samples ($r^2 = 0.6193 – 0.8965$), therefore a shared IC_{50} value of 3.547 ± 1.079 mM was calculated ($p = 0.9876$).

A concentration of 100 μM caffeine was chosen as a physiologically relevant level, and at this concentration only VAP-1 isolated from ALD livers was significantly inhibited from 105.8 fmol H_2O_2/min/μg protein (93.0 – 119.5 fmol H_2O_2/min/μg protein) to 89.1 fmol H_2O_2/min/μg protein (86.6 – 94.0 fmol H_2O_2/min/μg protein), $p \leq 0.05$ (Figure 3.14C). At a supraphysiological concentration of 5 mM, caffeine significantly inhibited VAP-1 from normal, ALD, NASH, AIH and NANB livers. When normalised and expressed as a proportion of total activity, all tested concentrations of caffeine significantly inhibited the amine oxidase reaction rate: from approximately 20% inhibition with 100 μM

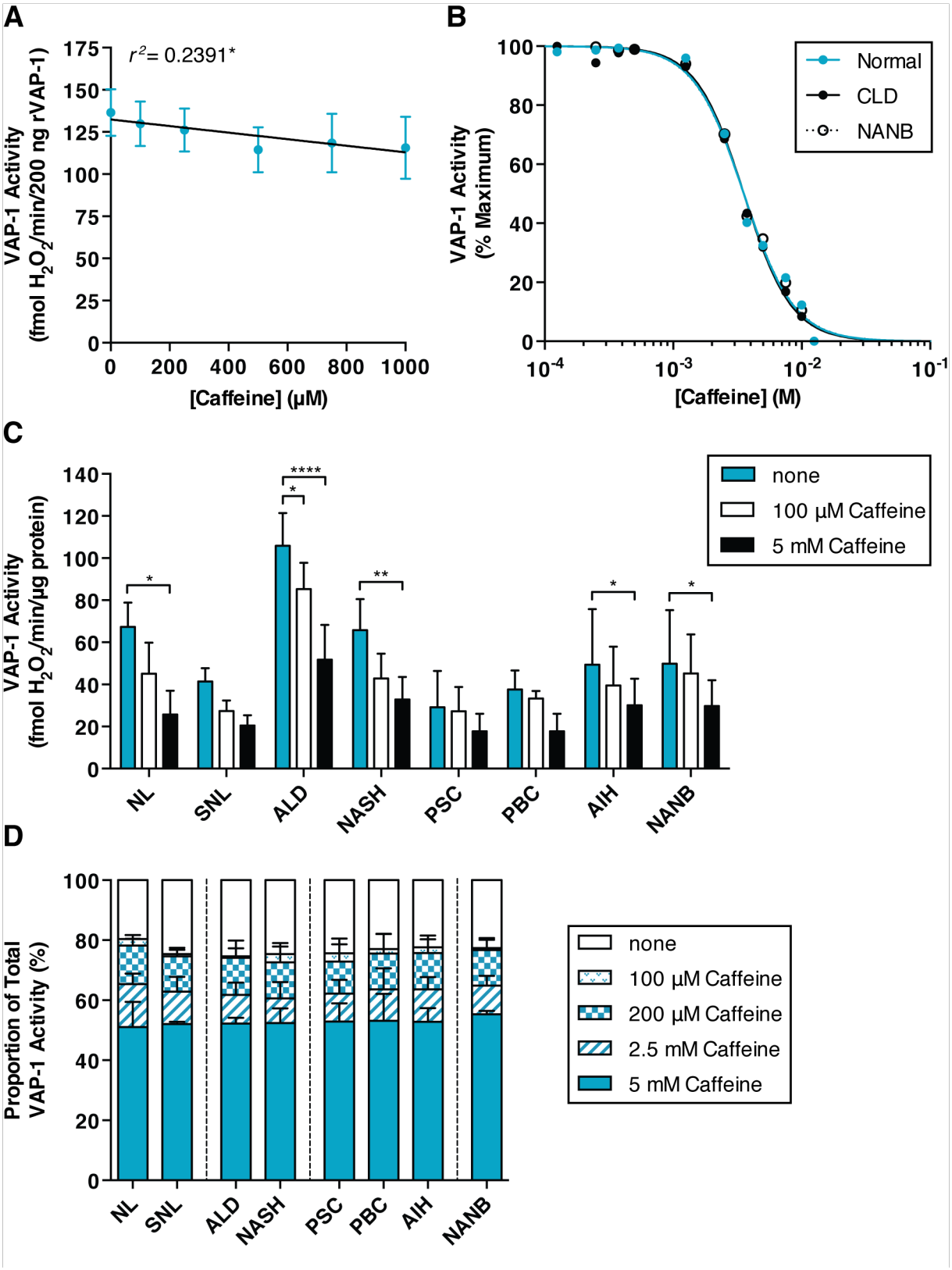

A
VAP-1 Activity
(fmol H2O2/min/200 ng rVAP-1)
r2= 0.2391*
[Caffeine] (µM)
B
VAP-1 Activity
(% Maximum)
Normal
CLD
NANB
[Caffeine] (M)
C
VAP-1 Activity
(fmol H2O2/min/µg protein)
none
100 µM Caffeine
5 mM Caffeine
NL
SNL
ALD
NASH
PSC
PBC
AIH
NANB
D
Proportion of Total
VAP-1 Activity (%)
none
100 µM Caffeine
200 µM Caffeine
2.5 mM Caffeine
5 mM Caffeine

Figure 3.14 Inhibitory effect of caffeine on hepatic VAP-1 activity. (**A**) Inhibition of 200 ng rVAP-1 by caffeine (*n* = 3). (**B**) Inhibition of VAP-1 captured from liver tissue by semicarbazide. CLD represents combined tissue samples from ALD, NASH, PSC and PBC (*n* = 3). (**C**) Amine oxidase activity of VAP-1 captured from human liver tissue in the presence and absence of 100 µM and 5 mM caffeine (*n* = 5). (**D**) Proportion of total VAP-1 activity inhibited by 100 µM, 200 µM, 2.5 mM and 5 mM caffeine across liver tissue samples (*n* = 5). Data shown as mean (SD) (**A**), mean (**B**) and median (IQR) and were analysed by two-way ANOVA with Holm-Sidak post-hoc correction (**C**). * $p \leq 0.05$, ** $p \leq 0.01$, **** $p \leq 0.0001$.

there was no significant difference in caffeine response between disease samples.

Previous studies have suggested that caffeine may interfere with the Amplex UltraRed reaction used within this study (Carpéné et al., 2016). Figure 3.15A shows an H_2O_2 standard curve used within these experiments with and without 200 µM caffeine. If the overall slopes were identical there would be a 3.6% chance of randomly choosing data points with slopes this different ($p = 0.0364$), therefore suggesting that caffeine has had an effect on the assay. However, the difference in slope of 2.4% is considerably less than the approximately 25% inhibition of VAP-1 activity elicited by the same concentration of caffeine.

Another dietary methylxanthine, theobromine, was also examined for any potential inhibitory function against VAP-1. Due to the poor solubility of this compound, the effect on inhibition of amine oxidase activity could only tested up to 875 µM concentration. Theobromine did not exhibit any reliable inhibitory function over this concentration range and therefore no dose-response curve could be generated (Figure 3.15B).

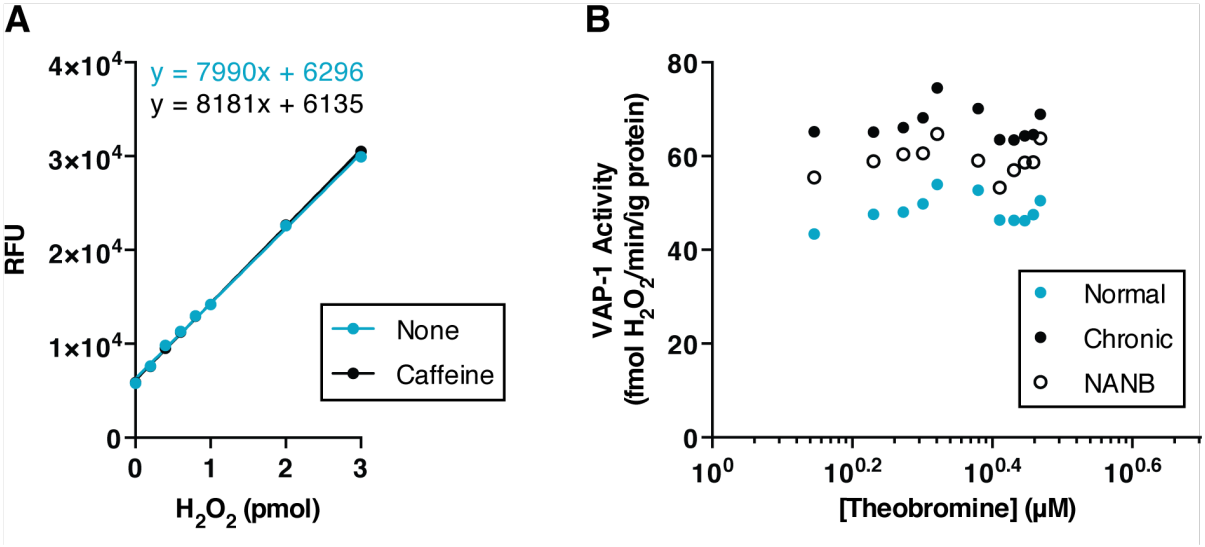


Figure 3.15 Optimisation of methylxanthines and amine oxidase activity. (**A**) Amplex UltraRed H_2O_2 standard curve in the presence and absence of 200 µM caffeine (n = 3). Lines of best fit were significantly different $p \leq 0.05$ (**B**) Inhibition of VAP-1 captured from liver tissue by theobromine. CLD represents combined tissue samples from ALD, NASH, PSC and PBC (n = 3). Data points represent mean values.

3.3 Discussion

The focus of this chapter was *to determine and compare hepatic VAP-1 expression during health and across inflammatory liver diseases.* The distribution of hepatic VAP-1 was first examined by immunohistochemical staining of healthy and diseased human livers, which demonstrated distinct centrilobular localisation with staining isolated to regions of high vascularity, HSEC and the fibrotic scar. This was additionally supported by qPCR analysis of *AOC3* expression in HSEC, HSCs and aLMFs.

The study was then extended in order to characterise and directly compare the localisation, expression and activity of hepatic VAP-1 between normal livers and seven different hepatic pathologies. Qualitative analysis of VAP-1 localisation demonstrated similar expression patterns across the different diseases, which was supported by similar proportions of VAP-1-positive tissue following semi-quantitative analysis. Expression of *AOC3* mRNA, however, was elevated in the tissue of chronically inflamed livers compared to healthy control, which correlated with the extent of hepatic fibrosis. Conversely, the enzyme activity of VAP-1 was lower in the diseased cohort despite analysis of the same patient samples in each of these investigations. These results appear highly contradictory with somewhat ambiguous correlations, which may demonstrate the complex nature of VAP-1 expression and the relationship between the different forms and splice variants. However, they may also highlight limitations of the experimental techniques employed.

This chapter finally characterised the enzyme activity of hepatic VAP-1 further, focussing on the potency of three mechanistically dissimilar inhibitors: semicarbazide, LJP-1586 and caffeine. Each molecule was capable of at least partially inhibiting hepatic VAP-1 activity in a dose-dependant manner. Furthermore, VAP-1 isolated from chronically diseased livers was equally sensitive to inhibition from each of the molecules. However, VAP-1 from NANB livers exhibited a slightly reduced activity in the presence of LJP-1586 compared to other livers. This may highlight a distinct functional difference of VAP-1 within acutely damaged livers, although it might also be an experimental artefact created by low numbers in the sample population.

3.3.1 Distribution of hepatic VAP-1

Weston and colleagues recently described the distribution of hepatic VAP-1 in human livers. They found vascular expression of VAP-1 in both normal liver and in tissue taken from patients with simple steatosis, with a predominantly endothelial distribution observed (Weston et al., 2015). In end-stage CLD - specifically NASH, PBC, PSC and ALD - increased immunohistochemical staining was also detected within neovessels and stromal cells of the fibrotic scar: the first demonstration of a role for VAP-1 in liver fibrosis.

The study by Weston and colleagues was extended in this thesis to also include a larger number of samples from different aetiologies, with the addition of AIH, and the first demonstration of VAP-1 expression in liver tissue taken from patients with NANB hepatic injury. The expression studies herein confirmed the vascular distribution of VAP-1 across all tissue samples, with a lack of VAP-1 on biliary structures and strong staining within the fibrotic lesion. This is also consistent with the original vascular description of VAP-1 on inflamed rheumatoid synovium (Salmi and Jalkanen, 1992) and more recent identification on HSEC (Lalor et al., 2002). Interestingly, scanning large areas of tissue sections (10–20 mm) with the use of the Zeiss Axio Scan.Z1 highlighted previously hidden staining patterns. In particular the striking centrilobular VAP-1 expression in normal and mildly steatotic samples that is lost upon the parenchymal disruption by the fibrotic septa. The reason for this differential expression is unclear, although similar zone 3 expression is seen in other molecules that are implicated in leukocyte migration, such as JAM-1 (Khandoga et al., 2005) and caveolin-1 (Ogi et al., 2003). However, zone 3 of the hepatic acinus is lowest in dietary amine composition and oxygen levels. A recent study demonstrated that the enzyme activity of murine adipocyte VAP-1 is reduced under hypoxic conditions, similar to centrilobular sinusoids (Repessé et al., 2015). This may suggest lower *in situ* VAP-1 activity within normal livers, however this is beyond the scope of this study.

The data shown here confirm the previous findings that VAP-1 is expressed in endothelial and stellate cells but is not detectable in cholangiocytes or hepatocytes (Weston et al., 2015). Stellate cells share an intimate relationship with sinusoidal endothelial cells by acting as pericytes, therefore contributing to the regulation of endothelial differentiation and function (Friedman, 2008). Quiescent stellate cells proliferate and differentiate into activated myofibroblasts during injury and

subsequently deposit ECM during fibrogenesis. ECM deposition is also important for angiogenesis, which in combination with the VAP-1-positive neovessels supports previous work implicating VAP-1 in this process (Marttila-Ichihara et al., 2010, 2009; Noda et al., 2008). The data shown here also confirms the *de novo* synthesis of *AOC3* mRNA by non-activated HSCs from normal liver tissue as well as *in vivo*-activated aLMFs from chronically diseased tissue, consistent with recent publications (Hsia et al., 2016; Weston et al., 2013). HSCs also secrete enzymatically active VAP-1 that may act as a potent leukocyte chemotactic factor, contributing to inflammation in CLD (Weston et al., 2015).

3.3.2 Characterisation of VAP-1 expression and activity

The aim of this chapter was to evaluate differences between the functional characteristics of VAP-1 within normal liver tissue and that of most major liver diseases. This direct comparison of VAP-1 between normal and seven discrete liver aetiologies represents the most comprehensive study to date. The liver samples were also broadly divided into subclasses of disease (normal and mildly steatotic livers; the steatotic diseases; autoimmune diseases and the acute disorder non-A non-B hepatitis) to discover whether commonality existed in regarding VAP-1 expression and function. Liver tissue from each patient was analysed in terms of the proportion of VAP-1-positive stained tissue, *AOC3* mRNA expression and VAP-1 enzyme activity, in the hope of highlighting any changes during the different disease states.

Quantification of the immunohistochemical staining demonstrated no significant difference in the total area of VAP-1-positive normal tissue compared to tissue from any of the investigated diseases. VAP-1 coverage was also independent of the extent of fibrosis, despite the strong and dense staining associated with the lesions. This therefore suggests a fundamental reorganisation of VAP-1 within fibrotic tissue: shifting from primarily sinusoidal to a more septal expression without affecting the total VAP-1-positive area. It is therefore likely that the proportion of VAP-1-positive sinusoids decreases with increased fibrosis. The simple thresholding analysis employed for this quantification allowed for full analysis of the incredibly large images of tissue sections but did not contain information pertaining to variations in staining intensity. This binary method of analysing staining above a defined threshold, although widely utilised, is not necessarily proportional to total protein expression (Jensen, 2013). Western blot

analysis would be more effective for this purpose, however while certain antibody clones worked well for overexpressing cell lines (Weston et al., 2013) it was not possible to obtain consistent results using liver tissue during the course of this study, despite using a range of extraction buffers and blotting conditions. The data shown here is therefore not necessarily contrary to previous suggestions that hepatic VAP-1 is increased in NANB and chronically diseased liver tissue (Tuncer et al., 2013; Weston et al., 2015).

Consistent with this, VAP-1 gene expression was significantly higher in chronic liver disease compared to normal samples when all patient data was combined. The differences in expression between normal and single disease aetiologies, however, did not amount to statistical significance. A contributing factor to this was the large variation in mRNA expression between patients within the same disease group. This may be in part due to variations in housekeeping gene expression between the diseases, however *18S* and *SFRS4* were chosen as those least effected by fibrosis and steatosis (Boujedidi et al., 2012). Likewise, by normalising to two housekeeping genes it was hoped that variations would be further minimised. Interpatient variability and delays in processing the liver once it had been removed from the patient may also be indicative of factors additional to disease aetiology that influence gene expression. Delays were particularly problematic when processing normal livers, which were often transported between several hospitals before finally being rejected for transplant. Maximum efforts were taken to ensure that these livers were as close to normal as possible by selecting only those with low steatosis, inflammation and fibrosis, however no definitive test is available to determine the 'normality' of this tissue. Unlike many other studies, no tissue was used from sites distal to resected tumours due to evidence suggesting VAP-1 expression is altered in these conditions, such as hepatocellular carcinoma (Yoong et al., 1998).

Gene expression correlated more strongly with picrosirius red staining, suggesting the extent of fibrosis as a dominant factor. This may be due to increased numbers of *AOC3*-expressing aLMFs or may be related to additional factors such as the extent of inflammatory infiltrate or vascularisation. Unfortunately these data were not collected for NANB samples due to the acute nature of the conditions. However, they often present as acute on a background of chronic liver disease and may therefore provide interesting information regarding the importance of fibrosis to VAP-1 gene expression in this condition. It was also not possible to source additional tissue for comparison from other acute liver injuries, such as POD, due to restrictions with ethics. These tissues are

thought to exhibit differential expression of cell adhesion molecule including VAP-1 and would therefore be of interest to investigate in subsequent studies (Tuncer et al., 2013). Regardless of mechanism, increased VAP-1 expression in diseased samples provides support for a role in the propagation of liver disease.

A somewhat unexpected finding was that levels of *AOC3* mRNA did not correlate with the quantification of VAP-1 staining. It is possible that this is an artefact of the method of quantification employed and that VAP-1 staining intensity also increased in each of the diseases, as discussed. Alternatively, HSCs, aLMFs and HSEC are thought to secrete soluble VAP-1 and increased serum sVAP-1 levels have been well documented during CLD (Kurkijärvi et al., 2000, 1998; Weston et al., 2015). It therefore stands to reason that although VAP-1 gene expression is raised during disease, much of this may be secreted from the liver into the circulation, reducing the levels detectable by immunohistochemistry. This is consistent with transgenic mouse studies that were able to recapitulate serum VAP-1 levels in VAP-1^{KO} mice by inducing endothelium-specific expression of VAP-1 (Stolen et al., 2004). However, the precise mechanism of soluble VAP-1 production still remains elusive.

Secretion of VAP-1 in its soluble form may also be an explanation for some of the observed reduction in VAP-1 activity demonstrated across the liver diseases compared to normal liver. Soluble VAP-1, particularly through its enzyme activity, can act as a promigratory signal for leukocytes (Weston et al., 2015). Therefore if diseased livers secrete sVAP-1, this may exacerbate inflammation and lead to further damage. However this is unlikely to be the major contributor to loss of function as VAP-1 activity negatively correlated with mRNA expression. This finding, however, may implicate the recently discovered splice variant of VAP-1, VAP-1Δ3, that is present within the liver but devoid of any amine oxidase activity (Kaitaniemi et al., 2013). Preliminary unpublished data from our lab appears to suggest that this truncated form of VAP-1 is expressed in ALD, AIH, PSC and PBC tissue but is absent from normal tissue. It is therefore possible that VAP-1Δ3 is capable of dimerising with VAP-1, thereby diminishing the total enzymatic activity. Neither TK8-14 nor TK8-18 are able to discriminate between the two variants; therefore while immunohistochemical analysis would appear identical the enzyme activity would be reduced in proportion to the amount of TK8-18-captured VAP-1Δ3 (Kaitaniemi et al., 2013). On the contrary, the probe used for qPCR analysis spans exons 2 and 3 and may therefore be incapable of binding and detecting the splice

variant that lacks exon 3. However, if the probe is able to bind to VAP-1Δ3 then it is not possible to discern whether the increase in *AOC3* mRNA corresponds to VAP-1 or VAP-1Δ3.

Reduced VAP-1 activity has also been demonstrated during acute carrageen-induced inflammation and chronic adjuvant-induced arthritis (Tábi et al., 2013). The authors suggested a potential inactivation of VAP-1 following engagement with extravasating leukocytes, possibly via internalisation to previously described intracellular granules (Jaakkola et al., 2000; Salmi et al., 1993). A similar mechanism may also be occurring within the diseased liver tissue, which may also explain why VAP-1 did not fully colocalise with CD31 in the fluorescent immunohistochemistry shown here.

The reduced amine oxidase activity within diseased livers may also indicate the presence of an inhibitor within these tissues. Unidentified endogenous VAP-1 inhibitors have been described in both human serum and rat cytosol and may therefore be present during liver disease (Buffoni et al., 1983; Obata and Nakashima, 2016). Similarly, elastin is a known endogenous inhibitor of VAP-1 and is actively synthesised by HSCs and LMFs in the diseased liver and is key for the development of fibrosis (Kanta, 2016; Olivieri et al., 2010). VAP-1 activity trended towards negative correlation with extent of fibrosis, which would therefore result in more elastin and resultant inhibition of activity. Although equally this effect may be due to more tightly bound VAP-1 in fibrotic tissues, therefore dissociation during sample preparation would be less effective and yield lower activities. It is also not possible to exclude any of the wide range of substances that are administered during or prior to surgery that may inhibit VAP-1 function. In line with this, normal tissue is likely to have increased ischemic period prior to tissue processing that may allow sufficient time for dissociation or metabolism of VAP-1 inhibitors.

A major limitation of these data is the small sample sizes within each disease group. Increased patient numbers may have highlighted subtle differences in VAP-1 that are currently masked by outliers and statistical analysis with low power. Similarly, the small sample size was more sensitive to variations in selection of tissue samples for analysis: ideally this should have been from regions bearing similar vascular, stromal and fibrotic volume to be directly comparable. In reality this approach was not feasible and tissue was therefore selected at random. Patient samples were also collected following transplant and therefore represent end-stage aetiologies, as it is not ethically

feasible to sample patients prior to this. It is therefore unfortunately not possible to draw conclusions about hepatic VAP-1 in pre-cirrhotic livers and whether changes occur gradually or rapidly after a particular trigger. Novel imaging techniques are currently in development that may provide insight into VAP-1 in patients across the spectrum of disease, such as tracking labelled VAP-1-binding peptides via positron emission tomography (Autio et al., 2011; Li et al., 2013; Silvola et al., 2016). These will hopefully provide valuable replacements for murine models, which have proven difficult to assess for VAP-1 by immunohistochemistry and enzyme activity in the past.

3.3.3 Inhibition of hepatic VAP-1

VAP-1 is emerging as a potentially important therapeutic target in many different inflammatory conditions including liver disease (Lalor et al., 2007). One particular area of interest is the inhibition of VAP-1 amine oxidase activity due to the lower manufacturing costs and ease of administration in the clinic (Foot et al., 2013; Marttila-Ichihara et al., 2010; O'Rourke et al., 2008; Schilter et al., 2015). The development of the VAP-1 activity assay provided an excellent platform to examine the effect of inhibitors on hepatic VAP-1 and to discover whether similar sensitivities were demonstrated across all disease aetiologies. Although Amplex UltraRed assays have been previously used to assess VAP-1 activity, this work constitutes one of the first efforts to reduce potential confounding factors. In particular, reducing activity from other copper-containing amine oxidases, lysyl oxidases and monoamine oxidases with high levels of similarity in terms of structure and specificity for substrates and inhibitors.

Very little is known about the pharmacodynamics of human VAP-1 and the archetypal hydrazine-based inhibitor, semicarbazide, however there appears to be variation between VAP-1 from different sources. This may be due to altered glycosylation between VAP-1 derived from different tissues, which has been previously shown to affect the amine oxidase activity and therefore may also affect inhibition (Maula et al., 2005). For example, one study estimated a ten-fold difference in IC_{50} values of semicarbazide and VAP-1 from human serum and saphenous vein, respectively (Mészáros et al., 2000). In the studies presented here no differences in IC_{50} were observed between pooled disease samples; however low coefficients of determination indicate that subtle shifts in dose-response curves may have been obscured. This notwithstanding, the aim of these studies were to compare and contrast the inhibitory effect across disease aetiologies

rather than obtain absolute measures of potency. At the inhibitory concentration of 0.5 mM, similar levels of VAP-1 inhibition were recorded in liver tissue from all diseases. This concentration should inhibit the majority of VAP-1 activity, however there is a similar level of apparent residual activity across all samples, which is likely to correspond to auto-oxidation of the Amplex UltraRed detection system.

The VAP-1-specific inhibitor LJP-1586 has a reported IC_{50} of 27 nM and 43 nM in human umbilical cord and rVAP-1, respectively (O'Rourke et al., 2007). The high specificity for VAP-1 also means that inhibition of other amine oxidases has only been recorded above 2.2 μM (O'Rourke et al., 2007). 500 nM was therefore chosen as a concentration that would effectively inhibit all VAP-1 activity while exhibiting minimal off-target effects. VAP-1 isolated from NANB tissue demonstrated significantly lower sensitivity to LJP-1586 at this concentration than VAP-1 from normal livers, whereas no differences were seen between the chronic diseases. As the only acute liver disease within the cohort, this may indicate a conformational change of VAP-1 within these livers that renders it less susceptible to inhibition. The active site of VAP-1 is controlled by a cavity between the D3 and D4 domains, the size of which dictates substrate specificity (Airenne et al., 2005). Murine VAP-1 has an enlarged active site with wider entrance (Yraola et al., 2006), which may determine the observed increased susceptibility to competitive inhibition by LJP-1586 (O'Rourke et al., 2007). An opposite conformational change within this region of VAP-1 expressed by NANB livers may therefore decrease the accessibility of LJP-1586 without affecting entry of the smaller semicarbazide molecule, or simply alter the binding affinity of the inhibitors. VAP-1 antibodies used in previous studies have increased VAP-1 activity, likely due to conformational change, therefore the opposite may also be possible; however no such molecules have been described to the author's knowledge (Salmi et al., 2001). Similarly, altered glycosylation of VAP-1 may also affect activity, and therefore also inhibition (Maula et al., 2005).

Pretreatment of VAP-1 with LJP-1586 prior to activity measurement produced a lower baseline activity rate and corresponding increased total inhibition. This time-dependent inhibition has not previously been documented for LJP-1586; despite similar observations with semicarbazide and other VAP-1 inhibitors (Lizcano et al., 1996; Wang et al., 2006). However, more in depth analysis, such as Kitz and Wilson, is required for

confirmation of this property prior to any decisive clinical implications (Kitz and Wilson, 1962).

Over the past 25 years many epidemiological studies have consistently demonstrated that increased coffee consumption by patients suffering from chronic liver disease is linked to a reduced risk of cirrhosis and a lower incidence of HCC development (Cadden et al., 2007; Torres and Harrison, 2013). Treatment with coffee also decreased liver inflammation and fibrosis in both a rat CCl_4 model (Shi et al., 2010) and murine TAA model of injury (Arauz et al., 2013). Similar effects have also been observed following the provision of caffeine alone in both the TAA model (Shim et al., 2013) and a model of ALD (Lv et al., 2010) suggesting that caffeine may be the active ingredient driving the response. A study by Olivieri and Tipton demonstrated that caffeine is also an inhibitor of the bovine form of VAP-1 (Olivieri and Tipton, 2011), which provided a possible mechanism of action of caffeine in reducing fibrosis through direct effects on VAP-1. This was supported by *in vivo* studies demonstrating inhibition of hepatic VAP-1 activity following a 25-day course of caffeine treatment in Wistar rats (Che et al., 2012). The data presented within this thesis describe a dose-dependent inhibition of both recombinant and liver tissue-derived human VAP-1 activity by caffeine for the first time, albeit with approximately forty fold lower potency compared to semicarbazide. These data also demonstrated that VAP-1 from different liver diseases exhibited similar sensitivities to inhibition by caffeine, however there was approximately 30% margin of error, which may have obscured subtle differences.

A recent study suggested that caffeic acid might interfere with peroxidase-dependent fluorometric assays such as those used by Olivieri and Tipton and within this study (Carpéné et al., 2016). Carpéné and colleagues suggested that caffeic acid prevented H_2O_2 from reacting with the chromogenic mixture thus artificially lowering the fluorescent readout and mimicking inhibition. This effect was exhibited in the nanomolar range, with almost 100% inhibition of H_2O_2 at the caffeine concentrations used within this thesis. This may suggest that this effect is either an artefact of the older Amplex Red reaction that is not present in the improved Amplex UltraRed assay, or a property of caffeic acid that is not shared with caffeine. Regardless, the careful controls used in this study suggested that any inhibition of the coupled reaction by caffeine was small relative to the effects observed on the amine oxidase-catalysed reaction. However

future confirmatory assays utilising ^{14}C-labelled benzyamine or similar systems may be required.

It is of course difficult to approximate the concentration of caffeine within the sinusoids following coffee consumption that would be available to inhibit HSEC-expressed VAP-1. An average cup of coffee contains approximately 80 mg caffeine and increases serum caffeine concentrations to approximately 10–50 μM (Lelo et al., 1986), however sinusoidal concentrations are likely to be higher due to their proximity to the gut. Patients suffering from liver disease also have decreased caffeine clearance compared to healthy controls and would therefore have higher serum concentrations with longer half-life (McDonagh et al., 1991). The lowest inhibitory concentration of caffeine used in this study, 100 μM, may represent the higher end of the theoretical physiological spectrum of sinusoidal concentrations of patients suffering from liver disease following a single cup of coffee. At this concentration VAP-1 activity was significantly decreased by approximately 20%. Serum concentrations of caffeine exceeding 500 μM are considered lethal; therefore values above this can be considered supraphysiological (Winek et al., 2001). This being said, the mechanism of caffeine inhibition of VAP-1 is still unclear, therefore a cumulative effect may occur over time without the need for high concentrations within the sinusoids. However, it is therefore unlikely that this is the sole explanation for the observed better prognosis of patients with CLD with increased coffee consumption, although it may well be a contributing factor. A likely ulterior mechanism of action is antagonism of the adenosine receptor A2a (Feld et al., 2015), which inhibits hepatic stellate cell function and subsequent fibrosis (Wang et al., 2014).

The solubility of theobromine limited the investigation into its inhibitory action on VAP-1; however there are many other physiologically relevant xanthine-derivatives that may be of interest. The majority of caffeine is metabolised by CYP450 to paraxanthine with a small minority forming theophylline, both of which may act as inhibitors of VAP-1. Interestingly, the latter is used as a treatment for conditions such as chronic obstructive pulmonary disease and asthma due to its brochodilatory effects via phosphodiesterase inhibition and adenosine receptor antagonism (Barnes, 2013). However, theophylline also appears to have several other anti-inflammatory effects including reducing lymphocytic infiltration into bronchial epithelium of asthmatics (Jaffar et al., 1996). The high expression of VAP-1 within the lungs makes this an intriguing molecule to investigate and may implicate VAP-1 in its immunomodulatory function.

Different patient cohorts were used in the LJP-1586 inhibition studies compared to the semicarbazide and caffeine studies, which resulted in distinct differences in peak non-inhibited amine oxidase activity between the data sets. In the latter cohort, VAP-1 from ALD livers exhibited considerably higher activity than the other disease groups. It is unclear whether this is patient specific or due to unrepresentative sampling of highly vascularised liver tissue. Low patient numbers during these experiments meant that the data was susceptible to statistical outliers. However, a clear difference was highlighted between normal and chronically diseased tissue, which will hopefully power future studies to determine statistically significant differences within a robust dataset.

3.3.4 Chapter summary

The data presented here are consistent with the current knowledge of the hepatic localisation of VAP-1. They also illustrate the complex nature of liver disease and how variable the activity and expression of VAP-1 is across the spectrum of disease. Changes in VAP-1 expression and activity in patients with chronic liver disease were clear, although the data suggest that changes are common between all liver disease aetiologies and do not appear to be disease-specific. Fluctuations in VAP-1 function during disease are therefore likely dictated by factors that are also not disease-specific, such as extent of fibrosis, extent of inflammatory infiltrate or changes occurring prior to end-stage disease. Similarly, activity of VAP-1 expressed in chronically diseased liver tissue and sensitivity to inhibition are similar to that of normal tissue, implying little or no modification occurs to the molecule itself during the disease states. One exception is VAP-1 isolated from NANB livers, which differed in terms of sensitivity to inhibition but this requires further examination and extension to other acute liver injury settings such as POD to fully elucidate. These data show that VAP-1 inhibition may be a successful therapy across liver diseases and is not limited to those currently under clinical trial, such as PSC. VAP-1 from all livers tested was also sensitive to inhibition by physiological levels of caffeine, providing a potential contributory factor for the hepatoprotective effects previously documented.

4

THE ROLE OF VAP-1 IN LEUKOCYTE FUNCTION

4.1 Introduction

VAP-1 was first identified as a surface-expressed molecule capable of mediating lymphocyte binding to HEV (Salmi and Jalkanen, 1992) but has since been implicated in the adhesion of a variety of leukocytes to many other human tissues including ischemic heart (Jaakkola et al., 2000), inflamed skin (Arvilommi et al., 1996) and the gut (Salmi et al., 1993). The expression of VAP-1 by HSEC has also led to several investigations into its adhesive function within the sinusoids of the liver. Initial experiments clearly demonstrated that antibody blockade of VAP-1 reduced adhesion of lymphocytes to frozen liver tissue sections (McNab et al., 1996). However, only one study to date has been able to replicate these findings using cultured human HSEC under flow conditions (Lalor et al., 2002). The most recent of which found that VAP-1 antibody blockade had no impact at all on lymphocyte adhesion to HSEC (Tuncer et al., 2013)

whereas other studies have suggested that while total adhesion is unaffected, the fraction of transmigrated cells is reduced (Edwards et al., 2005; Lalor et al., 2007; Shetty et al., 2011). This may be due to functional differences in VAP-1 expressed by different tissues, for example smooth muscle-derived VAP-1 does not appear to interact with lymphocytes (Jaakkola et al., 1999). Tissue-specific differences in the adhesive function of VAP-1 may also explain the somewhat contradictory literature on which leukocyte subsets are recruited by VAP-1. For example anti-VAP-1 antibody does not significantly reduce the adhesion of neutrophils to human tonsil HEV (Salmi and Jalkanen, 1992), whereas adhesion of the same cell population to human myocardial endothelium is reduced by 60% (Jaakkola et al., 2000). Furthermore, inhibition of VAP-1 amine oxidase activity with SMIs has also been reported to reduce leukocyte adhesion to a variety of tissues, although there is no apparent synergistic or additive effect exhibited upon combined inhibition (Koskinen et al., 2004; Lalor et al., 2002; Marttila-Ichihara et al., 2006; Salmi et al., 2001). This highlights a clear need for thorough investigation into the tissue-specific activity of VAP-1 and its role in leukocyte-endothelium interactions, particularly due to the potential therapeutic value of VAP-1 inhibition for inflammatory conditions. VAP-1 evidently has an intimate relationship with leukocytes due to its function as an adhesion molecule, however studies of VAP-1 expression by hematopoietic cells have been largely absent. The first paper describing VAP-1 demonstrated a lack of *AOC3* expression in a series of leukocyte cell lines by flow cytometric analysis and very little follow up work has been conducted since, highlighting a clear gap in our current understanding (Salmi and Jalkanen, 1992).

In this chapter, the adhesive functionality of hepatic VAP-1 is interrogated to determine not only an insight into the mechanistic functions of VAP-1-mediated adhesion, but also the leukocyte specificity (if any) afforded by expression of the adhesin, and the role soluble VAP-1 may play in this process. As a consequence of these studies this chapter then focuses on the expression of VAP-1 by neutrophils and the functional significance of this finding.

4.2 Results

4.2.1 VAP-1 and hepatic leukocyte recruitment

4.2.1.1 Effect of VAP-1 inhibition on lymphocyte recruitment to HSEC

Flow-based adhesion assays are a useful tool for examining leukocyte-endothelial interactions *in vitro* by closely replicating conditions experienced *in vivo*. During the assay leukocytes are flowed over endothelium and the interactions between the cells are observed in real time by phase-contrast microscopy. Leukocytes that interact with the endothelial monolayer are classified as rolling, firmly adherent (round), transmigrating (shape-changed light or dark as they progress) or fully transmigrated across the monolayer. In order to effectively model the inflamed liver microenvironment, peripheral blood lymphocytes (PBLs) or subsets thereof were flowed over TNFα-stimulated HSEC at a low flow rate comparable to that within the hepatic sinusoids (0.05 Pa, or 0.5 dyne/cm^2). HSEC were pretreated with inhibitors of VAP-1 prior to the assay to elucidate its involvement in the hepatic lymphocyte adhesion cascade.

Antibody blockade of endothelial VAP-1 using the well-described function blocking clone TK8-14 did not yield any change in the proportion of adherent PBLs compared to IMC (Figure 4.1A) nor did it affect the distribution of cells that were round, shape-changed or transmigrated (Figure 4.1B). Inhibition of VAP-1 amine oxidase activity with either semicarbazide or caffeine also had no effect on total PBL adhesion (Figure 4.1A). The number of round cells was decreased by approximately 30% upon inhibition with either semicarbazide or caffeine, although this was not statistically significant (Figure 4.1C and 4.1D). Semicarbazide and caffeine did not have detrimental effects on HSEC viability at the concentrations used within the assay (250 μM and 200 μM, respectively), however caffeine caused cell death at higher concentrations as measured by live cell imaging (Figure 4.2).

4.2.1.2 Effect of serum on lymphocyte recruitment to HSEC

Flow-based adhesion assays are routinely carried out using HSEC growth media, which is supplemented with heat-inactivated human serum (56°C for 30 minutes), vascular endothelial growth factor and hepatocyte growth factor (Curbishley et al., 2005; Edwards et al., 2005; Lalor et al., 2007). The addition of serum provides the cells with a large

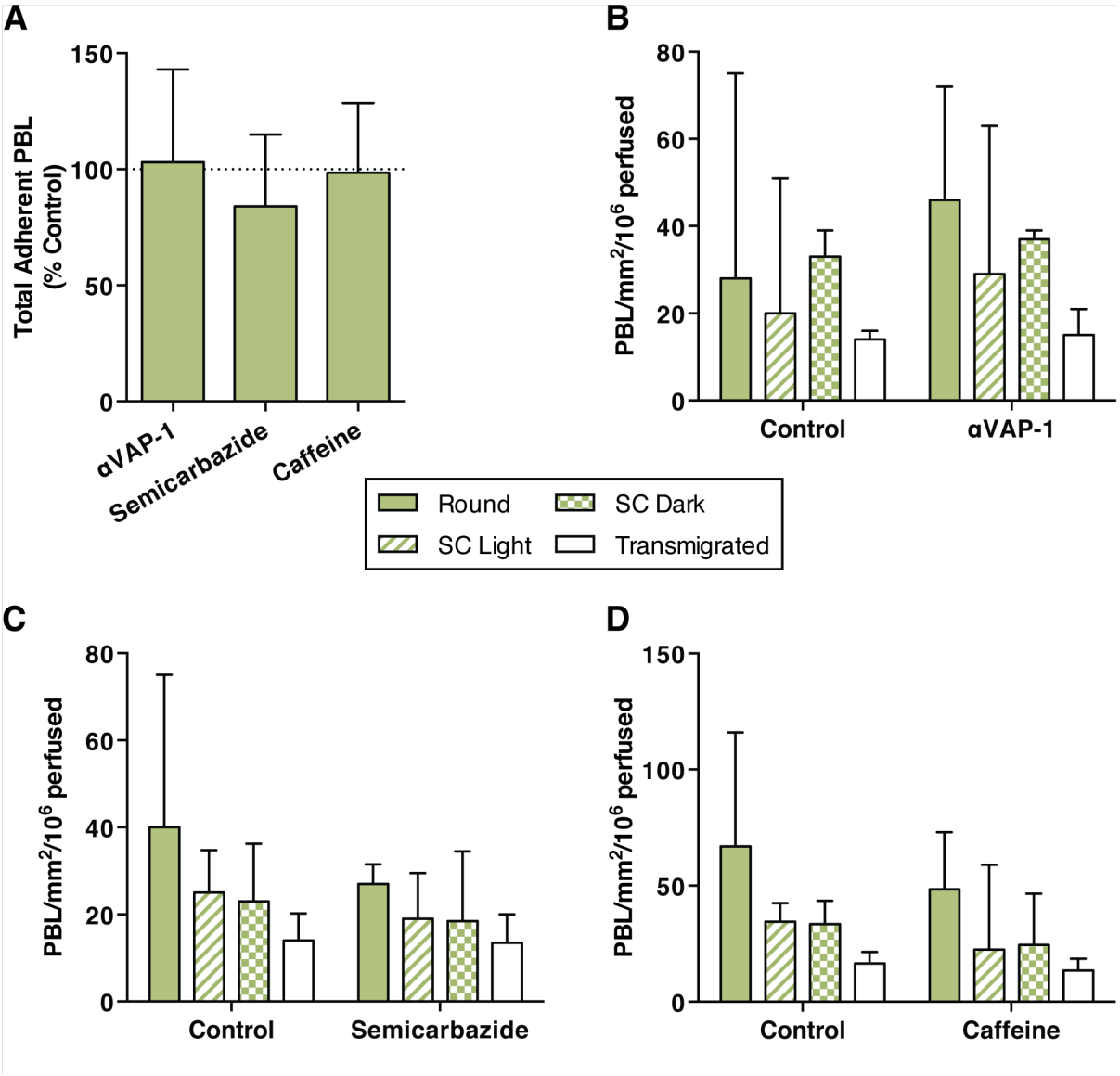


Figure 4.1 Effect of VAP-1 inhibition on adhesion of PBLs to stimulated HSEC. PBLs were perfused over TNFα-stimulated HSEC at a shear flow rate comparable to that within the sinusoids. (**A**) The total number of adherent cells was assessed following 20 min treatment with anti-VAP-1 antibody (TK8-14, 10 μg/mL) or the amine oxidase inhibitors semicarbazide (250 μM) and caffeine (250 μM). Extent of leukocyte migration was quantified as either round (adherent), shape-changed (SC) light or dark (transmigrating) or transmigrated in the presence of (**B**) anti-VAP-1 antibody (TK8-14, 10 μg/mL), (**C**) semicarbazide (250 μM) or (**D**) caffeine (200 μM) compared to isotype-matched (**A**) or media (**C** & **D**) control (*n* = 3-5 different PBL and HSEC donors; 10-12 fields of view each). Data shown as median (IQR) and were analysed by KW test with Dunn's post-hoc correction (**A**) and two-way ANOVA with Holm-Sidak post-hoc correction (**B**, **C** & **D**). All nonsignificant from control.

proportion of the nutrients required for normal functioning, however it is an ill-defined mixture of many components with large batch variability (Brunner et al., 2010). Furthermore, this serum is likely to provide a form of VAP-1, although to the author's knowledge this has not been assessed. Flow-based adhesion assays were therefore used to discern whether the presence of this serum was important for lymphocyte recruitment

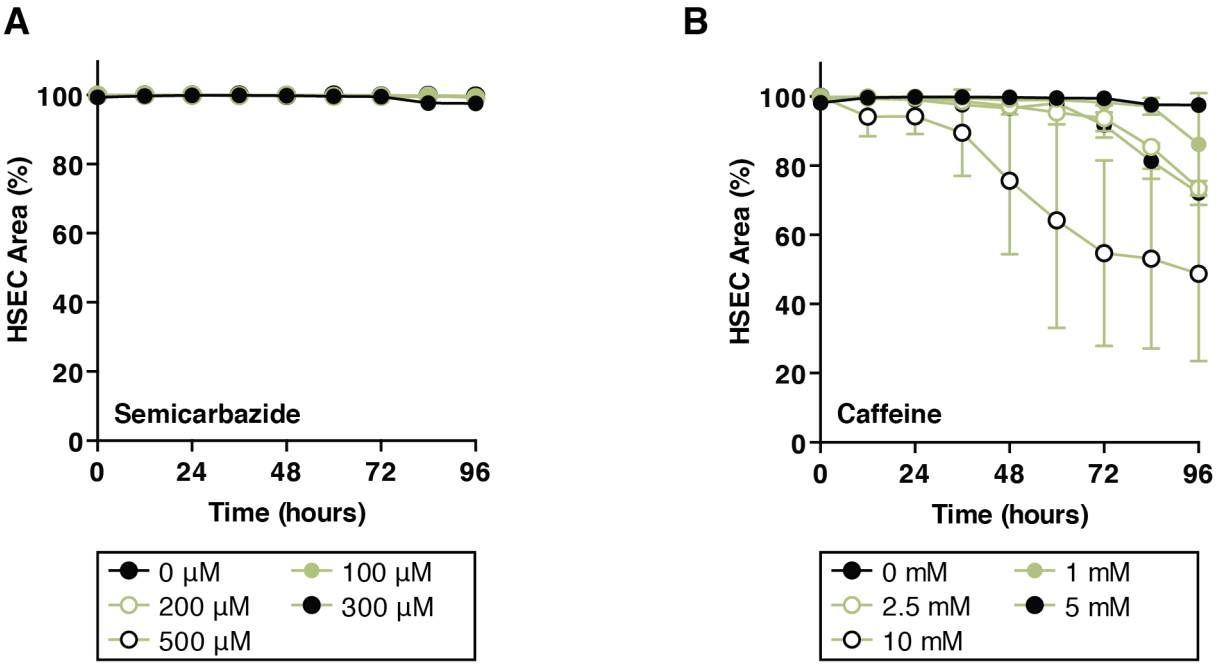


Figure 4.2 HSEC viability in the presence of VAP-1 inhibitors. Confluent HSEC monolayers were incubated with different concentrations of (**A**) semicarbazide or (**B**) caffeine in complete HSEC media for 96 hours in a CellIQ machine. Viability was assessed every 12 hours by calculating the total area covered by HSEC in each field of view ($n = 2$). Data shown as mean (SD).

to HSEC and in particular, the function of VAP-1. All assays were carried out with identical flow media consisting of BSA-supplement basal media.

HSEC cultured in media supplemented with human serum (HS) or foetal calf serum (FCS) for 24 hours prior to assaying supported the adhesion of over three times as many PBLs than HSEC treated with bovine serum albumin (BSA) (Figure 4.3A). Low numbers of PBLs also adhered to HSEC cultured in serum-free optimized leukocyte media commonly used to maintain GMP-grade cell preparations, although still over twice as many as BSA alone (TexMACS). Treatment of HSEC with blocking antibodies against VAP-1 and VCAM-1 elicited comparable non-significant reductions in PBL adhesion in both serum-containing media and TexMACS (Figure 4.3B). The proportion of PBLs that underwent complete transmigration was greatest across HSEC supplemented with human serum or BSA (approximately 25%) compared to FCS or TexMACS (Figure 4.3C).

Culture of HSEC with media supplemented with 10% FCS, BSA or TexMACS exhibited reduced viability after 24 hours (Figure 4.4A), however this effect was mitigated by supplementing the media with growth factors (Figure 4.4B).

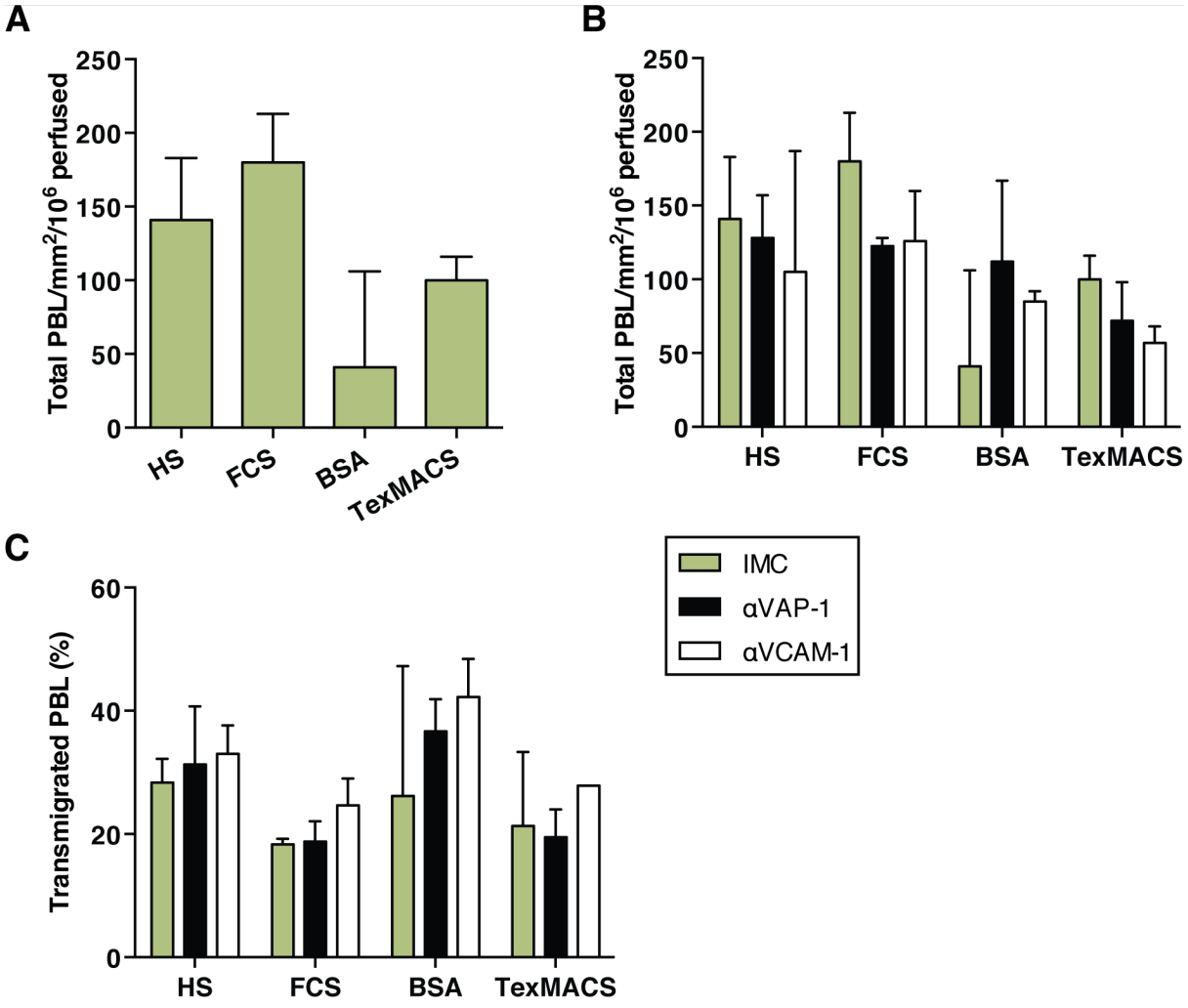


Figure 4.3 Effect of media on adhesion of PBLs to stimulated HSEC. PBLs were perfused over TNFα-stimulated HSEC at a shear flow rate comparable to that within the sinusoids. (**A**) The total number of adherent cells was assessed following culture in either TexMACS serum-free media or endothelial serum-free media supplemented with human serum (HS, 10%), foetal calf serum (FCS, 10%) or bovine serum albumin (BSA, 0.5%). (**B**) Extent of leukocyte adhesion or (**C**) proportion of cells that underwent transmigration was quantified following 20 min treatment with anti-VAP-1 antibody (TK8-14, 10 μg/mL) or anti-VCAM-1 antibody (10 μg/mL) compared to isotype-matched control (IMC). All media was supplemented with VEGF and HGF growth factors (n = 3 different PBL and HSEC donors; 10-12 fields of view each). Data shown as median (IQR) and were analysed by KW test with Dunn's post-hoc correction (**A**) and two-way ANOVA with Holm-Sidak post-hoc correction (**B** & **C**). All nonsignificant from IMC.

4.2.1.3 Effect of VAP-1 inhibition on recruitment of leukocyte subsets

Inhibition of VAP-1 had no significant effect on the adhesion of mixed PBL populations to HSEC. The studies were therefore extended to determine whether inhibition affected the adhesion of $CD4^+$ lymphocytes, $CD8^+$ lymphocytes, NK cells or neutrophils individually; cell subsets that have previously been shown to use VAP-1 for recruitment

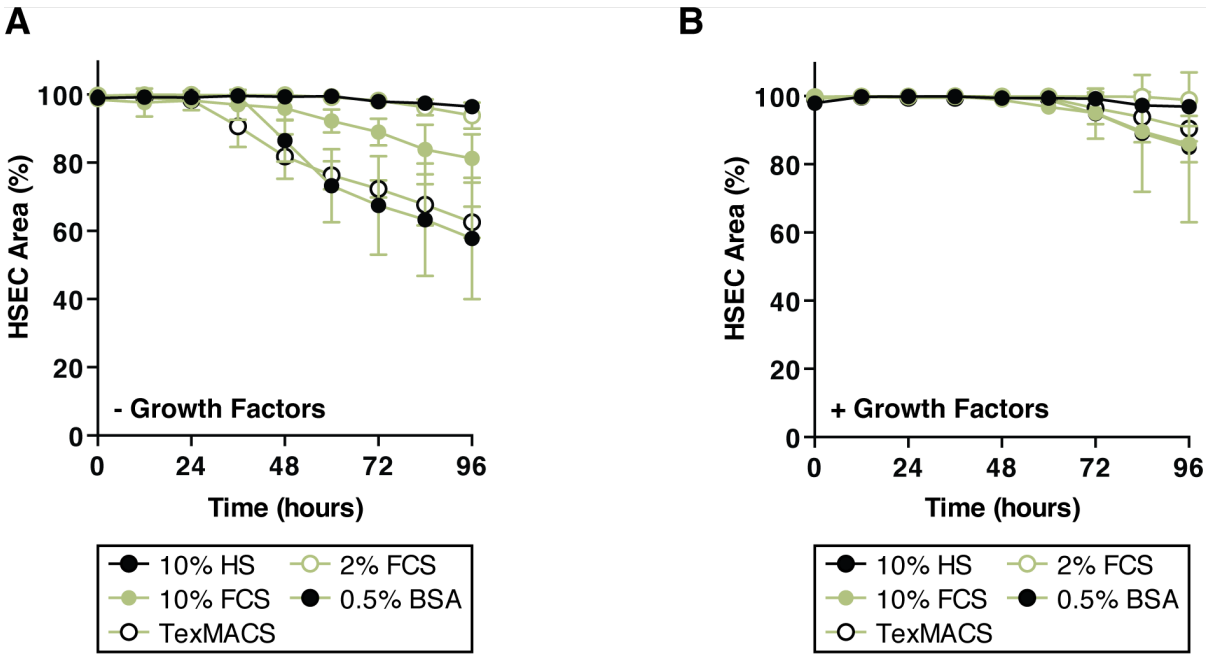


Figure 4.4 HSEC viability in the presence of different culture media. (**A**) Confluent HSEC monolayers were cultured in either TexMACS serum-free media or endothelial serum-free media supplemented with human serum (HS, 10%), foetal calf serum (FCS, 2% or 10%) or bovine serum albumin (BSA, 0.5%) for 96 hours in a CellIQ machine. (**A**) Media either did not contain growth factors or (**B**) was supplemented with VEGF (10 µg/mL) and HGF (10 µg/mL). Viability was assessed every 12 hours by calculating the total area covered by HSEC in each field of view (n = 3). Data shown as mean (SD).

in human *in vitro* studies or animal models. Flow-based adhesion assays were used to study these purified leukocyte subsets in isolation to highlight any effects that may have been previously obscured. Inhibition of VAP-1 with a function-blocking antibody, LJP-1586 or both did not significantly alter the total adhesion of any of the leukocyte subsets (Figure 4.5). Treatment with anti-VCAM-1 antibody reduced adhesion of T cells by approximately 40%, although this was not statistically significant. Similarly, none of the treatments significantly altered the proportion of cells that were rolling, round, transmigrating or fully transmigrated (Figure 4.6). Both anti-VAP-1 and LJP-1586 treatment did, however, lower the number of shape-changed transmigrating neutrophils non-significantly (Figure 4.6D).

To determine whether the leukocyte subsets were capable of binding to VAP-1, each cell population was also flowed over recombinant protein adsorbed onto ibidi flow chambers in place of the endothelial monolayer, using similar flow media to cell-based assays. $CD4^+$ and $CD8^+$ lymphocytes and NK cells adhered to recombinant VCAM-1 (rVCAM-1) but not recombinant VAP-1 (rVAP-1) in isolation (Figure 4.7). The addition of rVAP-1 in

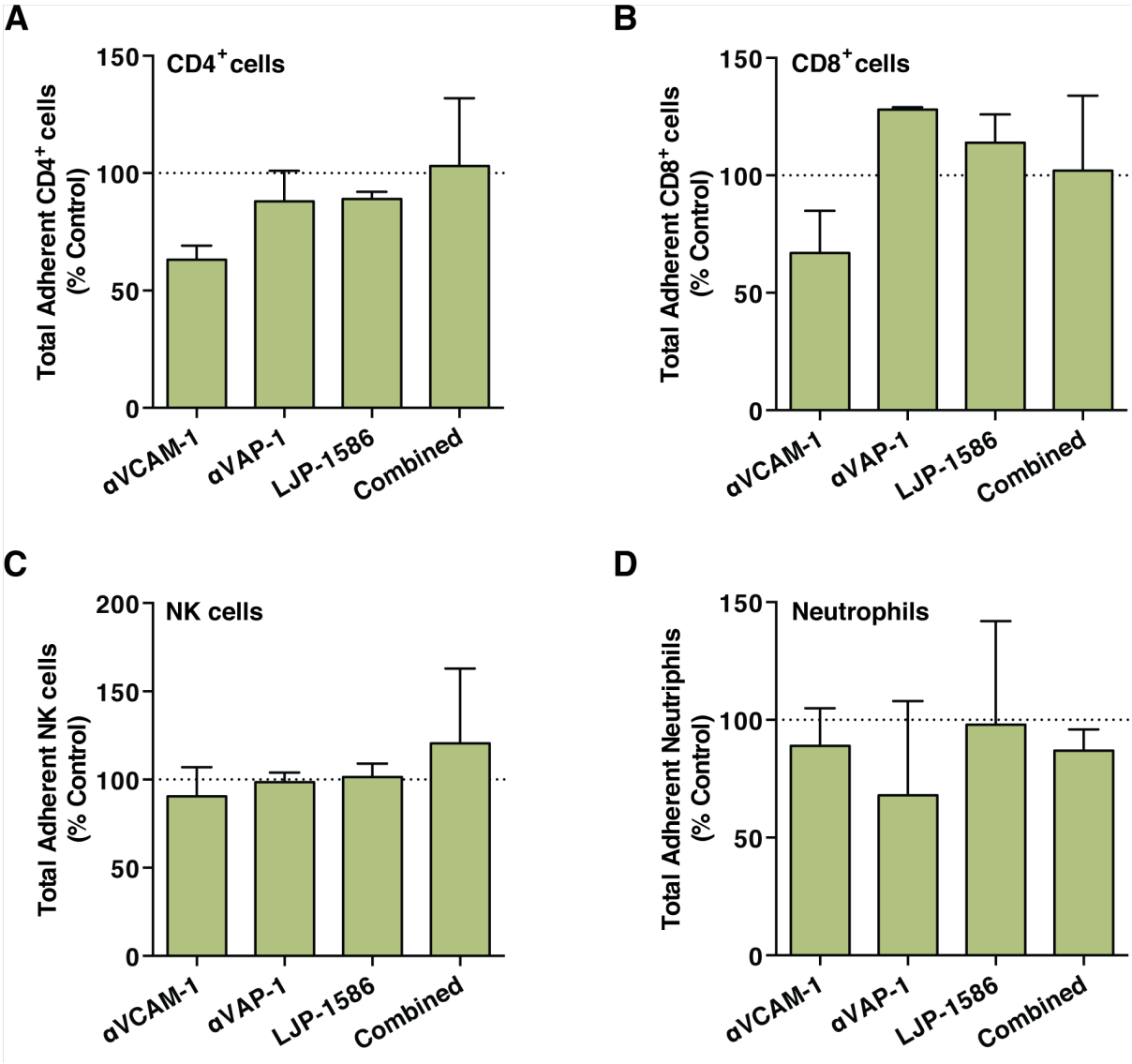


Figure 4.5 Effect of VAP-1 inhibition on adhesion of leukocyte subsets to stimulated HSEC. (**A**) $CD4^+$ lymphocytes, (**B**) $CD8^+$ lymphocytes, (**C**) NK cells or (**D**) neutrophils were perfused over TNFα-stimulated HSEC at a shear flow rate comparable to that within the sinusoids. The total number of adherent cells was assessed following 20 min treatment with: anti-VCAM-1 antibody (10 µg/mL); anti-VAP-1 antibody (TK8-14, 10 µg/mL); the VAP-1-specific amine oxidase inhibitor LJP-1586 (500 nM); or TK8-14 and LJP-1586 combined (n = 3 different leukocyte and HSEC donors; 10-12 fields of view each). Results were normalised to control containing mouse IgG_1 and IgG_{2a}. Data shown as median (IQR) and were analysed by KW test with Dunn's post-hoc correction. All nonsignificant from control.

combination with rVCAM-1 also exerted no additive effect on adhesion, and in fact when added sequentially adhesion was diminished. This may have been due to rVAP-1 occupying area that may have been otherwise filled with VCAM-1. The proportion of cells that were rolling, round or shape-changed also remained unchanged for these cells in each lane (Figure 4.8). However, neutrophils were capable of binding to rVAP-1, with

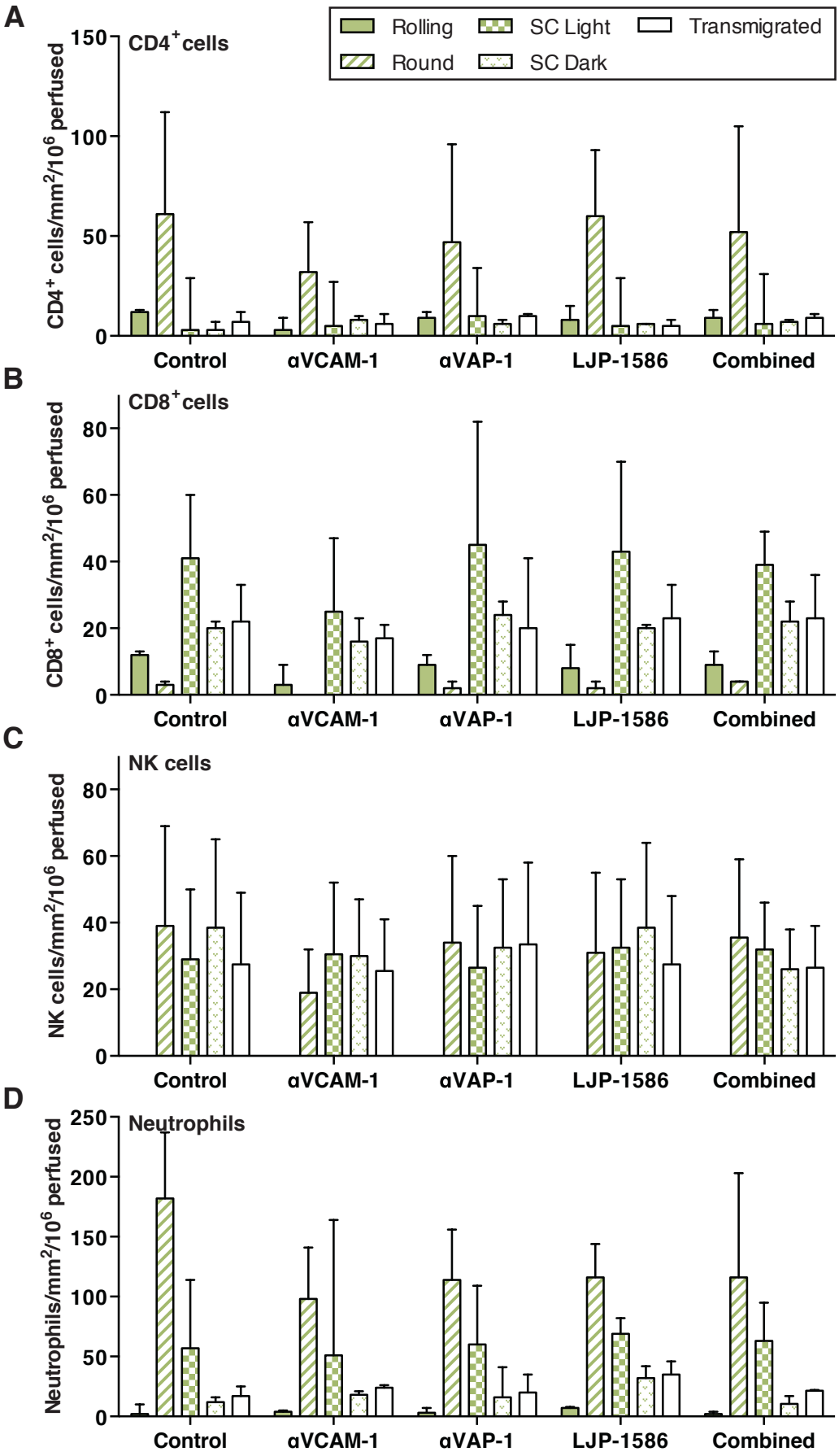

A
CD4+cells
Rolling
Round
SC Light
SC Dark
Transmigrated
CD4+ cells/mm2/10^6 perfused
150
100
50
0
Control
αVCAM-1
αVAP-1
LJP-1586
Combined
B
CD8+cells
CD8+ cells/mm2/10^6 perfused
80
60
40
20
0
Control
αVCAM-1
αVAP-1
LJP-1586
Combined
C
NK cells
NK cells/mm2/10^6 perfused
80
60
40
20
0
Control
αVCAM-1
αVAP-1
LJP-1586
Combined
D
Neutrophils
Neutrophils/mm2/10^6 perfused
250
200
150
100
50
0
Control
αVCAM-1
αVAP-1
LJP-1586
Combined

Figure 4.6 Effect of VAP-1 inhibition on migration of leukocyte subsets across stimulated HSEC. (**A**) $CD4^+$ lymphocytes, (**B**) $CD8^+$ lymphocytes, (**C**) NK cells or (**D**) neutrophils were perfused over TNFα-stimulated HSEC at a shear flow rate comparable to that within the sinusoids Extent of leukocyte migration was quantified as either round (adherent), shape-changed (SC) light or dark (transmigrating) or transmigrated following 20 min treatment with: anti-VCAM-1 antibody (10 µg/mL); anti-VAP-1 antibody (TK8-14, 10 µg/mL); the VAP-1-specific amine oxidase inhibitor LJP-1586 (500 nM); or TK8-14 and LJP-1586 combined (n = 3 different leukocyte and HSEC donors; 10-12 fields of view each). Results were normalised to control containing mouse IgG_1 and IgG_{2a}. Data shown as median (IQR) and were analysed by two-way ANOVA with Holm-Sidak post-hoc correction. All nonsignificant from IMC.

similar numbers of cells adhering to rVCAM-1 and rVAP-1 as seen in Figure 4.7D (93 cells/mm^2/10^6 perfused (70 – 132 cells/mm^2/10^6 perfused) and 86 cells/mm^2/10^6 perfused (63 – 112 cells/mm^2/10^6 perfused) to rVCAM-1 and rVAP-1, respectively). There were also a higher proportion of shape-changed neutrophils in all three of the rVAP-1-containing lanes compared to rVCAM-1 alone, indicative of a more activated phenotype (Figure 4.8D). Similarly to other cell types, no additive effect was observed when rVAP-1 and rVCAM-1 were applied in combination. However, unlike the other cells, neutrophils almost adhered equally as well when the adhesion molecules were added sequentially, possibly indicating mechanistic contribution from both proteins.

4.2.1.4 Effect of TNFα on VAP-1 expression by HSEC

To investigate why neutrophils are capable of binding rVAP-1 but were not affected by VAP-1 blockade or inhibition, the expression of VAP-1 by HSEC observed in Chapter 3 was examined further. qPCR analysis found that expression of *AOC3* mRNA was lower in HSEC stimulated with the proinflammatory cytokines TNFα and IFNϒ (Figure 4.9A). This effect was not

replicated at the protein level by Western Blot analysis, however differences in loading controls may have obscured these results (Figure 4.9B). The amine oxidase activity of VAP-1 present in lysates of TNFα-stimulated HSEC was also lower than that of unstimulated cells (Figure 4.9C). These data, while not conclusive, suggest that VAP-1 may be downregulated in HSEC upon stimulation with pro-inflammatory mediators.

4.2.1.5 Transfection of HSEC with GFP-VAP-1

To further investigate the role of VAP-1 in leukocyte migration, HSEC were transfected with a plasmid encoding an N-terminal green fluorescent protein (GFP)-VAP-1 fusion

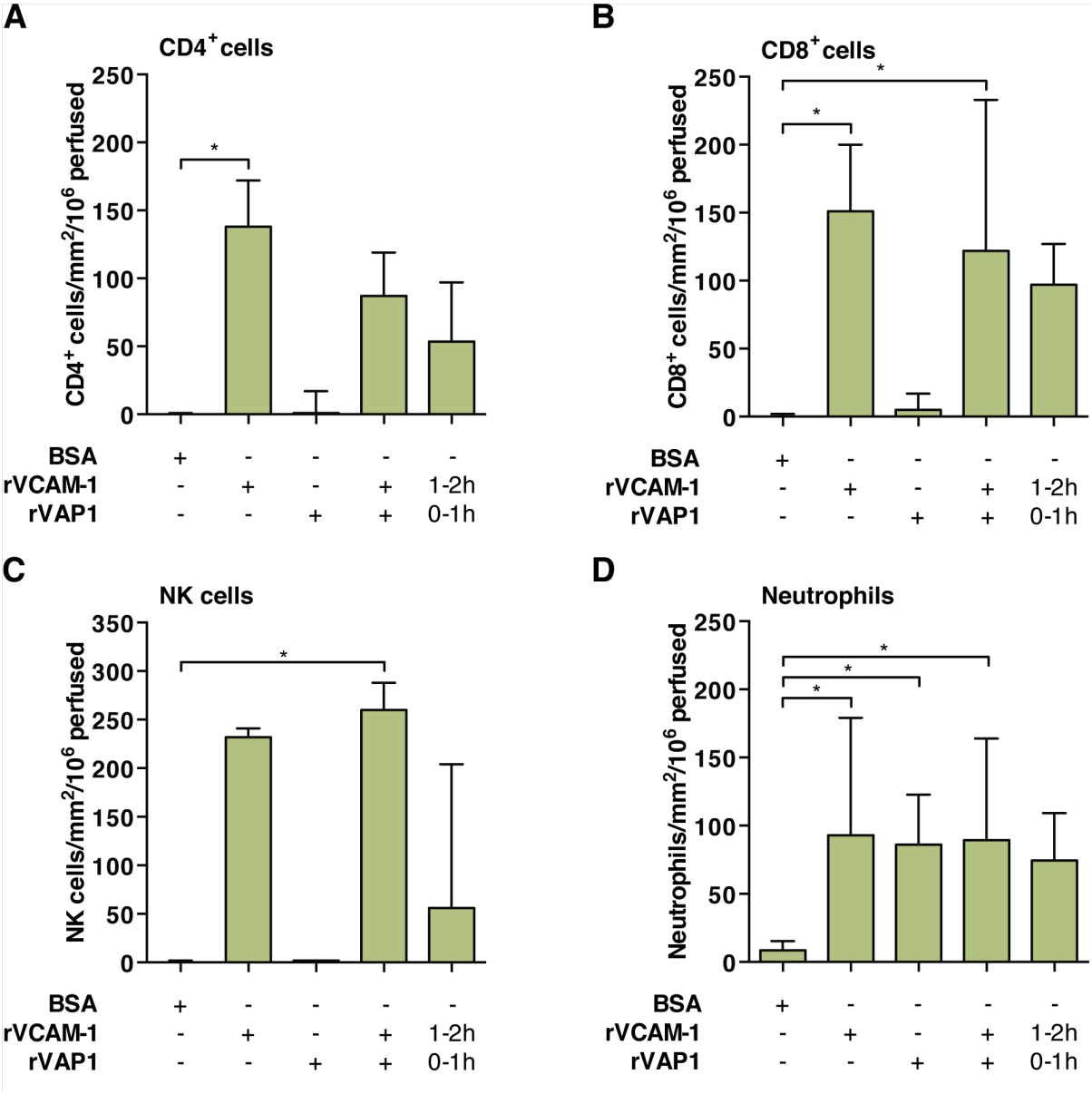


Figure 4.7 Adhesion of leukocyte subsets to recombinant adhesion molecules. (**A**) $CD4^+$ lymphocytes, (**B**) $CD8^+$ lymphocytes, (**C**) NK cells or (**D**) neutrophils were perfused over recombinant protein at a shear flow rate comparable to that within the sinusoids and total number of adherent cells assessed. Lanes were coated with: 1% BSA; recombinant human VCAM-1 (10 µg/mL); recombinant human VAP-1 (10 µg/mL); rVCAM-1 (10 µg/mL) and rVAP-1 (10 µg/mL) combined; or coated for one hour with rVAP-1 (10 µg/mL), washed and incubated for an additional hour with rVCAM-1 (10 µg/mL). All lanes were blocked with BSA (1%, 30 min) prior to assay (n = 3-4 different donors; 10-12 fields of view each). Data shown as median (IQR) and were analysed by KW test with Dunn's post-hoc correction. * $p \leq 0.05$.

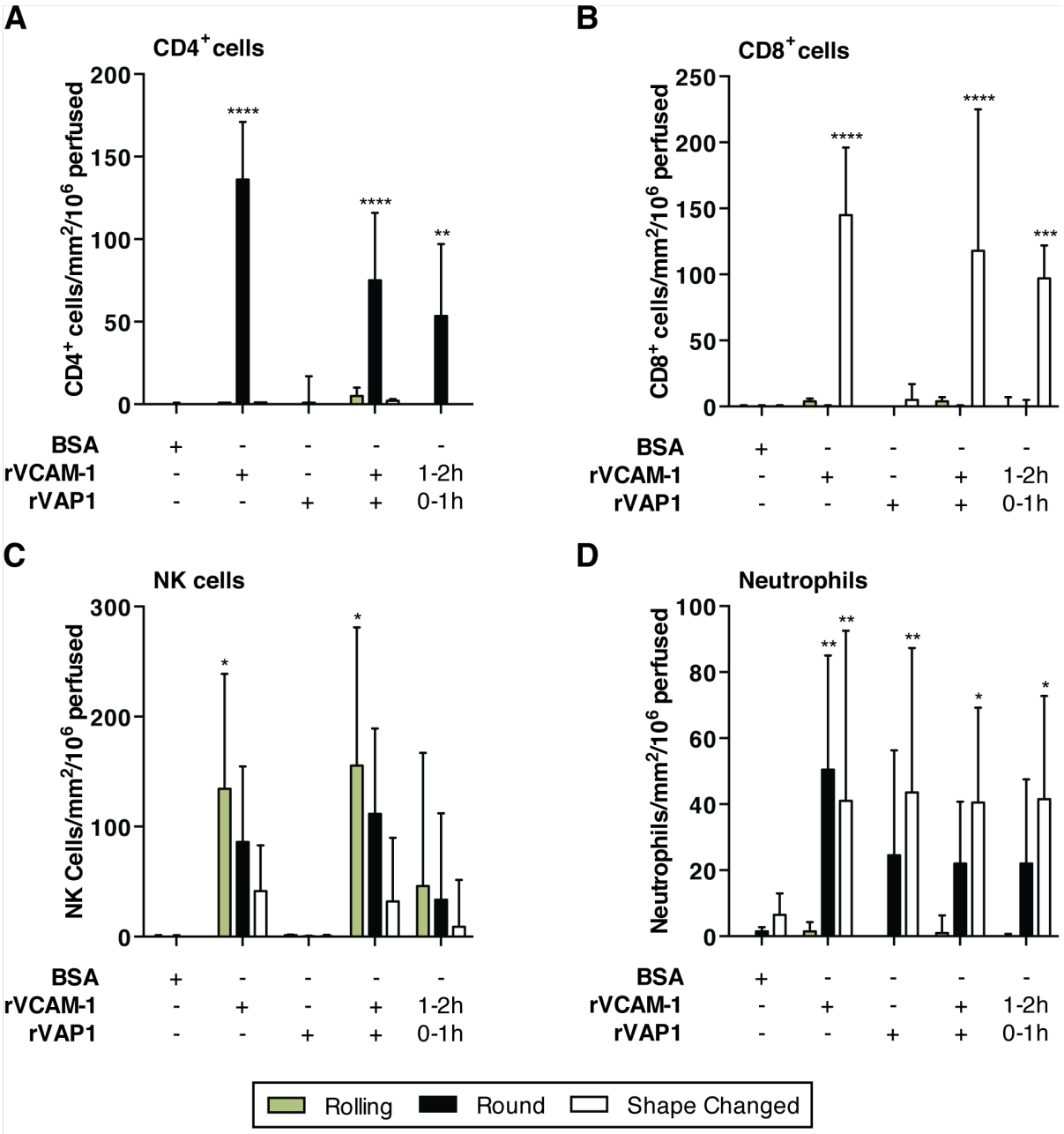


Figure 4.8 Interaction of leukocyte subsets with recombinant adhesion molecules. (**A**) $CD4^+$ lymphocytes, (**B**) $CD8^+$ lymphocytes, (**C**) NK cells or (**D**) neutrophils were perfused over recombinant protein at a shear flow rate comparable to that within the sinusoids and total proportion of cells rolling, adherent (round) or adherent and shape-changed was assessed. Lanes were coated with: 1% BSA; recombinant human VCAM-1 (10 µg/mL); recombinant human VAP-1 (10 µg/mL); rVCAM-1 (10 µg/mL) and rVAP-1 (10 µg/mL) combined; or coated for one hour with rVAP-1 (10 µg/mL), washed and incubated for an additional hour with rVCAM-1 (10 µg/mL). All lanes were blocked with BSA (1%, 30 min) prior to assay (n = 3-4 different donors; 10-12 fields of view each). Data shown as median (IQR) and were analysed by two-way ANOVA with Holm-Sidak post-hoc correction. * $p \leq 0.05$, ** $p \leq 0.01$, *** $p \leq 0.001$, **** $p \leq 0.0001$.

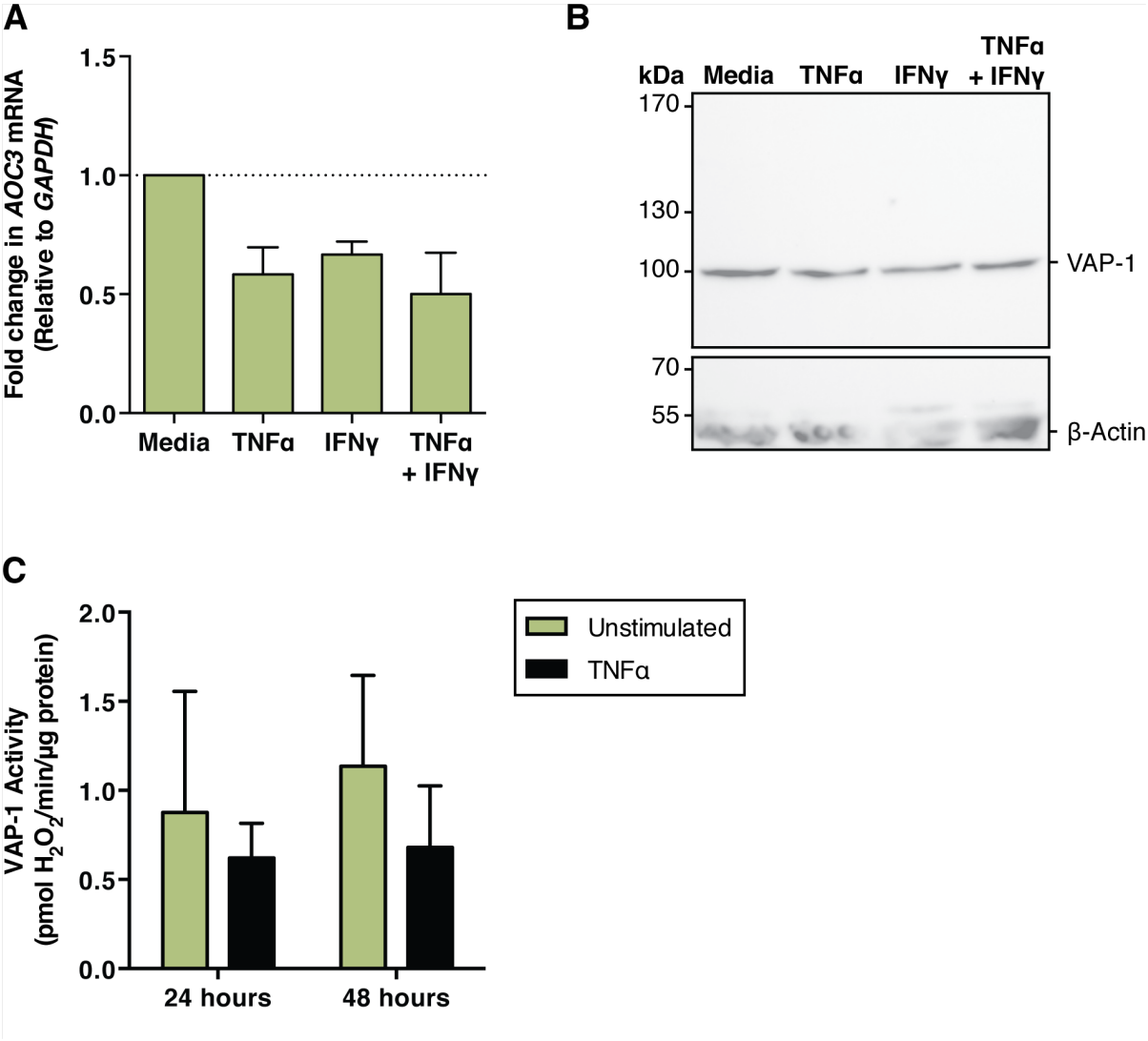


Figure 4.9 Effect of proinflammatory stimulation on HSEC VAP-1 expression. HSEC were stimulated for 24 hours with TNFα (10 ng/mL), IFNγ (10 ng/mL) or both in combination (10 ng/mL each) and subsequently analysed for (**A**) *AOC3* mRNA expression by qPCR and (**B**) VAP-1 protein expression by Western Blot analysis. (**B**) Unstimulated HSEC or those stimulated with TNFα (10 ng/mL) for 24 or 48 hours were lysed and VAP-1 amine oxidase activity assessed by antibody capture Amplex UltraRed assay (*n* = 3 different HSEC donors). Data shown as median (IQR) and were analysed by KW test with Dunn's post-hoc correction (**A**) and two-way ANOVA with Holm-Sidak post-hoc correction (**C**). All nonsignificant from unstimulated control.

protein. Endotoxin free plasmids encoding two forms of GFP-labelled VAP-1 were used: wild-type GFP-VAP-1^{WT} and an enzymatically inactive form, GFP-VAP-1^{Y471F}, created through a point mutation of the active site tyrosine. Cells were transfected using 5 ng of VAP-1 plasmid or 2 ng of positive control plasmid, pmaxGFP, per 10^6 cells via electroporation-based nucleofection using a Nucleofector 2b device. Several nucleofection programs, varying in pulse shape and duration, were recommended by Lonza for the transfection of HSEC and were subsequently assessed for transfection frequency and

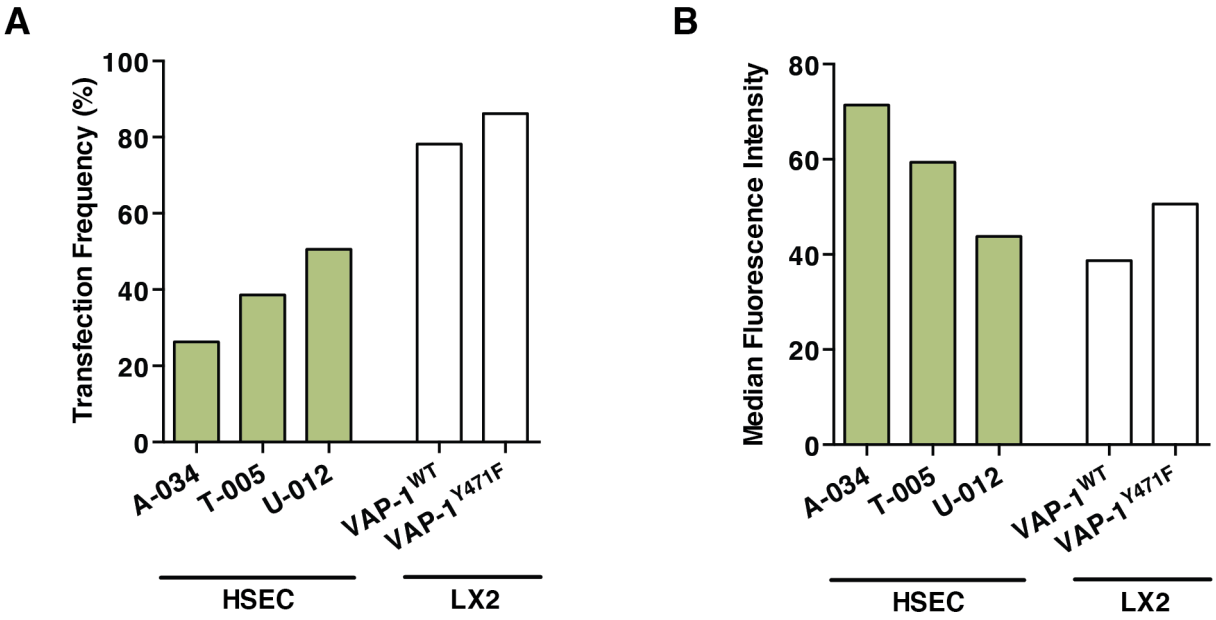
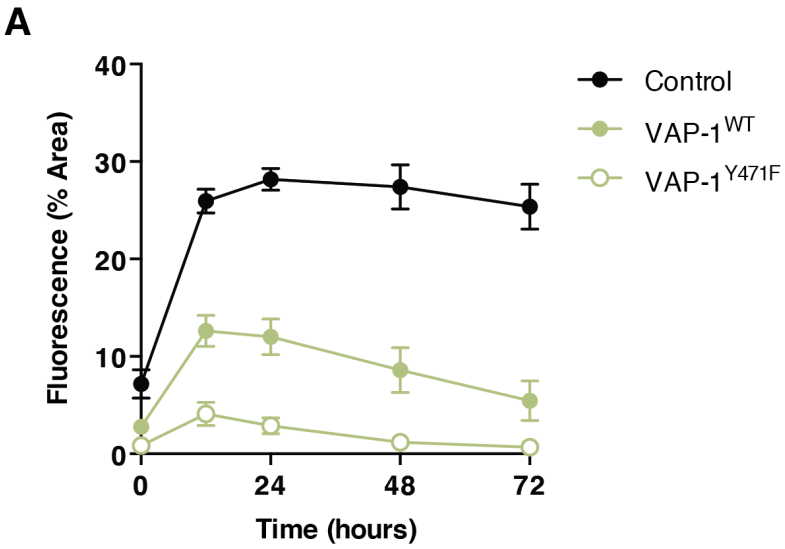


Figure 4.10 Optimisation of HSEC nucleofection with GFP-VAP-1. HSEC were nucleofected with GFP-VAP-1^{WT} plasmid using protocols A-034, T-005 or U-012 and evaluated by flow cytometry to characterise (**A**) frequency of transfection and (**B**) median fluorescence intensity. These were compared to stably-transfected LX2 cell lines. All cells were gated on the live population prior to analysis of nucleofection efficiency (n = 1).

fluorescence intensity via flow cytometry after 24 hours (Figure 4.10). All cells were gated on the live population prior to analysis of nucleofection efficiency. Program T-005 was deemed most appropriate as it demonstrated a good compromise between frequency (38.6%) of transfection and intensity of the expressed product. The stably transfected LX2 HSC cell line population, which had been selected for uptake of plasmid via blasticidin resistance, exhibited approximately 80% positivity. The non-selected HSEC therefore demonstrated lower transfection efficiencies than these values across all nucleofection programs, although mean fluorescence intensity was 1.53 times greater. Unlike the LX2 cell line, HSEC were not stably transfected with either of the GFP-VAP-1 plasmids: fluorescence peaked at approximately 12 hours after nucleofection but steadily decreased thereafter (Figure 4.11). Cells transfected with GFP-VAP-1^{WT} exhibited a higher peak fluorescent area than GFP-VAP-1^{Y471F}, indicative of a higher transfection rate, higher levels of expression, or both (Figure 4.11A).

To confirm that the transfected VAP-1 was catalytically active in these cells the activity of surface exposed membrane-bound VAP-1 was measured via Amplex UltraRed assay after fixing the transfected cells without permeabilisation (Figure 4.12). Amine oxidase activity was determined with and without the presence of semicarbazide and the


A
Fluorescence (% Area)
40
30
20
10
0
0
24
48
72
Time (hours)
Control
VAP-1WT
VAP-1Y471F

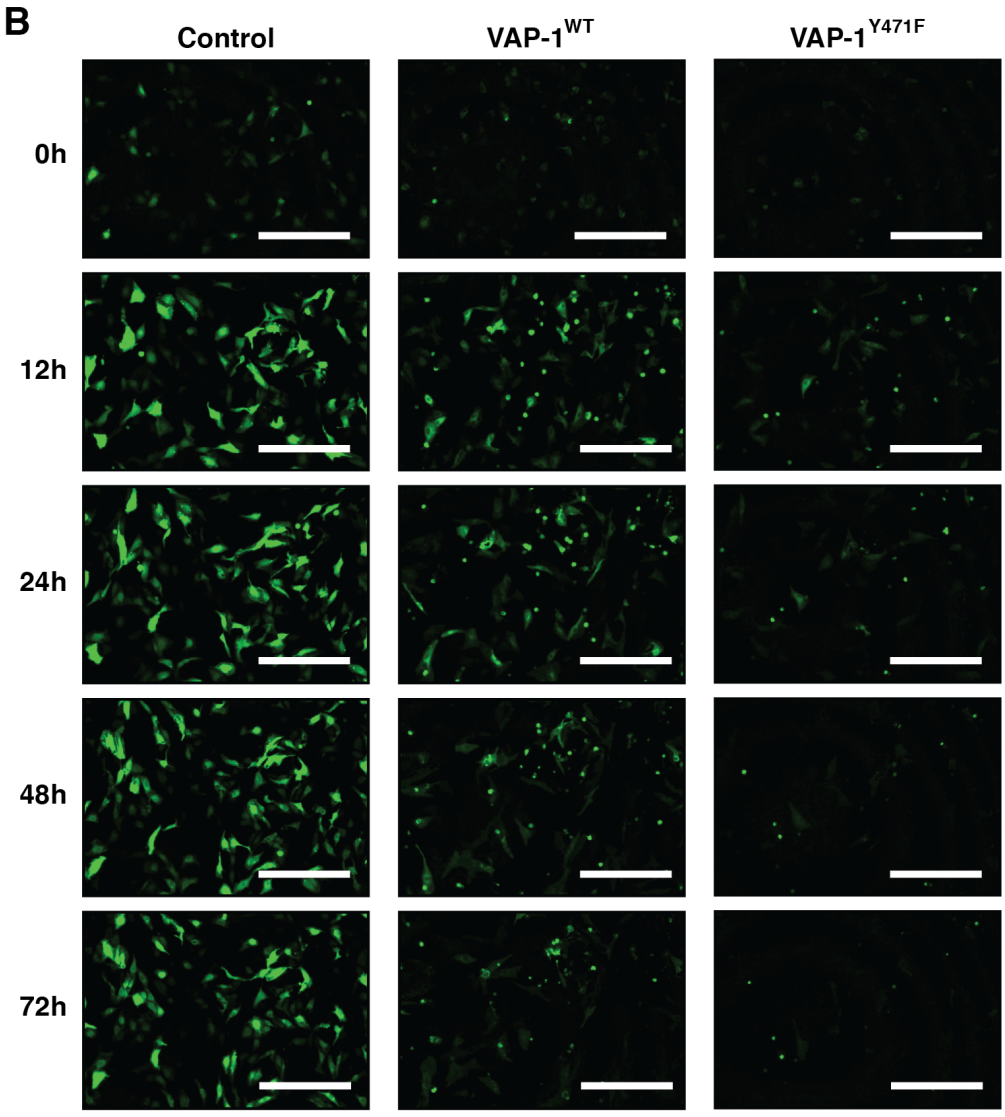

B
Control
VAP-1WT
VAP-1Y471F
0h
12h
24h
48h
72h

Figure 4.11 HSEC expression of GFP-VAP-1 over time. HSEC were nucleofected with plasmids encoding GFP-VAP-1^{WT}, GFP-VAP-1^{Y471F} or pmaxGFP control and expression evaluated by fluorescence imaging up to 72 hours post-transfection. (**A**) Quantification of total fluorescence area of (**B**) fluorescent images (n = 4). Data shown as mean (SD). White bar: 400 µm.

difference between these values was described as VAP-1 activity (semicarbazide-corrected activity). Endothelial cells have been proposed as a source of soluble VAP-1 (Stolen et al., 2004); therefore it was of interest to assess whether transfected VAP-1 was released from the overexpressing cells. This was achieved by measuring the VAP-1 activity of transfected cell-conditioned media by antibody-capture Amplex UltraRed assays, also semicarbazide-correcting for additional specificity. A human embryonic kidney 293 (HEK293) cell line was used as a control. Transfection of HEK293 cells with GFP-VAP-1^{WT} yielded increased cell surface VAP-1 activity of approximately 0.5 nmol H_2O_2/min per well at 24 hours and 2 nmol H_2O_2/min by 48 hours (Figure 4.12A). Whereas VAP-1 activity of GFP-VAP-1^{Y471F}-transfected HEK293 cells was comparable to cells transfected with no plasmid. In contrast, membrane VAP-1 activity of HSEC was broadly similar between cells transfected with GFP-VAP-1^{WT}, GFP-VAP-1^{Y471F}, pmaxGFP control or no plasmid (Figure 4.12C). This was approximately ten-fold lower than the activity of VAP-1^{WT}-transfected HEK293 cells and was comparable to VAP-1^{Y471F}-transfected HEK293 cells at 48 hours. Activity within conditioned media was very low for both cell types (below 150 fmol H_2O_2/min/µl media) regardless of which plasmid was used (Figure 4.12B and 4.12D). This was taken to indicate that no VAP-1 was released into the media from either cell type under the conditions tested.

The addition of TNFα had little effect on VAP-1 activity within the HSEC membrane or surrounding media (figure 4.12C and 4.12D). Similarly, TNFα had no measurable effect on protein expression or rate of reduction in fluorescence, as demonstrated by confocal microscopy (Figure 4.13). These images also revealed a similar localisation of GFP-VAP^{WT} and GFP-VAP-1^{Y471F}: primarily punctate fluorescence, focused in the perinuclear region with limited cell surface expression that was unaffected by the presence of TNFα.

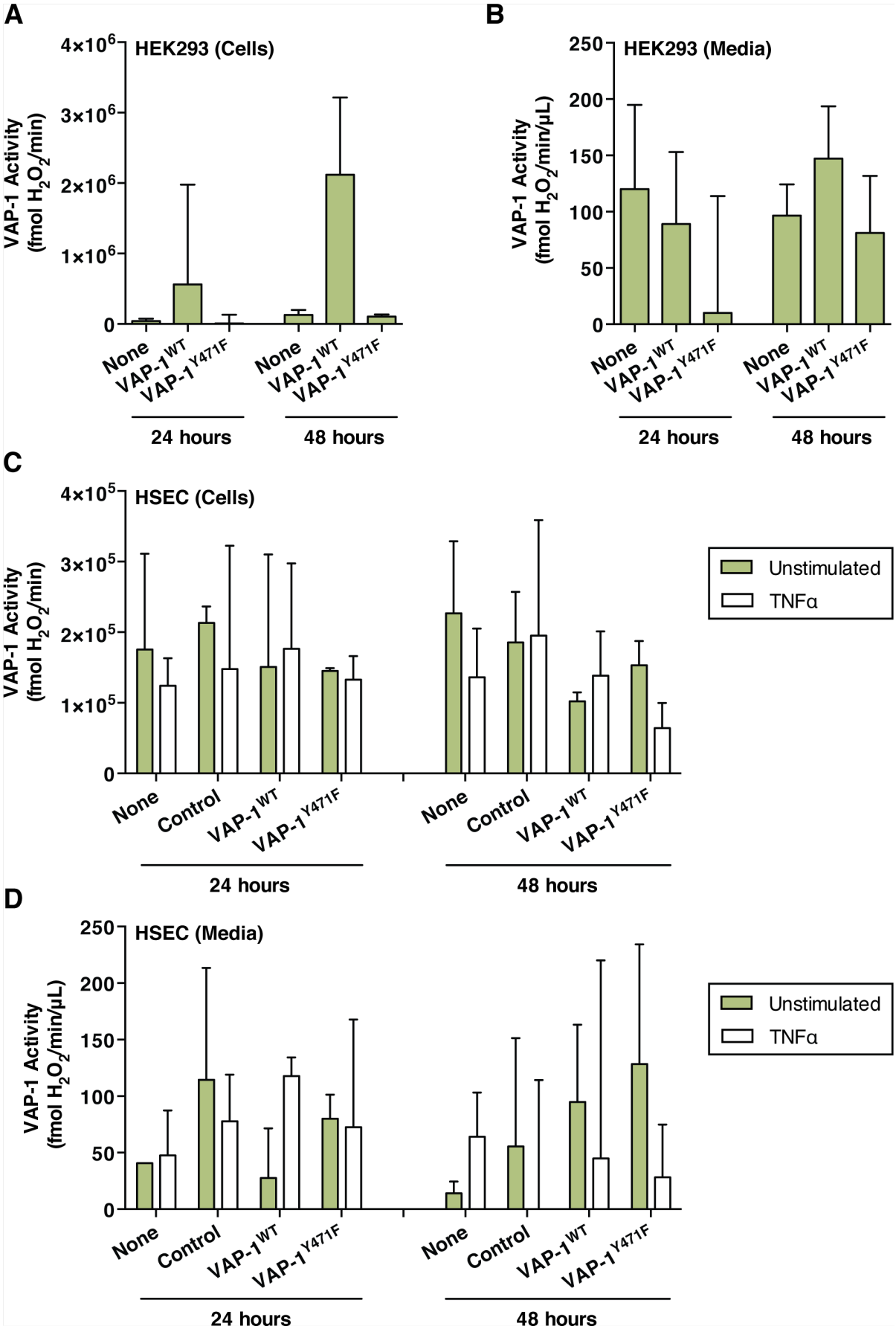

A
HEK293 (Cells)
VAP-1 Activity (fmol H_2O_2/min)
4×10^6
3×10^6
2×10^6
1×10^6
0
None
VAP-1^WT
VAP-1^Y471F
None
VAP-1^WT
VAP-1^Y471F
24 hours
48 hours
B
HEK293 (Media)
VAP-1 Activity (fmol H_2O_2/min/µL)
250
200
150
100
50
0
None
VAP-1^WT
VAP-1^Y471F
None
VAP-1^WT
VAP-1^Y471F
24 hours
48 hours
C
HSEC (Cells)
VAP-1 Activity (fmol H_2O_2/min)
4×10^5
3×10^5
2×10^5
1×10^5
0
Unstimulated
TNFα
None
Control
VAP-1^WT
VAP-1^Y471F
None
Control
VAP-1^WT
VAP-1^Y471F
24 hours
48 hours
D
HSEC (Media)
VAP-1 Activity (fmol H_2O_2/min/µL)
250
200
150
100
50
0
Unstimulated
TNFα
None
Control
VAP-1^WT
VAP-1^Y471F
None
Control
VAP-1^WT
VAP-1^Y471F
24 hours
48 hours

Figure 4.12 VAP-1 enzyme activity following transfection with GFP-VAP-1. (**A**) Untransfected HEK293 cell line (none) or cells transfected with plasmids encoding GFP-VAP-1^{WT}, GFP-VAP-1^{Y471F} or pmaxGFP control were analysed for surface VAP-1 amine oxidase activity 24 or 48 hours post transfection by Amplex UltraRed assay. (**B**) The culture media of untransfected or transfected HEK293 cells was also assayed for VAP-1 activity via antibody capture Amplex UltraRed assay. (**C**) HSEC were similarly assayed for surface VAP-1 activity or (**D**) presence of VAP-1 in conditioned culture media with or without stimulation with TNFα (10 ng/mL) (n = 3 different HSEC donors or HEK293 technical repeats). Data shown as median (IQR) and were analysed by KW test with Dunn's post-hoc correction (**A & B**) and two-way ANOVA with Holm-Sidak post-hoc correction (**C** & **D**). All nonsignificant.

4.2.1.6 Neutrophil recruitment to GFP-VAP-1-transfected HSEC

Neutrophils were the only leukocytes to bind to rVAP-1 in our assays (Figure 4.7), therefore this leukocyte subset were chosen for further investigations with VAP-1 overexpressing cells. The interactions between neutrophils and HSEC expressing GFP-VAP-1 plasmids were investigated by flow-based adhesion assay.

Neutrophils bound preferentially to HSEC transfected with GFP-VAP-1^{WT} compared to those transfected with a positive control plasmid (119% (109 – 122%) total adhesion), although this was not statistically significant (Figure 4.14A). The positive control used in this instance was pLifeAct-Ruby, which encodes a short peptide that binds to filamentous actin and is not thought to affect any other cellular processes (Riedl et al., 2008). Neutrophil adherence to VAP-1^{Y471F}-transfected HSEC was comparable to control (98% (91 – 107%)), suggesting the importance of VAP-1 activity for adhesion. Interestingly, VAP-1^{Y471F}-transfected HSEC exhibited more round neutrophils and fewer shape-changed cells bound suggesting that the enzyme activity may be less critical for initial binding to the HSEC and more important for subsequent transmigration (Figure 4.14B).

The small differences in adhesion observed within this assay may be due to a lack of VAP-1 protein being posted on the HSEC membrane. To examine other interactions that may take place as the neutrophils interact with the endothelium flow-based adhesion assays were carried out with simultaneous visualisation using a confocal microscope. This allowed for the interactions of neutrophils with GFP-VAP-1^{WT} to be viewed in real time and without artefacts of fixation. Confocal microscopy revealed that GFP-VAP-1^{WT} was more concentrated at sites of neutrophil interaction and appeared to form a "cup-like" structure around the neutrophil. This was observed at cell junctions during

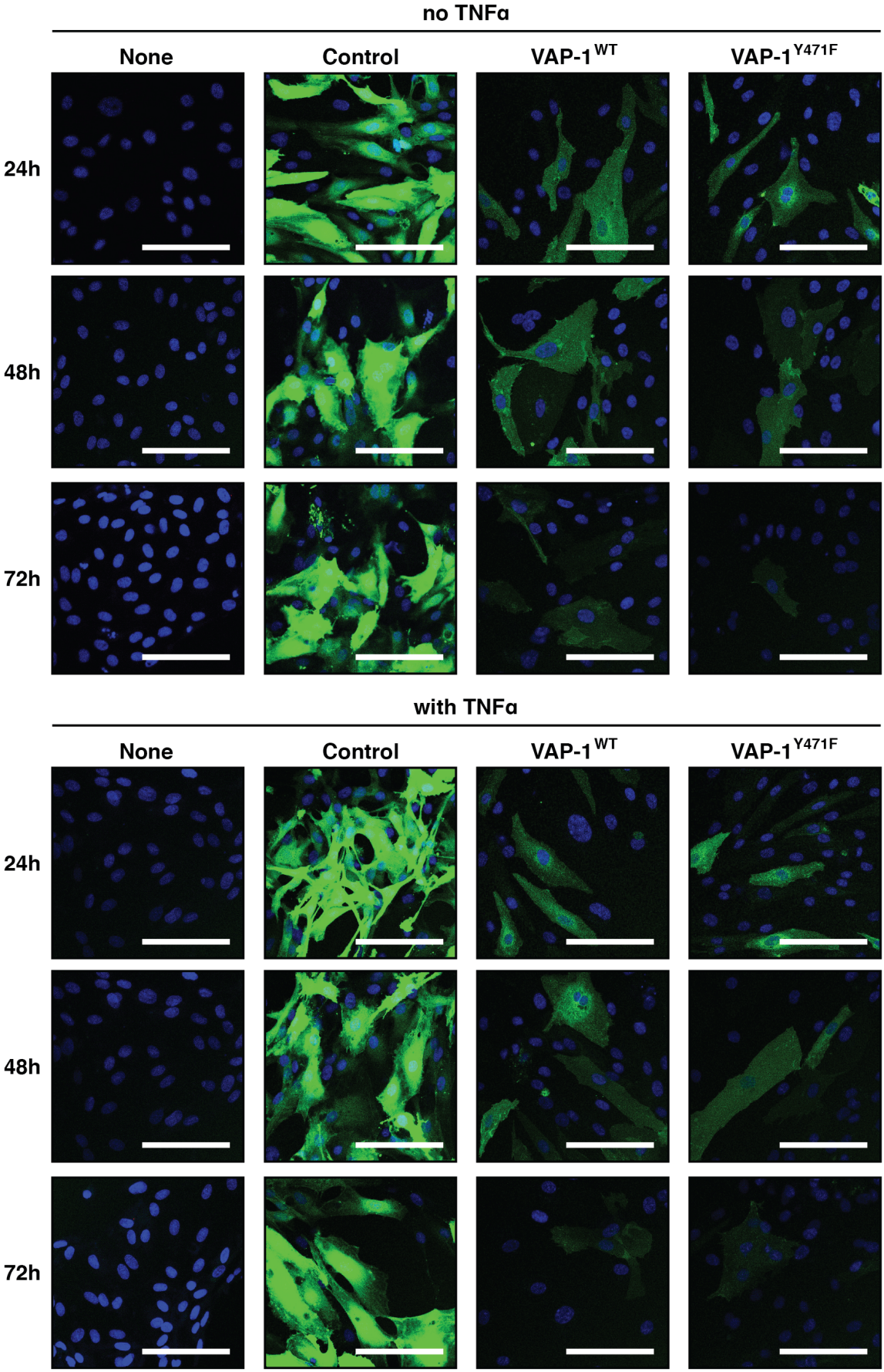

no TNFα
None
Control
VAP-1 WT
VAP-1 Y471F
24h
48h
72h
with TNFα
None
Control
VAP-1 WT
VAP-1 Y471F
24h
48h
72h

Figure 4.13 Expression patterns of GFP-VAP-1 in HSEC. Untransfected HSEC or cells transfected with plasmids encoding GFP-VAP-1^{WT}, GFP-VAP-1^{Y471F} or pmaxGFP (green) were cultured with or without TNFα (10 ng/mL) for 72 hours and imaged by confocal microscopy every 24 hours to evaluate the intracellular localisation of GFP. Nuclei were identified by incubation with DAPI (blue). Representative images of three replicates. White bar: 100 μm.

paracellular migration (Figure 4.15) and also during transcellular migration (Figure 4.16A).

The accumulation of GFP-VAP-1^{WT} was dynamic: moving with the neutrophil as it crawled along the endothelium with highest concentrations at the leading edge of travel (Figure 4.16A and 4.16B). The accumulation occurred within minutes and dissipated equally as fast following the interaction (Figure 4.16B and 4.16C). There also appeared to be direct contact between the GFP-VAP-1^{WT} and neutrophil, which remained even after the neutrophil had moved away, as seen in Figure 4.16C. Some neutrophils were also GFP-VAP^{WT}-positive, suggesting a passing of protein between the endothelium and neutrophil (Figure 4.15).

4.2.1.7 Effect of rVAP-1 on neutrophil recruitment to HSEC

HSEC can function as antigen presenting cells (APCs) and are therefore capable of taking up antigen from their surroundings and presenting it at their surface. To investigate whether this was possible with VAP-1, and moreover whether this may facilitate leukocyte binding, HSEC were pretreated for 20 minutes with rVAP-1 prior to flow-based adhesion assay. Treatment of HSEC with 0.5 μg/mL or 1 μg/mL rVAP-1 increased neutrophil binding by 38% and 58%, respectively (Figure 4.17A). Higher concentrations of rVAP-1 did not lead to further increases in neutrophil adhesion, with 5 μg/mL promoting adherence to the same level as 0.5 μg/mL (38%) and a reduction of 19% with 10 μg/mL when compared to the untreated control. This effect appeared to be specific to VAP-1 since the addition of rVCAM-1 had no effect on adherence. This may suggest active uptake and presentation rather than passive binding of the protein on the HSEC glycocalyx or VAP-1-binding receptors on the HSEC surface. However, the bell-shaped curve observed is similar to that of a chemokine action, possibly indicating a similar function of VAP-1 following immobilisation on the glycocalyx. The bell-shaped trend was largely reflected in changes in rolling and round-shaped adherent cells, with rVAP-1 titration having little effect on the proportion of cells that were shape-changed or

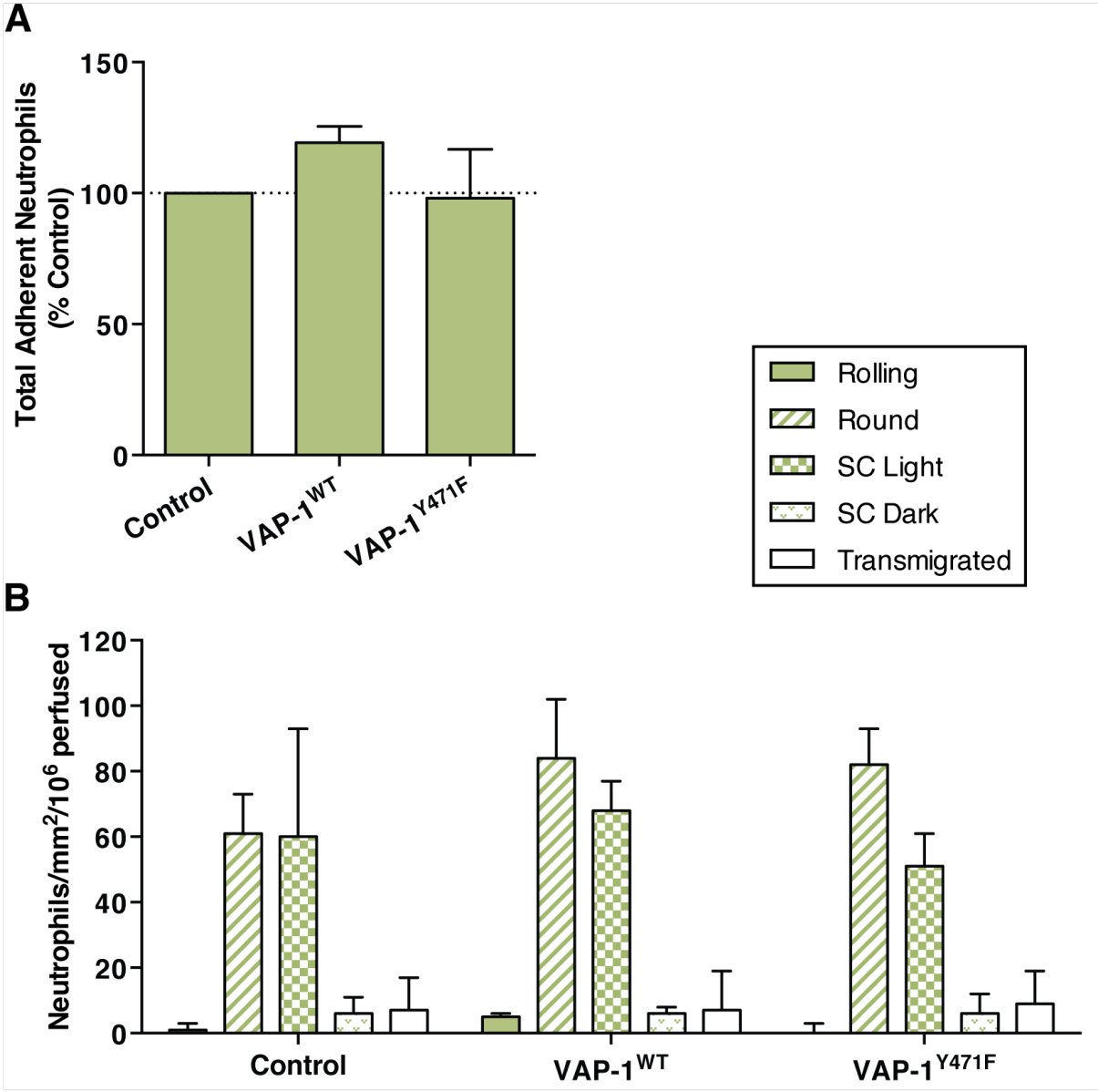


Figure 4.14 Effect of GFP-VAP-1 overexpression on adhesion of neutrophils to stimulated HSEC. Neutrophils were perfused over TNFα-stimulated HSEC transfected with plasmids encoding GFP-VAP-1^{WT}, GFP-VAP-1^{Y471F} or pLifeAct-Ruby at a shear flow rate comparable to that within the sinusoids. (**A**) The total number of adherent cells was assessed and (**B**) the extent of leukocyte migration was quantified as either round (adherent), shape-changed (SC) light or dark (transmigrating) or transmigrated (n = 3 different neutrophil and HSEC donors; 10-12 fields of view each). Data shown as mean (SD) and were analysed by KW test with Dunn's post-hoc correction (**A**) and two-way ANOVA with Holm-Sidak post-hoc correction (**B**). All nonsignificant from control.

transmigrated (Figure 4.17B). This observation implicates VAP-1 in adhesion rather than migration in these studies. Subsequent immunohistochemical analysis of these assays demonstrated that adherent neutrophils were positive for VAP-1 (figure 4.17C). VAP-1 staining of neutrophils was most intense when HSEC were incubated with 5 μg/mL rVAP-1, although cells were also positive in the absence of exogenous rVAP-1.

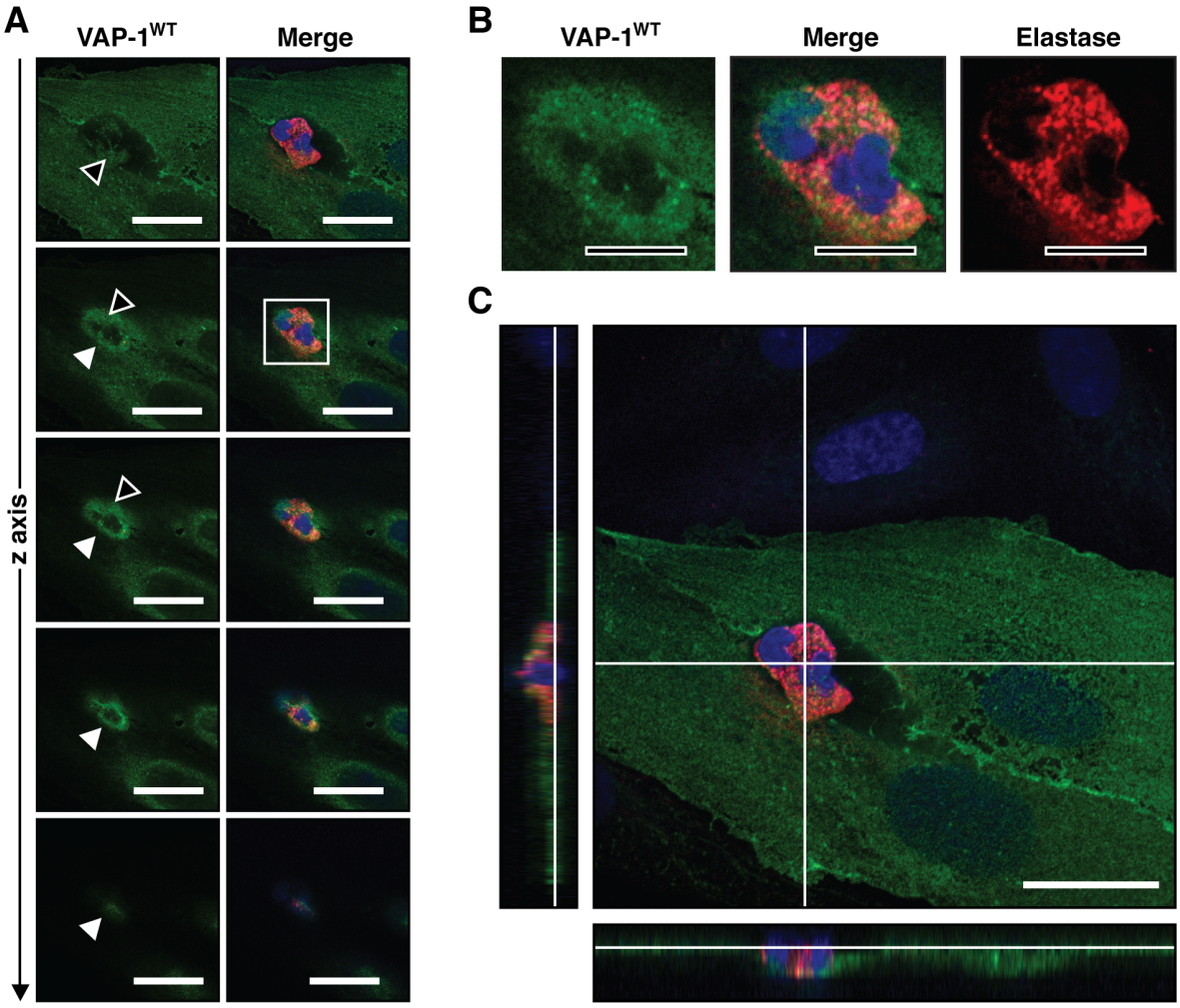


Figure 4.15 Z-stack analysis of neutrophil interaction with GFP-VAP-1^{WT}. HSEC were transfected with a plasmid encoding GFP-VAP-1^{WT}, stimulated with TNFα and neutrophils (red) were perfused over continuously at a shear flow rate comparable to that within the sinusoids. Interactions of neutrophils with GFP-VAP-1^{WT} (green) were assessed in real time through the full thickness of the HSEC monolayer by confocal microscopy. Nuclei were identified by incubation with DRAQ5 (blue). (**A**) Confocal images taken through the depth of the HSEC monolayer (z axis) at 1 µm intervals. High concentrations of GFP-VAP-1^{WT} are indicated by white arrowheads, potential presence of GFP within neutrophil is indicated by black arrowheads. (**B**) Magnification of white boxed region in (A) to highlight colocalisation of Neutrophil Elastase and GFP-VAP-1^{WT}. (**C**) z-stacked image illustrating the cup-like formation of VAP-1 around the neutrophil. Representative image from 3 experiments. White bar: 20 µm, black bar: 5 µm.

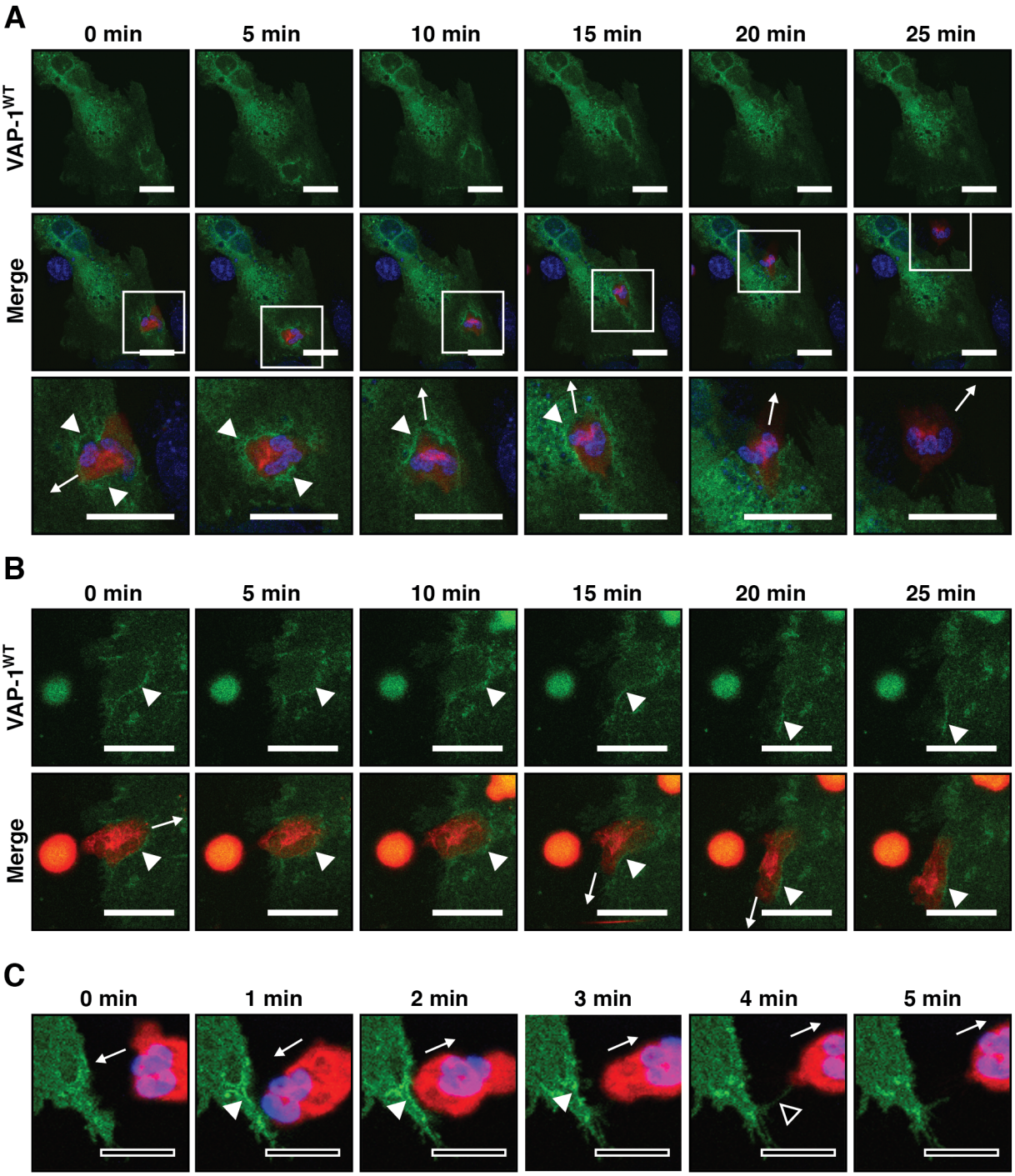


Figure 4.16 Time-lapse analysis of neutrophil interaction with GFP-VAP-1^{WT}. HSEC were transfected with a plasmid encoding GFP-VAP-1^{WT}, stimulated with TNFα and neutrophils (red) were perfused over continuously at a shear flow rate comparable to that within the sinusoids. Interactions of neutrophils with GFP-VAP-1^{WT} (green) were assessed in real time. Nuclei were identified by incubation with DRAQ5 (blue). (**A**) Neutrophil crawling along the HSEC surface while encompassed with GFP-VAP-1^{WT}, (**B**) Neutrophil interacting with GFP-VAP-1^{WT}-positive 'pocket'. (**C**) Neutrophil interacting with region of high GFP-VAP-1^{WT} concentration. Direction of neutrophil travel indicated by white arrows. High concentrations of GFP-VAP-1^{WT} are indicated by white arrowheads, Black arrowhead indicates region of maintained intercellular interaction. White box represents region of magnification Representative image from 3 experiments. White bar: 20 µm, black bar: 10 µm.

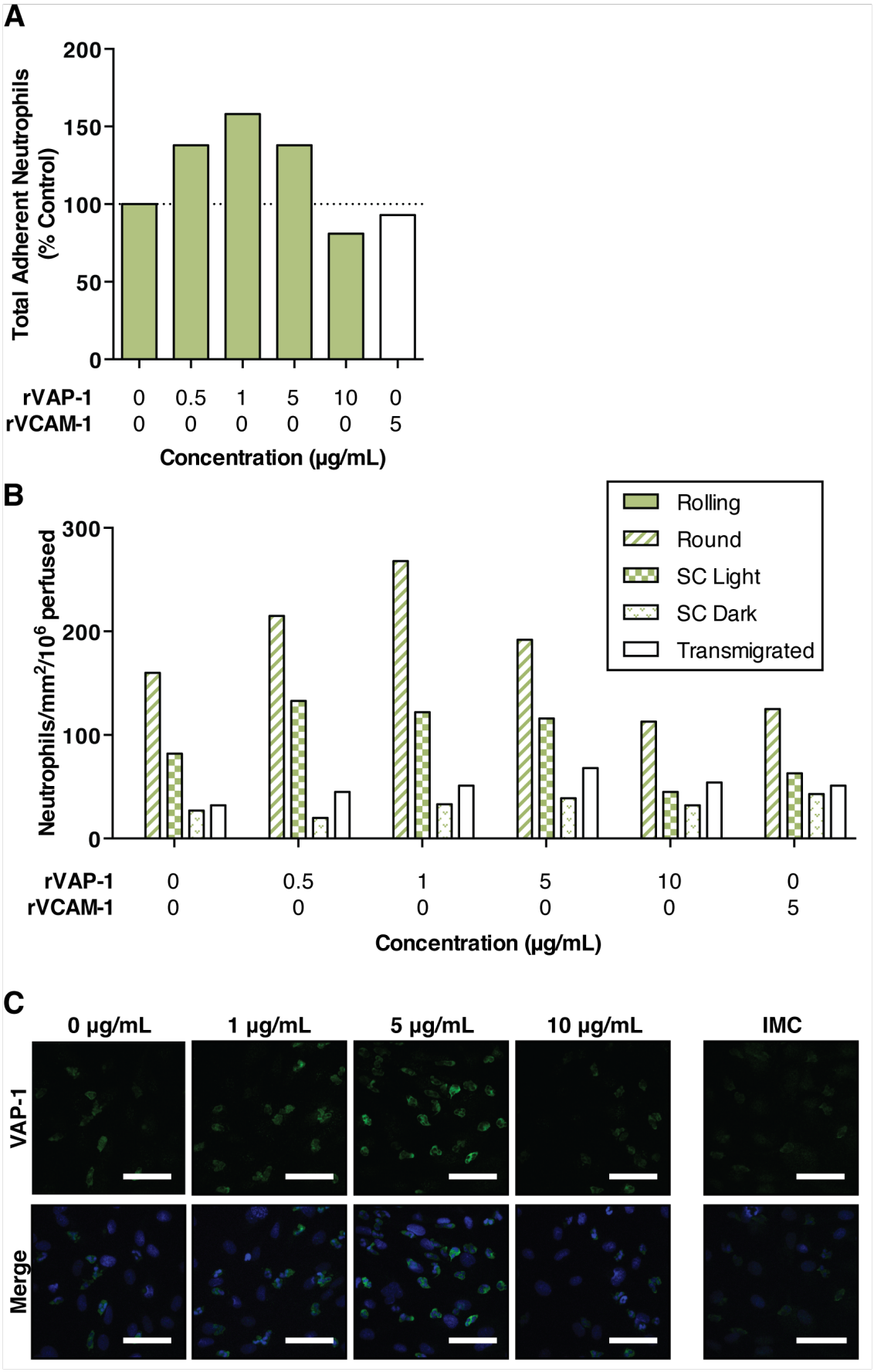

A
Total Adherent Neutrophils (% Control)
200
150
100
50
0
rVAP-1 0 0.5 1 5 10 0
rVCAM-1 0 0 0 0 0 5
Concentration (µg/mL)
B
Neutrophils/mm2/10^6 perfused
300
200
100
0
Rolling
Round
SC Light
SC Dark
Transmigrated
rVAP-1 0 0.5 1 5 10 0
rVCAM-1 0 0 0 0 0 5
Concentration (µg/mL)
C
0 µg/mL
1 µg/mL
5 µg/mL
10 µg/mL
IMC
VAP-1
Merge

Figure 4.17 Effect of rVAP-1 on adhesion of neutrophils to stimulated HSEC. Neutrophils were perfused over TNFα-stimulated HSEC at a shear flow rate comparable to that within the sinusoids following 20 min incubation with rVAP-1 (0-10 μg/mL) or rVCAM-1 (10 μg/mL). (**A**) The total number of adherent cells was assessed and (**B**) the extent of leukocyte migration was quantified as either round (adherent), shape-changed (SC) light or dark (transmigrating) or transmigrated (*n* = 1; 10-12 fields of view). (**C**) Immunohistochemical analysis of slides after fixation for the presence of VAP-1 (green). Nuclei were identified with DAPI (blue). IMC = isotype-matched control. White bar: 50 μm.

4.2.2 VAP-1 and neutrophil function

4.2.2.1 Neutrophil expression of VAP-1

Immunohistochemical analyses of neutrophils were conducted to determine whether granulocytes are capable of constitutive VAP-1 expression or are only capable of taking up exogenous protein. No VAP-1 expression by neutrophils (as indicated by neutrophil elastase immunoreactivity) was detected within either the sinusoids of the cirrhotic liver or by those that had migrated to the fibrotic scar (Figure 4.18A). Isolated peripheral blood neutrophils, however, stained positively for VAP-1 *in vitro* (Figure 4.18B). VAP-1-positivity was lost following

stimulation of neutrophils with phorbol myristate acetate (PMA) for 4 hours to induce the formation of neutrophil extracellular traps (NETs). To investigate whether other proinflammatory molecules induced similar downregulation of VAP-1 protein expression, isolated neutrophils were incubated with TNFα and LPS both separately or in combination. The cells were subsequently analysed for VAP-1 expression by immunohistochemistry. Only neutrophils that were not treated with proinflammatory stimuli stained positively for VAP-1 (Figure 4.19).

To exclude the possibility that the immunofluorescent staining observed for VAP-1 in neutrophils was an artefact caused by non-specific binding of the anti-VAP-1 antibody, the expression of the VAP-1 gene product (*AOC3*) by neutrophils and other peripheral blood leukocyte populations was determined by qPCR. Neutrophils were consistently found to express *AOC3*, however no expression was detectable in $CD4^+$ and $CD8^+$ T cells, NK cells, B cells or $CD14^+$ monocytes (Figure 4.20A). Incubation of neutrophils with either TNFα or IFNϒ resulted in approximately half the expression of *AOC3* mRNA compared to untreated cells (Figure 4.20B).

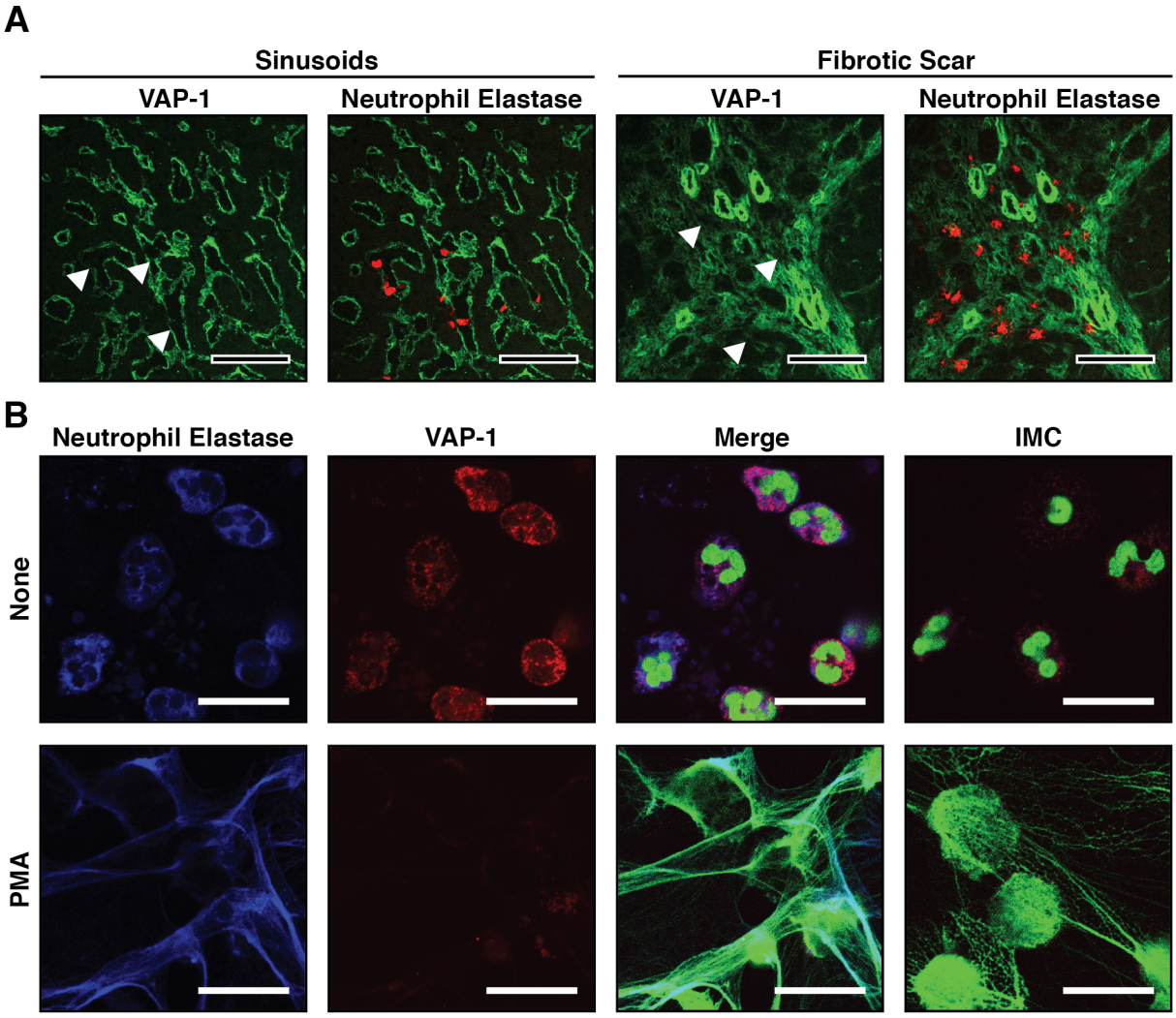


Figure 4.18 VAP-1 expression by human neutrophils. (**A**) Immunohistochemical analysis of neutrophils (red) within an ALD liver section for VAP-1 expression (green). White arrows indicate the location of neutrophils. (**B**) Immunohistochemical analysis of *ex vivo* peripheral blood neutrophils for the expression of neutrophil elastase (blue) and VAP-1 (red) either untreated or stimulated with PMA (25 nM) to form NETs (identified by Sytox Green stain). IMC = isotype-matched control. Black bar: 100 µm, white bar: 20 µm.

Peripheral blood neutrophils were then lysed and analysed for total cell VAP-1 amine oxidase activity via antibody capture Amplex UltraRed assay. Antibody capture was used in order to reduce any interfering H_2O_2 production from other neutrophil processes. To further ensure that VAP-1-specific H_2O_2 production was being measured, activity was assessed in the presence and absence of the amine oxidase inhibitor LJP-1586, and VAP-1 activity was recorded as the difference between the two values (LJP-1586-corrected activity). Neutrophil lysates were found to contain enzymatically active VAP-1 (Figure 4.21A). Conditioned media from neutrophil cell culture also contained enzymatically active VAP-1, suggesting that VAP-1 is secreted by the cells

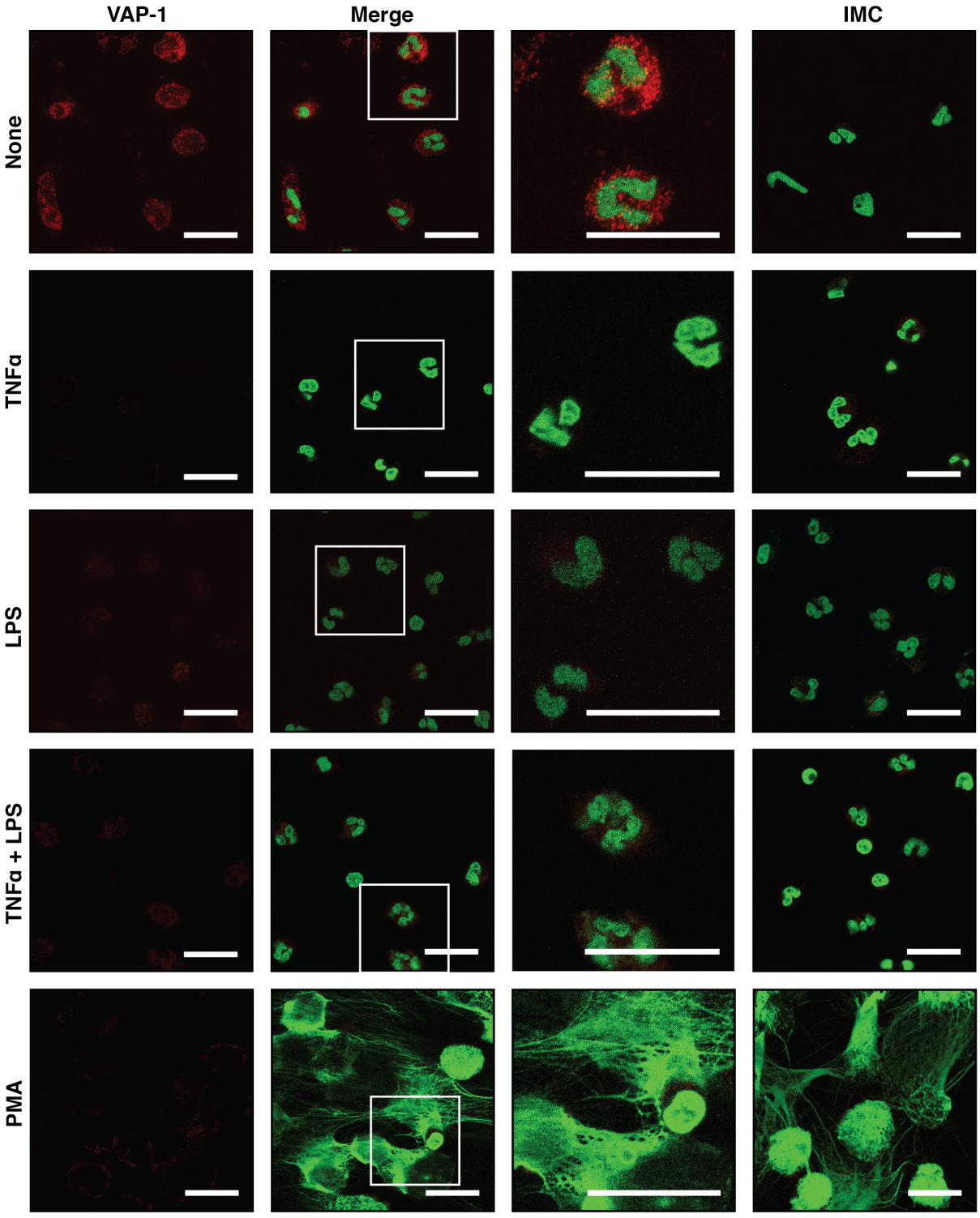


Figure 4.19 Effect of stimulation on VAP-1 expression by human neutrophils. Immunohistochemical analysis of *ex vivo* peripheral blood neutrophils for the expression of VAP-1 (red) either untreated or following stimulation for 4 hours with proinflammatory molecules: TNFα (10 ng/mL), LPS (100 ng/mL), TNFα and LPS in combination or PMA (25 nM). DNA was identified by Sytox Green stain. IMC = isotype-matched control. White box indicates magnified region. White bar: 20 µm.

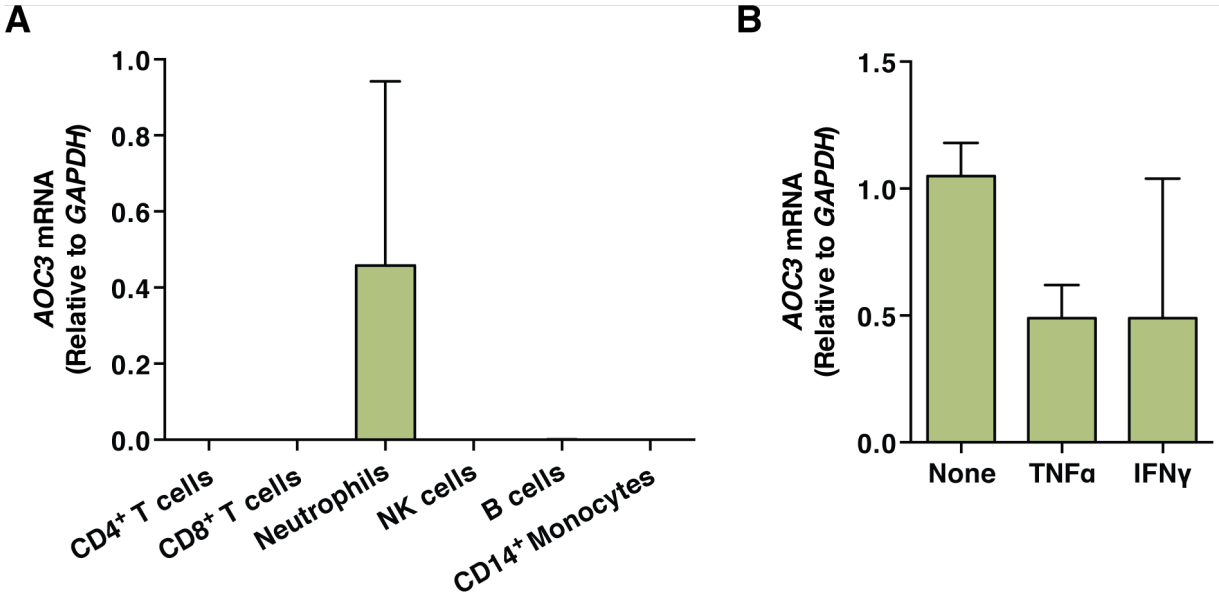


Figure 4.20 Expression of *AOC3* mRNA by human leukocytes. (**A**) *Ex vivo* human peripheral blood leukocyte subsets were analysed for *AOC3* mRNA expression by qPCR analysis (n = 3-8). (**B**) Effect of 4 hour stimulation with TNFα (10 ng/mL) or IFNγ (10 ng/mL) on *AOC3* mRNA expression by human peripheral blood neutrophils (n = 3). Data shown as mean (SD) (**A**) and median (IQR) (**B**) and were analysed by KW test with Dunn's post-hoc correction (**B**). All nonsignificant in (**B**).

(Figure 4.21B). Pre-incubation of neutrophils with either TNFα or IFNϒ reduced both the intracellular and secreted VAP-1 activity, although only the reduction by IFNϒ reached statistical significance in both cases ($p \leq 0.05$). The secretion of enzymatically active VAP-1 was also independent of adherence to HSEC and was unaffected by stimulation of the HSEC with either TNFα or LPS for 24 hours prior to the assay (Figure 4.21C).

4.2.2.2 Effect of inhibiting neutrophil VAP-1 on recruitment

Following the discovery that neutrophils express catalytically active VAP-1, it was important to elucidate whether this could impact on neutrophil recruitment. Recombinant VAP-1 flow-based adhesion assays were employed for this purpose, during which the neutrophils, rVAP-1 or both were pretreated with LJP-1586. Inhibition of rVAP-1 had a slight effect on the number of adherent neutrophils (131% (109 - 140%) compared to untreated control) whereas treatment of the neutrophils with LJP-1586 resulted in an almost two-fold increase in the total number of adherent cells (186% (165 - 227%) of control, $p \leq 0.05$) as seen in Figure 4.22A. Incubation of neutrophils with LJP-1586 also increased adhesion to HSEC by 18% (17 - 23%), although

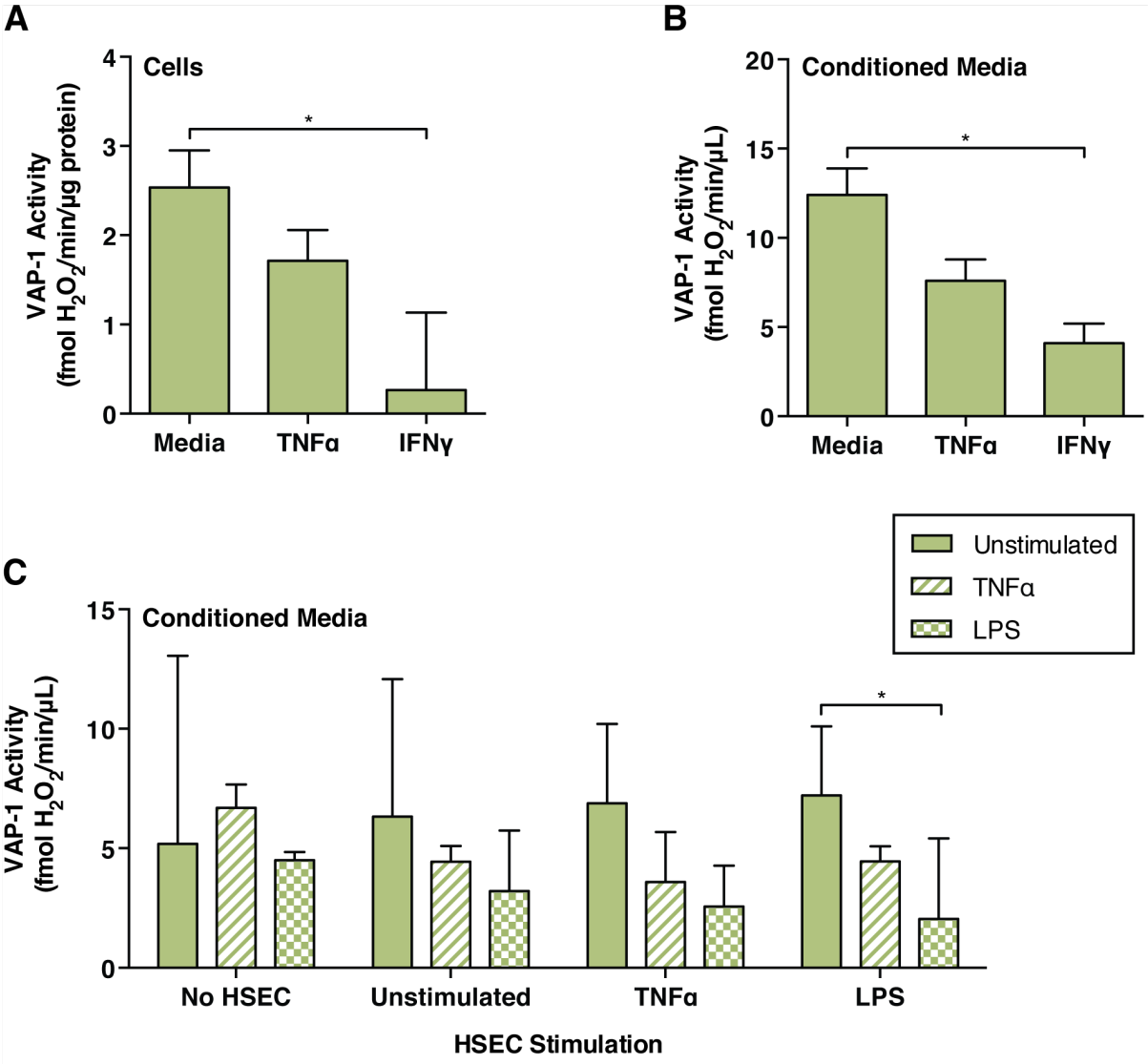


Figure 4.21 VAP-1 amine oxidase activity of human neutrophils. *Ex vivo* peripheral blood neutrophils were stimulated for 4 hours with TNFα (10 ng/mL) or IFNγ (10 ng/mL) before being analysed for VAP-1 amine oxidase activity by antibody-capture Amplex UltraRed assay either (**A**) intracellular following lysis or (**B**) within the cell-conditioned culture media. (**C**) Unstimulated neutrophils or cells stimulated with TNFα (10 ng/mL) or LPS (10 µg/mL) were cocultured for 4 hours with HSEC that were either unstimulated or stimulated with TNFα (10 ng/mL) or LPS (10 ng/mL) or no HSEC. Cell-conditioned media was assessed for VAP-1 amine oxidase activity by antibody-capture Amplex UltraRed assay (n = 3 different donors). Data shown as median (IQR) and were analysed by KW test with Dunn's post-hoc correction (**A** & **B**) and two-way ANOVA with Holm-Sidak post-hoc correction (**C**). * $p \leq 0.05$.

this was not statistically significant (Figure 4.22B). Inhibition of neutrophil VAP-1 made no clear difference to the proportion of cells that were at different stages in the leukocyte adhesion cascade (Figure 4.22C).

4.2.2.3 Neutrophil VAP-1 activity and ROS production

The respiratory burst is critical to the cytotoxic function of neutrophils and can be modulated by the presence of H_2O_2 (Winn et al., 1991). To investigate whether the amine oxidase activity of VAP-1 may also affect this process, neutrophils were stimulated with PMA in the presence or absence of LJP-1586. Extracellular H_2O_2 production was measured by Amplex UltraRed assay as an indication of respiratory burst (Figure 4.23). Inhibition of neutrophil VAP-1 activity had no effect on the rate of H_2O_2 production of either PMA-stimulated or unstimulated cells. Neutrophil H_2O_2 production was then compared between those isolated from the bone marrow of mice that express the catalytically inactive form of VAP-1 ($SSAO^{KO}$) and WT C57/BL6 mice (Figure 4.23C and 4.23D). $SSAO^{KO}$ neutrophils exhibited elevated H_2O_2 production compared to those from WT mice (Figure 4.23C and 4.23D). This difference was most apparent when cells were treated with PMA: $SSAO^{KO}$ mice exhibited a 32% greater H_2O_2 production rate (1.28 pmol H_2O_2/min/WT neutrophil and 1.69 pmol H_2O_2/min/$SSAO^{KO}$ neutrophil). However, these data represent only a single experimental repeat ($n = 1$).

Given that inhibition of neutrophil VAP-1 activity had a limited effect on function, neutrophils were subsequently stimulated with PMA in the presence of VAP-1 substrates to determine whether an increase in VAP-1 activity affected H_2O_2 production. Benzylamine and cysteamine were chosen as good non-physiological and physiological substrates of VAP-1, respectively, and histamine was chosen as a poor substrate with physiological relevance to neutrophils. The presence of benzylamine and histamine resulted in a significant ($p \leq 0.0001$) reduction of over 60% the resting-state H_2O_2 generation (Figure 4.24A and 4.24B). Benzylamine also reduced the rate of H_2O_2 production when stimulated with PMA by 34.8% (29.7 – 39.9%), $p \leq 0.05$. This effect of benzylamine was reversed by the inhibition of VAP-1 with LJP-1586, resulting in an increase in H_2O_2 production (Figure 4.24C and 4.24D).

Cysteamine increased the production rate of H_2O_2 by over two-fold during the resting state ($p \leq 0.0001$) but did not significantly affect the rate upon stimulation with PMA

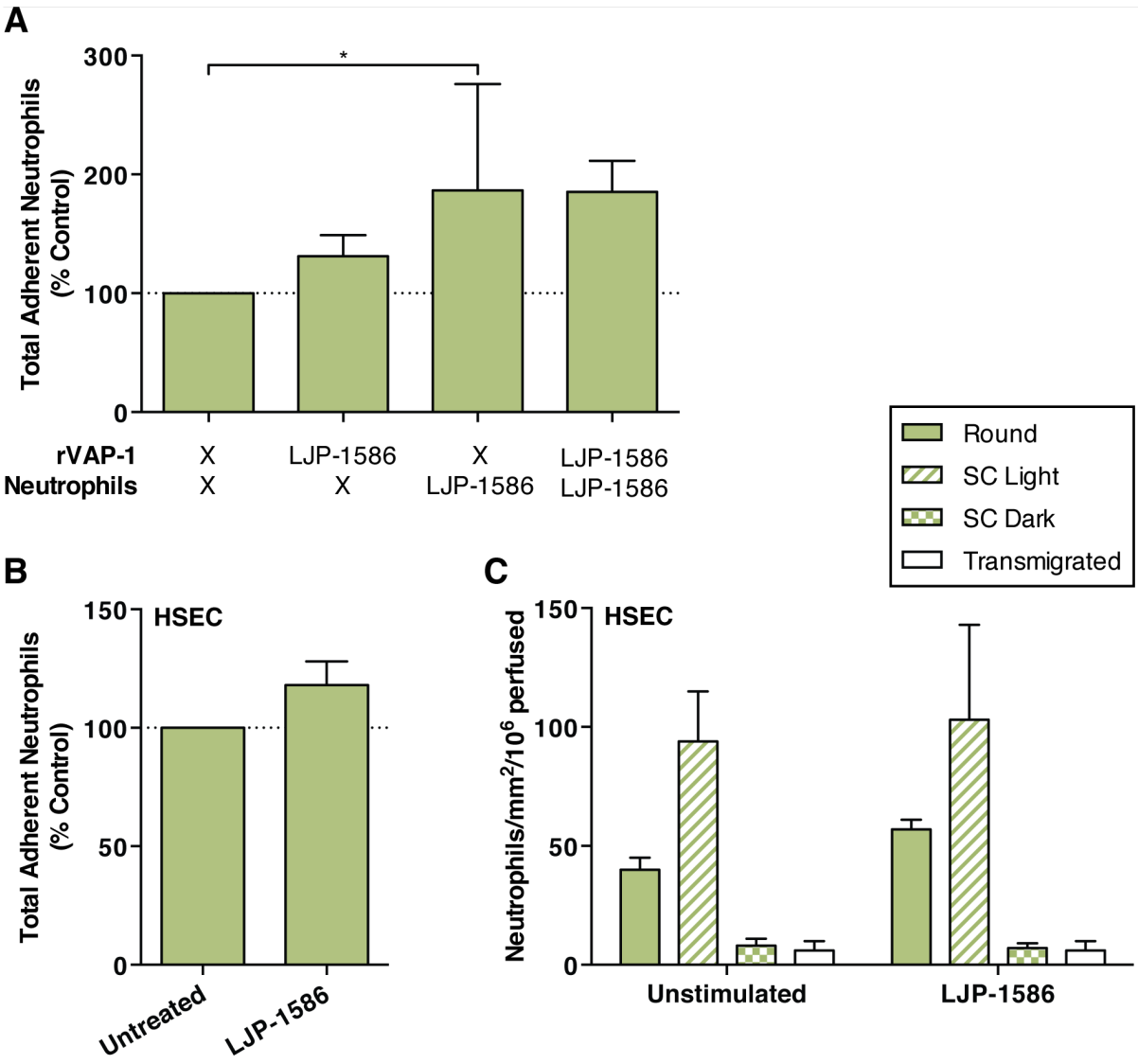


Figure 4.22 Effect of VAP-1 inhibition on neutrophil adhesion. (**A**) Neutrophils were perfused over recombinant human VAP-1 at a shear flow rate comparable to that within the sinusoids: rVAP-1, the neutrophils or both were incubated with LJP-1586 for 1 hour prior to assay. The total number of adherent cells was assessed following 1-hour treatment of rVAP-1, neutrophils or both with LJP-1586 (500 nM) (n = 4 different neutrophil donors; 10-12 field of view each). Neutrophils were also perfused over TNFα-stimulated HSEC after their incubation for 1 hour with LJP-1586 (500 nM) and either (**B**) the total number of adherent cells was assessed or (**C**) extent of leukocyte migration was quantified as either round (adherent), SC light or dark (transmigrating) or transmigrated (n = 3 different neutrophil and HSEC donors; 10-12 fields of view each). Data shown as median (IQR) and were analysed by KW test with Dunn's post-hoc correction (**A** & **B**) and two-way ANOVA with Holm-Sidak post-hoc correction (**C**). * $p \leq 0.05$.

(Figure 4.24A and 4.24B). However, the fluorescent reading of the Amplex UltraRed assay appeared to be affected by the presence of cysteamine, indicated by the increase in fluorescence over time in the presence of constant H_2O_2 concentration (Figure 4.24E). It is unclear to what degree this may affect the results shown.

4.2.2.4 Effect of rVAP-1 on neutrophil ROS production

Neutrophils are exposed to sVAP-1 within the circulation and appear to be able to uptake VAP-1 protein from their surrounding, therefore the consequences of

extracellular VAP-1 on H_2O_2 production was investigated. Extracellular H_2O_2 was measured using the Amplex UltraRed Assay while neutrophils were stimulated with PMA, TNFα or LPS in the presence or absence of rVAP-1 within the culture media. Neutrophils treated with rVAP-1 exhibited approximately 10-30% lower rates of H_2O_2 production regardless of stimuli, although this was not statistically significant (Figure 4.25A and 4.25B). This effect was not observed when mouse bone marrow neutrophils were treated with mouse rVAP-1 *ex vivo* and was not affected by the catalytic activity of the VAP-1 they expressed (Figure 4.25C and 4.25D).

4.2.2.5 Neutrophil VAP-1 activity and NETosis

The release of neutrophil extracellular traps (NETs) is an important effector function of neutrophils with the purpose of trapping and killing pathogens. NETs are primarily formed of nuclear chromatin coated with histones and many granular antimicrobial proteins such as neutrophil elastase (Remijsen et al., 2011). The amount of cell-free DNA (cfDNA) can therefore be measured fluorometrically and used as a measure of NETosis (Hampson et al., 2016). This method was employed to assess whether endogenous VAP-1 activity affected NETosis. Inhibition of VAP-1 did not significantly alter the amount of cfDNA in response to stimulation with PMA, although in the presence of a VAP-1 inhibitor neutrophils showed a trend for marginally increased levels of NETosis (Figure 4.26A and 4.26B). Similarly, no difference in cfDNA was observed between neutrophils from WT or $SSAO^{KO}$ mice (Figure 4.26C and 4.26D). Interestingly, the murine bone-marrow neutrophils did not respond to stimuli in the same way or to the same extent as did human peripheral blood neutrophils: similar levels of cfDNA were recorded in stimulated and unstimulated cells. However, these data only represent a single experiment so therefore may not be representative of true responses.

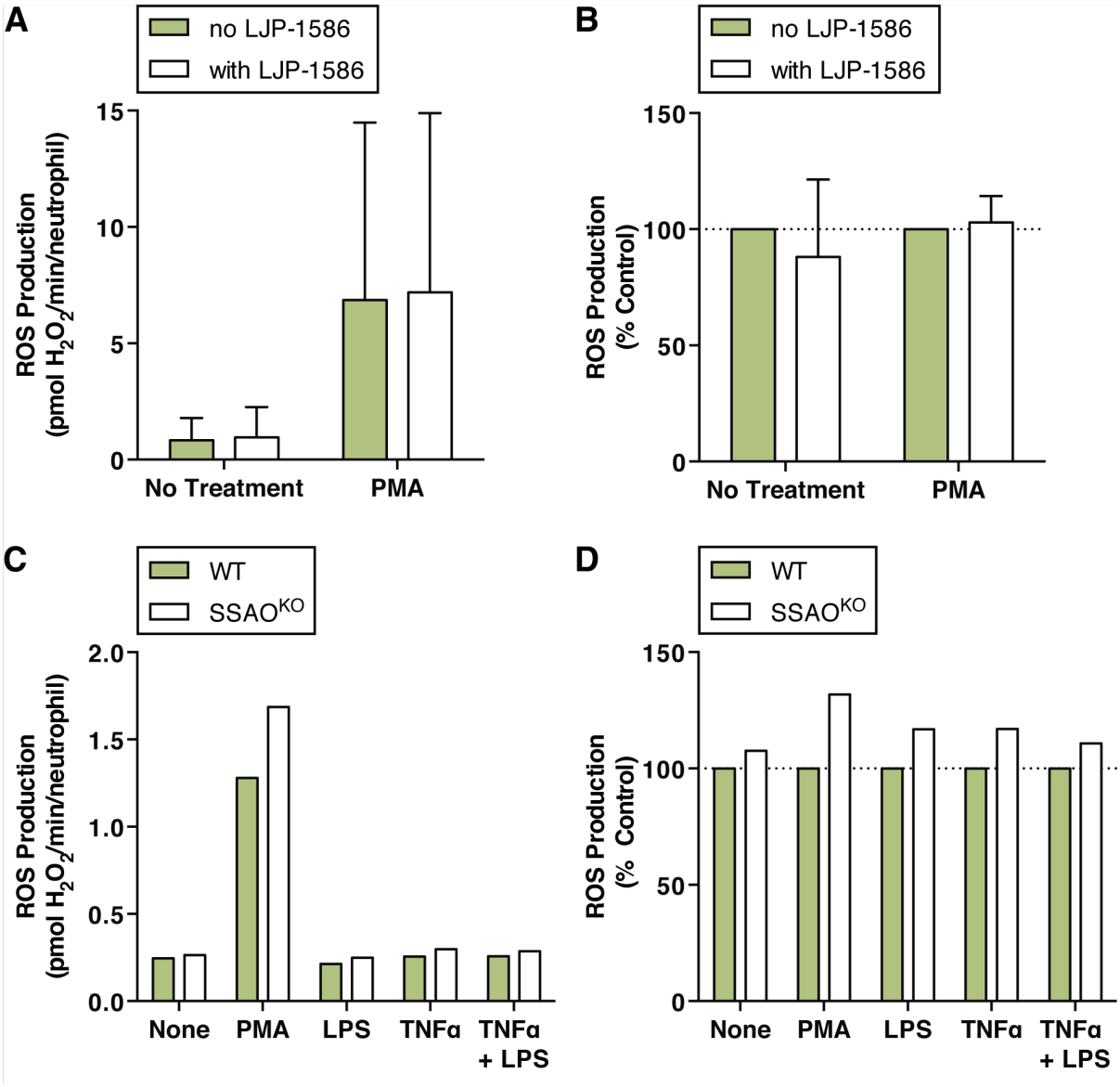


Figure 4.23 Effect of VAP-1 amine oxidase inhibition on neutrophil ROS production. (**A**) *Ex vivo* human peripheral blood neutrophils were stimulated with PMA (25 nM) for 4 hours in the presence or absence of LJP-1586 (500 nM). Extracellular H_2O_2 production was assessed by Amplex UltraRed assay and (**B**) normalised to untreated control (n = 4). (**C**) *Ex vivo* murine bone marrow neutrophils from WT or SSAO^{KO} animals were stimulated with PMA (25 nM), LPS (100 ng/mL), TNFα (10 ng/mL) or TNFα and LPS combined for 4 hours. Extracellular H_2O_2 production was assessed by Amplex UltraRed assay and (**D**) normalised to control (n = 1). Data shown as median (IQR) where applicable and were analysed by two-way ANOVA with Holm-Sidak post-hoc correction (**A** & **B**). All nonsignificant compared to control.

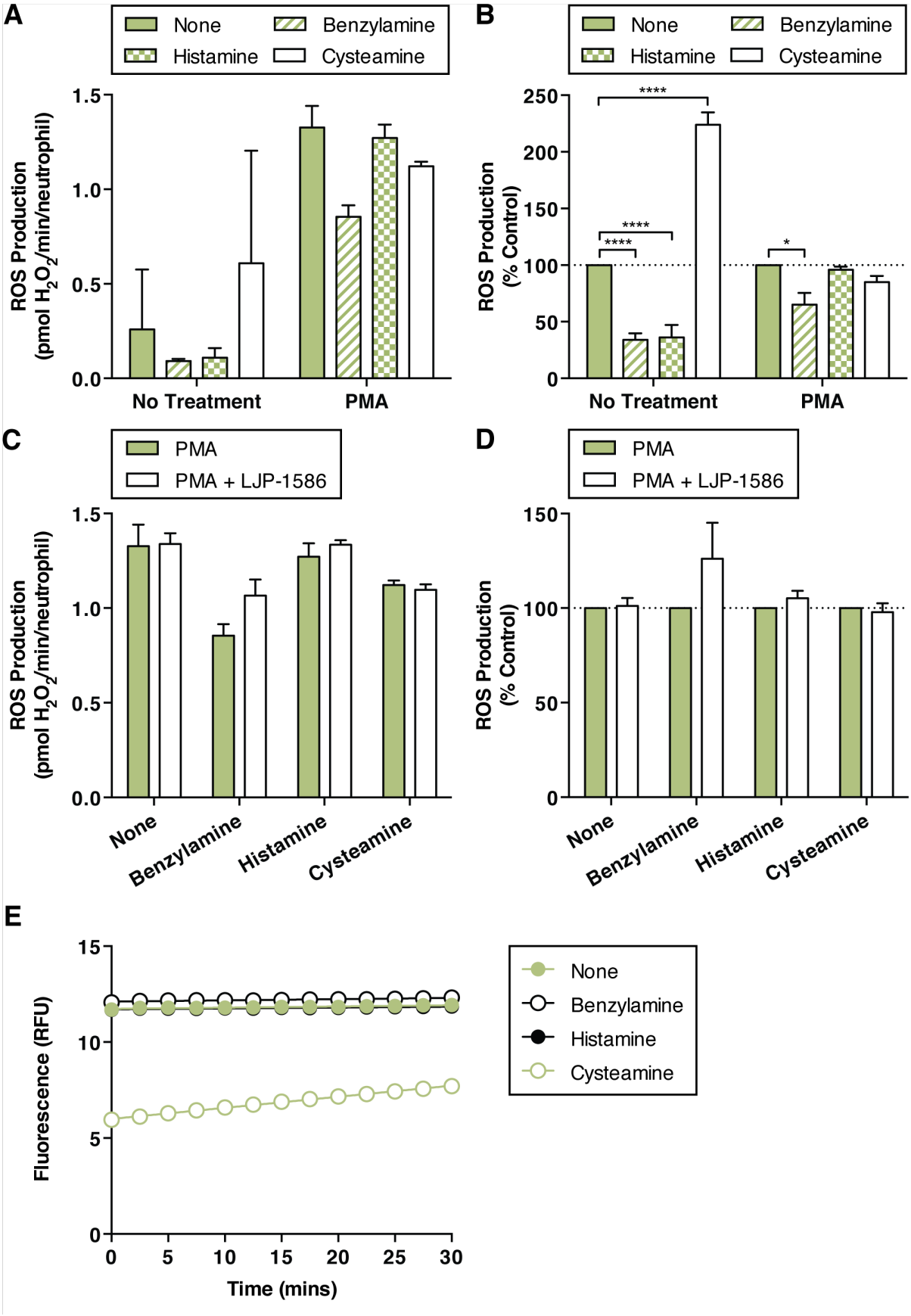

A
None
Benzylamine
Histamine
Cysteamine
ROS Production (pmol H_2O_2/min/neutrophil)
1.5
1.0
0.5
0.0
No Treatment
PMA
B
None
Benzylamine
Histamine
Cysteamine
ROS Production (% Control)
250
200
150
100
50
0
****
****
****
*
No Treatment
PMA
C
PMA
PMA + LJP-1586
ROS Production (pmol H_2O_2/min/neutrophil)
1.5
1.0
0.5
0.0
None
Benzylamine
Histamine
Cysteamine
D
PMA
PMA + LJP-1586
ROS Production (% Control)
150
100
50
0
None
Benzylamine
Histamine
Cysteamine
E
Fluorescence (RFU)
15
10
5
0
0
5
10
15
20
25
30
Time (mins)
None
Benzylamine
Histamine
Cysteamine

Figure 4.24 Effect of VAP-1 substrates on neutrophil ROS production. (**A**) *Ex vivo* human peripheral blood neutrophils were stimulated with PMA (25 nM) for 4 hours in the presence or absence of VAP-1 substrates benzylamine, histamine and cysteamine (100 nM). Extracellular H_2O_2 production assessed by Amplex UltraRed assay and (**B**) normalised to untreated control (n = 3). (**C**) Neutrophils were stimulated with PMA in the presence or absence of VAP-1 substrates and LJP-1586 (500 nM). Extracellular H_2O_2 production assessed by Amplex UltraRed assay and (**D**) normalised to untreated control (n = 3). (**E**) Impact of VAP-1 substrates on the Amplex UltraRed assay was assessed by incubation with 3 µM H_2O_2 (n = 3 technical repeats). Data shown as median (IQR) and were analysed by two-way ANOVA with Holm-Sidak post-hoc correction. * $p \leq 0.05$, **** $p \leq 0.0001$.

The presence of VAP-1 substrates did not affect the amount of cfDNA released by untreated human neutrophils, however the presence of cysteamine almost abolished the NET-stimulating effect of PMA to levels comparable to untreated cells (116.9 ng/mL (107.9 – 127 4 ng/mL) PMA alone and 53.9 ng/mL (48.1 – 57.8 ng/mL) with PMA and cysteamine, $p \leq 0.01$) as seen in Figure 4.26E and 4.26F. Benzylamine also reduced the amount of cfDNA produced by PMA-stimulated neutrophils by 32.0% (25.4 – 32.1%), although this was not statistically significant ($p \geq 0.05$).

4.2.2.6 Effect of rVAP-1 on NETosis

The cfDNA assay was then used to assess the effect of exogenous VAP-1 on NETosis. The presence of rVAP-1 within the media significantly reduced the amount of cfDNA produced by human peripheral blood neutrophils in response to proinflammatory stimuli (Figure 4.27). This effect was most pronounced upon stimulation with PMA (193.2 ng/mL (124.8 – 237.3 ng/mL) with PMA alone and 101.1 ng/mL (71.3 – 135.9 ng/mL) with PMA and rVAP-1, $p \leq 0.01$), however cfDNA levels were lower in all treatment groups in the presence of rVAP-1.

NETosis follows the rapid condensation of intracellular chromatin, which may require the citrullination of histone 3 (H3) by PAD4. It was therefore of interest to discern whether rVAP-1 affected this process. Neutrophils were stimulated with PMA, LPS and TNFα in the presence or absence of rVAP-1 and subsequently analysed for the presence of citrullinated histone 3 (CitH3) by immunohistochemistry (Figure 4.28). The number of neutrophils that expressed CitH3 above a defined threshold was then calculated by ImageJ analysis (Figure 4.29A). The presence of rVAP-1 significantly increased the proportion of CitH3-positive cells in untreated neutrophils and those stimulated with

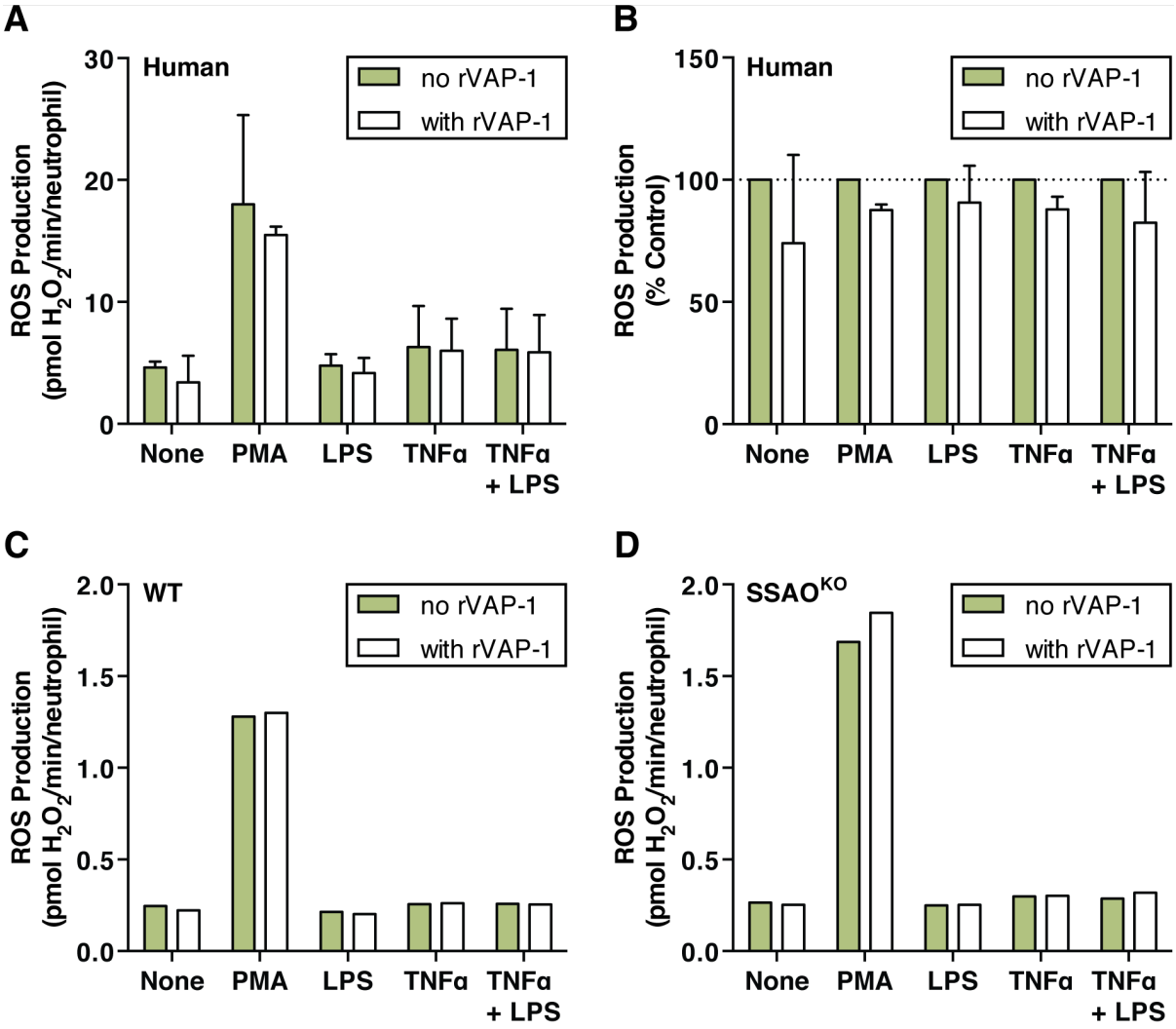


Figure 4.25 Effect of recombinant VAP-1 protein on neutrophil ROS production. (**A**) *Ex vivo* human peripheral blood neutrophils were stimulated with PMA (25 nM) LPS (100 ng/mL), TNFα (10 ng/mL) or TNFα and LPS combined for 4 hours in the presence or absence of recombinant human VAP-1 (500 ng/mL). Extracellular H_2O_2 production was assessed by Amplex UltraRed assay and (**B**) normalised to untreated control (n = 5). *Ex vivo* murine bone marrow neutrophils from (**C**) WT or (**D**) SSAO^{KO} animals were stimulated with PMA, LPS, TNFα or TNFα and LPS combined for 4 hours in the presence or absence of recombinant murine VAP-1 (500 ng/mL). Extracellular H_2O_2 production was assessed by Amplex UltraRed assay (n = 1). Data shown as median (IQR) where applicable and were analysed by two-way ANOVA with Holm-Sidak post-hoc correction (**A** & **B**). All nonsignificant compared to control.

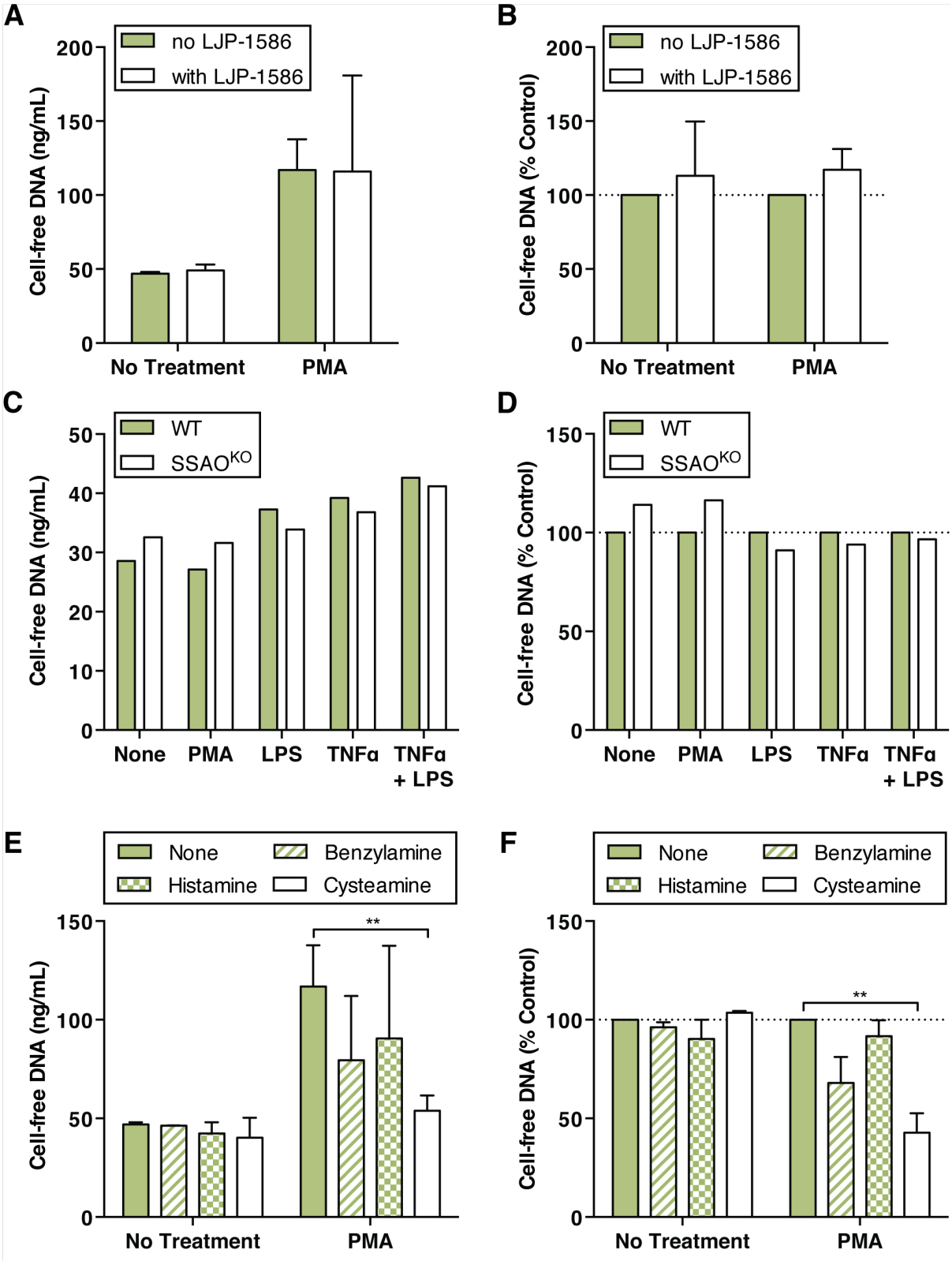

A
no LJP-1586
with LJP-1586
Cell-free DNA (ng/mL)
200
150
100
50
0
No Treatment
PMA
B
no LJP-1586
with LJP-1586
Cell-free DNA (% Control)
200
150
100
50
0
No Treatment
PMA
C
WT
SSAOKO
Cell-free DNA (ng/mL)
50
40
30
20
10
0
None
PMA
LPS
TNFα
TNFα + LPS
D
WT
SSAOKO
Cell-free DNA (% Control)
150
100
50
0
None
PMA
LPS
TNFα
TNFα + LPS
E
None
Benzylamine
Histamine
Cysteamine
Cell-free DNA (ng/mL)
150
100
50
0
**
No Treatment
PMA
F
None
Benzylamine
Histamine
Cysteamine
Cell-free DNA (% Control)
150
100
50
0
**
No Treatment
PMA

Figure 4.26 Effect of VAP-1 amine oxidase activity on NET production. (**A**) *Ex vivo* human peripheral blood neutrophils were stimulated with PMA (25 nM) for 4 hours in the presence or absence of LJP-1586 (500 nM). NET production was assessed by measuring cell-free DNA via Sytox Green fluorometric assay and (**B**) normalised to untreated control (n = 3). (**C**) *Ex vivo* murine bone marrow neutrophils from WT or SSAO^{KO} animals were stimulated with PMA (25 nM), LPS (100 ng/mL), TNFα (10 ng/mL) or TNFα and LPS combined for 4 hours. NET production was assessed by measuring cell-free DNA via Sytox Green fluorometric assay and (**D**) normalised to control (n = 1). (**E**) *Ex vivo* human peripheral blood neutrophils were stimulated with PMA (25 nM) for 4 hours in the presence or absence of VAP-1 substrates benzylamine, histamine and cysteamine (100 nM). NET production was assessed by measuring cell-free DNA via Sytox Green fluorometric assay and (**F**) normalised to untreated control (n = 3). Data shown as medina (IQR) where applicable and were analysed by two-way ANOVA with Holm-Sidak post-hoc correction (**A**, **B**, **C** & **D**). ** $p \leq 0.01$.

PMA or TNFα and LPS ($p \leq 0.05$). Conversely, rVAP-1 did not affect CitH3 expression in cells treated with TNFα or LPS alone.

The decondensed nuclei of NETosing neutrophils lose their lobulation and begin to swell prior to release of extracellular DNA (Fuchs et al., 2007). NET-forming cells can therefore be quantified by size analysis of immunohistochemical images (Hosseinzadeh et al., 2012). This form of analysis also includes those neutrophils that are yet to release the NETs but have undergone decondensation. The average nuclear size of neutrophils stimulated with TNFα and LPS was significantly reduced in the presence of rVAP-1 but not when stimulated with other proinflammatory mediators (Figure 4.29B). Similarly, the proportion of nuclei over 100 μm^2 (considered NET-forming) was reduced by over 95% ($p \leq 0.0001$; Figure 4.29C). Conversely, the presence of rVAP-1 increased the proportion of NET-forming cells when stimulated with PMA ($p \leq 0.05$).

To determine whether the effects of rVAP-1 on NETosis were a result of endogenous VAP-1 activity, the production of cfDNA by WT murine neutrophils was compared to those from SSAO^{KO} animals. NETosis by WT neutrophils was reduced in the presence of murine rVAP-1 in a similar fashion to that of human peripheral blood neutrophils (Figure 4.30A). However, the addition of murine rVAP-1 had no effect on NETosis of SSAO^{KO} neutrophils in most conditions (Figure 4.30B). Interestingly, rVAP-1 appeared to decrease the cfDNA produced by neutrophils stimulated with TNFα and LPS in combination to great degree in cells from both WT and SSAO^{KO} animals. However, these data only represent a single experiment.

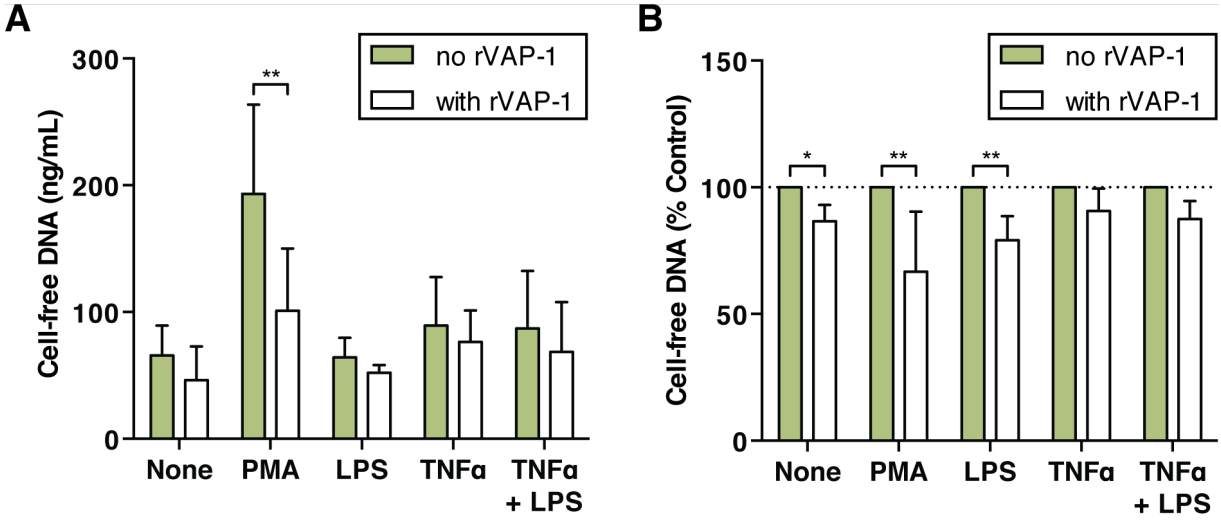


Figure 4.27 Effect of recombinant VAP-1 protein on human NET production. (**A**) *Ex vivo* human peripheral blood neutrophils were stimulated with PMA (25 nM) LPS (100 ng/mL), TNFα (10 ng/mL) or TNFα and LPS combined for 4 hours in the presence or absence of recombinant human VAP-1 (500 ng/mL). NET production was assessed by measuring cell-free DNA via Sytox Green fluorometric assay and (**B**) normalised to untreated control (n = 6). Data shown as median (IQR) and were analysed by two-way ANOVA with Holm-Sidak post-hoc correction. * $p \leq 0.05$, ** $p \leq 0.01$.

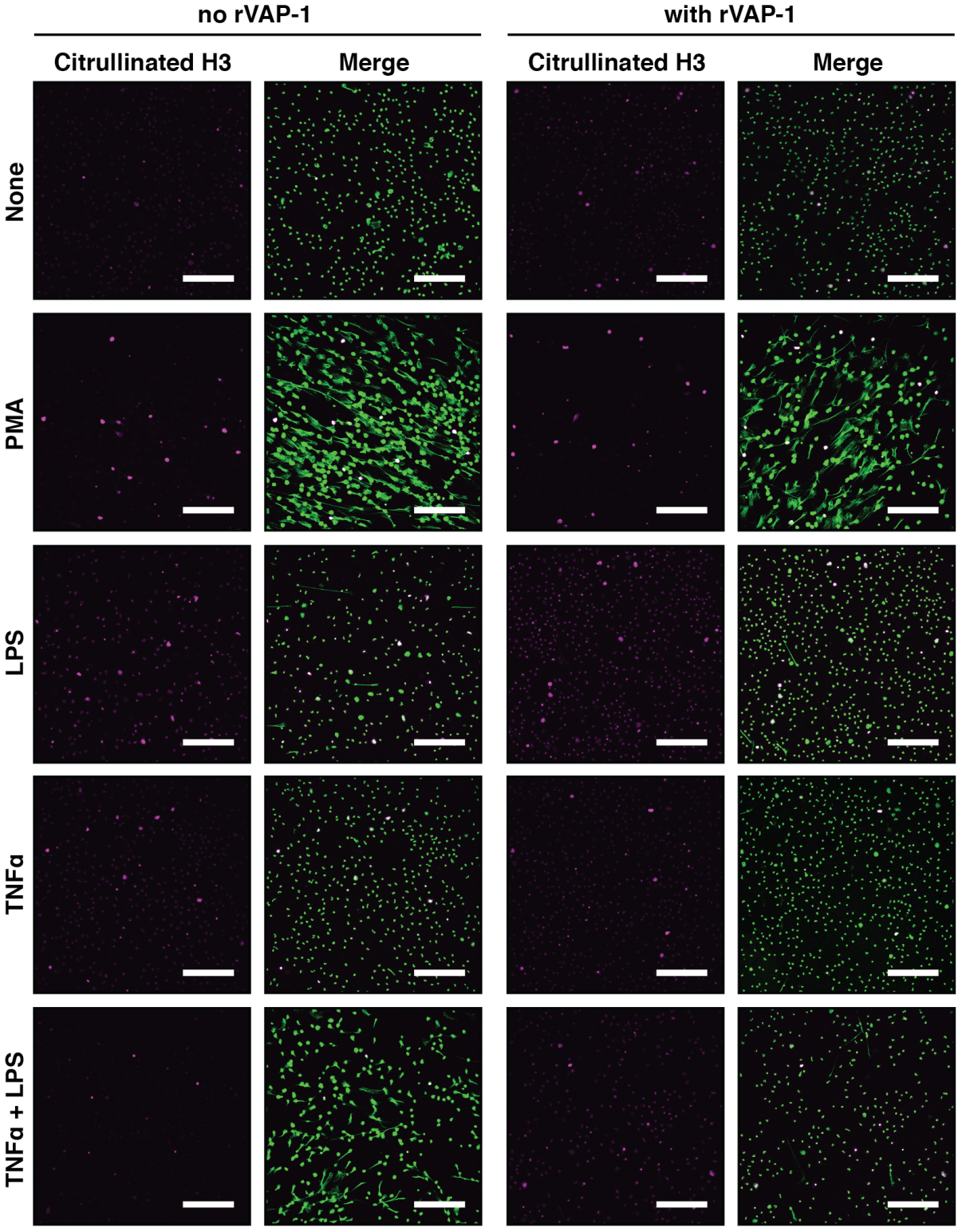


Figure 4.28 Effect of recombinant VAP-1 protein on histone 3 citrullination. *Ex vivo* human peripheral blood neutrophils were stimulated with PMA (25 nM), LPS (100 ng/mL), TNFα (10 ng/mL) or TNFα and LPS combined for 4 hours in the presence or absence of recombinant human VAP-1 (500 ng/mL). Cells were subsequently analysed via immunohistochemistry for the presence of citrullinated histone 3 (pink) and DNA visualised with Sytox Green. White bar: 200 µm.

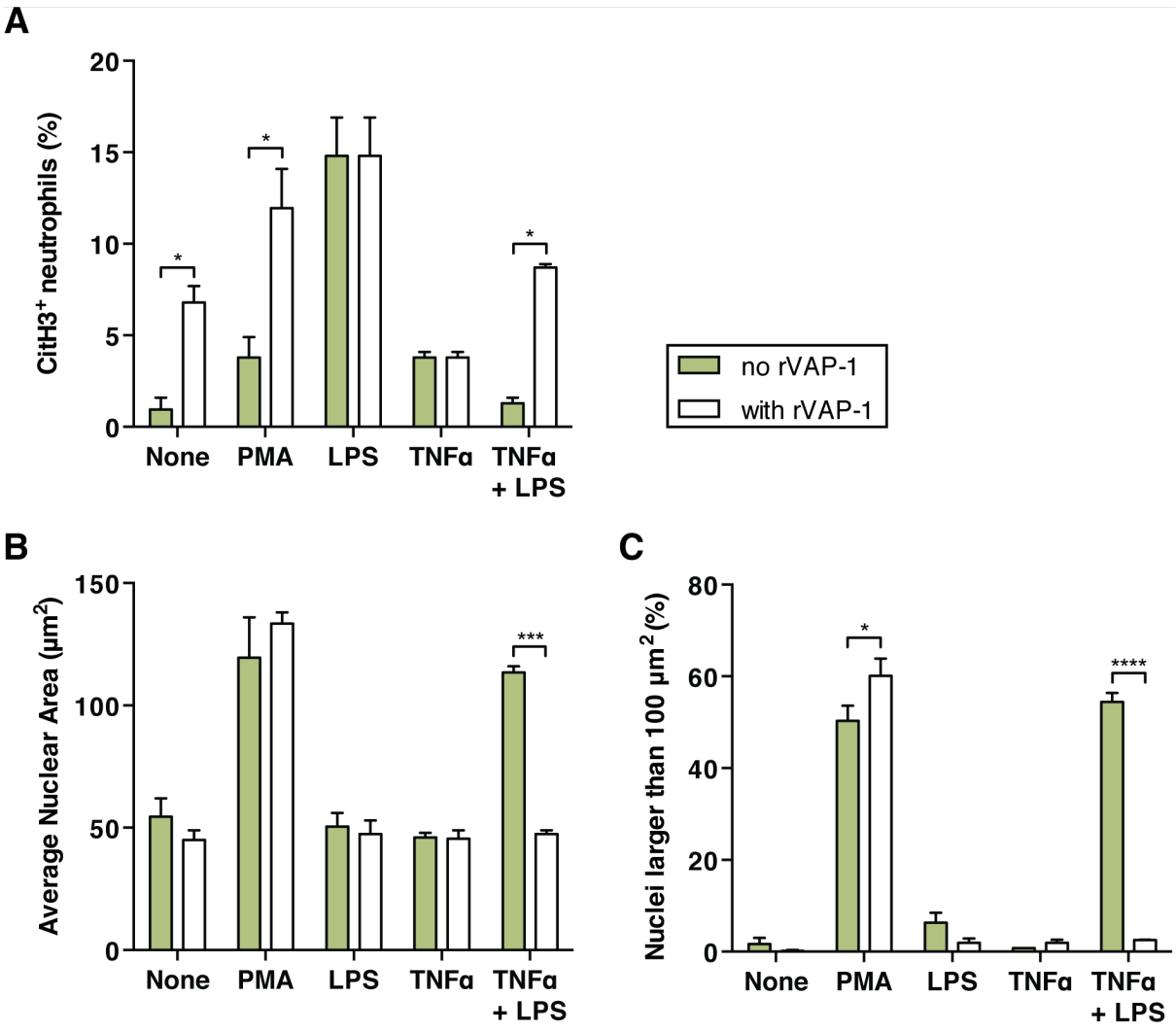


Figure 4.29 Effect of recombinant VAP-1 protein on NETosis. *Ex vivo* human peripheral blood neutrophils were stimulated with PMA (25 nM), LPS (100 ng/mL), TNFα (10 ng/mL) or TNFα and LPS combined for 4 hours in the presence or absence of recombinant human VAP-1 (500 ng/mL). (**A**) Cells were analysed via immunohistochemistry for the presence of citrullinated histone 3 and quantified by ImageJ analysis. (**B**) Nuclei were visualised with Sytox Green and the size of each nucleus enumerated and (**C**) expressed as the proportion of nuclei larger than 100 µm^2 (n = 3 fields of view). Data shown as median (IQR) and were analysed by two-way ANOVA with Holm-Sidak post-hoc correction. * $p \leq 0.05$, *** $p \leq 0.001$, **** $p \leq 0.0001$.

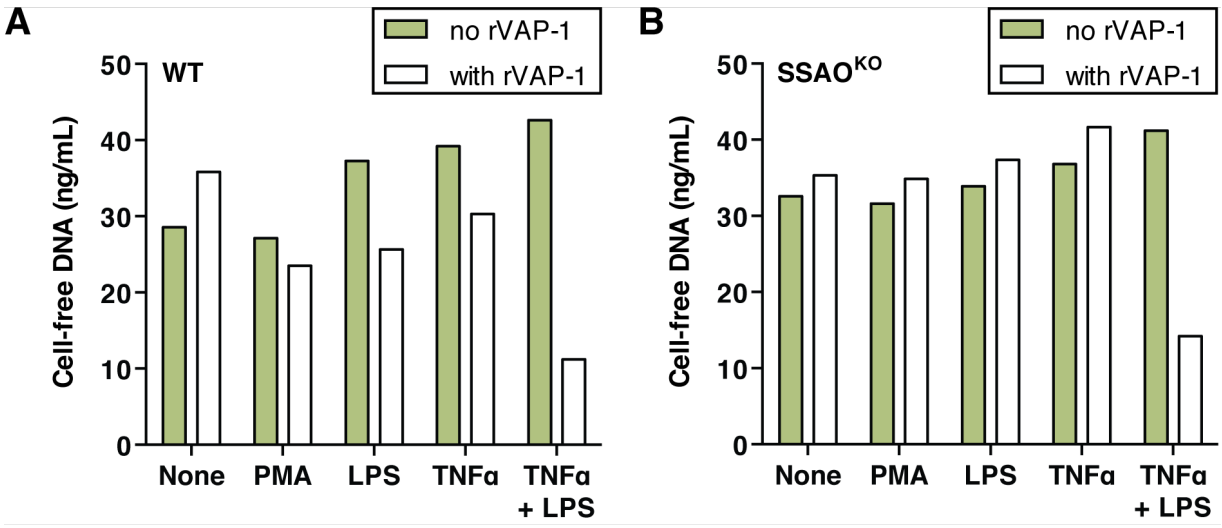


Figure 4.30 Effect of recombinant VAP-1 protein on murine NET production. *Ex vivo* murine bone marrow neutrophils from (**A**) WT or (**B**) $SSAO^{KO}$ animals were stimulated with PMA (25 nM), LPS (100 ng/mL), TNFα (10 ng/mL) or TNFα and LPS combined for 4 hours in the presence or absence of recombinant murine VAP-1 (500 ng/mL). NET production was assessed by measuring cell-free DNA via Sytox Green fluorometric assay ($n = 1$).

4.3 Discussion

The focus of Chapter 4 was to first *interrogate the adhesin functionality of hepatic VAP-1* and then to *investigate the effect of VAP-1 on neutrophil function.*

Flow-based adhesion assays were used to model hepatic lymphocyte recruitment to HSEC *in vitro* and thereby examine the effect of VAP-1 inhibition on this process. These experiments exhibited no clear effect of anti-VAP-1 antibody or small molecule inhibitors on the recruitment of mixed PBLs or isolated subsets to the HSEC monolayer. These findings were supported by additional assays in which T cells and NK cells were not capable of binding and adhering to catalytically active rVAP-1 protein in isolation under flow conditions.

Contrary to the other leukocyte subsets that were examined, neutrophils were effectively captured from flow by rVAP-1 protein. Interestingly, this result that could not be replicated using HSEC and inhibitors of VAP-1. However, further examination of *AOC3* expression and VAP-1 activity in HSEC exhibited downregulation following stimulation with proinflammatory cytokines. It is therefore possible that insufficient VAP-1 was expressed to support adhesion in the TNFα-stimulated HSEC, which may provide an explanation for these contrasting findings.

In order to effectively study any potential neutrophil-VAP-1 interactions it was necessary to ensure high levels of VAP-1 expression within the HSEC while also mimicking an inflammatory state. The cells were therefore transfected with GFP-labelled VAP-1 plasmids. Fluorescent imaging evidenced the successful, although somewhat inconsistent, expression that was unaffected by TNFα; however neutrophil recruitment by the HSEC was still not significantly altered. Despite this, closer inspection of the neutrophil-HSEC interaction clearly demonstrated an intimate relationship: GFP-VAP-1 was highly concentrated at sites of neutrophil contact, which moved with the neutrophils as they traversed the monolayer in transmigratory cup-like structures.

Immunohistochemical analysis revealed that human peripheral blood neutrophils express VAP-1 *ex vivo*, both at the mRNA and protein level. This highly novel finding was the focus of the second part of Chapter 4, with the aim to elucidate some of the functional consequences of neutrophil-derived VAP-1. Amine oxidase activity assays confirmed that the VAP-1 was catalytically active and suggested it was also secreted

from the cells. Enzyme activity was reduced following proinflammatory stimulation, which correlated with a reduction in mRNA production and reduced detection by immunofluorescence. This may also explain why VAP-1 was not detected on intrahepatic neutrophils when examining tissue sections from patients suffering from inflammatory liver disease.

Inhibition of neutrophil-derived VAP-1 did not measurably affect the production of ROS or the ability of neutrophils to undergo NETosis. However, the addition of VAP-1 substrates negatively affected both of these critical effector functions. Neutrophils produced significantly less cell-free DNA following PMA-stimulation in the presence of cysteamine and both basal and PMA-stimulated H_2O_2 production was reduced in the presence of benzylamine. Furthermore, Inhibition of VAP-1 catalytic activity abrogated the inhibitory effect of benzylamine on ROS production. Interestingly, the addition of rVAP-1 also reduced both ROS and NET production, although this only reached statistical significance in the latter. These data suggest that VAP-1 enzyme activity is important for the regular functioning of neutrophils.

4.3.1 Hepatic lymphocyte recruitment via VAP-1

The adhesin function of VAP-1 is well documented in several human tissues, including lymph nodes (Salmi et al., 1998), inflamed synovium (Salmi et al., 1997) and the lungs (Singh et al., 2003). The constitutive expression of VAP-1 by HSEC may suggest that a similar function is also exerted within the sinusoids. However, the data presented here demonstrated no significant effect of VAP-1 inhibition on total lymphocyte adhesion to the HSEC monolayer by SMI or antibody blockade, which corroborates the findings of previous studies (Edwards et al., 2005; Lalor et al., 2007; Shetty et al., 2011; Tuncer et al., 2013). That being said, these previous studies reported that treatment with anti-VAP-1 antibody resulted in a reduction in the proportion of cells that transmigrated across the endothelial monolayer, which was not corroborated by the findings presented within this study.

The discrepancy between the current data and other work may be due to the use of different antibodies: whereas most previous studies used the murine IgM clone 1B2, the newly commercially available IgG_{2a} clone TK8-14 was used herein. TK8-14 is capable of reducing leukocyte adhesion to other endothelial monolayers, but others have also been

unable to replicate this finding in HSEC cells (Jalkanen and Salmi, 2001). This may highlight structural differences between VAP-1 expressed by HSEC and other endothelial cells. Interestingly, the 1B2 antibody also has other documented binding partners, which may affect its function in these assays (Salmi et al., 1997). It is clear from these data that the presence of serum, either human or bovine, facilitates leukocyte adhesion in some manner. Cells were viable for approximately 72 hours with all growth factor-supplemented media, suggesting that non-viability is unlikely to be the cause. It is therefore more probable that one or more of the constituents of the ill-defined serum mixture are required to facilitate adhesion of leukocytes. The finding that rVAP-1 increased adhesion of neutrophils to HSEC may implicate soluble VAP-1 in this process and would be of interest for further investigation.

The current findings may also differ from previous work because of differences in apparatus. The flow-based adhesion assays conducted within this investigated utilised an ibidi system that was specifically designed for this purpose, whereas more rudimentary set-ups were used for all past assays. Edwards et al. used homemade parallel plate flow chambers (Edwards et al., 2005) whereas others used glass capillaries (Lalor et al., 2007; Shetty et al., 2011; Tuncer et al., 2013). It is therefore possible that the material the HSEC were culture on impacted on the function of these cells or the leukocytes as they flowed to and over the monolayer. During these assays the cells were also cultured in open dishes and therefore exposed to contamination such as by endotoxin.

This study also demonstrated that $CD4^+$ and $CD8^+$ lymphocytes (as well as NK cells) were unable to bind directly to rVAP-1 protein under flow conditions. This may be evidence to suggest that these cells are not recruited in a VAP-1-dependent manner, which may provide an explanation as to why PBL adhesion to HSEC was unaffected by VAP-1 inhibition. Correspondingly, $CD4^+$ and $CD8^+$ T cells do not express Siglec 9 or 10, which are proposed VAP-1 ligands (Aalto et al., 2011; Kivi et al., 2009). However, adhesion via Siglec molecules is thought to be enzyme activity-dependent (Elovaara et al., 2016), whereas only antibody blockade of VAP-1 has been previously shown to effectively reduce lymphocyte adhesion to human endothelium (Salmi et al., 1998, 1997). In a murine Con A model of liver injury only T_h2 $CD4^+$ lymphocyte adhesion was reduced by anti-VAP-1 antibody (Bonder et al., 2005). Similarly, adhesion of $CD4^+$ lymphocytes is reduced in *Aoc3*$^{-/-}$ mice compared to WT during chronic CCl_4, chronic MCD diet, chronic

WLM (Weston et al., 2015) and acute Con A models of liver injury (Lee et al., 2013). This supports previous suggestions that VAP-1 is not involved in the initial tethering of lymphocytes but is involved in transmigration, therefore requiring additional molecules to recruit lymphocytes from flow (Edwards et al., 2005; Lalor et al., 2007; Shetty et al., 2011; Tuncer et al., 2013). Similarly, the first paper describing a functional role for VAP-1 demonstrated that lymphocytes adhered to immunopurified VAP-1 protein under static conditions (Salmi and Jalkanen, 1992), which differs from the current findings shown in Figure 4.7. This may also highlight differences between the source of VAP-1 molecules: if lymphocytes interact with VAP-1 then is likely via N-glycosylated residues on the molecules surface (Maula et al., 2005), and it is highly probable that the commercially available rVAP-1 used in this study is aberrantly glycosylated by the host *Spodoptera frugiperda* and therefore may not support adhesion. Furthermore, unpublished data from our research group has also found that recombinant VAP-1 produced in Chinese hamster ovary cells is also unable to bind to lymphocytes in similar assays. A similar line of reasoning is also thought to explain the lack of adhesive capacity demonstrated by VAP-1 of smooth muscle cell origin (Jaakkola et al., 1999). However contamination of the purified VAP-1 used in the original assays with other molecules that may support adhesion cannot be excluded (Salmi and Jalkanen, 1992), particularly as the 1B2 antibody used for the immunoaffinity purification step was found to bind to an unrelated protein sequence (Salmi et al., 1997).

Flow-based adhesion assays provide a useful reconstruction of leukocyte recruitment in the presence of shear stress and allow analysis of adhesion under well-defined force. However, they are subject to many variables that can affect the repeatability of the data. For instance the use of primary human cells is thought to resemble conditions most similar to those *in vivo*, yet they are highly variable and in isolation do not mimic the environment of the hepatic sinusoid precisely, such as lack of stromal cells and interactions with Kupffer cells. Results shown in Chapter 3 of this thesis demonstrated disease-specific variability in VAP-1 expression that could affect the outcomes of adhesion assays. However, unpublished observations from this group suggest that once cultured, HSEC revert to a similar "*in vitro* phenotype" regardless of disease. One source of variation is the fact that each experiment was repeated with HSEC and PBL from different donors to reduce the effect from any one HSEC-PBL pairing that may skew the data. This may account for the spread of data exhibited here, which may have obscured

subtle differences in adhesion. Factors such as the method of cell isolation, passage number, cell density and growth conditions can affect the cell phenotype, including expression of adhesion molecules and this impacts on the results of the assay. This study also demonstrated the importance of serum for leukocyte migration across HSEC; therefore batch variation may also affect the outcome of assays. For this reason all of these factors were kept as similar between repeats as possible, although this was a challenge when dealing with primary cells that relied on liver transplants for tissue and the availability of a pool of donors for the isolation of leukocytes. The assay also fundamentally relies on the correct and consistent identification of immune cells at different stages of migration by phase-contrast microscopy. This is a difficult method of analysis that can easily skew the data and mask subtle differences between treatments. Furthermore, a critical characteristic of leukocyte recruitment within the liver is the narrow diameter of the sinusoids, which provides a large surface area for interactions to occur and maximises the interactions between the cells. In these assay HSEC are grown as a flat monolayer and the slide has a height of 0.4 mm, almost two hundred times greater than the sinusoidal diameter.

Flow-based adhesion assays are routinely carried out using TNFα-stimulated HSEC to mimic the inflammatory environment of the liver (Edwards, 2005), however this study found that this reduced the expression of VAP-1. A similar dose-dependent reduction in *AOC3* mRNA levels has been previously recorded in adipocytes, which corresponded to a reduction in total protein level and enzyme activity (Mercier et al., 2003). In the present study, downregulation of VAP-1 expression by TNFα may have resulted in insufficient levels to observe any significant changes in adhesion by VAP-1 inhibition. This may also explain the difficulties associated with identifying VAP-1 within HSEC by immunohistochemistry. Interestingly, the single previous study that demonstrated a significant reduction in lymphocyte adhesion to HSEC with anti-VAP-1 found that TNFα did not affect surface VAP-1 expression when measured by ELISA (Lalor et al., 2002). The constant level of surface VAP-1 found in that study may explain why anti-VAP-1 had the effect of immune cell recruitment that was not seen in the present experiments; however the previous study was also conducted under static conditions and in both cases used a different anti-VAP-1 clone (1B2). Furthermore, TNFα also increases expression of ICAM-1 and CD18 in HSEC, which facilitate leukocyte recruitment and may negate the

need for VAP-1 to be present for the recruitment of inflammatory cells (Sakamoto et al., 1997).

4.3.2 Overexpression of GFP-VAP-1

The recent development of the GFP-VAP-1 fusion protein by Weston and colleagues has allowed for real-time *in vitro* visualisation of VAP-1 within live cells (Weston et al., 2013). Transfection of HSEC with GFP-VAP-1 was used in this study to examine the involvement of VAP-1 in neutrophil adhesion to the sinusoids. HSEC are particularly difficult to transfect by traditional lipid-based approaches (Weston et al., 2013) therefore nucleofection provided a useful alternative. Nucleofection also has additional benefits to more traditional methods, such as being less damaging and therefore preserving a more physiological state (Livingston et al., 2012). Unfortunately transfection efficiencies were also low when employing nucleofection, with few cells exhibiting strong GFP-VAP-1 expression despite extensive optimisation steps. Accordingly, plasmid incorporation into the host genome was also low, demonstrated by the gradual reduction in VAP-1 expression. Fluorescence was almost completely lost by 72 hours post-transfection, which is in line with previously recorded VAP-1 turnover *in vivo* (O'Rourke et al., 2007; Vainio et al., 2005). HSEC also exhibit high level of scavenging activity, therefore rapid plasmid turnover was not unexpected (Elvevold et al., 2004).

VAP-1 amine oxidase activity could only be detected at very low levels within the media of transfected endothelial cells, thereby suggesting that the diminished fluorescent signal was due to degradation rather than secretion. Similar findings have been observed in untransfected endothelial cells *in vitro* (Salmi and Jalkanen, 1995) and confocal imaging of transfected HSEC showed that a large proportion of the protein was present in lysosomes (Weston et al., 2013). This is contrary to murine *in vivo* studies that demonstrated an endothelial origin of sVAP-1 (Stolen et al., 2004), thus suggesting the critical presence of an additional factor required for secretion; this may be a metalloproteinase as suggested for soluble VAP-1 derived from adipocytes (Abella et al., 2004) and retinal capillary endothelial cells (Murata et al., 2012).

Cell-surface VAP-1 enzyme activity on HSEC was much lower than that of HEK293 cells transfected with GFP-VAP-1^{WT}. In correlation with this, immunohistochemical analysis of transfected HSEC found that very little GFP-VAP-1^{WT} and GFP-VAP-1^{Y471F} localised

to the cell surface, with most located within intracellular structures. This may contribute to the low activity levels of VAP-1 recorded at the surface. Weston et al. also noted this localisation in their original study using these constructs, recording specific localisation to ER, Golgi and early endosomes (Weston et al., 2013). Although this may be a difference in processing brought about by the addition of GFP, several other studies have also previously suggested an intracellular localisation of native VAP-1 within endothelium (Salmi and Jalkanen, 1995; 2011). During inflammation VAP-1 may be rapidly mobilised to the cell surface (Jalkanen and Salmi, 2001), however TNFα had no effect on VAP-1 localisation in this study. If scarcely any VAP-1 is expressed on the surface of cultured HSEC it may explain why inhibition had little effect on leukocyte adhesion.

4.3.3 Hepatic neutrophil recruitment via VAP-1

Early neutrophil recruitment is key to the pathologies of various liver diseases including NASH (Rensen et al., 2012), ALD (Jaeschke, 2002) and acute inflammatory liver injury (Ramaiah and Jaeschke, 2007). Accumulation of neutrophils within the sinusoids is typically the first step in the progression of these diseases (Jaeschke and Smith, 1997). The results herein represent, to the author's knowledge, the first investigation into the role of VAP-1 in the adhesion of neutrophils within the human liver. This study found that inhibition of VAP-1 had no significant effect on neutrophil adhesion to HSEC *in vitro* under flow conditions (Figure 4.5). Murine *in vivo* studies had previously shown a reduction in rolling neutrophils within the post-sinusoidal venules when mice suffering from Con A-induced liver injury were administered anti-VAP-1 (Bonder et al., 2005). However, most neutrophils involved in the injury process extravasate from the sinusoids and not postsinusoidal venules (Jaeschke and Smith, 1997). The role of VAP-1 in neutrophil adhesion to other tissues is also quite well evidenced: VAP-1 antibody blockade reduced adhesion to human tonsil HEV (Salmi and Jalkanen, 1992) and myocardium endothelium (Jaakkola et al., 2000) as well as extravasation across inflamed murine peritoneum (Kirton et al., 2005; Merinen et al., 2005). Inhibition of VAP-1 enzyme activity also reduced neutrophil adhesion to murine cornea (Nakao et al., 2011), lung endothelium (Schilter et al., 2015) and to sites of rat adjuvant-induced arthritis (Marttila-Ichihara et al., 2006), inflamed air pouches (Koskinen et al., 2004)

and kidneys following ischemic reperfusion injury (Tanaka et al., 2017). However, these studies may also raise important cross-species variation in VAP-1 activity.

This study demonstrated for the first time that neutrophils are capable of adhering to rVAP-1 protein under conditions of flow, supporting the notion that either TNFα-stimulated HSEC express insufficient levels of VAP-1, that VAP-1 expressed by HSEC is incapable of supporting adhesion or that a binding partner protein or small molecule renders the VAP-1 unable to bind to neutrophils. The idea that the levels of VAP-1 are insufficient to support adhesion may be somewhat refuted by the finding that even when GFP-VAP-1^{WT} was overexpressed this conferred only a slight non-significant increase in adhesion, possibly because transfection efficiencies were low and most GFP-VAP-1 did not localise to the cell surface. In support of a role for the enzyme activity of VAP-1 in facilitating neutrophil adhesion, overexpression of GFP-VAP-1^{Y471F} did not promote recruitment of neutrophils, highlighting the importance of enzyme activity for this process. HSEC were also treated with TNFα in these assays, which did not affect the distribution of GFP-VAP-1, but would have upregulated the expression of other adhesion molecules such as hyaluronan or ICAM-1, thereby possibly obscuring any effect of GFP-VAP-1 expression (McDonald et al., 2008; Sakamoto et al., 1997).

The fact that rVAP-1 supported neutrophil adhesion but did not support adhesion of NK cells or lymphocyte clearly highlights distinct functional adhesive mechanisms between the cells. This may suggest that lymphocytes require additional accessory molecules to support their tethering, whereas neutrophils do not. For example Lalor and colleagues found an additive effect of blocking PBL adhesion to TNFα-stimulated HSEC with antibodies against VAP-1 and ICAM-1 in combination (Lalor et al., 2002). If rVAP-1 does not support lymphocyte adhesion due to aberrant glycosylation then these findings suggest this is not fundamental for neutrophil adhesion but is critical for lymphocyte interactions, as previously suggested (Maula et al., 2005). However, the proposed VAP-1 ligand Siglec-9 is expressed exclusively on cells of the myeloid lineage and is therefore absent from lymphocytes and NK cells (Aalto et al., 2011; Zhang et al., 2000). Previous work from our group has also demonstrated that $CD16^{+}$ monocytes, which express Siglec-9, adhere to HSEC in a VAP-1-dependent manner (Aspinall et al., 2010). Interestingly, the VAP-1-Siglec-9 interaction has recently been proposed to occur via a sialic acid-binding domain of Siglec-9 (Elovaara et al., 2016). This would therefore

suggest that the rVAP-1 used in the current experiments contain some level of sialylation for the interaction to take place.

Incubation of HSEC with rVAP-1 promoted neutrophil adhesion whereas incubation with rVCAM-1 did not. HSEC *in vivo* are capable of antigen uptake and presentation to leukocytes as part of the tolerogenic immune environment of the liver (Schurich et al., 2009). Likewise HSEC are capable of actively endocytosing large proteins, such as BSA (Smedsrød et al., 1990). It is therefore possible that rVAP-1 is actively taken up from the media and presented to neutrophils, thus facilitating adhesion. It is also possible, however, that VAP-1 was specifically captured on the HSEC surface by a previously uncharacterised binding partner or by the glycocalyx (Curbishley et al., 2005). However, it is widely believed that the latter takes approximately one week to fully form following trypsinisation and may therefore not be present during these assays. The uptake of VAP-1 could be examined in future assays by repetition in the presence of endocytosis inhibitors.

The increased neutrophil adhesion in the presence of rVAP-1 may explain why VAP-1 appears to play a more substantial role in leukocyte migration within the liver *in vivo* than *in vitro*: increased serum VAP-1 concentrations like those observed during CLD may result in increased uptake and presentation of VAP-1 and subsequent increased leukocyte migration to the liver. This may also be a contributing factor to the finding that the presence of VAP-1-containing serum increased leukocyte adhesion by almost three-fold (Figure 4.3). Furthermore, inhibition of VAP-1 had a more pronounced effect on migration in the presence of serum, although this was not statistically significant. Previous studies by Kurkijärvi and colleagues found also that preincubating leukocytes with human serum increased adhesion to VAP-1-transfected cells, an effect that was reversed when serum was depleted of VAP-1, implicating a VAP-1-VAP-1 interaction (Kurkijärvi et al., 1998).

Observation of flow-based adhesion assays using confocal microscopy demonstrated GFP-VAP-1^{WT} accumulation at sites of neutrophil adhesion, suggesting an active role in the interaction. The structures presenting VAP-1 to the neutrophils were highly similar to previously described 'transmigratory cups': docking structures on the apical surface of endothelium (Carman and Springer, 2004). These features were first described as actin-rich ICAM-1- and VCAM-1-containing structures that anchor and partially

embrace migrating leukocytes (Barreiro et al., 2002). Colocalisation of ICAM-1 and VAP-1 staining has previously been documented surrounding $CD4^+$ lymphocytes adherent to HSEC although it was not clear if these were simply an experimental artefact (Shetty et al., 2011). Interestingly, transmigratory cups contain high levels of caveolin-1 (Carman and Springer, 2004), which also colocalises with VAP-1 in smooth muscle cells (Jaakkola et al., 1999) and adipocytes (Souto et al., 2003). It is thought that these structures assemble following the initial engagement of endothelial-cell adhesion molecules with their cognate ligands and guide extravasation (Carman and Springer, 2004). Unfortunately no transmigrating neutrophils were captured during the course of this study. However, the images collected demonstrate higher levels of GFP-$VAP\text{-}1^{WT}$ at the leading edge of the migrating cell. This is consistent with previous immunohistochemical identification of VAP-1 at sites of transmigrating lymphocytes (Shetty et al., 2011). Upon activation with their ligands leukocytes become polarised: chemokine receptors are redistributed to the cellular front and adhesion receptors toward the rear pole (Vicente-Manzanares and Sánchez-Madrid, 2004). It is therefore possible that VAP-1 is involved in interactions with exploratory filopodia and lamellipodia at the front of the migrating cell, facilitating leukocyte crawling along the luminal surface. VAP-1 may therefore also function in determining the mechanism of diapedesis as transmigratory cups are thought to be involved in the transcellular mechanism rather than paracellular route (Shetty et al., 2011).

4.3.4 Expression of VAP-1 by neutrophils

The first paper describing VAP-1 as an adhesion molecule stated that peripheral blood lymphocytes, monocytes, NK cells and granulocytes were all negative for VAP-1 expression as measured by FACS analysis using the 1B2 clone antibody (Salmi and Jalkanen, 1992). This is referenced through much of the literature with little additional evidence in support. On the contrary, this study identifies for the first time that VAP-1 is produced by peripheral blood neutrophils of healthy individuals at both the mRNA and protein levels. Of note, expression of *AOC3* mRNA has been recorded during other studies, but was not highlighted. For example Jiang and colleagues investigated the transcriptomes of neutrophils from healthy individuals and those suffering from juvenile idiopathic or cystic fibrosis and identified *AOC3* as one of nearly 8,000 genes that were expressed in all samples (Jiang et al., 2015). Similarly, databases such as the European

Bioinformatics Institute (EMBL-EBI) Gene Expression Atlas and the Scripps Research Institute 'BioGPS' also list neutrophils as *AOC3* expressers.

Assessing neutrophil expression of VAP-1 at the protein level was hindered by nonspecific binding of detection antibodies to Fc receptors on the cell surface, resulting in positive IMC signals. This was minimised by the addition of blocking steps in the staining procedure and was accounted for by adjusting the fluorescent detection threshold but this may have obscured subtle changes in expression. However following careful controls, VAP-1 did not appear to localise to the neutrophil surface but was instead intracellular in nature. The observed punctate staining of VAP-1 may be indicative of granular localisation similar to that reported in endothelial and smooth muscle cells (Salmi et al., 1993). Neutrophil granules are highly heterogeneous with distinct protein content and function, therefore the clarification of which of these contain VAP-1 may provide valuable information as to the functional consequence of VAP-1 expression. Interestingly, AOC1 (also known as histaminase) is found within the lumen of neutrophil specific granules where it is involved in the degradation of histamine (Ringel et al., 1984). Specific granules are MPO-negative and rich in antibiotic substances and thus participate mainly in antimicrobial activities by mobilising to either the phagosome or exterior of the cell (Faurschou and Borregaard, 2003). The findings of this study demonstrated that neutrophil-derived VAP-1 is catalytically active; therefore it is possible that VAP-1 is also involved in the degradation of amines such as the bacterial-derived cysteamine and aminoacetone following phagocytosis of these cells. Neutrophils also express abundant Vanin-1 both on their surface and within granules, which may also provide an additional source of cysteamine through the generation of pantothenate from pantetheine (Nitto and Onodera, 2013).

Neutrophils are also able to secrete AOC1, which then binds to endothelial cell and fibroblast receptors where it can carry out its function in histamine degradation (Baenziger et al., 1994). During the present study neutrophils were also shown to secrete catalytically active VAP-1, a potential factor in why bone tissue is a significant contributor to serum VAP-1 levels (Ekblom et al., 1999). The secreted VAP-1 may function similarly to AOC1 and catabolise local concentrations of toxic amines, such as bacterial-derived cysteamine. Additionally, treatment of HSEC with rVAP-1 resulted in increased adhesion of neutrophils to the monolayer; therefore secreted VAP-1 may also promote adhesion of leukocytes. This would result in an additive effect whereby local

concentrations of neutrophils would promote and facilitate the recruitment of additional cells.

The punctate VAP-1 staining may also indicate a mitochondrial distribution for VAP-1. Neutrophils express the mitochondrial enzyme ALDH2 (Jiang et al., 2015), which was recently proposed to be a VAP-1 binding partner (Ke et al., 2016). ALDH2 is critical in the catabolism of dopamine following its deamination by MAOA and MAOB (Arreola et al., 2016). Dopamine is also a good substrate for VAP-1 and may therefore also play a role in its catabolism (Shen et al., 2012). Neutrophil function is modulated by dopamine via expression of several dopamine receptors (McKenna et al., 2002), activation of which can result in reduced phagocytic activity, ROS production, chemotaxis (Wenisch et al., 1996) and the expression of adhesion molecules (Sookhai et al., 2000) therefore VAP-1 may also be involved in these processes.

Interestingly, this study also demonstrated a reduction in VAP-1 expression upon stimulation of neutrophils with proinflammatory mediators, similar to that observed for HSEC. This was recorded at both the mRNA and protein levels and corresponded to a reduction in VAP-1 activity. Responses of human neutrophils to TNFα, IFNϒ, LPS and PMA are complex and multifactorial, however VAP-1 expression was lowered under all conditions studied. Correspondingly, treatment of retinal capillary endothelial cells with TNFα *in vitro* also leads to a reduction in VAP-1 protein, although this was due to secretion into the culture media as sVAP-1 and did not affect mRNA production (Murata et al., 2012). This is likely the explanation for why tissue-resident neutrophils have not been previously seen to express VAP-1: high levels of proinflammatory mediators within inflamed tissue leads to decreased VAP-1 expression as the neutrophils migrate into the tissue. Interestingly the physical interaction between neutrophils and HSEC did not appear to affect VAP-1 expression, regardless of whether the HSEC had been prestimulated with proinflammatory molecules. This may suggest that the act of migration itself does not alter the expression of VAP-1.

4.3.5 Neutrophil-derived VAP-1 and recruitment

Neutrophils can adhere to rVAP-1 protein; therefore it was of interest to investigate whether neutrophil-derived VAP-1 was also involved in this process. Somewhat unexpectedly, inhibition of neutrophil VAP-1 enzyme activity resulted in an

approximately two-fold increase in adhesion to rVAP-1 protein and a slight, non-significant increase in adhesion to TNFα-stimulated HSEC. This is in conflict with most previous data that suggests inhibition of endothelial VAP-1 results in reduced leukocyte recruitment *in vitro* (Lalor et al., 2002; Salmi and Jalkanen, 2006). Furthermore, several studies have also demonstrated reduced neutrophil recruitment *in vivo* in the presence of systemic VAP-1 inhibitors, to which neutrophils would also be exposed (Foot et al., 2013; Nakao et al., 2011; Schilter et al., 2015). However, all *in vivo* inflammatory models would also drive the upregulation of proinflammatory molecules such as TNFα, which according to the results shown here would lower neutrophil VAP-1 expression and potentially quench the increase in adhesion caused by VAP-1 inhibition.

Immunohistochemical analysis showed that VAP-1 was not surface-expressed and inhibition of rVAP-1 had little effect on neutrophil adhesion; together these results suggest an indirect effect of VAP-1 inhibition, such as the amine oxidase activity of VAP-1 removing an amine with pro-adhesive properties or producing an aldehyde with anti-adhesive properties. This effect would then be reversed upon addition of the inhibitor. One possible pathway may be the interaction of biogenic amines with trace amine-associated receptors (TAARs), which are expressed on a variety of leukocytes and peripheral tissues and are thought to be involved in several processes including migration (Babusyte et al., 2013).

4.3.6 Functional consequence of neutrophil VAP-1 expression

One of the primary effector functions of neutrophils is their ability to rapidly release cytotoxic ROS produced via NADPH oxidase (NOX) during the respiratory burst. This generation of ROS is also thought to be a critical step in the formation of extracellular traps during NETosis (Fuchs et al., 2007; Steinberg and Grinstein, 2007). The results of this study found that inhibition of human neutrophil VAP-1 activity had no effect on PMA-stimulated ROS production or NETosis. However, incubation of neutrophils with VAP-1 amine substrates or rVAP-1 protein resulted in lower rates of ROS production and total NET formation.

The reduction in both ROS and NETosis in the presence of rVAP-1 was independent of inflammatory stimuli and was proportionally similar across conditions. However a constant concentration of rVAP-1 was used throughout the study therefore the

dose-dependent nature of this response cannot be determined. The concentration of rVAP-1 used (500 ng/mL) was within the physiological range of sVAP-1 in human serum; falling between concentrations found in normal serum and the elevated levels of patients suffering from NASH (Weston et al., 2015). Interestingly, the neutrophils from patients with NASH exhibit increased ROS production *ex vivo* compared to those from healthy individuals (Inzaugarat et al., 2011) whereas those from patients suffering acute liver failure - who have decreased sVAP-1 concentrations (Kurkijärvi et al., 2000) - exhibit reduced ROS production (Clapperton et al., 1997). Although this may suggest an inverse correlation between ROS production and sVAP-1 levels, there is no additional evidence that this relationship is causative and is probably due to additional factors. For example, the increased ROS produced by neutrophils from ALD patients is caused by elevated LPS concentrations within the serum (Mookerjee et al., 2007).

During this study neutrophils were shown to secrete sVAP-1, which may subsequently act similarly to rVAP-1 and reduce ROS production and NETosis thereby dampening the response of other local neutrophils in a VAP-1-dependent feedback loop. During inflammation, when an immune response is required, local increased concentrations of proinflammatory stimuli would downregulate neutrophil VAP-1 expression. In turn, this would reduce the secretion of VAP-1, removing the modulation of neutrophil effector functions. Assuming membrane-bound VAP-1 can also elicit the same response as soluble VAP-1 then ROS production and NETosis would be reduced within the sinusoids. This may contribute to the tolerogenic environment within the liver by reducing inappropriate responses of circulating neutrophils to harmless commensals.

The addition of VAP-1 substrates also reduced ROS production and NETosis, however the extent of this effect varied between amines. Histamine is the poorest VAP-1 substrate and accordingly demonstrated the least effect on neutrophil function of the three examined amines, despite playing a role in normal neutrophil function (Alcañiz et al., 2013). Although benzylamine is a non-physiological substrate for VAP-1, it consistently led to reduced ROS production and NETosis in response to PMA. In addition, inhibition of VAP-1 activity reversed the benzylamine-induced modulation of ROS production. Together, these data indicate that VAP-1 activity is critical to this observed effect and may therefore exert these effects via a product of this reaction. H_2O_2 is known to modulate the respiratory burst of human neutrophils, however only at micromolar concentrations and not upon stimulation with PMA so is unlikely to be the only active

product (Winn et al., 1991). Benzaldehyde – the product of benzylamine oxidation - may therefore have an inhibitory function on neutrophil effector function. Aminobenzaldehyde is thought to inhibit neutrophil elastase and proteinase 3 within azurophilic granules; therefore benzaldehyde may also act in a similar manner (Hwang et al., 2015).

Cysteamine is a good physiological substrate of VAP-1 (Shen et al., 2012) and the high expression of Vanin-1 and -2 by neutrophils means that it is also readily available (Nitto and Onodera, 2013). Cysteamine exhibited the largest reduction of NETosis in response to PMA but comparatively also dramatically increased ROS production in resting cells. Interestingly, a similar effect has been observed by treatment of neutrophils with ammonia: impaired neutrophil phagocytosis and increasing oxidative burst (Shawcross et al., 2008). However, this may be a cysteamine-specific effect, for example cysteamine is an inhibitor of the rate-limiting enzyme in glutathione synthesis, γ-glutamylcysteine synthase. Glutathione is crucial for the detoxification of H_2O_2 that has diffused into the cytosol from ROS produced by NOX enzymes (Franco et al., 2007). The recorded increase in H_2O_2 production may therefore be a result of decreased glutathione available to scavenge any that leaks. However, it may also have simply been an experimental artefact caused by cysteamine interacting with the Amplex UltraRed assay due to its strong reducing properties.

The results shown here found that the addition of rVAP-1, benzylamine or cysteamine reduced PMA-induced NETosis and ROS production in a similar manner; therefore a common mechanism of action is likely. PMA directly activates neutrophil protein kinase C (PKC) (Castagna et al., 1982), which then phosphorylates components of NOX (Bouin et al., 1998; Kramer et al., 1988), activating the enzyme thereby inducing the production of superoxide and subsequently H_2O_2 (Chessa et al., 2010). This is also thought to be a key stage in NETosis, although the mechanism is yet to be fully elucidated, as outlined in Figure 4.31 (Fuchs et al., 2007; Steinberg and Grinstein, 2007). It is therefore possible that the aldehyde products of the VAP-1-catalysed reaction elicited an inhibitory function on ROS production and therefore NETosis. In murine macrophages, two physiological aldehydes, acetaldehyde and acrolein, have been found to bind to an atypical isoform of PKC, PKCζ, resulting in its translocation to the nucleus (Yao et al., 2010). Once in the nucleus, PKCζ forms a complex with the CREB-binding protein (CBP) and acetylated RelA-p65, which causes phosphorylation and acetylation of histones on

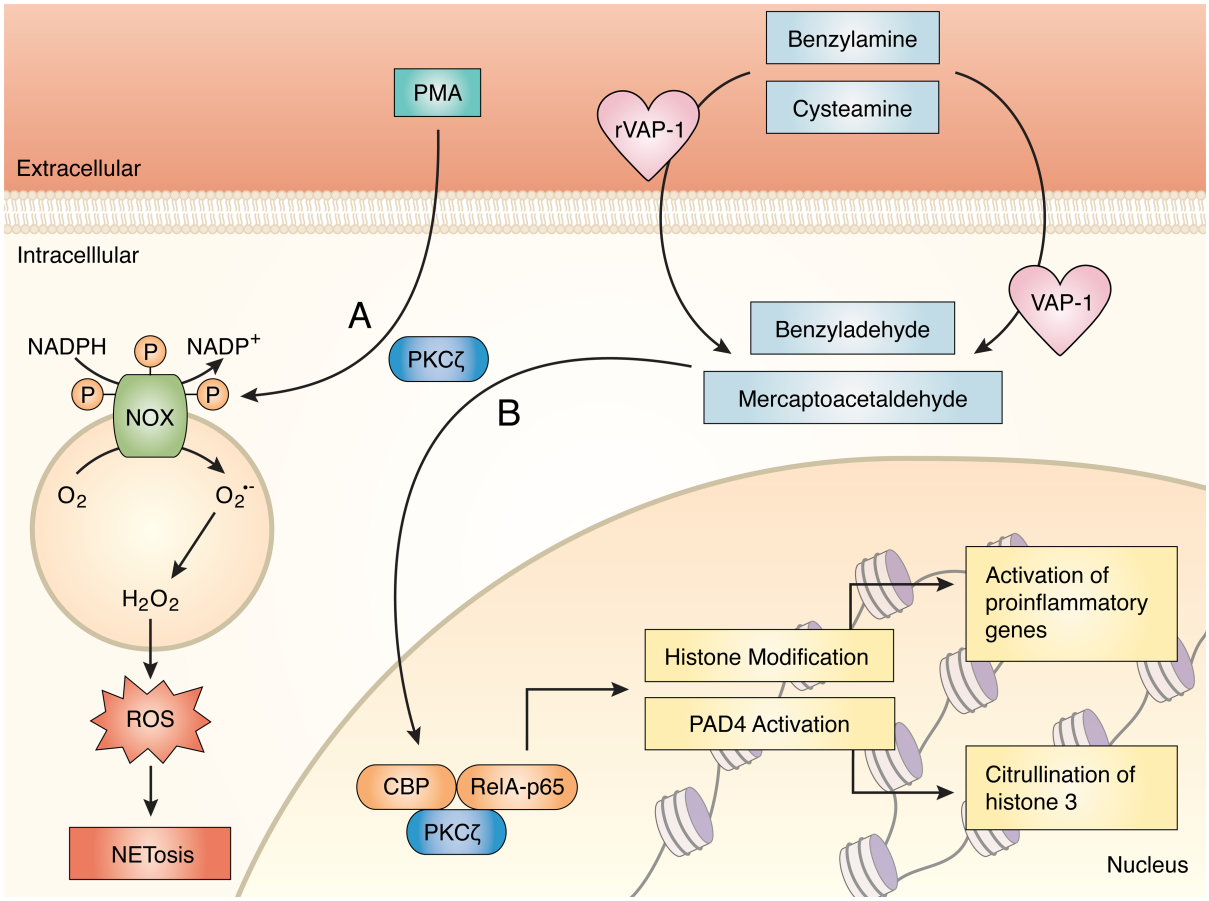


Figure 4.31 A possible mechanism of VAP-1 in NETosis. (**A**) Protein Kinase C subtype ζ (PKCζ) is activated by PMA, which in turn activates phagosomal NADPH oxidase (NOX) thereby promoting the production of ROS. This is thought to be a critical step in the formation of NETs. (**B**) Aldehydes produced by the amine oxidase activity of VAP-1 may bind to PKCζ, resulting in its translocation to the nucleus. Nuclear PKCζ forms a complex with the CREB-Binding Protein (CBP) and RelA-p65, which induces posttranslational modifications of histones at the promoters of proinflammatory genes such as IL-6 and CXCL2. This also results in PAD4 activation and subsequent citrullination of histone 3, which may also be involved in NETosis. Therefore VAP-1 activity may reduce ROS production and NETosis while promoting the citrullination of histone 3.

the promoters of proinflammatory genes (Yao et al., 2010). Interestingly, specific inhibition of PKCζ in neutrophils results in inhibition of PMA-induced NETosis (Neeli and Radic, 2013). Therefore mercaptoacetaldyde and benzaldehyde produced by VAP-1 during oxidation of cysteamine and benzylamine, respectively, may also promote the translocation of PKCζ to the nucleus. The sequestering of PKCζ may therefore reduce its availability to activate NOX, thereby decreasing the generation of ROS and NETs, as shown in Figure 4.31.

Immunohistochemical analysis of NET-forming neutrophils revealed very low numbers of CitH3-positive cells following PMA stimulation. This is line with other recent evidence suggesting citrullination of PAD4 may not be a prerequisite of NETosis (Douda et al.,

2015; Neeli and Radic, 2013). Interestingly, the addition of rVAP-1 increased the number of CitH3-positive neutrophils in these experiments, despite reducing the total number of cells undergoing NETosis. PKCζ is an activator of PAD4 (Neeli and Radic, 2013), which is located within the nucleus (Rohrbach et al., 2012). The addition of VAP-1 may therefore increase the local concentration of aldehydes, resulting in the translocation of PKCζ to the nucleus and resulting in activation of PAD4 and citrullination of H3.

This hypothesis could be examined by western blot analysis of neutrophils lysates following treatment with benzylamine, cysteamine, benzaldehyde and mercaptoacetaldyde in combination with LJP-1586 for colocalisation of PKCζ, CBP and RelA-p65. Similarly, immunohistochemical analysis of PKCζ localisation following treatment and analysis of nuclear PKCζ-activated gene expression by qPCR, such as CXCL2 and IL-6, may also provide useful insights (Yao et al., 2010).

Although only representing a single experiment, the murine neutrophil data revealed measurable differences in responses between cells of mouse and human origin. Murine neutrophils are thought to produce NETs in a similar NOX-dependent manner in response to PMA, but PMA can also promote autophagy in these cells (Remijsen et al., 2011). This may explain why PMA-stimulation increased ROS production within this study, but very little cell-free DNA was detected. The fact that rVAP-1 reduced this low levels may therefore also indicate a role for VAP-1 in autophagy, but this is purely speculative. Interestingly, unlike the human experiments, murine-specific rVAP-1 did not reduce ROS production of mouse neutrophils in response to stimulation despite also being catalytically active. This may suggest fundamental differences between the two organisms, for example murine neutrophils may not express *Aoc3* mRNA. This was unfortunately not completed in the course of this study but may be a prerequisite for the effect exerted by rVAP-1. Similarly, this may highlight important differences between bone marrow-derived and peripheral neutrophils, for example peripheral cells would be exposed to both serum and membrane-bound VAP-1 prior to isolation. However, further experiments are required to elucidate the true mechanism.

4.3.7 Chapter summary

The data presented here support previous findings that inhibition of VAP-1 does not affect leukocyte adhesion to human HSEC *in vitro* (Edwards et al., 2005; Lalor et al.,

2007; Shetty et al., 2011; Tuncer et al., 2013). However, unlike most of these studies, no change in the proportion of cells that transmigrated was observed (Edwards et al., 2005; Lalor et al., 2007; Shetty et al., 2011). Similarly, no effect was exhibited when individual leukocyte subsets were investigated in isolation. It is unclear whether this is a true representation of *in vivo* hepatic conditions or whether the stimulation of HSEC with TNFα in these experiments simply downregulated VAP-1 expression, thus muting effects of inhibition.

Interestingly, neutrophils adhered to rVAP-1 protein in *in vitro* flow assays, whereas $CD4^+$ and $CD8^+$ lymphocytes and NK cells did not. Treatment of HSEC with rVAP-1 also increased neutrophil adhesion, which was not replicated by the addition of rVCAM-1, suggesting a VAP-1-specific effect. Overexpression of GFP-VAP-1^{WT} conferred only a slight increase in neutrophil adhesion to the HSEC monolayer, but transfection with the enzyme-inactive form (GFP-VAP-1^{Y471F}) had no effect. Neutrophils closely associated with the HSEC-expressed GFP-VAP-1^{WT} protein as they crawled along the monolayer, and VAP-1 appeared to form a transmigratory cup structure. Together, these data highlight an intimate interaction between neutrophils and VAP-1 within the sinusoids.

The data shown here also suggest for the first time that human neutrophils express and secrete VAP-1 protein, which is downregulated in the presence of pro-inflammatory stimulation. Furthermore, inhibition of neutrophil VAP-1 increased adhesion to rVAP-1 by two fold and non-significantly increased adhesion to HSEC. This inhibition did not affect the production of ROS or extracellular traps. However, the addition of recombinant VAP-1 protein or VAP-1 substrates (benzylamine and cysteamine) exerted a significant reduction in ROS production and NETosis.

5

THE ROLE OF VAP-1 IN ACUTE LIVER DISEASE

5.1 Introduction

Neutrophils play a pivotal role as part of the innate immune system, mediating inflammation as part of the first line of host defence. Following hepatic injury, neutrophils are rapidly guided to the site of damage by signalling molecules that are released from dead or dying hepatocytes, such as TNFα, IL-8 and CXC chemokines (Antoniades et al., 2008; Faouzi et al., 2001; Zou et al., 2009). However, once within the parenchyma neutrophils often exacerbate the injury through release of cytotoxic ROS (Bilzer and Lauterburg, 1991; Gujral et al., 2004) and proteases capable of activating additional cytokines (Niehörster et al., 1990), chemokines (Yamaguchi et al., 2000), growth factors and their receptors (Wiedow and Meyer-Hoffert, 2005). The local upregulation of these inflammatory mediators often causes collateral damage that

contributes to and often dominates the pathogenic mechanism of acute inflammatory liver injury and subsequent liver failure (Xu et al., 2014). The complex relationship between neutrophils and VAP-1 highlighted in Chapter 4 therefore raises the question of how VAP-1 may also be involved in the development of acute liver disease.

Liver failure arising from acute hepatic injury is rare, with an incidence of fewer than 10 cases per million people per annum (Bernal, 2013; Bower, 2007). However, although rare it is associated with a particularly high mortality rate. Despite dramatic improvements in prognosis over the last 20 years (Germani et al., 2012), only 15% of patients survive without transplantation (Tessier et al., 2002). Acute liver failure (ALF) therefore accounts for approximately 8% of liver transplantation in Europe (Adam et al., 2012), highlighting a clear need for further research and the development of novel therapeutic strategies.

The rarity of ALF, along with its unpredictable and rapid onset has meant that large clinical trials are next to impossible (Lee et al., 2012). Animal models have therefore provided a useful tool to gain insight into the mechanisms of the disease. The most common causes of ALF in the Western world are NANB and drug-induced hepatitis (Bernal et al., 2010). As NANB hepatitis is a diagnosis of exclusion, no animal models of this disease are currently available whereas several models of acute drug-induced injury are available: the most commonly employed of which are induced by the administration of hepatotoxins, such as paracetamol, carbon tetrachloride (CCl_4) or thioacetamide (TAA). The heterogeneity of ALF means that no model perfectly and reliably replicates the human condition, however each of the models induce reversible acute hepatotoxicity resulting in the formation of necrotic lesions and an inflammatory response, as observed in man (Rahman and Hodgson, 2000).

Very little is known about the role of VAP-1 during acute hepatitis. Hepatic VAP-1 expression is thought to be elevated during human paracetamol-induced ALF (Tuncer et al., 2013) despite the concentration of sVAP-1 being unaffected (Kurkijärvi et al., 2000). Antibody blockade of VAP-1 has also been shown to reduce inflammation and disease severity in an acute Con A model of injury (Bonder et al., 2005; Lee et al., 2013). However, Con A-induced hepatitis is immune-cell mediated therefore it is difficult to draw direct comparison to drug-induced disease mechanisms in both murine and human systems.

In this chapter, the role of VAP-1 in an acute model of liver injury is investigated. Specifically the hepatotoxic effect of CCl_4 is compared and contrasted between WT mice and those expressing the catalytically inactive variant of VAP-1, VAP-1^{Y471F} (referred to as $SSAO^{KO}$ animals) to examine the involvement of VAP-1 amine oxidase activity in acute hepatitis.

5.2 Results

5.2.1 Acute murine CCl_4 hepatotoxicity

An initial pilot study was conducted to examine the acute toxic effect of CCl_4 on the liver of wild-type (WT) mice. This study aimed to ensure a robust and repeatable response was generated to maximise the potential for highlighting potentially subtle differences in later experiments. Similarly, the pilot aimed to determine an approximate time course of injury to advise future experiments. During this study, CCl_4 or mineral oil control (1 mL/kg) was administered into the peritoneum of five WT C57/BL6 mice. The animals were sacrificed by cervical dislocation at either 48 or 72 hours following injection and analysed for signs of hepatotoxicity.

5.2.1.1 Hepatotoxicity of CCl_4

Serum ALT levels were first analysed as an indicator of hepatocyte injury by aspirating blood via cardiac puncture prior to sacrifice (Figure 5.1). ALT concentrations were significantly elevated at 48 hours post-CCl_4 administration compared to control animals that received mineral oil vehicle alone (1569 IU/L (1084 – 2223 IU/L) and 25 IU/L (24 - 26 IU/L), respectively; $p \leq 0.01$). However, by 72 hours following CCl_4 injection serum ALT levels had decreased to levels comparable to control serum from animals that received vehicle alone.

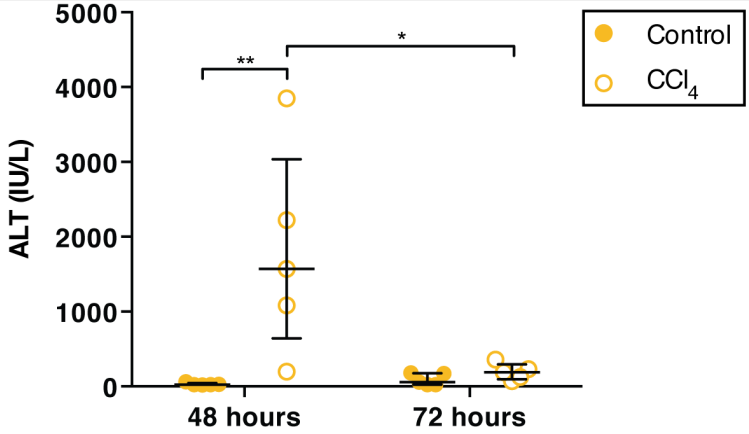


Figure 5.1 Effect of CCl_4 on serum ALT concentrations of WT mice. CCl_4 (1 mL/kg) or mineral oil control was administered to WT C57/BL6 mice via IP injection. Blood was drawn via cardiac puncture at 48 or 72 hours following injection and serum analysed for ALT concentration (n = 5). Data shown as median (IQR) and were analysed by two-way ANOVA with Tukey's post-hoc correction. * $p \leq 0.05$, ** $p \leq 0.01$.

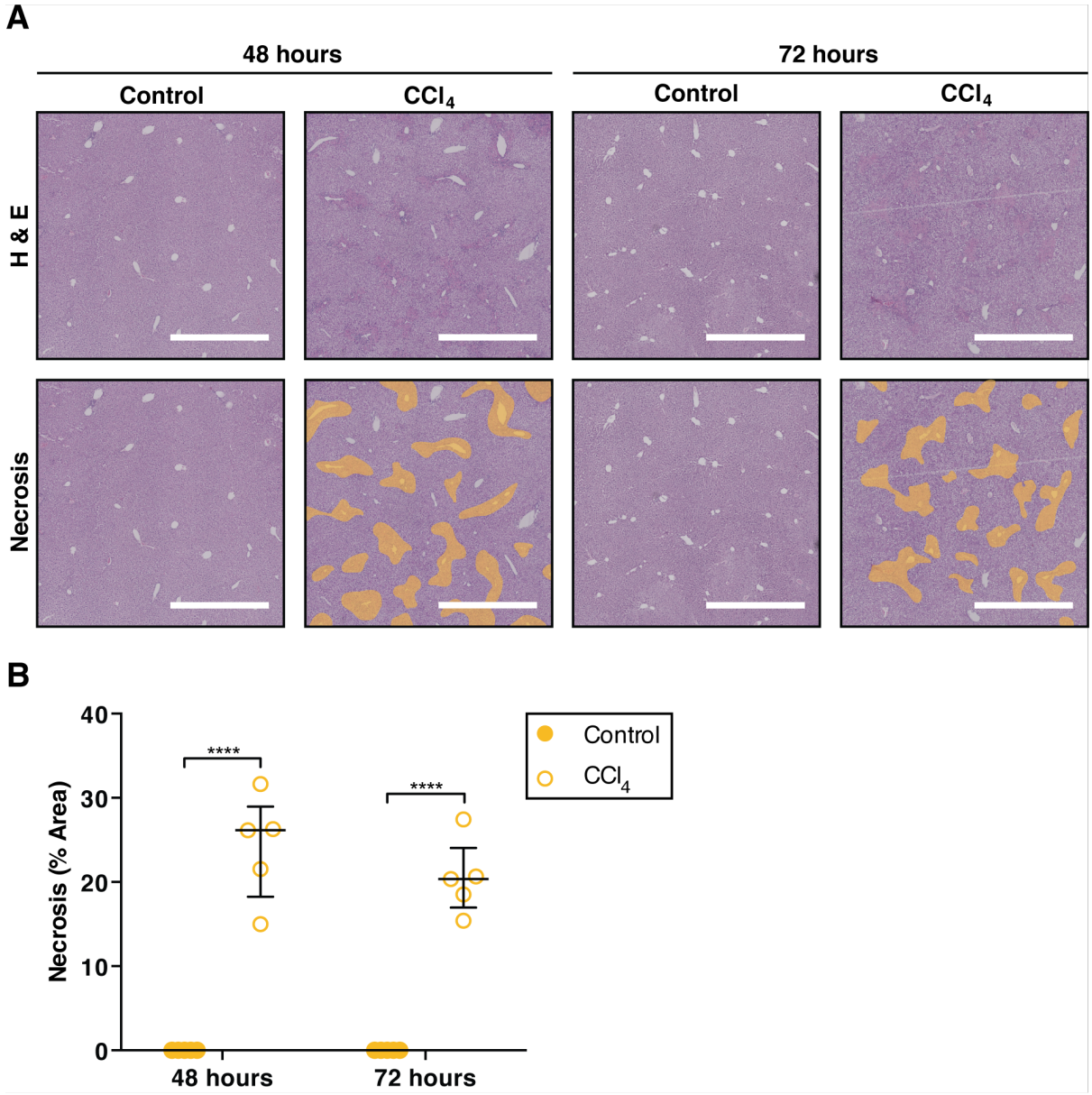


Figure 5.2 Effect of CCl_4 on hepatic necrosis of WT mice. WT C57/BL6 mice were treated with CCl_4 (1 mL/kg) or mineral oil control via IP injection and sacrificed 48 or 72 hours later. (**A**) Livers were stained with haematoxylin and eosin (H & E) and areas of necrosis were highlighted (yellow). Scale bar: 1 mm. (**B**) Necrotic areas were quantified by ImageJ analysis ($n = 5$). Data shown as median (IQR) and were analysed by two-way ANOVA with Tukey's post-hoc correction. **** $p \leq 0.0001$.

Following sacrifice, the livers of CCl_4-treated and control animals were harvested for analysis. Haematoxylin and Eosin (H & E) stain revealed many large areas (approximately 0.25 mm^2) of necrotic liver tissue in CCl_4-treated animals, which were absent from the tissue of control animals (Figure 5.2A). Necrotic areas were primarily centrilobular and radiated from central blood vessels with some bridging between vessels. The area of necrotic tissue was similar at both 48 and 72 hours post-injury,

constituting 26.1% (21.5 – 26.3%) and 20.3% (18.5 – 20.7%) of total hepatic area, respectively (Figure 5.2B). These necrotic areas also stained positive for the cleaved form of caspase-3, indicative of cells undergoing apoptosis (Figure 5.3A). Correspondingly, the livers of mice treated with CCl_4 also exhibited significantly raised levels of cleaved caspase-3 at both 48 and 72 hours post-injury compared to control animals, representing 5.2% (3.3 – 6.1%) and 7.0% (6.3 – 7.6%) of total hepatic area, respectively (Figure 5.3B).

5.2.1.2 Hepatic regeneration following acute CCl_4 injury

To determine the rate of hepatic regeneration following CCl_4 injury, murine liver tissue was assessed for the expression of the proliferation marker Ki67 by immunohistochemistry (Figure 5.4A). The livers of CCl_4-treated mice contained significantly elevated numbers of Ki67-expressing cells than control animals at both 48 hours (2.92% (2.25 – 3.39%) and 0.2% (0.16 – 0.24%), respectively; $p \leq 0.0001$) and 72 hours (3.19% (3.07 – 3.37%) and 0.39% (0.24 – 0.59%), respectively; $p \leq 0.0001$) post-administration, demonstrating similar levels of expression at both time points (Figure 5.4B). Ki67-expressing cells were clustered in a centrilobular distribution at sites of CCl_4-induced liver damage. Hepatic regeneration was also assessed by Western blot analysis of proliferating cell nuclear antigen (PCNA). The liver tissue recovered from mice that had received CCl_4 demonstrated raised levels of PCNA, consistent with changes in Ki67, whereas expression was below the limit of detection in control livers (Figure 5.5).

5.2.1.3 Inflammatory response to acute CCl_4 injury

One prominent feature of acute liver injury is the rapid infiltration of inflammatory cells to the hepatic parenchyma. To determine the extent of this intrahepatic recruitment, tissue sections were stained for the presence of the pan-leukocyte marker CD45 following administration of CCl_4 or mineral oil dosing. Liver tissue from CCl_4-treated mice exhibited higher levels of $CD45^+$ cells than control animals, although this difference was only significant at 72 hours post-injection (CCl_4: 4.75% (3.75 – 5.29%); Control: 0.60% (0.43 – 0.66%); $p \leq 0.01$) as seen in Figure 5.6B. The area of CD45-positivity was therefore also significantly greater at 72 hours after injury than at 48 hours (4.75% (3.75 – 5.29%) and 1.14% (0.94 – 1.28%), respectively; $p \leq 0.05$) suggesting continued influx of cells to this time point. The $CD45^+$ cells were observed clustered around blood vessels at

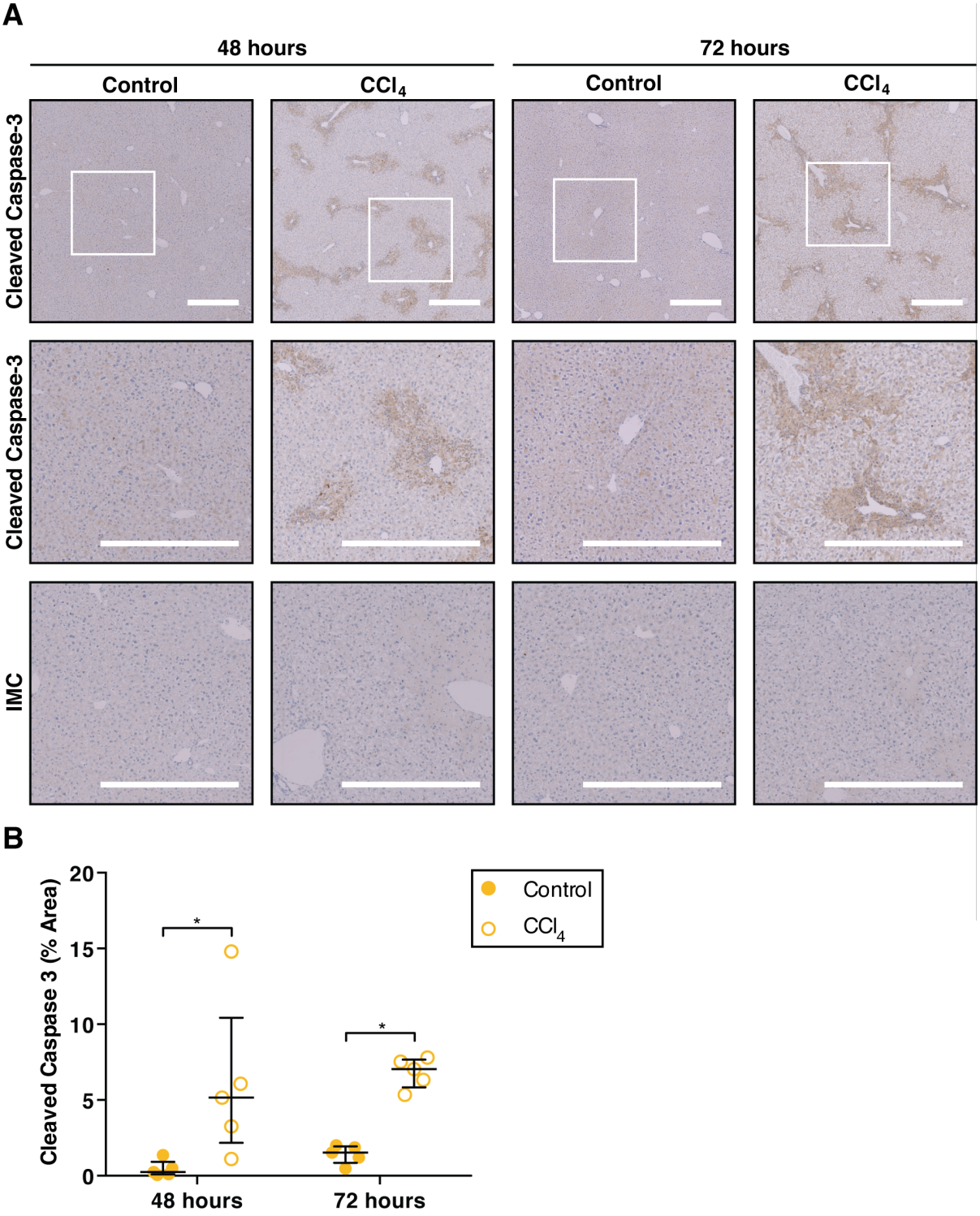


Figure 5.3 Effect of CCl_4 on hepatic cleaved caspase-3 expression of WT mice. WT C57/BL6 mice were treated with CCl_4 (1 mL/kg) or mineral oil control via IP injection and sacrificed 48 or 72 hours later. (**A**) Livers were stained for the presence of the cleaved form of caspase-3 (brown) and counterstained with haematoxylin to visualise nuclei (blue). Middle panel represents enlargement of white boxed region in upper panel. Scale bar: 500 µm. (**B**) Staining was quantified by ImageJ analysis (n = 5). Data shown as median (IQR) and were analysed by two-way ANOVA with Tukey's post-hoc correction. * $p \leq 0.05$.

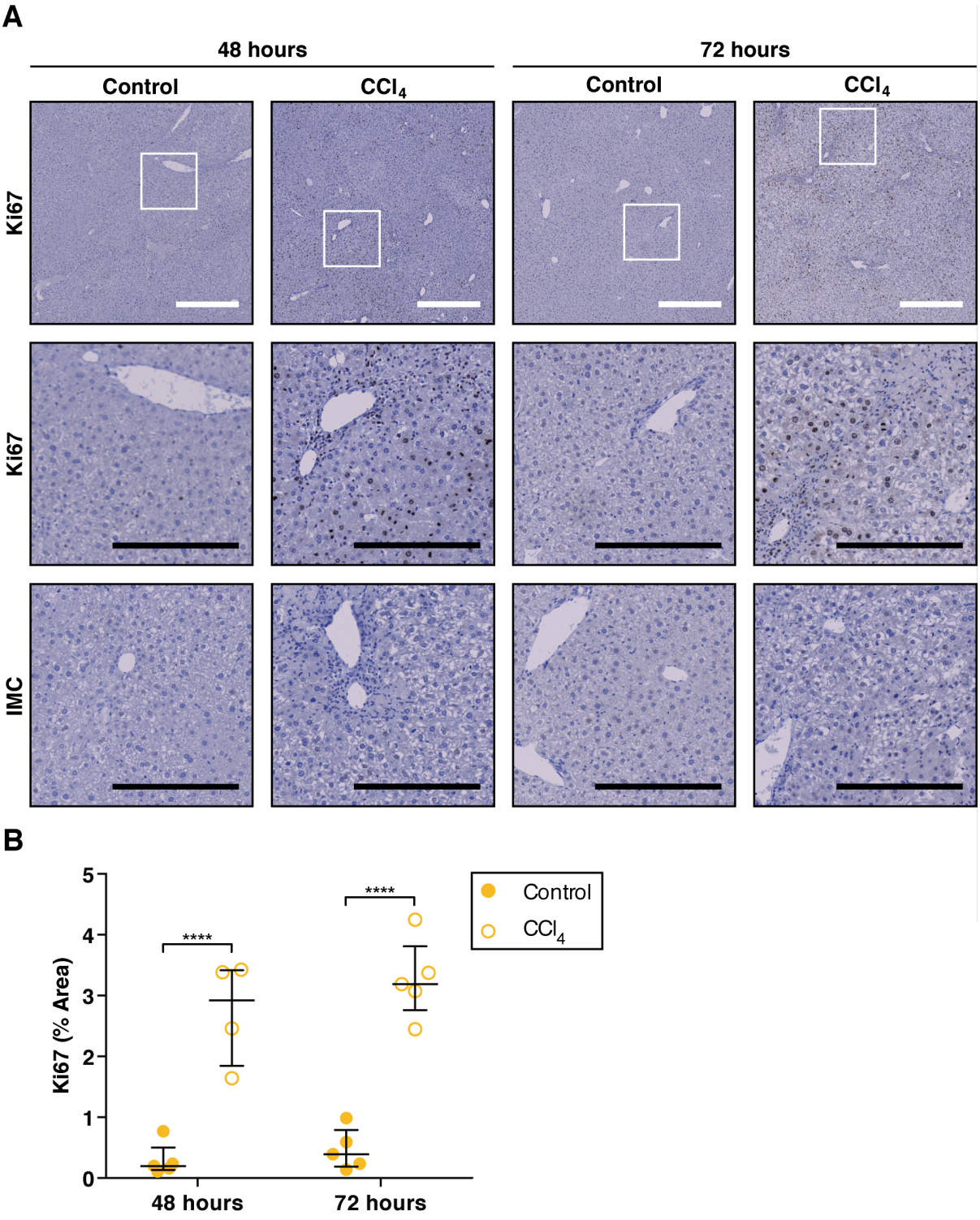


Figure 5.4 Effect of CCl_4 on hepatic Ki67 expression of WT mice. WT C57/BL6 mice were treated with CCl_4 (1 mL/kg) or mineral oil control via IP injection and sacrificed 48 or 72 hours later. (**A**) Livers were stained for the presence of Ki67 (black) and counterstained with haematoxylin to visualise nuclei (blue). Middle panel represents enlargement of white boxed region in upper panel. White scale bar: 500 µm; Black scale bar: 250 µm. (**B**) Staining was quantified by ImageJ analysis (n = 5, although one 48 hour CCl_4 section was damaged and therefore not able to be quantified). Data shown as median (IQR) and were analysed by two-way ANOVA with Tukey's post-hoc correction. **** $p \leq 0.0001$.

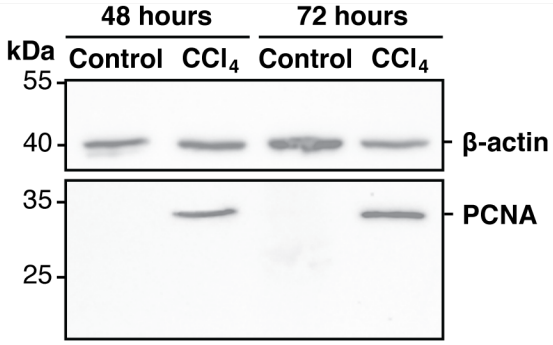


Figure 5.5 Effect of CCl_4 on hepatic PCNA expression of WT mice. WT C57/BL6 mice were treated with CCl_4 (1 mL/kg) or mineral oil control via IP injection and sacrificed 48 or 72 hours later. Sections of liver were analysed for the presence of proliferating cell antibody by Western blot. β-actin was used as a loading control. Representative blot from two replicates.

sites of injury, limited to areas of apoptosis/necrosis, with very few migrating further into the parenchyma (Figure 5.6A).

Although immunohistochemistry can provide useful information about the distribution of intrahepatic leukocytes, it can only give an approximation of the extent of infiltration in terms of percentage area. Furthermore, analysis of leukocyte subsets is labour intensive and subject to sampling bias. Flow cytometry was therefore employed to determine the immunophenotype of the hepatic infiltrate following acute CCl_4 injury. Liver tissue was perfused *in situ* with PBS following sacrifice by cervical dislocation prior to harvesting to flush any peripheral blood out of the organ. The liver tissue was then placed in RPMI and first mechanically and then collagenase digested to dissociate the leukocytes from parenchymal tissue. The cells were subsequently separated on a density gradient before undergoing flow cytometric analysis.

The isolated cell population was divided in two and analysed using either a lymphoid or myeloid antibody panel. During flow cytometry, all leukocytes were first crudely selected from the heterogeneous population of cells corresponding to their size (forward scatter, FS) and internal complexity (side scatter, SC). Single live cells were then selected utilising pulse width characteristics (Figure 5.7A) and leukocytes defined as all remaining live $CD45^+$ cells. The gating strategy for the lymphoid antibody panel (Figure 5.7B) was used to immunophenotype the $CD3^+$ T cell population: specifically $CD4^+$ T helper cells, $CD8^+$ cytotoxic T cell and $CD49b^+$ NKT cells. Similarly this panel allowed for characterisation of $CD3^-CD49b^+$ NK cells and $CD3^-CD19^+$ B cells. The myeloid antibody panel was used to define two subsets: myeloid-derived suppressor-like cells

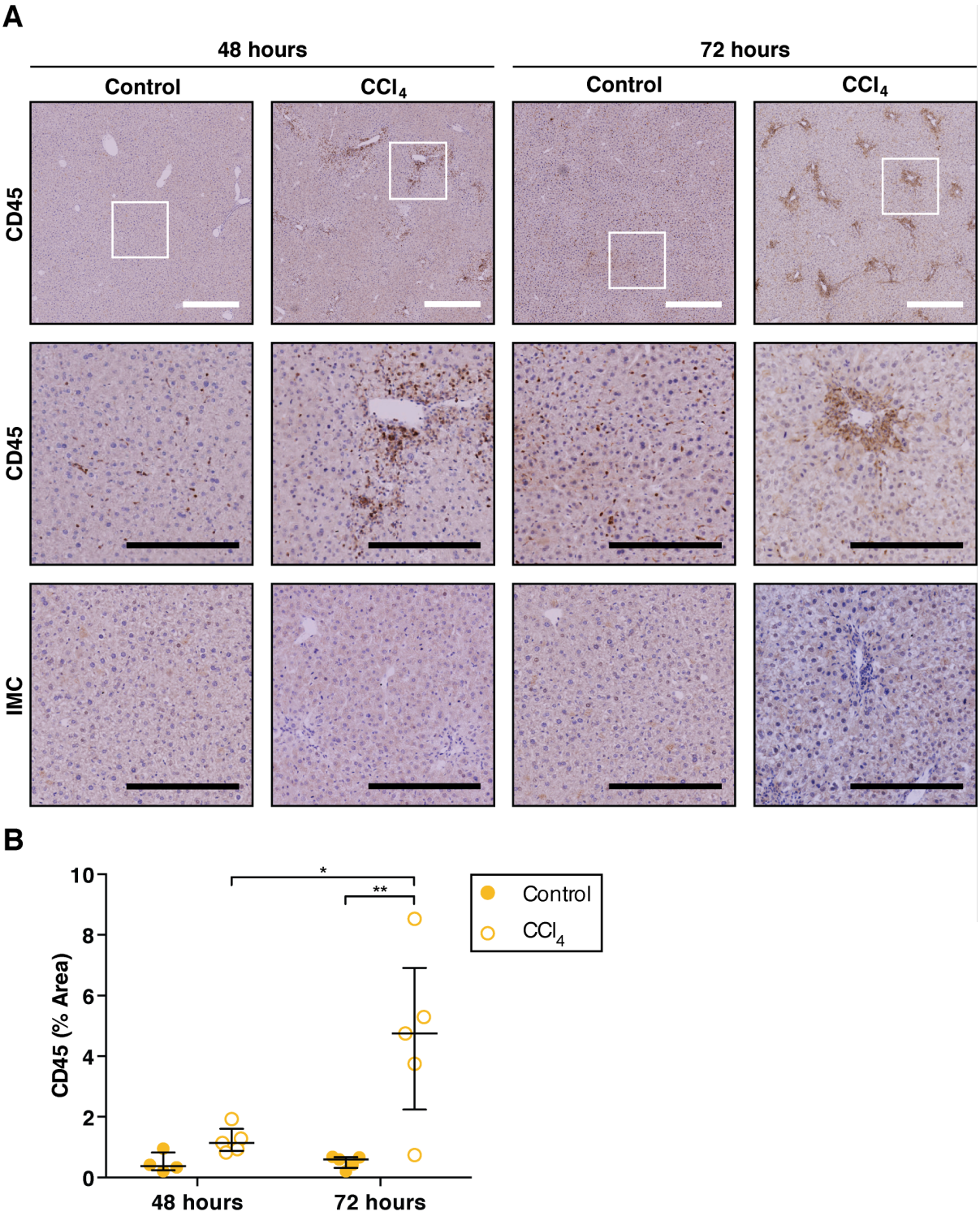


Figure 5.6 Effect of CCl_4 on infiltrating hepatic $CD45^+$ cells in WT mice. WT C57/BL6 mice were treated with CCl_4 (1 mL/kg) or mineral oil control via IP injection and sacrificed 48 or 72 hours later. (**A**) Livers were stained for the presence of CD45 (brown) and counterstained with haematoxylin to visualise nuclei (blue). Middle panel represents enlargement of white boxed region in upper panel. White scale bar: 500 µm; Black scale bar: 250 µm. (**B**) Staining was quantified by ImageJ analysis (n = 5). Data shown as median (IQR) and were analysed by two-way ANOVA with Tukey's post-hoc correction. * $p \leq 0.05$, ** $p \leq 0.01$.

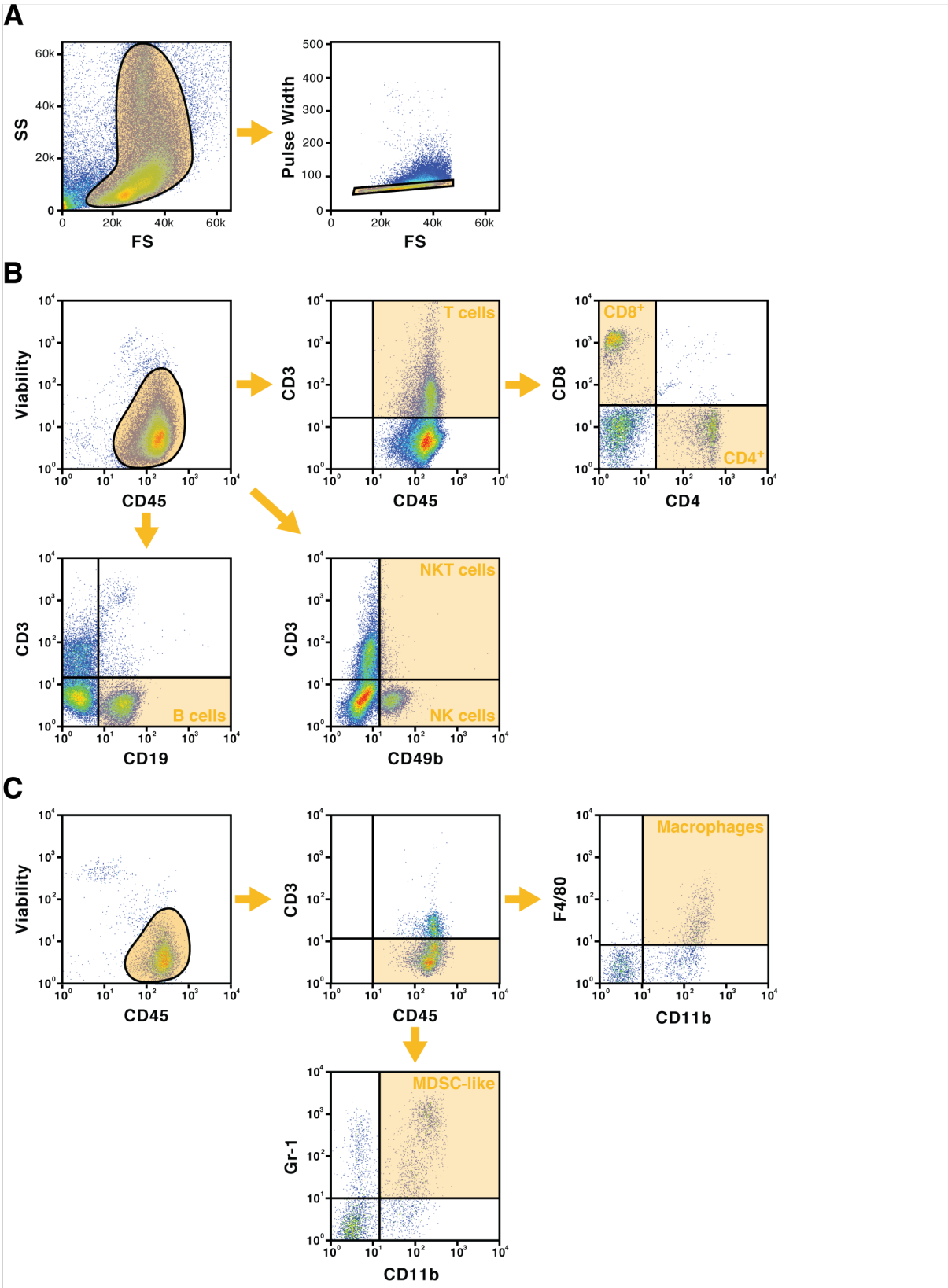

A
SS
FS
Pulse Width
FS
B
Viability
CD45
CD3
CD45
T cells
CD8
CD4
CD8+
CD4+
CD3
CD19
B cells
CD3
CD49b
NKT cells
NK cells
C
Viability
CD45
CD3
CD45
F4/80
CD11b
Macrophages
Gr-1
CD11b
MDSC-like

Figure 5.7 Gating strategy for phenotypic analysis of WT murine intrahepatic leukocytes by flow cytometry. (**A**) All cells were first gated on the leukocyte population using FS and SS characteristics and then single cells utilising pulse width. (**B**) All lymphoid cells were first gated on live leukocytes. T cells were designated at $CD3^+$ and further classified as $CD4^+$ and $CD8^+$. NKT cells were classified as $CD3^+$ and $CD49^+$. B cells and NK cells were both $CD3^-$ populations that were positive for CD19 or CD49b, respectively. (**C**) All myeloid cells were also first gated on live leukocytes and then gated as $CD3^-$ populations. Macrophages were positive for both F4/80 and CD11b and were further subdivided into Gr-1^{hi} and Gr-1^{low} populations. MDSC-like cells were Gr-1^+ and $CD11b^+$.

(MDSC-like) and macrophages. $CD3^-CD11b^+Gr\text{-}1^+$ MDSCs are a heterogeneous population of cells of the myeloid lineage that are capable of supressing T cell function and are induced during hepatitis (Hegde et al., 2011; Sarra et al., 2013). Although $CD11b^+Gr\text{-}1^+$ cells are generally considered as murine MDSCs, at present there are no combinations of markers unique to these cells (Bronte et al., 2016). Therefore MDSC-like terminology is used throughout this study to refer to this subset of cells. The $CD3^-CD11b^+F4/80^+$ macrophages also analysed using the myeloid antibody panel were further subdivided by relative intensity of the pan Ly6C/Ly6G marker, Gr-1. Evidence has shown that Ly-$6C^{hi}$ murine macrophages have proinflammatory activity whereas Ly-$6C^{low}$ macrophages have an immunomodulatory phenotype (Heymann et al., 2009; Ramachandran et al., 2012); therefore intensity of Gr-1 was used as an approximate classification of these cells during the pilot investigation.

The proportions of both $CD4^+$ and $CD8^+$ T cells were significantly lower in the livers of CCl_4-treated mice at 48 and 72 hours post-injury than in the livers of control animals (Figure 5.8B and 5.8C). At 48 hours, $CD4^+$ and $CD8^+$ T cells both represented approximately 10% of total $CD45^+$ cells. However, by 72 hours the proportion of $CD8^+$ cells was decreased to 5.8% (5.6 – 6.1%), whereas $CD4^+$ cells remained constant. Interestingly the addition of CCl_4 did not affect the proportion of NKT cells or B cells within the liver (Figure 5.8F and 5.8D). However, the proportion of intrahepatic NK Cells was significantly higher at 48 hours in CCl_4-treated mice than control animals ($p \leq 0.01$), but these levels returned to baseline by 72 hours (Figure 5.8E). Similarly, macrophages (both proinflammatory and proresolution subtypes) and MDSC-like cells were all elevated at 48 hours after the administration of CCl_4, but had normalised to levels similar to those seen in control mice by 72 hours (Figure 5.9).

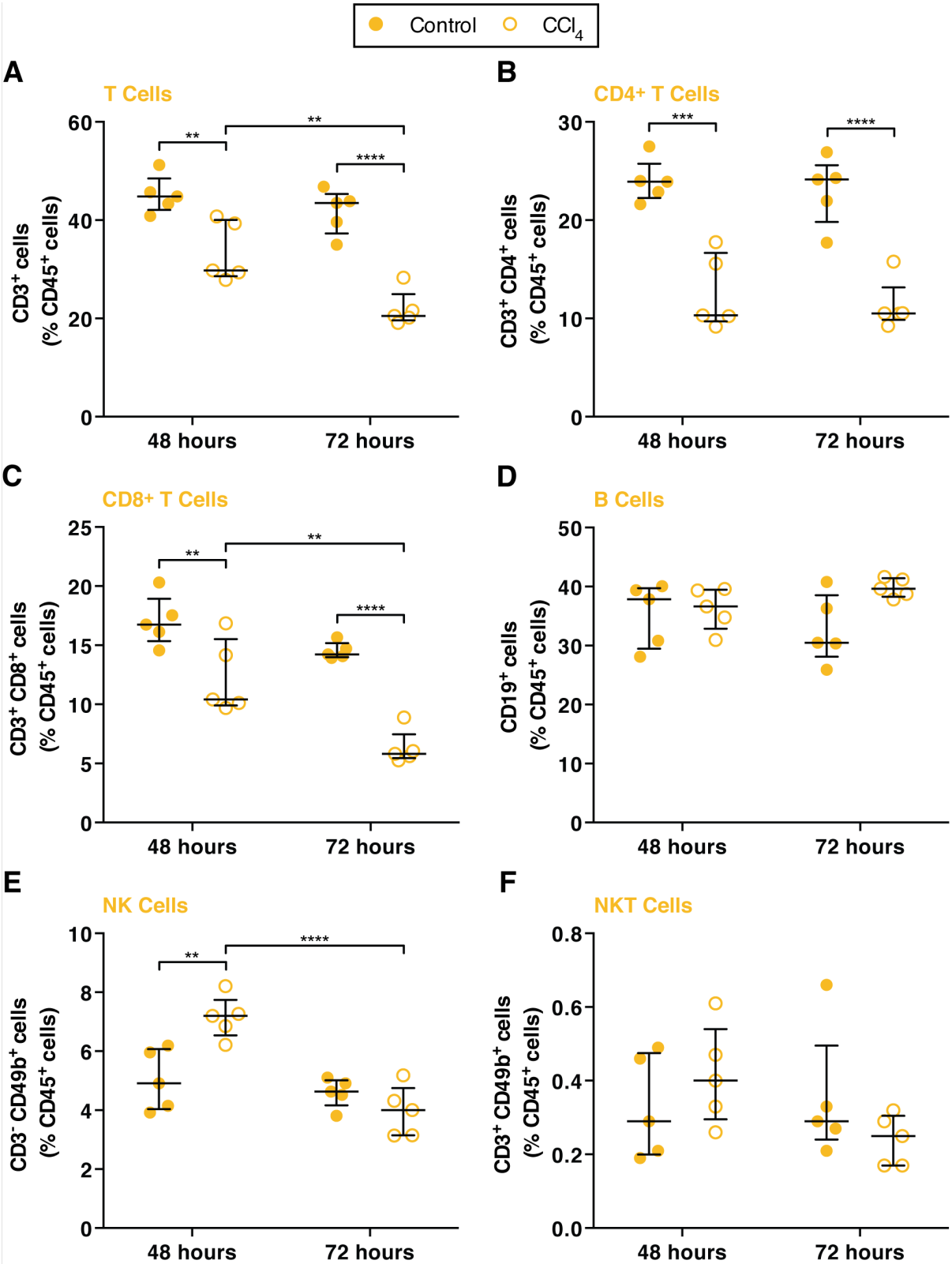


Figure 5.8 Effect of CCl_4 on intrahepatic lymphoid cells of WT mice. WT C57/BL6 mice were treated with CCl_4 (1 mL/kg) or mineral oil control via IP injection and sacrificed 48 or 72 hours later. Intrahepatic leukocytes were isolated and phenotyped by flow cytometry. (**A**) $CD3^+$ T cells. (**B**) $CD3^+CD4^+$ helper T cells. (**C**) $CD3^+CD8^+$ cytotoxic T cells. (**D**) $CD3^-CD19^+$ B cells. (**E**) $CD3^-CD49b^+$ NK cells. (**F**) $CD3^+CD49b^+$ NKT cells ($n = 5$). Data shown as median (IQR) and were analysed by two-way ANOVA with Tukey's post-hoc correction. ** $p \leq 0.01$, *** $p \leq 0.001$, **** $p \leq 0.0001$.

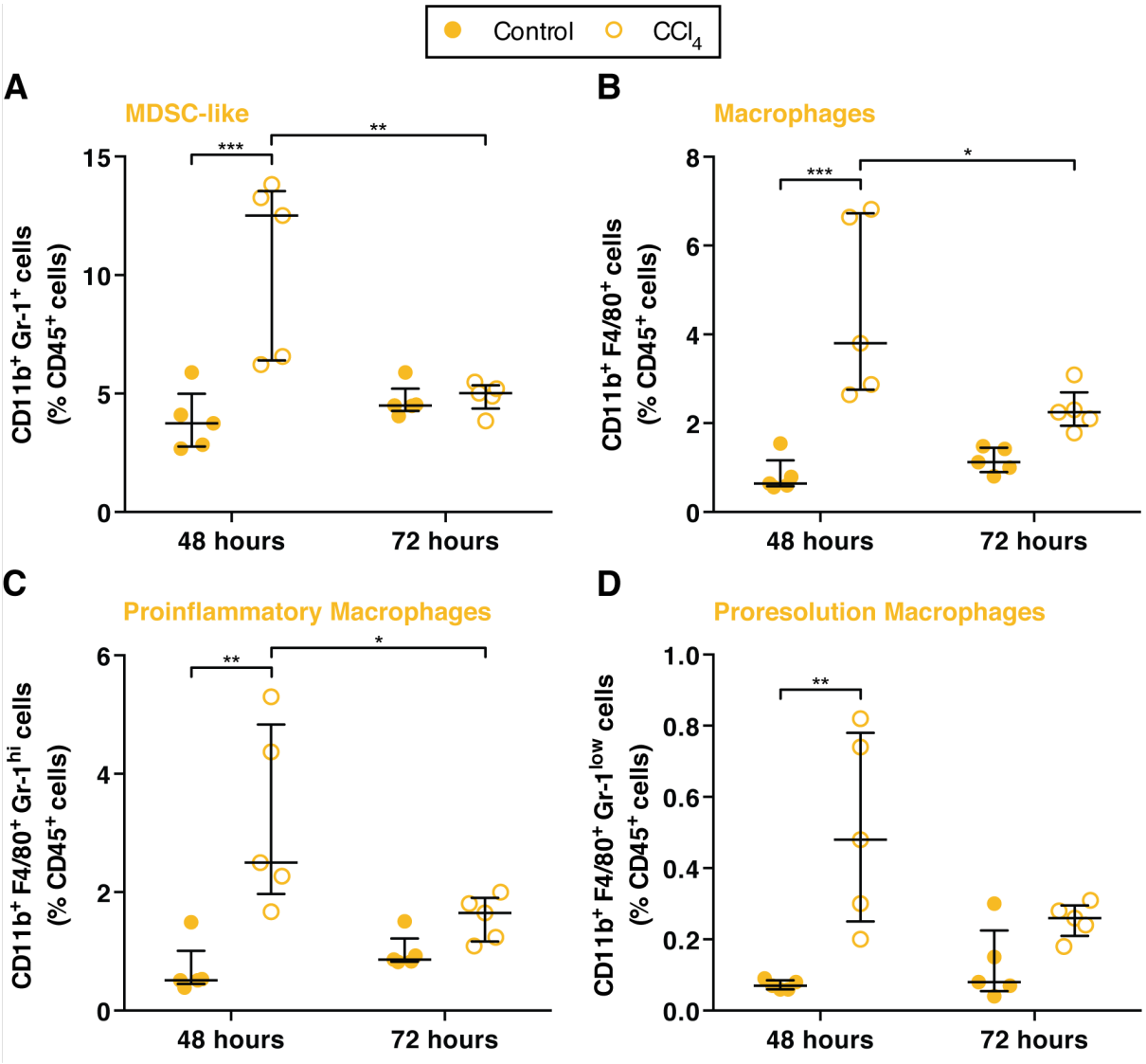


Figure 5.9 Effect of CCl_4 on intrahepatic myeloid cells of WT mice. WT C57/BL6 mice were treated with CCl_4 (1 mL/kg) or mineral oil control via IP injection and sacrificed 48 or 72 hours later. Intrahepatic leukocytes were isolated and phenotyped by flow cytometry. (**A**) $CD11b^+Gr\text{-}1^+$ MDSC-like cells. (**B**) $CD11b^+F4/80^+$ Macrophages. (**C**) $CD11b^+F4/80^+Gr\text{-}1^{hi}$ Proinflammatory Macrophages. (**D**) $CD11b^+F4/80^+Gr\text{-}1^{hi}$ Proresolution Macrophages (n = 5). Data shown as median (IQR) and were analysed by two-way ANOVA with Tukey's post-hoc correction. * $p \leq 0.05$, ** $p \leq 0.01$, *** $p \leq 0.001$.

The proportions of intrahepatic leukocytes observed during this preliminary experiment were in line with results from previous studies (Karlmark et al., 2009). Similarly, the immunohistochemical data was also in line with current literature. It was therefore confidently concluded that the model had been effectively and reliably reproduced and could be extended to investigate the role of VAP-1 in this injury mechanism.

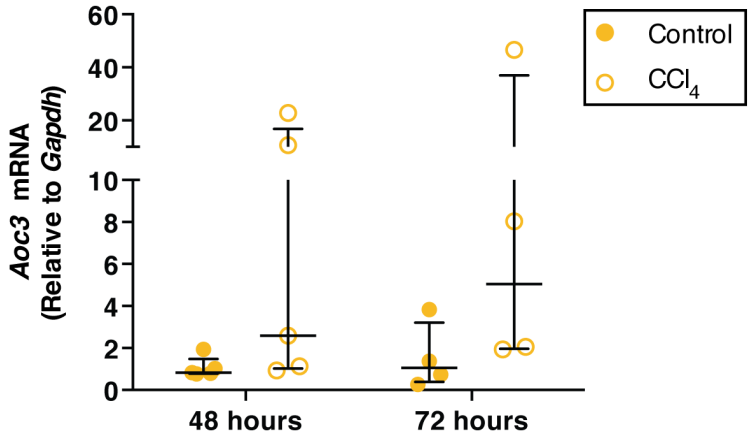


Figure 5.10 Effect of CCl_4 on hepatic *Aoc3* expression of WT mice. WT C57/BL6 mice were treated with CCl_4 (1 mL/kg) or mineral oil control via IP injection and sacrificed 48 or 72 hours later. Livers were analysed for the expression of *Aoc3* mRNA and normalised to *Gapdh* expression (n = 4-5). Data shown as median (IQR) and were analysed by two-way ANOVA with Tukey's post-hoc correction. All differences were nonsignificant.

5.2.1.4 Hepatic VAP-1 during acute CCl_4 injury

In Chapter 3 changes in hepatic VAP-1 expression were observed during human chronic liver diseases. To examine whether similar changes occurred during acute CCl_4 toxicity, *Aoc3* mRNA expression was initially quantified by qPCR analysis. The range of hepatic *Aoc3* expression was considerably higher between CCl_4-treated animals compared to control: two animals exhibited elevated expression relative to *Gapdh* at both time points, however these animals did not demonstrate any obvious correlating factors in the other assays (Figure 5.10). The remaining animals exhibited *Aoc3* expression more comparable to control levels, although median values were elevated non-significantly.

The data in Chapter 1 found that human CLDs exhibited altered VAP-1 amine oxidase activity, therefore antibody-capture Amplex UltraRed assays were also employed to assess changes in murine hepatic VAP-1 activity during acute CCl_4 toxicity. Several VAP-1 antibody clones were screened for use in the immunosorbence assay, with only one, clone 7-106, effectively captured murine rVAP-1 (Figure 5.11A). However, only 62% of total uncaptured rVAP-1 activity was recorded. Both captured and non-captured activities were therefore recorded when measuring hepatic VAP-1 activity in subsequent experiments in order to ensure that any loss of activity was consistent and proportional. VAP-1-specific activity was defined as the difference between amine oxidase activities

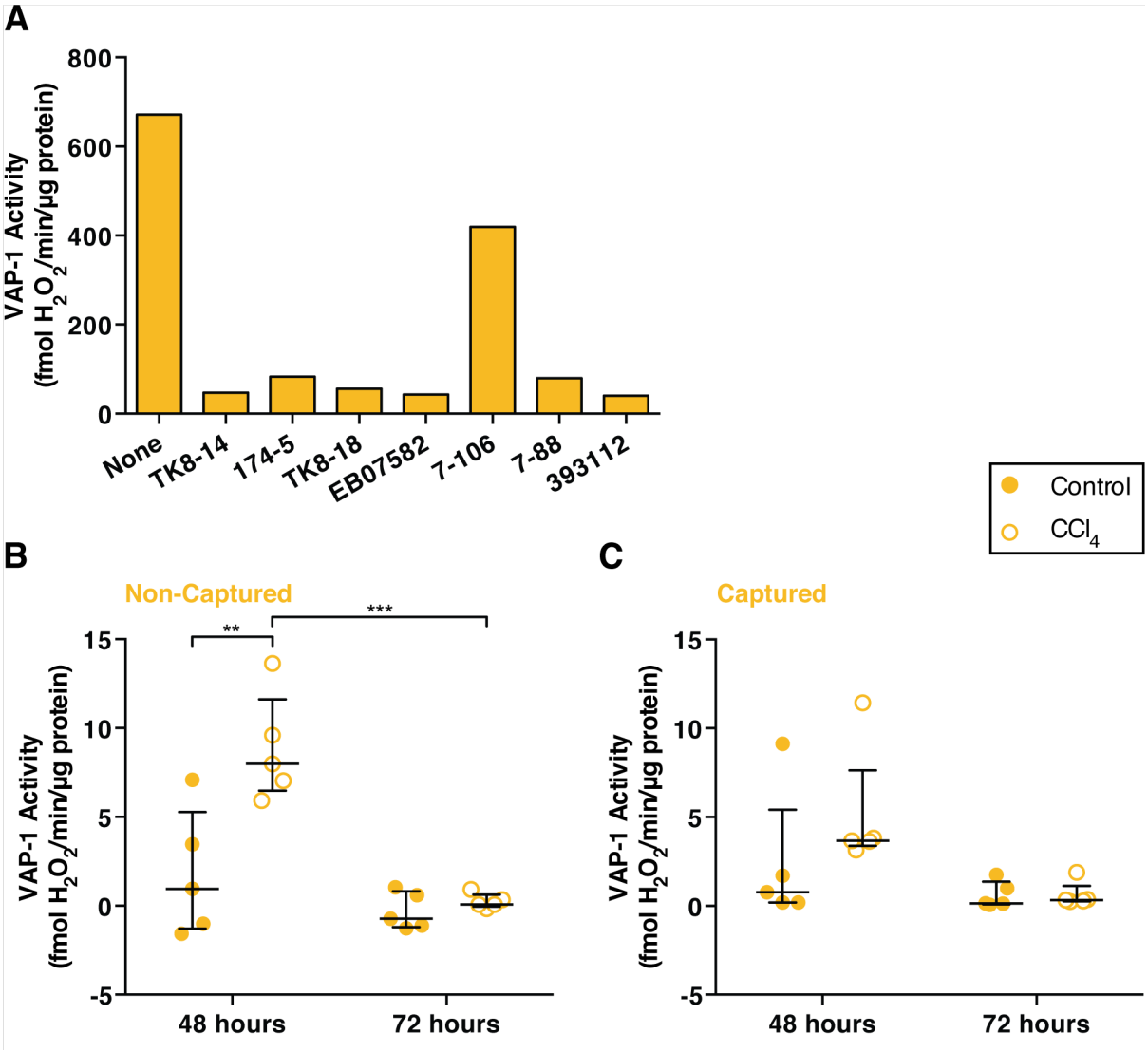


Figure 5.11 Effect of CCl_4 on hepatic VAP-1 enzyme activity of WT mice. (**A**) Optimisation of murine antibody capture Amplex UltraRed assay. Amine oxidase activity of 1µg murine rVAP-1 either uncaptured or following capture with different VAP-1 antibody clones (n = 2). (**B**) WT C57/BL6 mice were treated with CCl_4 (1 mL/kg) or mineral oil control via IP injection and sacrificed 48 or 72 hours later. Hepatic VAP-1 activity was calculated as the difference in amine oxidase activity with and without the presence of LJP-1586 using Amplex UltraRed assay or (**C**) following capture with antibody clone 7-106 (n = 5). Data shown as median (IQR) and were analysed by two-way ANOVA with Tukey's post-hoc correction (**B** and **C**). ** $p \leq 0.01$, *** $p \leq 0.001$.

recorded in the absence and presence of LJP-1586 (LJP-1586-corrected activity) to ensure VAP-1-specificity.

VAP-1 activity was elevated in mice that received CCl_4 compared to control at 48 hours following the administration of CCl_4, although this difference was only statistically significant in the non-captured fraction (CCl_4: 7.99 fmol H_2O_2/min/µg protein (7.04 – 9.59 fmol H_2O_2/min/µg protein); Control: 0.96 fmol H_2O_2/min/µg protein (-1.00 –

3.47 fmol H_2O_2/min/μg protein); $p \leq 0.01$) as seen in Figure 5.11B and 5.11C. By 72 hours this elevation had normalised to levels comparable to that of untreated control livers.

The positive results of this initial pilot study therefore suggested that VAP-1 might contribute to the inflammatory response in acute liver injury. It was therefore of interest to examine this role through the use of $SSAO^{KO}$ animals. Furthermore, VAP-1 activity was highest at 48 hours post-injury therefore suggesting maximum changes in activity are likely to be observed at his time point.

5.2.2 Role of VAP-1 activity in acute murine CCl_4 hepatotoxicity

To examine the role of VAP-1 amine oxidase activity during acute CCl_4 injury, 1 mL/kg CCl_4 was administered into the peritoneum of seven WT C57/BL6 control mice or $SSAO^{KO}$ animals. The animals were then sacrificed at 48 hours following injection and analysed for signs of hepatotoxicity.

5.2.2.1 Hepatic VAP-1 in $SSAO^{KO}$ mice following acute CCl_4 injury

Amplex UltraRed activity assays were employed to confirm that the livers of $SSAO^{KO}$ mice were devoid of VAP-1 enzyme activity. The liver tissue taken from all seven $SSAO^{KO}$ mice were found to exhibit little to no amine oxidase activity, which was significantly lower than the activity recorded in WT livers (Figure 5.12A and 5.12B). The WT hepatic VAP-1 activity was also consistent between this and the previous cohort examined during the preliminary investigation, demonstrating good repeatability and reliability of the assay. To examine whether hepatic VAP-1 expression levels were comparable between WT and $SSAO^{KO}$ mice following CCl_4 administrations, hepatic *Aoc3* mRNA expression was also quantified by qPCR analysis. The results of this assay confirmed that both WT and $SSAO^{KO}$ animals expressed similar levels of VAP-1 expression relative to *Gapdh* (Figure 5.12C).

5.2.2.2 Hepatotoxicity of CCl_4 in $SSAO^{KO}$ mice

Hepatocyte injury was assessed following the administration of CCl_4 to WT and $SSAO^{KO}$ animals by measuring serum ALT and AST levels. Serum concentrations of both enzymes were non-significantly lower within $SSAO^{KO}$ mice compared to WT, suggestive of less hepatocyte injury in enzyme-deficient animals (Figure 5.13A and 5.13B).

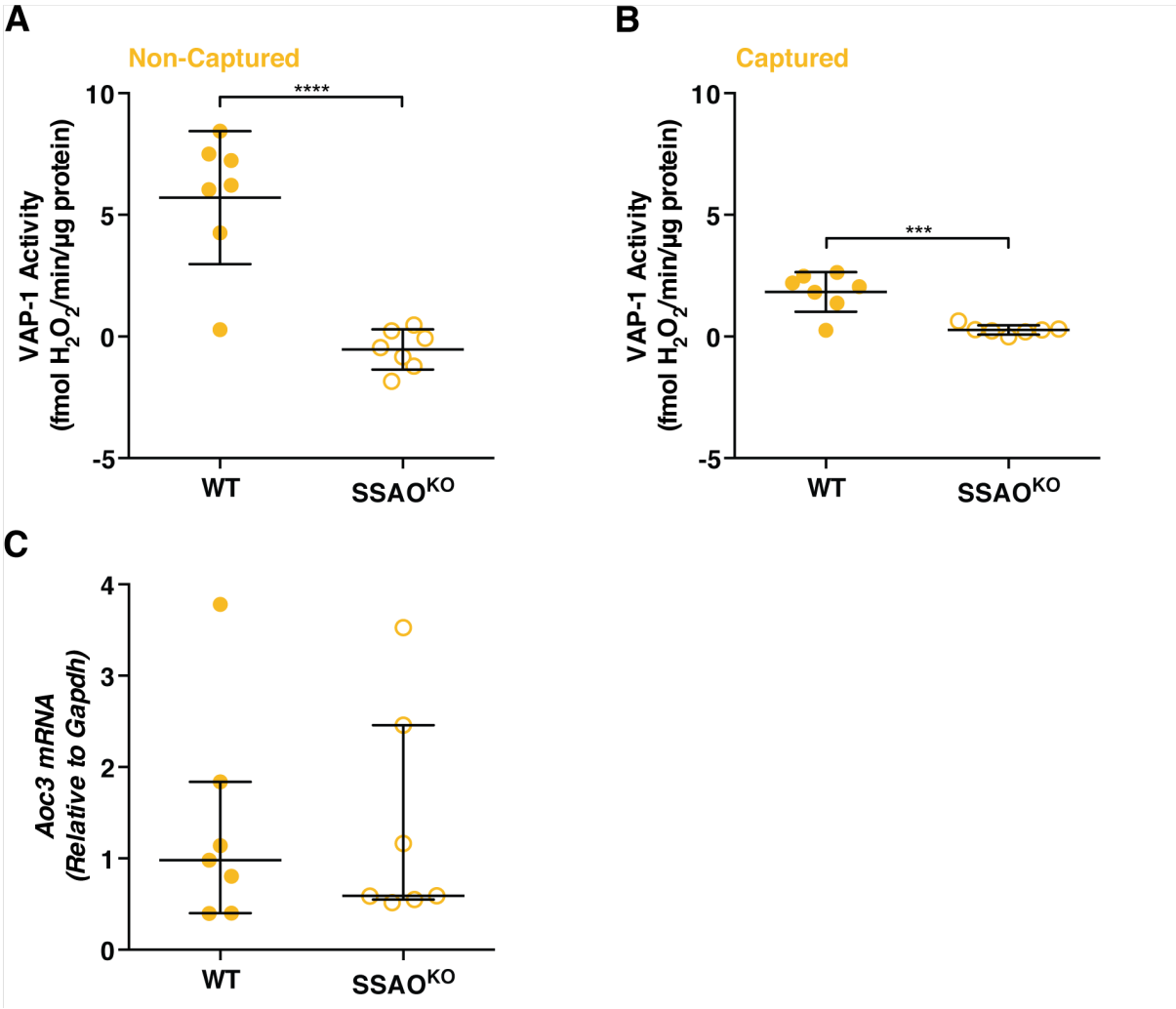


Figure 5.12 Effect of CCl_4 on hepatic VAP-1 of WT and SSAO^{KO} mice. WT C57/BL6 or SSAO^{KO} mice were treated with CCl_4 (1 mL/kg) via IP injection and sacrificed 48 hours later. (**A**) Hepatic VAP-1 activity was calculated as the difference in amine oxidase activity with and without the presence of LJP-1586 using Amplex UltraRed assay or (**B**) following capture with antibody clone 7-106. (C) Livers were analysed for the expression of *Aoc3* mRNA and normalised to *Gapdh* expression (n = 7). Data shown as mean (SD) were analysed by t test (**A** & **B**) and median (IQR) and analysed by Mann-Witney test (**C**). *** $p \leq 0.001$, **** $p \leq 0.0001$.

The extent of hepatic necrosis following CCl_4 injection was assessed by H & E staining of liver tissue sections. Liver tissue from SSAO^{KO} and WT animals both exhibited large centrilobular necrotic lesions (Figure 5.14A). The extent of injury, as indicated by the area of liver tissue that consisted of necrotic lesion, was highly similar between both SSAO^{KO} and WT mice (30.5% (24.1 – 31.9%) and 29.5% (26.0 – 30.1%), respectively).

Analysis of immunohistochemistry for cleaved caspase-3 revealed expression within necrotic lesions of both SSAO^{KO} and WT livers following CCl_4 injury (Figure 5.15A). Quantification of this staining revealed a greater median amount of cleaved-caspase 3

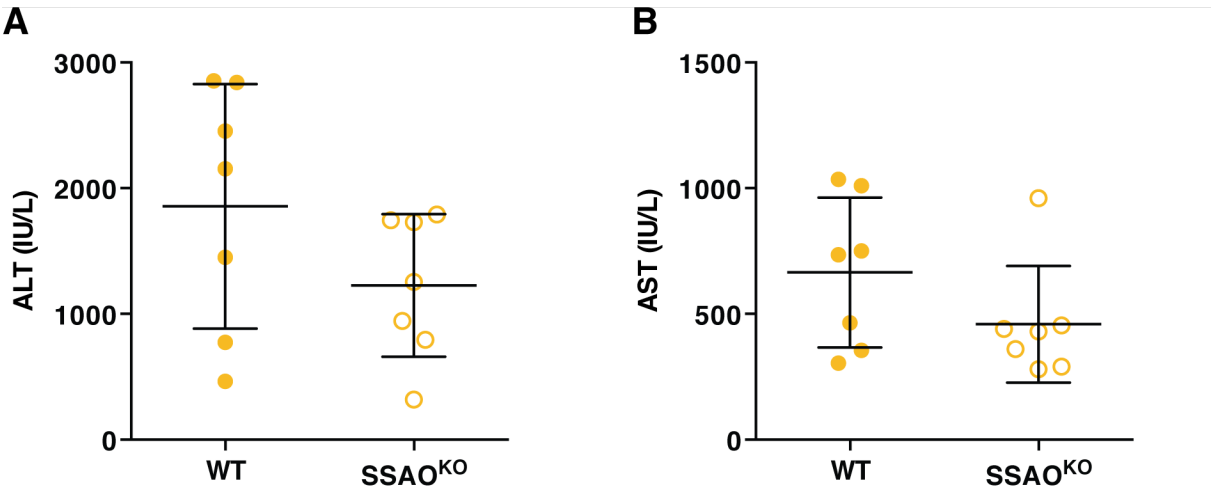


Figure 5.13 Effect of CCl_4 on serum liver enzyme concentrations of WT and $SSAO^{KO}$ mice. WT C57/BL6 or $SSAO^{KO}$ mice were treated with CCl_4 (1 mL/kg) via IP injection. Blood was drawn via cardiac puncture at 48 following injection and serum analysed for (**A**) ALT and (**B**) AST concentration ($n = 7$). Data shown as mean (SD) and were analysed by *t* test. No significant differences.

staining in $SSAO^{KO}$ livers compared to WT, however statistical significance was not reached due to two WT livers that exhibited particularly high levels. The exact cause of these outliers was not clear and did not appear to correlate with other measured variables.

5.2.2.3 Hepatic regeneration in $SSAO^{KO}$ mice following acute CCl_4 injury

To examine whether VAP-1 activity affected hepatic regeneration following CCl_4 injury, murine liver tissue from WT and $SSAO^{KO}$ animals was assessed for the expression of Ki67 by immunohistochemistry. Proliferating Ki67-expressing cells were clustered within centrilobular regions, at sites of CCl_4-induced liver damage but were also found throughout the parenchyma (Figure 5.16A). The liver of $SSAO^{KO}$ mice contained significantly lower numbers of Ki67-expressing cells than WT animals (1.6% (1.3 – 1.9%) and 2.8% (2.6 – 3.1%), respectively; $p \leq 0.001$) indicative of higher levels of proliferation (Figure 5.16B). This appeared to be primarily spread across the parenchyma, relating to hepatocyte proliferation. Accordingly, the livers of $SSAO^{KO}$ mice also expressed significantly less PCNA than WT animals ($p \leq 0.05$), as demonstrated by Western blot analysis, confirming a lower proliferative capacity (Figure 5.17).

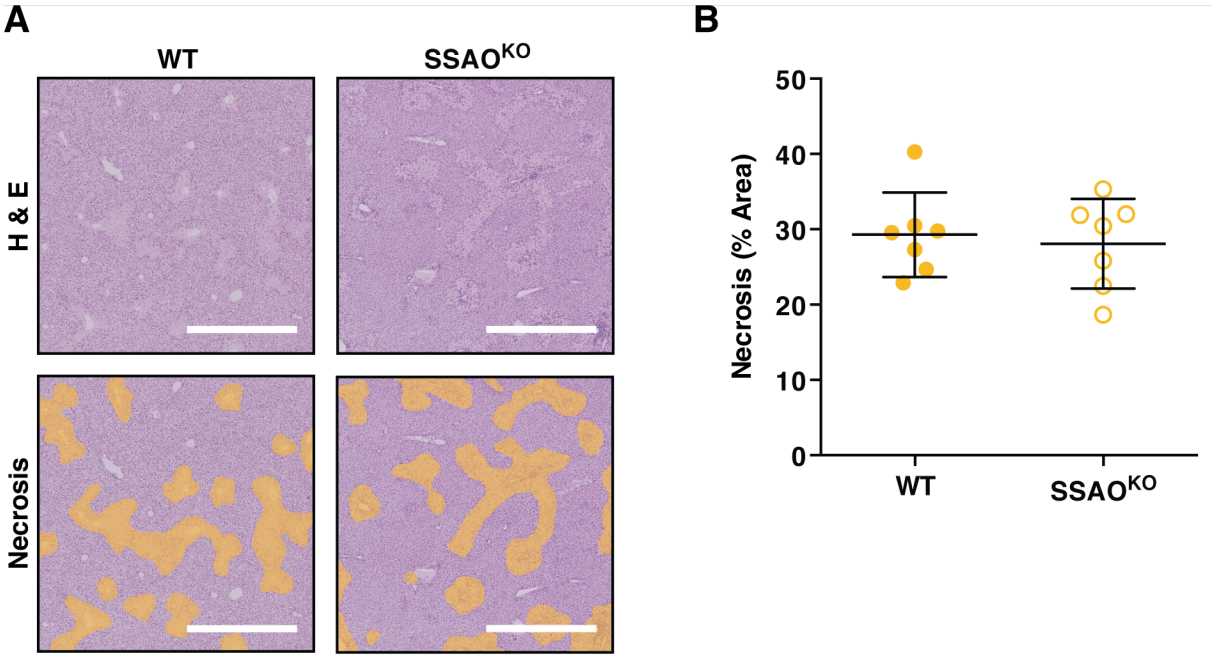


Figure 5.14 Effect of CCl_4 on hepatic necrosis of WT and $SSAO^{KO}$ mice. WT C57/BL6 or $SSAO^{KO}$ mice were treated with CCl_4 (1 mL/kg) via IP injection and sacrificed 48 hours later. (**A**) Livers were stained with haematoxylin and eosin (H & E) and areas of necrosis were highlighted (yellow). Scale bar: 1 mm. (**B**) Necrotic areas were quantified by ImageJ analysis (n = 7). Data shown as mean (SD) and were analysed by t test. No significant difference.

5.2.2.4 Inflammatory response of $SSAO^{KO}$ mice to acute CCl_4 injury

To investigate whether lacking VAP-1 enzyme activity affected the recruitment of leukocytes to the liver following CCl_4 injury, liver sections from $SSAO^{KO}$ mice were compared to those from WT animals. Immunohistochemical analysis of intrahepatic $CD45^+$ cells revealed no conspicuous difference between the $SSAO^{KO}$ and WT animals: both exhibited high numbers of centrilobular leukocytes but limited numbers within the parenchyma (Figure 5.18A). Quantification of the staining also suggested similar total leukocytic infiltrate between the animals, although the range between $SSAO^{KO}$ animals was greater (Figure 5.18B).

To discover whether recruitment of individual leukocyte subsets was affected by the lack of VAP-1 enzyme activity, intrahepatic leukocytes were phenotyped via flow cytometry using a modified myeloid panel to that for the pilot WT experiment (Figure 5.19). Within this panel, individual Ly6C and Ly6G antibodies were used in place of the pan marker Gr-1. This allowed for the identification of $Ly6G^+$ neutrophils and for more accurate classification of macrophages as either proinflammatory ($Ly6C^{hi}$) or proresolution

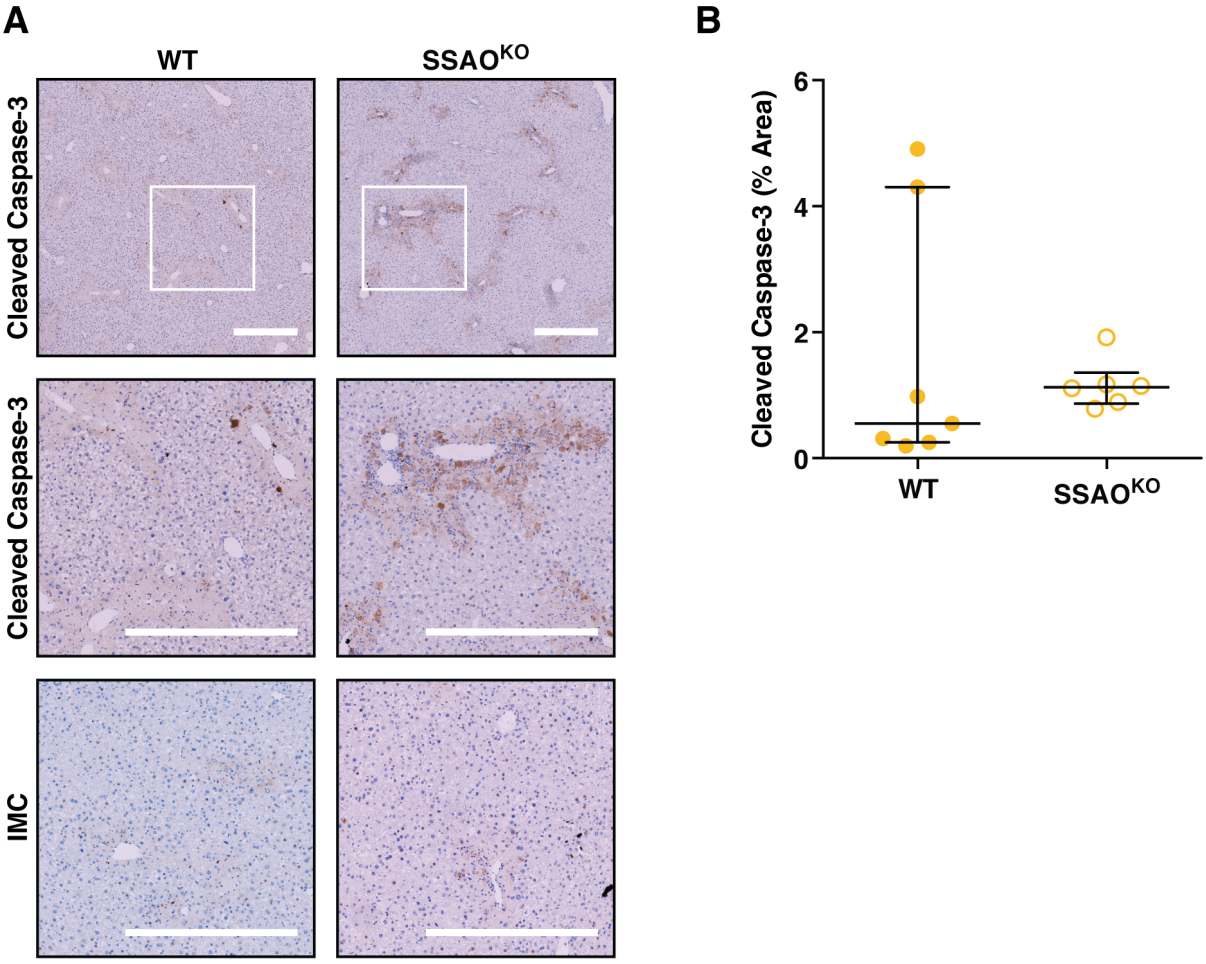


Figure 5.15 Effect of CCl_4 on hepatic cleaved caspase-3 expression of WT and SSAO^{KO} mice. WT C57/BL6 or SSAO^{KO} mice were treated with CCl_4 (1 mL/kg) via IP injection and sacrificed 48 hours later. (**A**) Livers were stained for the presence of the cleaved form of caspase-3 (brown) and counterstained with haematoxylin to visualise nuclei (blue). Middle panel represents enlargement of white boxed region in upper panel. Scale bar: 500 µm. (**B**) Staining was quantified by ImageJ analysis (n = 7). Data shown as median (IQR) and were analysed by Mann-Whitney test. No significant difference.

(Ly6C^{low}). Furthermore this also allowed for the more precise description of MDSC subsets from the heterogeneous MDSC-like population: as either CD11b^{+}Ly6G^{+}Ly6C^{low} polymorphonuclear-MDSCs (PMN-MDSCs) or CD11b^{+}Ly6G-Ly6C^{hi} monocyte-MDSCs (M-MDSCs) (Peranzoni et al., 2010).

The proportions of most intrahepatic lymphoid subsets in SSAO^{KO} mice were similar to WT, with no difference in the proportion of CD4^{+} and CD8^{+} T cells, B cells or NK cells (Figure 5.20). However, the proportion NKT cells were elevated in SSAO^{KO} livers, representing 0.87% (0.75 – 0.96%) of total intrahepatic leukocytes compared to 0.73% (0.59 – 0.76%) in WT livers ($p \leq 0.05$). Likewise, the intrahepatic faction of PMN- and

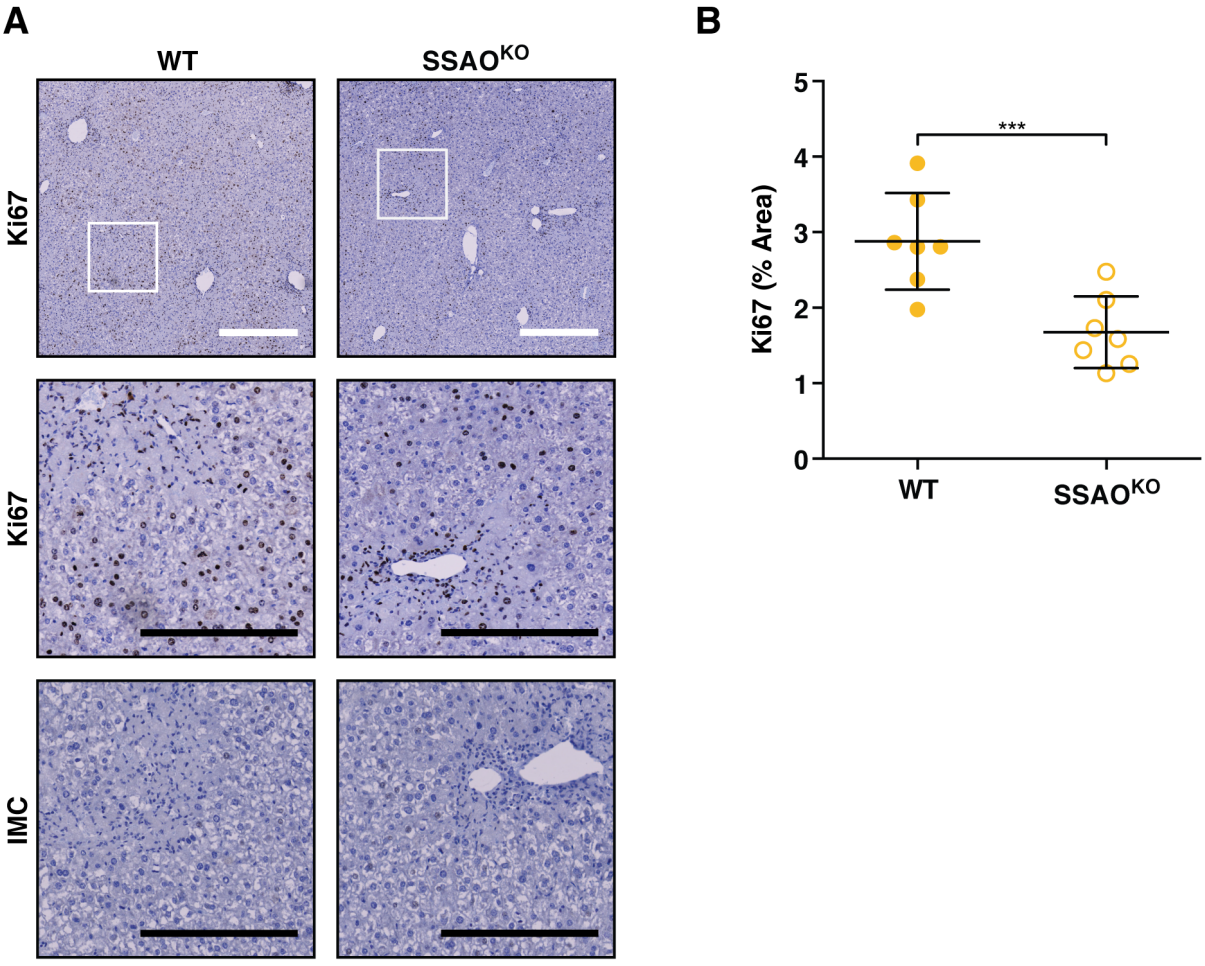


Figure 5.16 Effect of CCl_4 on hepatic Ki67 expression of WT and SSAO^{KO} mice. WT C57/BL6 or SSAO^{KO} mice were treated with CCl_4 (1 mL/kg) via IP injection and sacrificed 48 hours later. (**A**) Livers were stained for the presence of Ki67 to visualise nuclei (black) and counterstained with haematoxylin (blue). Middle panel represents enlargement of white boxed region in upper panel. White scale bar: 500 µm; Black scale bar: 250 µm. (**B**) Staining was quantified by ImageJ analysis ($n = 7$). Data shown as mean (SD) and were analysed by *t* test. *** $p \leq 0.001$.

M-MDSCs, both proinflammatory and proresolution macrophages and neutrophils were all elevated in the livers of SSAO^{KO} mice compared to WT, although this only reached statistical significance for proresolution macrophages as seen in Figure 5.21 (WT: 5.7% (5.32 – 7.38%); SSAO^{KO}: 10.8% (9.0 – 13.1%); $p \leq 0.05$).

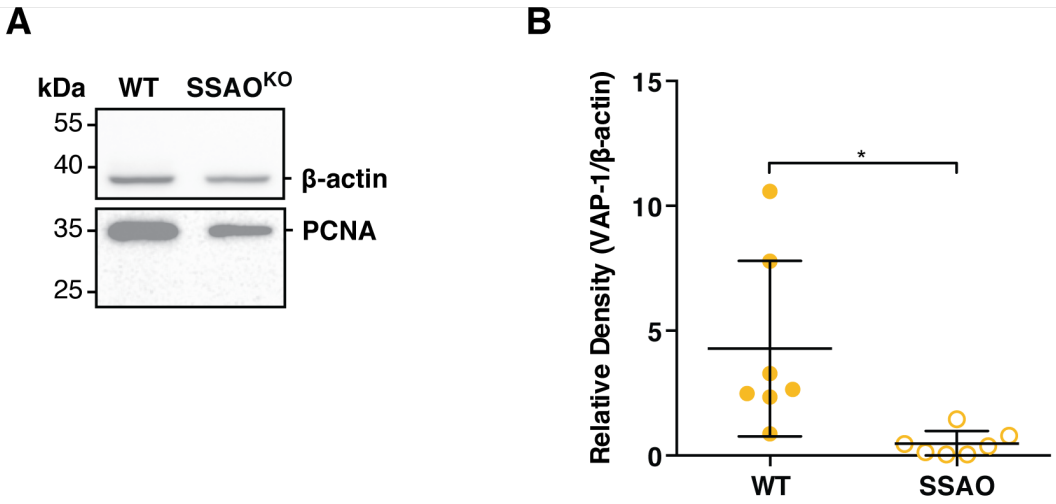


Figure 5.17 Effect of CCl_4 on hepatic PCNA expression of WT and SSAO^{KO} mice. WT C57/BL6 or SSAO^{KO} mice were treated with CCl_4 (1 mL/kg) via IP injection and sacrificed 48 hours later. (**A**) Sections of liver were analysed for the presence of proliferating cell antibody by Western blot. β-actin was used as a loading control. (**B**) Densitometry of Western blot analysis (n = 7). Data shown as mean (SD) and were analysed by t test. * $p \leq 0.05$.

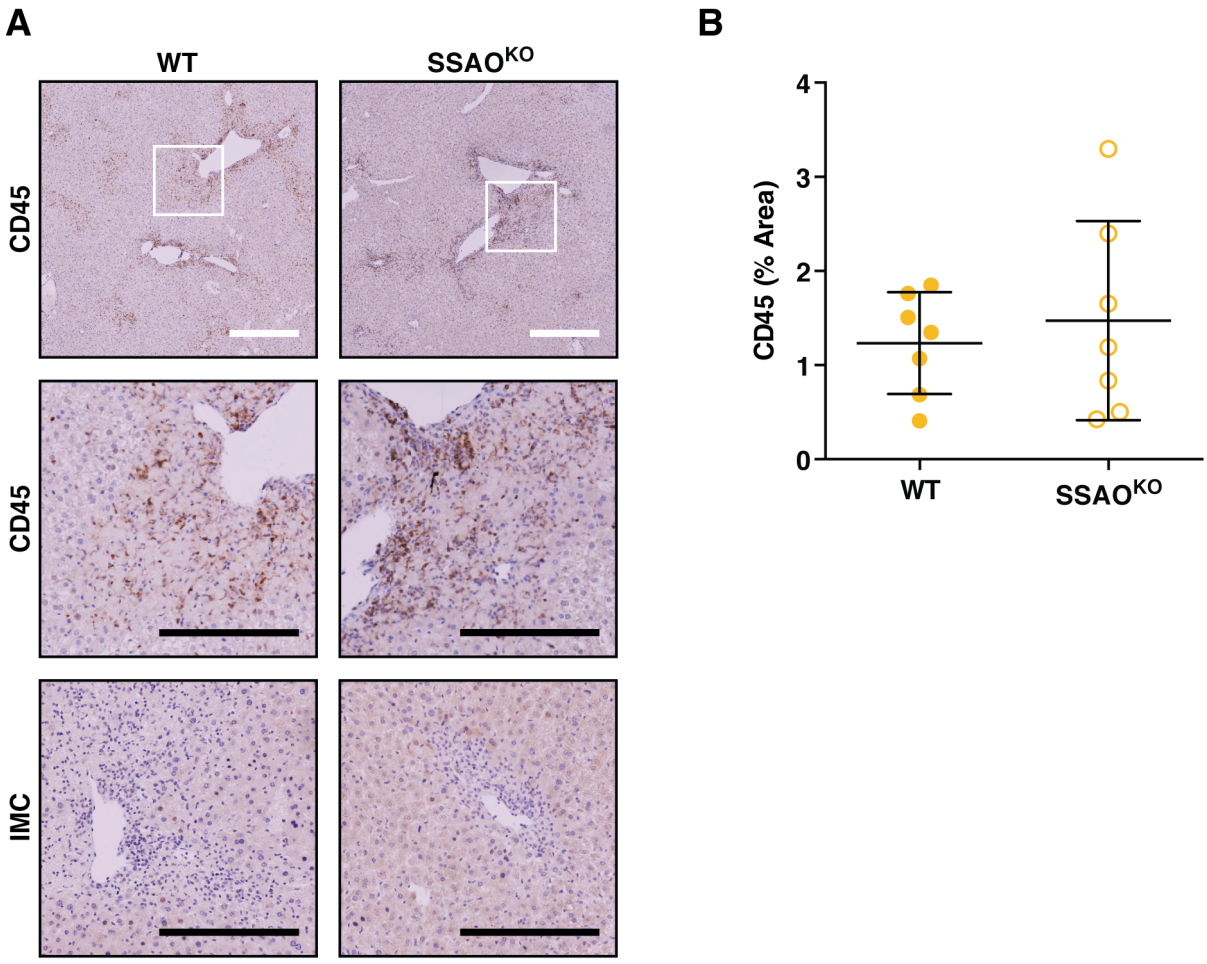


Figure 5.18 Effect of CCl_4 on infiltrating hepatic CD45$^+$ cells in WT and SSAO^{KO} mice. WT C57/BL6 or SSAO^{KO} mice were treated with CCl_4 (1 mL/kg) via IP injection and sacrificed 48 hours later. (**A**) Livers were stained for the presence of CD45 (brown) and counterstained with haematoxylin to visualise nuclei (blue). Middle panel represents enlargement of white boxed region in upper panel. White scale bar: 500 µm; Black scale bar: 250 µm. (**B**) Staining was quantified by ImageJ analysis (*n* = 7). Data shown as mean (SD) and were analysed by *t* test. No significant difference.

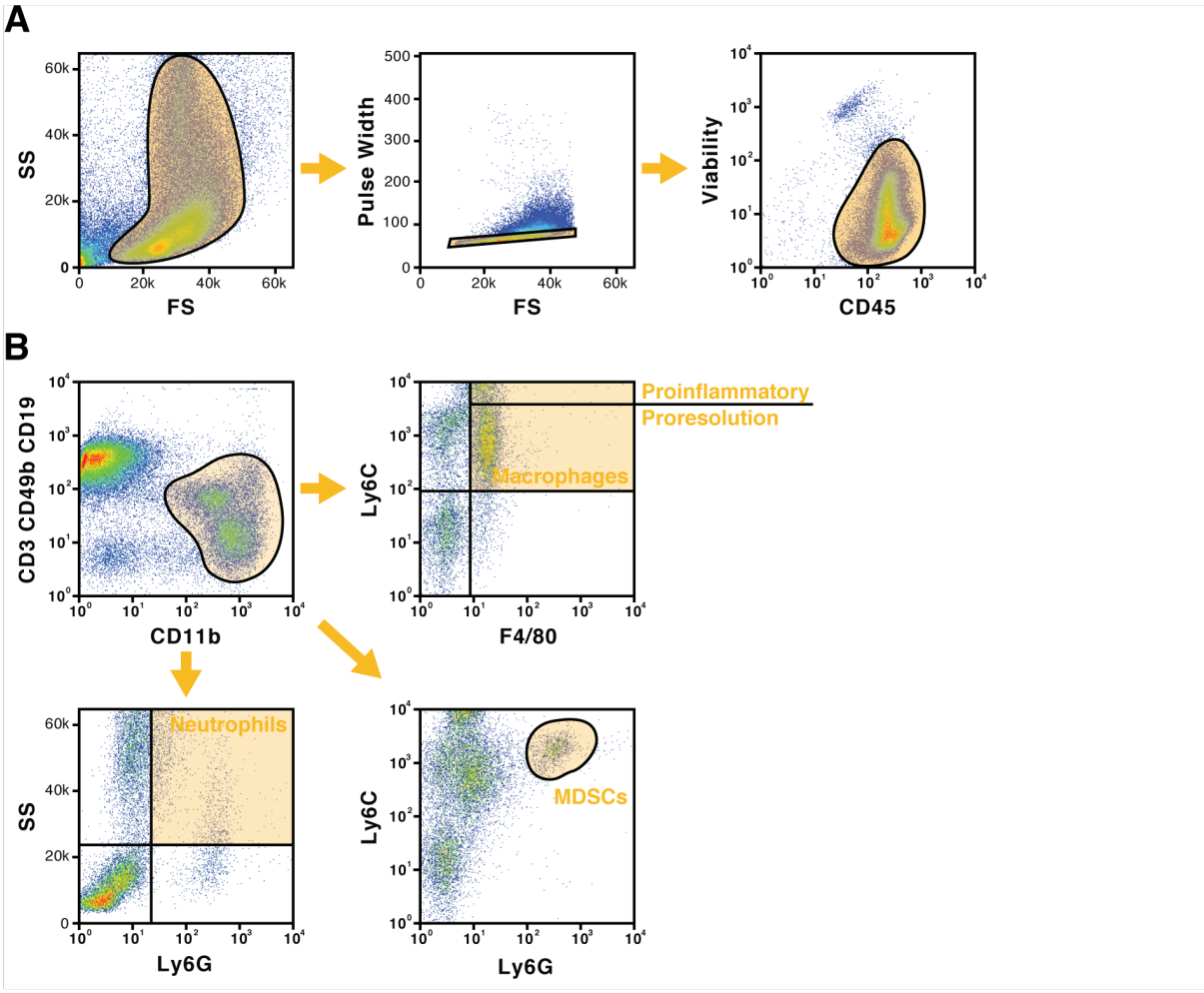


Figure 5.19 Gating strategy for phenotypic analysis of WT and SSAO^{KO} murine intrahepatic myeloid leukocytes by flow cytometry. (**A**) All cells were first gated on the leukocyte population using FS and SS characteristics, then single cells utilising pulse width and finally live cells. (**B**) All myeloid leukocytes were first gated as CD11b+ and CD3-CD49b^{-}CD19^{-} populations. Macrophages were designated as F4/80^{+}Ly6C^{+} and further classified as Ly6C^{hi} (proinflammatory) and CD6C^{low} (proresolution). Neutrophils were characterised due to their SS properties and as Ly6G^{+} whereas MDSCs were Ly6C^{+}Ly6G^{+}. Lymphoid populations were characterised as in Figure 5.7B.

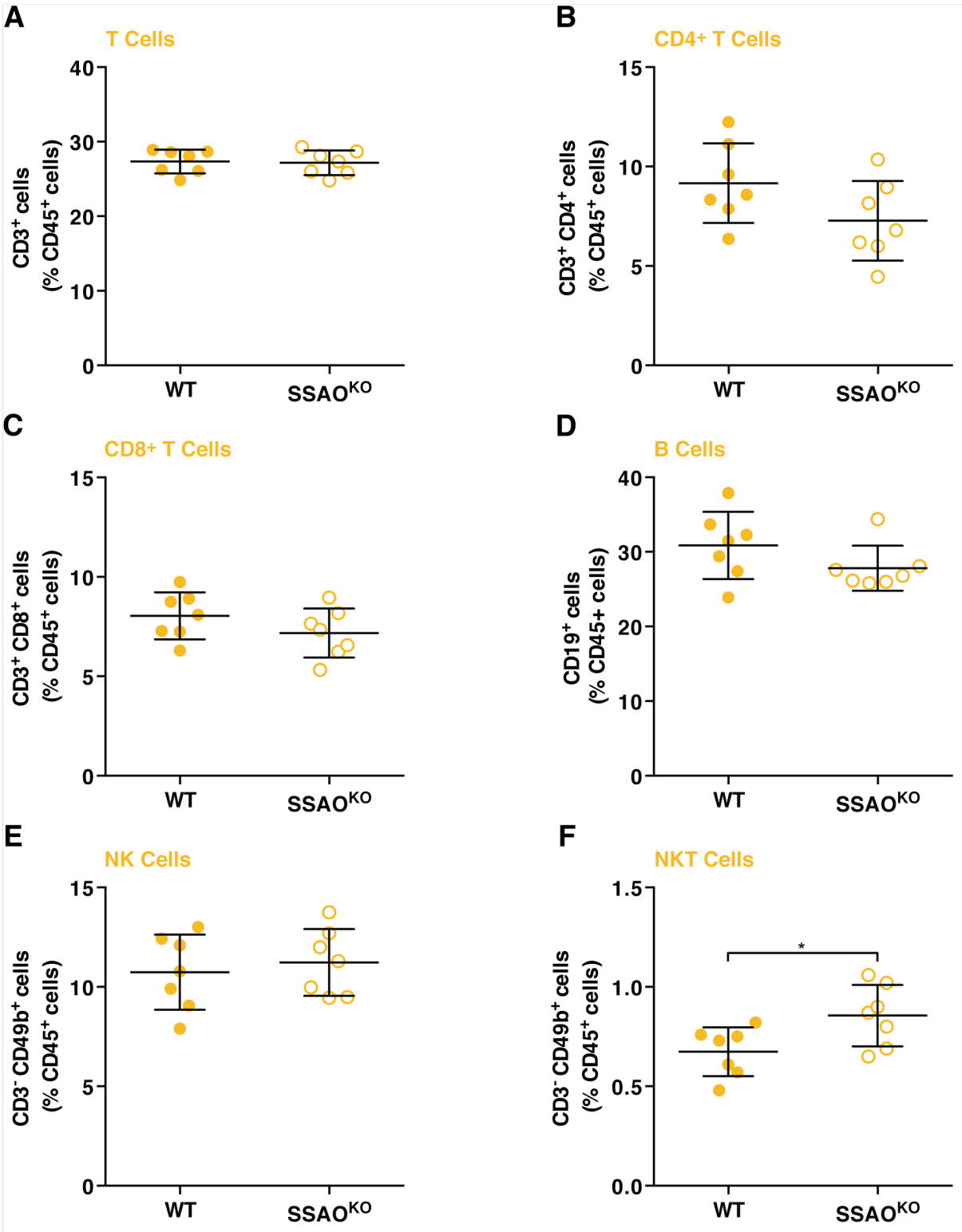


Figure 5.20 Effect of CCl_4 on intrahepatic lymphoid cells of WT and SSAO^{KO} mice. WT C57/BL6 or SSAO^{KO} mice were treated with CCl_4 (1 mL/kg via IP injection and sacrificed 48 hours later. Intrahepatic leukocytes were isolated and phenotyped by flow cytometry. (**A**) $CD3^+$ T cells. (**B**) $CD3^+CD4^+$ helper T cells. (**C**) $CD3^+CD8^+$ cytotoxic T cells. (**D**) $CD3^-CD19^+$ B cells. (**E**) $CD3^-CD49b^+$ NK cells. (**F**) $CD3^+CD49b^+$ NKT cells ($n = 7$). Data shown as mean (SD) and were analysed by *t* test. * $p \leq 0.05$.

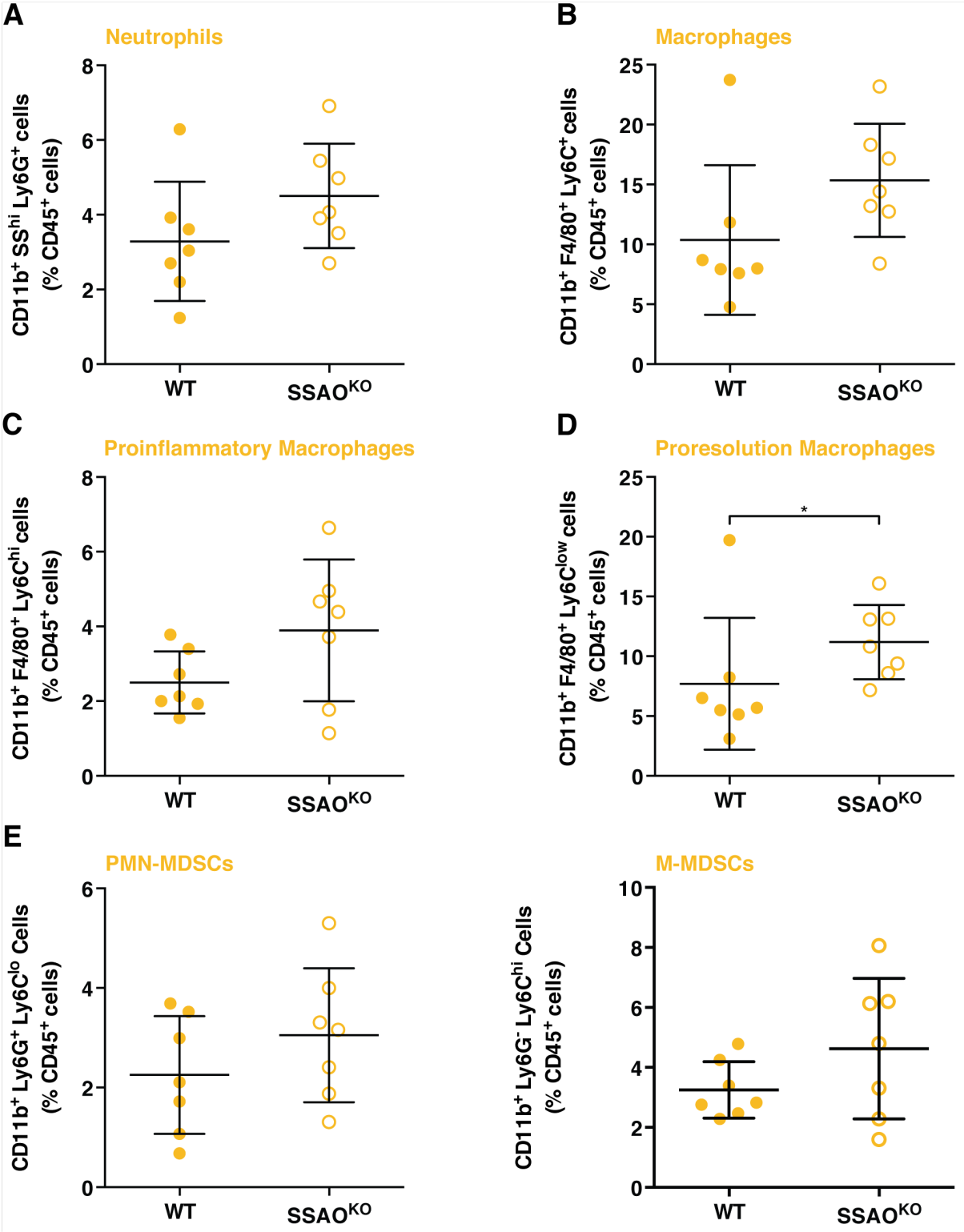


Figure 5.21 Effect of CCl_4 on intrahepatic myeloid cells of WT and $SSAO^{KO}$ mice. WT C57/BL6 or $SSAO^{KO}$ mice were treated with CCl_4 (1 mL/kg via IP injection and sacrificed 48 hours later. Intrahepatic leukocytes were isolated and phenotyped by flow cytometry. (A) $CD11b^+Ly6C^+Ly6G^+$ MDSCs. (**B**) $CD11b^+F4/80^+Ly6C^+$ Macrophages. (**C**) $CD11b^+F4/80^+Ly6C^{hi}$ Proinflammatory Macrophages. (**D**) $CD11b^+F4/80^+Ly6C^{low}$ Proresolution Macrophages. (**E**) $CD11b^+SS^{hi}Ly6G^{hi}$ Neutrophils ($n = 7$). Data shown as mean (SD) and were analysed by *t* test. * $p \leq 0.05$.

5.3 Discussion

The aim of Chapter 5 was *to investigate the role of VAP-1 amine oxidase activity in a murine model of acute liver injury*, specifically *t*he acute CCl_4-induced liver injury model. Wild-type animals were initially used to characterise the injury and to examine any changes in VAP-1 over the course of the pathology. These preliminary investigations demonstrated that hepatic damage peaked at approximately 48 hours post CCl_4 injection, as demonstrated by elevated serum ALT concentrations, total necrosis and cleaved caspase-3 immunohistochemistry. The proportion of intrahepatic NK cells and those of the myeloid lineage were also elevated at the 48 hour time point, although total $CD45^+$ staining peaked 24 hours later. Ki-67 staining and β-actin expression analysis both indicated that hepatic regeneration had begun by the 48-hour point and was further heightened at 72 hours. These data suggest that between 48 and 72 hours the damage had peaked and the liver had then entered the resolution stage. Interestingly, hepatic VAP-1 mRNA was also elevated in approximately half of the injured animals at both time points, whereas the catalytic activity was greater in all injured animals at 48 hours, but reduced to basal levels by 72 hours.

The acute CCl_4 model was then extended to enzyme-deficient $SSAO^{KO}$ animals to contrast how the liver injury differs in these animals compared to those that express the catalytically active form. The 48-hour time point was chosen as the point of maximal injury measured in WT animals, therefore greatest potential divergence. As expected, $SSAO^{KO}$ animals exhibited little to no VAP-1 enzyme activity but expressed comparable levels of VAP-1 mRNA to their wild-type littermates. The extent of liver injury following CCl_4 administration was highly similar between the two sets of mice, as evidenced by no significant difference in serum ALT and AST concentrations, hepatic necrosis or cleaved caspase-3 expression. Interestingly, both hepatic Ki67 staining and β-actin expression were lower in $SSAO^{KO}$ livers compared to WT, indicative of an impeded regenerative capacity. This contrasted with the elevated proportion of intrahepatic proresolution macrophages observed in the $SSAO^{KO}$ animals, however these cells formed a considerably larger fraction of the total liver leukocytes compared to during the preliminary investigations. $SSAO^{KO}$ livers also contained a significantly higher proportion of NKT cells compared to WT, although these numbers were more consistent with the characterisation study.

5.3.1 Acute murine liver injury model suitability

Acute human liver failure has an incidence of fewer than 10 cases per million persons per year in the Western world (Bower et al., 2007). This low prevalence in combination with the unpredictable nature of presentation has meant that acquiring fresh tissue samples for analysis during the course of this work has not been possible. Murine models therefore offered a useful tool for the investigation into the potential role of VAP-1 during acute liver injury. Furthermore, the availability of $SSAO^{KO}$ mice allowed investigations into the role of VAP-1 enzyme activity that would not be possible with human samples without prophylactic treatment with VAP-1 inhibitors.

Acute human liver injury can be the consequence of a variety of aetiologies but one of the commonest causes in the Western world is paracetamol overdose. While paracetamol can be used to induce liver injury in mice, there is often a lack of reproducibility reflected by unpredictable dose response and time to death (Newsome et al., 2000). Other models of acute liver injuries have therefore been historically used to study drug-induced hepatitis, perhaps the most common of which is acute CCl_4 toxicity. While paracetamol induces hepatic damage principally through oxidative stress, CCl_4 is metabolised within hepatocytes to produce highly reactive trichloromethyl radicals (McGill et al., 2012). These radicals react with and inactivate a whole host of biological molecules, inducing centrilobular necrosis and inflammation (Benedetti et al., 1974; Boll et al., 2001; Slater et al., 1964). Compared to other models, acute CCl_4 injury is relatively well characterised, is highly reproducible and immunogenic. For these reasons it was chosen as the model for investigating the consequences of VAP-1 function during acute liver injury.

5.3.2 Characterisation of acute hepatic CCl_4 injury and regeneration

During the pilot investigation, WT mice treated with CCl_4 clearly demonstrated signs of hepatic injury as indicated by increased serum ALT concentrations and large cleaved capase-3-positive centrilobular necrotic lesions. CCl_4 injury has a rapid onset: ALT concentrations are generally thought to peak approximately 24 hours after injection and begin to steadily decrease thereafter (Horiguchi et al., 2010; Huang, 2012; Karlmark et al., 2009; et al., 2013). The serum ALT values measured herein were consistent with these previous findings; demonstrating elevation at 48 hours post-administration of CCl_4 that was reduced to levels comparable to untreated mice by 72 hours. Increased serum ALT levels correlated with the development of large centrilobular necrotic lesions within

the livers of CCl_4-treated mice at 48 and 72 hours as indicated by immunohistochemistry, which are characteristic of CCl_4 hepatotoxicity. The identification of cleaved caspase-3 within these lesions also indicated the presence of cells undergoing apoptosis at both time points, consistent with previous characterisation of the hepatotoxic action of CCl_4 (Shi et al., 1998). The lesions also stained positive for the proliferation marker Ki67, indicating that hepatic regeneration had already commenced by 48 hours, which was also corroborated by Western blot analysis of PCNA.

The data presented here demonstrated similar levels of damage and regeneration at 48 and 72 hours post-administration. It is likely that these data points represent the reparative process following initial injury. This is in keeping with previous studies that have shown peak injury to occur around 24 hours after administration of CCl_4, which is followed by resolution by approximately 72 hours (Huang, 2012; Karlmark et al., 2009; Shi et al., 1998) or longer in some cases (Wehr et al., 2013). Without earlier time points this cannot be verified in the current model, however my data clearly indicate that CCl_4 induces hepatic necrosis and proliferation by at least 48 hours following administration.

5.3.3 Consequence of VAP-1 activity during injury and regeneration

These studies represent the first investigation into the role of VAP-1 amine oxidase activity in acute CCl_4 injury, which was achieved by induction of hepatic injury in $SSAO^{KO}$ mice. Interestingly, the extent of hepatic damage experienced by these animals was not vastly different to that of WT mice, demonstrated by the non-significant differences in serum ALT or AST, size of necrotic lesions or the presence of cleaved caspase-3. This was comparable to previous studies that found that the provision of an SSAO inhibitor had no effect of serum ALT concentration in a murine Con A-induced model of acute hepatic injury (Lee et al., 2013).

Interestingly, cellular proliferation following CCl_4-induced damage was significantly lower in the livers of $SSAO^{KO}$ mice compared to WT as indicated by both Ki67 immunohistochemistry and PCNA Western blot analysis. To the authors knowledge this is the first indication that VAP-1 may be implicated in hepatic regeneration. Weston and colleagues previously found similar levels of resolution between *Aoc3*$^{-/-}$, WT mice treated with VAP-1 antibody and WT control animals following chronic CCl_4 injury (Weston et al., 2015). This may highlight the importance of the enzyme activity of VAP-1 in hepatic

regeneration, which may mediate its effect through a number of related proliferative processes. For example VAP-1 inhibition can inhibit angiogenesis in murine models of cornea inflammation (Nakao et al., 2011) and melanoma (Marttila-Ichihara et al., 2010, 2009). Similarly to the chronic CCl_4 model, these effects on angiogenesis cannot be replicated by antibody blockade. This may be somewhat counterintuitive as H_2O_2 is traditionally thought to induce hepatocyte toxicity (Mavier et al., 1988; Ruch et al., 1989; Xu et al., 1997), however recent data suggest that at lower concentrations it is able to stimulate proliferation. Pharmacological lowering of intrahepatic H_2O_2 levels has been shown to reduce the extent of foetal hepatocyte proliferation and delays the onset of liver regeneration (Bai et al., 2015). Similarly, low concentrations of H_2O_2 are capable of stimulating the proliferation and transformation of liver oval cells *in vitro* (Wang and Yuan-de, 2001). The anti-proliferative effects of VAP-1 inhibition and that seen in $SSAO^{KO}$ animals herein may therefore be due to the reduction of hepatic H_2O_2, which may have important consequences for the future therapeutic value of VAP-1 enzyme inhibitors.

5.3.4 Characterisation of the acute inflammatory response to CCl_4 injury

The primary purpose of this thesis was to investigate the role of VAP-1 in hepatic inflammation; therefore the hepatic inflammatory response to CCl_4 was of great interest. The experimental time points were chosen in order to observe optimal change in leukocyte composition within the liver, following previously reported peak infiltration at 48 hours and recovery at around 72 hours post-CCl_4 infusion (Karlmark et al., 2009). On the contrary, immunohistochemistry appeared to suggest that maximum $CD45^+$ leukocyte infiltration occurred at 72 hours after administration of CCl_4 in WT animals. Furthermore, there was no significant difference between control and CCl_4-treated mice at 48 hours in terms of total leukocyte infiltration. $CD45^+$ staining of CCl_4-treated mouse livers at 72 hours post-injury did not, however, appear to be confined to single cells as in the images at 48 hours. This may indicate an issue during the staining procedure that may have artificially raised the quantified values of total staining area.

Flow cytometry allowed for more robust and full phenotypic analysis of intrahepatic leukocytes in WT animals following CCl_4 injury at 48 and 72 hours and results were broadly similar to previously published data. The size of the intrahepatic cytotoxic and helper T cell fractions were significantly lower in CCl_4-injured mice than control animals

at both the recorded time points. Although this is consistent with previous acute CCl_4 studies (Wehr et al., 2013) the opposite is seen during acute murine Con A injury (Lee et al., 2013), acute human liver injury (Ishida et al., 2002; Krenkel et al., 2014) and chronic CCl_4 injury (Weston et al., 2015). Acute CCl_4 toxicity does not induce generalised lymphopenia; therefore the precise reason for the observed reduction is unknown (Saba et al., 2010). However, it is possible that lymphocytes are sequestered to other damaged organs such as the kidneys or lungs. This is supported by the observed continued reduction in $CD8^+$ T cells to 72 hours after injection, which is beyond the active hepatotoxic action of CCl_4.

While the lymphoid fraction was decreased following CCl_4 administration, the proportion of intrahepatic myeloid cells was significantly raised at 48 hours. This increase was also in keeping with the literature, although previous studies also demonstrated increases in the proportion of classical macrophages ($CD11b^+F4/80^+$) of up to 50% total $CD45^+$ cells (Karlmark et al., 2009; Wehr et al., 2013). The greatly expanded macrophage population is also seen during acute human liver injury, such as paracetamol overdose (Antoniades et al., 2012). It is therefore possible that these cells were somehow lost during the preparation of the livers, perhaps through adhesion to plastic. It is also possible that these cells were associated with others, such as other macrophages or those of the parenchyma, and therefore gated out early in the flow cytometry analysis.

Ly-$6C^{hi}$ murine macrophages are thought to be analogous to $CD14^{hi}CD16^{low}$ cells in human and are considered to have proinflammatory activity whereas Ly-$6C^{low}$ macrophages are analogous to $CD14^{low}CD16^{hi}$ immunomodulatory human monocytes that can differentiate into tissue-resident macrophages (Heymann et al., 2009; Ramachandran et al., 2012). The pan-Ly6C/Ly6G marker Gr-1 was used to differentiate these populations during the initial experiments of this study on WT animals, an approach that has been reported previously (Karlmark et al., 2009). It is possible that Ly6G-expressing granulocytes would also be included in the $Gr\text{-}1^+$ population, however gating on F4/80-positivity as well as forward and side-scatter properties should have minimised this contamination. Both $Gr\text{-}1^{hi}$ and $Gr\text{-}1^{low}$ subsets exhibited similar trends although the numbers of proinflammatory macrophages was approximately ten-fold greater. These cells may be precursors to intrahepatic macrophages and are critical to the development of hepatic fibrosis by activation of HSCs (Karlmark et al., 2009). The release of $Gr\text{-}1^{hi}$ proinflammatory cells from the bone marrow and influx to the liver is

regulated by CCL2, abolishment of which dramatically reduced fibrosis in chronic CCl_4 injury (Engel et al., 2008; Karlmark et al., 2009). However upregulation of CCR2 would also be expected to result in increased migration of lymphocytes and NK cells which too migrate via the CCR2/CCL2 axis (Karlmark et al., 2008). This was not observed in this study suggesting additional mechanism of action. The proportion of immunoregulatory MDSC-like cells was also increased and formed a considerably higher proportion of the intrahepatic leukocyte fraction than proinflammatory macrophages. MDSCs are thought to be recruited to the liver via CXCR2 (Zhang et al., 2014), the ligand of which is upregulated on most hepatic cells during injury, including hepatocytes, KCs, HSCs, HSEC and BEC (Kuboki et al., 2008). MDSCs therefore accumulate in the liver during a range of acute models of injury, including Con A- (Hegde et al., 2011), LPS- (Sarra et al., 2013) and picryl chloride-induced hepatitis (Liu et al., 2014). Interestingly, murine HSCs are capable of inducing $CD11b^{+}Gr\text{-}1^{+}$ cells from bone marrow-derived cells through uncharacterised soluble mediators (Chou et al., 2011). It is therefore possible that at least a proportion of the observed intrahepatic MDSC fraction might be a differentiated rather than recruited population, formed as a direct consequence of $Gr\text{-}1^{hi}$ proinflammatory monocyte-activated HSCs. The soluble mediators may even be sVAP-1 secreted from HSCs (Weston et al., 2015). Once within the liver, MDSCs are capable of inhibiting lymphocyte proliferation (Sarra et al., 2013), which may also explain the decreased proportion of these cells compared to untreated livers that contain fewer MDSCs. This would also suggest that a large fraction of the lymphocyte population is also derived from proliferation rather than recruitment.

To phenotype liver-infiltrating leukocytes following CCl_4 injury the leukocyte population were first separated from other hepatic cell types. Different methods of isolation are known to affect the proportion of cells detected (Dong et al., 2004). A combination of enzymatic digestion and mechanical dissection was employed during this study in order to yield the largest possible fraction of leukocytes. However, enzymatic digestion with collagenase and DNase has been reported to decrease the surface expression of molecules such as NK1.1 and CD49b (Dong et al., 2004). This may therefore mean that true changes in NK and NKT cell populations were obscured, which may account for the low numbers of detected NKT cells. Similarly, this may also explain why no change was observed in this population following CCl_4 injury, in conflict with previously reported data (Wehr et al., 2013).

5.3.5 Consequence of VAP-1 activity on inflammatory response

In the previous chapter, VAP-1 inhibition was found to have no effect on leukocyte recruitment to human HSEC during *in vitro* flow-based adhesion assays. Correspondingly, immunohistochemistry indicated that the livers of $SSAO^{KO}$ animals exhibited no statistically significant difference in leukocyte infiltration following CCl_4 injury compared to WT animals. However, the range of infiltration between $SSAO^{KO}$ mice was greater than that between WT animals, therefore more sensitive methods of analysis may be required to elucidate any subtle differences. For example the addition of counting beads during flow cytometric analysis would allow for more precise enumeration of the hepatic infiltrate, or expansion of the flow cytometry panel to include additional inflammatory cell subsets such as regulatory T cells. Although the 48-hour time point elicited the greater total hepatic leukocyte fraction in the pilot study, it is likely that this was not the exact point of maximal influx. Extension of the study to include more time points may therefore also amplify any differences between the WT and $SSAO^{KO}$ animals.

Although the proportion of total intrahepatic T cells was almost identical between WT and $SSAO^{KO}$ mice, the livers of the latter did contain non-significantly fewer $CD4^+$ cells. Mice deficient in VAP-1 (*Aoc3*$^{-/-}$) or those treated with a VAP-1 antibody cocktail also demonstrate impaired $CD4^+$ recruitment, in particular those of the T_h2 lineage, during acute Con A hepatitis (Bonder et al., 2005; Lee et al., 2013). This may highlight the importance of both enzymatic activity and adhesin functionality for the recruitment of these cells, or perhaps that peak differences occur at a time earlier or later than the 48-hour time point sampled. Conversely, *Aoc3*$^{-/-}$ mice, those treated with VAP-1 antibody and the $SSAO^{KO}$ animals used in this study all showed no difference in total $CD8^+$ cell recruitment during acute hepatic injury (Bonder et al., 2005; Lee et al., 2013). However, it is important to remember that whereas Con A is a T cell-mediated model of injury, lymphocyte numbers are reduced during CCl_4 injury. Therefore while both CCl_4 and Con A induce acute hepatotoxicity, their mechanisms of action are discrete. Despite this, these murine results appear to be opposite of what is observed in human HEV and lymph nodes, where antibody blockade of VAP-1 is thought to strongly reduce the adhesion of $CD8^+$ but not $CD4^+$ T cells (Salmi et al., 1998, 1997).

This study was the first investigation into the role of VAP-1 in the hepatic recruitment of B cells, $CD49b^+$ cells and myeloid cells during acute liver injury. The intrahepatic

fraction of B cells and NK cells was similar between $SSAO^{KO}$ and WT mice, suggesting that VAP-1 enzyme activity is not essential for their recruitment. Interestingly, the proportion of intrahepatic NKT cells was higher in enzyme-deficient animals. This was comparable to the myeloid subsets, all of which were elevated in the livers of $SSAO^{KO}$ mice despite only reaching statistical significance for $Ly6C^{low}$ macrophages. The proportion of these proresolution macrophages was considerably higher than during earlier experiments using Gr-1 as a marker, whereas the proportion of $Ly6C^{hi}$ cells was similar. The reason for this difference is unclear as the opposite might be expected due to the cross reactivity of Gr-1 for both Ly6G and Ly6C.

CCl_4 hepatotoxicity is thought to induce the rapid recruitment of $Ly6C^{hi}$ cells to the liver (Karlmark et al., 2009). However, upon infiltration $Ly6C^{hi}$ cells can differentiate into $Ly6C^{low}$ phenotype, possibly facilitated by phagocytosis of cellular debris (Ramachandran et al., 2012). Therefore the significantly increased $Ly6^{low}$ population observed during this study could be a result of infiltrated $Ly6C^{hi}$ cells that have undergone this phenotypic switch to promote healing of the damaged liver. This could implicate VAP-1 in this differentiation process: the amine oxidase activity may retain the cells in a $Ly6C^{hi}$ phenotype therefore removal of this activity results in increased differentiation. This appears to be a more feasible explanation than lack of VAP-1 enzyme activity promotes the transmigration of $Ly6C^{low}$ cells into the liver, particularly as inhibition of VAP-1 via SMI has also been shown to reduce macrophage adhesion to inflamed murine cornea and aorta (Nakao et al., 2011; Silvola et al., 2016). Interestingly, the $Ly6C^{low}$ cells also demonstrate increased expression of metalloproteinases including MMP9 (Ramachandran et al., 2012), which is thought to mediate the protein cleavage of VAP-1 from retinal capillary endothelial cells (Murata et al., 2012). This might mean that $SSAO^{KO}$ mice would exhibit increased sVAP-1 concentrations compared to WT control. If sVAP-1 is the soluble mediator capable of inducing MDSCs, this may also contribute to the elevated levels within $SSAO^{KO}$ liver thereby indicating that enzyme activity is not required for this activation. This would also mean that both $Ly6C^{low}$ proresolution and $Ly6C^{hi}$ proinflammatory macrophages are capable of inducing MDSC differentiation, through increased MMP9 and cleavage of the membrane-bound form or activation of HSCs, respectively.

Inclusion of Ly6C and Ly6G antibodies allowed for the sub-classification of the MDSC fraction as either PMN- or monocyte-related. During acute Con A injury there are twice

as many intrahepatic PMN-MDSCs than M-MDSCs (Murata et al., 2012), however the reverse was found in both WT and $SSAO^{KO}$ mice herein. Interestingly the M-MDSC population is thought to be the only one capable of suppressing T cell function and limiting liver injury, as demonstrated in Con A hepatitis (Zhu et al., 2014) and *Tgfβ1*$^{-/-}$ mice (Cripps et al., 2010). However, both subpopulations of MDSCs were slightly elevated in $SSAO^{KO}$ livers compared to WT. The proportion of PMN- and M-MDSCs was relatively consistent between animals, despite exhibiting a large range between animals; in particular the two $SSAO^{KO}$ animals that exhibited the lowest proportion of PMN-MDSCs also had the lowest proportion of M-MDSCs. Interestingly, these same two animals were the outliers that demonstrated the lowest proportion of $Ly6C^{hi}$ proinflammatory macrophages. This is consistent with the previously described theory that intrahepatic $Ly6C^{hi}$ macrophages activate HSCs, which then induce the differentiation of other myeloid cells to MDSCs.

The use of Ly6C and Ly6G antibodies also allowed for the examination of intrahepatic neutrophils, which was not possible during the pilot study. Neutrophils are readily recruited to the liver during acute CCl_4 injury and may be key drivers of hepatotoxicity (Louis et al., 1998; Saba et al., 2010; Toriumi et al., 2013). However, the total proportion of neutrophils was considerably lower than would be expected, thereby potentially suggesting that these cells were lost in the isolation process. Although neutrophils have a much greater buoyant density than other mononuclear cells, they should still have been retained on 1.09 g/mL gradient used (Marchi et al., 2014), although it is still possible that they were not. In this case the fraction of cells measured in these experiments may relate to immature or activated neutrophils, which display altered buoyancy in density gradients (Dumitru et al., 2012). If $Ly6C^{hi}$ macrophages can differentiate into $Ly6C^{low}$ phenotype following phagocytosis, it is also possible that the neutrophils have been engulfed by macrophages. This may also contribute an explanation as to the increased numbers of $Ly6C^{low}$ cells. However, WT mice did not demonstrate increased numbers of intrahepatic neutrophils compared to $SSAO^{KO}$. Regardless, the recorded proportion of intrahepatic neutrophils was elevated in $SSAO^{KO}$ mice compared to WT. This is reminiscent of earlier experiments during which incubation of neutrophils with VAP-1 SMI elicited increased adhesion of cells to rVAP-1 protein under flow conditions. It is not certain whether or not murine neutrophils

express VAP-1, however if so then the expression of the catalytically inactive form may act in a similar fashion to treatment with VAP-1 SMI, thereby increasing adhesion.

5.3.6 Changes in hepatic VAP-1 during acute CCl_4 hepatotoxicity

The examination of chronically diseased human livers in the third chapter of this thesis did not detect any statistically significant changes in *AOC3* mRNA expression between healthy control and specific diseases. Significance was only reached following the increase in sample size by combining all samples from chronic conditions. A similar result was also demonstrated in the livers of WT mice treated with CCl_4: increased average expression levels that did not reach statistical significance. However, there was wide variation between the animals at both 48 and 72 hours, therefore half the mice exhibited greatly increased levels while the remainder were similar to control. This could be due to non-representative liver sampling as only small sections of liver were processed for mRNA expression. It is therefore possible that the composition differed between samples: with highly vascularised areas of tissue expected to exhibit higher VAP-1 expression. Similarly, if murine neutrophils also express catalytically active VAP-1, regions of the liver with increased cellular infiltrate may also contribute to spurious readings. However, during experiments with enzyme-deficient animals, the livers of both $SSAO^{KO}$ and WT mice exhibited almost identical VAP-1 expression after treatment with CCl_4, with relative values more comparable to untreated control animals in the first experiments. Unfortunately, lack of effective murine VAP-1 staining antibodies has meant that this method of detection was not possible and time restraints meant that qPCR analysis was not undertaken. It was demonstrated in Chapter 4 that proinflammatory mediators might downregulate VAP-1, therefore timing is critical in order to identify changes in VAP-1 expression by qPCR. The amine oxidase activities may therefore be a superior method of analysis, particularly in the absence of effective antibodies for detecting murine VAP-1 by Western blot. However, without simultaneous analysis of CCl_4-treated and untreated $SSAO^{KO}$ animals it is not possible to draw firm conclusions from these data. Subsequent investigations are therefore required.

Although VAP-1 mRNA expression was not significantly increased during CCl_4 hepatotoxicity, the enzyme activity of VAP-1 clearly was. It has been historically difficult to examine hepatic murine VAP-1 activity, and to the authors knowledge this demonstrates the first reported example. Similar trends were observed using both the

antibody capture and non-capture methods, although the captured activity was consistently lower than unbound sample. The captured fraction of activity represented approximately 60% of uncaptured activity, which is also comparable to the ratio observed during optimisation with rVAP-1. It is therefore likely that 7-106 decreases substrate access to the active site by steric hindrance, non-favourable orientation or by inducing a conformational change in the protein. Correcting the values of non-captured VAP-1 to LJP-1586-inhibited activity clearly reduced interference from other amine oxidases without the need for additional inhibitors, and demonstrated the lack of activity for $SSAO^{KO}$ livers as expected. The non-captured assay therefore appears to give the most representative value and should be used in future assays.

The slight increase in VAP-1 expression and the increase in VAP-1 activity demonstrated during acute CCl_4 injury in WT mice in the pilot study does not appear to be directly linked to the observed changes in intrahepatic leukocyte populations. This can be assumed due to the similar proportions of lymphoid subtypes in the livers of injured $SSAO^{KO}$ animals whereas the populations of myeloid subsets were further increased.

5.3.7 Chapter Summary

These studies represent the first investigation into the role of VAP-1 in acute murine CCl_4 hepatotoxicity. CCl_4 induced hepatocyte apoptosis in WT mice within the first 48 hours, which continued to 72 hours after injection. The liver injury induced corresponding reparative proliferation and an influx of intrahepatic leukocytes of the myeloid lineage, but reduced the fraction of intrahepatic lymphoid cells. Interestingly hepatic VAP-1 expression was slightly elevated following injury and VAP-1 enzyme activity was significantly higher.

$SSAO^{KO}$ mice exhibited similar levels of injury to WT animals at 48 hours after injury, but markers of hepatic regeneration were markedly reduced. Conversely, the proportion of proresolution macrophages within the livers of $SSAO^{KO}$ mice was elevated compared to WT livers whereas all other differences in infiltrate were not statistically significant.

Although these studies provide an interesting insight into the role of VAP-1 in acute hepatic injury, additional studies may answer some of the questions that have been raised. Extension to include both earlier and later time points would allow full

characterisation of the response to injury and hopefully highlight differences between $SSAO^{KO}$ and WT animals that were not statistically significant in this study. The changes in VAP-1 expression observed following CCl_4 injury could not be directly linked to changed in leukocyte recruitment, therefore extension to include the full VAP-1-deficient *Aoc3*$^{-/-}$ animals would allow for comparison of amine oxidase activity and adhesin functionality of VAP-1 to fully examine this function. These results of this study did suggest that VAP-1 activity might play a role in macrophage differentiation, which could be examined through subsequent *in vitro* coculture assays. Similarly assays may also elucidate whether sVAP-1 is indeed HSC-derived the soluble mediator capable of inducing the differentiation of MDSCs within the liver.

Despite differences between murine and human systems, the therapeutic implications of these data are unclear. Prophylactic treatment is not possible for most cases of acute liver disease, although this may be possible for acute-on-chronic conditions such as NANB. Inhibition of VAP-1 appears to induce expansion of the intrahepatic proresolution macrophages and immunomodulatory MDSC fractions, which may aid in recovery, although regenerative capacity of the liver may also be reduced. Further extension of these studies into other models of acute liver injury and examination of later time points may provide additional valuable insight into the translational relevance of VAP-1 therapy for acute injury.

6

CONCLUSIONS AND FUTURE WORK

6.1 Overview

Endothelial cells that line the hepatic sinusoids form a physical barrier between the hepatic parenchyma and the sinusoidal lumen and are therefore capable of mediating the hepatic immune response. HSEC are highly specialised to facilitate the tolerance of harmless commensals and food-borne antigens from the gastrointestinal tract while also supporting the recruitment of leukocytes from peripheral blood. VAP-1, an amine oxidase and adhesion molecule, is constitutively expressed by these cells and plays an important role in the leukocyte adhesion mechanism. As such VAP-1 has been implicated in the pathogenesis of inflammatory liver disease.

Since the discovery of VAP-1 25 years ago, a large body of literature has grown describing the functions of this many-faceted protein. However, many of the studies have reported conflicting results regarding the mechanism of action, which leukocytes are capable of interaction and the extent to which expression and activity promote and maintain an inflammatory environment. The intention of this thesis was to examine VAP-1 in a hepatic setting by investigating expression across a spectrum of liver diseases and to interrogate some of its functions within the liver with a view to understand more about the mechanism of action.

6.2 Summary of principle findings

6.2.1 VAP-1 and human liver disease

VAP-1 is thought to play a crucial role in homeostasis of the liver and as such it has been implicated in the pathogenesis of both acute and chronic inflammatory liver disease. However, much of this work has been conducted in murine models of injury with relatively little work examining human tissue. Recent evidence suggests that hepatic expression of VAP-1 is elevated during NASH, ALD, PSC and PBC (Karim et al., 2014; Weston et al., 2015), with corresponding raised levels of sVAP-1 (Kurkijärvi et al., 2000, 1998; Weston et al., 2015). Soluble VAP-1 activity is also demonstrably higher in hepatic compared to portal veins during chronic liver disease, thereby suggesting the liver as a possible source (Kurkijärvi et al., 2000).

The studies presented in Chapter 3 examined VAP-1 expression and enzyme activity across a spectrum of chronic liver diseases and NANB hepatitis. Expression of VAP-1 was localised to centrilobular sinusoids and the fibrotic scar, with expression primarily limited to HSEC, HSCs and myofibroblasts, which is line with previous studies (Weston et al., 2015). This localisation was unchanged during disease although expression was increased during chronic cirrhosis and correlated with extent of fibrosis. Conversely, activity levels of VAP-1 were reduced in chronically diseased liver tissue, although no single disease aetiology was significantly different from healthy control. The data in Chapter 3 also demonstrated that VAP-1 isolated from healthy and diseased livers was sensitive to inhibition to a similar degree. The data showed that hepatic VAP-1 was effectively inhibited by semicarbazide, LJP-1586 and - for the first time in man - caffeine in a dose-dependant manner.

6.2.2 VAP-1 and leukocyte function

VAP-1 has dual functions: as an amine oxidase and as a glycosylated adhesion molecule (Salmi and Jalkanen, 2001). The ability of VAP-1 to facilitate leukocyte adhesion has been clearly demonstrated using several human endothelial monolayers including lymph node (Salmi et al., 1998), inflamed synovium (Salmi et al., 1997) and lung tissue (Singh et al., 2003). Inhibition of amine oxidase activity or antibody blockade reduced the adhesive capacity of VAP-1, although no synergistic or additive effect has been found in combined inhibition studies (Koskinen et al., 2004; Lalor et al., 2002; Marttila-Ichihara et al., 2006; Salmi et al., 2001). However, there have been several contradictory findings regarding the function of VAP-1 expressed by HSEC within the liver in regards to its ability to support leukocyte adhesion and transmigration (Edwards et al., 2005; Lalor et al., 2007; Shetty et al., 2011; Tuncer et al., 2013).

The data in Chapter 4 describe an investigation into the adhesive capacity of VAP-1 expressed by HSEC. In line with previous studies, inhibition of VAP-1 by either SMI or blocking antibody had no effect on the total adhesion of leukocytes to the HSEC monolayer (Edwards et al., 2005; Lalor et al., 2007; Shetty et al., 2011; Tuncer et al., 2013). However, unlike several of these studies, no change in the proportion of cells that transmigrated was observed (Edwards et al., 2005; Lalor et al., 2007; Shetty et al., 2011). Furthermore, no effect was highlighted when, for the first time, $CD4^+$ and $CD8^+$ T cells, NK cells or neutrophils were examined in isolation. Overexpression of GFP-VAP^{WT} conferred a slight increase in the adhesion of neutrophils to the HSEC monolayer, potentially indicating that the previous results were a consequence of TNFα-induced downregulation of VAP-1 on the HSEC surface. Interestingly, the neutrophils intimately interacted with the GFP-VAP^{WT} protein as they crawled along the monolayer, and VAP-1 appeared to form transmigratory cup structures that have been previously identified to facilitate adhesion (Carman and Springer, 2004).

Chapter 4 also demonstrated that neutrophils were capable of adhering to commercially available recombinant VAP-1 protein under flow conditions, whereas other subsets were not. Subsequent analysis revealed for the first time that human neutrophils also express and secrete catalytically active VAP-1 protein, which is downregulated following proinflammatory stimulation. This finding was corroborated by databases such as the European Bioinformatics Institute (EMBL-EBI) Gene Expression Atlas and the Scripps Research Institute 'BioGPS' and other studies investigating the transcriptomes of

neutrophils, although the significance was not highlighted at the time of publication (Jiang et al., 2015). Inhibition of neutrophil VAP-1 induced a two-fold increase in adhesion to rVAP-1 protein and elevated adhesion to HSEC under flow conditions, although the latter was not statistically significant, but did not affect the production of ROS or extracellular traps. However, the addition of rVAP-1 protein or VAP-1 substrates (benzylamine and cysteamine) exerted a significant reduction in ROS production and NETosis.

6.2.3 VAP-1 and acute murine liver injury

VAP-1 has been implicated in the pathogenesis of most liver diseases, however relatively little work has investigated its function in acute liver injury. Hepatic VAP-1 expression is thought to be elevated during paracetamol-induced ALF (Tuncer et al., 2013), however data shown in Chapter 3 demonstrated that VAP-1 was not significantly affected during NANB hepatitis. Unfortunately, these conditions are rare, unpredictable and have a rapid onset therefore tissue samples are scarce and large clinical trials are next to impossible (Lee et al., 2012). Animal models of acute liver injury have therefore provided a useful tool to gain insight into the mechanism of the disease.

Murine studies described in Chapter 5 examined the acute hepatotoxic effect of CCl_4 and the role of VAP-1 during this process. A single IP injection of CCl_4 induced centrilobular apoptosis and necrosis within 48 hours, which corresponded to a significant increase in cellular proliferation and expansion of intrahepatic leukocytes of the myeloid lineage. The injury also induced an elevation in hepatic VAP-1 expression and activity. Compared to WT animals, mice expressing the catalytically inactive form of VAP-1 ($SSAO^{KO}$) experienced similar levels of VAP-1 expression and hepatic injury following the administration of CCl_4, but exhibited a marked reduction in regenerative proliferation. Interestingly, the proportion of proresolution macrophages within the livers of $SSAO^{KO}$ mice was also elevated compared to WT livers, and demonstrated slight nonsignificant increases in other myeloid cell types.

6.3 Study limitations

The strong links between the Centre for Liver Research at the University of Birmingham and the Liver Transplant Unit at the Queen Elizabeth Hospital has allowed for the use of human liver tissue samples for this study. Working with patient samples provides a

valuable insight into *in vivo* conditions but also has several limitations, the most notable of which is that all patient samples used in this study have been acquired following liver transplantation. This means that all samples are limited to end-stage liver disease, therefore preventing comment on whether VAP-1 expression is altered in the pre-cirrhotic state. Often these patients present with multiple aetiologies therefore selection of patients with single diagnoses for this study was particularly challenging. Similarly, normal liver samples were acquired from donor tissue that was rejected for transplant. The reasons for rejection are highly varied and although samples were selected following careful examination by a pathologist, pre-existing conditions cannot be discounted fully. Factors such as age, gender and other extraneous factors such as smoking status may affect the expression of VAP-1 (and presence of circulating sVAP-1), which was also not accounted for within this study. This interpatient variability is most likely responsible for the large range between samples observed in Chapter 3. Similarly, inter-patient variability is likely to have affected the characteristic of the isolated HSEC used within this study. However, this was a compromise that was made in order to recapitulate *in vivo* conditions as closely as possible.

6.4 Translational implications

The implication of amine oxidases in many inflammatory conditions has highlighted this family of proteins as potentially valuable therapeutic targets. Particular interest has been paid to VAP-1 due to its restricted expression in combination with the upregulation of serum concentrations during a diverse range of inflammatory process, including: multiple sclerosis (Airas et al., 2006; Yanaba et al., 2013), atherosclerosis (Karádi et al., 2002), Psoriasis vulgaris (Ataseven and Kesli, 2016; Madej et al., 2007; Nemati et al., 2013), atopic eczema (Madej et al., 2006), chronic kidney disease (Lin et al., 2008), type II diabetes (Elliott et al., 1991; Garpenstrand et al., 1999; Hayes and Clarke, 1990; Li et al., 2009), end stage renal disease (Li et al., 2016) and of course liver disease (Kurkijärvi et al., 2000, 1998; Tuncer et al., 2013; Weston et al., 2015). Furthermore, inhibition of VAP-1 has demonstrated suppression of inflammation and reduced leukocyte recruitment to inflamed tissue during many animal disease models, including: ulcerative colitis (Salter-Cid et al., 2005), arthritis (Marttila-Ichihara et al., 2006; Tábi et al., 2013), uveitis (Noda et al., 2008) diabetic retinopathy (Noda et al., 2009), chronic obstructive pulmonary disease (Jarnicki et al., 2016), ischemic heart disease (Jaakkola et al., 2000)

and a range of chronic (Weston et al., 2015) and acute liver diseases (Bonder et al., 2005; Lee et al., 2013). This has encouraged the development of many therapeutic anti-VAP-1 antibodies and SMIs in the hope of treating these conditions. Of particular interest are the inhibitor PXS4728A, recently acquired by Boehringer Ingelheim from Pharmaxis, and the humanised antibody BTT1023 (Timolumab) developed by Biotie Therapies (now acquired by Acorda Therapeutics). The former has recently successfully passed through a Phase I clinical trial and is soon to enter Phase II for the treatment of NASH whereas a current phase II clinical trial is currently underway in Birmingham using BTT1023 for the treatment of PSC. The findings of this thesis therefore add to the growing body of literature describing hepatic VAP-1 and may be of particular therapeutic relevance.

The proposed hepatoprotective functionality of VAP-1 inhibition is via the reduction of leukocyte migration into the liver. All chronic liver diseases have a strong inflammatory component, in particular the autoimmune diseases such as PSC - one reason that it was chosen for the current clinical trial. However, the similarity in VAP-1 expression across the diseases demonstrated in Chapter 3 would suggest that the therapeutics might also be of benefit for the treatment of other chronic liver diseases. The VAP-1 isolated from each of the diseases also demonstrated similar sensitivities to inhibition, thereby indicating similar pharmacokinetics and potential drug efficacy between the conditions.

The present study found that VAP-1 inhibition had no effect on adhesion of T cells, neutrophils or NK cells to HSEC, in line with previous findings (Edwards et al., 2005; Lalor et al., 2007; Shetty et al., 2011; Tuncer et al., 2013). Data within Chapter 4 also demonstrated that neutrophils were capable of adhering to rVAP-1 protein in isolation and that overexpression of GFP-VAP-1^{WT} or incubation with rVAP-1 also increased the proportion of adherent neutrophils to the HSEC monolayer. Together, these data may suggest HSEC-derived VAP-1 is not capable of supporting leukocyte adhesion, comparative to that expressed by smooth muscle cells (Jaakkola et al., 1999), due to aberrant surface N-glycosylation (Maula et al., 2005) or intracellular rather than extracellular localisation (Weston et al., 2013). These data may therefore suggest that VAP-1 inhibition will not be efficacious in reducing leukocyte recruitment to the liver in the current clinical trials. That being said, the results of this study may be an *in vitro* artefact of the flow-based adhesion assay, such as the difference between leukocyte migration across plastic-adherent HSEC compared to *in vivo* conditions where hepatocytes and hepatic stroma form the basal layer and the interactions occur in a

milieu of pro- and anti-inflammatory molecules. These cells and molecules may provide additional factors during injury that are absent in the HSEC monoculture. The observed results may be also ascribed to downregulation of VAP-1 following TNFα stimulation, as documented in Chapter 4. Although TNFα concentrations are also constitutively elevated within the liver during cirrhosis (Hammam et al., 2013), HSEC may be refractory following repeat exposure, similar to that observed with LPS (Uhrig et al., 2005). While total VAP-1 mRNA production was elevated in the chronic livers examined in Chapter 3, expression was primarily focussed within the fibrotic septa, with loss demonstrated across parenchymal HSEC compared to control tissue. This may be due to downregulation but may also due to release of soluble VAP-1, as suggested by transgenic murine studies (Stolen et al., 2004), thereby acting as the source of the elevated serum VAP-1 levels during chronic disease (Kurkijärvi et al., 2000, 1998; Tuncer et al., 2013; Weston et al., 2015). Soluble VAP-1 is capable of altering the adhesive status of leukocytes and promoting diapedesis (Kurkijärvi et al., 1998), which may be a contributing factor to the reduced adhesion in the absence of serum described in Chapter 4. Soluble VAP-1 can also act directly as a chemoattractant, which is critically dependent on the amine oxidase activity (Tanaka et al., 2017; Weston et al., 2015). Therefore, if soluble VAP-1 is released from HSEC during inflammation and subsequently facilitates leukocyte adhesion, treatment with SMIs may prove efficacious in the ongoing trials.

Somewhat counterintuitively, the murine studies herein found that lack of VAP-1 amine oxidase activity resulted in elevated expansion of intrahepatic myeloid cells during acute injury. In particular the proportion of restorative cells was increased including proresolution macrophages and immunomodulatory MDSCs. The underlying mechanism of how enzyme activity-deficient VAP-1 is linked to an increase in these cell populations is unclear. Proinflammatory macrophages are rapidly recruited to the liver following injury (Karlmark et al., 2009), therefore it is possible that the amine oxidase activity of VAP-1 is capable of maintaining the proinflammatory phenotype of these cells: removal of this activity would therefore result in increased differentiation to the $Ly6C^{low}$ proresolution phenotype observed in the livers of $SSAO^{KO}$ mice. Ly6Clow macrophages may also induce the cleavage of membrane-bound VAP-1 via expression of MMP9 (Ramachandran et al., 2012) as observed in retinal capillary endothelial cells (Murata et al., 2012). Despite differences between murine and human systems, this may indicate that inhibition of VAP-1 may result in increased sVAP-1 during acute injury. The

infiltrated Ly6^{hi} proinflammatory population are also capable of activating local HSCs (Karlmark et al., 2009), which is turn induce the differentiation of MDSCs via unknown soluble mediators (Chou et al., 2011). It is possible that this mediator is VAP-1 (Weston et al., 2015), in which case both Ly6^{hi} and Ly6^{low} macrophages could induce increases in sVAP-1 through separate mechanisms. The consequences of these data in terms of hepatic regeneration and recovery are unclear as while hepatic proliferation was reduced, the extent of injury was comparable between SSAO^{KO} mice and those expressing catalytically active VAP-1. SSAO^{KO} animals are also more directly comparable to prophylactic VAP-1 inhibition, which is not possible in a clinical setting. The complex mechanisms of VAP-1 inhibition may therefore elicit unexpected effects during the PXS4728A trial.

This study demonstrated for the first time that human neutrophils express catalytically active VAP-1. Inhibition of neutrophil VAP-1 with LJP-1586 increased adhesion of this immune cell subset to rVAP-1 and potentially also to an HSEC monolayer. Previously unpredictable consequences may therefore arise from treating NASH patients with PXS4728A, as this will also affect the recruitment of patient neutrophils to all VAP-1-expressing tissues. However, the inflammatory conditions experienced during PSC and NASH may downregulate VAP-1 within the neutrophils, therefore ameliorating any effect of inhibition. This could be examined *in vitro* by extension of the neutrophil flow-based adhesion assays to include pretreatment combinations of proinflammatory cytokines and VAP-1 SMI. Inhibition of VAP-1 did not affect the neutrophil effector functions examined in this study, although this list was not exhaustive. Further work is required in this area to examine the effect on functions such as phagocytosis or secretion of granule contents. It is also not possible to speculate on the effect of antibody blockade of VAP-1 neutrophil function from the current data and the consequence of this for the current clinical trial.

6.5 Future work

The literature surrounding VAP-1 is highly contradictory but one conclusion can be definitively drawn - the physiological role of VAP-1 in health and disease is clearly complex. Despite the fact that clinical trials are now underway, there is still a clear need for further examination of this protein to elucidate the full implications of its functionality. Future studies may hope to investigate some of the following:

Extension of hepatic VAP-1 characterisation

- The number of samples used within this study were limited and warrant extension to include much larger cohorts in hope of elucidating true differences in hepatic VAP-1 expression and activity in health and disease.
- Quantification of hepatic VAP-1 via Western blot or ELISA would be desirable in order to yield a more accurate determination of differences at the protein level during health and disease.
- Immunohistochemical analysis of VAP-1 within cultured HSEC has been historically difficult, with no previous studies clearly demonstrating effective antibody staining. While GFP-tagged VAP-1 is a useful tool, the GFP protein may interfere with endogenous VAP-1 processing. The use of FLAG-tagged proteins may therefore yield more successful results for examining native-state VAP-1 within these cells. This may confirm whether any protein is surface-expressed or, as seen within this study, the majority is intracellular and not capable of interacting with leukocytes.

Leukocyte recruitment via VAP-1

- During this study it was only possible to examine the role of VAP-1 in the recruitment of $CD4^+$ and $CD8^+$ lymphocytes, NK cells and neutrophils to HSEC. VAP-1 has been implicated in the recruitment of the majority of leukocytes; therefore extension of this panel would be of interest, in particular to include the examination of T_h1 and T_h2 lymphocyte and macrophage subsets.
- These studies demonstrated that only neutrophils were capable of adhering to rVAP-1 protein. It is unclear whether this was a true representation of binding capacities or an artefact of the protein expressed by *S. frugiperda*, perhaps caused by aberrant glycosylation. Future studies may therefore examine the glycosylation of hepatic VAP-1 and that expressed by *S. frugiperda* via size exclusion chromatography, isoelectric capillary electrophoresis, or mass spectrometry. Furthermore it would be of interest to affinity-purify VAP-1 from human livers and use this in the flow-based adhesion assays to assess the binding capacity of hepatic VAP-1 in isolation.
- GFP-VAP-1^{WT} expressed by HSEC formed a transmigratory cup around adhered neutrophils. Further characterisation of this structure would allow for

comparison to those previously described. In particular, immunohistochemical staining for markers such as ICAM-1, LFA-1 and VE-cadherin may elucidate the functional role (Carman and Springer, 2004). Similarly, it appeared that VAP-1 may be involved in the intraluminal crawling process in transfected cells, therefore kinetic analysis of this process in the presence or absence of inhibitors may highlight subtle changes in this process.

- Only a single replicate was conducted examining the effects of soluble VAP-1 on the recruitment of neutrophils to HSEC. This is a potentially exciting study and may link the elevated sVAP-1 levels observed during disease with the increase in inflammation. Confirmatory replicates of these experiments are required and extension to examine the mechanism of action may be of great therapeutic interest.
- Normothermic machine liver perfusion (NMLP) systems offer an exciting opportunity for whole human organ models. These machines offer permit the perfusion of donor livers to maintain liver function post transplant, but can also be used to perfuse labelled leukocytes and examine recruitment throughout the whole organ. Blocking VAP-1 activity with antibodies and SMIs represent an advanced flow-based adhesion assay, minimising *in vitro* artefacts.

Consequence of neutrophil VAP-1 expression

- This study represents the first indication that neutrophils express VAP-1, however the full extent of this expression is unclear. Confirmation at the protein level by Western blot would be a critical first assay, but also extension to other organisms such as murine neutrophils. Future analysis of subcellular localisation through immunohistochemistry and subcellular fractionation would also provide useful insight into the possible function of this expression.
- These studies demonstrated downregulation of neutrophil VAP-1 in the presence of TNF and IFN. These proinflammatory molecules are elevated in the liver during CLD; therefore VAP-1 may be chronically downregulated in neutrophils during these diseases. The physiological relevance of this is of great importance in order to elucidate the functional consequence of VAP-1 inhibitor therapies. Additional analysis of neutrophil adhesion to HSEC *in vitro* in the presence of various pro- and anti-inflammatory mediators and inhibitors may provide some

mechanistic insight. Furthermore, analysis of neutrophils from patients suffering from CLD for VAP-1 expression would be of particular interest.

- SMI inhibition of VAP-1 had no effect on neutrophil ROS or NET production, however incubation with rVAP-1 and VAP-1 substrates reduced these processes. A PKCζ-dependent mechanism of action was proposed, however this was purely speculative. Full interrogation of this theory may be of great therapeutic interest and would provide useful insight into the still elusive mechanism of NETosis. Furthermore, extension to analyse additional neutrophil effector functions would be of interest, such as phagocytosis.

Extension of acute CCl_4 studies

- $SSAO^{KO}$ animals provided a useful tool for examining the enzymatic function of VAP-1. However, some studies have suggested that the amine oxidase activity is not important for leukocyte recruitment. Extension of these studies to include VAP-1-deficient (*Aoc3*$^{-/-}$) animals would therefore allow for further examination into the role of VAP-1 in CCl_4 hepatotoxicity.
- It is likely that the observed reduction in hepatic proliferation of $SSAO^{KO}$ mice was an H_2O_2-dependent effect, however this was beyond the scope of the present study. Further investigation into the true mechanism of action may provide useful insight into the role of hepatic VAP-1, which may be relevant beyond murine models of acute hepatotoxicity.

REFERENCES

Aalto, Autio, Kiss, Elima, Nymalm, Veres, Marttila-Ichihara, Elovaara, Saanijoki, Crocker, Maksimow, Bligt, Salminen, Salmi, Roivainen and Jalkanen. (2011). Siglec-9 is a novel leukocyte ligand for vascular adhesion protein-1 and can be used in PET imaging of inflammation and cancer. *Blood*, 118 (13), p.3725–3733. doi:10.1182/blood-2010-09-311076.

Abdel-Misih, S. and Bloomston, M. (2010). Liver Anatomy. *Surgical Clinics of North America*, 90 (4), p.643–653. doi:10.1016/j.suc.2010.04.017.

Abella, A., García-Vicente, S., Viguerie, N., Ros-Baró, A., Camps, M., Palacín, M., Zorzano, A. and Marti, L. (2004). Adipocytes release a soluble form of VAP-1/SSAO by a metalloprotease-dependent process and in a regulated manner. *Diabetologia*, 47 (3), p.429–438. doi:10.1007/s00125-004-1346-2.

Abella, A., Marti, L., Camps, M., Claret, M., Fernández-Alvarez, J., Gomis, R., Gumà, A., Viguerie, N., Carpéné, C., Palacín, M., Testar, X. and Zorzano, A. (2003). Semicarbazide-sensitive amine oxidase/vascular adhesion protein-1 activity exerts an antidiabetic action in Goto-Kakizaki rats. *Diabetes*, 52 (4), p.1004–1013. doi:10.2337/diabetes.52.4.1004.

Adam, R., Karam, V., Delvart, V., O'Grady, J., Mirza, D., Klempnauer, J., Castaing, D., Neuhaus, P., Jamieson, N., Salizzoni, M., Pollard, S., Lerut, J., Paul, A., Garcia-Valdecasas, J. C., Rodríguez, F. S. and Burroughs, A. (2012). Evolution of indications and results of liver transplantation in Europe. A report from the European Liver Transplant Registry (ELTR). *Journal of hepatology*, 57 (3), p.675–688. doi:10.1016/j.jhep.2012.04.015.

Adams, D. and Eksteen, B. (2006). Aberrant homing of mucosal T cells and extra-intestinal manifestations of inflammatory bowel disease. *Nature Reviews Immunology*, 6 (3), p.244–251. doi:10.1038/nri1784.

Adams, D. H. and Shaw, S. (1994). Leucocyte-endothelial interactions and regulation of leucocyte migration. *Lancet (London, England)*, 343 (8901), p.831–836.

Adler, M., Taylor, S., Okebugwu, K., Yee, H., Fielding, C., Fielding, G. and Poles, M. (2011). Intrahepatic natural killer T cell populations are increased in human hepatic steatosis. *World journal of gastroenterology*, 17 (13), p.1725–1731. doi:10.3748/wjg.v17.i13.1725.

Ager, A. and May, M. (2015). Understanding high endothelial venules: Lessons for cancer immunology. *OncoImmunology*, 4 (6), p.e1008791. doi:10.1080/2162402X.2015.1008791.

Ahlenstiel, G., Titerence, R. H., Koh, C., Edlich, B., Feld, J. J., Rotman, Y., Ghany, M. G.,

Hoofnagle, J. H., Liang, T. J., Heller, T. and Rehermann, B. (2010). Natural killer cells are polarized toward cytotoxicity in chronic hepatitis C in an interferon-alfa-dependent manner. *Gastroenterology*, 138 (1), p.325–35.e1–2. doi:10.1053/j.gastro.2009.08.066.

Airas, L., Mikkola, J., Vainio, J. M., Elovaara, I. and Smith, D. J. (2006). Elevated serum soluble vascular adhesion protein-1 (VAP-1) in patients with active relapsing remitting multiple sclerosis. *Journal of neuroimmunology*, 177 (1-2), p.132–135. doi:10.1016/j.jneuroim.2006.05.014.

Aird, WC. (2007). Phenotypic heterogeneity of the endothelium II. Representative vascular beds. *Circulation research*. doi:10.1161/01.RES.0000255690.03436.ae.

Airenne, T., Nymalm, Y., Kidron, H., Smith, D., Pihlavisto, M., Salmi, M., Jalkanen, S., Johnson, M. and Salminen, T. (2005). Crystal structure of the human vascular adhesion protein-1: Unique structural features with functional implications. *Protein Science*, 14 (8), p.1964–1974. doi:10.1110/ps.051438105.

Alcañiz, L., Vega, A., Chacón, P., Bekay, R., Ventura, I., Aroca, R., Blanca, M., Bergstralh, D. and Monteseirin, J. (2013). Histamine production by human neutrophils. *The FASEB Journal*, 27 (7), p.2902–2910. doi:10.1096/fj.12-223867.

Alvaro, D., Mancino, M., Glaser, S., Gaudio, E., Marzioni, M., Francis, H. and Alpini, G. (2007). Proliferating Cholangiocytes: A Neuroendocrine Compartment in the Diseased Liver. *Gastroenterology*, 132 (1), p.415–431. doi:10.1053/j.gastro.2006.07.023.

Amadei, B., Urbani, S., Cazaly, A., Fisicaro, P., Zerbini, A., Ahmed, P., Missale, G., Ferrari, C. and Khakoo, S. I. (2010). Activation of natural killer cells during acute infection with hepatitis C virus. *Gastroenterology*, 138 (4), p.1536–1545. doi:10.1053/j.gastro.2010.01.006.

Anstee, Q. M. and Goldin, R. D. (2006). Mouse models in non-alcoholic fatty liver disease and steatohepatitis research. *International journal of experimental pathology*, 87 (1), p.1–16. doi:10.1111/j.0959-9673.2006.00465.x.

Anstee, Q. M., Targher, G. and Day, C. P. (2013). Progression of NAFLD to diabetes mellitus, cardiovascular disease or cirrhosis. *Nature reviews. Gastroenterology & hepatology*, 10 (6), p.330–344. doi:10.1038/nrgastro.2013.41.

Antoniades, C. G., Berry, P. A., Wendon, J. A. and Vergani, D. (2008). The importance of immune dysfunction in determining outcome in acute liver failure. *Journal of hepatology*, 49 (5), p.845–861. doi:10.1016/j.jhep.2008.08.009.

Antoniades, C. G., Quaglia, A., Taams, L. S., Mitry, R. R., Hussain, M., Abeles, R., Possamai, L. A., Bruce, M., McPhail, M., Starling, C., Wagner, B., Barnardo, A., Pomplun, S., Auzinger, G., Bernal, W., Heaton, N., Vergani, D., Thursz, M. R. and Wendon, J. (2012). Source and characterization of hepatic macrophages in acetaminophen-induced acute liver failure in humans. *Hepatology*, 56 (2), p.735–746. doi:10.1002/hep.25657.

Apolinario, A., Majano, P. L., Alvarez-Pérez, E., Saez, A., Lozano, C., Vargas, J. and García-Monzón, C. (2002). Increased expression of T cell chemokines and their receptors in chronic hepatitis C: relationship with the histological activity of liver disease. *The American journal of gastroenterology*, 97 (11), p.2861–2870. doi:10.1111/j.1572-0241.2002.07054.x.

Arauz, J., Moreno, M., Cortés-Reynosa, P., Salazar, E. and Muriel, P. (2013). Coffee attenuates fibrosis by decreasing the expression of TGF-β and CTGF in a murine model of liver damage. *Journal of Applied Toxicology*, 33 (9), p.970–979. doi:10.1002/jat.2788.

Arreola, R., Alvarez-Herrera, S., Pérez-Sánchez, G., Becerril-Villanueva, E., Cruz-Fuentes, C., Flores-Gutierrez, E., Garcés-Alvarez, M., de la Cruz-Aguilera, D., Medina-Rivero, E., Hurtado-Alvarado, G., Quintero-Fabián, S. and Pavón, L. (2016). Immunomodulatory Effects Mediated by Dopamine. *Journal of Immunology Research*, 2016, hindawi, p.1–31. doi:10.1155/2016/3160486.

Arvilommi, A.-M., Salmi, M., Kalimo, K. and Jalkanen, S. (1996). Lymphocyte binding to vascular endothelium in inflamed skin revisited: a central role for vascular adhesion protein-1 (VAP-1). *European Journal of Immunology*, 26 (4), p.825–833. doi:10.1002/eji.1830260415.

Asma, G. E., Langlois van den Bergh, R. and Vossen, J. M. (1984). Development of pre-B and B lymphocytes in the human fetus. *Clinical and experimental immunology*, 56 (2), p.407–414.

Aspinall, A. I., Curbishley, S. M., Lalor, P. F., Weston, C. J., Blahova, M., Liaskou, E., Adams, R. M., Holt, A. P. and Adams, D. H. (2010). CX(3)CR1 and vascular adhesion protein-1-dependent recruitment of CD16(+) monocytes across human liver sinusoidal endothelium. *Hepatology*, 51 (6), p.2030–2039. doi:10.1002/hep.23591.

Ataseven, A. and Kesli, R. (2016). Novel inflammatory markers in psoriasis vulgaris: vaspin, vascular adhesion protein-1 (VAP-1), and YKL-40. *Giornale italiano di dermatologia e venereologia : organo ufficiale, Societa italiana di dermatologia e sifilografia*, 151 (3), p.244–250.

Auffray, C., Fogg, D., Garfa, M., Elain, G., Join-Lambert, O., Kayal, S., Sarnacki, S., Cumano, A., Lauvau, G. and Geissmann, F. (2007). Monitoring of blood vessels and tissues by a population of monocytes with patrolling behavior. *Science*, 317 (5838), American Association for the Advancement of Science, p.666–670. doi:10.1126/science.1142883.

Baenziger, N. L., Dalemar, L. R., Mack, P. and Haddock, R. C. (1994). Histamine degradative uptake by cultured human pulmonary vascular endothelial cells utilizes an inflammatory cell diamine oxidase. *The Journal of biological chemistry*, 269 (52), p.32858–32864.

Bai, H., Zhang, W., Qin, X.-J., Zhang, T., Wu, H., Liu, J.-Z. and Hai, C.-X. (2015). Hydrogen Peroxide Modulates the Proliferation/Quiescence Switch in the Liver During Embryonic Development and Posthepatectomy Regeneration. *Antioxidants & Redox Signaling*, 22 (11), p.921–937. doi:10.1089/ars.2014.5960.

Baiocchi, L., LeSage, G., Glaser, S. and Alpini, G. (1999). Regulation of cholangiocyte bile secretion. *Journal of hepatology*, 31 (1), p.179–191.

Bajt, M. L., Farhood, A. and Jaeschke, H. (2001). Effects of CXC chemokines on neutrophil activation and sequestration in hepatic vasculature. *American journal of physiology. Gastrointestinal and liver physiology*, 281 (5), p.G1188–95.

Baker, S., Baker, R., Liu, W., Nowak, N. and Zhu, L. (2010). Role of Alcohol Metabolism in Non-Alcoholic Steatohepatitis. *PLoS ONE*, 5 (3), p.e9570. doi:10.1371/journal.pone.0009570.

Barreiro, O., Yanez-Mo, M., Serrador, J. M., Montoya, M. C., Vicente-Manzanares, M., Tejedor, R., Furthmayr, H. and Sanchez-Madrid, F. (2002). Dynamic interaction of VCAM-1 and ICAM-1 with moesin and ezrin in a novel endothelial docking structure for adherent leukocytes. *The Journal of cell biology*, 157 (7), p.1233–1245. doi:10.1083/jcb.200112126.

Bazil, V. (1995). Physiological enzymatic cleavage of leukocyte membrane molecules. *Immunology today*, 16 (3), p.135–140.

Benedetti, A., Bassotti, C., Rapino, K., Marucci, L. and Jezequel, A. M. (1996). A morphometric study of the epithelium lining the rat intrahepatic biliary tree. *Journal of hepatology*, 24 (3), p.335–342.

Benedetti, A., Ferrali, M., Chieli, E. and Comporti, M. (1974). A study of the relationships between carbon tetrachloride-induced lipid peroxidation and liver damage in rats pretreated with vitamin E. *Chemico-biological interactions*, 9 (2), p.117–134.

Benedetti, M., Tipton, K. and Whomsley, R. (2007). Amine oxidases and monooxygenases in the in vivo metabolism of xenobiotic amines in humans: has the involvement of amine oxidases been neglected? *Fundamental & Clinical Pharmacology*, 21 (5), p.467–480. doi:10.1111/j.1472-8206.2007.00498.x.

Bengsch, B., Martin, B. and Thimme, R. (2014). Restoration of HBV-specific CD8+ T cell function

by PD-1 blockade in inactive carrier patients is linked to T cell differentiation. *Journal of hepatology*, 61 (6), p.1212–1219. doi:10.1016/j.jhep.2014.07.005.

Berg, M., Wingender, G., Djandji, D., Hegenbarth, S., Momburg, F., Hämmerling, G., Limmer, A. and Knolle, P. (2006). Cross-presentation of antigens from apoptotic tumor cells by liver sinusoidal endothelial cells leads to tumor-specific CD8+ T cell tolerance. *European journal of immunology*, 36 (11), p.2960–2970. doi:10.1002/eji.200636033.

Bernal, W. (2003). Changing patterns of causation and the use of transplantation in the United kingdom. *Seminars in liver disease*, 23 (3), p.227–237. doi:10.1055/s-2003-42640.

Bernal, W., Auzinger, G., Dhawan, A. and Wendon, J. (2010). Acute liver failure. *The Lancet*, 376 (9736), p.190–201. doi:10.1016/S0140-6736(10)60274-7.

Berruyer, C., Martin, F. M., Castellano, R., Macone, A., Malergue, F., Garrido-Urbani, S., Millet, V., Imbert, J., Duprè, S., Pitari, G., Naquet, P. and Galland, F. (2004). Vanin-1-/- mice exhibit a glutathione-mediated tissue resistance to oxidative stress. *Molecular and cellular biology*, 24 (16), p.7214–7224. doi:10.1128/MCB.24.16.7214-7224.2004.

Bertolino, P., Schrage, A., Bowen, D. G., Klugewitz, K., Ghani, S., Eulenburg, K., Holz, L., Hogg, N., McCaughan, G. W. and Hamann, A. (2005). Early intrahepatic antigen-specific retention of naïve CD8+ T cells is predominantly ICAM-1/LFA-1 dependent in mice. *Hepatology*, 42 (5), p.1063–1071. doi:10.1002/hep.20885.

Bettelli, E., Oukka, M. and Kuchroo, V. K. (2007). T(H)-17 cells in the circle of immunity and autoimmunity. *Nature immunology*, 8 (4), p.345–350. doi:10.1038/ni0407-345.

Bilzer, M. and Lauterburg, B. H. (1991). Effects of hypochlorous acid and chloramines on vascular resistance, cell integrity, and biliary glutathione disulfide in the perfused rat liver: modulation by glutathione. *Journal of hepatology*, 13 (1), p.84–89.

Bilzer, M., Roggel, F. and Gerbes, A. L. (2006). Role of Kupffer cells in host defense and liver disease. *Liver international : official journal of the International Association for the Study of the Liver*, 26 (10), p.1175–1186. doi:10.1111/j.1478-3231.2006.01342.x.

Blachier, M., Leleu, H., Peck-Radosavljevic, M., Valla, D.-C. C. and Roudot-Thoraval, F. (2013). The burden of liver disease in Europe: a review of available epidemiological data. *Journal of hepatology*, 58 (3), p.593–608. doi:10.1016/j.jhep.2012.12.005.

Blomhoff, R., Green, M. H. and Norum, K. R. (1992). Vitamin A: physiological and biochemical processing. *Annual review of nutrition*, 12, p.37–57. doi:10.1146/annurev.nu.12.070192.000345.

Boettler, T., Spangenberg, H. C., Neumann-Haefelin, C., Panther, E., Urbani, S., Ferrari, C., Blum, H. E., von Weizsäcker, F. and Thimme, R. (2005). T cells with a CD4+CD25+ regulatory phenotype suppress in vitro proliferation of virus-specific CD8+ T cells during chronic hepatitis C virus infection. *Journal of virology*, 79 (12), p.7860–7867. doi:10.1128/JVI.79.12.7860-7867.2005.

Boll, M., Weber, L. W., Becker, E. and Stampfl, A. (2001). Mechanism of carbon tetrachloride-induced hepatotoxicity. Hepatocellular damage by reactive carbon tetrachloride metabolites. *Zeitschrift fur Naturforschung. C, Journal of biosciences*, 56 (7-8), p.649–659.

Bonder, C., Norman, U., Swain, M., Zbytnuik, L., Yamanouchi, J., Santamaria, P., Ajuebor, M., Salmi, M., Jalkanen, S. and Kubes, P. (2005). Rules of Recruitment for Th1 and Th2 Lymphocytes in Inflamed Liver: A Role for Alpha-4 Integrin and Vascular Adhesion Protein-1. *Immunity*, 23 (2), p.153–163. doi:10.1016/j.immuni.2005.06.007.

Boomsma, F and van Veldhuisen, DJ. (1997). Plasma semicarbazide-sensitive amine oxidase is elevated in patients with congestive heart failure. *Cardiovascular ….* doi:10.1016/S0008-6363(96)00209-X.

Bouin, A.-P., Grandvaux, N., Vignais, P. and Fuchs, A. (1998). p40 phox Is Phosphorylated on

Threonine 154 and Serine 315 during Activation of the Phagocyte NADPH Oxidase implication of a protein kinase c-type kinase in the phosphorylation process. *Journal of Biological Chemistry*, 273 (46), p.30097–30103. doi:10.1074/jbc.273.46.30097.

Boujedidi, H., Bouchet-Delbos, L., Cassard-Doulcier, A., Njiké-Nakseu, M., Maitre, S., Prévot, S., Dagher, I., Agostini, H., Voican, C., Emilie, D., Perlemuter, G. and Naveau, S. (2012). Housekeeping Gene Variability in the Liver of Alcoholic Patients. *Alcoholism: Clinical and Experimental Research*, 36 (2), p.258–266. doi:10.1111/j.1530-0277.2011.01627.x.

Bour, S., Caspar-Bauguil, S., Iffiú-Soltész, Z., Nibbelink, M., Cousin, B., Miiluniemi, M., Salmi, M., Stolen, C., Jalkanen, S., Casteilla, L., Pénicaud, L., Valet, P. and Carpéné, C. (2009). Semicarbazide-sensitive amine oxidase/vascular adhesion protein-1 deficiency reduces leukocyte infiltration into adipose tissue and favors fat deposition. *The American journal of pathology*, 174 (3), p.1075–1083. doi:10.2353/ajpath.2009.080612.

Bowen, D. G., McCaughan, G. W. and Bertolino, P. (2005). Intrahepatic immunity: a tale of two sites? *Trends in immunology*, 26 (10), p.512–517. doi:10.1016/j.it.2005.08.005.

Bower, W. A., Johns, M., Margolis, H. S., Williams, I. T. and Bell, B. P. (2007). Population-based surveillance for acute liver failure. *The American journal of gastroenterology*, 102 (11), p.2459–2463. doi:10.1111/j.1572-0241.2007.01388.x.

Braet, F. and Wisse, E. (2002). Structural and functional aspects of liver sinusoidal endothelial cell fenestrae: a review. *Comparative hepatology*, 1 (1), p.1. doi:10.1186/1476-5926-1-1.

Brinkmann, V., Reichard, U., Goosmann, C., Fauler, B., Uhlemann, Y., Weiss, D. S., Weinrauch, Y. and Zychlinsky, A. (2004). Neutrophil extracellular traps kill bacteria. *Science (New York, N.Y.)*, 303 (5663), p.1532–1535. doi:10.1126/science.1092385.

Bronte, V., Brandau, S., Chen, S.-H., Colombo, M., Frey, A., Greten, T., Mandruzzato, S., Murray, P., Ochoa, A., Ostrand-Rosenberg, S., Rodriguez, P., Sica, A., Umansky, V., Vonderheide, R. and Gabrilovich, D. (2016). Recommendations for myeloid-derived suppressor cell nomenclature and characterization standards. *Nature Communications*, 7, p.12150. doi:10.1038/ncomms12150.

Brunner, D., Frank, J., Appl, H., Schöffl, H., Pfaller, W. and Gstraunthaler, G. (2010). Serum-free cell culture: the serum-free media interactive online database. *ALTEX*, 27 (1), p.53–62.

Buffoni, F., Banchelli, G., Ignesti, G., Pirisino, R. and Raimondi, L. (1983). The presence of an inhibitor of benzylamine oxidase in human blood plasma. *Biochemical Journal*, 211 (3), Portland Press Limited, p.767–769.

Bukowski, J., Morita, C. and Brenner, M. (1999). Human γδ T Cells Recognize Alkylamines Derived from Microbes, Edible Plants, and Tea. *Immunity*, 11 (1), p.57–65. doi:10.1016/S1074-7613(00)80081-3.

Bull-Otterson, L., Feng, W., Kirpich, I., Wang, Y., Qin, X., Liu, Y., Gobejishvili, L., Joshi-Barve, S., Ayvaz, T. and Petrosino, J. (2013). Metagenomic analyses of alcohol induced pathogenic alterations in the intestinal microbiome and the effect of Lactobacillus rhamnosus GG treatment. *PloS one*, 8 (1), Public Library of Science, p.e53028. doi:10.1371/journal.pone.0053028.

Butcher, E. C. (1991). Leukocyte-endothelial cell recognition: three (or more) steps to specificity and diversity. *Cell*, 67 (6), p.1033–1036.

Butera, D., Marukian, S., Iwamaye, A. E., Hembrador, E., Chambers, T. J., Di Bisceglie, A. M., Charles, E. D., Talal, A. H., Jacobson, I. M., Rice, C. M. and Dustin, L. B. (2005). Plasma chemokine levels correlate with the outcome of antiviral therapy in patients with hepatitis C. *Blood*, 106 (4), p.1175–1182. doi:10.1182/blood-2005-01-0126.

Cadden, I. S., Partovi, N. and Yoshida, E. M. (2007). Review article: possible beneficial effects of coffee on liver disease and function. *Alimentary pharmacology & therapeutics*, 26 (1), p.1–8.

doi:10.1111/j.1365-2036.2007.03319.x.

Carman, C. V., Sage, P. T., Sciuto, T. E., de la Fuente, M. A., Geha, R. S., Ochs, H. D., Dvorak, H. F., Dvorak, A. M. and Springer, T. A. (2007). Transcellular diapedesis is initiated by invasive podosomes. *Immunity*, 26 (6), p.784–797. doi:10.1016/j.immuni.2007.04.015.

Carman, C. V. and Springer, T. A. (2004). A transmigratory cup in leukocyte diapedesis both through individual vascular endothelial cells and between them. *The Journal of cell biology*, 167 (2), p.377–388. doi:10.1083/jcb.200404129.

Carpéné, C., Hasnaoui, M., Balogh, B., Matyus, P., Fernández-Quintela, A., Rodríguez, V., Mercader, J. and Portillo, M. (2016). Dietary Phenolic Compounds Interfere with the Fate of Hydrogen Peroxide in Human Adipose Tissue but Do Not Directly Inhibit Primary Amine Oxidase Activity. *Oxidative Medicine and Cellular Longevity*, 2016, hindawi, p.1–15. doi:10.1155/2016/2427618.

Castagna, M., Takai, Y., Kaibuchi, K., Sano, K., Kikkawa, U. and Nishizuka, Y. (1982). Direct activation of calcium-activated, phospholipid-dependent protein kinase by tumor-promoting phorbol esters. *The Journal of biological chemistry*, 257 (13), p.7847–7851.

Cattaneo, M. (2004). Aspirin and Clopidogrel. *Arteriosclerosis, Thrombosis, and Vascular Biology*, 24 (11), p.1980–1987. doi:10.1161/01.ATV.0000145980.39477.a9.

Chan, J. R., Hyduk, S. J. and Cybulsky, M. I. (2001). Chemoattractants induce a rapid and transient upregulation of monocyte alpha4 integrin affinity for vascular cell adhesion molecule 1 which mediates arrest: an early step in the process of emigration. *The Journal of experimental medicine*, 193 (10), p.1149–1158.

Charlton, M, Krishnan, A and Viker, K. (2011). Fast food diet mouse: novel small animal model of NASH with ballooning, progressive fibrosis, and high physiological fidelity to the human condition. *American Journal of ….* doi:10.1152/ajpgi.00145.2011.

Che, B., Wang, L., Zhang, Z., Zhang, Y. and Deng, Y. (2012). Distribution and accumulation of caffeine in rat tissues and its inhibition on semicarbazide-sensitive amine oxidase. *NeuroToxicology*, 33 (5), p.1248–1253. doi:10.1016/j.neuro.2012.07.004.

Chen, J., Xi, J., Tian, Y., Bova, G. S. and Zhang, H. (2013). Identification, prioritization, and evaluation of glycoproteins for aggressive prostate cancer using quantitative glycoproteomics and antibody-based assays on tissue specimens. *Proteomics*, 13 (15), p.2268–2277. doi:10.1002/pmic.201200541.

Chen, M., Tabaczewski, P., Truscott, S. M., Van Kaer, L. and Stroynowski, I. (2005). Hepatocytes express abundant surface class I MHC and efficiently use transporter associated with antigen processing, tapasin, and low molecular weight polypeptide proteasome subunit components of antigen processing and presentation pathway. *Journal of immunology*, 175 (2), p.1047–1055.

Chessa, T., Anderson, K., Hu, Y., Xu, Q., Rausch, O., Stephens, L. and Hawkins, P. (2010). Phosphorylation of threonine 154 in p40phox is an important physiological signal for activation of the neutrophil NADPH oxidase. *Blood*, 116 (26), p.6027–6036. doi:10.1182/blood-2010-08-300889.

Chou, H.-S., Hsieh, C.-C., Yang, H.-R., Wang, L., Arakawa, Y., Brown, K., Wu, Q., Lin, F., Peters, M., Fung, J., Lu, L. and Qian, S. (2011). Hepatic stellate cells regulate immune response by way of induction of myeloid suppressor cells in mice. *Hepatology*, 53 (3), p.1007–1019. doi:10.1002/hep.24162.

Christen, U. and von Herrath, M. G. (2004). Induction, acceleration or prevention of autoimmunity by molecular mimicry. *Molecular immunology*, 40 (14-15), p.1113–1120. doi:10.1016/j.molimm.2003.11.014.

Chuang, Y.-H., Lan, R. and Gershwin, E. (2009). The immunopathology of human biliary cell

epithelium. *Seminars in Immunopathology*, 31 (3), springer, p.323–331. doi:10.1007/s00281-009-0172-5.

Claassen, M. A. A., de Knegt, R. J., Tilanus, H. W., Janssen, H. L. and Boonstra, A. (2010). Abundant numbers of regulatory T cells localize to the liver of chronic hepatitis C infected patients and limit the extent of fibrosis. *Journal of hepatology*, 52 (3), p.315–321. doi:10.1016/j.jhep.2009.12.013.

Clapperton, M., Rolando, N., Sandoval, L., Davies, E. and Willia, R. (1997). Neutrophil superoxide and hydrogen peroxide production in patients with acute liver failure. *European Journal of Clinical Investigation*, 27 (2), European Journal of Clinical Investigation, p.164–168. doi:10.1046/j.1365-2362.1997.920640.x.

Clark, S. R., Ma, A. C., Tavener, S. A., McDonald, B., Goodarzi, Z., Kelly, M. M., Patel, K. D., Chakrabarti, S., McAvoy, E., Sinclair, G. D., Keys, E. M., Allen-Vercoe, E., Devinney, R., Doig, C. J., Green, F. H. and Kubes, P. (2007). Platelet TLR4 activates neutrophil extracellular traps to ensnare bacteria in septic blood. *Nature medicine*, 13 (4), p.463–469. doi:10.1038/nm1565.

Collier, S. D. and Pruett, S. B. (2000). Mechanisms of suppression of poly I:C-induced activation of NK cells by ethanol. *Alcohol (Fayetteville, N.Y.)*, 21 (1), p.87–95.

Conklin, D. J., Langford, S. D. and Boor, P. J. (1998). Contribution of serum and cellular semicarbazide-sensitive amine oxidase to amine metabolism and cardiovascular toxicity. *Toxicological sciences : an official journal of the Society of Toxicology*, 46 (2), p.386–392. doi:10.1006/toxs.1998.2528.

Conklin, D., Prough, R., Juvan, P., Rezen, T., Rozman, D., Haberzettl, P., Srivastava, S. and Bhatnagar, A. (2011). Acrolein-induced dyslipidemia and acute-phase response are independent of HMG-CoA reductase. *Molecular Nutrition & Food Research*, 55 (9), p.1411–1422. doi:10.1002/mnfr.201100225.

Constantin, G., Majeed, M., Giagulli, C., Piccio, L., Kim, J. Y., Butcher, E. C. and Laudanna, C. (2000). Chemokines trigger immediate beta2 integrin affinity and mobility changes: differential regulation and roles in lymphocyte arrest under flow. *Immunity*, 13 (6), p.759–769.

Cover, C., Liu, J., Farhood, A., Malle, E., Waalkes, M. P., Bajt, M. L. and Jaeschke, H. (2006). Pathophysiological role of the acute inflammatory response during acetaminophen hepatotoxicity. *Toxicology and applied pharmacology*, 216 (1), p.98–107. doi:10.1016/j.taap.2006.04.010.

Cripps, J., Wang, J., Maria, A., Blumenthal, I. and Gorham, J. (2010). Type 1 T Helper Cells Induce the Accumulation of Myeloid-Derived Suppressor Cells in the Inflamed Tgfb1 Knockout Mouse Liver. *Hepatology*, 52 (4), p.1350–1359. doi:10.1002/hep.23841.

Crispe, I. N. (2009). The liver as a lymphoid organ. *Annual review of immunology*, 27, p.147–163. doi:10.1146/annurev.immunol.021908.132629.

Croner, R., Hoerer, E., Kulu, Y., Hackert, T., Gebhard, M.-M., Herfarth, C. and Klar, E. (2006). Hepatic platelet and leukocyte adherence during endotoxemia. *Critical Care*, 10 (1), p.R15. doi:10.1186/cc3968.

Curbishley, S., Eksteen, B., Gladue, R., Lalor, P. and Adams, D. (2005). CXCR3 Activation Promotes Lymphocyte Transendothelial Migration across Human Hepatic Endothelium under Fluid Flow. *The American Journal of Pathology*, 167 (3), p.887–899. doi:10.1016/S0002-9440(10)62060-3.

Curzio, M, Esterbauer, H and Dianzani, MU. (1984). Chemotactic activity of hydroxyalkenals on rat neutrophils. *International journal of tissue reactivity,* 7 (2), p. 137-142.

D'Ambrosio, D., Albanesi, C., Lang, R., Girolomoni, G., Sinigaglia, F. and Laudanna, C. (2002).

Quantitative differences in chemokine receptor engagement generate diversity in integrin-dependent lymphocyte adhesion. *Journal of immunology,*169 (5), p.2303–2312.

Daoust, R. and Cantero, A. (1959). The numerical proportions of cell types in rat liver during carcinogenesis by 4-dimethylaminoazobenzene (DAB). *Cancer research*, 19, Cancer research, p.757–762.

Davì, G and Patrono, C. (2007). Platelet activation and atherothrombosis. *New England Journal of Medicine*. doi:10.1056/NEJMra071014.

Deaciuc, I. V., Fortunato, F., D'Souza, N. B., Hill, D. B., Schmidt, J., Lee, E. Y. and McClain, C. J. (1999). Modulation of caspase-3 activity and Fas ligand mRNA expression in rat liver cells in vivo by alcohol and lipopolysaccharide. *Alcoholism, clinical and experimental research*, 23 (2), p.349–356.

Dejana, E. (2004). Endothelial cell–cell junctions: happy together. *Nature reviews Molecular cell biology*. doi:10.1038/nrm1357.

DeJarnett, Conklin, Riggs, Myers, O'Toole, Hamzeh, Wagner, Chugh, Ramos, Srivastava, Higdon, Tollerud, DeFilippis, Becher, Wyatt, McCracken, Abplanalp, Rai, Ciszewski, Xie, Yeager, Prabhu and Bhatnagar. (2014). Acrolein Exposure Is Associated With Increased Cardiovascular Disease Risk. *Journal of the American Heart Association*, 3 (4), p.e000934–e000934. doi:10.1161/JAHA.114.000934.

Diacovo, T. G., Puri, K. D., Warnock, R. A., Springer, T. A. and von Andrian, U. H. (1996). Platelet-mediated lymphocyte delivery to high endothelial venules. *Science (New York, N.Y.)*, 273 (5272), p.252–255.

Diehl, L., Schurich, A., Grochtmann, R., Hegenbarth, S., Chen, L. and Knolle, P. A. (2008). Tolerogenic maturation of liver sinusoidal endothelial cells promotes B7-homolog 1-dependent CD8+ T cell tolerance. *Hepatology,* 47 (1), p.296–305. doi:10.1002/hep.21965.

Dini, L. and Carla, E. C. (1998). Hepatic sinusoidal endothelium heterogeneity with respect to the recognition of apoptotic cells. *Experimental cell research*, 240 (2), p.388–393.

Doherty, D. G. and O'Farrelly, C. (2000). Innate and adaptive lymphoid cells in the human liver. *Immunological reviews*, 174, p.5–20.

Dominguez, M, Miquel, R, Colmenero, J and Moreno, M. (2009). Hepatic expression of CXC chemokines predicts portal hypertension and survival in patients with alcoholic hepatitis. *Gastroenterology*. 136 (5), p. 1639-1650.

Donaghy, L., Barry, F. J., Hunter, J. G., Stableforth, W., Murray, I. A., Palmer, J., Bendall, R. P., Elsharkawy, A. M. and Dalton, H. R. (2013). Clinical and laboratory features and natural history of seronegative hepatitis in a nontransplant centre. *European journal of gastroenterology & hepatology*, 25 (10), p.1159–1164. doi:10.1097/MEG.0b013e3283610484.

Dong, Z.-J. J., Wei, H.-M. M., Sun, R., Tian, Z.-G. G. and Gao, B. (2004). Isolation of murine hepatic lymphocytes using mechanical dissection for phenotypic and functional analysis of NK1.1+ cells. *World journal of gastroenterology*, 10 (13), p.1928–1933. doi:10.3748/wjg.v10.i13.1928.

Douda, D., Khan, M., Grasemann, H. and Palaniyar, N. (2015). SK3 channel and mitochondrial ROS mediate NADPH oxidase-independent NETosis induced by calcium influx. *Proceedings of the National Academy of Sciences*, 112 (9), p.2817–2822. doi:10.1073/pnas.1414055112.

Dumitru, C., Moses, K., Trellakis, S., Lang, S. and Brandau, S. (2012). Neutrophils and granulocytic myeloid-derived suppressor cells: immunophenotyping, cell biology and clinical relevance in human oncology. *Cancer Immunology, Immunotherapy*, 61 (8), p.1155–1167. doi:10.1007/s00262-012-1294-5.

Dunn, C., Peppa, D., Khanna, P., Nebbia, G., Jones, M., Brendish, N., Lascar, R. M., Brown, D., Gilson, R. J., Tedder, R. J., Dusheiko, G. M., Jacobs, M., Klenerman, P. and Maini, M. K.

(2009). Temporal analysis of early immune responses in patients with acute hepatitis B virus infection. *Gastroenterology*, 137 (4), p.1289–1300. doi:10.1053/j.gastro.2009.06.054.

Ebe, Y., Hasegawa, G., Takatsuka, H., Umezu, H., Mitsuyama, M., Arakawa, M., Mukaida, N. and Naito, M. (1999). The role of Kupffer cells and regulation of neutrophil migration into the liver by macrophage inflammatory protein-2 in primary listeriosis in mice. *Pathology international*, 49 (6), p.519–532.

Edwards, S., Lalor, P., Nash, G., Rainger and Adams, D. (2005). Lymphocyte traffic through sinusoidal endothelial cells is regulated by hepatocytes. *Hepatology,* 41 (3), p.451–459. doi:10.1002/hep.20585.

Ehlers, R., Ustinov, V., Chen, Z., Zhang, X., Rao, R., Luscinskas, F. W., Lopez, J., Plow, E. and Simon, D. I. (2003). Targeting platelet-leukocyte interactions: identification of the integrin Mac-1 binding site for the platelet counter receptor glycoprotein Ibalpha. *The Journal of experimental medicine*, 198 (7), p.1077–1088. doi:10.1084/jem.20022181.

Ekblom, J, Grönvall, JL and Garpenstrand, H. (1999). Is semicarbazide-sensitive amine oxidase in blood plasma partly derived from the skeleton? *Neurobiology (Bp),* 8 (2), p. 129-135.

El Hadri, K., Moldes, M., Mercier, N., Andreani, M., Pairault, J. and Feve, B. (2002). Semicarbazide-sensitive amine oxidase in vascular smooth muscle cells: differentiation-dependent expression and role in glucose uptake. *Arteriosclerosis, thrombosis, and vascular biology*, 22 (1), p.89–94. doi:10.1161/hq0102.101550.

Elliott, J., Fowden, A. L., Callingham, B. A., Sharman, D. F. and Silver, M. (1991). Physiological and pathological influences on sheep blood plasma amine oxidase: effect of pregnancy and experimental alloxan-induced diabetes mellitus. *Research in veterinary science*, 50 (3), p.334–339.

Elovaara, H., Parkash, V., Fair-Mäkelä, R., Salo-Ahen, O., Guédez, G., Bligt-Lindén, E., Grönholm, J., Jalkanen, S. and Salminen, T. (2016). Multivalent Interactions of Human Primary Amine Oxidase with the V and C22 Domains of Sialic Acid-Binding Immunoglobulin-Like Lectin-9 Regulate Its Binding and Amine Oxidase Activity. *PLOS ONE*, 11 (11), plos, p.e0166935. doi:10.1371/journal.pone.0166935.

Elvevold, K. H., Nedredal, G. I., Revhaug, A. and Smedsrød, B. (2004). Scavenger properties of cultivated pig liver endothelial cells. *Comparative hepatology*, 3 (1), p.4. doi:10.1186/1476-5926-3-4.

Emoto, M, Mittrücker, HW and Schmits, R. (1999). Critical role of leukocyte function-associated antigen-1 in liver accumulation of CD4+ NKT cells. *The Journal of Immunology,* 162 (9), p. 5094-5098.

Engel, D. R., Maurer, J., Tittel, A. P. P., Weisheit, C., Cavlar, T., Schumak, B., Limmer, A., van Rooijen, N., Trautwein, C., Tacke, F. and Kurts, C. (2008). CCR2 mediates homeostatic and inflammatory release of Gr1(high) monocytes from the bone marrow, but is dispensable for bladder infiltration in bacterial urinary tract infection. *Journal of immunology,* 181 (8), p.5579–5586.

Enrique-Tarancón, G., Castan, I., Morin, N., Marti, L., Abella, A., Camps, M., Casamitjana, R., Palacín, M., Testar, X., Degerman, E., Carpéné, C. and Zorzano, A. (2000). Substrates of semicarbazide-sensitive amine oxidase co-operate with vanadate to stimulate tyrosine phosphorylation of insulin-receptor-substrate proteins, phosphoinositide 3-kinase activity and GLUT4 translocation in adipose cells. *The Biochemical journal*, 350 Pt 1, p.171–180.

Enrique-Tarancón, G., Marti, L., Morin, N., Lizcano, J., Unzeta, M., Sevilla, L., Camps, M., Palacín, M., Testar, X., Carpéné, C. and Zorzano, A. (1998). Role of Semicarbazide-sensitive Amine Oxidase on Glucose Transport and GLUT4 Recruitment to the Cell Surface in Adipose Cells. *Journal of Biological Chemistry*, 273 (14), p.8025–8032. doi:10.1074/jbc.273.14.8025.

Epelman, S., Lavine, K. J. and Randolph, G. J. (2014). Origin and functions of tissue

macrophages. *Immunity*, 41 (1), p.21–35. doi:10.1016/j.immuni.2014.06.013.

Eriksson, E. E., Xie, X., Werr, J., Thoren, P. and Lindbom, L. (2001). Importance of primary capture and L-selectin-dependent secondary capture in leukocyte accumulation in inflammation and atherosclerosis in vivo. *The Journal of experimental medicine*, 194 (2), p.205–218.

Faouzi, S., Burckhardt, B. E., Hanson, J. C., Campe, C. B., Schrum, L. W., Rippe, R. A. and Maher, J. J. (2001). Anti-Fas induces hepatic chemokines and promotes inflammation by an NF-kappa B-independent, caspase-3-dependent pathway. *The Journal of biological chemistry*, 276 (52), p.49077–49082. doi:10.1074/jbc.M109791200.

Faurschou, M. and Borregaard, N. (2003). Neutrophil granules and secretory vesicles in inflammation. *Microbes and Infection*, 5 (14), p.1317–1327. doi:10.1016/j.micinf.2003.09.008.

Fava, G., Glaser, S., Francis, H. and Alpini, G. (2005). The Immunophysiology of Biliary Epithelium. *Seminars in Liver Disease*, 25 (03), thieme, p.251–264. doi:10.1055/s-2005-916318.

Feld, J., Lavoie, É., Michel, F. and Dranoff, J. (2015). I drink for my liver, Doc: emerging evidence that coffee prevents cirrhosis. *F1000Research*, 4, pmc, p.95. doi:10.12688/f1000research.6368.2.

Ferjančič, Š., Gil-Bernabé, A., Hill, S., Allen, P., Richardson, P., Sparey, T., Savory, E., McGuffog, J. and Muschel, R. (2013). VCAM-1 and VAP-1 recruit myeloid cells that promote pulmonary metastasis in mice. *Blood*, 121 (16), p.3289–3297. doi:10.1182/blood-2012-08-449819.

Ferri, S., Longhi, M. S., De Molo, C., Lalanne, C., Muratori, P., Granito, A., Hussain, M. J., Ma, Y., Lenzi, M., Mieli-Vergani, G., Bianchi, F. B., Vergani, D. and Muratori, L. (2010). A multifaceted imbalance of T cells with regulatory function characterizes type 1 autoimmune hepatitis. *Hepatology,* 52 (3), p.999–1007. doi:10.1002/hep.23792.

Filip, A., Pinzano, A., Bianchi, A., Fève, B., Jalkanen, S., Gillet, P., Mainard, D., Lacolley, P., Magdalou, J. and Mercier, N. (2016). Expression of the semicarbazide-sensitive amine oxidase in articular cartilage: its role in terminal differentiation of chondrocytes in rat and human. *Osteoarthritis and cartilage*, 24 (7), p.1223–1234. doi:10.1016/j.joca.2016.01.340.

Finger, E., Purl, K., Alon, R., Lawrence, M., von Andrian, U. and Springer, T. (1996). Adhesion through L-selectin requires a threshold hydrodynamic shear. *Nature*, 379 (6562), nature, p.266–269. doi:10.1038/379266a0.

Fisher, J. E., McKenzie, T. J., Lillegard, J. B., Yu, Y., Juskewitch, J. E., Nedredal, G. I., Brunn, G. J., Yi, E. S., Malhi, H., Smyrk, T. C. and Nyberg, S. L. (2013). Role of Kupffer cells and toll-like receptor 4 in acetaminophen-induced acute liver failure. *The Journal of surgical research*, 180 (1), p.147–155. doi:10.1016/j.jss.2012.11.051.

Fontana, E., Boucher, J., Marti, L., Lizcano, J. M., Testar, X., Zorzano, A. and Carpéné, C. (2001). Amine oxidase substrates mimic several of the insulin effects on adipocyte differentiation in 3T3 F442A cells. *The Biochemical journal*, 356 (Pt 3), p.769–777.

Foot, J., Yow, T., Schilter, H., Buson, A., Deodhar, M., Findlay, A., Guo, L., McDonald, I., Turner, C., Zhou, W. and Jarolimek, W. (2013). PXS-4681A, a Potent and Selective Mechanism-Based Inhibitor of SSAO/VAP-1 with Anti-Inflammatory Effects In Vivo. *Journal of Pharmacology and Experimental Therapeutics*, 347 (2), p.365–374. doi:10.1124/jpet.113.207613.

Forman, H., Maiorino, M. and Ursini, F. (2010). Signaling Functions of Reactive Oxygen Species. *Biochemistry*, 49 (5), p.835–842. doi:10.1021/bi9020378.

Fox-Robichaud, A. and Kubes, P. (2000). Molecular mechanisms of tumor necrosis factor alpha-stimulated leukocyte recruitment into the murine hepatic circulation. *Hepatology*, 31 (5), p.1123–1127. doi:10.1053/he.2000.6961.

Francis, H., Glaser, S., DeMorrow, S., Gaudio, E., Ueno, Y., Venter, J., Dostal, D., Onori, P.,

Franchitto, A., Marzioni, M., Vaculin, S., Vaculin, B., Katki, K., Stutes, M., Savage, J. and Alpini, G. (2008). Small mouse cholangiocytes proliferate in response to H1 histamine receptor stimulation by activation of the IP3/CaMK I/CREB pathway. *American Journal of Physiology - Cell Physiology*, 295 (2), p.C499–C513. doi:10.1152/ajpcell.00369.2007.

Franco, A., Barnaba, V., Natali, P., Balsano, C., Musca, A. and Balsano, F. (1988). Expression of class I and class II major histocompatibility complex antigens on human hepatocytes. *Hepatology*, 8 (3), p.449–454.

Franco, R., Schoneveld, O. J., Pappa, A. and Panayiotidis, M. I. (2007). The central role of glutathione in the pathophysiology of human diseases. *Archives of physiology and biochemistry*, 113 (4-5), p.234–258. doi:10.1080/13813450701661198.

Friedman, S. L. (2008). Hepatic stellate cells: protean, multifunctional, and enigmatic cells of the liver. *Physiological reviews*, 88 (1), p.125–172. doi:10.1152/physrev.00013.2007.

Fuchs, T., Abed, U., Goosmann, C., Hurwitz, R., Schulze, I., Wahn, V., Weinrauch, Y., Brinkmann, V. and Zychlinsky, A. (2007). Novel cell death program leads to neutrophil extracellular traps. *The Journal of Cell Biology*, 176 (2), p.231–241. doi:10.1083/jcb.200606027.

Furman, M. I., Benoit, S. E., Barnard, M. R., Valeri, C. R., Borbone, M. L., Becker, R. C., Hechtman, H. B. and Michelson, A. D. (1998). Increased platelet reactivity and circulating monocyte-platelet aggregates in patients with stable coronary artery disease. *Journal of the American College of Cardiology*, 31 (2), p.352–358.

Gale, R. P., Sparkes, R. S. and Golde, D. W. (1978). Bone marrow origin of hepatic macrophages (Kupffer cells) in humans. *Science (New York, N.Y.)*, 201 (4359), p.937–938.

Gao, D, Wei, C, Chen, L and Huang, J. (2004). Oxidative DNA damage and DNA repair enzyme expression are inversely related in murine models of fatty liver disease. *American Journal of Physiology - Gastrointestinal and Liver Physiology,* 287 (5), G1070-1077.

Gao, B. and Bataller, R. (2011). Alcoholic liver disease: pathogenesis and new therapeutic targets. *Gastroenterology*, 141 (5), p.1572–1585. doi:10.1053/j.gastro.2011.09.002.

Gao, B., Jeong, W.-I. I. and Tian, Z. (2008). Liver: An organ with predominant innate immunity. *Hepatology*, 47 (2), p.729–736. doi:10.1002/hep.22034.

García-Vicente, S., Abella, A., Viguerie, N., Ros-Baró, A., Camps, M., Testar, X., Palacín, M., Zorzano, A. and Marti, L. (2005). The release of soluble VAP-1/SSAO by 3T3-L1 adipocytes is stimulated by isoproterenol and low concentrations of TNFalpha. *Journal of physiology and biochemistry*, 61 (2), p.395–401.

Garetto, S., Trovato, A. E., Lleo, A., Sala, F., Martini, E., Betz, A. G., Norata, G. D., Invernizzi, P. and Kallikourdis, M. (2015). Peak inflammation in atherosclerosis, primary biliary cirrhosis and autoimmune arthritis is counter-intuitively associated with regulatory T cell enrichment. *Immunobiology*, 220 (8), p.1025–1029. doi:10.1016/j.imbio.2015.02.006.

Garpenstrand, H, Bergqvist, M, Brattström, D and Larsson, A. (2004). Serum semicarbazide-sensitive amine oxidase (SSAO) activity correlates with VEGF in non-small-cell lung cancer patients. *Medical Oncology*. http://link.springer.com/article/10.1385/MO:21:3:241.

Garpenstrand, H., Ekblom, J., Bäcklund, L. B., Oreland, L. and Rosenqvist, U. (1999). Elevated plasma semicarbazide-sensitive amine oxidase (SSAO) activity in Type 2 diabetes mellitus complicated by retinopathy. *Diabetic medicine : a journal of the British Diabetic Association*, 16 (6), p.514–521.

Gebhardt, R. (2014). Liver zonation: Novel aspects of its regulation and its impact on homeostasis. *World Journal of Gastroenterology*, 20 (26), pmc, p.8491. doi:10.3748/wjg.v20.i26.8491.

Geissmann, F., Cameron, T. O., Sidobre, S., Manlongat, N., Kronenberg, M., Briskin, M. J., Dustin, M. L. and Littman, D. R. (2005). Intravascular immune surveillance by CXCR6+ NKT cells patrolling liver sinusoids. *PLoS biology*, 3 (4), p.e113.

doi:10.1371/journal.pbio.0030113.

Germani, G., Theocharidou, E., Adam, R., Karam, V., Wendon, J., O'Grady, J., Burra, P., Senzolo, M., Mirza, D., Castaing, D., Klempnauer, J., Pollard, S., Paul, A., Belghiti, J., Tsochatzis, E. and Burroughs, A. (2012). Liver transplantation for acute liver failure in Europe: Outcomes over 20years from the ELTR database. *Journal of Hepatology*, 57 (2), p.288–296. doi:10.1016/j.jhep.2012.03.017.

Ghenghesh, KS and Drucker, DB. (1988). Gas liquid chromatography of amines produced by the Enterobacteriaceae. *Brazilian journal of medical and Biological Research,* 22 (6), p.653-665.

Giagulli, C., Ottoboni, L., Caveggion, E., Rossi, B., Lowell, C., Constantin, G., Laudanna, C. and Berton, G. (2006). The Src family kinases Hck and Fgr are dispensable for inside-out, chemoattractant-induced signaling regulating beta 2 integrin affinity and valency in neutrophils, but are required for beta 2 integrin-mediated outside-in signaling involved in sustained adhesion. *Journal of immunology*, 177 (1), p.604–611.

Giagulli, C., Scarpini, E., Ottoboni, L., Narumiya, S., Butcher, E. C., Constantin, G. and Laudanna, C. (2004). RhoA and zeta PKC control distinct modalities of LFA-1 activation by chemokines: critical role of LFA-1 affinity triggering in lymphocyte in vivo homing. *Immunity*, 20 (1), p.25–35.

Golden-Mason, L., Palmer, B., Klarquist, J., Mengshol, J. A., Castelblanco, N. and Rosen, H. R. (2007). Upregulation of PD-1 expression on circulating and intrahepatic hepatitis C virus-specific CD8+ T cells associated with reversible immune dysfunction. *Journal of virology*, 81 (17), p.9249–9258. doi:10.1128/JVI.00409-07.

Grant, A. J., Lalor, P. F., Hübscher, S. G., Briskin, M. and Adams, D. H. (2001). MAdCAM-1 expressed in chronic inflammatory liver disease supports mucosal lymphocyte adhesion to hepatic endothelium (MAdCAM-1 in chronic inflammatory liver disease). *Hepatology*, 33 (5), p.1065–1072. doi:10.1053/jhep.2001.24231.

Green, S., Smith, M., Hasley, R., Stephany, D., Harned, A., Nagashima, K., Abdullah, S., Pittaluga, S., Imamichi, T., Qin, J., Rupert, A., Ober, A., Lane, C. and Catalfamo, M. (2015). Activated platelet–T-cell conjugates in peripheral blood of patients with HIV infection. *AIDS*, 29 (11), p.1297–1308. doi:10.1097/QAD.0000000000000701.

Gregory, S. H., Cousens, L. P., van Rooijen, N., Döpp, E. A., Carlos, T. M. and Wing, E. J. (2002). Complementary adhesion molecules promote neutrophil-Kupffer cell interaction and the elimination of bacteria taken up by the liver. *Journal of immunology*, 168 (1), p.308–315.

Gubisne-Haberle. (2004). Protein Cross-Linkage Induced by Formaldehyde Derived from Semicarbazide-Sensitive Amine Oxidase-Mediated Deamination of Methylamine. *Journal of Pharmacology and Experimental Therapeutics*, 310 (3), p.1125–1132. doi:10.1124/jpet.104.068601.

Guidotti, LG, Inverso, D, Sironi, L, Lucia, D. P. and Fioravanti, J. (2015). Immunosurveillance of the liver by intravascular effector CD8+ T cells. *Cell*, 161 (3), p.486-500. doi:10.1016/j.cell.2015.03.005.

Gujral, J. S., Hinson, J. A., Farhood, A. and Jaeschke, H. (2004). NADPH oxidase-derived oxidant stress is critical for neutrophil cytotoxicity during endotoxemia. *American Journal of Physiology-Gastrointestinal and Liver Physiology*, 287 (1), Am Physiological Soc, p.G243–G252. doi:10.1152/ajpgi.00287.2003.

Guo, H., Callaway, J. B. and Ting, J. P. (2015). Inflammasomes: mechanism of action, role in disease, and therapeutics. *Nature medicine*, 21 (7), p.677–687. doi:10.1038/nm.3893.

Gupta, A. K., Joshi, M. B., Philippova, M., Erne, P., Hasler, P., Hahn, S. and Resink, T. J. (2010). Activated endothelial cells induce neutrophil extracellular traps and are susceptible to NETosis-mediated cell death. *FEBS letters*, 584 (14), p.3193–3197. doi:10.1016/j.febslet.2010.06.006.

Hamburger, S. A. and McEver, R. P. (1990). GMP-140 mediates adhesion of stimulated platelets to neutrophils. *Blood*, 75 (3), p.550–554.

Hammam, O., Mahmoud, O., Zahran, M., Sayed, A., Salama, R., Hosny, K. and Farghly, A. (2013). A Possible Role for TNF-α in Coordinating Inflammation and Angiogenesis in Chronic Liver Disease and Hepatocellular Carcinoma. *Gastrointestinal cancer research : GCR*, 6 (4), p.107–114.

Hampson, P., Dinsdale, R., Wearn, C., Bamford, A., Bishop, J., Hazeldine, J., Moiemen, N., Harrison, P. and Lord, J. (2016). Neutrophil Dysfunction, Immature Granulocytes, and Cell-free DNA are Early Biomarkers of Sepsis in Burn-injured Patients: A Prospective Observational Cohort Study. *Annals of Surgery*, 265 (6), p.1241-1249. doi:10.1097/SLA.0000000000001807.

Harada, K., Shimoda, S., Sato, Y., Isse, K., Ikeda, H. and Nakanuma, Y. (2009). Periductal interleukin-17 production in association with biliary innate immunity contributes to the pathogenesis of cholangiopathy in primary biliary cirrhosis. *Clinical and experimental immunology*, 157 (2), p.261–270. doi:10.1111/j.1365-2249.2009.03947.x.

Harburger, D. and Calderwood, D. (2009). Integrin signalling at a glance. *Journal of Cell Science*, 122 (2), p.159–163. doi:10.1242/jcs.018093.

Harris, E., McIntyre, T., Prescott, S. and Zimmerman, G. (2000). The Leukocyte Integrins. *Journal of Biological Chemistry*, 275 (31), p.23409–23412. doi:10.1074/jbc.R000004200.

Hayes, B. E. and Clarke, D. E. (1990). Semicarbazide-sensitive amine oxidase activity in streptozotocin diabetic rats. *Research communications in chemical pathology and pharmacology*, 69 (1), p.71–83.

Hegde, V. L., Nagarkatti, P. S. and Nagarkatti, M. (2011). Role of myeloid-derived suppressor cells in amelioration of experimental autoimmune hepatitis following activation of TRPV1 receptors by cannabidiol. *PloS one*, 6 (4), p.e18281. doi:10.1371/journal.pone.0018281.

Heit, B, Colarusso, P, Liu, L and Ballantyne, CM. (2006). Intraluminal crawling of neutrophils to emigration sites: a molecularly distinct process from adhesion in the recruitment cascade. Journal of Experimental *Medicine*. 203 (12), p.2569-2575. doi:10.1084/jem.20060925.

Helmy, K. Y., Katschke, K. J., Gorgani, N. N., Kljavin, N. M., Elliott, J. M., Diehl, L., Scales, S. J., Ghilardi, N. and van Lookeren Campagne, M. (2006). CRIg: a macrophage complement receptor required for phagocytosis of circulating pathogens. *Cell*, 124 (5), p.915–927. doi:10.1016/j.cell.2005.12.039.

Hernandez, M., Solé, M., Boada, M. and Unzeta, M. (2006). Soluble semicarbazide sensitive amine oxidase (SSAO) catalysis induces apoptosis in vascular smooth muscle cells. *Biochimica et biophysica acta*, 1763 (2), p.164–173. doi:10.1016/j.bbamcr.2005.11.017.

Heymann, F., Hamesch, K., Weiskirchen, R. and Tacke, F. (2015). The concanavalin A model of acute hepatitis in mice. *Laboratory animals*, 49 (1 Suppl), p.12–20. doi:10.1177/0023677215572841.

Heymann, F., Trautwein, C. and Tacke, F. (2009). Monocytes and macrophages as cellular targets in liver fibrosis. *Inflammation & allergy drug targets*, 8 (4), p.307–318. doi:10.2174/187152809789352230.

Hidalgo, A., Peired, A. J., Wild, M. K., Vestweber, D. and Frenette, P. S. (2007). Complete identification of E-selectin ligands on neutrophils reveals distinct functions of PSGL-1, ESL-1, and CD44. *Immunity*, 26 (4), p.477–489. doi:10.1016/j.immuni.2007.03.011.

Hintermann, E, Ehser, J and Christen, U. (2012). The CYP2D6 animal model: how to induce autoimmune hepatitis in mice. *JoVE (Journal of Visualized Experiments,* (60). pii: 3644. doi:10.3791/3644.

Hofmann, M. A., Drury, S., Fu, C., Qu, W., Taguchi, A., Lu, Y., Avila, C., Kambham, N., Bierhaus,

A., Nawroth, P., Neurath, M. F., Slattery, T., Beach, D., McClary, J., Nagashima, M., Morser, J., Stern, D. and Schmidt, A. M. (1999). RAGE mediates a novel proinflammatory axis: a central cell surface receptor for S100/calgranulin polypeptides. *Cell*, 97 (7), p.889–901.

Holdener, M, Hintermann, E and Bayer, M. (2008). Breaking tolerance to the natural human liver autoantigen cytochrome P450 2D6 by virus infection. *The Journal of Experimental Medicine,* 205 (6), p.1409-1422. doi:10.1084/jem.20071859.

Holt, M. P., Cheng, L. and Ju, C. (2008). Identification and characterization of infiltrating macrophages in acetaminophen-induced liver injury. *Journal of leukocyte biology*, 84 (6), p.1410–1421. doi:10.1189/jlb.0308173.

Horie, T., Ono, K., Nagao, K., Nishi, H., Kinoshita, M., Kawamura, T., Wada, H., Shimatsu, A., Kita, T. and Hasegawa, K. (2008). Oxidative stress induces GLUT4 translocation by activation of PI3-K/Akt and dual AMPK kinase in cardiac myocytes. *Journal of cellular physiology*, 215 (3), p.733–742. doi:10.1002/jcp.21353.

Horiguchi, N., Lafdil, F., Miller, A., Park, O., Wang, H., Rajesh, M., Mukhopadhyay, P., Fu, X., Pacher, P. and Gao, B. (2010). Dissociation between liver inflammation and hepatocellular damage induced by carbon tetrachloride in myeloid cell-specific signal transducer and activator of transcription 3 gene knockout mice. *Hepatology*, 51 (5), p.1724–1734. doi:10.1002/hep.23532.

Hosseinzadeh, A., Messer, P. K. and Urban, C. F. (2012). Stable Redox-Cycling Nitroxide Tempol Inhibits NET Formation. *Frontiers in immunology*, 3, p.391. doi:10.3389/fimmu.2012.00391.

Hritz, I, Mandrekar, P, Velayudham, A and Catalano, D. (2008). The critical role of toll-like receptor (TLR) 4 in alcoholic liver disease is independent of the common TLR adapter MyD88. *Hepatology,* 48 (4), p.1224-1231. doi:10.1002/hep.22470.

Hsia, L., Ashley, N., Ouaret, D., Wang, L., Wilding, J. and Bodmer, W. (2016). Myofibroblasts are distinguished from activated skin fibroblasts by the expression of AOC3 and other associated markers. *Proceedings of the National Academy of Sciences*, 113 (15), p.E2162–E2171. doi:10.1073/pnas.1603534113.

Hu, Z., Zhao, P., Zhang, K., Zang, L., Liao, H. and Ma, W. (2016). Evaluation of Serum Vascular Adhesion Protein-1 as a Potential Biomarker in Thyroid Cancer. *International journal of endocrinology*, 2016, p.6312529. doi:10.1155/2016/6312529.

Huang, A. J., Manning, J. E., Bandak, T. M., Ratau, M. C., Hanser, K. R. and Silverstein, S. C. (1993). Endothelial cell cytosolic free calcium regulates neutrophil migration across monolayers of endothelial cells. *The Journal of cell biology*, 120 (6), p.1371–1380.

Huang, H.-L. (2012). Hepatoprotective effects of baicalein against CCl 4 -induced acute liver injury in mice. *World Journal of Gastroenterology*, 18 (45), p.6605. doi:10.3748/wjg.v18.i45.6605.

Huo, Y., Hafezi-Moghadam, A. and Ley, K. (2000). Role of vascular cell adhesion molecule-1 and fibronectin connecting segment-1 in monocyte rolling and adhesion on early atherosclerotic lesions. *Circulation research*, 87 (2), p.153–159.

Hwang, T.-L., Wang, W.-H., Wang, T.-Y., Yu, H.-P. and Hsieh, P.-W. (2015). Synthesis and pharmacological characterization of 2-aminobenzaldehyde oxime analogs as dual inhibitors of neutrophil elastase and proteinase 3. *Bioorganic & Medicinal Chemistry*, 23 (5), p.1123–1134. doi:10.1016/j.bmc.2014.12.056.

Hyogo, H. and Yamagishi, S. (2008). Advanced glycation end products (AGEs) and their involvement in liver disease. *Current pharmaceutical design*, 14 (10), p.969–972.

Iannacone, M., Sitia, G., Isogawa, M., Marchese, P., Castro, M., Lowenstein, P., Chisari, F., Ruggeri, Z. and Guidotti, L. (2005). Platelets mediate cytotoxic T lymphocyte–induced liver damage. *Nature Medicine*, 11 (11), p.1167–1169. doi:10.1038/nm1317.

Ibusuki, R., Uto, H., Arima, S., Mawatari, S., Setoguchi, Y., Iwashita, Y., Hashimoto, S., Maeda, T., Tanoue, S., Kanmura, S., Oketani, M., Ido, A. and Tsubouchi, H. (2013). Transgenic expression of human neutrophil peptide-1 enhances hepatic fibrosis in mice fed a choline-deficient, L-amino acid–defined diet. *Liver International*, 33 (10), p.1549–1556. doi:10.1111/liv.12203.

Iffiú-Soltész, Wanecq, Prévot, Grès and Carpéné. (2010a). Histamine oxidation in mouse adipose tissue is controlled by the AOC3 gene-encoded amine oxidase. *Inflammation Research*, 59 (S2), springer, p.227–229. doi:10.1007/s00011-009-0129-0.

Iffiú-Soltész, Z., Wanecq, E., Lomba, A., Portillo, M. P., Pellati, F., Szöko, E., Bour, S., Woodley, J., Milagro, F. I., Alfredo Martinez, J., Valet, P. and Carpéné, C. (2010b). Chronic benzylamine administration in the drinking water improves glucose tolerance, reduces body weight gain and circulating cholesterol in high-fat diet-fed mice. *Pharmacological research*, 61 (4), p.355–363. doi:10.1016/j.phrs.2009.12.014.

Iigo, Y., Suematsu, M., Higashida, T., Oheda, J., Matsumoto, K., Wakabayashi, Y., Ishimura, Y., Miyasaka, M. and Takashi, T. (1997). Constitutive expression of ICAM-1 in rat microvascular systems analyzed by laser confocal microscopy. *The American journal of physiology*, 273 (1 Pt 2), p.H138–47.

Inzaugarat, M., Solari, N., Billordo, L., Abecasis, R., Gadano, A. and Cherñavsky, A. (2011). Altered Phenotype and Functionality of Circulating Immune Cells Characterize Adult Patients with Nonalcoholic Steatohepatitis. *Journal of Clinical Immunology*, 31 (6), p.1120–1130. doi:10.1007/s10875-011-9571-1.

Iredale, J. P., Benyon, R. C., Pickering, J., McCullen, M., Northrop, M., Pawley, S., Hovell, C. and Arthur, M. J. (1998). Mechanisms of spontaneous resolution of rat liver fibrosis. Hepatic stellate cell apoptosis and reduced hepatic expression of metalloproteinase inhibitors. *The Journal of clinical investigation*, 102 (3), p.538–549. doi:10.1172/JCI1018.

Irie, J., Wu, Y., Wicker, L. S., Rainbow, D., Nalesnik, M. A., Hirsch, R., Peterson, L. B., Leung, P. S., Cheng, C., Mackay, I. R., Gershwin, M. E. and Ridgway, W. M. (2006). NOD.c3c4 congenic mice develop autoimmune biliary disease that serologically and pathogenetically models human primary biliary cirrhosis. *The Journal of experimental medicine*, 203 (5), p.1209–1219. doi:10.1084/jem.20051911.

Ishida, Y., Kondo, T., Ohshima, T., Fujiwara, H., Iwakura, Y. and Mukaida, N. (2002). A pivotal involvement of IFN-gamma in the pathogenesis of acetaminophen-induced acute liver injury. *FASEB journal : official publication of the Federation of American Societies for Experimental Biology*, 16 (10), p.1227–1236. doi:10.1096/fj.02-0046com.

Jaakkola, K, Kaunismäki, K, Tohka, S and Yegutkin, G. (1999a). Human vascular adhesion protein-1 in smooth muscle cells. *The American journal of Pathology,* 155 (6), p.1953-1963.

Jaakkola, K., Jalkanen, S., Kaunismäki, K., Vänttinen, E., Saukko, P., Alanen, K., Kallajoki, M., Voipio-Pulkki, L. M. and Salmi, M. (2000a). Vascular adhesion protein-1, intercellular adhesion molecule-1 and P-selectin mediate leukocyte binding to ischemic heart in humans. *Journal of the American College of Cardiology*, 36 (1), p.122–129.

Jaakkola, K., Kaunismäki, K., Tohka, S., Yegutkin, G., Vänttinen, E., Havia, T., Pelliniemi, L., Virolainen, M., Jalkanen, S. and Salmi, M. (1999b). Human Vascular Adhesion Protein-1 in Smooth Muscle Cells. *The American Journal of Pathology*, 155 (6), p.1953–1965. doi:10.1016/S0002-9440(10)65514-9.

Jaakkola, K., Nikula, T., Holopainen, R., Vähäsilta, T., Matikainen, M.-T., Laukkanen, M.-L., Huupponen, R., Halkola, L., Nieminen, L., Hiltunen, J., Parviainen, S., Clark, M., Knuuti, J., Savunen, T., Kääpä, P., Voipio-Pulkki, L. and Jalkanen, S. (2000b). In Vivo Detection of Vascular Adhesion Protein-1 in Experimental Inflammation. *The American Journal of Pathology*, 157 (2), p.463–471. doi:10.1016/S0002-9440(10)64558-0.

Jaeschke, H. (2002). Neutrophil-mediated tissue injury in alcoholic hepatitis. *Alcohol (Fayetteville, N.Y.)*, 27 (1), p.23–27.

Jaeschke, H. and Smith, C. W. (1997). Mechanisms of neutrophil-induced parenchymal cell injury. *Journal of leukocyte biology*, 61 (6), p.647–653.

Jaffar, Z. H., Sullivan, P., Page, C. and Costello, J. (1996). Low-dose theophylline modulates T-lymphocyte activation in allergen-challenged asthmatics. *The European respiratory journal*, 9 (3), p.456–462.

Jalan, R., Chiara, F., Balasubramaniyan, V., Andreola, F., Khetan, V., Malago, M., Pinzani, M., Mookerjee, R. and Rombouts, K. (2016). Ammonia produces pathological changes in human hepatic stellate cells and is a target for therapy of portal hypertension. *Journal of Hepatology*, 64 (4), p.823–833. doi:10.1016/j.jhep.2015.11.019.

Jalkanen, S., Karikoski, M., Mercier, N., Koskinen, K., Henttinen, T., Elima, K., Salmivirta, K. and Salmi, M. (2007). The oxidase activity of vascular adhesion protein-1 (VAP-1) induces endothelial E- and P-selectins and leukocyte binding. *Blood*, 110 (6), p.1864–1870. doi:10.1182/blood-2007-01-069674.

Jalkanen, S. and Salmi, M. (2001). Cell surface monoamine oxidases: enzymes in search of a function. *The EMBO journal*, 20 (15), p.3893–3901. doi:10.1093/emboj/20.15.3893.

James, L. P., McCullough, S. S., Knight, T. R., Jaeschke, H. and Hinson, J. A. (2003). Acetaminophen toxicity in mice lacking NADPH oxidase activity: role of peroxynitrite formation and mitochondrial oxidant stress. *Free radical research*, 37 (12), p.1289–1297.

Janeway, C. A. and Medzhitov, R. (2002). Innate immune recognition. *Annual review of immunology*, 20, p.197–216. doi:10.1146/annurev.immunol.20.083001.084359.

Jarnicki, A. G., Schilter, H., Liu, G., Wheeldon, K., Essilfie, A.-T. T., Foot, J. S., Yow, T. T., Jarolimek, W. and Hansbro, P. M. (2016). The inhibitor of semicarbazide-sensitive amine oxidase, PXS-4728A, ameliorates key features of chronic obstructive pulmonary disease in a mouse model. *British journal of pharmacology*, 173 (22), p.3161–3175. doi:10.1111/bph.13573.

Jenne, C. N. and Kubes, P. (2013). Immune surveillance by the liver. *Nature immunology*, 14 (10), p.996–1006. doi:10.1038/ni.2691.

Jenne, C. N., Wong, C. H., Zemp, F. J., McDonald, B., Rahman, M. M., Forsyth, P. A., McFadden, G. and Kubes, P. (2013). Neutrophils recruited to sites of infection protect from virus challenge by releasing neutrophil extracellular traps. *Cell host & microbe*, 13 (2), p.169–180. doi:10.1016/j.chom.2013.01.005.

Jensen, E. (2013). Quantitative Analysis of Histological Staining and Fluorescence Using ImageJ. *The Anatomical Record*, 296 (3), p.378–381. doi:10.1002/ar.22641.

Jiang, K., Sun, X., Chen, Y., Shen, Y. and Jarvis, J. (2015). RNA sequencing from human neutrophils reveals distinct transcriptional differences associated with chronic inflammatory states. *BMC Medical Genomics*, 8 (1). doi:10.1186/s12920-015-0128-7.

John, B. and Crispe, I. N. (2004). Passive and active mechanisms trap activated CD8+ T cells in the liver. *Journal of immunology,* 172 (9), p.5222–5229.

Johnson, Z., Proudfoot, A. E. and Handel, T. M. (2005). Interaction of chemokines and glycosaminoglycans: a new twist in the regulation of chemokine function with opportunities for therapeutic intervention. *Cytokine & growth factor reviews*, 16 (6), p.625–636. doi:10.1016/j.cytogfr.2005.04.006.

Jungi, T. W., Spycher, M. O., Nydegger, U. E. and Barandun, S. (1986). Platelet-leukocyte interaction: selective binding of thrombin-stimulated platelets to human monocytes, polymorphonuclear leukocytes, and related cell lines. *Blood*, 67 (3), p.629–636.

Kaitaniemi, S., Grön, K., Elovaara, H., Salmi, M., Jalkanen, S. and Elima, K. (2013). Functional modulation of vascular adhesion protein-1 by a novel splice variant. *PloS one*, 8 (1), p.e54151. doi:10.1371/journal.pone.0054151.

Kansas, G. S. (1996). Selectins and their ligands: current concepts and controversies. *Blood*, 88 (9), p.3259–3287.

Kanta, J. (2016). Elastin in the Liver. *Frontiers in Physiology*, 7, frontiers. doi:10.3389/fphys.2016.00491.

Kanwar, S., Johnston, B. and Kubes, P. (1995). Leukotriene C4/D4 induces P-selectin and sialyl Lewis(x)-dependent alterations in leukocyte kinetics in vivo. *Circulation research*, 77 (5), p.879–887.

Kaplan, M. A., Kucukoner, M., Inal, A., Urakci, Z., Evliyaoglu, O., Firat, U., Kaya, M. and Isikdogan, A. (2014). Relationship between serum soluble vascular adhesion protein-1 level and gastric cancer prognosis. *Oncology research and treatment*, 37 (6), p.340–344. doi:10.1159/000362626.

Karádi, I, Mészáros, Z, Csányi, A and Szombathy, T. (2002). Serum semicarbazide-sensitive amine oxidase (SSAO) activity is an independent marker of carotid atherosclerosis. *Clinica chimica acta*. 323 (1-2), p.139-146.

Karikoski, M., Irjala, H., Maksimow, M., Miiluniemi, M., Granfors, K., Hernesniemi, S., Elima, K., Moldenhauer, G., Schledzewski, K., Kzhyshkowska, J., Goerdt, S., Salmi, M. and Jalkanen, S. (2009). Clever-1/Stabilin-1 regulates lymphocyte migration within lymphatics and leukocyte entrance to sites of inflammation. *European Journal of Immunology*, 39 (12), p.3477–3487. doi:10.1002/eji.200939896.

Karim, S., Liaskou, E., Fear, J., Garg, A., Reynolds, G., Claridge, L., Adams, D. H., Newsome, P. N. and Lalor, P. F. (2014). Dysregulated hepatic expression of glucose transporters in chronic disease: contribution of semicarbazide-sensitive amine oxidase to hepatic glucose uptake. *American journal of physiology. Gastrointestinal and liver physiology*, 307 (12), p.G1180–90. doi:10.1152/ajpgi.00377.2013.

Karlmark, K. R., Wasmuth, H. E., Trautwein, C. and Tacke, F. (2008). Chemokine-directed immune cell infiltration in acute and chronic liver disease. *Expert review of gastroenterology & hepatology*, 2 (2), p.233–242. doi:10.1586/17474124.2.2.233.

Karlmark, K. R., Weiskirchen, R., Zimmermann, H. W., Gassler, N., Ginhoux, F., Weber, C., Merad, M., Luedde, T., Trautwein, C. and Tacke, F. (2009). Hepatic recruitment of the inflammatory Gr1+ monocyte subset upon liver injury promotes hepatic fibrosis. *Hepatology*, 50 (1), p.261–274. doi:10.1002/hep.22950.

Katt, J., Schwinge, D., Schoknecht, T., Quaas, A., Sobottka, I., Burandt, E., Becker, C., Neurath, M. F., Lohse, A. W., Herkel, J. and Schramm, C. (2013). Increased T helper type 17 response to pathogen stimulation in patients with primary sclerosing cholangitis. *Hepatology*, 58 (3), p.1084–1093. doi:10.1002/hep.26447.

Katz, N. R. (1992). Metabolic heterogeneity of hepatocytes across the liver acinus. *The Journal of nutrition*, 122 (3 Suppl), p.843–849.

Katzenellenbogen, M, Mizrahi, L and Pappo, O. (2007). Molecular mechanisms of liver carcinogenesis in the mdr2-knockout mice. *Molecular Cancer Research,* 5 (11), p.1159-1170. doi:10.1158/1541-7786.MCR-07-0172.

Ke, M., Zhang, Y., Xiong, Y., Saeed, Y. and Deng, Y. (2016). Identification of protein complexes of microsomes in rat adipocytes by native gel coupled with LC-ESI-QTOF. *Molecular bioSystems*, 12 (4), p.1313–1323. doi:10.1039/C5MB00707K.

Kemik, O., Sümer, A., Kemik, A. S., Itik, V., Dulger, A. C., Purisa, S. and Tuzun, S. (2010). Human vascular adhesion proteın-1 (VAP-1): serum levels for hepatocellular carcinoma in

non-alcoholic and alcoholic fatty liver disease. *World journal of surgical oncology*, 8, p.83. doi:10.1186/1477-7819-8-83.

Kempka, G. and Kolb-Bachofen, V. (1988). Binding, uptake, and transcytosis of ligands for mannose-specific receptors in rat liver: an electron microscopic study. *Experimental cell research*, 176 (1), p.38–48.

Khandoga, A, Kessler, JS, Meissner, H and Hanschen, M. (2005a). Junctional adhesion molecule-A deficiency increases hepatic ischemia-reperfusion injury despite reduction of neutrophil transendothelial migration. *Blood*. 106 (2), 725-733.

Khandoga, A., Kessler, J. S., Meissner, H., Hanschen, M., Corada, M., Motoike, T., Enders, G., Dejana, E. and Krombach, F. (2005b). Junctional adhesion molecule-A deficiency increases hepatic ischemia-reperfusion injury despite reduction of neutrophil transendothelial migration. *Blood*, 106 (2), Blood, p.725–733. doi:10.1182/blood-2004-11-4416.

Kirton, C., Laukkanen, M.-L., Nieminen, A., Merinen, M., Stolen, C., Armour, K., Smith, D., Salmi, M., Jalkanen, S. and Clark, M. (2005). Function-blocking antibodies to human vascular adhesion protein-1: a potential anti-inflammatory therapy. *European journal of immunology*, 35 (11), p.3119–3130. doi:10.1002/eji.200535300.

Kiskin, N. I., Hellen, N., Babich, V., Hewlett, L., Knipe, L., Hannah, M. J. and Carter, T. (2010). Protein mobilities and P-selectin storage in Weibel-Palade bodies. *Journal of cell science*, 123 (Pt 17), p.2964–2975. doi:10.1242/jcs.073593.

Kiss, J., Jalkanen, S., Fülöp, F., Savunen, T. and Salmi, M. (2008). Ischemia-reperfusion injury is attenuated in VAP-1-deficient mice and by VAP-1 inhibitors. *European journal of immunology*, 38 (11), p.3041–3049. doi:10.1002/eji.200838651.

Kitz, R. and Wilson, I. B. (1962). Esters of methanesulfonic acid as irreversible inhibitors of acetylcholinesterase. *The Journal of biological chemistry*, 237, The Journal of biological chemistry, p.3245–3249.

Kivi, E., Elima, K., Aalto, K., Nymalm, Y., Auvinen, K., Koivunen, E., Otto, D., Crocker, P., Salminen, T., Salmi, M. and Jalkanen, S. (2009). Human Siglec-10 can bind to vascular adhesion protein-1 and serves as its substrate. *Blood*, 114 (26), p.5385–5392. doi:10.1182/blood-2009-04-219253.

Klugewitz, K and Blumenthal-Barby, F. (2002). Immunomodulatory effects of the liver: deletion of activated CD4+ effector cells and suppression of IFN-γ-producing cells after intravenous protein immunization. *The Journal of Immunology,* 169 (5), 2407-2413. doi:10.4049/jimmunol.169.5.2407.

Kmieć, Z. (2001). Cooperation of liver cells in health and disease. *Advances in anatomy, embryology, and cell biology*, 161, p.III–XIII, 1–151.

Knolle, P. A. and Limmer, A. (2003). Control of immune responses by savenger liver endothelial cells. *Swiss medical weekly*, 133 (37-38), p.501–506.

Knolle, P. A., Uhrig, A., Hegenbarth, S., Löser, E., Schmitt, E., Gerken, G. and Lohse, A. W. (1998a). IL-10 down-regulates T cell activation by antigen-presenting liver sinusoidal endothelial cells through decreased antigen uptake via the mannose receptor and lowered surface expression of accessory molecules. *Clinical and experimental immunology*, 114 (3), p.427–433.

Knolle, P. A. and Wohlleber, D. (2016). Immunological functions of liver sinusoidal endothelial cells. *Cellular & molecular immunology*, 13 (3), p.347–353. doi:10.1038/cmi.2016.5.

Knolle, P., Uhrig, A., Protzer, U., Trippler, M., Duchmann, R., zum Büschenfelde, K. and Gerken, G. (1998b). Interleukin-10 expression is autoregulated at the transcriptional level in human and murine kupffer cells. *Hepatology*, 27 (1), p.93–99. doi:10.1002/hep.510270116.

Konig, M. and Andrade, F. (2016). A Critical Reappraisal of Neutrophil Extracellular Traps and

NETosis Mimics Based on Differential Requirements for Protein Citrullination. *Frontiers in Immunology*, 7, frontiers. doi:10.3389/fimmu.2016.00461.

Koskinen, K., Vainio, P. J., Smith, D. J., Pihlavisto, M., Ylä-Herttuala, S., Jalkanen, S. and Salmi, M. (2004). Granulocyte transmigration through the endothelium is regulated by the oxidase activity of vascular adhesion protein-1 (VAP-1). *Blood*, 103 (9), p.3388–3395. doi:10.1182/blood-2003-09-3275.

Kramer, I. M., Verhoeven, A. J., van der Bend, R. L., Weening, R. S. and Roos, D. (1988). Purified protein kinase C phosphorylates a 47-kDa protein in control neutrophil cytoplasts but not in neutrophil cytoplasts from patients with the autosomal form of chronic granulomatous disease. *The Journal of biological chemistry*, 263 (5), p.2352–2357.

Krenkel, O., Mossanen, J. C. and Tacke, F. (2014). Immune mechanisms in acetaminophen-induced acute liver failure. *Hepatobiliary surgery and nutrition*, 3 (6), p.331–343. doi:10.3978/j.issn.2304-3881.2014.11.01.

Kubes, P. and Mehal, W. Z. (2012). Sterile inflammation in the liver. *Gastroenterology*, 143 (5), p.1158–1172. doi:10.1053/j.gastro.2012.09.008.

Kuboki, S., Shin, T., Huber, N., Eismann, T., Galloway, E., Schuster, R., Blanchard, J., Edwards, M. J. and Lentsch, A. B. (2008). Hepatocyte signaling through CXC chemokine receptor-2 is detrimental to liver recovery after ischemia/reperfusion in mice. *Hepatology*, 48 (4), p.1213–1223. doi:10.1002/hep.22471.

Kunkel, E. J. and Ley, K. (1996). Distinct phenotype of E-selectin-deficient mice. E-selectin is required for slow leukocyte rolling in vivo. *Circulation research*, 79 (6), p.1196–1204.

Kurkijärvi, R., Adams, D. H., Leino, R., Möttönen, T., Jalkanen, S. and Salmi, M. (1998). Circulating form of human vascular adhesion protein-1 (VAP-1): increased serum levels in inflammatory liver diseases. *Journal of immunology*, 161 (3), p.1549–1557.

Kurkijärvi, R., Yegutkin, G. G., Gunson, B. K., Jalkanen, S., Salmi, M. and Adams, D. H. (2000). Circulating soluble vascular adhesion protein 1 accounts for the increased serum monoamine oxidase activity in chronic liver disease. *Gastroenterology*, 119 (4), p.1096–1103.

Lalor, Herbert, Bicknell and Adams. (2013). Hepatic sinusoidal endothelium avidly binds platelets in an integrin-dependent manner, leading to platelet and endothelial activation and leukocyte recruitment. *AJP: Gastrointestinal and Liver Physiology*, 304 (5), p.G469–G478. doi:10.1152/ajpgi.00407.2012.

Lalor, P., Edwards, S., McNab, G., Salmi, M., Jalkanen, S. and Adams, D. (2002). Vascular adhesion protein-1 mediates adhesion and transmigration of lymphocytes on human hepatic endothelial cells. *Journal of immunology*, 169 (2), p.983–992. doi:10.1016/S0168-8278(01)80783-2.

Lalor, P. F., Lai, W. K., Curbishley, S. M., Shetty, S. and Adams, D. H. (2006). Human hepatic sinusoidal endothelial cells can be distinguished by expression of phenotypic markers related to their specialised functions in vivo. *World journal of gastroenterology*, 12 (34), p.5429–5439.

Lalor, P. F., Tuncer, C., Weston, C., Martin-Santos, A., Smith, D. J. and Adams, D. H. (2007). Vascular adhesion protein-1 as a potential therapeutic target in liver disease. *Annals of the New York Academy of Sciences*, 1110, p.485–496. doi:10.1196/annals.1423.051.

Lammert, F., Wang, D. Q., Hillebrandt, S., Geier, A., Fickert, P., Trauner, M., Matern, S., Paigen, B. and Carey, M. C. (2004). Spontaneous cholecysto- and hepatolithiasis in Mdr2-/- mice: a model for low phospholipid-associated cholelithiasis. *Hepatology*, 39 (1), p.117–128. doi:10.1002/hep.20022.

Lan, R. Y., Salunga, T. L., Tsuneyama, K., Lian, Z.-X. X., Yang, G.-X. X., Hsu, W., Moritoki, Y., Ansari, A. A., Kemper, C., Price, J., Atkinson, J. P., Coppel, R. L. and Gershwin, M. E. (2009). Hepatic IL-17 responses in human and murine primary biliary cirrhosis. *Journal of*

autoimmunity, 32 (1), p.43–51. doi:10.1016/j.jaut.2008.11.001.

Langford, S. D., Trent, M. B., Balakumaran and Boor, P. J. (1999). Developmental Vasculotoxicity Associated with Inhibition of Semicarbazide-Sensitive Amine Oxidase. *Toxicology and Applied Pharmacology*, 155 (3), p.237–244. doi:10.1006/taap.1998.8602.

Langford, Trent and Boor. (2002). Semicarbazide-sensitive amine oxidase and extracellular matrix deposition by smooth-muscle cells. *Cardiovascular Toxicology*, 2 (2), p.141-150. doi:10.1385/CT:2:2:141.

Lawrence, M. B., Kansas, G. S., Kunkel, E. J. and Ley, K. (1997). Threshold levels of fluid shear promote leukocyte adhesion through selectins (CD62L,P,E). *The Journal of cell biology*, 136 (3), p.717–727.

Lee, J., French, Morgan and French, S. (2014). The liver is populated by a broad spectrum of markers for macrophages. In alcoholic hepatitis the macrophages are M1 and M2. *Experimental and Molecular Pathology*, 96 (1), p.118–125. doi:10.1016/j.yexmp.2013.09.004.

Lee and Kubes. (2008). Leukocyte adhesion in the liver: distinct adhesion paradigm from other organs. *The Journal of Hepatology*, 48 (3), p.504-512.

Lee, W. M., Stravitz, R. T. and Larson, A. M. (2012). Introduction to the revised American Association for the Study of Liver Diseases Position Paper on acute liver failure 2011. *Hepatology*, 55 (3), p.965–967. doi:10.1002/hep.25551.

Lee, W.-Y. Y., Moriarty, T. J., Wong, C. H., Zhou, H., Strieter, R. M., van Rooijen, N., Chaconas, G. and Kubes, P. (2010). An intravascular immune response to Borrelia burgdorferi involves Kupffer cells and iNKT cells. *Nature immunology*, 11 (4), p.295–302. doi:10.1038/ni.1855.

Lee, W.-Y. Y., Salmi, M., Kelly, M. M., Jalkanen, S. and Kubes, P. (2013). Therapeutic advantage of anti-VAP-1 over anti-α4 integrin antibody in concanavalin a-induced hepatitis. *Hepatology*, 58 (4), p.1413–1423. doi:10.1002/hep.26469.

Lelo, A., Miners, J., Robson, R. and Birkett, D. (1986). Assessment of caffeine exposure: Caffeine content of beverages, caffeine intake, and plasma concentrations of methylxanthines. *Clinical Pharmacology & Therapeutics*, 39 (1), p.54–59. doi:10.1038/clpt.1986.10.

Lemmers, A., Moreno, C., Gustot, T., Maréchal, R., Degré, D., Demetter, P., de Nadai, P., Geerts, A., Quertinmont, E., Vercruysse, V., Le Moine, O. and Devière, J. (2009). The interleukin-17 pathway is involved in human alcoholic liver disease. *Hepatology*, 49 (2), p.646–657. doi:10.1002/hep.22680.

Leo, M. A. and Lieber, C. S. (1983). Hepatic fibrosis after long-term administration of ethanol and moderate vitamin A supplementation in the rat. *Hepatology*, 3 (1), p.1–11.

Lewinsohn, R. (1977). Human serum amine oxidase. Enzyme activity in severely burnt patients and in patients with cancer. *Clinica Chimica Acta*. 81 (3), p.247-256.

Ley, K., Laudanna, C., Cybulsky, M. and Nourshargh, S. (2007). Getting to the site of inflammation: the leukocyte adhesion cascade updated. *Nature Reviews Immunology*, 7 (9), nature, p.678–689. doi:10.1038/nri2156.

Li. (2003). Critical role of CXC chemokines in endotoxemic liver injury in mice. *Journal of Leukocyte Biology*, 75 (3), p.443–452. doi:10.1189/jlb.0603297.

Li, H.-Y. Y., Jiang, Y.-D. D., Chang, T.-J. J., Wei, J.-N. N., Lin, M.-S. S., Lin, C.-H. H., Chiang, F.-T. T., Shih, S.-R. R., Hung, C. S., Hua, C.-H. H., Smith, D. J., Vanio, J. and Chuang, L.-M. M. (2011). Serum vascular adhesion protein-1 predicts 10-year cardiovascular and cancer mortality in individuals with type 2 diabetes. *Diabetes*, 60 (3), p.993–999. doi:10.2337/db10-0607.

Li, H.-Y. Y., Lin, H.-A. A., Nien, F.-J. J., Wu, V.-C. C., Jiang, Y.-D. D., Chang, T.-J. J., Kao, H.-L. L., Lin, M.-S. S., Wei, J.-N. N., Lin, C.-H. H., Shih, S.-R. R., Hung, C.-S. S. and Chuang, L.-M.

M. (2016). Serum Vascular Adhesion Protein-1 Predicts End-Stage Renal Disease in Patients with Type 2 Diabetes. *PloS one*, 11 (2), p.e0147981. doi:10.1371/journal.pone.0147981.

Li, H.-Y. Y., Wei, J.-N. N., Lin, M.-S. S., Smith, D. J., Vainio, J., Lin, C.-H. H., Chiang, F.-T. T., Shih, S.-R. R., Huang, C.-H. H., Wu, M.-Y. Y., Hsein, Y.-C. C. and Chuang, L.-M. M. (2009). Serum vascular adhesion protein-1 is increased in acute and chronic hyperglycemia. *Clinica chimica acta; international journal of clinical chemistry*, 404 (2), p.149–153. doi:10.1016/j.cca.2009.03.041.

Li, Y.-I. I., Hung, J.-S. S., Yu, T.-Y. Y., Liou, J.-M. M., Wei, J.-N. N., Kao, H.-L. L., Chuang, L.-M. M., Shun, C.-T. T., Lee, P.-H. H., Lai, H.-S. S., Su, C.-Y. Y., Li, H.-Y. Y. and Liang, J.-T. T. (2014). Serum vascular adhesion protein-1 predicts all-cause mortality and cancer-related mortality in subjects with colorectal cancer. *Clinica chimica acta; international journal of clinical chemistry*, 428, p.51–56. doi:10.1016/j.cca.2013.10.024.

Li, Z. and Diehl, A. M. (2003). Innate immunity in the liver. *Current opinion in gastroenterology*, 19 (6), p.565–571.

Li, Z., Soloski, M. J. and Diehl, A. M. (2005). Dietary factors alter hepatic innate immune system in mice with nonalcoholic fatty liver disease. *Hepatology*, 42 (4), p.880–885. doi:10.1002/hep.20826.

Liang, W., Lindeman, J. H., Menke, A. L., Koonen, D. P., Morrison, M., Havekes, L. M., van den Hoek, A. M. and Kleemann, R. (2014). Metabolically induced liver inflammation leads to NASH and differs from LPS- or IL-1β-induced chronic inflammation. *Laboratory investigation; a journal of technical methods and pathology*, 94 (5), p.491–502. doi:10.1038/labinvest.2014.11.

Liaskou, E, Karikoski, M and Reynolds, GM. (2011). Regulation of MAdCAM-1 Expression in Human and Mice By VAP-1 Amine Oxidase Activity. *Hepatology,* 53 (2), p.661-672. doi:10.1002/hep.24085.

Lieber, CS, Leo, MA, Mak, KM, Xu, Y and Cao, Q. (2004). Acarbose attenuates experimental non-alcoholic steatohepatitis. *Biochemical and Biophysical Research Communications,* 315 (3), p.699-703.

Lieber, C. S. and DeCarli, L. M. (1986). The feeding of ethanol in liquid diets. *Alcoholism, clinical and experimental research*, 10 (5), p.550–553.

Limmer, A., Ohl, J., Kurts, C., Ljunggren, H. G., Reiss, Y., Groettrup, M., Momburg, F., Arnold, B. and Knolle, P. A. (2000). Efficient presentation of exogenous antigen by liver endothelial cells to CD8+ T cells results in antigen-specific T-cell tolerance. *Nature medicine*, 6 (12), p.1348–1354. doi:10.1038/82161.

Limmer, A., Ohl, J., Wingender, G., Berg, M., Jüngerkes, F., Schumak, B., Djandji, D., Scholz, K., Klevenz, A., Hegenbarth, S., Momburg, F., Hämmerling, G. J. J., Arnold, B. and Knolle, P. A. (2005). Cross-presentation of oral antigens by liver sinusoidal endothelial cells leads to CD8 T cell tolerance. *European journal of immunology*, 35 (10), p.2970–2981. doi:10.1002/eji.200526034.

Lin, M.-S. S., Li, H.-Y. Y., Wei, J.-N. N., Lin, C.-H. H., Smith, D. J., Vainio, J., Shih, S.-R. R., Chen, Y.-H. H., Lin, L.-C. C., Kao, H.-L. L., Chuang, L.-M. M. and Chen, M.-F. F. (2008). Serum vascular adhesion protein-1 is higher in subjects with early stages of chronic kidney disease. *Clinical biochemistry*, 41 (16-17), p.1362–1367. doi:10.1016/j.clinbiochem.2008.06.019.

Liu, Bi, Wang, Yang, Zhang, Wang, Liu, Lu, Zhang, Chen, Chu and Yang. (2014). Targeting S1P1 Receptor Protects against Murine Immunological Hepatic Injury through Myeloid-Derived Suppressor Cells. *The Journal of Immunology*, 192 (7), p.3068–3079. doi:10.4049/jimmunol.1301193.

Livak, K. J. and Schmittgen, T. D. (2001). Analysis of relative gene expression data using real-

time quantitative PCR and the 2(-Delta Delta C(T)) Method. *Methods*, 25 (4), p.402–408. doi:10.1006/meth.2001.1262.

Livingston, P., Strouse, B., Perry, H., Borjigin, M., Bialk, P. and Kmiec, E. B. (2012). Oligonucleotide delivery by nucleofection does not rescue the reduced proliferation phenotype of gene-edited cells. *Nucleic acid therapeutics*, 22 (6), p.405–413. doi:10.1089/nat.2012.0374.

Lizcano, de Arriba, F., Tipton and Unzeta. (1996). Inhibition of bovine lung semicarbazide-sensitive amine oxidase (SSAO) by some hydrazine derivatives. *Biochemical pharmacology*, 52 (2), p.187–195.

Lohr, H. F., Schlaak, J. F., Lohse, A. W., Bocher, W. O., Arenz, M., Gerken, G. and Buschenfelde, KM. (1996). Autoreactive CD4+ LKM specific and anticlonotypic T cell responses in LKM 1 antibody positive autoimmune hepatitis. *Hepatology*, 24 (6), p.1416–1421. doi:10.1002/hep.510240619.

Louis, H., Van Laethem, J. L., Wu, W., Quertinmont, E., Degraef, C., Van den Berg, K., Demols, A., Goldman, M., Le Moine, O., Geerts, A. and Devière, J. (1998). Interleukin-10 controls neutrophilic infiltration, hepatocyte proliferation, and liver fibrosis induced by carbon tetrachloride in mice. *Hepatology*, 28 (6), p.1607–1615. doi:10.1002/hep.510280621.

Lumsden, A. B., Henderson, J. M. and Kutner, M. H. (1988). Endotoxin levels measured by a chromogenic assay in portal, hepatic and peripheral venous blood in patients with cirrhosis. *Hepatology*, 8 (2), p.232–236.

Lv, X., Chen, Z., Li, J., Zhang, L., Liu, H., Huang, C. and Zhu, P. (2010). Caffeine protects against alcoholic liver injury by attenuating inflammatory response and oxidative stress. *Inflammation Research*, 59 (8), p.635–645. doi:10.1007/s00011-010-0176-6.

Lyles, GA and Chalmers, J. (1992). The metabolism of aminoacetone to methylglyoxal by semicarbazide-sensitive amine oxidase in human umbilical artery. *Biochemical pharmacology*. 43 (7), p.1409-1414.

Lyles, G. A. (1996). Mammalian plasma and tissue-bound semicarbazide-sensitive amine oxidases: biochemical, pharmacological and toxicological aspects. *The international journal of biochemistry & cell biology*, 28 (3), p.259–274.

Maciorkowska, D., Zbroch, E. and Malyszko, J. (2015). Circulating renalase, catecholamines, and vascular adhesion protein 1 in hypertensive patients. *Journal of the American Society of Hypertension : JASH*, 9 (11), p.855–864. doi:10.1016/j.jash.2015.08.002.

MacPhee, P. J., Schmidt, E. E. and Groom, A. C. (1995). Intermittence of blood flow in liver sinusoids, studied by high-resolution in vivo microscopy. *The American journal of physiology*, 269 (5 Pt 1), p.G692–8.

Madej, A., Reich, A., Orda, A. and Szepietowski, J. C. (2006). Expression of vascular adhesion protein-1 in atopic eczema. *International archives of allergy and immunology*, 139 (2), p.114–121. doi:10.1159/000090386.

Madej, A., Reich, A., Orda, A. and Szepietowski, J. C. (2007). Vascular adhesion protein-1 (VAP-1) is overexpressed in psoriatic patients. *Journal of the European Academy of Dermatology and Venereology : JEADV*, 21 (1), p.72–78. doi:10.1111/j.1468-3083.2006.01869.x.

Magyar, K., Mészáros, Z. and Mátyus, P. (2001). Semicarbazide-sensitive amine oxidase. Its physiological significance. *Pure and Applied Chemistry*, 73 (9), p.1393–1400. doi:10.1351/pac200173091393.

Maher, J. J. (1995). Rat hepatocytes and Kupffer cells interact to produce interleukin-8 (CINC) in the setting of ethanol. *The American journal of physiology*, 269 (4 Pt 1), p.G518–23.

Makgoba, M., Sanders, M., Luce, G., Dustint, M., Springer, T., Clark, E., Mannoni, P. and Shaw, S. (1988). ICAM-1 a ligand for LFA-1-dependent adhesion of B, T and myeloid cells. *Nature*, 331 (6151), p.86–88. doi:10.1038/331086a0.

Mamdouh, Z., Mikhailov, A. and Muller, W. A. (2009). Transcellular migration of leukocytes is mediated by the endothelial lateral border recycling compartment. *The Journal of experimental medicine*, 206 (12), p.2795–2808. doi:10.1084/jem.20082745.

Mancinelli, R., Franchitto, A., Gaudio, E., Onori, P., Glaser, S., Francis, H., Venter, J., DeMorrow, S., Carpino, G., Kopriva, S., White, M., Fava, G., Alvaro, D. and Alpini, G. (2010). After Damage of Large Bile Ducts by Gamma-Aminobutyric Acid, Small Ducts Replenish the Biliary Tree by Amplification of Calcium-Dependent Signaling and de Novo Acquisition of Large Cholangiocyte Phenotypes. *The American Journal of Pathology*, 176 (4), p.1790–1800. doi:10.2353/ajpath.2010.090677.

Marchi, Sesti-Costa, Chedraoui-Silva and Mantovani. (2014). Comparison of four methods for the isolation of murine blood neutrophils with respect to the release of reactive oxygen and nitrogen species and the expression of immunological receptors. *Comparative Clinical Pathology*, 23 (5), p.1469–1476. doi:10.1007/s00580-013-1808-3.

Marques, P. E., Amaral, S. S., Pires, D. A., Nogueira, L. L., Soriani, F. M., Lima, B. H., Lopes, G. A., Russo, R. C., Avila, T. V., Melgaço, J. G., Oliveira, A. G. G., Pinto, M. A., Lima, C. X., De Paula, A. M., Cara, D. C., Leite, M. F., Teixeira, M. M. and Menezes, G. B. (2012). Chemokines and mitochondrial products activate neutrophils to amplify organ injury during mouse acute liver failure. *Hepatology*, 56 (5), p.1971–1982. doi:10.1002/hep.25801.

Marttila-Ichihara, F., Auvinen, K., Elima, K., Jalkanen, S. and Salmi, M. (2009). Vascular adhesion protein-1 enhances tumor growth by supporting recruitment of Gr-1+CD11b+ myeloid cells into tumors. *Cancer research*, 69 (19), p.7875–7883. doi:10.1158/0008-5472.CAN-09-1205.

Marttila-Ichihara, F., Castermans, K., Auvinen, K., Oude Egbrink, M. G., Jalkanen, S., Griffioen, A. W. and Salmi, M. (2010). Small-molecule inhibitors of vascular adhesion protein-1 reduce the accumulation of myeloid cells into tumors and attenuate tumor growth in mice. *Journal of immunology*, 184 (6), p.3164–3173. doi:10.4049/jimmunol.0901794.

Marttila-Ichihara, F., Smith, D., Stolen, C., Yegutkin, G., Elima, K., Mercier, N., Kiviranta, R., Pihlavisto, M., Alaranta, S., Pentikäinen, U., Pentikäinen, O., Fülöp, F., Jalkanen, S. and Salmi, M. (2006). Vascular amine oxidases are needed for leukocyte extravasation into inflamed joints in vivo. *Arthritis and rheumatism*, 54 (9), p.2852–2862. doi:10.1002/art.22061.

Mathys, K. C., Ponnampalam, S. N., Padival, S. and Nagaraj, R. H. (2002). Semicarbazide-sensitive amine oxidase in aortic smooth muscle cells mediates synthesis of a methylglyoxal-AGE: implications for vascular complications in diabetes. *Biochemical and biophysical research communications*, 297 (4), p.863–869.

Matsuda, J. L., Mallevaey, T., Scott-Browne, J. and Gapin, L. (2008). CD1d-restricted iNKT cells, the 'Swiss-Army knife' of the immune system. *Current opinion in immunology*, 20 (3), p.358–368. doi:10.1016/j.coi.2008.03.018.

Matsuno, K., Ezaki, T., Kudo, S. and Uehara, Y. (1996). A life stage of particle-laden rat dendritic cells in vivo: their terminal division, active phagocytosis, and translocation from the liver to the draining lymph. *The Journal of experimental medicine*, 183 (4), p.1865–1878.

Maula, S., Salminen, T., Kaitaniemi, S., Nymalm, Y., Smith, D. and Jalkanen, S. (2005). Carbohydrates located on the top of the 'cap' contribute to the adhesive and enzymatic functions of vascular adhesion protein-1. *European Journal of Immunology*, 35 (9), p.2718–2727. doi:10.1002/eji.200526351.

Mavier, P., Guigui, B., Preaux, A. M., Rosenbaum, J., Lescs, M. C., Zafrani, E. S. and Dhumeaux, D. (1988). In vitro toxicity of hydrogen peroxide against normal vs. tumor rat hepatocytes: role of catalase and of the glutathione redox cycle. *Hepatology*, 8 (6), p.1673–1678.

McDonagh, Nathan, Bonavia, Moyle and Tanner. (1991). Caffeine clearance by enzyme multiplied

immunoassay technique: a simple, inexpensive, and useful indicator of liver function. *Gut*, 32 (6), p.681–684. doi:10.1136/gut.32.6.681.

McDonald, B., McAvoy, E., Lam, F., Gill, V., de la Motte, C., Savani, R. and Kubes, P. (2008). Interaction of CD44 and hyaluronan is the dominant mechanism for neutrophil sequestration in inflamed liver sinusoids. *The Journal of Experimental Medicine*, 205 (4), p.915–927. doi:10.1084/jem.20071765.

McDonald, B., Pittman, K., Menezes, G. B., Hirota, S. A., Slaba, I., Waterhouse, C. C., Beck, P. L., Muruve, D. A. and Kubes, P. (2010). Intravascular danger signals guide neutrophils to sites of sterile inflammation. *Science*, 330 (6002), p.362–366. doi:10.1126/science.1195491.

McDonald, B., Urrutia, R., Yipp, B. G., Jenne, C. N. and Kubes, P. (2012). Intravascular neutrophil extracellular traps capture bacteria from the bloodstream during sepsis. *Cell host & microbe*, 12 (3), p.324–333. doi:10.1016/j.chom.2012.06.011.

McEver, R. P. and Cummings, R. D. (1997). Perspectives series: cell adhesion in vascular biology. Role of PSGL-1 binding to selectins in leukocyte recruitment. *The Journal of clinical investigation*, 100 (3), p.485–491. doi:10.1172/JCI119556.

McGill, M. R., Sharpe, M. R., Williams, C. D., Taha, M., Curry, S. C. and Jaeschke, H. (2012). The mechanism underlying acetaminophen-induced hepatotoxicity in humans and mice involves mitochondrial damage and nuclear DNA fragmentation. *The Journal of clinical investigation*, 122 (4), p.1574–1583. doi:10.1172/JCI59755.

McKenna, F., McLaughlin, P. J., Lewis, B. J., Sibbring, G. C., Cummerson, J. A., Bowen-Jones, D. and Moots, R. J. (2002). Dopamine receptor expression on human T- and B-lymphocytes, monocytes, neutrophils, eosinophils and NK cells: a flow cytometric study. *Journal of neuroimmunology*, 132 (1-2), p.34–40.

McNab, Reeves, Salmi and Hubscher. (1996). Vascular adhesion protein 1 mediates binding of T cells to human hepatic endothelium. *Gastroenterology,* 110 (2), p.522-528.

Mercier, N, Moldes, M, Hadri, E. K. and Fève, B. (2003). Regulation of semicarbazide-sensitive amine oxidase expression by tumor necrosis factor-α in adipocytes: Functional consequences on glucose transport. *Journal of Pharmacology and Experimental Therapy,* 304 (3), p.1197-1207. doi:10.1124/jpet.102.044420.

Mercier, N., Moldes, M., El Hadri, K. and Fève, B. (2001). Semicarbazide-sensitive amine oxidase activation promotes adipose conversion of 3T3-L1 cells. *The Biochemical journal*, 358 (Pt 2), p.335–342.

Mercier, N., Osborne-Pellegrin, M., Hadri, K., Kakou, A., Labat, C., Loufrani, L., Henrion, D., Challande, P., Jalkanen, S., Fève, B. and Lacolley, P. (2006). Carotid arterial stiffness, elastic fibre network and vasoreactivity in semicarbazide-sensitive amine-oxidase null mouse. *Cardiovascular Research*, 72 (2), p.349–357. doi:10.1016/j.cardiores.2006.08.008.

Merinen, M., Irjala, H., Salmi, M., Jaakkola, I., Hänninen, A. and Jalkanen, S. (2005). Vascular adhesion protein-1 is involved in both acute and chronic inflammation in the mouse. *The American journal of pathology*, 166 (3), p.793–800. doi:10.1016/S0002-9440(10)62300-0.

Mészáros, Z., Csányi, A., Vallus, G., Szombathy, T., Karádi, I. and Magyar, K. (2000). Inhibitor sensitivity of human serum and vascular semicarbazide-sensitive amine oxidases. *Neurobiology*, 8 (2), p.215–223.

Middleton, J., Neil, S., Wintle, J., Clark-Lewis, I., Moore, H., Lam, C., Auer, M., Hub, E. and Rot, A. (1997). Transcytosis and surface presentation of IL-8 by venular endothelial cells. *Cell*, 91 (3), p.385–395.

Middleton, J., Patterson, A. M., Gardner, L., Schmutz, C. and Ashton, B. A. (2002). Leukocyte extravasation: chemokine transport and presentation by the endothelium. *Blood*, 100 (12), p.3853–3860. doi:10.1182/blood.V100.12.3853.

Millán, J., Hewlett, L., Glyn, M., Toomre, D., Clark, P. and Ridley, A. (2006). Lymphocyte transcellular migration occurs through recruitment of endothelial ICAM-1 to caveola- and F-actin-rich domains. *Nature Cell Biology*, 8 (2), p.113–123. doi:10.1038/ncb1356.

Mitchell, S. C. and Zhang, A. Q. (2001). Methylamine in human urine. *Clinica chimica acta; international journal of clinical chemistry*, 312 (1-2), p.107–114.

Mizutani, T., Shinoda, M., Tanaka, Y., Kuno, T., Hattori, A., Usui, T., Kuno, N. and Osaka, T. (2008). Autoantibodies Against CYP2D6 and Other Drug-Metabolizing Enzymes in Autoimmune Hepatitis Type 2. *Drug Metabolism Reviews*, 37 (1), p.235–252. doi:10.1081/DMR-200028798.

Moldes, M, Fève, B and Pairault, J. (1999). Molecular cloning of a major mRNA species in murine 3T3 adipocyte lineage differentiation-dependent expression, regulation, and identification as semicarbazide-sensitive amine oxidase. *Journal of Biological Chemistry*., 274 (14), p.9515-9523. doi:10.1074/jbc.274.14.9515.

Monteiro, J. P. P., Alves, M. G., Oliveira, P. F. and Silva, B. M. (2016). Structure-Bioactivity Relationships of Methylxanthines: Trying to Make Sense of All the Promises and the Drawbacks. *Molecules*, 21 (8). doi:10.3390/molecules21080974.

Mookerjee, R. P., Stadlbauer, V., Lidder, S., Wright, G. A., Hodges, S. J., Davies, N. A. and Jalan, R. (2007). Neutrophil dysfunction in alcoholic hepatitis superimposed on cirrhosis is reversible and predicts the outcome. *Hepatology)*, 46 (3), p.831–840. doi:10.1002/hep.21737.

Moreira, R. K. (2007). Hepatic stellate cells and liver fibrosis. *Archives of pathology & laboratory medicine*, 131 (11), p.1728–1734. doi:10.1043/1543-2165(2007)131

Morin, N, Lizcano, JM, Fontana, E, Marti, L and Smih, F. (2001). Semicarbazide-sensitive amine oxidase substrates stimulate glucose transport and inhibit lipolysis in human adipocytes. The Journal *of Pharmacology and Experimental Therapy*. 297 (2), p.563-572. http://jpet.aspetjournals.org/content/297/2/563.short.

Morland, C. M., Fear, J., McNab, G., Joplin, R. and Adams, D. H. (1997). Promotion of leukocyte transendothelial cell migration by chemokines derived from human biliary epithelial cells in vitro. *Proceedings of the Association of American Physicians*, 109 (4), p.372–382.

Morsy, M. A., Norman, P. J., Mitry, R., Rela, M., Heaton, N. D. and Vaughan, R. W. (2005). Isolation, purification and flow cytometric analysis of human intrahepatic lymphocytes using an improved technique. *Laboratory investigation; a journal of technical methods and pathology*, 85 (2), p.285–296. doi:10.1038/labinvest.3700219.

Munday, J., Kerr, S., Ni, J., Cornish, A. L., Zhang, J. Q., Nicoll, G., Floyd, H., Mattei, M. G., Moore, P., Liu, D. and Crocker, P. R. (2001). Identification, characterization and leucocyte expression of Siglec-10, a novel human sialic acid-binding receptor. *The Biochemical journal*, 355 (Pt 2), p.489–497.

Murata, M., Noda, K., Fukuhara, J., Kanda, A., Kase, S., Saito, W., Ozawa, Y., Mochizuki, S., Kimura, S., Mashima, Y., Okada, Y. and Ishida, S. (2012). Soluble Vascular Adhesion Protein-1 Accumulates in Proliferative Diabetic Retinopathy. *Investigative Opthalmology & Visual Science*, 53 (7), p.4055. doi:10.1167/iovs.12-9857.

Nakamoto, N., Cho, H., Shaked, A., Olthoff, K., Valiga, M. E., Kaminski, M., Gostick, E., Price, D. A., Freeman, G. J., Wherry, E. J. and Chang, K.-M. M. (2009). Synergistic reversal of intrahepatic HCV-specific CD8 T cell exhaustion by combined PD-1/CTLA-4 blockade. *PLoS pathogens*, 5 (2), p.e1000313. doi:10.1371/journal.ppat.1000313.

Nakao, S., Noda, K., Zandi, S., Sun, D., Taher, M., Schering, A., Xie, F., Mashima, Y. and Hafezi-Moghadam, A. (2011). VAP-1-mediated M2 macrophage infiltration underlies IL-1β- but not VEGF-A-induced lymph- and angiogenesis. *The American journal of pathology*, 178 (4), p.1913–1921. doi:10.1016/j.ajpath.2011.01.011.

Naveau, S., Chollet-Martin, S., Dharancy, S., Mathurin, P., Jouet, P., Piquet, M.-A. A., Davion, T., Oberti, F., Broët, P. and Emilie, D. (2004). A double-blind randomized controlled trial of infliximab associated with prednisolone in acute alcoholic hepatitis. *Hepatology*, 39 (5), p.1390–1397. doi:10.1002/hep.20206.

Neeli, I. and Radic, M. (2013). Opposition between PKC isoforms regulates histone deimination and neutrophil extracellular chromatin release. *Frontiers in Immunology*, 4 doi:10.3389/fimmu.2013.00038.

Nemati, H., Khodarahmi, R., Rahmani, A., Ebrahimi, A., Amani, M. and Eftekhari, K. (2013). Serum lipid profile in psoriatic patients: correlation between vascular adhesion protein 1 and lipoprotein (a). *Cell biochemistry and function*, 31 (1), p.36–40. doi:10.1002/cbf.2857.

Neumann, K., Erben, U., Kruse, N., Wechsung, K., Schumann, M., Klugewitz, K., Scheffold, A. and Kühl, A. (2015). Chemokine Transfer by Liver Sinusoidal Endothelial Cells Contributes to the Recruitment of CD4+ T Cells into the Murine Liver. *PLOS ONE*, 10 (6), p.e0123867. doi:10.1371/journal.pone.0123867.

Newsome, P. N., Plevris, J. N., Nelson, L. J. and Hayes, P. C. (2000). Animal models of fulminant hepatic failure: a critical evaluation. *Liver transplantation : official publication of the American Association for the Study of Liver Diseases and the International Liver Transplantation Society*, 6 (1), p.21–31. doi:10.1002/lt.500060110.

Nieminen, M., Henttinen, T., Merinen, M., Marttila-Ichihara, F., Eriksson, J. E. and Jalkanen, S. (2006). Vimentin function in lymphocyte adhesion and transcellular migration. *Nature cell biology*, 8 (2), p.156–162. doi:10.1038/ncb1355.

Niethammer, P., Grabher, C., Look, T. and Mitchison, T. (2009). A tissue-scale gradient of hydrogen peroxide mediates rapid wound detection in zebrafish. *Nature*, 459 (7249), p.996–999. doi:10.1038/nature08119.

Nishioji, K., Okanoue, T., Itoh, Y., Narumi, S., Sakamoto, M., Nakamura, H., Morita, A. and Kashima, K. (2001). Increase of chemokine interferon-inducible protein-10 (IP-10) in the serum of patients with autoimmune liver diseases and increase of its mRNA expression in hepatocytes. *Clinical and experimental immunology*, 123 (2), p.271–279.

Nitto, T. and Onodera, K. (2013). Linkage between coenzyme a metabolism and inflammation: roles of pantetheinase. *Journal of pharmacological sciences*, 123 (1), p.1–8.

Noda, K., Miyahara, S., Nakazawa, T., Almulki, L., Nakao, S., Hisatomi, T., She, H., Thomas, K. L., Garland, R. C., Miller, J. W., Gragoudas, E. S., Kawai, Y., Mashima, Y. and Hafezi-Moghadam, A. (2008a). Inhibition of vascular adhesion protein-1 suppresses endotoxin-induced uveitis. *FASEB journal : official publication of the Federation of American Societies for Experimental Biology*, 22 (4), p.1094–1103. doi:10.1096/fj.07-9377com.

Noda, K., Nakao, S., Zandi, S., Engelstädter, V., Mashima, Y. and Hafezi-Moghadam, A. (2009). Vascular adhesion protein-1 regulates leukocyte transmigration rate in the retina during diabetes. *Experimental eye research*, 89 (5), p.774–781. doi:10.1016/j.exer.2009.07.010.

Noda, K., She, H., Nakazawa, T., Hisatomi, T., Nakao, S., Almulki, L., Zandi, S., Miyahara, S., Ito, Y., Thomas, K., Garland, R., Miller, J., Gragoudas, E., Mashima, Y. and Hafezi-Moghadam, A. (2008b). Vascular adhesion protein-1 blockade suppresses choroidal neovascularization. *The FASEB Journal*, 22 (8), p.2928–2935. doi:10.1096/fj.07-105346.

Norris, S., Collins, C., Doherty, D. G., Smith, F., McEntee, G., Traynor, O., Nolan, N., Hegarty, J. and O'Farrelly, C. (1998). Resident human hepatic lymphocytes are phenotypically different from circulating lymphocytes. *Journal of hepatology*, 28 (1), p.84–90.

Notas, G., Kisseleva, T. and Brenner, D. (2009). NK and NKT cells in liver injury and fibrosis. *Clinical immunology*, 130 (1), p.16–26. doi:10.1016/j.clim.2008.08.008.

Nourshargh, S. and Alon, R. (2014). Leukocyte Migration into Inflamed Tissues. *Immunity*, 41 (5),

p.694–707. doi:10.1016/j.immuni.2014.10.008.

O'Rourke, A. M., Wang, E. Y., Miller, A., Podar, E. M., Scheyhing, K., Huang, L., Kessler, C., Gao, H., Ton-Nu, H.-T. T., Macdonald, M. T., Jones, D. S. and Linnik, M. D. (2008). Anti-inflammatory effects of LJP 1586 [Z-3-fluoro-2-(4-methoxybenzyl)allylamine hydrochloride], an amine-based inhibitor of semicarbazide-sensitive amine oxidase activity. *The Journal of pharmacology and experimental therapeutics*, 324 (2), p.867–875. doi:10.1124/jpet.107.131672.

O'Rourke, Wang, Salter-Cid, Huang, Miller, Podar, Gao, Jones and Linnik. (2007). Benefit of inhibiting SSAO in relapsing experimental autoimmune encephalomyelitis. *Journal of neural transmission*, 114 (6), p.845–849. doi:10.1007/s00702-007-0699-3.

O'Sullivan. (2004). Semicarbazide-Sensitive Amine Oxidases: Enzymes with Quite a Lot to Do. *NeuroToxicology*, 25 (1-2), p.303–315. doi:10.1016/S0161-813X(03)00117-7.

O'Sullivan, Davey, O'Sullivan and Tipton. (2007). Hydrogen peroxide derived from amine oxidation mediates the interaction between aminosugars and semicarbazide-sensitive amine oxidase. *Journal of Neural Transmission*, 114 (6), p.751–756. doi:10.1007/s00702-007-0683-y.

O'Sullivan, J., O'Sullivan, M., Tipton, K. F., Unzeta, M., Del Mar Hernandez, M. and Davey, G. P. (2003). The inhibition of semicarbazide-sensitive amine oxidase by aminohexoses. *Biochimica et biophysica acta*, 1647 (1-2), p.367–371.

Obata, T. and Nakashima, M. (2016). Evidence for existence of thyroid hormone inducible semicarbazide-sensitive amine oxidase (SSAO) in rat heart cytosol. *Indian Heart Journal*, 68 (2), p.225–230. doi:10.1016/j.ihj.2016.01.011.

Oertelt, S, Lian, ZX and Cheng, CM. (2006). Anti-mitochondrial antibodies and primary biliary cirrhosis in TGF-β receptor II dominant-negative mice. *The Journal of Immunology,* 177 (3), p.1655-1660. doi:10.4049/jimmunol.177.3.1655.

Ogi, Yokomori, H., Oda, M., Yoshimura, K., Nomura, M., Ohshima, S., Akita, M., Toda, K. and Ishii, H. (2003). Distribution and localization of caveolin-1 in sinusoidal cells in rat liver. *Medical Electron Microscopy*, 36 (1), p.33–40. doi:10.1007/s007950300004.

De Oliveira, C., de Marqueti, R., Cominetti, M., Vieira, E., Ribeiro, J., Pontes, C., Borghi-Silva, A. and Selistre-de-Araujo, H. (2014). Effects of Blocking αvβ3 integrin by a recombinant RGD disintegrin on remodeling of wound healing after induction of incisional hernia in rats. *Acta Cirurgica Brasileira*, 29, p.06–13. doi:10.1590/S0102-86502014001700002.

Olivieri, A., O'Sullivan, J., Fortuny, L., Vives, I. and Tipton, K. (2010). Interaction of l-lysine and soluble elastin with the semicarbazide-sensitive amine oxidase in the context of its vascular-adhesion and tissue maturation functions. *Biochimica et Biophysica Acta (BBA) - Proteins and Proteomics*, 1804 (4), p.941–947. doi:10.1016/j.bbapap.2010.01.003.

Olivieri, A., Rico, D., Khiari, Z., Henehan, G., O'Sullivan, J. and Tipton, K. (2011). From caffeine to fish waste: amine compounds present in food and drugs and their interactions with primary amine oxidase. *Journal of Neural Transmission*, 118 (7), p.1079–1089. doi:10.1007/s00702-011-0611-z.

Olivieri and Tipton. (2011). Inhibition of bovine plasma semicarbazide-sensitive amine oxidase by caffeine. *Journal of biochemical and molecular toxicology*, 25 (1), p.26–27. doi:10.1002/jbt.20356.

Olynyk, J. K., Matuschak, G. M., Lechner, A. J., Britton, R. S., Tredway, T. L., O'Neill, R. and Bacon, B. R. (1994). Differential production of TNF by Kupffer cells after phagocytosis of E. coli and C. albicans. *The American journal of physiology*, 267 (2 Pt 1), p.G213–9.

Oo, Y., Banz, V., Kavanagh, D., Liaskou, E., Withers, D., Humphreys, E., Reynolds, G., Lee-Turner, L., Kalia, N., Hubscher, S., Klenerman, P., Eksteen, B. and Adams, D. (2012). CXCR3-dependent recruitment and CCR6-mediated positioning of Th-17 cells in the

inflamed liver. *Journal of Hepatology*, 57 (5), p.1044–1051. doi:10.1016/j.jhep.2012.07.008.

Van Oosten, M., van de Bilt, E., de Vries, H. E., van Berkel, T. J. and Kuiper, J. (1995). Vascular adhesion molecule-1 and intercellular adhesion molecule-1 expression on rat liver cells after lipopolysaccharide administration in vivo. *Hepatology*, 22 (5), p.1538–1546.

Ott, I., Neumann, F. J., Gawaz, M., Schmitt, M. and Schömig, A. (1996). Increased neutrophil-platelet adhesion in patients with unstable angina. *Circulation*, 94 (6), p.1239–1246.

Pamuk, G. E. E., Turgut, B., Pamuk, O. N., Vural, O., Demir, M. and Cakir, N. (2007). Increased circulating platelet-leucocyte complexes in patients with primary Raynaud's phenomenon and Raynaud's phenomenon secondary to systemic sclerosis: a comparative study. *Blood coagulation & fibrinolysis : an international journal in haemostasis and thrombosis*, 18 (4), p.297–302. doi:10.1097/MBC.0b013e328010bd05.

Park, J.-J. J., Wong, D. K., Wahed, A. S., Lee, W. M., Feld, J. J., Terrault, N., Khalili, M., Sterling, R. K., Kowdley, K. V., Bzowej, N., Lau, D. T., Kim, W. R., Smith, C., Carithers, R. L., Torrey, K. W., Keith, J. W., Levine, D. L., Traum, D., Ho, S., Valiga, M. E., Johnson, G. S., Doo, E., Lok, A. S. and Chang, K.-M. M. (2016). Hepatitis B Virus--Specific and Global T-Cell Dysfunction in Chronic Hepatitis B. *Gastroenterology*, 150 (3), p.684–695.e5. doi:10.1053/j.gastro.2015.11.050.

Parker, G. A. and Picut, C. A. (2005). Liver immunobiology. *Toxicologic pathology*, 33 (1), p.52–62. doi:10.1080/01926230590522365.

Parsons, M. R., Convery, M. A., Wilmot, C. M., Yadav, K. D., Blakeley, V., Corner, A. S., Phillips, S. E., McPherson, M. J. and Knowles, P. F. (1995). Crystal structure of a quinoenzyme: copper amine oxidase of Escherichia coli at 2 A resolution. *Structure*, 3 (11), p.1171–1184.

Patel, K. D., Nollert, M. U. and McEver, R. P. (1995). P-selectin must extend a sufficient length from the plasma membrane to mediate rolling of neutrophils. *The Journal of cell biology*, 131 (6 Pt 2), p.1893–1902.

Patel, M., Keshavarzian, A., Kottapalli, V., Badie, B., Winship, D. and Fields, J. Z. (1996). Human neutrophil functions are inhibited in vitro by clinically relevant ethanol concentrations. *Alcoholism, clinical and experimental research*, 20 (2), p.275–283.

Patrick, Rullo, Beaudin, Liaw and Fox-Robichaud. (2007). Hepatic leukocyte recruitment in response to time-limited expression of TNF- and IL-1beta. *AJP: Gastrointestinal and Liver Physiology*, 293 (4), p.G663–G672. doi:10.1152/ajpgi.00070.2007.

Peppa, D., Micco, L., Javaid, A., Kennedy, P. T., Schurich, A., Dunn, C., Pallant, C., Ellis, G., Khanna, P., Dusheiko, G., Gilson, R. J. and Maini, M. K. (2010). Blockade of immunosuppressive cytokines restores NK cell antiviral function in chronic hepatitis B virus infection. *PLoS pathogens*, 6 (12), p.e1001227. doi:10.1371/journal.ppat.1001227.

Peranzoni, E., Zilio, S., Marigo, I., Dolcetti, L., Zanovello, P., Mandruzzato, S. and Bronte, V. (2010). Myeloid-derived suppressor cell heterogeneity and subset definition. *Current opinion in immunology*, 22 (2), p.238–244. doi:10.1016/j.coi.2010.01.021.

Petrasek, J., Csak, T., Ganz, M. and Szabo, G. (2013). Differences in innate immune signaling between alcoholic and non-alcoholic steatohepatitis. *Journal of Gastroenterology and Hepatology*, 28 (S1), p.93–98. doi:10.1111/jgh.12020.

Petrovic, A., Alpdogan, O., Willis, L., Eng, J., Greenberg, A., Kappel, B., Liu, C., Murphy, G., Heller, G. and van den Brink, M. (2004). LPAM (α4β7 integrin) is an important homing integrin on alloreactive T cells in the development of intestinal graft-versus-host disease. *Blood*, 103 (4), p.1542–1547. doi:10.1182/blood-2003-03-0957.

Phillipson, M, Heit, B, Parsons, SA and Petri, B. (2009). Vav1 is essential for mechanotactic crawling and migration of neutrophils out of the inflamed microvasculature. *The Journal of Immunology,* 182 (11), p.6870-6878. doi:10.4049/jimmunol.0803414.

Pillarisetty, V. G., Shah, A. B., Miller, G., Bleier, J. I. and DeMatteo, R. P. (2004). Liver dendritic cells are less immunogenic than spleen dendritic cells because of differences in subtype composition. *Journal of immunology*, 172 (2), p.1009–1017.

Politz, O., Gratchev, A., McCourt, P. A., Schledzewski, K., Guillot, P., Johansson, S., Svineng, G., Franke, P., Kannicht, C., Kzhyshkowska, J., Longati, P., Velten, F. W., Johansson, S. and Goerdt, S. (2002). Stabilin-1 and -2 constitute a novel family of fasciclin-like hyaluronan receptor homologues. *The Biochemical journal*, 362 (Pt 1), p.155–164.

Preiss, D. and Sattar, N. (2008). Non-alcoholic fatty liver disease: an overview of prevalence, diagnosis, pathogenesis and treatment considerations. *Clinical science*, 115 (5), p.141–150. doi:10.1042/CS20070402.

Puri, K. D., Doggett, T. A., Huang, C.-Y. Y., Douangpanya, J., Hayflick, J. S., Turner, M., Penninger, J. and Diacovo, T. G. (2005). The role of endothelial PI3Kgamma activity in neutrophil trafficking. *Blood*, 106 (1), p.150–157. doi:10.1182/blood-2005-01-0023.

Radziewicz, H, Ibegbu, CC and Fernandez, ML. (2007). Liver-infiltrating lymphocytes in chronic human hepatitis C virus infection display an exhausted phenotype with high levels of PD-1 and low levels of CD127 expression. *Journal of Virology,* 81 (6), p.2545-2553. doi:10.1128/JVI.02021-06.

Rahman, T. M. and Hodgson, H. J. (2000). Animal models of acute hepatic failure. *International journal of experimental pathology*, 81 (2), p.145–157. doi:10.1046/j.1365-2613.2000.00144.x.

Raimondi, L, Pirisino, R, Banchelli, G, Ignesti, G, Conforti, L and Buffoni, F. (1990). Cultured preadipocytes produce a semicarbazide-sensitive amine oxidase (SSAO) activity. *The Journal of Neural Transmission (supplementary),* 32, p.331–336. doi:10.1007/978-3-7091-9113-2_44.

Rakhmilevich, A. L. (1995). Neutrophils are essential for resolution of primary and secondary infection with Listeria monocytogenes. *Journal of leukocyte biology*, 57 (6), p.827–831.

Ramachandran, P., Pellicoro, A., Vernon, M. A., Boulter, L., Aucott, R. L., Ali, A., Hartland, S. N., Snowdon, V. K., Cappon, A., Gordon-Walker, T. T., Williams, M. J., Dunbar, D. R., Manning, J. R., van Rooijen, N., Fallowfield, J. A., Forbes, S. J. and Iredale, J. P. (2012). Differential Ly-6C expression identifies the recruited macrophage phenotype, which orchestrates the regression of murine liver fibrosis. *Proceedings of the National Academy of Sciences of the United States of America*, 109 (46), p.E3186–95. doi:10.1073/pnas.1119964109.

Ramaiah, S. K. and Jaeschke, H. (2007). Hepatic neutrophil infiltration in the pathogenesis of alcohol-induced liver injury. *Toxicology mechanisms and methods*, 17 (7), p.431–440. doi:10.1080/00952990701407702.

Rao, R. (2009). Endotoxemia and gut barrier dysfunction in alcoholic liver disease. *Hepatology*. doi:10.1002/hep.23009.

Reddy, J. K. (2001). III. Peroxisomal -oxidation, PPAR , and steatohepatitis. *American Journal of Physiology-Gastrointestinal and Liver Physiology*, 281 (6), p.G1333–G1339. http://ajpgi.physiology.org/content/281/6/G1333.short.

Remijsen, Kuijpers, Wirawan, Lippens, Vandenabeele and Berghe, V. (2011). Dying for a cause: NETosis, mechanisms behind an antimicrobial cell death modality. *Cell Death & Differentiation*, 18 (4), p.581–588. doi:10.1038/cdd.2011.1.

Rensen, S., Bieghs, V., Xanthoulea, S., Arfianti, E., Bakker, J., Shiri-Sverdlov, R., Hofker, M., Greve, J. and Buurman, W. (2012). Neutrophil-Derived Myeloperoxidase Aggravates Non-Alcoholic Steatohepatitis in Low-Density Lipoprotein Receptor-Deficient Mice. *PLoS ONE*, 7 (12), p.e52411. doi:10.1371/journal.pone.0052411.

Rensen, S., Slaats, Y., Nijhuis, J., Jans, A., Bieghs, V., Driessen, A., Malle, E., Greve, J. and Buurman, W. (2009). Increased Hepatic Myeloperoxidase Activity in Obese Subjects with Nonalcoholic Steatohepatitis. *The American Journal of Pathology*, 175 (4), p.1473–1482.

doi:10.2353/ajpath.2009.080999.

Reth, M. (2002). Hydrogen peroxide as second messenger in lymphocyte activation. *Nature immunology*, 3 (12), p.1129–1134. doi:10.1038/ni1202-1129.

Rhee. (2006). CELL SIGNALING: H2O2, a Necessary Evil for Cell Signaling. *Science*, 312 (5782), p.1882–1883. doi:10.1126/science.1130481.

Ringel, E. W., Soter, N. A. and Austen, K. F. (1984). Localization of histaminase to the specific granule of the human neutrophil. *Immunology*, 52 (4), p.649–658.

Rivera, C. A., Adegboyega, P., van Rooijen, N., Tagalicud, A., Allman, M. and Wallace, M. (2007). Toll-like receptor-4 signaling and Kupffer cells play pivotal roles in the pathogenesis of non-alcoholic steatohepatitis. *Journal of hepatology*, 47 (4), p.571–579. doi:10.1016/j.jhep.2007.04.019.

Rohrbach, A., Slade, D., Thompson, P. and Mowen, K. (2012). Activation of PAD4 in NET formation. *Frontiers in Immunology*, 3. doi:10.3389/fimmu.2012.00360.

Rose, S., Misharin, A. and Perlman, H. (2012). A novel Ly6C/Ly6G-based strategy to analyze the mouse splenic myeloid compartment. *Cytometry. Part A: the journal of the International Society for Analytical Cytology*, 81 (4), p.343–350. doi:10.1002/cyto.a.22012.

Roychowdhury, S., Chiang, D. J., McMullen, M. R. and Nagy, L. E. (2014). Moderate, chronic ethanol feeding exacerbates carbon-tetrachloride-induced hepatic fibrosis via hepatocyte-specific hypoxia inducible factor 1α. *Pharmacology research & perspectives*, 2 (5), p.e00061. doi:10.1002/prp2.61.

Ruch, R., Crist, K. and Klaunig, J. (1989). Effects of culture duration on hydrogen peroxide-induced hepatocyte toxicity. *Toxicology and Applied Pharmacology*, 100 (3), p.451–464. doi:10.1016/0041-008X(89)90293-7.

Saba, AB, Oyagbemi, AA and Azeez, OI. (2010). Amelioration of carbon tetrachloride-induced hepatotoxicity and haemotoxicity by aqueous leaf extract of Cnidoscolus aconitifolius in rats. *Nigerian Journal of Physiological Sciences*. 25 (2), p.139-147.

Sakamoto, S., Okanoue, T., Itoh, Y., Sakamoto, K., Nishioji, K., Nakagawa, Y., Yoshida, N., Yoshikawa, T. and Kashima, K. (1997). Intercellular adhesion molecule-1 and CD18 are involved in neutrophil adhesion and its cytotoxicity to cultured sinusoidal endothelial cells in rats. *Hepatology*, 26 (3), p.658–663. doi:10.1053/jhep.1997.v26.pm0009303496.

Sallisalmi, M., Tenhunen, J., Yang, R., Oksala, N. and Pettilä, V. (2012). Vascular adhesion protein-1 and syndecan-1 in septic shock. *Acta anaesthesiologica Scandinavica*, 56 (3), p.316–322. doi:10.1111/j.1399-6576.2011.02578.x.

Salmi, M and Jalkanen, S. (1992a). A 90-kilodalton endothelial cell molecule mediating lymphocyte binding in humans. *Science*, 257 (5075), p.1407-1409.

Salmi, Hellman and Jalkanen. (1998). The role of two distinct endothelial molecules, vascular adhesion protein-1 and peripheral lymph node addressin, in the binding of lymphocyte subsets to human lymph nodes. *Journal of immunology*, 160 (11), p.5629–5636.

Salmi and Jalkanen. (1996). Human vascular adhesion protein 1 (VAP-1) is a unique sialoglycoprotein that mediates carbohydrate-dependent binding of lymphocytes to endothelial cells. *The Journal of experimental medicine*, 183 (2), p.569–579.

Salmi, Kalimo and Jalkanen. (1993). Induction and function of vascular adhesion protein-1 at sites of inflammation. *The Journal of Experimental Medicine*, 178 (6), p.2255–2260. doi:10.1084/jem.178.6.2255.

Salmi, M. and Jalkanen, S. (1992b). A 90-kilodalton endothelial cell molecule mediating lymphocyte binding in humans. *Science*, 257 (5075), Science, p.1407–1409.

Salmi, M. and Jalkanen, S. (1995). Different forms of human vascular adhesion protein 1 (VAP 1)

in blood vessels in vivo and in cultured endothelial cells: implications for lymphocyte endothelial cell adhesion models. *European journal of immunology*, 25 (10), p.2803–2812. doi:10.1002/eji.1830251014.

Salmi, M. and Jalkanen, S. (2001). VAP-1: an adhesin and an enzyme. *Trends in immunology*, 22 (4), p.211–216.

Salmi, M. and Jalkanen, S. (2006). Developmental regulation of the adhesive and enzymatic activity of vascular adhesion protein-1 (VAP-1) in humans. *Blood*, 108 (5), p.1555–1561. doi:10.1182/blood-2005-11-4599.

Salmi, M., Smith, D. J., Bono, P., Leu, T., Hellman, J., Matikainen, M. T. and Jalkanen, S. (1997a). A mouse molecular mimic of human vascular adhesion protein-1. *Molecular immunology*, 34 (16-17), p.1227–1236.

Salmi, M., Tohka, S., Berg, E. L., Butcher, E. C. and Jalkanen, S. (1997b). Vascular adhesion protein 1 (VAP-1) mediates lymphocyte subtype-specific, selectin-independent recognition of vascular endothelium in human lymph nodes. *The Journal of experimental medicine*, 186 (4), p.589–600.

Salmi, M., Yegutkin, G. G., Lehvonen, R., Koskinen, K., Salminen, T. and Jalkanen, S. (2001). A cell surface amine oxidase directly controls lymphocyte migration. *Immunity*, 14 (3), p.265–276. doi:10.1016/S1074-7613(01)00108-X.

Salmi, Rajala and Jalkanen. (1997c). Homing of mucosal leukocytes to joints. Distinct endothelial ligands in synovium mediate leukocyte-subtype specific adhesion. *The Journal of clinical investigation*, 99 (9), p.2165–2172. doi:10.1172/JCI119389.

Salmi, Tohka and Jalkanen. (2000a). Human Vascular Adhesion Protein-1 (VAP-1) Plays a Critical Role in Lymphocyte-Endothelial Cell Adhesion Cascade Under Shear. *Circulation Research*, 86 (12), p.1245–1251. doi:10.1161/01.RES.86.12.1245.

Salmi, Tohka and Jalkanen. (2000b). Human Vascular Adhesion Protein-1 (VAP-1) Plays a Critical Role in Lymphocyte-Endothelial Cell Adhesion Cascade Under Shear. *Circulation Research*, 86 (12), p.1245–1251. doi:10.1161/01.RES.86.12.1245.

Salminen, T. A., Smith, D. J., Jalkanen, S. and Johnson, M. S. (1998). Structural model of the catalytic domain of an enzyme with cell adhesion activity: human vascular adhesion protein-1 (HVAP-1) D4 domain is an amine oxidase. *Protein engineering*, 11 (12), p.1195–1204.

Salter-Cid, L. M., Wang, E., O'Rourke, A. M., Miller, A., Gao, H., Huang, L., Garcia, A. and Linnik, M. D. (2005). Anti-inflammatory effects of inhibiting the amine oxidase activity of semicarbazide-sensitive amine oxidase. *The Journal of pharmacology and experimental therapeutics*, 315 (2), p.553–562. doi:10.1124/jpet.105.089649.

Santoso, S., Sachs, U. J., Kroll, H., Linder, M., Ruf, A., Preissner, K. T. and Chavakis, T. (2002). The junctional adhesion molecule 3 (JAM-3) on human platelets is a counterreceptor for the leukocyte integrin Mac-1. *The Journal of experimental medicine*, 196 (5), p.679–691. doi:10.1084/jem.20020267.

Sarra, M., Cupi, M., Bernardini, R., Ronchetti, G., Monteleone, I., Ranalli, M., Franzè, E., Rizzo, A., Colantoni, A., Caprioli, F., Maggioni, M., Gambacurta, A., Mattei, M., Macdonald, T., Pallone, F. and Monteleone, G. (2013). IL-25 prevents and cures fulminant hepatitis in mice through a myeloid-derived suppressor cell-dependent mechanism. *Hepatology*, 58 (4), p.1436–1450. doi:10.1002/hep.26446.

Sato, T., Habtezion, A., Beilhack, A., Schulz, S., Butcher, E. and Thorlacius, H. (2006). Short-term homing assay reveals a critical role for lymphocyte function-associated antigen-1 in the hepatic recruitment of lymphocytes in graft-versus-host disease. *Journal of Hepatology*, 44 (6), p.1132–1140. doi:10.1016/j.jhep.2005.11.042.

Schenkel, A. R., Mamdouh, Z. and Muller, W. A. (2004). Locomotion of monocytes on endothelium

is a critical step during extravasation. *Nature immunology*, 5 (4), p.393–400. doi:10.1038/ni1051.

Schildberg, F. A., Hegenbarth, S. I., Schumak, B., Scholz, K., Limmer, A. and Knolle, P. A. (2008). Liver sinusoidal endothelial cells veto CD8 T cell activation by antigen-presenting dendritic cells. *European journal of immunology*, 38 (4), p.957–967. doi:10.1002/eji.200738060.

Schilter, H., Collison, A., Russo, R., Foot, J., Yow, T., Vieira, A., Tavares, L., Mattes, J., Teixeira, M. and Jarolimek, W. (2015). Effects of an anti-inflammatory VAP-1/SSAO inhibitor, PXS-4728A, on pulmonary neutrophil migration. *Respiratory Research*, 16 (1). doi:10.1186/s12931-015-0200-z.

Schnoor, M., Lai, F. P., Zarbock, A., Kläver, R., Polaschegg, C., Schulte, D., Weich, H. A., Oelkers, J. M., Rottner, K. and Vestweber, D. (2011). Cortactin deficiency is associated with reduced neutrophil recruitment but increased vascular permeability in vivo. *The Journal of experimental medicine*, 208 (8), p.1721–1735. doi:10.1084/jem.20101920.

Schrage, A., Wechsung, K., Neumann, K., Schumann, M., Schulzke, J.-D., Engelhardt, B., Zeitz, M., Hamann, A. and Klugewitz, K. (2008). Enhanced T cell transmigration across the murine liver sinusoidal endothelium is mediated by transcytosis and surface presentation of chemokines. *Hepatology*, 48 (4), p.1262–1272. doi:10.1002/hep.22443.

Schulte, D., Küppers, V., Dartsch, N., Broermann, A., Li, H., Zarbock, A., Kamenyeva, O., Kiefer, F., Khandoga, A., Massberg, S. and Vestweber, D. (2011). Stabilizing the VE-cadherin-catenin complex blocks leukocyte extravasation and vascular permeability. *The EMBO journal*, 30 (20), p.4157–4170. doi:10.1038/emboj.2011.304.

Schurich, A., Böttcher, J. P., Burgdorf, S., Penzler, P., Hegenbarth, S., Kern, M., Dolf, A., Endl, E., Schultze, J., Wiertz, E., Stabenow, D., Kurts, C. and Knolle, P. (2009). Distinct kinetics and dynamics of cross-presentation in liver sinusoidal endothelial cells compared to dendritic cells. *Hepatology*, 50 (3), p.909–919. doi:10.1002/hep.23075.

Schurich, A., Khanna, P., Lopes, A. R., Han, K. J., Peppa, D., Micco, L., Nebbia, G., Kennedy, P. T., Geretti, A.-M. M., Dusheiko, G. and Maini, M. K. (2011). Role of the coinhibitory receptor cytotoxic T lymphocyte antigen-4 on apoptosis-Prone CD8 T cells in persistent hepatitis B virus infection. *Hepatology*, 53 (5), p.1494–1503. doi:10.1002/hep.24249.

Schwelberger. (2010). Structural organization of mammalian copper-containing amine oxidase genes. *Inflammation Research*, 59 (S2), p.223–225. doi:10.1007/s00011-009-0135-2.

Schwelberger, H. G. (2007). The origin of mammalian plasma amine oxidases. *Journal of neural transmission*, 114 (6), p.757–762. doi:10.1007/s00702-007-0684-x.

Scoazec, J.-Y. and Feldmann, G. (1994). The cell adhesion molecules of hepatic sinusoidal endothelial cells. *Journal of Hepatology*, 20 (2), p.296–300. doi:10.1016/S0168-8278(05)80072-8.

Sebode, M., Peiseler, M., Franke, B., Schwinge, D., Schoknecht, T., Wortmann, F., Quaas, A., Petersen, B.-S., Ellinghaus, E., Baron, U., Olek, S., Wiegard, C., Weiler-Normann, C., Lohse, A., Herkel, J. and Schramm, C. (2014). Reduced FOXP3+ regulatory T cells in patients with primary sclerosing cholangitis are associated with IL2RA gene polymorphisms. *Journal of Hepatology*, 60 (5), p.1010–1016. doi:10.1016/j.jhep.2013.12.027.

Seki, E. and Brenner, D. A. (2008). Toll-like receptors and adaptor molecules in liver disease: update. *Hepatology*, 48 (1), p.322–335. doi:10.1002/hep.22306.

Senoo, H. (2004). Structure and function of hepatic stellate cells. *Medical electron microscopy : official journal of the Clinical Electron Microscopy Society of Japan*, 37 (1), p.3–15. doi:10.1007/s00795-003-0230-3.

Sharma, P., Kumar, A., Sharma, B. C. and Sarin, S. K. (2009). Infliximab monotherapy for severe alcoholic hepatitis and predictors of survival: an open label trial. *Journal of hepatology*, 50

(3), p.584–591. doi:10.1016/j.jhep.2008.10.024.

Shattil, S. J. (2005). Integrins and Src: dynamic duo of adhesion signaling. *Trends in cell biology*, 15 (8), p.399–403. doi:10.1016/j.tcb.2005.06.005.

Shawcross, D. L., Wright, G. A., Stadlbauer, V., Hodges, S. J., Davies, N. A., Wheeler-Jones, C., Pitsillides, A. A. and Jalan, R. (2008). Ammonia impairs neutrophil phagocytic function in liver disease. *Hepatology*, 48 (4), p.1202–1212. doi:10.1002/hep.22474.

Shen, S., Wertz, D. and Klinman, J. (2012). Implication for Functions of the Ectopic Adipocyte Copper Amine Oxidase (AOC3) from Purified Enzyme and Cell-Based Kinetic Studies. *PLoS ONE*, 7 (1), p.e29270. doi:10.1371/journal.pone.0029270.

Sheth, K. and Bankey, P. (2001). The liver as an immune organ. *Current opinion in critical care*, 7 (2), p.99–104.

Shetty, S., Weston, C., Adams, D. and Lalor, P. (2014). A Flow Adhesion Assay to Study Leucocyte Recruitment to Human Hepatic Sinusoidal Endothelium Under Conditions of Shear Stress. *Journal of Visualized Experiments : JoVE*, (85), p.51330. doi:10.3791/51330.

Shetty, S., Weston, C., Oo, Y., Westerlund, N., Stamataki, Z., Youster, J., Hubscher, S., Salmi, M., Jalkanen, S., Lalor, P. and Adams, D. (2011). Common lymphatic endothelial and vascular endothelial receptor-1 mediates the transmigration of regulatory T cells across human hepatic sinusoidal endothelium. *Journal of immunology*, 186 (7), p.4147–4155. doi:10.4049/jimmunol.1002961.

Shi, J, Aisaki, K, Ikawa, Y and Wake, K. (1998). Evidence of hepatocyte apoptosis in rat liver after the administration of carbon tetrachloride. *The American journal of pathology*. 153 (2), p.515-525.

Shi, H., Dong, L., Zhang, Y., Bai, Y., Zhao, J. and Zhang, L. (2010). Protective effect of a coffee preparation (Nescafe pure) against carbon tetrachloride-induced liver fibrosis in rats. *Clinical nutrition*, 29 (3), p.399–405. doi:10.1016/j.clnu.2009.12.007.

Shi, M., Wei, G., Pan, W. and Tabel, H. (2004). Trypanosoma congolense infections: antibody-mediated phagocytosis by Kupffer cells. *Journal of leukocyte biology*, 76 (2), p.399–405. doi:10.1189/jlb.1003500.

Shih, Y.-H., Chang, K.-W., Chen, M., Yu, C.-C., Lin, D.-J., Hsia, S.-M., Huang, H.-L. and Shieh, T.-M. (2013). Lysyl oxidase and enhancement of cell proliferation and angiogenesis in oral squamous cell carcinoma. *Head & Neck*, 35 (2), p.250–256. doi:10.1002/hed.22959.

Shim, S. G., Jun, D. W., Kim, E. K., Saeed, W. K., Lee, K. N., Lee, H. L., Lee, O. Y., Choi, H. S. and Yoon, B. C. (2013). Caffeine attenuates liver fibrosis via defective adhesion of hepatic stellate cells in cirrhotic model. *Journal of gastroenterology and hepatology*, 28 (12), p.1877–1884. doi:10.1111/jgh.12317.

Shin, E.-C. C., Sung, P. S. and Park, S.-H. H. (2016). Immune responses and immunopathology in acute and chronic viral hepatitis. *Nature reviews. Immunology*, 16 (8), p.509–523. doi:10.1038/nri.2016.69.

Shiratori, Y., Takada, H., Hikiba, Y., Nakata, R., Okano, K., Komatsu, Y., Niwa, Y., Matsumura, M., Shiina, S. and Omata, M. (1993). Production of chemotactic factor, interleukin-8, from hepatocytes exposed to ethanol. *Hepatology*, 18 (6), p.1477–1482.

Shulman, Shinder, Klein, Grabovsky and Yeger. (2009). Lymphocyte crawling and transendothelial migration require chemokine triggering of high-affinity LFA-1 integrin. *Immunity,* 30 (3), p.384-396. doi:10.1016/j.immuni.2008.12.020.

Silvola, J. M., Virtanen, H., Siitonen, R., Hellberg, S., Liljenbäck, H., Metsälä, O., Ståhle, M., Saanijoki, T., Käkelä, M., Hakovirta, H., Ylä-Herttuala, S., Saukko, P., Jauhiainen, M., Veres, T. Z., Jalkanen, S., Knuuti, J., Saraste, A. and Roivainen, A. (2016). Leukocyte trafficking-associated vascular adhesion protein 1 is expressed and functionally active in

atherosclerotic plaques. *Scientific reports*, 6, p.35089. doi:10.1038/srep35089.

Simon, S. I., Hu, Y., Vestweber, D. and Smith, C. W. (2000). Neutrophil tethering on E-selectin activates beta 2 integrin binding to ICAM-1 through a mitogen-activated protein kinase signal transduction pathway. *Journal of immunology*, 164 (8), p.4348–4358.

Singbartl, K., Thatte, J., Smith, M. L., Wethmar, K., Day, K. and Ley, K. (2001). A CD2-green fluorescence protein-transgenic mouse reveals very late antigen-4-dependent CD8+ lymphocyte rolling in inflamed venules. *Journal of immunology*, 166 (12), p.7520–7526.

Singh, B., Tschernig, T., van Griensven, M., Fieguth, A. and Pabst, R. (2003). Expression of vascular adhesion protein-1 in normal and inflamed mice lungs and normal human lungs. *Virchows Archiv : an international journal of pathology*, 442 (5), p.491–495. doi:10.1007/s00428-003-0802-6.

Sitia, G., Iannacone, M., Aiolfi, R., Isogawa, M., van Rooijen, N., Scozzesi, C., Bianchi, M., von Andrian, U., Chisari, F. and Guidotti, L. (2011). Kupffer Cells Hasten Resolution of Liver Immunopathology in Mouse Models of Viral Hepatitis. *PLoS Pathogens*, 7 (6), plos, p.e1002061. doi:10.1371/journal.ppat.1002061.

Slaba, I., Wang, J., Kolaczkowska, E., McDonald, B., Lee, W.-Y. Y. and Kubes, P. (2015). Imaging the dynamic platelet-neutrophil response in sterile liver injury and repair in mice. *Hepatology*, 62 (5), p.1593–1605. doi:10.1002/hep.28003.

Slater, T. F., Sträuli, U. D. and Sawyer, B. C. (1964). Changes in liver nucleotide concentrations in experimental liver injury. 1. Carbon tetrachloride poisoning. *The Biochemical journal*, 93 (2), p.260–266.

Smedsrød, B., Pertoft, H., Gustafson, S. and Laurent, T. C. (1990). Scavenger functions of the liver endothelial cell. *The Biochemical journal*, 266 (2), p.313–327.

Smith, D. J., Salmi, M., Bono, P., Hellman, J., Leu, T. and Jalkanen, S. (1998). Cloning of vascular adhesion protein 1 reveals a novel multifunctional adhesion molecule. *The Journal of experimental medicine*, 188 (1), p.17–27. doi:10.1084/jem.188.1.17.

Smith-Mungo, L. I. and Kagan, H. M. (1998). Lysyl oxidase: properties, regulation and multiple functions in biology. *Matrix biology : journal of the International Society for Matrix Biology*, 16 (7), p.387–398.

Solé, M. and Unzeta, M. (2011). Vascular cell lines expressing SSAO/VAP-1: a new experimental tool to study its involvement in vascular diseases. *Biology of the cell*, 103 (11), p.543–557. doi:10.1042/BC20110049.

Son, G., Kremer, M. and Hines, I. N. (2010). Contribution of gut bacteria to liver pathobiology. *Gastroenterology research and practice*, 2010. doi:10.1155/2010/453563.

Sookhai, S., Wang, J. H., Winter, D., Power, C., Kirwan, W. and Redmond, H. P. (2000). Dopamine attenuates the chemoattractant effect of interleukin-8: a novel role in the systemic inflammatory response syndrome. *Shock*, 14 (3), p.295–299.

Souto, R., Vallega, G., Wharton, J., Vinten, J., Tranum-Jensen, J. and Pilch, P. (2003). Immunopurification and Characterization of Rat Adipocyte Caveolae Suggest Their Dissociation from Insulin Signaling. *Journal of Biological Chemistry*, 278 (20), p.18321–18329. doi:10.1074/jbc.m211541200.

Spahr, L., Rubbia-Brandt, L., Frossard, J.-L. L., Giostra, E., Rougemont, A.-L. L., Pugin, J., Fischer, M., Egger, H. and Hadengue, A. (2002). Combination of steroids with infliximab or placebo in severe alcoholic hepatitis: a randomized controlled pilot study. *Journal of hepatology*, 37 (4), p.448–455.

Spencer, M., Hamp, T., Reid, R., Fischer, L., Zeisel, S. and Fodor, A. (2011). Association Between Composition of the Human Gastrointestinal Microbiome and Development of Fatty Liver With Choline Deficiency. *Gastroenterology*, 140 (3), p.976–986.

doi:10.1053/j.gastro.2010.11.049.

Spruss, A., Kanuri, G., Wagnerberger, S., Haub, S., Bischoff, S. C. and Bergheim, I. (2009). Toll-like receptor 4 is involved in the development of fructose-induced hepatic steatosis in mice. *Hepatology,* 50 (4), p.1094–1104. doi:10.1002/hep.23122.

Starkel, P. and Leclercq, I. A. (2011). Animal models for the study of hepatic fibrosis. *Best practice & research. Clinical gastroenterology*, 25 (2), p.319–333. doi:10.1016/j.bpg.2011.02.004.

Steinberg and Grinstein. (2007). Unconventional Roles of the NADPH Oxidase: Signaling, Ion Homeostasis, and Cell Death. *Science's STKE*, 2007 (379), p.pe11–pe11. doi:10.1126/stke.3792007pe11.

Steinhoff, G., Behrend, M., Schrader, B., Duijvestijn, A. M. and Wonigeit, K. (1993). Expression patterns of leukocyte adhesion ligand molecules on human liver endothelia. Lack of ELAM-1 and CD62 inducibility on sinusoidal endothelia and distinct distribution of VCAM-1, ICAM-1, ICAM-2, and LFA-3. *The American journal of pathology*, 142 (2), p.481–488.

Stolen, C. M., Yegutkin, G. G., Kurkijärvi, R., Bono, P., Alitalo, K. and Jalkanen, S. (2004). Origins of serum semicarbazide-sensitive amine oxidase. *Circulation research*, 95 (1), p.50–57. doi:10.1161/01.RES.0000134630.68877.2F.

Stolen, C., Marttila-Ichihara, F., Koskinen, K., Yegutkin, G., Turja, R., Bono, P., Skurnik, M., Hänninen, A., Jalkanen, S. and Salmi, M. (2005). Absence of the endothelial oxidase AOC3 leads to abnormal leukocyte traffic in vivo. *Immunity*, 22 (1), p.105–115. doi:10.1016/j.immuni.2004.12.006.

Stone, J. R. and Collins, T. (2002). The role of hydrogen peroxide in endothelial proliferative responses. *Endothelium : journal of endothelial cell research*, 9 (4), p.231–238.

Sutti, S., Jindal, A., Locatelli, I., Vacchiano, M., Gigliotti, L., Bozzola, C. and Albano, E. (2014). Adaptive immune responses triggered by oxidative stress contribute to hepatic inflammation in NASH. *Hepatology*, 59 (3), p.886–897. doi:10.1002/hep.26749.

Syn, W.-K. K., Oo, Y. H., Pereira, T. A., Karaca, G. F., Jung, Y., Omenetti, A., Witek, R. P., Choi, S. S., Guy, C. D., Fearing, C. M., Teaberry, V., Pereira, F. E., Adams, D. H. and Diehl, A. M. (2010). Accumulation of natural killer T cells in progressive nonalcoholic fatty liver disease. *Hepatology*, 51 (6), p.1998–2007. doi:10.1002/hep.23599.

Szabo, G. and Csak, T. (2012). Inflammasomes in liver diseases. *Journal of hepatology*, 57 (3), p.642–654. doi:10.1016/j.jhep.2012.03.035.

Szabo, G., Mandrekar, P., Girouard, L. and Catalano, D. (1996). Regulation of human monocyte functions by acute ethanol treatment: decreased tumor necrosis factor-alpha, interleukin-1 beta and elevated interleukin-10, and transforming growth factor-beta production. *Alcoholism, clinical and experimental research*, 20 (5), p.900–907.

Sørensen, K. K., Simon-Santamaria, J., McCuskey, R. S. and Smedsrød, B. (2015). Liver Sinusoidal Endothelial Cells. *Comprehensive Physiology*, 5 (4), p.1751–1774. doi:10.1002/cphy.c140078.

Tábi, T., Szökő, E., Mérey, A., Tóth, V., Mátyus, P. and Gyires, K. (2013). Study on SSAO enzyme activity and anti-inflammatory effect of SSAO inhibitors in animal model of inflammation. *Journal of neural transmission*, 120 (6), p.963–967. doi:10.1007/s00702-012-0961-1.

Tabibian, J. H., Masyuk, A. I., Masyuk, T. V., O'Hara, S. P. and LaRusso, N. F. (2013). Physiology of cholangiocytes. *Comprehensive Physiology*, 3 (1), p.541–565. doi:10.1002/cphy.c120019.

Taïeb, J., Delarche, C., Ethuin, F., Selloum, S., Poynard, T., Gougerot-Pocidalo, M.-A. A. and Chollet-Martin, S. (2002). Ethanol-induced inhibition of cytokine release and protein degranulation in human neutrophils. *Journal of leukocyte biology*, 72 (6), p.1142–1147.

Tajiri, K., Shimizu, Y., Tsuneyama, K. and Sugiyama, T. (2009). Role of liver-infiltrating

CD3+CD56+ natural killer T cells in the pathogenesis of nonalcoholic fatty liver disease. *European journal of gastroenterology & hepatology*, 21 (6), p.673–680. doi:10.1097/MEG.0b013e32831bc3d6.

Takagi. (2004). Structural basis for ligand recognition by RGD (Arg-Gly-Asp)-dependent integrins. *Biochemical Society Transactions*, 32 (3), p.403–406. doi:10.1042/BST0320403.

Takai, S., Kimura, K., Nagaki, M., Satake, S., Kakimi, K. and Moriwaki, H. (2005). Blockade of neutrophil elastase attenuates severe liver injury in hepatitis B transgenic mice. *Journal of virology*, 79 (24), p.15142–15150. doi:10.1128/JVI.79.24.15142-15150.2005.

Tamura, Adachi, Osuga, J. -i., Ohashi, Yahagi, Sekiya, Okazaki, Tomita, Iizuka, Shimano, Nagai, Kimura, Tsujimoto and Ishibashi. (2003). FEEL-1 and FEEL-2 Are Endocytic Receptors for Advanced Glycation End Products. *Journal of Biological Chemistry*, 278 (15), p.12613–12617. doi:10.1074/jbc.M210211200.

Tanaka, S., Tanaka, T., Kawakami, T., Takano, H., Sugahara, M., Saito, H., Higashijima, Y., Yamaguchi, J., Inagi, R. and Nangaku, M. (2017). Vascular adhesion protein-1 enhances neutrophil infiltration by generation of hydrogen peroxide in renal ischemia/reperfusion injury. *Kidney International*. doi:10.1016/j.kint.2017.01.014.

Tanaka, Y., Adams, D. H., Hubscher, S., Hirano, H., Siebenlist, U. and Shaw, S. (1993). T-cell adhesion induced by proteoglycan-immobilized cytokine MIP-1 beta. *Nature*, 361 (6407), p.79–82. doi:10.1038/361079a0.

Tavassoli, M., Kishimoto, T. and Kataoka, M. (1986). Liver endothelium mediates the hepatocyte's uptake of ceruloplasmin. *The Journal of cell biology*, 102 (4), p.1298–1303.

Tedder, T. F., Steeber, D. A., Chen, A. and Engel, P. (1995). The selectins: vascular adhesion molecules. *FASEB journal : official publication of the Federation of American Societies for Experimental Biology*, 9 (10), p.866–873.

Tessier, G., Villeneuve, E. and Villeneuve, J.-P. P. (2002). Etiology and outcome of acute liver failure: experience from a liver transplantation centre in Montreal. *Canadian journal of gastroenterology*, 16 (10), p.672–676.

Tetri, LH, Basaranoglu, M and Brunt, EM. (2008). Severe NAFLD with hepatic necroinflammatory changes in mice fed trans fats and a high-fructose corn syrup equivalent. *American Journal of Physiology-Gastrointestinal and Liver Physiology*. 295 (5), p.G987-995. doi:10.1152/ajpgi.90272.2008.

Thomson, A. W. and Knolle, P. A. (2010). Antigen-presenting cell function in the tolerogenic liver environment. *Nature reviews. Immunology*, 10 (11), p.753–766. doi:10.1038/nri2858.

Tilg, H., Jalan, R., Kaser, A., Davies, N. A., Offner, F. A., Hodges, S. J., Ludwiczek, O., Shawcross, D., Zoller, H., Alisa, A., Mookerjee, R. P., Graziadei, I., Datz, C., Trauner, M., Schuppan, D., Obrist, P., Vogel, W. and Williams, R. (2003). Anti-tumor necrosis factor-alpha monoclonal antibody therapy in severe alcoholic hepatitis. *Journal of hepatology*, 38 (4), p.419–425.

Tipton, KF and Benedetti, S. M. (2001). Amine oxidases and the metabolism of xenobiotics. *Enzyme systems that metabolise drugs and other xenobiotics*. Wiley, Chichester, UK, p.95-146.

Tipton, KF, O'sullivan, MI and Davey, GP. (2003). It can be a complicated life being an enzyme. *Biochemical Society Transactions*. 31 (3), p.711-715. doi:10.1042/bst0310711.

Tjandra, K, Sharkey, KA and Swain, MG. (2000). Progressive development of a Th1-type hepatic cytokine profile in rats with experimental cholangitis. *Hepatology*. doi:10.1002/hep.510310204.

Toiyama, Y., Miki, C., Inoue, Y., Kawamoto, A. and Kusunoki, M. (2009). Circulating form of human vascular adhesion protein-1 (VAP-1): decreased serum levels in progression of colorectal cancer and predictive marker of lymphatic and hepatic metastasis. *Journal of surgical oncology*, 99 (6), p.368–372. doi:10.1002/jso.21246.

Tokita, D., Sumpter, T. L., Raimondi, G., Zahorchak, A. F., Wang, Z., Nakao, A., Mazariegos, G. V., Abe, M. and Thomson, A. W. (2008). Poor allostimulatory function of liver plasmacytoid DC is associated with pro-apoptotic activity, dependent on regulatory T cells. *Journal of hepatology*, 49 (6), p.1008–1018. doi:10.1016/j.jhep.2008.07.028.

Toriumi, K., Horikoshi, Y., Yoshiyuki Osamura, R., Yamamoto, Y., Nakamura, N. and Takekoshi, S. (2013). Carbon tetrachloride-induced hepatic injury through formation of oxidized diacylglycerol and activation of the PKC/NF-κB pathway. *Laboratory investigation; a journal of technical methods and pathology*, 93 (2), p.218–229. doi:10.1038/labinvest.2012.145.

Torres, D. M. and Harrison, S. A. (2013). Is it time to write a prescription for coffee? Coffee and liver disease. *Gastroenterology*, 144 (4), p.670–672. doi:10.1053/j.gastro.2013.02.015.

Trivedi, P. J., Tickle, J., Vesterhus, M. N., Eddowes, P. J., Bruns, T., Vainio, J., Parker, R., Smith, D., Liaskou, E., Thorbjørnsen, L. W., Hirschfield, G. M., Auvinen, K., Hubscher, S. G., Salmi, M., Adams, D. H. and Weston, C. J. (2017). Vascular adhesion protein-1 is elevated in primary sclerosing cholangitis, is predictive of clinical outcome and facilitates recruitment of gut-tropic lymphocytes to liver in a substrate-dependent manner. *Gut*. doi:10.1136/gutjnl-2016-312354.

Tsukamoto, H., French, S. W., Benson, N., Delgado, G., Rao, G. A., Larkin, E. C. and Largman, C. (1985). Severe and progressive steatosis and focal necrosis in rat liver induced by continuous intragastric infusion of ethanol and low fat diet. *Hepatology*, 5 (2), p.224–232.

Tuncer, C., Oo, Y., Murphy, N., Adams, D. and Lalor, P. (2013). The regulation of T-cell recruitment to the human liver during acute liver failure. *Liver international : official journal of the International Association for the Study of the Liver*, 33 (6), p.852–863. doi:10.1111/liv.12182.

Uhrig, A., Banafsche, R., Kremer, M., Hegenbarth, S., Hamann, A., Neurath, M., Gerken, G., Limmer, A. and Knolle, P. A. (2005). Development and functional consequences of LPS tolerance in sinusoidal endothelial cells of the liver. *Journal of leukocyte biology*, 77 (5), p.626–633. doi:10.1189/jlb.0604332.

Urban, C., Ermert, D., Schmid, M., Abu-Abed, U., Goosmann, C., Nacken, W., Brinkmann, V., Jungblut, P. and Zychlinsky, A. (2009). Neutrophil Extracellular Traps Contain Calprotectin, a Cytosolic Protein Complex Involved in Host Defense against Candida albicans. *PLoS Pathogens*, 5 (10), p.e1000639. doi:10.1371/journal.ppat.1000639.

Urbani, S, Amadei, B, Fisicaro, P and Pilli, M. (2005). Heterologous T cell immunity in severe hepatitis C virus infection. *The Journal of Experimental Medicine,* 201 (5), p. 675-680. doi:10.1084/jem.20041058.

Vainio, P., Kortekangas-Savolainen, O., Mikkola, J., Jaakkola, K., Kalimo, K., Jalkanen, S. and Veromaa, T. (2005). Safety of Blocking Vascular Adhesion Protein-1 in Patients with Contact Dermatitis. *Basic & Clinical Pharmacology & Toxicology*, 96 (6), p.429–435. doi:10.1111/j.1742-7843.2005.pto_96605.x.

Valente, T., Solé, M. and Unzeta, M. (2008). SSAO/VAP-1 protein expression during mouse embryonic development. *Developmental dynamics : an official publication of the American Association of Anatomists*, 237 (9), p.2585–2593. doi:10.1002/dvdy.21682.

Verma, S., Szmitko, P. and Ridker, P. (2005). C-reactive protein comes of age. *Nature Clinical Practice Cardiovascular Medicine*, 2 (1), p.29–36. doi:10.1038/ncpcardio0074.

Vierling, J. M. (2001). Animal models for primary sclerosing cholangitis. *Best practice & research. Clinical gastroenterology*, 15 (4), p.591–610. doi:10.1053/bega.2001.0207.

Volpes, R., van den Oord, J. and Desmet, V. (1992). Vascular adhesion molecules in acute and chronic liver inflammation. *Hepatology*, 15 (2), p.269–275. doi:10.1002/hep.1840150216.

Wakabayashi, K., Yoshida, K., Leung, P. S., Moritoki, Y., Yang, G.-X. X., Tsuneyama, K., Lian, Z.-

X. X., Hibi, T., Ansari, A. A., Wicker, L. S., Ridgway, W. M., Coppel, R. L., Mackay, I. R. and Gershwin, M. E. (2009). Induction of autoimmune cholangitis in non-obese diabetic (NOD).1101 mice following a chemical xenobiotic immunization. *Clinical and experimental immunology*, 155 (3), p.577–586. doi:10.1111/j.1365-2249.2008.03837.x.

Wallace, Hamesch, Lunova, Kim, Weiskirchen, Strnad and Friedman. (2015). Standard Operating Procedures in Experimental Liver Research: Thioacetamide model in mice and rats. *Laboratory Animals*, 49 (1 Suppl), p.21–29. doi:10.1177/0023677215573040.

Wang, E., Gao, H., Salter-Cid, L., Zhang, J., Huang, L., Podar, E., Miller, A., Zhao, J., O'Rourk, A. and Linnik, M. (2006a). Design, Synthesis, and Biological Evaluation of Semicarbazide-Sensitive Amine Oxidase (SSAO) Inhibitors with Anti-inflammatory Activity. *Journal of Medicinal Chemistry*, 49 (7), p.2166–2173. doi:10.1021/jm050538l.

Wang, J.-H. H., Batey, R.-G. G. and George, J. (2006b). Role of ethanol in the regulation of hepatic stellate cell function. *World journal of gastroenterology*, 12 (43), p.6926–6932.

Wang, S. and Yuan-de, QW. (2001). Role of Hydrogen Peroxide in Promoting Proliferation and Transformation of Rat Liver Oval Cell Line *Acta Academiae Medicinae Sinicae*. 23 (4), p.346-350.

Wang, Y., Li, M., Stadler, S., Correll, S., Li, P., Wang, D., Hayama, R., Leonelli, L., Han, H., Grigoryev, S. A., Allis, C. D. and Coonrod, S. A. (2009). Histone hypercitrullination mediates chromatin decondensation and neutrophil extracellular trap formation. *The Journal of cell biology*, 184 (2), p.205–213. doi:10.1083/jcb.200806072.

Wang, Y., Wysocka, J., Sayegh, J., Lee, Y.-H. H., Perlin, J. R., Leonelli, L., Sonbuchner, L. S., McDonald, C. H., Cook, R. G., Dou, Y., Roeder, R. G., Clarke, S., Stallcup, M. R., Allis, C. D. and Coonrod, S. A. (2004). Human PAD4 regulates histone arginine methylation levels via demethylimination. *Science*, 306 (5694), p.279–283. doi:10.1126/science.1101400.

Wang, Y.-C. C., Li, H.-Y. Y., Wei, J.-N. N., Lin, M.-S. S., Shih, S.-R. R., Hua, C.-H. H., Smith, D. J., Vanio, J. and Chuang, L.-M. M. (2013). Serum vascular adhesion protein-1 level is higher in smokers than non-smokers. *Annals of human biology*, 40 (5), p.413–418. doi:10.3109/03014460.2013.788679.

Ward, S. T., Weston, C. J., Shepherd, E. L., Hejmadi, R., Ismail, T. and Adams, D. H. (2016). Evaluation of serum and tissue levels of VAP-1 in colorectal cancer. *BMC cancer*, 16, p.154. doi:10.1186/s12885-016-2183-7.

Warren, A., Le Couteur, D. G., Fraser, R., Bowen, D. G., McCaughan, G. W. and Bertolino, P. (2006). T lymphocytes interact with hepatocytes through fenestrations in murine liver sinusoidal endothelial cells. *Hepatology*, 44 (5), p.1182–1190. doi:10.1002/hep.21378.

Wedemeyer, H, He, XS and Nascimbeni, M. (2002). Impaired effector function of hepatitis C virus-specific CD8+ T cells in chronic hepatitis C virus infection. *The Journal of* Immunology, 169 (6), p.3447-3458. doi:10.4049/jimmunol.169.6.3447.

Wehr, A., Baeck, C., Heymann, F., Niemietz, P. M., Hammerich, L., Martin, C., Zimmermann, H. W., Pack, O., Gassler, N., Hittatiya, K., Ludwig, A., Luedde, T., Trautwein, C. and Tacke, F. (2013). Chemokine receptor CXCR6-dependent hepatic NK T Cell accumulation promotes inflammation and liver fibrosis. *Journal of immunology*, 190 (10), p.5226–5236. doi:10.4049/jimmunol.1202909.

Wenisch, C., Parschalk, B., Weiss, A., Zedwitz-Liebenstein, K., Hahsler, B., Wenisch, H., Georgopoulos, A. and Graninger, W. (1996). High-dose catecholamine treatment decreases polymorphonuclear leukocyte phagocytic capacity and reactive oxygen production. *Clinical and diagnostic laboratory immunology*, 3 (4), p.423–428.

Weston, C. J., Shepherd, E. L., Claridge, L. C., Rantakari, P., Curbishley, S. M., Tomlinson, J. W., Hubscher, S. G., Reynolds, G. M., Aalto, K., Anstee, Q. M., Jalkanen, S., Salmi, M., Smith, D. J., Day, C. P. and Adams, D. H. (2015). Vascular adhesion protein-1 promotes liver

inflammation and drives hepatic fibrosis. *The Journal of clinical investigation*, 125 (2), p.501–520. doi:10.1172/JCI73722.

Weston, C., Shepherd, E. and Adams, D. (2013). Cellular localization and trafficking of vascular adhesion protein-1 as revealed by an N-terminal GFP fusion protein. *Journal of Neural Transmission*, 120 (6), p.951–961. doi:10.1007/s00702-013-1003-3.

Wiedow, O. and Meyer-Hoffert, U. (2005). Neutrophil serine proteases: potential key regulators of cell signalling during inflammation. *Journal of internal medicine*, 257 (4), p.319–328. doi:10.1111/j.1365-2796.2005.01476.x.

Wieland, S. F. and Chisari, F. V. (2005). Stealth and cunning: hepatitis B and hepatitis C viruses. *Journal of virology*, 79 (15), p.9369–9380. doi:10.1128/JVI.79.15.9369-9380.2005.

Wigg, AJ, Roberts-Thomson, IC and Dymock, RB. (2001). The role of small intestinal bacterial overgrowth, intestinal permeability, endotoxaemia, and tumour necrosis factor α in the pathogenesis of non-alcoholic steatohepatitis. *Gut*. 48 (2), p.206-211. doi:10.1136/gut.48.2.206.

Wigg, A. J., Gunson, B. K. and Mutimer, D. J. (2005). Outcomes following liver transplantation for seronegative acute liver failure: experience during a 12-year period with more than 100 patients. *Liver transplantation : official publication of the American Association for the Study of Liver Diseases and the International Liver Transplantation Society*, 11 (1), p.27–34. doi:10.1002/lt.20289.

Williams, C. D., Bajt, M. L., Farhood, A. and Jaeschke, H. (2010). Acetaminophen-induced hepatic neutrophil accumulation and inflammatory liver injury in CD18-deficient mice. *Liver international : official journal of the International Association for the Study of the Liver*, 30 (9), p.1280–1292. doi:10.1111/j.1478-3231.2010.02284.x.

Williams, C., Stengel, J., Asike, M., Torres, D., Shaw, J., Contreras, M., Landt, C. and Harrison, S. (2011). Prevalence of Nonalcoholic Fatty Liver Disease and Nonalcoholic Steatohepatitis Among a Largely Middle-Aged Population Utilizing Ultrasound and Liver Biopsy: A Prospective Study. *Gastroenterology*, 140 (1), p.124–131. doi:10.1053/j.gastro.2010.09.038.

Williams, R., Aspinall, R., Bellis, M., Camps-Walsh, G., Cramp, M., Dhawan, A., Ferguson, J., Forton, D., Foster, G., Gilmore, I., Hickman, M., Hudson, M., Kelly, D., Langford, A., Lombard, M., Longworth, L., Martin, N., Moriarty, K., Newsome, P., O'Grady, J., Pryke, R., Rutter, H., Ryder, S., Sheron, N. and Smith, T. (2014). Addressing liver disease in the UK: a blueprint for attaining excellence in health care and reducing premature mortality from lifestyle issues of excess consumption of alcohol, obesity, and viral hepatitis. *Lancet*, 384 (9958), p.1953–1997. doi:10.1016/S0140-6736(14)61838-9.

Winau, F., Hegasy, G., Weiskirchen, R., Weber, S., Cassan, C., Sieling, P. A., Modlin, R. L., Liblau, R. S., Gressner, A. M. and Kaufmann, S. H. (2007). Ito cells are liver-resident antigen-presenting cells for activating T cell responses. *Immunity*, 26 (1), p.117–129. doi:10.1016/j.immuni.2006.11.011.

Winek, C. L., Wahba, W. W., Winek, C. L. and Balzer, T. W. (2001). Drug and chemical blood-level data 2001. *Forensic science international*, 122 (2-3), p.107–123. doi:10.1016/S0379-0738(01)00483-2.

Winn, J. S., Guille, J., Gebicki, J. M. and Day, R. O. (1991). Hydrogen peroxide modulation of the respiratory burst of human neutrophils. *Biochemical pharmacology*, 41 (1), p.31–36.

Wolf, M. J., Adili, A., Piotrowitz, K., Abdullah, Z., Boege, Y., Stemmer, K., Ringelhan, M., Simonavicius, N., Egger, M., Wohlleber, D., Lorentzen, A., Einer, C., Schulz, S., Clavel, T., Protzer, U., Thiele, C., Zischka, H., Moch, H., Tschöp, M., Tumanov, A. V., Haller, D., Unger, K., Karin, M., Kopf, M., Knolle, P., Weber, A. and Heikenwalder, M. (2014). Metabolic activation of intrahepatic CD8+ T cells and NKT cells causes nonalcoholic steatohepatitis and liver cancer via cross-talk with hepatocytes. *Cancer cell*, 26 (4), p.549–564.

doi:10.1016/j.ccell.2014.09.003.

Wong, VW, Won, GL, Chim, AM, Chu, WC and Yeung, DK. (2013). Treatment of nonalcoholic steatohepatitis with probiotics. A proof-of-concept study. *Annals of Hepatology*, 12 (2), p.256-262.

Wong, J., Johnston, B., Lee, S. S., Bullard, D. C., Smith, C. W., Beaudet, A. L. and Kubes, P. (1997). A minimal role for selectins in the recruitment of leukocytes into the inflamed liver microvasculature. *The Journal of clinical investigation*, 99 (11), p.2782–2790. doi:10.1172/JCI119468.

Wong, M., Saad, S., Zhang, J., Gross, S., Jarolimek, W., Schilter, H., Chen, J., Gill, A., Pollock, C. and Wong, M. (2014). Semicarbazide-sensitive amine oxidase (SSAO) inhibition ameliorates kidney fibrosis in a unilateral ureteral obstruction murine model. *American Journal of Physiology - Renal Physiology*, 307 (8), p.F908–F916. doi:10.1152/ajprenal.00698.2013.

Xu, H., Testai, F. D., Valyi-Nagy, T., N Pavuluri, M., Zhai, F., Nanegrungsunk, D., Paisansathan, C. and Pelligrino, D. A. (2015). VAP-1 blockade prevents subarachnoid hemorrhage-associated cerebrovascular dilating dysfunction via repression of a neutrophil recruitment-related mechanism. *Brain research*, 1603, p.141–149. doi:10.1016/j.brainres.2015.01.047.

Xu, R., Huang, H., Zhang, Z. and Wang, F.-S. S. (2014). The role of neutrophils in the development of liver diseases. *Cellular & molecular immunology*, 11 (3), p.224–231. doi:10.1038/cmi.2014.2.

Xu, Y., Bradham, C., Brenner, D. A. and Czaja, M. J. (1997). Hydrogen peroxide-induced liver cell necrosis is dependent on AP-1 activation. *The American journal of physiology*, 273 (4 Pt 1), p.G795–803.

Yamaguchi, Y., Ohshiro, H., Nagao, Y., Odawara, K., Okabe, K., Hidaka, H., Ishihara, K., Uchino, S., Furuhashi, T., Yamada, S., Mori, K. and Ogawa, M. (2000). Urinary trypsin inhibitor reduces C-X-C chemokine production in rat liver ischemia/reperfusion. *The Journal of surgical research*, 94 (2), p.107–115. doi:10.1006/jsre.2000.5999.

Yanaba, K., Yoshizaki, A., Muroi, E., Ogawa, F., Shimizu, K. and Sato, S. (2013). Increased circulating soluble vascular adhesion protein-1 levels in systemic sclerosis: association with lower frequency and severity of interstitial lung disease. *International journal of rheumatic diseases*, 16 (4), p.442–447. doi:10.1111/1756-185X.12094.

Yang, L., Kowalski, J. R., Zhan, X., Thomas, S. M. and Luscinskas, F. W. (2006). Endothelial cell cortactin phosphorylation by Src contributes to polymorphonuclear leukocyte transmigration in vitro. *Circulation research*, 98 (3), p.394–402. doi:10.1161/01.RES.0000201958.59020.1a.

Yao, H., Hwang, J., Moscat, J., Diaz-Meco, M., Leitges, M., Kishore, N., Li, X. and Rahman, I. (2010). Protein Kinase Cζ Mediates Cigarette Smoke/Aldehyde- and Lipopolysaccharide-induced Lung Inflammation and Histone Modifications. *Journal of Biological Chemistry*, 285 (8), p.5405–5416. doi:10.1074/jbc.M109.041418.

Yasuda, H., Toiyama, Y., Ohi, M., Mohri, Y., Miki, C. and Kusunoki, M. (2011). Serum soluble vascular adhesion protein-1 is a valuable prognostic marker in gastric cancer. *Journal of surgical oncology*, 103 (7), p.695–699. doi:10.1002/jso.21877.

Yin, M, Wheeler, MD, Kono, H, Bradford, BU and Gallucci, RM. (1999). Essential role of tumor necrosis factor α in alcohol-induced liver injury in mice. *Gastroenterology*. 117 (4), p.942-952.

Yoong, McNab, Hübscher and Adams. (1998). Vascular adhesion protein-1 and ICAM-1 support the adhesion of tumor-infiltrating lymphocytes to tumor endothelium in human hepatocellular carcinoma. *Journal of immunology*, 160 (8), p.3978–3988.

You, Q., Cheng, L., Kedl, R. M. and Ju, C. (2008). Mechanism of T cell tolerance induction by murine hepatic Kupffer cells. *Hepatology*, 48 (3), p.978–990. doi:10.1002/hep.22395.

Young, SN, Davis, BA and Gauthier, S. (1982). Precursors and metabolites of phenylethylamine,

m and p-tyramine and tryptamine in human lumbar and cisternal cerebrospinal fluid. *Journal of Neurology*. 45 (7), p.633-639.

Yraola, F., García-Vicente, S., Fernández-Recio, J., Albericio, F., Zorzano, A., Marti, L. and Royo, M. (2006). New Efficient Substrates for Semicarbazide-Sensitive Amine Oxidase/VAP-1 Enzyme: Analysis by SARs and Computational Docking. *Journal of Medicinal Chemistry*, 49 (21), acs, p.6197–6208. doi:10.1021/jm051076e.

Yu, T.-Y. Y., Li, H.-Y. Y., Jiang, Y.-D. D., Chang, T.-J. J., Wei, J.-N. N., Lin, C.-M. M., Chu, C.-C. C. and Chuang, L.-M. M. (2014). Serum vascular adhesion protein-1 level predicts risk of incident cancers in subjects with type II diabetes. *Cancer epidemiology, biomarkers & prevention : a publication of the American Association for Cancer Research, cosponsored by the American Society of Preventive Oncology*, 23 (7), p.1366–1373. doi:10.1158/1055-9965.EPI-14-0023.

Zanger, U. and Schwab, M. (2013). Cytochrome P450 enzymes in drug metabolism: Regulation of gene expression, enzyme activities, and impact of genetic variation. *Pharmacology & Therapeutics*, 138 (1), p.103–141. doi:10.1016/j.pharmthera.2012.12.007.

Zhang, H., Stolz, D. B., Chalasani, G. and Thomson, A. W. (2013). Hepatic B cells are readily activated by Toll-like receptor-4 ligation and secrete less interleukin-10 than lymphoid tissue B cells. *Clinical and experimental immunology*, 173 (3), p.473–479. doi:10.1111/cei.12126.

Zhang, J. Q., Nicoll, G., Jones, C. and Crocker, P. R. (2000). Siglec-9, a novel sialic acid binding member of the immunoglobulin superfamily expressed broadly on human blood leukocytes. *The Journal of biological chemistry*, 275 (29), p.22121–22126. doi:10.1074/jbc.M002788200.

Zhang, Y., Bi, Y., Yang, H., Chen, X., Liu, H., Lu, Y., Zhang, Z., Liao, J., Yang, S., Chu, Y., Yang, R. and Liu, G. (2014). mTOR limits the recruitment of CD11b+Gr1+Ly6Chigh myeloid-derived suppressor cells in protecting against murine immunological hepatic injury. *Journal of leukocyte biology*, 95 (6), p.961–970. doi:10.1189/jlb.0913473.

Zhao, X., Kuja-Panula, J., Rouhiainen, A., Chen, Y., Panula, P. and Rauvala, H. (2011). High mobility group box-1 (HMGB1; amphoterin) is required for zebrafish brain development. *The Journal of biological chemistry*, 286 (26), p.23200–23213. doi:10.1074/jbc.M111.223834.

Zhu, L, Baker, SS, Gill, C, Liu, W and Alkhouri, R. (2013). Characterization of gut microbiomes in nonalcoholic steatohepatitis (NASH) patients: a connection between endogenous alcohol and NASH. *Hepatology*, 57 (2), p.601-609. doi:10.1002/hep.26093.

Zhu, K., Zhang, N., Guo, N., Yang, J., Wang, J., Yang, C., Yang, C., Zhu, L., Xu, C., Deng, Q., Zhu, R., Wang, H., Chen, X., Shi, Y., Li, Y. and Leng, Q. (2014). SSChighCD11bhighLy-6ChighLy-6Glow myeloid cells curtail CD4 T cell response by inducible nitric oxide synthase in murine hepatitis. *The International Journal of Biochemistry & Cell Biology*, 54, p.89–97. doi:10.1016/j.biocel.2014.07.005.

Zimmermann, T., Müller, A., Machnik, G., Franke, H., Schubert, H. and Dargel, R. (1987). Biochemical and morphological studies on production and regression of experimental liver cirrhosis induced by thioacetamide in Uje: WIST rats. *Zeitschrift fur Versuchstierkunde*, 30 (5-6), p.165–180.

Ziol, M., Tepper, M., Lohez, M., Arcangeli, G., Ganne, N., Christidis, C., Trinchet, J. C., Beaugrand, M., Guillet, J. G. and Guettier, C. (2001). Clinical and biological relevance of hepatocyte apoptosis in alcoholic hepatitis. *Journal of hepatology*, 34 (2), p.254–260.

Zorzano, A., Abella, A., Marti, L., Carpéné, C., Palacín, M. and Testar, X. (2003). Semicarbazide-sensitive amine oxidase activity exerts insulin-like effects on glucose metabolism and insulin-signaling pathways in adipose cells. *Biochimica et biophysica acta*, 1647 (1-2), p.3–9.

Zou, Z., Li, B., Xu, D., Zhang, Z., Zhao, J.-M. M., Zhou, G., Sun, Y., Huang, L., Fu, J., Yang, Y., Jin, L., Zhang, W., Zhao, J., Sun, Y., Xin, S. and Wang, F.-S. S. (2009). Imbalanced intrahepatic cytokine expression of interferon-gamma, tumor necrosis factor-alpha, and

interleukin-10 in patients with acute-on-chronic liver failure associated with hepatitis B virus infection. *Journal of clinical gastroenterology*, 43 (2), p.182–190. doi:10.1097/MCG.0b013e3181624464.